U.S. Department
of Transportation
**National Highway
Traffic Safety
Administration**

NHTSA

DOT HS 813 269

September 2022

Rear-Seat Frontal Crash Protection Research With Application to Vehicles With Automated Driving Systems, Volume 1

Disclaimer

This publication is distributed by the U.S. Department of Transportation, National Highway Traffic Safety Administration, in the interest of information exchange. The opinions, findings and conclusions expressed in this publication are those of the authors and not necessarily those of the Department of Transportation or the National Highway Traffic Safety Administration. The United States Government assumes no liability for its content or use thereof. If trade or manufacturer's names or products are mentioned, it is because they are considered essential to the object of the publication and should not be construed as an endorsement. The United States Government does not endorse products or manufacturers.

NOTE: This report is published in the interest of advancing motor vehicle safety research. While the report may provide results from research or tests using specifically identified motor vehicle models, it is not intended to make conclusions about the safety performance or safety compliance of those motor vehicles, and no such conclusions should be drawn.

Suggest APA Format Citation:

Hardy, W. N., Kemper, A. R., Untaroiu, C. D., Albert, D. L., Meng, Y., Yates, K. M., Guettler, A. J., Bianco, S. T., Boyle, D. M., Tatem, W. M., & Chaka, M. (2022, September). *Rear-seat frontal crash protection research with application to vehicles with automated driving systems, Volume 1* (DOT HS 813 269). National Highway Traffic Safety Administration.

Technical Report Documentation Page

1. Report No.	2. Government Accession No.	3. Recipient's Catalog No.
DOT HS 813 269		

4. Title and Subtitle	5. Report Date
Rear Seat Frontal Crash Protection Research with Application to Vehicles with Automated Driving Systems, Volume 1	September 2022
	6. Performing Organization Code

7. Author(s)	8. Performing Organization Report No.
Warren N. Hardy, Andrew R. Kemper, Costin D. Untaroiu, Devon L. Albert, Yunzhu Meng, Keegan M. Yates, Allison J. Guettler, Samuel T. Bianco, David M. Boyle, Whitney M. Tatem, Michelle Chaka	

9. Performing Organization Name and Address	10. Work Unit No. (TRAIS)
Virginia Tech Transportation Institute 3500 Transportation Research Plaza (0536) Blacksburg, VA 2406	11. Contract or Grant No.

12. Sponsoring Agency Name and Address	13. Type of Report and Period Covered
National Highway Traffic Safety Administration 1200 New Jersey Avenue SE Washington, DC 20590	Final Report
	14. Sponsoring Agency Code

15. Supplementary Notes

The Contract Officer Representative is Ellen Lee.

16. Abstract

This report explores crash outcomes when tests designed for frontal crash protection are run with rear-seat 50th-percentile male occupants. Seven vehicle bucks were constructed for use in sled testing. Twenty-five tests were conducted using a 1.4-MN Seattle Safety ServoSled. Three crash pulses were used for each vehicle: an "NCAP85" pulse (NCAP pulse scaled to delta V of 56 km/h), a "scaled" pulse (NCAP pulse scaled to delta V of 32 km/h), and a "generic" pulse that was the average of the scaled pulses. A THOR-50M ATD was positioned in the left-rear seat. The THOR-50M standard abdomen was replaced with a prototype abdomen containing dual pressure sensors. A Hybrid III ATD was positioned in the right-rear seat. Injury metrics were evaluated for both ATDs and injury risk was estimated for all metrics. Sixteen out of 25 tests resulted in some degree of submarining in the THOR-50M dummy. The Hybrid III did not submarine during any test. Hybrid III and THOR-50M responses were compared for tests having relatively better or worse occupant protection performance. Restraint system characteristics were examined. To assess the validity of ATD FE models, tests from six vehicles were modeled and then quantitatively compared to the test data and injury risks. The FE models performed well enough for use in parametric studies

17. Key Words	18. Distribution Statement
ADS, ADS-DV, Automated Driving System, Federal Motor Vehicle Safety Standards, FMVSS, regulations, rear-seat safety, occupant restraint, IARVs, injury risk, submarining, Hybrid III, THOR-50M, finite element models	Document is available to the public from the DOT, BTS, National Transportation Library, Repository & Open Science Access Portal, rosap.ntl.bts.gov.

19 Security Classif. (of this report)	20. Security Classif. (of this page)	21 No. of Pages	22. Price
Unclassified	Unclassified	460	

Form DOT F 1700.7 (8-72) Reproduction of completed page authorized

Table of Contents

Executive Summary **1**

Report Contents 5
Summary Conclusion 6

Introduction **7**

Objective **9**

Approach **10**

1. Real-World Problem Scoping **12**

Quantify Rear-Seated Passenger Injury Incidence and Risk 12
Assess ADS-DV Occupant Seating Preference 19
Select Late-Model Vehicles Spanning a Range of Potential Rear-Seat Safety Performance 19
Summary Remarks 22

2. Platform and ATD Modeling, and Vehicle Selection **23**

Seat Reconstruction 23
ATD FEM Positioning and Settling 24
Impact Simulations 26
Results: Relative Safety Performance Assessment of Simulated Vehicles 28
Vehicle Selection for Sled Testing 29
Summary Remarks 30

3. Test Buck Preparation **31**

Summary Remarks 32

4. ATD Sled Testing **33**

ATD Positioning Procedure 33
Paired ATD Sled Tests using Vehicle Bucks 35
Results 42
Summary Remarks 73

5. ATD FEM Verification and Validation **75**

Results 77
Injury Metrics and Assessed Injury Probabilities From FE Simulations 81
Summary Remarks 86

Concluding Remarks **87**

References **88**

Appendix A. V1 Buck Development **A-1**

Appendix B. V6 Buck Development **B-1**

Appendix C. V10 Buck Development **C-1**

Appendix D. V13 Buck Development **D-1**

Appendix E. V14 Buck Development **E-1**

Appendix F. V15 Buck Development F-1
Appendix G. V19 Buck Development G-1
Appendix H. Sled Acceleration Pulses for All Tests H-1
Appendix I. Test-Specific Issues I-1
Appendix J. Pre- and Post-Test Images J-1
Appendix K. Select Data Traces From Test FRS-V1-1 ..... K-1
Appendix L. Select Data Traces From Test FRS-V1-2 ..... L-1
Appendix M. Select Data Traces From Test FRS-V1-3 ..... M-1
Appendix N. Select Data Traces From Test FRS-V6-1 ..... N-1
Appendix O. Select Data Traces From Test FRS-V6-2 ..... O-1
Appendix P. Select Data Traces From Test FRS-V6-4 ..... P-1
Appendix Q. Select Data Traces From Test FRS-V10-1 ..... Q-1
Appendix R. Select Data Traces From Test FRS-V10-2 ..... R-1
Appendix S. Select Data Traces From Test FRS-V10-3 ..... S-1
Appendix T. Select Data Traces From Test FRS-V13-1 ..... T-1
Appendix U. Select Data Traces From Test FRS-V13-2 ..... U-1
Appendix V. Select Data Traces From Test FRS-V13-3 ..... V-1
Appendix W. Select Data Traces From Test FRS-V14-1 ..... W-1
Appendix X. Select Data Traces From Test FRS-V14-2 ..... X-1
Appendix Y. Select Data Traces From Test FRS-V14-3 ..... Y-1
Appendix Z. Select Data Traces From Test FRS-V14-4 ..... Z-1
Appendix AA. Select Data Traces From Test FRS-V15-1 ..... AA-1
Appendix BB. Select Data Traces From Test FRS-V15-2 ..... BB-1
Appendix CC. Select Data Traces From Test FRS-V15-3 ..... CC-1
Appendix DD. Select Data Traces From Test FRS-V15-4 ..... DD-1
Appendix EE. Select Data Traces From Test FRS-V19-1 ..... EE-1
Appendix FF. Select Data Traces From Test FRS-V19-2 ..... FF-1
Appendix GG. Select Data Traces From Test FRS-V19-3 ..... GG-1
Appendix HH. Select Data Traces From Test FRS-V19-4 ..... HH-1
Appendix II. PeakTables of Data Peaks Organized by Vehicle Series II-1
Appendix JJ. Tables of IARVs and Injury Risk Organized by Vehicle Test Series JJ-1
Appendix KK. PeakTables of Diferences Between Data Peaks and IARVs of Repeat Tests KK-1

Appendix LL. ATD X-Z VICON Excursion Plots for Generic Tests LL-1

Appendix MM. ATD X-Z VICON Excursion Plots for Scaled Tests..... MM-1

Appendix NN. ATD X-Z VICON Excursion Plots for NCAP85 TESTS..... NN-1

Appendix OO. TABLES OF ATD Peak X AND Z VICON Excursions Organized by Vehicle..... OO-1

Appendix PP. ATD X-Z Peak HIP Excursion Frames for Generic Tests PP-1

Appendix QQ. ATD X-Z Peak HIP X Excursion Frames for Scaled Tests..... QQ-1

Appendix RR. ATD X-Z Peak HIP X Excursion Frames for NCAP85 TESTS RR-1

Table of Figures

Figure 2-1. FARO Surface of V10 Seat and Simplified Seat Geometry 23
Figure 2-2. Seat Force – Displacement: Measurement Point and Estimated Curve (V13) 24
Figure 2-3. Position of HIII and THOR-50M ATD FEM Prior to Settling in Seat 25
Figure 2-4. Example of ATD FEM (a) Prior to and (b) After Settling 25
Figure 2-5. (a) HIII and (b) THOR-50M in Seats With Belts Fit 26
Figure 2-6. OIM Values With the HIII (a, c) and THOR (b, d) ATD FEMs at 150 ms (a, b) and 110 ms (c, d) 29
Figure 2-7. Injury Metrics With the HIII (a, c) and THOR (b, d) ATD FEMs at 150 ms (a, b) and 110 ms (c, d) 30
Figure 4-1. THOR Resultant Head (Left) and Chest Acceleration (Right) for V15-1 & V15-2 45
Figure 4-2. THOR Upper Neck (Left) and T12 (Right) Fx For V15-1 & V15-2 45
Figure 4-3. THOR Upper Neck (Left) and T12 (Right) Fz for V15-1 & V15-2 45
Figure 4-4. THOR Upper Neck (Left) and T12 (Right) My for V15-1 & V15-2 46
Figure 4-5. THOR Left (Left) and Right (Right) ASIS Fx for V15-1 & V15-2 46
Figure 4-6. THOR UR (Left) and LR (Right) Resultant Chest Deflection for V15-1 & V19-2 46
Figure 4-7. THOR Resultant Head (Left) and Chest Accelerations (Right) for V19-3 & V19-4 47
Figure 4-8. THOR Resultant Pelvis Accelerations for V19-3 & V19-4 47
Figure 4-9. THOR Upper Neck (Left) and T12 (Right) Fx for V19-3 & V19-4 47
Figure 4-10. THOR Upper Neck (Left) and T12 (Right) Fz for V19-3 & V19-4 48
Figure 4-11. THOR Upper Neck (Left) and T12 (Right) My for V19-3 & V19-4 48
Figure 4-12. THOR Left (Left) and Right (Right) ASIS Fx for V19-3 & V19-4 48
Figure 4-13. THOR UR (Left) and LR (Right) Resultant Chest Deflection for V19-3 & V19-4 49
Figure 4-14. THOR Left (Left) and Right (Right) Abdominal Pressures for V19-3 & V19-4 49
Figure 4-15. HIII Resultant Head (Left) and Chest Accelerations (Right) for V19-3 & V19-4 49
Figure 4-16. HIII Resultant Pelvis Accelerations for V19-3 & V19-4 50
Figure 4-17. HIII Upper Neck (Left) and Lumbar (Right) Fx for V19-3 & V19-4 50
Figure 4-18. HIII Upper Neck (Left) and Lumbar (Right) Fz for V19-3 & V19-4 50
Figure 4-19. HIII Upper Neck (Left) and Lumbar (Right) My for V19-3 & V19-4 51
Figure 4-20. HIII Chest Deflection for V19-3 & V19-4 51
Figure 4-21. HIII Versus THOR Resultant Head (Left) and Chest (Right) Accelerations for V13-2 52
Figure 4-22. HIII Versus THOR Resultant Pelvis Accelerations for V13-2 52
Figure 4-23. HIII Versus THOR Upper Neck (Left) and Lumbar (Right) Fx for V14-4 52
Figure 4-24. HIII Versus THOR Upper Neck (Left) and Lumbar (Right) Fz for V14-4 53
Figure 4-25. HIII Versus THOR Upper Neck (Left) and Lumbar (Right) My for V14-4 53

Figure 4-26. HIII Versus THOR Outer (Left) and Inner (Right) Shoulder Belt Forces for V14-4 53
Figure 4-27. HIII Versus THOR Resultant Head (Left) and Chest (Right) Accelerations for V13-2 54
Figure 4-28. HIII Versus THOR Resultant Pelvis Accelerations for V13-2 54
Figure 4-29. HIII Versus THOR Upper Neck (Left) and Lumbar (Right) Fx for V13-2 54
Figure 4-30. HIII Versus THOR Upper Neck (Left) and Lumbar/T12 (Right) Fz for V13-2 55
Figure 4-31. HIII Versus THOR Upper Neck (Left) and Lumbar (Right) My for V13-2 55
Figure 4-32. HIII Versus THOR Outer (Left) and Inner (Right) Shoulder Belt Forces for V13-2 55
Figure 4-33. Post-Test Pictures of Test FRS-V13-1, Which Involved Moderate Submarining of the THOR Dummy, Partial Departure of the Pelvis From the Seat Bottom, and Slouching of the Dummy During/After Seat Belt Unloading 59
Figure 4-34. Lap Belt Loads (Left) From Test FRS-V13-1, Which Show the Rapid Drop in Seat Belt Tension When the Belt Slips off the ASIS Followed by a Lower Load Plateau as the Belt Loads the Abdomen, and Elevated and Extended ABISUP Pressures (Right) 59
Figure 4-35. ASIS X-Direction Loads (Left) and Y-Axis Moments (Right) From Test FRS-V13-1, Which Show the Rapid Drop in Lap Belt Interaction With the ASIS When the Belt Slips off the ASIS and Into the Abdomen 59
Figure 4-36. Post-Test Pictures of Test FRS-V15-2, Which Involved Minor Submarining of the THOR Dummy With the Belt Penetrating the Abdomen on the Right (Inboard) Side 60
Figure 4-37. Lap Belt Loads (Left) From Test FRS-V15-2, Which Exhibit a Relative Low Peak Load for the Right (Submarined) Side, snd ABISUP Pressures (Right) Showing a Substantially Elevated Response on the Right Side 60
Figure 4-38. ASIS X-Direction Loads (Left) and Y-Axis Moments (Right) From Test FRS-V15-2, Which Show the Rapid Drop in Lap Belt Interaction With the ASIS When the Belt Slips off the Right ASIS, But Not the Left ASIS, and Into the Abdomen 61
Figure 4-39. Peak Resultant Head Accelerations for HIII (Left) and THOR (Right) 62
Figure 4-40. HIC15 for HIII (Left) and THOR (Right) 62
Figure 4-41. BrIC for HIII (Left) and THOR (Right) 62
Figure 4-42. BrIC Injury Risk for HIII (Left) and THOR (Right) 63
Figure 4-43. HIII (Left) and THOR (Right) Upper Neck Fore/Aft Load (Fx) 63
Figure 4-44. HIII (Left) and THOR (Right) Upper Neck Tension/Compression Load (Fz) 64
Figure 4-45. HIII (Left) and THOR (Right) Upper Neck Flexion/Extension Moment (My) 64
Figure 4-46. HIII (Left) and THOR (Right) Lower Neck Fore/Aft Load (Fx) 65
Figure 4-47. HIII (Left) and THOR (Right) Lower Neck Tension/Compression Load (Fz) 65
Figure 4-48. HIII (Left) and THOR (Right) Lower Neck Flexion/Extension Moment (My) 65
Figure 4-49. Nij for HIII (Left) and THOR (Right) 66
Figure 4-50. Nij AIS 3+ Injury Risk for HIII (Left) and THOR (Right) 66
Figure 4-51. HIII (Left) and THOR (Right) Peak Resultant Chest Acceleration 67
Figure 4-52. HIII (Left) and THOR (Right) Peak Resultant Chest Acceleration 3ms Clip 67

Figure 4-53. Peak Chest Deflection for HIII (Left) and THOR (Right) 68
Figure 4-54. Thoracic AIS 3+ Injury Risk for a 40-Year-Old Based on HIII Max Deflection (Left) and Risk Functions From Craig et al. (2020)/Federal Register (2015) for THOR (Right) 69
Figure 4-55. Thoracic AIS 3+ Injury Risk for a 35-Year-Old Based on HIII Max Deflection (Left) and Risk Functions From Craig et al. (2020)/Federal Register (2015) for THOR (Right) 69
Figure 4-56. THOR Thoracic AIS 3+ Injury Risk for a 45-Year-Old (Left) and 55-Year-Old (Right) Based on Max Deflection Using the Risk Function From the Federal Register (2015) 69
Figure 4-57. THOR Thoracic AIS 3+ Injury Risk for a 35-Year-Old (Left) and a 40-Year-Old (Right) Based on PCA Score 70
Figure 4-58. HIII Lumbar (Left) and THOR T12 (Right) Fore/Aft Load (Fx) 71
Figure 4-59. HIII Lumbar (Left) and THOR T12 (Right) Tension/Compression Load (Fz) 71
Figure 4-60. HIII Lumbar (Left) and THOR T12 (Right) Flexion/Extension Moment (My) 72
Figure 4-61. Peak Resultant Pelvis Accelerations for HIII (Left) and THOR (Right) 72
Figure 4-62. Peak Left/Right Abdominal Pressures for THOR Tests With the ABISUP 73
Figure 5-1. THOR (a,b) and HIII (c,d) in the Vehicle 14 NCAP85 Sled Test at 100 ms 80
Figure 5-2. Head (a) and Hip (b) Excursion for a Non-Submarining Case With the HIII ATD FEM (V14 NCAP85) 80
Figure 5-3. Head (a) and Hip (b) Excursion for a Submarining Case With the THOR ATD FEM (V13 NCAP85) 81
Figure A-1. The Completed V1 Buck on Casters A-2
Figure A-2. Frontal View of the V1 Buck A-2
Figure A-3. Anchor Point Reinforcement Detail on the V1 Buck A-3
Figure A-4. Underside of the V1 Buck Showing Detachable Seat Track and Frame Support A-3
Figure A-5. The Seat Track and Frame Reinforcement A-4
Figure A-6. Retractor Location Reinforcement on the V1 Buck A-4
Figure A-7. Rear Seat and Retractor Reinforcement of the V1 Buck A-5
Figure A-8. Rear Seat Reinforcement of the V1 Buck A-5
Figure A-9. Rear Seat Reinforcement Structure Beneath the DAS Plates of the V1 Buck A-6
Figure A-10. Reinforcement of the Interior Front of the V1 Buck. A-6
Figure B-1. The Completed V6 Buck on Casters B-2
Figure B-2. Front V6 Buck Detail (Left) and Second Row Seating and Floor Detail (Right) B-2
Figure B-3. Rear of V6 Buck Showing Seat and Structural Supports B-3
Figure B-4. Internal V6 Buck Rear Structural Detail B-3
Figure B-5. Underneath V6 Buck Rear Seat and Anchor Reinforcements B-4
Figure B-6. Underneath V6 Buck Rear Reinforcement Details B-4
Figure B-7. Reinforcement Over the “Stow-And-Go” Recess in the V6 Buck B-5

Figure C-1. The Completed V10 Buck Mounted to the Deck of the Servosled C-2
Figure C-2. Front Reinforcement Structure Detail of the V10 Buck C-2
Figure C-3. Rear Reinforcement Structure and Seat Support in the V10 Buck C-3
Figure C-4. Interior Detail of Rear Structural Reinforcement and Restraint Support C-3
Figure C-5. Exterior Detail of Rear Structural Reinforcement and Restraint Support C-4
Figure C-6. Underneath V10 Buck Rear Seat and Anchor Reinforcements C-4
Figure D-1. Lateral Perspective of the V13 Buck on the Sled D-2
Figure D-2. Oblique Perspective of the V13 Buck on the Sled D-2
Figure D-3. Frontal Perspective of the V13 Buck on the Sled D-3
Figure D-4. Detail of the Rear Seat and Retractor Reinforcement on the V13 Buck D-3
Figure E-1. The Completed V14 Buck on Casters E-2
Figure E-2. Frontal View of the V14 Buck E-2
Figure E-3. Front Reinforcement Detail of the V14 Buck E-3
Figure E-4. Underside of the V14 Buck Anchor Point and Seat Pan Reinforcements E-3
Figure E-5. Detail of the V14 Buck Seat Pan Reinforcement From Below E-4
Figure E-6. Detail of the V14 Buck Seat Pan Reinforcement From Above E-4
Figure E-7. Retractor Location Reinforcement on the V14 Buck E-5
Figure E-8. Posterior View of the V14 Buck Showing Seatback Reinforcement E-5
Figure F-1. The Completed V15 Buck on the Sled F-2
Figure F-2. Lateral View of the V15 Buck on the Sled Under the Lights F-2
Figure F-3. Frontal View of the V15 Buck on the Sled Under the Lights F-3
Figure F-4. Posterior Oblique View of the V15 Buck on the Sled Showing Seatback Reinforcement and DAS Mounting Plates F-3
Figure F-5. Underside of the V15 Buck on the Sled F-4
Figure F-6. Seat Pan Reinforcement of the V15 Buck F-4
Figure F-7. Fuel Tank Access Structural Reinforcement on the V15 Buck F-5
Figure F-8. Urethane Foam Support of the Fuel Tank Access Cover F-5
Figure G-1. Lateral Perspective of the V19 Buck on the Sled With ATDs Installed G-2
Figure G-2. Frontal Aspect of the V19 Buck G-2
Figure G-3. Rear of V19 Buck Showing Seat Back Reinforcement G-3
Figure G-4. Underside of the V19 Buck Showing Rear Supports G-3
Figure G-5. Rear Seat and Anchor Reinforcement on the V19 Buck G-4
Figure G-6. Detail of Rear Anchor and Seat Support Structure on the V19 Buck G-4
Figure I-1. The Reinforced Seat Bottom Structure Used for Tests V1-1 and V1-2 (Left): An Original Equipment Frame Was Used for Test V1-3 (Right), Which Was an NCAP85 Test I-2

Figure I-2. Test V6-2 THOR-50M Seat Pedestal Mounting Bracket Separated and Deformed: The Pedestals for Both ATDs Were Realigned and Reinforced for Test V6-3 ..... I-3

Figure I-3. Test V6-2 THOR-50M Seat Pedestal Mounting Bracket Separated and Deformed: The Pedestals for Both ATDs Were Realigned and Reinforced for Test V6-3 ..... I-3

Figure I-4. Test V6-2, THOR-50M Inboard Rear-Seat Pedestal Anchor Pulled Through Bracket (Left), Deformed Anchor Bolt and Washer in Pedestal Riser (Middle), and Deformed Anchor Bolt and Washer in Pedestal Riser (Right): A Grade 9 Bolt Was Used for Test V6-3, and a Small Plate Was Used Instead of a Washer I-4

Figure I-5. Test V6-2 THOR-50M Seat Pedestal Mounting Bracket Separated and Deformed: The Pedestals for Both ATDs Were Realigned and Reinforced by Welding for Test V6-3 ..... I-4

Figure I-6. Test V6-3 Target (Tgt.) and Acquired (Acq.) Sled Pulses: There Is a 5-g Anomaly at the Start of the Pulse, Approximately 10 ms in Duration. When Compared to a Time-Shifted Target, the Remainder of the Acquired Pulse Aligns I-5

Figure I-7. Test V6-3 Torn Shoulder Belt (Both Sides Shown) for the THOR-50M: The Belt Was Torn During Interaction With the T1 Accelerometer Mount and the Z-Direction Accelerometer Was Damaged I-6

Figure I-8. Post Test V6-3 THOR-50M Final Posture Without the Shoulder Belt I-6

Figure I-9. Test V6-3 Broken THOR-50M Left Knee Clevis, in (Left) and out (Right) of the ATD I-7

Figure I-10. Post Test V6-3 THOR-50M Damaged Knee Slider Potentiometer Mounting Brackets (Both Knees), Which Were Removed for Subsequent Tests I-7

Figure I-11. New Seat Pedestals and Reinforcing Weldments Used for Test V6-4 for Both ATDs I-8

Figure I-12. New Reinforced Pedestals Installed for Test V6-4 (Left), Inboard Rear Grade 9 Anchor Bolt and Load-Distribution Plate Used for Both ATDs for Tests V6-3 and V6-4 ..... I-8

Figure I-13. Various Perspectives of the T1 Accelerometer Mount Shroud Implemented for THOR-50M for Use in Test V6-4 ..... I-9

Figure I-14. THOR-50M T1 Accelerometer Mount Shroud Installed for Test V-4: It Was Designed to Keep the T1 Mount From Cutting the Shoulder Belt I-10

Figure I-15. The THOR-50M T1 Accelerometer Mount Shroud Protects the Shoulder Belt When It Slips Between the Neck and Shoulder I-10

Figure I-16. THOR-50M Left Shoulder Supplemental Bib (Leather) Installed to Help Keep the Shoulder Belt From Slipping Between the Neck and Shoulder During Test V6-4 ..... I-10

Figure I-17. Revised D-Ring Slider Position Used for the THOR-50M and HIII for Test V6-4: The Slider Is Two Positions (2 Inches) From the Top Location, Which Was Used for the Previous Three V6 Tests I-11

Figure I-18. Post Test V6-4 THOR-50M Posture: The Shoulder Belt Slipped Between the Neck and Shoulder but Did Not Get Cut, and the Knees Did Not Over-Rotate Appreciably I-12

Figure I-19. During Test V6-4 the Shoulder Belt Slipped Past the Collar and Leather Bib Installed on the THOR-50M and Was Trapped Between the T1 Accelerometer Mount Shroud and the Shoulder I-12

Figure I-20. During Test V6-4 the Shoulder Belt Folded Over on Itself as It Was Trapped by the Shoulder of THOR-50M I-13

Figure I-21. The THOR-50M T1 Accelerometer Mount and Shroud Were Damaged During Test V6-4: The Mount Locating Pin and Retaining Bolt Were Compromised I-13

Figure I-22. THOR-50M Collar Damage From Test V6-4 ..... I-13

Figure I-23. Different Perspectives of the Locating Block Used to Position the T1 Accelerometer Mount on the Right Side of the THOR-50M Without Any Pins: This Block Was Used for All V10 Tests I-14

Figure I-24. The T1 Accelerometer Mount Locating Block Installed on the Right Side of the THOR-50M Spine Box, Both Without and With Accelerometers I-15

Figure I-25. Repair of the THOR-50M Collar Prior to Test V10-1 ..... I-15

Figure I-26. Damage to Seat Bottom Structures During Test V10-1 ..... I-16

Figure I-27. The Toes of the THOR-50M Contacted the Riser for the Front Seat During Test V10-2: Video Frame at Contact (Left) and Finale Posture (Right). This Minor Contact Did Not Affect the Test Results I-17

Figure I-28. Ramps Installed for Both ATDs in Buck V10 Prior to Test V10-3: These Ramps Were Designed to Prevent Contact Between the Dummy Toes and the Front Seat Riser I-18

Figure I-29. The Expanded Bib Covering the Shoulder of the THOR-50M for Test V10-3 (Left), and the T1 Shroud Used to Fill the Space on the Left Side of the Dummy (Right) I-18

Figure I-30. Damage to the THOR-50M Collar Repair From Test V10-3 ..... I-19

Figure I-31. Damage to the THOR-50M ABISUP Abdomen During Test V10-3: All Damage Was Minor, and Was Related to Seams and Corners of the ABISU I-19

Figure I-32. Seat Bottom Damage From Test V10-3 ..... I-19

Figure I-33. Details of Seat Bottom Damage From Test V10-3 ..... I-20

Figure I-34. Damage to Seat Bottom Supports From Test V13-2 (Left and Right Outboard) I-21

Figure I-35. Incorrect Data Appearing in a DAS “Data Channel” (Black Trace) and the Correct Signal Having an Incorrect Scale Factor Applied Appearing in the “Swapped Channel” (Red Trace) I-22

Figure I-36. An Example of Completely Corrected, Spliced, and Processed Data Recovered after A DAS Failure (the “Filled” Red Trace). the Effect of Filling the Data Gap Can be Seen by Comparing to the Red Trace to the Black (“Unfilled”) Trace I-22

Figure I-37. Damage to the Pelvis Flesh of the THOR-50M From Test 15-4 (Left), and Subsequent Repair (Right) I-24

Figure I-38. Loose Bolts in the Thorax of the THOR-50M Discovered After Test V19- I-25

Figure I-39. Loose Bolts at the Thoracoabdominal Junction of the THOR-50M Discovered After Test V19-3 ..... I-25

Figure I-40. Collection of Robust Repairs Made to the THOR-50M ABISUP Between Tests: Damage Typically Occurred at the Seams and Corners of the ABISUP I-26

Figure J-1. Pre-Test Images for Vehicle V1, Test 1 (Generic Pulse) J-2

Figure J-2. Post-Test Images for Vehicle V1, Test 1 (Generic Pulse) J-3

Figure J-3. Pre-Test Images for Vehicle V1, Test 2 (Specific/Scaled Pulse) J-4

Figure J-4. Post-Test Images for Vehicle V1, Test 2 (Specific/Scaled Pulse) J-5

Figure J-5. Pre-Test Images for Vehicle V1, Test 3 (NCAP85 Pulse J-6

Figure J-6. Post-Test Images for Vehicle V1, Test 3 (NCAP85 Pulse) J-7

Figure J-7. Pre-Test Images for Vehicle V6, Test 1 (Generic Pulse) J-8
Figure J-8. Post-Test Images for Vehicle V6, Test 1 (Generic Pulse) J-9
Figure J-9. Pre-Test Images for Vehicle V6, Test 2 (Specific/Scaled) J-10
Figure J-10. Post-Test Images for Vehicle V6, Test 2 (Specific/Scaled) J-11
Figure J-11. Pre-Test Images for Vehicle V6, Test 3 (NCAP85) J-12
Figure J-12. Post-Test Images for Vehicle V6, Test 3 (NCAP85) J-13
Figure J-13 Pre-Test Images for Vehicle V6, Test 4 (NCAP85 Repeat) J-14
Figure J-14. Post-Test Images for Vehicle V6, Test 4 (NCAP85 Repeat) J-15
Figure J-15. Pre-Test Images for Vehicle V10, Test 1 (Generic Pulse) J-16
Figure J-16. Post-Test Images for Vehicle V10, Test 1 (Generic Pulse) J-17
Figure J-17. Pre-Test Images for Vehicle V10, Test 2 (Specific/Scaled) J-18
Figure J-18. Post-Test Images for Vehicle V10, Test 2 (Specific/Scaled) J-19
Figure J-19. Pre-Test Images for Vehicle V10, Test 3 (NCAP85) J-20
Figure J-20. Post-Test Images for Vehicle V10, Test 3 (NCAP85) J-21
Figure J-21. Pre-Test Images for Vehicle V13, Test 1 (Specific/Scaled Pulse) J-22
Figure J-22. Post-Test Images for Vehicle V13, Test 1 (Specific/Scaled Pulse) J-23
Figure J-23. Pre-Test Images for Vehicle V13, Test 2 (NCAP85 Pulse) J-24
Figure J-24. Post-Test Images for Vehicle V13, Test 2 (NCAP85 Pulse) J-25
Figure J-25. Pre-Test Images for Vehicle V13, Test 3 (Generic Pulse) J-26
Figure J-26. Pre-Test Images for Vehicle V13, Test 3 (Generic Pulse) J-27
Figure J-27. Pre-Test Images for Vehicle V14, Test 1 (Generic Pulse) J-28
Figure J-28. Post-Test Images for Vehicle V14, Test 1 (Generic Pulse) J-29
Figure J-29. Pre-Test Images for Vehicle V14, Test 2 (Specific/Scaled Pulse) J-30
Figure J-30. Post-Test Images for Vehicle V14, Test 2 (Specific/Scaled Pulse) J-31
Figure J-31. Pre-Test Images for Vehicle V14, Test 3 (NCAP85 Pulse) J-32
Figure J-32. Post-Test Images for Vehicle V14, Test 3 (NCAP85 Pulse) J-33
Figure J-33. Pre-Test Images for Vehicle V14, Test 4 (NCAP85 Pulse), Repeat J-34
Figure J-34. Post-Test Images for Vehicle V14, Test 4 (NCAP85 Pulse), Repeat J-35
Figure J-35. Pre-Test Images for Vehicle V15, Test 1 (Generic Pulse and THOR Standard Abdomen) J-36
Figure J-36. Post-Test Images for Vehicle V15, Test 1 (Generic Pulse and THOR Standard Abdomen) J-37
Figure J-37. Pre-Test Images for Vehicle V15, Test 2 (Specific/Scaled Pulse) J-38
Figure J-38. Post-Test Images for Vehicle V15, Test 2 (Specific/Scaled Pulse) J-39
Figure J-39. Pre-Test Images for Vehicle V15, Test 3 (NCAP85 Pulse) J-40
Figure J-40. Post-Test Images for Vehicle V15, Test 3 (NCAP85 Pulse), Repeat J-41

Figure J-41. Pre-Test Images for Vehicle V15, Test 4 (NCAP85 Pulse), Repeat J-42
Figure J-42. Post-Test Images for Vehicle V15, Test 4 (Generic Pulse), Repeat J-43
Figure J-43 Pre-Test Images for Vehicle V19, Test 1 (Generic Pulse) J-44
Figure J-44. Post-Test Images for Vehicle V19, Test 1 (Generic Pulse) J-45
Figure J-45. Pre-Test Images for Vehicle V19, Test 2 (Specific/Scaled Pulse) J-46
Figure J-46. Post-Test Images for Vehicle V19, Test 2 (Specific/Scaled Pulse) J-47
Figure J-47. Pre-Test Images for Vehicle V19, Test 3 (NCAP Pulse) J-48
Figure J-48. Post-Test Images for Vehicle V19, Test 3 (NCAP Pulse) J-49
Figure J-49. Pre-Test Images for Vehicle V19, Test 4 (NCAP Pulse), Repeat J-50
Figure J-50. Post-Test Images for Vehicle V19, Test 4 (NCAP Pulse), Repeat J-51
Figure LL-1. HIII (Left) and THOR (Right) Head Excursions (Generic Tests) LL-2
Figure LL-2. HIII (Left) and THOR (Right) Shoulder Excursions (Generic Tests) LL-2
Figure LL-3. HIII (Left) and THOR (Right) Hip Excursions (Generic Tests) LL-2
Figure LL-4 HIII (Left) and THOR (Right) Knee Excursions (Generic Tests) LL-3
Figure MM-1. HIII (Left) and THOR (Right) Head Excursions (Scaled/Specific Tests) MM-2
Figure MM-2. HIII (Left) and THOR (Right) Shoulder Excursions (Scaled/Specific Tests) MM-2
Figure MM-3. HIII (Left) and THOR (Right) Hip Excursions (Scaled/Specific Tests) MM-2
Figure MM-4. HIII (Left) and THOR (Right) Knee Excursions (Scaled/Specific Tests) MM-3
Figure NN-1. HIII (Left) and THOR (Right) Head Excursions (NCAP85 Tests) NN-2
Figure NN-2. HIII (Left) and THOR (Right) Shoulder Excursions (NCAP85 Tests) NN-2
Figure NN-3. HIII (Left) and THOR (Right) Hip Excursions (NCAP85 Tests) NN-2
Figure NN-4. HIII (Left) and THOR (Right) Knee Excursions (NCAP85 Tests) NN-3
Figure PP-1. Test FRS-V1-1 HIII (Left) and THOR (Right) at Peak Hip Excursion PP-2
Figure PP-2. Test FRS-V6-1 HIII (Left) and THOR (Right) at Peak Hip Excursion PP-2
Figure PP-3. Test FRS-V10-1 HIII (Left) and THOR (Right) at Peak Hip Excursion PP-2
Figure PP-4. Test FRS-V13-3 HIII (Left) and THOR (Right) at Peak Hip Excursion PP-3
Figure PP-5. Test FRS-V14-1 HIII (Left) and THOR (Right) at Peak Hip Excursion PP-3
Figure PP-6. Test FRS-V15-2 HIII (Left) and THOR (Right) at Peak Hip Excursion PP-3
Figure PP-7. Test FRS-V19-1 HIII (Left) and THOR (Right) at Peak Hip Excursion PP-4
Figure QQ-1. Test FRS-V1-2 HIII (Left) and THOR (Right) at Peak Hip Excursion QQ-2
Figure QQ-2. Test FRS-V6-2 HIII (Left) and THOR (Right) at Peak Hip Excursion QQ-2
Figure QQ-3. Test FRS-V10-2 HIII (Left) and THOR (Right) at Peak Hip Excursion QQ-2
Figure QQ-4. Test FRS-V13-1 HIII (Left) and THOR (Right) at Peak Hip Excursion QQ-3
Figure QQ-5. Test FRS-V14-2 HIII (Left) and THOR (Right) at Peak Hip Excursion QQ-3
Figure QQ-6. Test FRS-V15-3 HIII (Left) and THOR (Right) at Peak Hip Excursion QQ-3

Figure QQ-7. Test FRS-V19-2 HIII (Left) and THOR (Right) at Peak Hip Excursion.....QQ-4
Figure RR-1. Test FRS-V1-3 HIII (Left) and THOR (Right) at Peak Hip Excursion RR-2
Figure RR-2. Test FRS-V6-3 HIII (Left) and THOR (Right) at Peak Hip Excursion RR-2
Figure RR-3. Test FRS-V6-4 HIII (Left) and THOR (Right) at Peak Hip Excursion RR-2
Figure RR-4. Test FRS-V10-3 HIII (Left) and THOR (Right) at Peak Hip Excursion RR-3
Figure RR-5. Test FRS-V13-2 HIII (Left) and THOR (Right) at Peak Hip Excursion RR-3
Figure RR-6. Test FRS-V14-3 HIII (Left) and THOR (Right) at Peak Hip Excursion RR-3
Figure RR-7. Test FRS-V14-4 HIII (Left) and THOR (Right) at Peak Hip Excursion RR-4
Figure RR-8. Test FRS-V15-4 HIII (Left) and THOR (Right) at Peak Hip Excursion RR-4
Figure RR-9. Test FRS-V19-3 HIII (Left) and THOR (Right) at Peak Hip Excursion RR-4
Figure RR-10. Test FRS-V19-4 HIII (Left) and THOR (Right) at Peak Hip Excursion RR-5

Table of Tables

Table 1-1. Risk of Fatal Injury for Restrained Rear-Seat Passenger Vehicle Occupants and RR of Fatality for Rear- Versus Front-Seat Restrained Passenger Involved in Frontal Impacts by Occupant Age and Vehicle Model Year 18

Table 1-2. Characteristics Used to Evaluate Vehicles 20

Table 1-3. Ranking of Vehicles Based on Crash and Anti-Submarining Performance 22

Table 2-1. Vehicle FE Model Information: Main Characteristics 23

Table 2-2. Nij Critical Values (Federal Register, 2015) 27

Table 4-1. The Matrix of FRS Tests Conducted 37

Table 4-2. Buck-to-Vehicle Map 37

Table 4-3. Limits and Intercepts/Critical Values for Nij Calculations 40

Table 4-4. The Standard Deviations (in mm) in Three Dimensions for the Seat Bight and Dummy H-Point Locations for Both ATDs 42

Table 4-5. Assessment of THOR-50M Submarining in FRS Series of Second-Row Sled Tests 57

Table 4-6. Sources of Submarining Evidence for the FRS Tests. A Plus Sign (+) Indicates a Positive Sign of Submarining. 58

Table 5-1. Limits and Intercepts/Critical Values for Nij Calculations 76

Table 5-2. CORA Scores for Generic (G), Scaled (S), and NCAP85 (N) Pulse Simulations With the HIII ATD FEM 78

Table 5-3. CORA Scores for Generic (G), Scaled (S), and NCAP85 (N) Pulse Simulations With the THOR Dummy 79

Table 5-4. Injury Metrics for Generic, Scaled, and NCAP85 Pulse Simulations With the HIII ATD FEM 82

Table 5-5. Injury Risks for Generic, Scaled, and NCAP85 Pulse Simulations With the HIII ATD FEM .. 83

Table 5-6. Injury Metrics for Generic, Scaled, and NCAP85 Pulse Simulations With the THOR ATD FEM 84

Table 5-7. Injury Risks for Generic, Scaled, and NCAP85 Pulse Simulations With the THOR ATD FEM 85

Table 5-8. Average Error for Each Injury Metrics 86

Table I-1. List of Signals Affected by DAS Channel Scrambling and Data Dropouts I-23

Table II-1. Data Peaks for Test Series FRS-V1 ..... II-2

Table II-2. Data Peaks for Test Series FRS-V6 ..... II-3

Table II-3. Data Peaks for Test Series FRS-V10 ..... II-4

Table II-4. Data Peaks for Test Series FRS-V13 ..... II-5

Table II-5. Data Peaks for Test Series FRS-V14 ..... II-6

Table II-6. Data Peaks for Test Series FRS-V15 ..... II-7

Table II-7. Data Peaks for Test Series FRS-V19 ..... II-8

Table OO-1. FRS-V1 Test Series Peak X and Z Direction Excursions in CM.....OO-2
Table OO-2. FRS-V6 Test Series Peak X and Z Direction Excursions in CM.....OO-2
Table OO-3. FRS-V10 Test Series Peak X and Z Direction Excursions in CM.....OO-2
Table OO-4. FRS-V13 Test Series Peak X and Z Direction Excursions in CM.....OO-3
Table OO-5. FRS-V14 Test Series Peak X and Z Direction Excursions in CM.....OO-3
Table OO-6. FRS-V15 Test Series Peak X and Z Direction Excursions in CM.....OO-3
Table OO-7. FRS-V19 Test Series Peak X and Z Direction Excursions in CM.....OO-4

Executive Summary

The research described in this report represents a proactive examination of the crash dummy behaviors observed when tests designed for frontal crash protection are run with anthropomorphic test devices (ATDs) in rear-seat positions. The project focus is the assessment of the 50th-percentile male response kinematics and kinetics in the second-row rear seat using ATDs and finite element models (FEMs). ATD and FEM injury predictions are examined as well.

The rear-seat frontal occupant protection explored in this report seeks to advance safety in vehicles driven by human drivers and vehicles also equipped with automated driving systems (ADSs). The research stemmed from work investigating technical translation options to address potential unnecessary or unintended regulatory barriers[1] to innovative new vehicle designs appearing in vehicles equipped with ADSs that lack manually operated driving controls.[2] ADS-dedicated vehicles (ADS-DVs) are designed to be operated exclusively by SAE level 4 or level 5 ADS[3] systems at maturity. The *FMVSS considerations for vehicles with automated driving systems: Volume 2* report (Chaka et al., 2021) included an analysis of FMVSS No. 208 and developed technical translation options. These translations included the possibility of mirroring the "passenger" (front right outboard seat) requirements to the left front outboard seat for ADS-DVs. While the options only included front-row seats, the potential considerations noted that "ADS-DV developments may be changing the role of the rear seat to be more like that of the front seat, affecting FMVSS No. 208 in particular." The potential consideration refers to the potential shift in occupancy rates from what is observed on the roads with human-driven vehicles today to potential seating preference in an ADS-DV shifting to the rear seat. The described research is designed to further the understanding of rear seat frontal occupant protection for forward-facing second-row seats regardless of the driver.

The objective of this research task is to support a potential translation of FMVSS No. 208 that would extend additional elements of the standard to occupants behind the front row. This consideration is predicated on the following points.

- Frontal collisions account for the majority of injuries and fatalities in motor vehicle collisions.
- It is assumed for the work that ADS-DVs subjected to FMVSS No. 208 will continue to use conventional seating configurations, and while unconventional seating configurations, such as rear facing front seats or reclining seats are being considered, they are out of the scope of this exploration.
- A number of recent studies have shown that occupant protection levels in motor vehicle collisions are disproportionately lower for rear-seat occupants as compared to front-seat

[1] The use of the term "regulatory barrier" in this report always refers to "an unintended and unnecessary regulatory barrier" because the technical translation process does not remove, reduce, or otherwise alter performance standards of the FMVSS under consideration.

[2] FMVSS considerations for vehicles with automated driving systems: Volume 1 (Blanco et al., 2020) and FMVSS considerations for vehicles with automated driving systems: Volume 2 (Chaka et al, 2021).

[3] As defined in SAE International Standard J3016, Taxonomy and Definitions for Terms Related to Driving Automation Systems for On-Road Motor Vehicles, June 2018.

occupants (Kuppa et al., 2005; Mitchell et al., 2015; Bilston et al., 2010; Durbin et al., 2015).

- It is hypothesized that occupants of ADS-DVs may self-select a rear-seat location, particularly in a rideshare environment, which could lead to higher rear-seat occupancy rates and thus an adverse effect on the annual number of occupant injuries and fatalities in the rear seat.
- The biofidelity of ATDs in this crash mode, efficacy of the corresponding injury metrics, and effectiveness of standard and advanced safety restraints cannot currently be evaluated because there is limited biomechanical response data for post mortem human surrogates (PMHS) in the rear seat during frontal collisions.

The outcomes of this research will be documented in two volumes. Volume 1 includes the ATD test results and presents a comparison and assessment of ATD FEMs. Volume 2 report will include a comparison of vehicle design and vehicle safety performance, a comparison of rear/second-row occupant protection performance to known front/first-row data, a parametric analysis of vehicle design characteristics, PMHS testing, Global Human Body Models Consortium FEM comparisons, and an analysis of rear seat characteristics of the existing "on the road" vehicle fleet.

There are five specific goals for this project.

1. Evaluate the expected incidences and outcomes of rear-seat (second row) occupants in an ADS-DV with conventional (forward-facing) seats.
2. Develop candidate positioning procedures for rear-seat ATDs for frontal crash testing.
3. Assess candidate injury criteria for rear-seat occupants for frontal crash testing.
4. Assess ATD performance for rear-seat (second row) occupants for frontal crash testing (with associated PMHS testing).
5. Assess ATD FEM and human body model FEM performance for the rear-seat (second row) occupants in frontal crash testing.

This report documents Volume 1 of the research effort, which is associated with the FMVSS 200-series, and has the following primary components: real-world problem scoping; platform/ATD modeling and test vehicle selection; test buck preparation; ATD sled testing; and ATD FEM verification and validation. These research components are designed to help delineate the boundaries of potential issues to be encountered as a result of occupants being seated anywhere other than in the front row of an ADS-DV. These efforts will provide the foundation for and inform future PMHS testing and subsequent comparison to the ATD tests to evaluate the injury-prediction capabilities of the ATDs for the rear seat and human body modeling.

For real-world problem scoping, a thorough literature review was performed to estimate the extent to which people will self-select the rear seat as their preferred seating location in an ADS-DV, understand the epidemiology associated with rear-seat occupants, understand the current state knowledge of rear-seat ATD frontal crash testing, and understand the current state of knowledge of rear-seat PMHS frontal crash testing. Next, data from the National Automotive Sampling System–Crashworthiness Data System (NASS-CDS) and the Fatality Analysis Reporting System (FARS) were used to quantify the difference in injury risk for front- and rear-seat occupants in frontal passenger vehicle crashes. During the timeframe selected for the study, 13.9 percent of occupants were seated in the rear row (includes second and third row in a vehicle with three rows) during a tow-away crash. The overall risk of serious injury as defined using the

Abbreviated Injury Scale (AIS3+) to these rear-seat occupants was 1.4 percent. When looking specifically at frontal crashes (the most common impact direction), an estimated 12.7 percent of involved occupants were rear-seated, and their risks of serious injury and fatality were 0.9 percent and 0.3 percent, respectively. In newer vehicles (model year [MY] 2007 and newer) involved in frontal crashes, the risk of fatality for rear-seat occupants was greater than for front-seat occupants. This suggests a potential disparity between front- and rear-seat restraint performance, which could be related to factors such as pretensioners and load limiters, air bags, restraint system geometry, and seat characteristics. When looking at the risk and relative risk (RR) of fatality in frontal impacts, this issue of elevated risk in the rear seats seems to be of greatest concern for older adults (55 and older). These results may suggest that the advances in rear-seat occupant protection have not kept pace with advances for the front seat, reinforcing the need for additional research related to rear-seat crash performance.

The second component of this portion of the research effort involved vehicle platform and ATD modeling as well as test vehicle selection. Late model vehicles available in the 2018 New Car Assessment Program (NCAP) post-test inventories were examined with an emphasis on seat and restraint system characteristics, restraint geometry, and seat belt routing. The collection of package information was used in conjunction with available real-world crash data and engineering assessment to determine which vehicles to consider for finite element (FE) modeling, based on perceived crash performance and anti-submarining performance. This subset of vehicles encompasses a perceived continuum of safety performance ranging from relatively worse to relatively better. Eight vehicle packages in the middle of the ranking list were selected for modeling evaluation to help inform the test vehicle selection. FEMs of the seats and restraints were created based on geometric data reconstructed from the vehicle inspections. Each vehicle's unique frontal NCAP crash pulse was used along with the Test Device for Human Occupant Restraint, or THOR-50M (v1.6), and Hybrid III (v1.0.7) 50th percentile male ATD FEMs models from Humanetics Innovative Solutions, Inc., to evaluate occupant protection performance. Based on the initial rankings of vehicles and the modeling results, a total of seven vehicles were selected for sled buck fabrication. These selected vehicles represented a wide range of performance. The output of this selection process resulted in vehicles spanning a range of second and/or third-row safety performance.

The objective of the third research component was to acquire vehicles and fabricate sled bucks from each vehicle. Seven vehicles were retrieved from NCAP/FMVSS post-test inventory with approval from NHTSA. Once the vehicles were obtained, the drivetrain, suspension, and unneeded interior components were removed. Then, each vehicle body was reinforced with steel tubing. The mid-sized sedans received an exoskeleton. After reinforcing the vehicle bodies, provisions for mounting the bucks to the sled were implemented. In addition, mounting plates for data acquisition components were fabricated and welded to the bucks. Finally, the bucks were painted with flat paint to help reduce sheen, which causes issues with the VICON motion tracking system.

The fourth research component involved performing frontal sled tests with the Hybrid III 50th percentile male ATD and the THOR-50M ATD seated in the rear seat of the test bucks that were fabricated as a part of the previous research component. Three crash pulses were used for each vehicle. First, each vehicle-specific NCAP crash pulse was scaled to a delta V of 56 km/h by scaling the pulse down to 85 percent of the original. This is referred to as the "NCAP85" pulse. Next, a "scaled" pulse was created by scaling the delta V to 32 km/h. Finally, a "generic" scaled

pulse was created by averaging the scaled pulses of the selected vehicles. Twenty-five tests were then conducted on a 1.4 MN Seattle Safety ServoSled using seven different bucks. It should be noted that 4 tests were repeated: one to compare the standard THOR-50M abdomen to the ABISUP (ABdominal Injury and SUbmarining Prediction) abdomen, one due to a data acquisition failure, one due to issues with bolts loosening in the THOR-50M, and one due to shoulder belt failure for THOR. The ABISUP is the alternative abdomen for the THOR-50M. Designed to replace the standard THOR-50M abdomen and instrumentation, it is a foam insert that has two fluid-filled reservoirs, each fitted with an internal pressure transducer.

For each test, the THOR-50M ATD was seated in the left rear seat, while the Hybrid III ATD was seated in the right. Several resources were leveraged to help develop procedures for positioning the 50th percentile dummies in an outboard, second-row seat. The available procedures were reconciled with the capabilities of the dummies, differences between front and rear seat geometries and adjustability, and differences between the dummies to develop a repeatable procedure for a limited range of ATD postures in the rear seat. For the THOR-50M ATD, all but one test was performed with the ABISUP abdomen. The matched generic scaled tests with the standard THOR abdomen and ABISUP abdomen showed that the ABISUP abdomen did not have a considerable effect on the response of the THOR, and that both the THOR and testing procedures were extremely repeatable.

The matched NCAP85 tests performed before and after tightening the spine bolts in the THOR-50M showed that the bolt looseness did not have a considerable effect on the response, and that the THOR-50M, Hybrid III, and testing procedures were very repeatable. Sixteen out of 25 tests resulted in some degree of submarining in the THOR-50M dummy, two of which were severe. The Hybrid III did not submarine during any test. The comparison between the Hybrid III and THOR-50M responses for an NCAP85 test that had good occupant protection performance and no submarining for either ATD showed that the shape, polarity, and phasing of the data were similar between the two ATDs. The comparison between the Hybrid III and THOR-50M responses for NCAP85 tests in which the THOR experienced severe submarining—while the Hybrid-III did not submarine—showed that the shape of the curves differed between ATDs for a number of variables, that the polarity of the lower neck forces and lumbar or T12 (twelfth thoracic vertebra analog) axial force differed between the ATDs, and that the similarity/dissimilarity in the magnitudes of a given measurement varied between parameters.

When comparing between the scaled and generic pulses for a given vehicle and ATD, there were no substantial differences in peak measurements or injury risks between the two pulses, which were generally below the respective injury thresholds. In general, for both ATDs, all peak measurements and injury risks were greater for the NCAP85 tests than those for the scaled and generic pulses.

The similarity in the magnitude and polarity of a given measurement between the two ATDs varied between parameters and vehicles. For the Hybrid III NCAP85 tests, the Brain Injury Criterion (BrIC) threshold was exceeded for five vehicles, the Neck Injury Criterion (Nij) threshold was exceeded for two vehicles, the peak chest acceleration injury threshold was exceeded for one vehicle, and the maximum chest deflection injury risk threshold (40 years old) was exceeded for three vehicles. For the THOR-50M NCAP85 tests, the 15-ms Head Injury Criterion (HIC15) injury threshold was exceeded for two vehicles, the BrIC injury threshold was exceeded for three vehicles, the Nij injury threshold was exceeded for three vehicles, and the

max chest deflection injury risk threshold (40 years old) was exceeded for one vehicle that had load limiters and pretensioners).

The ATD results showed that vehicle pretensioners and load limiters generally were associated with lower peak resultant head accelerations, head injury risks, and upper neck forces/moments for the NCAP85 tests. The thoracic response of the Hybrid III showed some sensitivity to the presence of pretensioners and load limiters; chest acceleration, deflection, and injury risks were lower for vehicles with pretensioners or load limiters. However, the thoracic response of the THOR-50M did not show a clear sensitivity to the presence of pretensioners and load limiters. In fact, the largest thoracic deflections and injury risks were observed in one vehicle with pretensioners and load limiters, while the lowest deflections and injury risks were observed in a third vehicle with pretensioners and load limiters. It is important to note that three of the other vehicles had moderate to severe submarining for the THOR-50M, which could have resulted in a different load path between the belt and occupant. In regard to submarining, it was found that pretensioners and load limiters did not eliminate occurrences of submarining; one of three vehicles with pretensioners and load limiters demonstrated submarining. Conversely, three of four vehicles without pretensioners and load limiters demonstrated submarining, two of which demonstrated severe submarining during the NCAP85 test related to seat pan/bottom designs that employed no substantive submarining mitigation strategy.

The fifth research component is comprised of an ATD modeling effort and an ongoing PMHS testing and human-body FE modeling planning effort. To assess the validity of the ATD FEMs, the tests from six vehicles were modeled and then quantitatively compared to the test data and injury risks. The methods for these simulations were similar to those used for the initial simulations. However, the positioning data and seat belt load cell data from the physical tests were used to update models. The simulations reasonably replicated the experimental data with average CORrelation and Analysis (Gehre et al., 2009), or CORA, scores of 0.69 and 0.64 for the Hybrid III and THOR-50M, respectively. The highest scores were usually recorded in head/chest/pelvis acceleration, the lowest in vertical forces of lumbar/T12. The simulation excursions showed better agreement with the test data in the cases without submarining. In terms of injury predictions, the dummy models usually over-predicted the test data, with the lowest errors in generic tests and the highest errors in NCAP85 tests. The average relative errors for each injury metric between simulation results and test data were consistent (0.1–0.3) except the max Nij for THOR (0.5). Based on the CORA scores and the average relative errors associated with the injury metrics, the FEMs performed well enough to be used in parametric studies of restraint systems.

The ongoing portion of this research, in combination with the fourth component, will inform future PMHS testing, and subsequent comparison to the ATD tests. This involves developing and considering options for PMHS tests, comparison between PMHS and ATD test results, and human-body FE modeling of the PMHS tests. The ATD testing has generated the information required to select four vehicle bucks to use in PMHS sled testing.

Report Contents

This report presents the methodologies, results, and analyses associated with each of the five primary research components focused on rear-seat occupant protection. These research components were developed in support of the specific objectives and goals of this study. As mentioned, this work will provide the foundation for and inform future PMHS testing,

subsequent comparison to the ATD tests to evaluate the injury-prediction capabilities of the ATDs for the rear seat, and human body modeling. Each of the five research components is organized as a separate section of the report. These sections are the following.

1. Real-world problem scoping
2. Platform and ATD modeling, and test vehicle selection
3. Test buck preparation
4. ATD sled testing
5. ATD FEM verification and validation

Section 1 presents the findings of a literature review focused on estimating the extent to which people will self-select the rear seat as their preferred seating location in an ADS-DV. In addition, the quantification of rear-seat passenger injury incidence and risk is presented through both a summary of current rear seat frontal ATD and PMHS sled testing literature and an analysis of NASS-CDS and FARS data. Further, the methods used to rank and select late-model vehicles spanning a range of potential rear-seat safety performance are explained. Section 2 describes the FEM simulations of vehicle specific NCAP tests that were performed for nine vehicle platforms, using the Hybrid III 50th percentile male ATD and THOR-50M ATD FEMs, to evaluate occupant protection performance and aid in the final test vehicle selection. Section 3 addresses the final selection of seven test vehicles, which span a range of second-row safety performance, and the methodology used to fabricate sled bucks from each vehicle. Section 4 covers the Hybrid III 50th percentile male ATD and THOR-50M ATD rear-seat frontal sled testing methods, results, and subsequent comparisons between the ATDs for the seven vehicles and three different crash pulses. Section 5 summarizes results from ATD FE simulations of the sled tests performed for six of the vehicle bucks. The computational and empirical results are quantitatively compared to assess the validity of the ATD models' use in the rear seat.

Summary Conclusion

The methodologies, results, and analyses associated with this phase of the research study were developed to focus on improving the state of knowledge in regard to rear-seat occupant protection, developing ATD testing procedures for rear-seat frontal sled tests, and evaluating the efficacy of ATD FEMs and their respective injury criteria. This first step provides the foundational work required to prepare for PMHS testing, which is critical for evaluating the efficacy of the candidate ATDs, ATD FEMs, and their respective injury criteria. The findings of this research further support the importance of addressing rear-seat occupant safety in both standard vehicles and ADS-DVs, and provide a wealth of critical information that will inform the consideration of translation of FMVSS No. 208 to extend elements of the standard to occupants behind the front row.

Introduction

As automated driving systems advance, vehicles equipped with these systems may lack manually operated driving controls (e.g., steering wheel and pedals). These ADS-dedicated vehicles are designed to be operated exclusively by an SAE level 4 or level 5 ADS.[4] These innovative new vehicle designs may change conventional seating patterns (i.e., human driver always seating in the front left outboard seat). Although unconventional seating configurations, such as rear-facing front seats, swiveling front seats, and reclining seats, have been proposed for future ADS-DVs, none has moved beyond the prototype stage. Significant research and development efforts would be needed to address the suitability of current anthropomorphic test devices and injury criteria for demonstrating occupant protection of these innovative designs. Therefore, occupant compartment configurations are not expected to change much in the near future and the first step in addressing occupant protection is exploring the forward-facing, second-row rear seat. This research stemmed from work investigating technical translation options to address potential unnecessary or unintended regulatory barriers[5] to innovative new vehicle designs appearing in vehicles equipped with ADSs that lack manually operated driving controls. The described research represents a proactive examination of the frontal-crash protection for rear-seat occupants regardless of the driver type (e.g., human or ADS). The project focus is the assessment of a 50th-percentile male in the second-row rear seat using ATDs and finite element models.

The starting point for the research was the *FMVSS Considerations for Vehicles With Automated Driving Systems: Volume 2* report (Chaka et al., 2021), which analyzed and developed technical translation options for FMVSS No. 208, Occupant Crash Protection, for conventional (forward-facing) seating. This standard specifies requirements for the protection of occupants in frontal crashes. The translations considered the "driver's designated seating position" (i.e., a human driver seated in the left-front outboard position) as a "passenger designated seating position," mirroring the front right outboard seat requirements to the left front outboard seat for ADS-DVs. While the options only included front-row seats, the potential considerations noted that "ADS-DV developments may be changing the role of the rear seat to be more like that of the front seat, affecting FMVSS No. 208 in particular." To further explain, there may be a shift in occupancy rates from front seats to rear seats in an ADS-DV. While, technical translation considerations formed the basis for the rear-seat frontal occupant crash research discussed in this report, the findings may be applicable beyond ADS-DVs.

FMVSS No. 208 and NHTSA's 5-Star consumer safety ratings program, NCAP, full-frontal rigid barrier tests are focused on adult occupants in the front seat for frontal crash protection, as they do not include the evaluation of occupant safety for rear-seat occupants (other than requirements for seat belts at rear-designated seating positions, or DSPs). FMVSS No. 214 currently evaluates occupant protection for rear-seat occupants during side impact collisions with the use of the SID-IIs 5th percentile adult female ATD. Historically, there has been a lower percentage of rear-seat versus front-seat occupancy on U.S. roadways (Trowbridge & Kent, 2009). Some have hypothesized that occupants of ADS-DVs are likely to self-select a rear-seat

[4] As defined in SAE International Standard J3016, Taxonomy and Definitions for Terms Related to Driving Automation Systems for On-Road Motor Vehicles, June 2018

[5] The use of the term "regulatory barrier" in this report always refers to "an unintended and unnecessary regulatory barrier" because the technical translation process does not remove, reduce, or otherwise alter performance standards of the FMVS under consideration.

location, particularly in a rideshare environment. In fact, a recent study focused on seating preference in highly automated vehicles (HAVs) reported that participants preferred sitting in the rear seat in both conventional (65.6%) and face-to-face seating configurations (77.6%) (Nie et al., 2020). In addition, rideshare applications may be an initial implementation of ADS technology and may represent a larger portion of the ADS-DV consumer experience moving forward.

Rideshare companies believe sharing vehicles can make transportation less expensive than personal car ownership as well as more convenient due to the reduced time and money spent on parking (Fulton, 2015; Hughes, 2017). Personal cars tend to be rarely used, remaining parked more than 95 percent of the time (Shoup, 2005) or used inefficiently (e.g., driven by the driver alone). Automated driving technology might potentially be safer, more cost-, time-, and space-efficient, and better for the environment. Given that the frontal region is the most frequent initial impact location for fatal and injured occupants in motor vehicle collisions (Traffic Safety Facts 2018 Annual Report, Table 99 [NCSA, 2020]) and that the increased use of ADS-DVs could lead to an increased percentage of rear-seat occupancy, it may be important to consider further rear-seat occupant protection in frontal collisions. Therefore, this research effort is focused on rear-seat occupant protection during frontal crashes in support of the FMVSS Considerations for Automated Driving Systems project, specifically the FMVSS No. 208 technical translations. In the following, "rear seat" specifically refers to second-row seating positions or occupants.

If there were no change in occupant protection requirements, the hypothesized propensity of occupants to sit in the rear of ADS-DVs could have a considerable adverse effect on the number of occupant injuries and fatalities. Studies have shown that occupant protection in motor vehicle collisions is worse for adult rear-seat occupants compared to adult front-seat occupants (Kuppa et al., 2005; Mitchell et al., 2015). Overall, the fact that the risk of injury in frontal collisions is higher for rear-seat occupants than for front-seat occupants, especially in newer vehicles with advanced restraints in the front row and for older occupants, warrants consideration of improved rear-seat safety performance and evaluation. There have been a number of studies aimed at evaluating the effectiveness of the standard and advanced safety restraints for rear-seat occupants during frontal sled tests using ATDs. These studies compared rear-seat occupant protection offered by standard three-point belts equipped with advanced features (including retractor pretensioners, progressive load limiters, and inflatable seat belts) and found substantial reductions in rear-seat ATD injury measures with the use of advanced restraints (Forman et al., 2008, 2010; Sundararajan et al., 2011; Hu et al., 2015, 2017; Beck et al., 2014; and Tavakoli et al., 2015). Further, the possibility of occupants submarining the safety lap belt remains a concern in some of these tests. Fewer studies were found to have evaluated the biomechanical response of post-mortem human subjects (PMHS) in frontal, rear-seat, or sled tests against which the biofidelity of ATDs in this crash mode can be checked (Michaelson et al., 2008; Forman et al., 2009; Sundararajan et al., 2011; Luet et al., 2012; and Uriot et al., 2015). To date there has not been a study or series of studies examining rear seat-safety performance for a range of vehicles that attempt to connect that performance to real-world exposure and risk. In addition, there has not been a study to evaluate the appropriateness of ATD performance for rear-seat risk assessment by comparison to PMHS damage responses under a range of conditions in matched testing, nor has there been an in-depth effort to assess commercially available ATD FEM performance in the rear seat for frontal crashes. These are needed to provide a clearer picture of potential current risk to a rear-seat passenger.

Objective

The objective of this research task is to support a potential translation of FMVSS No. 208 that would extend additional elements of the standard to occupants behind the front row. This research objective was developed in collaboration with NHTSA. This research is based on the potential change in seating preference in an ADS-DV and is predicated on five points.

1. According to data from NHTSA's Traffic Safety Facts annual report (NCSA, 2020), frontal collisions account for the majority of injuries and fatalities in motor vehicle collisions.
2. It is expected that ADS-DVs will continue to use conventional seating configurations, and it is unknown when unconventional seating configurations will become more prevalent.
3. A number of recent studies have shown that occupant protection in motor vehicle collisions is disproportionately lower for rear-seat occupants compared to front-seat occupants, which is likely due to the fact that the frontal collision occupant protection tests are biased to the front seat (Kuppa et al., 2005; Bilston et al., 2010; Durbin et al., 2015).
4. It is hypothesized that occupants of ADS-DVs are likely to self-select a rear-seat location, particularly in a rideshare environment, which could lead to higher rear-seat occupancy rates and, thus, a considerable increase in the annual number of occupant injuries and fatalities.
5. The biofidelity of ATDs in this crash mode, efficacy of the corresponding injury metrics, and effectiveness of standard and advanced safety restraints cannot currently be evaluated because there is limited biomechanical response data for PMHS in the rear seat during frontal collisions.

In summary, ADS-DV developments may be changing the role of the rear seat to be more like that of the front seat, thereby affecting the efficacy of FMVSS No. 208 in particular. Therefore, the following effort seeks to achieve the following specific goals:

- Evaluate the expected incidences and outcomes of rear-seat (second row) occupants in an ADS-DV with conventional forward-facing seats.
- Develop candidate dummy positioning procedures for rear-seat ATDs for FMVSS No. 208 frontal crash testing.
- Assess candidate injury criteria for rear-seat occupants for FMVSS No. 208 frontal crash testing.
- Assess ATD performance for rear-seat (second row) occupants for FMVSS No. 208 frontal crash testing (associated with long-term research and PMHS testing).
- Assess ATD FEM and human body model FEM performance for the rear-seat (second row).

Approach

The first phase of the research effort associated with the FMVSS 200-series has five primary components. These research components are designed to help delineate the boundaries of potential issues that might be encountered as a result of occupants being seated behind the front row of an ADS-DV. The five primary components of this effort:

1. Real-world problem scoping
2. Platform/ATD modeling, and test vehicle selection
3. Test buck preparation
4. ATD sled testing
5. ATD FEM verification and validation

The organization of the five primary research components and their respective sections are illustrated in Figure 1. The output from each of the components feeds into the next in a logical progression. These efforts will inform options for future PMHS testing and subsequent comparison to the ATD tests to evaluate the injury-prediction capabilities of the ATDs for the rear seat and human body modeling.

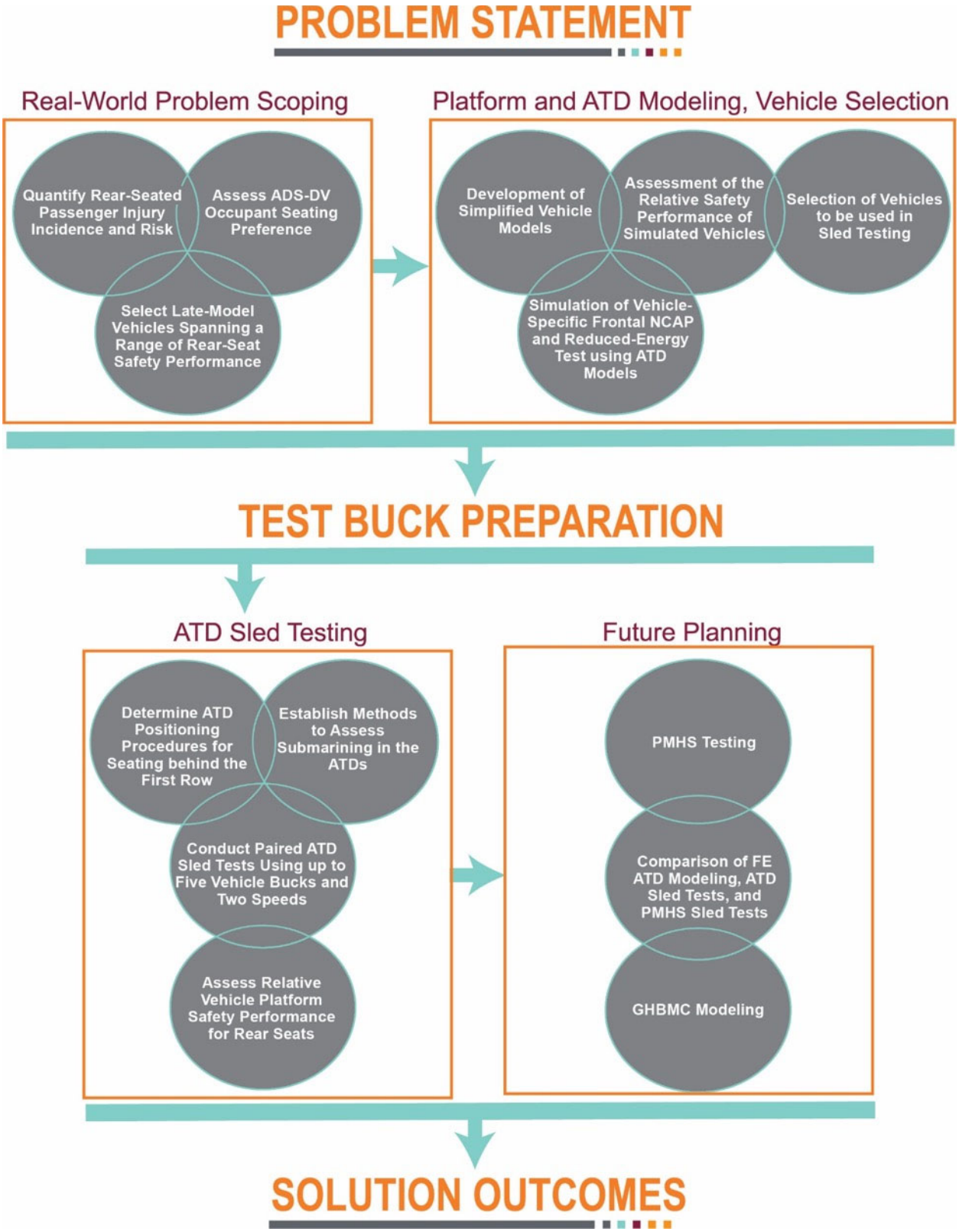

Figure 1. Sequencing and Flow of the Five Primary Research Components

1. Real-World Problem Scoping

This study initially examined the current risk to second-row occupants in frontal crashes by quantifying rear-seat passenger injury incidence and probability. It continued by estimating the extent to which people would self-select the rear seat as their preferred seating location in an ADS-DV. A primary aspect of the initial effort was the inspection of late-model vehicles to approximate relative crash performance characteristics based upon rear-seat package geometry and restraint system attributes. This was done to provide a set of vehicles to model, and a subsequent smaller set of vehicles to test, that spanned a range of potential rear-seat safety performance.

Quantify Rear-Seated Passenger Injury Incidence and Risk

The objective of this section is to better understand how current passenger seating distribution influences injury incidence and risk in frontal crashes. This knowledge will provide a baseline indication of rear-seat crash exposure and performance and will demonstrate the relative importance of frontal crash protection to rear-seat occupants in the absence of ADS-DV transportation. A literature review and a study on the differential injury risk between front and rear-seat occupants in frontal crashes are presented as follows.

Literature Review

An assessment of FMVSS technical translations indicates there is a critical knowledge gap in how to assess the injury risk for rear-seat occupants in frontal collisions. The current U.S. protection regulation for frontal impacts, FMVSS No. 208, and the NCAP full-frontal rigid barrier test are focused on the front seat and do not include the evaluation of occupant safety for rear-seat occupants. FMVSS No. 208 prescribes frontal crash test procedures, which include a full-frontal crash. In this test, each subject vehicle impacts a fixed, rigid concrete barrier at a velocity of approximately 56.3 km/h (35 mph) with 100 percent overlap. The standard specifies belted and unbelted performance requirements for the 50th percentile male and 5th percentile female Hybrid III ATDs in the driver and front outboard passenger seating positions.

FMVSS No. 208 also prescribes a frontal offset crash test. In this test each subject vehicle is propelled into a deformable barrier at a 40 percent offset at a velocity of approximately 40 km/h (25 mph). Subject vehicles may be tested on either the driver or passenger side, and their performance is evaluated on the impacted side (either the driver or the front passenger) from the responses recorded by a 5th percentile female Hybrid III ATD seated in the tested location. There are no ATD performance requirements for the rear seats for either this offset test or the previously described full-frontal impact test.

Trowbridge and Kent (2009) reported that only 12.9 percent of person-trips had rear-seat occupants. However, approximately 34.5 billion trips have been traveled annually and 399 billion vehicle miles were traveled with a rear-seat passenger, which indicates that the national at-risk exposure remains high (Bose et al., 2017). It has been reported that rear-seat occupants account for 23 percent of occupants with injuries and about 9 percent of fatalities in the publicly available database of tow-away crashes (Bilston et al., 2010). However, the percentage of rear-seat passengers may increase dramatically in the future with the increasing prevalence of ADS-DVs on the roadway. The rationale behind this is that with the advent of vehicles with high-level ADSs (level 4) and full automation (level 5), which do not require occupants to have any driving

involvement in certain or all conditions, passengers may elect to sit in the rear seat for increased comfort, perceived safety, and peace of mind. In fact, a recent survey study focused on seating preference in HAVs reported that "the rear seat was preferred in both the conventional (65.6%) and "face-to-face mode" seating configurations (77.6%), largely due to the fact that customers subjectively viewed it as being safer than sitting in a front seat in case of collisions" (Nie et al., 2020). The tendency of passengers to sit in the rear seat may be especially true for taxi services that use HAVs with level 4 or 5 automation, since passengers may have a psychological predisposition to sit the rear seat of a taxi that pulls up to the curb on the passenger side. In a study by Nemire (2017), it was reported that 91% of taxi passengers and 81% of rideshare passengers were rear-seat passengers.

The potential increase in the percentage of rear-seat occupants could lead to an increase in the number of occupant injuries and fatalities, since a number of recent studies have shown that occupant protection in motor vehicle collisions is worse for rear-seat adult occupants compared to front-seat adult occupants. Durbin et al. (2015) evaluated all crashes from 2007 to 2012 involving MY 2000-and-newer passenger vehicles in the NASS–CDS and FARS. It was reported that "after controlling for occupant age and gender, the relative risk of death for restrained rear-row occupants was significantly higher than that of front-seat occupants in MY 2007-and-newer vehicles and significantly higher in rear- and right-side impact crashes." Kuppa et al. (2005) compared the responses of 5th female and 50th male Hybrid III ATDs in the rear seats to those in the front seats during full-frontal vehicle crash tests into rigid barriers at 48 km/h and 56 km/h, and reported that ATDs in the rear seat had considerably higher head, neck, and chest injury risks. In addition, the percentage of ATD tests that had injury measures that exceeded threshold levels was substantially higher for rear-seat occupants (0–100% depending on the injury metric and crash speed) compared to front-seat occupants (0–12%).

Mitchell et al. (2015) evaluated injured rear- versus front-seat car passengers in the same vehicle from 2001 to 2011 in New South Wales, Australia, and reported that rear-seat passengers sustained higher severity injuries compared to front-seat passengers traveling in the same vehicle. In the study, information regarding the type of restraint, such as whether the seat belt was a shoulder and lap belt or lap-only, was not recorded. Mitchell et al. (2015) also reported that when only head-on vehicle-to-vehicle crashes were considered, the adjusted risk ratios of rear seat compared to front-seat occupants were significantly higher for the neck (2.12), and for the abdomen, lower back, lumbar spine, and pelvis (8.1), but were significantly lower for the upper extremities (0.59). Bilston et al. (2010) estimated the relative injury risk for front- and rear-seat occupants by matching front and rear occupants within a single vehicle in the same crash using NASS data from 1993 to 2007. Bilston et al. (2010) reported that the front and rear seats offered similar levels of protection in older vehicles (1990–1996) for occupants 16 to 50 years old. However, in newer model vehicles (1997–2007) the rear seat carried a higher risk of injury than the front seat (relative risk = 2.01 to 3.16). Overall, the fact that the risk of injury in frontal collisions is higher for rear-seat occupants than for front-seat occupants, especially in newer vehicles and for older occupants, illustrates that there is a need for improved rear-seat safety restraint system performance and evaluation.

A number of studies have evaluated the effectiveness of standard and advanced safety restraint systems for rear-seat occupants during frontal sled tests using ATDs. Forman et al. (2008) performed matched 29 km/h and 48 km/h frontal, rear seat, ATD sled tests with standard three-point belts and three-point belts with a retractor pretensioner and progressive load limiter using a

6-year-old Hybrid III, 5th female Hybrid III, 50th male Hybrid III, and 50th male THOR-NT. The results showed that the combined load limiter and pretensioner belt resulted in reduced peak chest deflections with little to no increase in head excursion and reduced pelvic excursion. Forman et al. (2010) performed 29 km/h and 48 km/h frontal, rear seat, ATD sled tests with an inflatable seat belt ("airbelt") using a 50th male Hybrid III ATD and compared the results to the previously performed 50th male Hybrid III ATD tests using combined load limiter and pretensioner three-point belts and reported that the airbelt resulted in significantly lower chest deflections and flexion moments in the lower neck. Similarly, Sundararajan et al. (2011) evaluated the effectiveness of a rear seat inflatable seat belt relative to a standard three-point seat belt during 56 km/h frontal sled tests with a 50th male Hybrid III, and reported that the inflatable belt resulted in reduced forward head excursions and peak chest deflections relative to the standard belt. Hu et al. (2015, 2017) performed matched frontal, rear seat, ATD sled tests with various combinations of safety restraint systems (standard three-point belts, four-point belts, retractor and/or buckle pretensioners, load limiters [constant load limiter, progressive load limiter, or switchable load limiter], inflatable three-point belt, bag in roof, and bag in front seat) using a 6-year-old Hybrid III, 5th female Hybrid III, 50th male THOR-NT, 95th male Hybrid III. The two crash pulses ("soft" and "severe") were based on U.S. NCAP frontal barrier tests. The data showed that the baseline three-point belt system resulted in many injury measures exceeding injury assessment reference values (IARVs). However, the data from the tests with the soft crash pulse showed that the advanced-belt-only condition (i.e., three-point belt, constant load limiter, retractor pretensioner, anchor pretensioner, and dynamic locking tongue) and an advanced-belt-plus-bag-in-front-seat condition reduced all the injury measures below the IARVs for all four ATDs. For the severe crash pulse, both advanced restraint systems reduced nearly all the injury measures for all ATDs, except for the THOR-50M. This was chiefly related to the maximum chest deflection measured in the THOR. The lower quadrant of the chest nearest to the seat belt buckle tended to experience larger deflection, while deflection in the upper thorax was typically reduced, as were other measures in the THOR.

Beck et al. (2014) performed a series of 45.8 km/h frontal sled tests with a 5th female Hybrid III ATD in the rear seat. In this study the authors used a typical sedan that was modified to allow for different anchorage positions for the upper belt, different seat belt buckle lengths, anti-submarining or flat seat pans, and seat belt pretensioner with load limiters. Beck et al. (2014) reported that posture (upright versus slouched) had the strongest effect on submarining, and that combined pretensioner and load limiter belts reduced head excursion, femur excursion, and chest deflections but did not prevent submarining. The anti-submarining seat pan reduced all injury measures, except pelvic rotation, for the upright posture. Submarining was observed in the upright posture with the flat seat pan and high inboard anchorage position, but not with the anti-submarining seat pan. Submarining was observed in the slouched posture tests regardless of the seat pan type. Longer seat belt buckle lengths resulted in submarining and increased femur excursions. Finally, the upper belt anchorage location affected the ATD response. Specifically, anchorage positions resulting in poor belt geometry (either low, wide or high inboard positions) increased both chest injury measures and occupant submarining relative to standard upper anchorage position; i.e., the belt across the center of the chest and shoulder.

Tavakoli et al. (2015) performed 56 km/h frontal, rear seat, ATD sled tests with three-point belts with varying combinations of pretensioners and load limiters using a 5th female Hybrid III, and 50th male Hybrid III. The results showed that the implementation of pretensioners affected both the pelvis acceleration and the chest acceleration for the 5th female Hybrid III and 50th male

Hybrid III. Use of a pretensioner belt aided the most in reducing occupant indices. There was a 50-percent improvement in HIC15 with the use of a pretensioner belt and the pretensioner belt showed approximately 50 percent of the baseline 36-ms Head Injury Criterion (HIC36) values. When load limiters were used in conjunction with pretensioners there was an additional 30 percent reduction in HIC and a 15-percent reduction in head and chest accelerations.

To the authors' knowledge, there have been five studies that have evaluated the biomechanical responses of PMHS in frontal, rear seat sled tests. Michaelson et al. (2008) performed 48 km/h, frontal, rear seat sled tests with three ~50th male PMHS (n = 3), a standard three-point belt, and a vehicle seat designed to be representative of a 2004 mid-sized sedan. All PMHS had severe chest injuries (AIS 4), cervical spine injuries between AIS 1 and AIS 5, thoracic or lumbar spine injuries between AIS 1 and AIS 3, and submarining. Forman et al. (2009) performed matched sled tests (48 km/h, frontal, rear seat) with three (n = 3) ~50th male PMHS and the same vehicle seat as Michaelson et al. (2008), but used three-point belts with a retractor pretensioner and progressive load limiter. The authors reported that the combined load limiter and pretensioner belt resulted in reduced shoulder belt tension, spine acceleration, and pelvic excursion, but increased forward torso rotation and shoulder belt pay out. One load limiter and pretensioner belt test resulted in submarining. Similar average maximum normalized chest deflections and mid-sternum deflections were observed for both belt types. The PMHS tests with the load limiter and pretensioner belt resulted in moderate to severe chest injuries (AIS 2, 4, and 4), one serious cervical spine injury (AIS 3), and moderate thoracic spine injuries (AIS 0, 2, 2). However, due to differences in age and bone quality between the two test groups and the limited sample size, no definitive conclusions could be made in regard to the injury outcomes with respect to restraint type.

Sundararajan et al. (2011) evaluated the effectiveness of a rear-seat inflatable seat belt relative to a standard three-point seat belt during 56 km/h frontal sled tests with four (n = 4) 50th male PMHS and four (n = 4) small female PMHS, and reported that the inflatable belt resulted in reduced forward head excursions, peak chest deflections, rib fractures, and cervical spine injuries relative to the standard belt. Luet et al. (2012) performed sled tests at 40 km/h and 50 km/h, using a custom made seat with an adjustable rigid seat pan and flat seat back with 10 cm of vehicle seat foam on it, with eight male PMHS (n = 9), eight male and one female PMHS (n = 1), which were all similar in size. Two belts were used to mimic a three-point belt in order to prevent the compromise of the tests' repeatability. The authors reported iliac wing fractures in five out of nine PMHS subjects. The fractures occurred at the Anterior-Superior Iliac Spine (ASIS) level where the lap belt was situated during testing. The authors also reported discrepancies between the biofidelity of the Hybrid II and Hybrid III 50th male ATD versus a PMHS subject when submarining occurred. Uriot et al. (2015) performed sled tests on eight male PMHS (n = 8) at 40 km/h and 50 km/h with three-point load limiter belts in the front and rear seat configuration using a custom made seat with an adjustable seat pan and flat back. There was no submarining observed in the front seat configuration. However, all subjects sustained pelvic fractures and demonstrated submarining in the rear seat configuration. The belt to pelvis angle was found to be one of the key parameters for submarining. It was noted that it was not possible to dissociate iliac wing fractures from submarining. The authors reported that the rear seat configuration resulted in more liver and spleen injuries than the front seat configuration. In regard to the observed thoracic skeletal injuries (i.e., rib fractures), five PMHS had AIS 4 injuries and three PMHS had AIS 3 injuries. Lung laceration AIS 3–4 injuries occurred in five

PMHS tests. Every PMHS had AIS 2 injuries to the pleurae, and six PMHS had AIS 2-3 lumbar spine injuries.

Given that there are currently no U.S. regulatory tests that assess rear-seat occupant safety, the design of the rear seat, rear seat safety restraints, and consequently occupant protection, can vary drastically between vehicle manufacturers and between makes and models for a given vehicle manufacturer. Kuppa et al. (2005) reported that head injury criterion (HIC15) values for rear-seat occupants varied considerably between five full-frontal vehicle crash tests into a rigid barrier at 48 km/h and 56 km/h, with some tests resulting in HIC values above the injury threshold. Although previous ATD and PMHS studies have shown that advanced and/or optimized rear-seat safety restraint systems could potentially improve rear-seat occupant protection in frontal collisions, these studies are very limited. Nearly all these previous studies evaluated only one type of rear seat and one belt anchorage configuration within the given study. While Beck et al. (2014) evaluated different seat pans and upper belt anchorage configurations, the authors only evaluated the responses of the 5th female Hybrid III ATD and noted that the configurations that were evaluated may not be representative of all vehicle configurations. Additionally, the effect of the lap belt anchorage configurations in the rear seat has not been evaluated. Also, there are only a limited number of rear-seat occupant tests and test configurations using a PMHS or the 50th male THOR-NT ATD, and only one series of rear seat tests with the newest version of the 50th male THOR ATD (THOR-50M), or the 5th female THOR ATD (THOR-05F). A study conducted by Crandall (2013) included a series of 48 km/h rear-seat sled tests using the most updated version of the THOR-50M. Nine frontal-impact rear-seat tests were performed using three different restraint systems. Three tests employed OEM belts with no advanced restraints—three had seat belt pretensioners and load-limiters, and three had inflatable belts. Only one buck was tested (2000 Taurus with a bench-style rear seat) and average peak chest deflection (IR-TRACC measurements) and peak seat belt loads were the only metrics reported. The inflatable belt was found to produce the lowest chest deflections and seat belt loads. Finally, there are currently no standard rear-seat positioning procedures for PMHSs or ATDs.

Differential Injury Risk Between Front and Rear-Seat Occupants in Frontal Crashes

The aim of this study was to quantify the difference in injury risk for front- and rear-seat occupants in frontal passenger vehicle crashes. In a frontal collision, the historical wisdom has been that rear-seat occupants are at a lower risk of injury in frontal crashes than their front seat counterparts. However, as previously discussed, recent studies have suggested otherwise. Further, significant advances in passive safety countermeasures, such as advanced air bags, seat belt pretensioners, load limiters, and structural improvements primarily benefit front-seat occupants. In addition, U.S. regulatory emphasis on occupant protection in frontal crashes has focused exclusively on front-seat occupants. With the safety advances and regulatory emphasis on front-seat occupant protection, protection of front-seat occupants has surpassed the protection of those in the rear seat. While existing studies provide valuable insight into the potential increased risk to rear-seat occupants, a more complete picture captured using more-recent data is needed. A reexamination is needed of the differential injury risk between front and rear-seat occupants in frontal crashes.

Methodology

The following study was based upon data from the NASS-CDS and FARS. Cases were extracted from both databases for all crashes occurring during case years 1999–2015 involving MY 2000 and newer passenger vehicles. The vehicle model year restriction of 2000 and later was imposed to help ensure that all vehicles in the resulting dataset were equipped with frontal air bags. Additionally, selected vehicles must have been within the most recent 10 model years relative to the crash year, as many crash details are not available in NASS-CDS for vehicles older than 10 years. FARS data on occupants involved in selected cases were substituted for the weighted sample of comparable NASS-CDS fatal cases in order to produce a combined injury dataset with exact fatality counts. When calculating risk estimates, fatalities were obtained from FARS and estimates of the total occupant exposure were extracted from NASS-CDS.

Variables of interest in this study that may affect the risk of injury to occupants include occupant age, occupant sex, vehicle model year, and vehicle type. All of these variables were treated categorically in this study. That is, occupant age was categorized into seven groups: 0–3 years, 4–8 years, 9–12 years, 13–19 years, 20–54 years, and 55 years and older. These were chosen both for consistency with previous studies and to reflect the age groups that are recommended to use the different restraint systems, such as the various additive child restraint systems. Furthermore, the vehicle model years were categorized as 2000–2002, 2003–2006, and 2007–2016. These MY categorizations were chosen to reflect the air bag technology present in the case vehicles. Model year 2000–2002 vehicles were primarily equipped with single-stage frontal air bags, and MY 2003–2006 vehicles reflect the phase-in period for advanced multi-stage frontal air bags. By MY 2011, all vehicles were equipped with advanced frontal air bags.

The intent of this study was in part to probe the effect that recent changes in vehicle restraint systems have had on injury risk. Therefore, occupants in this analysis were limited to those who were taking full advantage of a vehicle's safety systems by wearing their seat belt. This included children using additive protective equipment, such as a child restraint system.

Statistical Analysis

The combined CDS-FARS dataset was used along with logistic regression modeling to compute the relative risk (RR) of fatality for restrained rear versus front passenger seat occupants (i.e., non-drivers) adjusting for occupant age, occupant gender, impact direction, vehicle model year, and vehicle type. In this study, odds ratios from logistic regression are reported as the adjusted RRs. Odds ratios are a good approximation of RRs when the outcome of interest is uncommon, as fatalities are in this study.

All analyses were performed in R and SAS v9.4. The combined CDS-FARS dataset retained the NASS-CDS sampling weights, with case weights in FARS set to 1 as it is a census database. All proportion (weighted %) and risk analyses use these sampling weights, unless otherwise noted.

Results

During the timeframe selected for the study using NASS-CDS, an estimated 13.9 percent of occupants were seated in the rear row (includes second and third row in vehicles with three rows) during a tow-away crash. The overall risk of serious injury (AIS3+) to these rear-seat occupants was 1.4 percent. When looking specifically at frontal crashes, the most common impact

direction, an estimated 12.7 percent of involved occupants were rear-seated, and their risk of serious injury and fatality was 0.9 percent and 0.3 percent, respectively.

Risk of Fatality in the Rear Row in Frontal Impacts

Table 1-1 shows the sample of 2,242 restrained rear-row occupants who were fatally injured in frontal impacts over the time period of study and estimates the risk of fatal injury for restrained rear-row occupants by age and vehicle model year. The RR of fatality for rear- versus front-row (non-driver) restrained occupants is provided as well. Restrained rear-seat occupants 55 and older display a significantly higher risk of fatal injury (1.62%) in frontal crashes than their younger counter parts (average of 0.14%). This also holds true when looking at the RR of fatal injury. More importantly, there was significant evidence that restrained rear-row occupants in MY 2007 and newer vehicles are at a higher risk of fatality than front-row occupants (RR 1.36, 95% confidence interval [CI] 1.23-1.49). When comparing this RR to earlier model year categories, the trend was clear. The RR of fatal injury for rear versus front-seat occupants has been increasing in newer model year vehicles.

Table 1-1. Risk of Fatal Injury for Restrained Rear-Seat Passenger Vehicle Occupants and RR of Fatality for Rear- Versus Front-Seat Restrained Passenger Involved in Frontal Impacts by Occupant Age and Vehicle Model Year

Sample Characteristic	Number WWith Fatal Injury in Rear Seat *N* = 2,242 (Weighted%)	Risk of Fatal Injury in Rear Seat (95% CI)	RR of Fatal Injury (95% CI) for Rear Versus Front Seat
Occupant Age			
0–3	390 (17.40)	0.14% (0.13–0.15)	0.24 (0.16–0.36)
4–8	341 (15.21)	0.10% (0.09–0.12)	0.47 (0.37–0.60)
9–12	158 (7.05)	0.10% (0.08–0.11)	0.92 (0.71–1.21)
13–19	286 (12.76)	0.14% (0.12–0.15)	0.78 (0.68–0.90)
20–54	432 (19.27)	0.22% (0.20–0.24)	0.81 (0.73–0.90)
55+	635 (28.32)	1.62% (1.50–1.75)	1.44 (1.32–1.57)
Vehicle Model Year			
2000–2002	662 (29.53)	0.15% (0.14–0.16)	0.75 (0.68–0.82)
2003–2006	878 (39.16)	0.19% (0.17–0.20)	0.97 (0.89–1.05)
≥ 2007	702 (31.31)	0.21% (0.19–0.23)	1.36 (1.23–1.49)

Discussion

In newer vehicles (MY 2007+) involved in frontal crashes, the risk of fatality for rear-seat occupants was found to be greater than for front-seat occupants. This suggests a discrepancy between front and rear seat restraint performance. In contrast, for older vehicles (MY 2000–2006), there was no statistically significant difference in fatality risk between front- and rear-seat occupants. When looking at the risk and RR of fatality in frontal impacts, this issue of an elevated risk in the rear seats seems to primarily be a concern for older adults 55 and older.

Assess ADS-DV Occupant Seating Preference

The objective of this section of Real-World Problem Scoping is to better understand how passenger seating distribution might change as ADS-DVs become more prevalent. This knowledge will assist in determining the nature of the exposure of ADS-DV passengers and the relative importance of rear-seat frontal crash protection.

To assess occupant seating preference, a search for literature on occupant seating preference in ADS-DVs was performed. To date, there is very little literature on this topic, but seating preference is continually being researched. In Nemire (2017), seat belt use by adult rear-seat passengers in taxis and rideshare vehicles was investigated. Participants in the study were drivers and passengers from the general public in Las Vegas, Nevada, and San Francisco, California. Although occupant seating preference was not the primary focus of the study, of the 187 passengers observed in taxis and rideshare vehicles, 165 were rear-seat passengers. In terms of percentages, 91 percent of taxi passengers were rear passengers and 81 percent of rideshare passengers were rear passengers. In a recent study by Nie et al., (2020), seating preference in HAVs and occupant safety awareness were assessed for 1,018 people in China using a survey. This study reported that the majority of participants indicated that they would prefer to sit in the rear seat in both the conventional (65.6%) and face-to-face seating configurations (77.6%). The authors noted that this was largely due to the fact that people subjectively viewed the rear seat as being safer than the front seat in the event of a motor vehicle collision.

Intuitively, there are many reasons an occupant might select a front or rear seat. These include motion sickness (an occupant may feel more comfortable further from/closer to the front of the vehicle while in motion), perceived safety (sitting further from the front of the vehicle may be perceived to be safer in a frontal crash), habit (a passenger is often seated in the front seat for current vehicles that always have a driver), or adequate space (more leg room in the front seats of most vehicles, captain's chair in the second row of a minivan, etc.). In a rideshare environment, occupants might select a rear seat for many reasons, including being unfamiliar with the driver, being able to talk with a friend/colleague, or being in the habit of sitting in the rear seat of a taxi. The percentage of rear-seat occupants in these scenarios can be assumed to be much higher than the current rear seating rates in vehicles where there is always a driver.

Select Late-Model Vehicles Spanning a Range of Potential Rear-Seat Safety Performance

The objective of this section was to examine the spectrum of current safety performance for seating behind the front row by selecting a set of late-model passenger cars to model and test. Given the wide range of package geometry and restraint system characteristics behind the front row, it was anticipated that there would be an equally wide range of occupant safety performance. For example, there are substantial differences in seat bottom lengths, seat pan angles, seat belt types (i.e., most vehicles employ basic seat belts/retractors, while only some employ pretensioners, load limiters, or inflatable belts), and seat belt routing configurations among vehicles.

Survey of NCAP Vehicle Inventories

The 2018 NCAP post-test vehicle inventories were surveyed to determine which vehicles were available for inspection. Crash-testing facilities typically have repositories in which vehicles that have been tested are stored prior to transfer to a salvage yard. Although the available vehicles

were already crash tested in a frontal NCAP mode, they were inspected to ensure that there was no structural deformation of the rear occupant compartment and that all seat structures and restraints were intact.

Select Sedans, SUVs/Crossovers, and Minivans for Inspection

The available vehicles were screened and a more-limited set of vehicles was selected for further examination. The emphasis of this work was on passenger vehicles. Specifically, these included sedans, SUV/crossovers, and minivans. There are more rear-seat occupants in minivans (based on vehicle miles driven), but the majority of AIS3+ injuries for rear-seat occupants occur in sedans, followed by SUVs, for all ages (Bose et al., 2017). A total of 23 vehicles were selected from the available NCAP and FMVSS No. 208 testing at the Transportation Research Center (TRC), Karco, and MGA Research Corporation. This list of vehicles represented the initial subset of vehicles for testing.

Examine Vehicles' Package Characteristics, Restraint Geometry, and Seat Belt Routing

The package (seat and restraint system) characteristics, restraint geometry, and seat belt routing of the vehicles included in the initial subset were examined. To begin examining the subset of vehicles, a representative ~50th percentile male occupant sat in the second row of actual vehicles. The restraint and seat characteristics listed in Table 1-2 were documented.

Table 1-2. Characteristics Used to Evaluate Vehicles

Restraint Characteristics	• Belt anchor point locations (including D-rings, retractors) • Presence of load limiters, pretensioners, inflatable restraints • Seat belt routing
Seat Characteristics	• Seat back angle (when fixed) • Seat bottom angle and length • Seat pan geometry (including riser height) • Seat cushion stiffness • Relative headrest position

This task was used to inform the down-selection to a subset of vehicles for further consideration. Previous studies documenting rear-seat geometry and safety performance were examined to assist in this process. However, the focus of this study was vehicles from the past one or two model years that were available for inspection and testing.

A FARO Arm was used to establish the vehicle origin and coordinate system before being used to digitize the 3D locations of specific vehicle features. A number of 3D point coordinates were recorded on the floor pan, riser, seat pan, seat bottom and back cushions, and headrest. 3D point coordinates were also taken to quantify the locations of the anchor points and retractors. The 3D point coordinates for the belts, buckles, and anatomical landmarks were obtained from a roughly 50th percentile male subject sitting in the left second-row seat. The point clouds taken for the vehicles were then converted to surfaces (IGES files) to generate models.

Establish a Subset of Vehicles for Further Examination via FE Modeling

The collection of package information was used in conjunction with available real-world crash data and engineering assessments (similar to Beck et al., 2014) to determine which vehicles to consider for FE modeling. This subset of vehicles encompasses a perceived continuum of safety performance ranging from relatively worse to relatively better. Engineering judgment was used to evaluate certain variables associated with ATD crash performance measurements to down-select an initial subset of approximately eight vehicles for FE modeling.

The crash performance measurements included neck loads, chest deflection, lumbar loads, and pelvis acceleration. Each of these measurements has associated variables or parameters of the seat or restraint system that affect the relative ATD performance for each vehicle. For example, the chest deflection measurement was associated with the shoulder belt location on the clavicle, a retractor with a pretensioner or with a pretensioner and a constant force retractor, or load limiter, and the presence of a steep ramp, anti-submarining bar (sub bar), or box at the end of the seat pan. The lumbar load measurement can be associated with the lap belt angle, seat foam stiffness, the presence of an anti-submarining bar, a combination of foam stiffness and the sub bar, and a box section or drop off at the end of the seat pan ramp. For each measurement, a vehicle was assigned a score from low (worse ATD performance) to high (better ATD performance) by summing the relative influence of each associated variable. Similarly, submarining parameters (e.g., lap belt angle, seat foam stiffness, seat surface to floor height, anti-submarining bar, etc.) were used to assess the anti-submarining performance of each vehicle.

The crash performance and anti-submarining performance were combined to determine an overall score for each vehicle and used to rank the vehicles from theoretical worst performer to theoretical best performer. The scores for each vehicle (assigned an ID number of V# for identification during the assessment) are shown in Table 1-3. V1 ranked the lowest. A range of vehicles were selected for further analysis using modeling, as indicated by the dark shading in Table 1-3. Modeling was used to better differentiate between vehicles to aid in the selection of a subset for testing.

Table 1-3. Ranking of Vehicles Based on Crash and Anti-Submarining Performance

Vehicle ID	Vehicle	Sub + Crash (6 to 320)	Crash (0 to 200)	Submarining (6 to 120)
V1	2018 Audi Q5	92	55	37
V13	2017 Mazda Cx-3	120	59	61
V4	2018 Cadillac XT5	132	85	47
V9	2017 Hyundai Elantra	155	90	65
V3	2017 Buick Envision	156	100	56
V12	2018 Lincoln Continental	156	105	51
V17	2018 Subaru Impreza	161	105	56
V19	2018 Toyota Camry	165	115	50
V8	2018 Honda Odyssey	166	124	42
V20	2017 Toyota Prius	166	114	52
V10	2018 Hyundai Santa Fe	167	129	38
V11	2018 Jeep Compass	172	129	43
V15	2018 Nissan Maxima	175	129	46
V5	2018 Chevrolet Bolt	176	124	52
V16	2018 Nissan Rogue	177	130	47
V7	2018 Honda Accord	180	124	56
V18	2018 Subaru Legacy	185	135	50
V6	2017 Chrysler Pacifica	186	135	51
V2	2018 BMW X1	190	135	55
V14	2018 Mercedes GLC 300	221	140	81

Summary Remarks

Concerning seating preference, the literature indicated that people preferred to sit in rear seats in HAVs with conventional seating (66%), HAVs with face-to-face seating (78%), non-automated taxis (91%), and non-automated rideshares (81%). Regarding RR between rear- and front-seat occupants experiencing a frontal crash, the analysis of NASS-CDS and FARS showed that 13.9 percent of occupants were seated in rear rows (includes second and third row in a vehicle with three rows) during tow-away crashes. The overall risk of serious injury (AIS3+) to these rear-seat occupants was 1.4%. When looking specifically at frontal crashes, the most common impact direction, an estimated 12.7 percent of involved occupants were rear-seated, and their risk of serious injury and fatality were 0.9% and 0.3%, respectively. In newer vehicles (MY 2007+) involved in frontal crashes, the risk of fatality for rear-seat occupants was greater than for front-seat occupants. This suggests a discrepancy between front- and rear-seat restraint performance. When looking at the risk and RR of fatality in frontal impacts, this issue of an elevated risk in the rear seats seems to primarily be a concern for older adults 55 and older.

Rear seat and rear restraint characteristics and geometries were measured for 21 vehicles. This information combined with crash test results was used to rank the relative safety performance for the rear seat. From these vehicles, nine were selected for subsequent modeling in an effort to select a subset of vehicles to use for testing in the laboratory.

2. Platform and ATD Modeling, and Vehicle Selection

Based on the preliminary examination of current rear-seat safety performance in the late-model passenger cars performed in the previous Section 1, eight vehicle packages were selected for modeling evaluation. These vehicles spanned a range of passenger vehicles. Vehicle rear-seat FEMs were created based on geometric data reconstructed from the 3D point coordinates.

Seat Reconstruction

The FE seat models (Table 2-1) of selected vehicles were created based on geometric data reconstructed from 3D point coordinates. First, a scan was taken to note the position of the seat bottom surface, seat back surface, and floor. Next, a scan was taken with a passenger wearing the seat belt to note the path of the seat belt as well as the location of important components such as the buckle, D-ring, retractor, and anchors. Finally, the seat bottom cushion was removed, and a detailed scan was taken of the underlying seat pan. The resulting scans were then used to construct enclosed seat geometries in computer-aided design (CAD) software (Rhinoceros, v5.0, Robert McNeel & Associates, Seattle, WA). An example of an initial scan and the resulting seat geometry is shown in Figure 2-1.

Table 2-1. Vehicle FE Model Information: Main Characteristics

Vehicle	Seat bottom angle (°)	Seat stiffness (N/mm)	Other
V15	17	10	
V14	19	12	Pretensioner/load limiter
V19	13	10	Pretensioner/load limiter
V5	20	10	
V10	11	7	Spring seat bottom
V9	18	17	
V12	21	13	
V13	11	7	

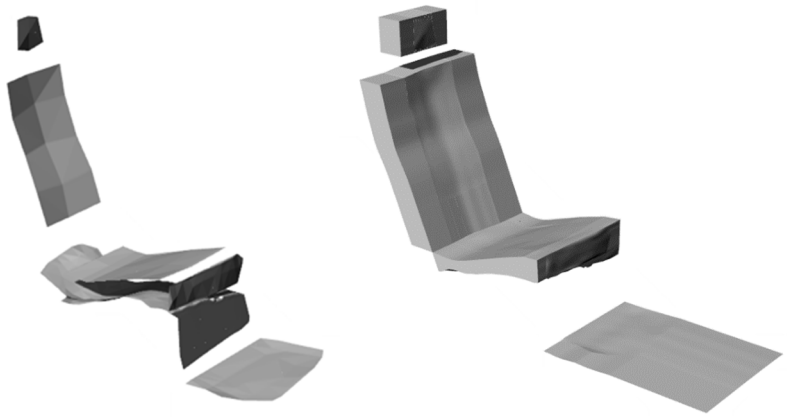

Figure 2-1. FARO Surface of V10 Seat and Simplified Seat Geometry

The geometries were then meshed using Hypermesh (v13.0, Altair, Troy, MI) with primarily hexahedral elements. For one of the seats modeled (V10), there was a spring-type seat bottom, which was modeled by fitting pictures of the seat bottom to the CAD geometry to capture the geometry of the springs with greater detail. The springs were modeled using compliant beam elements with the diameter based on images/field measurements and a steel stiffness of 207 GPa. For all other seats, the seat pan was modeled as rigid. The stiffness of the seat foam was measured quasi-statically in the vehicles with a rigid plate impactor. Force displacement curves were estimated by scaling an exemplar curve (Wietholter et al., 2016) to the stiffness measured on each seat (Figure 2-2). These curves were converted to rough engineering stress-strain curves by dividing the force by the area of the plate, and the displacement by the average thickness of the seat cushion. The stress-strain curves were then used as the inputs to the material model (*MAT_LOW_DENSITY_FOAM in LS-DYNA).

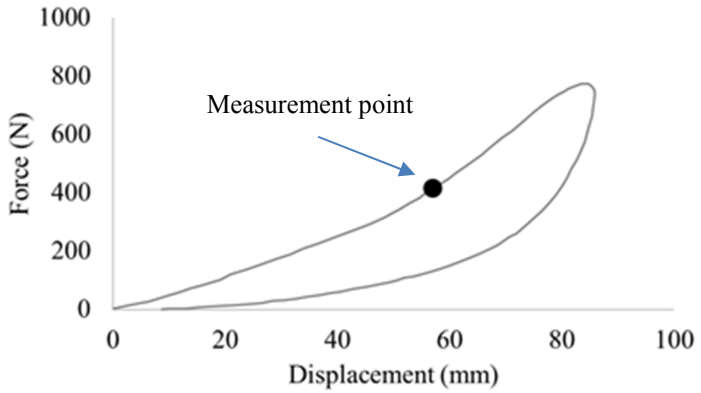

Figure 2-2. Seat Force – Displacement: Measurement Point and Estimated Curve (V13)

ATD FEM Positioning and Settling

The THOR-50M (v1.6) and Hybrid III (HIII) (v1.0.7) 50th percentile male ATD FEMs from Humanetics Innovative Solutions, Inc. (Farmington Hills, MI) were used to evaluate the seats (Figure 2-3). While both validated dummy models correspond to a 50th percentile male, these models have different methods of evaluating injury risks. Since the rear seat is often much smaller than the front seat, the ATD FEM did not always fit well when added in the standard driver posture.

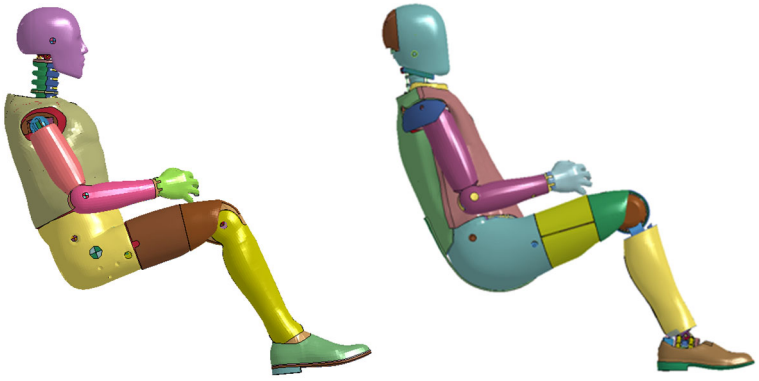

Figure 2-3. Position of HIII and THOR-50M ATD FEM Prior to Settling in Seat

To position the ATD FEMs prior to seating, slight modifications were made from the Humanetics release (driver) posture (Figure 2-4 and Figure 2-5). These changes were made to create a balance between preserving the ideal front-seat posture and creating a posture that worked for all vehicle rear seats. First, the arms were rotated downward to place the hands on the thighs. Then, the lower legs were flexed to -75 degrees, and the feet were positioned as parallel to the floor as possible. These moves were performed using the marionette method (Humanetics Innovative Solutions, 2018) to eliminate the need for manual effort to remove penetration in the flesh components at the joints. The ATD FEMs were then settled into the seat models. To allow for consistent comparison of the simulations, the following procedure was used for each seat. First, the ATD FEM was moved as far back and down into the seat as possible without any penetration occurring between the ATD FEM and the seat. Next, the entire ATD FEM was raised until the feet no longer penetrated the floor. Finally, the ATD FEMs were settled by applying gravity during a 250-ms simulation in LS-DYNA. ATD FEM and seat node locations and stresses were saved from these simulations. The ATD FEM posture was largely preserved from before the simulation, with the main differences in the lower leg, as the foot was able to slide into a natural position. The final step before impact simulations was the fitting of the seat belt. The fabric of the seat belt was routed following the path from the 3D point coordinate data using the LS-PREPOST (Livermore Software Technology Corporation [LSTC], v. 4.3.14) BeltFit tool.

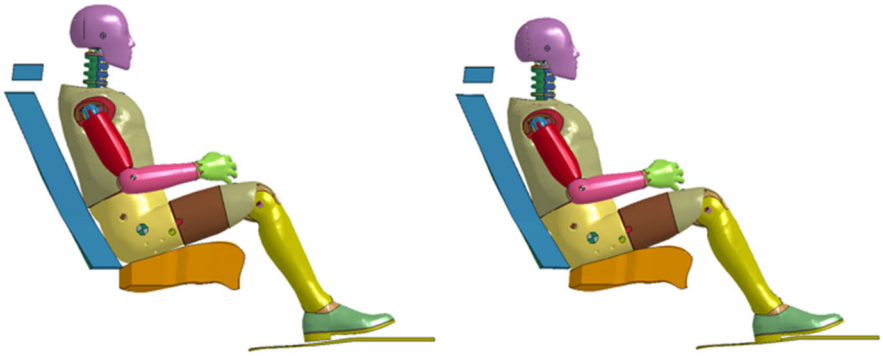

(a) (b)

Figure 2-4. Example of ATD FEM (a) Prior to and (b) After Settling

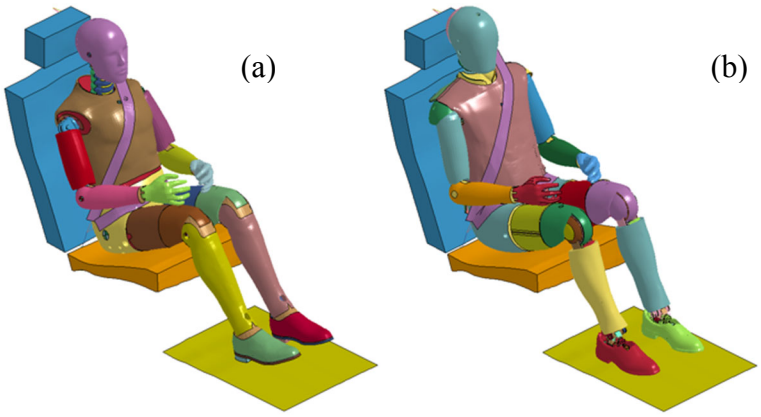

Figure 2-5. (a) HIII and (b) THOR-50M in Seats With Belts Fit

Impact Simulations

Each vehicle's unique frontal NCAP crash pulse was applied to the floor of the vehicle. The floor was rigidly coupled to the seat pan/seat back support as well as the seat belt components. The crash was simulated for 150 ms, by which time all injury metrics had peaked, and all simulations had run to completion. Overall, the motion of the ATD FEMs was similar in all cases but some differences were observed. Since the seats were modeled in isolation without a seat in front, the ATD FEM's legs were free to move upward. Therefore, some simulations showed the ATD FEM's head contacting the knee around 125 ms into the simulation, leading to large accelerations late in the simulation in the head and neck. Since interaction with the front seat in current vehicles might prevent head-knee impact (in current seat configurations), injury risks were calculated up to 110 ms (before head-knee impact) as well as the entire simulation (150 ms). It is also important to note that the head-knee impact occurred well after the maximum forward head and pelvis excursion while the ATD FEM was rebounding back from the restraints.

To examine injury risk, several injury measures were investigated: HIC15, BrIC (Takhounts et al., 2013), Nij (Eppinger et al., 1999, 2000), max chest deflection, and max femur force. Injury metrics were evaluated using Equation 2-1 through Equation 2-5. For the both the THOR-50M FEM and the Hybrid III FEM, Nij was calculated using the forces and moments that were outputted from the virtual upper-neck load cell, for which no compensation of flexion/extension is required to obtain the correct moment about the occipital condyles for Hybrid III. Nij was calculated using the critical values shown in Table 2-2. Risk of an AIS3+ injury was calculated for each of these metrics in the Hybrid III and THOR models (Takata, 2017; Kleinberger et al., 1998). Injury risk in the THOR chest, however, was calculated with a default age of 45 (Poplin et al., 2017). Additionally, to summarize injury risk, the Occupant Injury Metric (OIM) AIS3+ (Takata, 2017), which uses the risk of AIS3+ injury to one or more body regions as defined by the previously mentioned metrics, was calculated for each simulation. Injury probabilities were evaluated using Equation 2-6 to Equation 2-12.

HIC15 HIII & THOR-50M (Federal Register, 2015)	$HIC_{15} = \left\{(t_2 - t_1)\left[\frac{1}{(t_2-t_1)}\int_{t_1}^{t_2} a(t)dt\right]^{2.5}\right\}\max$	Equation 2-1
BrIC HIII & THOR-50M (Federal Register, 2015; Takhounts et al., 2013)	$BrIC = \sqrt{\left(\frac{max(\lvert w_x \rvert)}{w_{xc}}\right)^2 + \left(\frac{max(\lvert w_y \rvert)}{w_{yc}}\right)^2 + \left(\frac{max(\lvert w_z \rvert)}{w_{zc}}\right)^2}$ Where: w_{xc}=66.25 rad/s, w_{yc}=56.45 rad/s, w_{zc}=42.87 rad/s.	Equation 2-2
Nij HIII & THOR-50M (Eppinger et al., 1999, 2000)	$N_{ij} = \left(\frac{F_z}{F_{zc}}\right) + \left(\frac{M_y}{M_{yc}}\right)$	Equation 2-3
Chest Deflection THOR-50M (Federal Register, 2015)	$R_{max} = \max(UL_{max}, UR_{max}, LL_{max}, LR_{max})$ Where: $\{U/L\lvert R/L\}_{max} =$ $max\left(\sqrt{[L/R]X^2_{[U/L]S} + [L/R]Y^2_{[U/L]S} + [L/R]Z^2_{[U/L]S}}\right)$	Equation 2-4 Equation 2-5

Table 2-2. Nij Critical Values (Federal Register, 2015)

ATD FEM	Criterion	Peak Limits		Nij Intercepts/Critical Values (F_{zc}, M_{yc})			
		F_{zc}		F_{zc}		M_{yc}	
	Nij	Tension	Comp	Tension	Comp	Flexion	Extension
		(N)	(N)	(N)	(N)	(Nm)	(Nm)
HIII 50th M	Nij	4170	-4000	6806	-6160	310	-135
THOR 50th M	Nij	4170	-4000	2520	-3640	48	-72

HIC15 HIII & THOR-50M (Federal Register, 2015)	$p(AIS3+) = \Phi(\frac{ln(HIC) - 7.45231}{.73998})$	Equation 2-6
BrIC HIII & THOR-50M (Federal Register, 2015; Takata, 2017)	$p(AIS3+) = 1 - e^{-\left[\frac{BrIC}{0.987}\right]^{2.84}}$	Equation 2-7
Nij HIII & THOR-50M (Federal Register, 2008)	$p(AIS3+) = \frac{1}{1 + e^{3.227 - 1.969 N_{ij}}}$	Equation 2-8
Chest Deflection HIII (Federal Register, 2008)	$p(AIS3+) = \frac{1}{1+e^{10.5456 - 1.568*(\delta_{max})^{0.4612}}}$	Equation 2-9
Chest Deflection THOR-50M (Poplin et al., 2017)	$p(AIS3+) = 1 - e^{-\left[\frac{R_{max}}{e^{4.7775 - 0.0171*(age)}}\right]^{3.356}}$	Equation 2-10
Femur Load (Takata, 2017; Kleinberger et al., 1998)	$p(AIS3+) = \frac{1}{1+e^{4.9795 - .326 F_{max}}}$	Equation 2-11

OIM HIII & THOR-50M (Takata., 2017)	$p(AIS3+) = 1 - (1 - p(HIC) * (1p(BrIC)) * \left(1 - p(Nij)\right) * (1 - p(Chest\ Deflection)) * (1 - p(Femur\ Force))$	Equation 2-12

Results: Relative Safety Performance Assessment of Simulated Vehicles

Overall, trends were very similar between the Hybrid III and THOR-50M simulations, with the best performance seen in the two vehicles with pretensioners (V14 and V19). Good performance was also seen with vehicles that had a steep seat pan angle (V5 and V12). The OIM from the THOR simulations was generally higher than the Hybrid III simulations (Figure 2-6). Much of this difference can be attributed to the different injury probabilities to the chest, likely due to the differences in how chest deflections are measured by the Hybrid III and THOR ATD FEMs (single x deflection versus four 3D measurements), and differences in the derivations of the risk functions for the two dummies.

The AIS3+ injury risk according to each body injury metric is also shown (Figure 2-7). Again, similar trends are seen between the Hybrid III and THOR simulations. For Hybrid III, the head was more likely to hit the knee at the end of simulation than for THOR. Disregarding these impacts, HIC was fairly low for most vehicles. BrIC was by far the metric predicting the highest risk of injury in all cases, with an injury risk range from 0.2 to 0.98 for the Hybrid III and from 0.4 to 0.98 for the THOR (when calculated for the first 110 ms). Nij and chest deflection showed a moderate risk level (3%–26%) for all simulations, with an outlier in the Hybrid III simulation with V10, which showed a higher injury risk (63%) due to Nij. To better estimate the head and neck injuries for rear occupants, a review of all corresponding injury criteria with and without head contact may be beneficial. Finally, injury risk of the femur was low in all cases (<10%). Overall, the vehicles with pretensioners (V14 and V19) performed the best, followed by V5 and V12 which also performed well. Vehicle V10 performed the worst, particularly in terms of BrIC and Nij. ATD pelvises reached the rigid support at the front edge of the seat (~ 70 ms) and stopped moving forward, later generating a large relative head rotation.

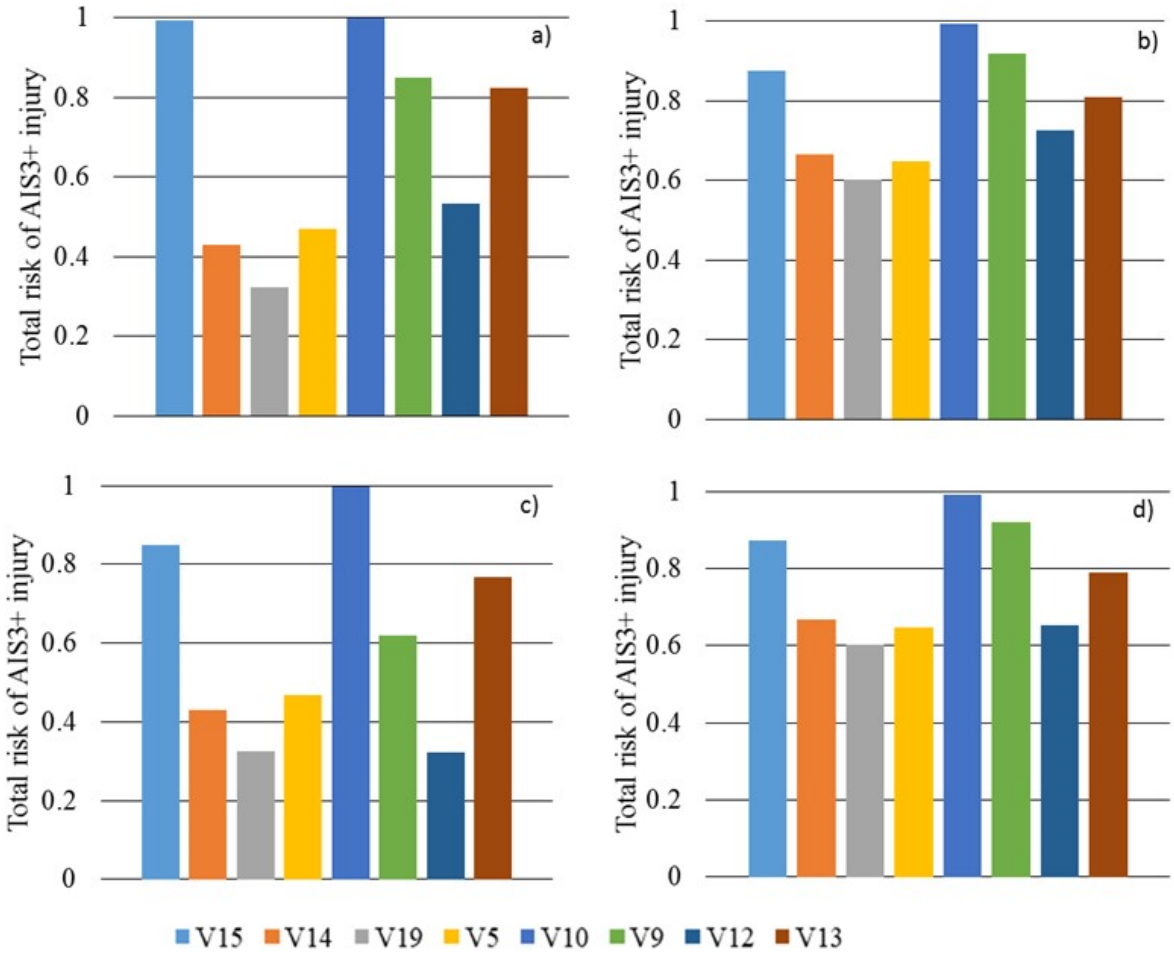

Note: In simulations where the ATD FEM's head contacted the knee, these impacts occurred at roughly 125 ms.

Figure 2-6. OIM Values With the HIII (a, c) and THOR (b, d) ATD FEMs at 150 ms (a, b) and 110 ms (c, d)

Vehicle Selection for Sled Testing

Based on the rankings of vehicles in Table 1-3, two of the lowest performing vehicles (V1, V13) with different vehicle characteristics and two of the highest performing vehicles (V6, V14) with different vehicle characteristics were selected for physical testing. Three vehicles were also selected from the middle performing vehicles in Table 1-3. These corresponded to the highest (V19) and two lowest (V10, V15) ranked vehicles based on the modeling results. It should be noted that not all vehicles were modeled. It is also of interest to note that V19 and V15 were similar vehicles, the former having advanced restraints, and the latter lacking them.

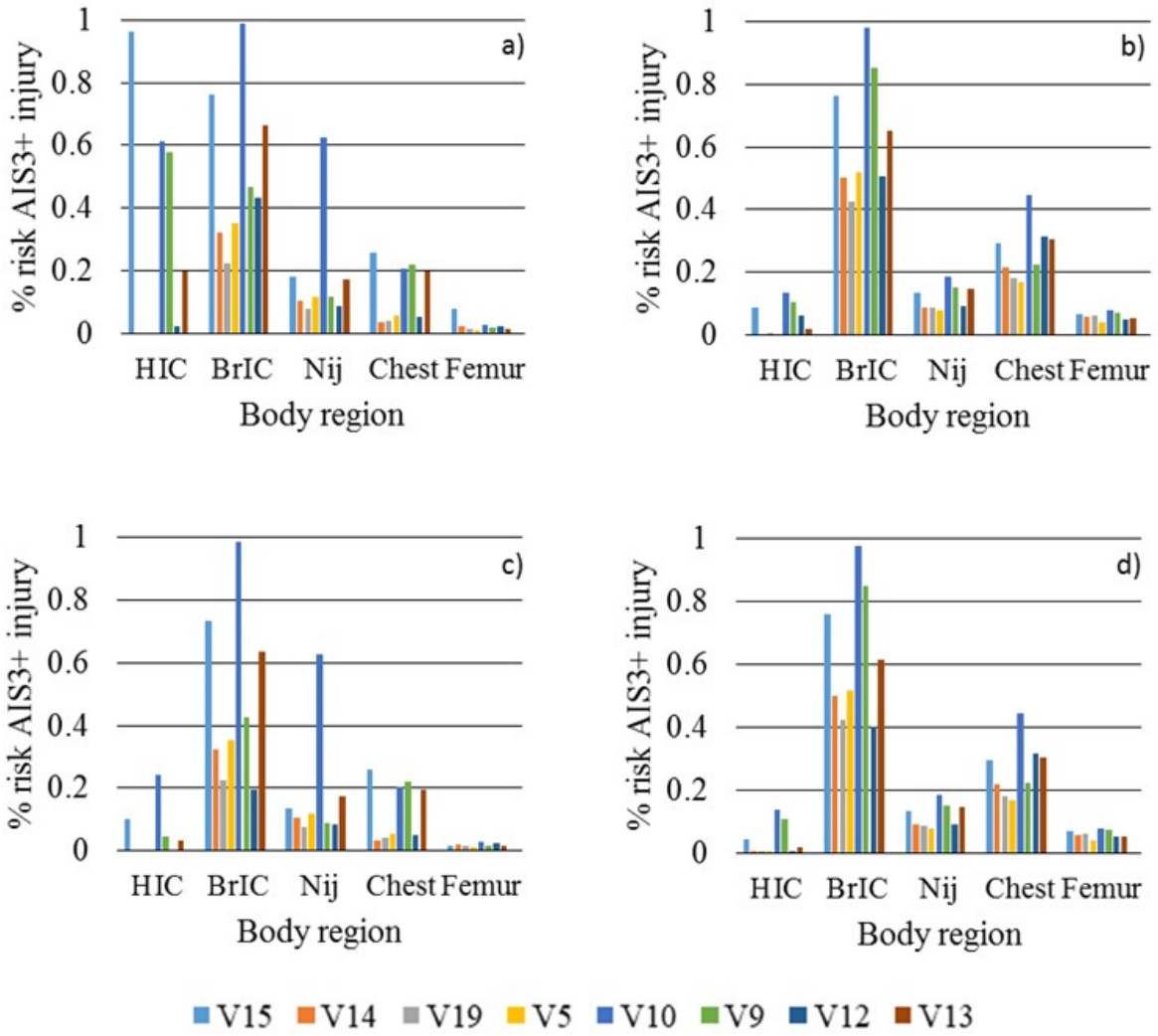

Note: In simulations where the ATD FEM's head contacted the knee, these impacts occurred at roughly 125 ms.

Figure 2-7. Injury Metrics With the HIII (a, c) and THOR (b, d) ATD FEMs at 150 ms (a, b) and 110 ms (c, d)

Summary Remarks

Nine vehicle simulations were conducted using vehicle-specific rear-seat properties, restraint characteristics, and NCAP pulses. Commercially available computational representations of both the Hybrid III and THOR-50M ATDs were used. The trends exhibited by both virtual ATD FEMs were similar, and resulted in similar assessments of the relative crash safety performance for the rear seat as the algorithm that was applied to the crash data and measured vehicle characteristics. This provided confidence in the techniques employed, and helped to discriminate between vehicles to the degree required to select the specific vehicles for sled testing. Seven vehicles were selected for testing based on a combination of the findings in Section 2 and these modeling results.

3. Test Buck Preparation

Multiple sled bucks were fabricated using vehicles that had undergone frontal barrier testing. The vehicles acquired were those indicated by the combined outcomes of the safety performance characteristics assessment (predicted performance rankings) and the FE modeling efforts. Seven vehicles were retrieved from NCAP post-test storage, with NHTSA approval. Three test bucks were fabricated representing the middle-, top-, and bottom-ranked vehicles: V15, V14, and V1. Bucks for V19 and V13, which are middle- and bottom-ranked vehicles, were fabricated also. Refer to Appendix A for V1, 0 for V6, 0 for V10, Appendix D for V13, Appendix E for V14, Appendix F for V15, and Appendix G for V19. A number of steps were involved in the fabrication of these test bucks. First, the windows, doors, engine, transmission, suspension, wheels, axles, fuel tank, fuel lines, brake lines, unneeded interior components, etc., were removed. Then, the vehicle body was reinforced with steel tubing (front, undercarriage, seat belt anchor points, seat pans, and seat back). The mid-sized sedans received exoskeletons (V15, V19). The mid-sized SUVs did not require exoskeletons due to the increased stiffness of the vehicle bodies, but were reinforced at the front, rear, and anchors. Unlike V14 and V15, which have fixed sheet metal seat pans, V1 has a sliding rear seat frame that required special attention to reinforce. After reinforcing the vehicle bodies, mounting plates to bolt the bucks to the sled were fabricated and welded to the steel tubing on the underside of the reinforced vehicle bodies. In addition, mounting plates to bolt data acquisition components to the vehicle were fabricated and welded to the steel tubing used to reinforce the rear seat backs (i.e., in the trunk of the vehicle). Finally, the bucks were painted with flat paint to help reduce sheen, which causes issues with the VICON motion tracking system.

V6 and V10, which were the last two bucks to be fabricated, required the removal of substantially more material to be able to achieve the vehicle-specific NCAP pulse speed during sled testing. Fortunately, the remaining structure of these vehicles was very stiff. These vehicles had three rows, and it was the second row that was tested. The second-row seats had adjustable seatback angles. The seatback angles were set to the average fixed angle measured in the other vehicles' bucks.

For each buck, the front row of seats was eliminated. This was done for several reasons. First, inclusion of these seats would introduce too many uncontrolled variables into the test results. Even if the mid-track position was used consistently, the seatbacks would be spaced differently from the rear seat and from the floor for each vehicle. Further, characteristics such as seat resistance to load and moment, and material properties would be different. In addition, the response of the front seats would be modulated by the nature of the occupants in those seats, and their interaction with the seats and restraint systems, which would affect the position and orientation of the seat backs at a given instant in time, and the rear-seat occupants' interaction with the seat backs. It would not be possible to create a consistent or repeatable interaction scenario, complicating interpretation of the results obtained from rear-seat surrogates. While the front seats would affect the lower-extremity response the most, the lower extremities were not a focus of this study. While the effect on submarining incidence and extent is unknown, it can be assumed to be small for many cases. However, without the front seats in place, the emphasis is placed upon the nature of the rear seat, rear restraints, and geometry. Finally, without front seats in place, the occupant compartment becomes more representative of that which might be expected in future novel seating configurations for which rear and front-seat occupants are facing

each other. The removal of the front seats has the added benefit of providing improved visualization of the tests via high-speed video.

Summary Remarks

Seven bucks were developed for use in sled testing. The bucks were designed for repeated use. All restraint anchor points were reinforced. The less-rigid bucks were outfitted with an exoskeleton frame. The first row of seats was removed for each buck. The roof of each buck was removed to facilitate video recording from overhead.

4. ATD Sled Testing

Prior to conducting sled tests, it was necessary to develop appropriate positioning procedures for the Hybrid III 50th percentile male ATD and the THOR-50M ATD for seating locations other than the first row. Both ATDs were acquired as government-provided hardware. A reliable method of assessing the occurrence of submarining in the dummies was also necessary. Once the positioning procedures and submarining assessment methods were developed, sled tests using the previously fabricated vehicle bucks were conducted. The Hybrid III 50th percentile male ATD and the THOR-50M were used simultaneously in each buck for each test. The ATD test results are used as a physical assessment of relative vehicle platform safety performance for seating locations behind the first row in frontal crashes. This provides the first step toward empirical delineation of the boundaries of potential issues to be encountered as a result of occupants being seated in locations other than in the front row of ADS-DVs during frontal crashes.

ATD Positioning Procedure

Since there are currently no official procedures for positioning the Hybrid III or THOR 50th percentile dummies in the rear seat, several steps were taken to develop a new draft procedure for the current study. First, various front and rear seat ATD positioning documents were reviewed. Positioning procedures are well established for the Hybrid III in the front-left outboard (driver's DSP) location as part of 49 C.F.R. § 571.208. In addition, there are draft positioning procedures, which were provided by NHTSA, for the THOR 50th percentile dummies in the front-left outboard (i.e., driver's DSP) and front-right outboard (i.e., right front passenger) locations. There are also procedures for positioning small female dummies, such as the Hybrid III 5th-percentile female, in the rear seat (Docket NHTSA-2015-0119, IIHS-2012). The resources listed above were leveraged to help develop draft procedures for positioning the Hybrid III and THOR 50th percentile dummies in an outboard, second-row seat. The available procedures were reconciled with the capabilities of the dummies, differences between front and rear seat geometries and adjustability, and differences between the dummies, to develop a repeatable procedure to assume a limited range of ATD postures in the rear seat. A mid-sized sedan was used to develop the initial procedures listed below. Tilt sensors were used to measure the knee, head, and pelvis angles to ensure they were within the tolerance of the target angles.

50th Percentile Male ATD Positioning Procedure for Rear-Seat Outboard Positions

- Set up FARO Arm and define the local coordinate system such that the X, Y, and Z axes are positive in the directions specified in SAE J211.
- Set headrest to full upward position.
- Mark right-left centerline of the headrest and thigh bolster with fabric marker.
- Determine the location of the seat bight (i.e., intersection of seat back and seat bottom).
    - Place large square (~3 ft x 4 ft) on centerline of thigh bolster such that the square is in the X-Z plane.
    - Check that the square is in-line with the centerline of both headrest and thigh bolster.
        - If there is a gap between the top of the square and the headrest, place a metal ruler on the side of the top of the square to bridge the gap. Be sure to account for the lateral offset of the metal ruler when centering the square on the head restraint.

        - Move square rearward until the lowest, rearmost corner of the square contacts the seat back and/or the raised portion of the thigh bolster (if applicable).
        - The corner of the square contacting the seat back (i.e., lowest, rearmost corner) is defined as the seat bight.
        - Digitize the location of the seat bight with the FARO Arm.
        - Digitize center lines of the headrest and thigh bolster.
- Place ATD in outboard seat.
- Set joint torques to 1 g.
- Push pelvis full rearward into the seat.
- Position ATD in the center of the seat using headrest and thigh bolster right-left centerlines.
- Check pelvis angle.
    - Targets:
        - Hybrid III 50th Male = 22.5 ± 2.5º
        - THOR 50th Male = 33 ± 2.5º
- If pelvis angle is not within tolerance, adjust until the angle is within tolerance.
- Check head angle.
    - Targets:
        - Hybrid III 50th Male = 0 ± 0.5º
        - THOR 50th Male = 0 ± 0.5º
- If head angle is not within tolerance, adjust until the angle is within tolerance.
- Recheck pelvis angle.
- If pelvis angle is not within tolerance, then repeat previous steps until both the pelvis angle and head angle are within tolerance.
- Set knee angles (i.e., angle between the thigh and shank).
    - Targets:
        - Hybrid III 50th Male = 100 ± 5º
        - THOR 50th Male = 100 ± 5º
- Place soles of the feet/shoes as flat as possible on the floor.
- Ensure thighs, shanks, and feet are in-line (in the sagittal plane).
- Recheck pelvis and head angles.
- If pelvis and head angles are not within tolerance, then repeat previous steps until the pelvis, head, and knee angles are within tolerance.
- Set the knee-to-knee distance.
    - Targets:
        - Hybrid III 50th Male = 269 mm between outer knee clevises
        - THOR 50th Male = 225 mm between knee centerlines
- Place shoulder belt around outboard arm, but do not buckle.
- Place hands on the distal portion of the thighs.
    - Palm resting on anterior/lateral portion of the thigh
    - Thumbs placed at the midline (sagittal plane) of thigh
    - Result is an arm angle of ~50º from horizontal (~40° from vertical)
- Recheck pelvis, head, and knee angles.
- If angles are not within tolerance, adjust position until all angles are within tolerance.
- Measure the H-point

    - Evaluate the X, Y, and Z distances from the H-point to the seat bight.
    - If positioning an ATD for a repeat test, verify that the H-point is within +/- 12mm of the average relative distances from the seat bight in all three directions.
    - If, for a repeat test, the H-point is not within +/- 12mm of the average relative distances from the seat bight in all three directions, repeat the previous positioning steps to bring the H-point as close as possible to being within +/- 12 mm of the relative distances from the seat bight in all three directions, and all other conditions are met.
- Digitize H-point.
- Place belt around ATD and buckle.
- Place seat belt tension load cells on belt.
    - Upper shoulder belt (outboard)
    - Lower shoulder belt (inboard)
    - Lap belt (outboard)
- If D-ring height adjustment is available, position in the highest detent.
- Position seat belt load cells to minimize interaction with ATD, minimize interaction with vehicle components, and minimize shoulder belt sag between D-ring and shoulder.
- Place 2–4 lbs of tension on lap belt.
- Position shoulder belt on chest.
- Pull and release shoulder belt from retractor 4x.
- Digitize all relevant points on the ATD with FARO Arm (relevant points were based on a spreadsheet provided by the Vehicle Research and Testing Center [VRTC]).

Paired ATD Sled Tests using Vehicle Bucks

Frontal sled tests were conducted with the Hybrid III 50th percentile male ATD and the THOR-50M ATD seated in the rear seat of the test bucks that were fabricated as described in the previous Section 3. Three crash pulses were used for each vehicle. First, each vehicle-specific NCAP crash pulse, obtained from NCAP test results in a NHTSA repository, was reduced to a delta V of 56 km/h by scaling the pulse down to 85 percent of the original. This is referred to as the "NCAP85" pulse. Next, a lower-energy impact was created by scaling the delta V to 32 km/h, i.e. ~57% of the original (32/56 = 0.5714). This is referred to as the "scaled" pulse. Finally, the spulses were averaged for each of the selected vehicles (n = 7) at each point in time, resulting in a "generic" pulse used for all vehicles.

After fabricating the test bucks, a number of practice runs were performed to tune the sled performance for the desired sled pulses. For each practice run, an empty test buck (i.e., no seat, dummies, data acquisition system [DAS], etc.) was attached to the sled along with ballast weight (i.e., weight to account for all the components not on the sled that would be on the sled for a full test). The sled pulses acquired during tuning were nearly identical to the target pulses for each buck. During these practice runs, the performance of newly fabricated onboard camera outriggers was evaluated. Based on the initial tests, modifications to the outriggers were made to provide additional reinforcement and the ability to accommodate all of the bucks. The high-speed video setup included five views: right onboard camera, left onboard camera, front onboard camera, stationary overhead camera, and a stationary left-lateral view camera. In addition to high-speed video, the feasibility of using the VICON capture system was evaluated. Specifically, there were concerns about the ability to obtain adequate lines-of-sight to markers on the ATDs due to the

obstructions caused by the vehicle body and camera outriggers. Based on these feasibility checks, it was determined that VICON would be able to reasonably quantify the ATD kinematics in the vehicles, and the system was used for all tests.

Twenty-five tests were then conducted using seven different bucks. All tests were run on a Seattle Safety ServoSled at Virginia Tech. For each test, the THOR-50M ATD (S/N DO9798) was seated in the left rear seat, while the Hybrid III 50th percentile male ATD (S/N 043) was seated in the right. The position of each ATD was recorded using a FARO arm. A strap was then added in front of the feet to prevent excessive excursion of the legs. New OEM seat belt hardware and seat pan fabric/cushions were used for all tests. Two abdomens were used for THOR: the standard abdomen and the ABISUP. The ABISUP, designed to replace the standard THOR-50M abdomen and instrumentation, is a foam insert that has two fluid-filled reservoirs, each fitted with an internal pressure transducer.

Three pulses were applied: generic (low speed), scaled/specific (low speed), and NCAP85. The actual sled acceleration pulses for all tests are provided in Appendix H. Table 4-1 provides the matrix of tests conducted. Both ATDs were qualified by NHTSA prior to the start of testing, and between the 16th and 17th tests. The order of testing is indicated in Table 4-1 in the "Test Sequence" column. Table 4-2 maps the buck vehicle numbers to the make, model, and year of each vehicle. The test designations are FRS-Vehicle#-Test#. For example, the first test conducted was FRS-V15-1. This test used the standard abdomen to THOR, and the generic sled pulse. Test FRS-V15-2 was a comparison test using the ABISUP and the generic sled pulse. These two tests served to demonstrate that the ABISUP did not affect the kinematics and kinetics of THOR. Comparisons of peak signal values, peak injury metrics and probabilities, and peak excursions are provided in Table KK-4 through Table KK-6. None of the comparisons for the THOR-50M was appreciably different from those associated with the Hybrid III. A notable exception is the T12 X-direction load, which is expected to be very different given the difference in the way the standard abdomen and the ABISUB interface with this region of the ATD. Specific traces are compared in the results of this section. Qualitatively, the comparisons are very strong. Therefore, the ABISUP was employed for all subsequent tests to avoid damaging the Infra-Red Telescoping Rod for the Assessment of Chest Compression (IR-TRACC) instrumentation in the standard abdomen, as it was not known if these devices could tolerate submarining events at high speeds. For the chest and abdomen for test FRS-V15-1, and for the chest for all other tests, the IR-TRACC post-processing followed the practice outlined in the Procedures for Assembly, Disassembly, and Inspection (PADI) document for the THOR-50M.

Three tests were repeated. Test FRS-V19-4 was a repeat of Test FRS-V19-3, Test FRS-V14-4 was a repeat of Test FRS-V14-3, and Test FRS-V6-4 was a repeat of Test FRS-V6-3. After Test FRS-V19-3, it was noted that several bolts in the THOR were coming loose. Test FRS-V19-4 was conducted for comparison and to provide confidence in all previously collected data. Test FRS-V14-4 was conducted because of a DAS failure during Test FRS-V14-3. There was a subsequent DAS failure during Test FRS-V14-4, but the data were successfully reconstructed. Test FRS-V6-4 was conducted because of a shoulder belt failure in which the T1 (first thoracic vertebra analog) accelerometer block cut the belt completely for the THOR during Test FRS-V6-3. Specific issues associated with some of the tests are described in Appendix I. These issues include problems with the ATDs, DAS, restraint systems, and buck structure.

Table 4-1. The Matrix of FRS Tests Conducted

Buck	Pretensioner/ Load Limiter	Test #	Test Sequence	Pulse	Abdomen	Note
V1	Y/Y	1	6	Generic	ABISUP	
		2	7	Scaled	ABISUP	
		3	17	NCAP85	ABISUP	
V6	N/N	1	19	Generic	ABISUP	
		2	20	Scaled	ABISUP	THOR seat anchor pulled
		3	21	NCAP85	ABISUP	THOR shoulder belt ripped
		4	22	NCAP85	ABISUP	FRS-V6-3 repeat
V10	N/N	1	23	Generic	ABISUP	
		2	24	Scaled	ABISUP	
		3	25	NCAP85	ABISUP	Toe ramp installed
V13	N/N	1	12	Scaled	ABISUP	
		2	13	NCAP85	ABISUP	
		3	18	Generic	ABISUP	
V14	Y/Y	1	4	Generic	ABISUP	
		2	5	Scaled	ABISUP	
		3	14	NCAP85	ABISUP	DAS failure (THOR side)
		4	15	NCAP85	ABISUP	FRS-V14-3 repeat
V15	N/N	1	1	Generic	Standard	
		2	2	Generic	ABISUP	
		3	3	Scaled	ABISUP	
		4	16	NCAP85	ABISUP	Reused FRS-V15-3 fabric
V19	Y/Y	1	8	Generic	ABISUP	
		2	9	Scaled	ABISUP	
		3	10	NCAP85	ABISUP	THOR integrity issues
		4	11	NCAP85	ABISUP	FRS-V19-3 repeat

Table 4-2. Buck-to-Vehicle Map

Buck	Make	Model	Year
V1	Audi	Q5	2018
V6	Chrysler	Pacifica	2017
V10	Hyundai	Santa Fe	2018
V13	Mazda	CX-3	2017
V14	Mercedes	GLC 300	2018
V15	Nissan	Maxima	2018
V19	Toyota	Camry	2018

Frangible Abdomen Exploration

The feasibility of using the Frangible Abdomen (Rouhana et al., 1989, 1990) to assess submarining in the Hybrid III ATD was evaluated. Unfortunately, this endeavor did not yield promising results. The standard Frangible Abdomen requires the chest potentiometer to be removed and does not allow for the use of the lumbar load cell. To avoid eliminating the standard method to quantify chest deflection in the Hybrid III, various alternative support brackets and foam geometry designs were tested in an attempt to provide a foam structure large enough to assess submarining while not causing any conflicts with the chest potentiometer. However, the research team was not able to develop a reasonable version (a support structure that could accommodate enough foam to reasonably assess submarining) that did not conflict with the chest potentiometer assembly and could be used with the lumbar load cell. While the alternative Frangible Abdomen design developed allows it to be used with the lumbar load cell and may work for the scaled-down sled pulses, it would not work at higher speeds/extreme flexion due to the potential interaction with the chest potentiometer. Furthermore, the Frangible abdomen only provides a piece of the submarining picture. Specifically, additional data and video are often required to truly assess the incidence of submarining, especially in cases of mild to moderate submarining.

Instrumentation and Data Acquisition

Both the Hybrid III and THOR ATDs were fully instrumented. However, only a subset of instrumentation is of strong importance to this study. Each ATD had three linear accelerometers and three angular rate sensors in the head, as well as upper and lower-neck six-axis load cells. The Hybrid III ATD had the standard chest potentiometer, chest and pelvis accelerometer blocks (three accelerometers each), and lumbar load cell. In comparison, the THOR ATD had T6 (sixth thoracic vertebra analog) and pelvis accelerometer blocks, four IR-TRACCs in the chest, a T12 load cell, ASIS load cells, and either the standard abdomen (with two IR-TRACCs) or the ABISUP (two pressures). To further quantify the interactions between the ATDs and the vehicle restraints, three load cells positioned at the shoulder, inboard lap (low on the shoulder strap), and outboard lap were placed on each seat belt.

Data were collected with G5 and TDAS Pro DASs (Tiny Data Acquisition System, Diversified Technical Systems, [DTS], Seal Beach, CA) using 20,000 samples per second. All DAS, VICON, and camera systems were synchronized and triggered by a DTS Timer Output Module signal after receiving a signal from the sled system.

High-speed videos (1,250 fps, 400 μs exposure) were captured at five views: right and left onboard lateral perspectives of each dummy, frontal onboard, off-board overhead, and an off-board side view of the entire event.

Data were processed to SAE J211 specifications, after short duration electrostatic discharge (ESD) and cable-pull related spikes were removed (short duration interpolation). Corrupted data (Test FRS-V14-4) were reconstructed by reassembling data segments and applying known scaling correction factors. Relatively short-duration missing data segments were filled using either cubic or linear interpolation, or data splicing. When present, these gaps occurred at the start of the data traces, so no subsequent analyses were affected by these techniques.

Occupant motion data were collected using a 1,000-fps VICON motion analysis system (VICON Motion Systems, Oxford, UK), consisting of 16 MX T-20 cameras. The Hybrid III, THOR-50M,

vehicle buck, and sled deck were instrumented with 37, 39, 4, and 8 retroreflective markers, respectively, for a total of 88 markers per test. The markers were placed on each ATD to quantify the motion of key anatomical landmarks. The trajectories of each of these markers were converted to the reference frame of the sled and to the SAE J211 sign convention. Then, the trajectories were converted into excursions by subtracting the initial location of each marker at the beginning of the test from the marker's location throughout the duration of the test. Excursions of interest were calculated for the head center of gravity (CG), outboard shoulder, outboard hip, and outboard knee for each ATD. The peak X and Z excursions were calculated for each location of interest, and the excursions were truncated to whichever peak excursion occurred later before plotting. Sight lines were lost before peak excursion for some body regions during some tests, particularly for the THOR during the high-speed tests.

Head Injury Metrics and Injury Risk Calculations

Head injury risk was assessed using HIC15 and BrIC for both ATDs. HIC15 was calculated using Equation 4-1, where the injury threshold was equal to 700 (NHTSA, 2005; Federal Register, 2015). Hybrid III BrIC and BrIC AIS3+ injury risk were calculated using Equation 4-2 and Equation 4-3 (Federal Register, 2015). BrIC and BrIC risk for the THOR-50M were calculated using Equation 4-2 and Equation 4-4 (Craig, et al., 2020). The BrIC risk functions for each ATD were chosen based on the ATD-specific literature at the time of study execution (Federal Register, 2015 for the Hybrid III and Craig et al., 2020 for the THOR-50M). Additionally, Takhounts et al. (2013) recommends Equation 4-3 to be used when calculating BrIC risk.

HIII & THOR-50M (Federal Register, 2015; Craig, et al., 2020)	$HIC_{15} = \left\{(t_2 - t_1)\left[\frac{1}{(t_2 - t_1)}\int_{t_1}^{t_2} a(t)dt\right]^{2.5}\right\}_{\max}$	Equation 4-1
HIII & THOR-50M (Federal Register, 2015; Takhounts et al., 2013)	$BrIC = \sqrt{\left(\frac{max(\lvert w_x \rvert)}{w_{xc}}\right)^2 + \left(\frac{max(\lvert w_y \rvert)}{w_{yc}}\right)^2 + \left(\frac{max(\lvert w_z \rvert)}{w_{zc}}\right)^2}$ **Where:** w_{xc}=66.25 rad/s, w_{yc}=56.45 rad/s, w_{zc}=42.87 rad/s	Equation 4-2
HIII (Federal Register, 2015; Takhounts et al., 2013)	$p(AIS3+) = 1 - e^{-\left[\frac{BrIC}{0.987}\right]^{2.84}}$	Equation 4-3
THOR-50M (Craig, et al., 2020)	$p(AIS\ 3+) = 1 - e^{-\left(\frac{BrIC - 0.523}{0.531}\right)^{1.8}}$	Equation 4-4

Neck Injury Metrics and Injury Risk Calculations

Nij and the corresponding risk of an AIS3+ neck injury were calculated for each ATD and using Equation 4-5 for both ATDs, Equation 4-6 for the Hybrid III, and Equation 4-7 for the THOR-50M, and the critical values specific to each ATD (Table 4-3; Eppinger et al., 2000; NHTSA, 2005; Federal Register, 2008; Federal Register, 2015; Craig et al., 2020). The injury threshold/limit for Nij was equal to 1.0 for both ATDs (NHTSA, 2005). The threshold of 1.0 was used for both ATDs because the loads and moments are normalized with respect to the ATD specific critical intercept values. This does not affect the threshold value of 1 developed for normalized Nij, which considers the combined effect of axial load and flexion/extension moments. However, it should be recognized that a Nij value of 1.0 for the Hybrid III and for the THOR-50M does not represent identical risk. For the THOR-50M, Nij was calculated using the forces and moments at the upper load cell. For the Hybrid III, Nij was calculated using the corrected moment about the occipital condyles.

HIII & THOR-50M (Eppinger et al., 1999, 2000)	$N_{ij} = \left(\frac{F_z}{F_{zc}}\right) + \left(\frac{M_y}{M_{yc}}\right)$	Equation 4-5
HIII (Federal Register, 2008)	$p(AIS3+) = \frac{1}{1 + e^{3.227 - 1.969 N_{ij}}}$	Equation 4-6
THOR-50M (Craig et al., 2020)	$p(AIS3+) = \frac{1}{1 + e^{6.047 - 5.44 N_{ij}}}$	Equation 4-7

Table 4-3. Limits and Intercepts/Critical Values for Nij Calculations

ATD	Criterion	Peak Limits		Nij Intercepts/Critical Values (F_{zc}, M_{yc})			
		F_{zc}		F_{zc}		M_{yc}	
	Nij	Tension	Comp	Tension	Comp	Flexion	Extension
		(N)	(N)	(N)	(N)	(Nm)	(Nm)
HIII 50th M	Nij	4170	-4000	6806	-6160	310	-135
THOR 50th M	Nij	4170	-4000	4200	-4520	60	-79.2

Chest Injury Metrics and Injury Risk Calculations

For the Hybrid III 50th percentile male ATD, the risk of sustaining an AIS3+ thoracic injury was calculated using Equation 4-8 and the peak deflection from the Hybrid III chest potentiometer (δmax;). An age of 40 years was used for this equation, which yields the same equation as the one used for the U.S. Frontal NCAP85 thoracic injury risk function (Equation 4-9; Federal Register, 2008). In addition, the peak deflection threshold (63 mm) and peak thoracic acceleration threshold (60 g) specified in FMVSS No. 208 were also used to assess thoracic injury risk for the Hybrid III ATD (NHTSA, 2005). Values for 3 ms clip chest acceleration were included for historical completeness and comparison.

HIII (Laituri et al., 2005)	$p(AIS3+) = \frac{1}{1+e^{12.597-0.05861(Age)-1.568*(\delta_{max})^{0.4612}}}$	Equation 4-8
HIII (Federal Register, 2008)	$p(AIS3+) = \frac{1}{1+e^{10.5456-1.568*(\delta_{max})^{0.4612}}}$ **Where:** δmax = max(HIII sternum deflection)	Equation 4-9

For the THOR-50M ATD, the risk of sustaining an AIS3+ injury was calculated using the overall maximum resultant deflection (Rmax) and Principal Component Analysis (PCA) score, both of which are multi-point thoracic injury criteria. The injury risk based on Rmax was calculated using Equation 4-12 (Federal Register, 2015) based upon Equation 4-10 and Equation 4-11 (Federal Register, 2015; Craig et al., 2020). An age of 40 years was used for this thoracic injury criterion in Equation 4-12, which yielded Equation 4-13 (Craig et al., 2020). In addition, the injury risk based on the peak resultant deflection (Rmax) was calculated using Equation 4-12 for ages 40-, 45-, and 55-years-old (Federal Register 2015) and using Equation 4-14 for 40-years-old (Poplin et al., 2017). Finally, the injury risk based on the PCA score was calculated using Equation 4-20 based upon Equation 4-15 through Equation 4-19. In addition to the deflection-based injury metrics, the peak thoracic acceleration threshold (60 g) specified in FMVSS No. 208 (NHTSA, 2005) was used to evaluate the THOR-50M responses, and values for the 3 ms clip chest acceleration were included for comparison to the Hybrid III results.

THOR-50M (Federal Register, 2015; Craig et al., 2020)	$R_{max} = \max(UL_{max}, UR_{max}, LL_{max}, LR_{max})$ Where: $\{U/L\|R/L\}_{max} = max\left(\sqrt{[L/R]X^2_{[U/L]S} + [L/R]Y^2_{[U/L]S} + [L/R]Z^2_{[U/L]S}}\right)$	Equation 4-10 Equation 4-11
THOR-50M (Federal Register, 2015)	$p(AIS3+) = 1 - e^{-\left[\frac{R_{max}}{e^{4.7276-0.0166*(age)}}\right]^{2.977}}$	Equation 4-12
THOR-50M (Craig et al., 2020)	$p(AIS3+) = 1 - e^{-\left[\frac{R_{max}}{58.183}\right]^{2.977}}$	Equation 4-13
THOR-50M (Poplin et al., 2017)	$p(AIS3+) = 1 - e^{-\left[\frac{R_{max}}{e^{4.7775-0.0171*(age)}}\right]^{3.356}}$	Equation 4-14
THOR-50M (Federal Register, 2015)	$PCA\ Score = 0.485\left(\frac{up_{tot}}{17.509}\right) + 0.499\left(\frac{low_{tot}}{15.526}\right) + 0.493\left(\frac{up_{dif}}{10.479}\right) + 0.522\left(\frac{low_{dif}}{11.996}\right)$ **Where:** $up_{tot} = \|UL\|max + \|UR\|max$ $up_{dif} = \|UL - UR\|max$ $low_{tot} = \|LL\|max + \|LR\|max$ $low_{dif} = \|LL - LR\|max$	Equation 4-15 Equation 4-16 Equation 4-17 Equation 4-18 Equation 4-19
THOR-50M (Federal Register, 2015)	$p(AIS3+) = 1 - e^{-\left[\frac{PCA\ Score}{e^{2.6092-0.0113*(age)}}\right]^{4.4444}}$	Equation 4-20

Results

All pre-test conditions and post-test configurations are documented photographically for both dummies for all tests in Appendix J. Various perspectives are provided for each dummy.

Seat Bight and H-Point Location Repeatability

The ability to position ATDs in a repeatable fashion is important for the reduction of experimental variance in dummy testing. The seat bight and H-point locations were measured for each dummy for each test. For a given vehicle, the target position specification was ±12 mm from the average point. Table 4-4 shows the standard deviation in three directions of the seat bight and H-point locations in millimeters. If the seat and the dummy are positioned consistently with respect to the sled coordinate system, then the H-point location will be consistent with respect to the seat bight. The standard deviation of the difference between the H-point and seat bight location is provided for each vehicle. These values indicate that the dummies were positioned similarly in the buck seats between tests using the same vehicle, which likely contributed to the repeatability observed between tests that had to be rerun due to DAS or ATD issues.

Table 4-4. The Standard Deviations (in mm) in Three Dimensions for the Seat Bight and Dummy H-Point Locations for Both ATDs

Vehicle		Seat Bight		H-Point		Difference	
		HIII	THOR	HIII	THOR	HIII	THOR
V1	X	6.41	2.69	2.86	8.36	5.97	5.79
	Y	0.53	2.30	1.49	2.93	1.84	3.56
	Z	2.36	6.16	7.96	2.13	5.65	4.57
V6	X	5.19	5.16	3.61	4.05	3.69	7.26
	Y	4.84	3.00	5.62	6.40	2.47	4.55
	Z	5.87	7.44	6.05	3.49	4.68	9.69
V10	X	3.60	4.64	4.22	9.73	7.39	7.39
	Y	2.41	2.30	4.32	0.36	4.94	5.36
	Z	2.41	5.44	4.12	4.49	5.36	7.27
V13	X	1.27	0.15	3.30	3.03	2.33	2.93
	Y	1.02	1.41	5.00	0.82	4.85	1.63
	Z	2.54	3.32	5.32	3.96	4.23	4.03
V14	X	3.46	1.62	4.32	9.54	7.28	8.83
	Y	4.81	3.02	4.35	6.74	5.55	8.37
	Z	6.86	3.44	4.23	5.14	3.59	8.12
V15	X	9.21	1.03	8.69	4.66	13.64*	4.63
	Y	6.05	4.89	5.72	2.67	8.29	4.29
	Z	15.37*	6.98	9.87	6.68	18.65*	4.92

Vehicle		Seat Bight		H-Point		Difference	
		HIII	THOR	HIII	THOR	HIII	THOR
V19	X	2.74	2.75	10.30	6.20	10.00	3.18
	Y	1.78	1.44	4.02	4.55	1.15	5.84
	Z	2.51	2.33	5.31	5.76	7.75	4.07

*Exceeds ±12-mm tolerance specification

Data Traces

Select data traces from both dummies for all tests are provided in Appendix K through Appendix HH. Specifically, those signals involved in IARV calculation or injury risk estimation are plotted. Other important channels, such as lower neck loads and lumbar/T12 loads, are provided as well.

Appendix A catalogs the data peaks, organized by vehicle number. Appendix JJ tabulates the IARVs that were evaluated and injury risks that were estimated. These parameters are used in subsequent analysis and comparison between vehicles.

Motion Data

The ATD X-Z plane excursion plots derived from the VICON data are presented in Appendix KK for the generic pulse tests, in Appendix MM for the scaled/specific pulse tests, and in Appendix NN for the NCAP85 tests. The peak X- and Z-direction excursions are provided in Appendix OO. Appendix PP through Appendix RR contain high-speed video frames corresponding to the time of peak hip X-direction excursion.

A few observations can be made from inspection of the VICON results. First, there was little difference in ATD excursions between the generic and scaled/specific low-speed tests within each vehicle. Repeated high-speed tests resulted in similar excursions for both ATDs, particularly for the Hybrid III. The high-speed (NCAP85) tests resulted in greater head and shoulder forward excursions for both ATDs, regardless of vehicle. At the hip, the high-speed tests resulted in greater forward excursions for the THOR-50M, except for V6 where the scaled/specific test resulted in a slightly higher excursion than the high-speed test. Depending on the vehicle, the forward hip excursions for the Hybrid III during the high-speed tests were either greater than the low-speed tests (V1, V6, V10, V13, and V19) or similar in magnitude (V14 and V15). High-speed tests resulted in greater knee forward excursions for both ATDs regardless of vehicle, with the exception of the THOR in V6.

When comparing the Hybrid III and THOR-50M, the THOR-50M had greater X and Z excursions at the head than did the Hybrid III for all vehicles. At the shoulder, hip, and knee, the THOR-50M had greater X-direction excursions than the Hybrid III.

When comparing between vehicles for the generic sled pulse, it was found that V14 (advanced restraints) produced the lowest X-direction excursions at the head and shoulders for both ATDs. V1 (advanced restraints) produced the lowest X-direction excursions for the hip and knee. The vehicle that produced the greatest X-direction excursions varied depending on ATD and body region. V10 (no advanced restraints) produced the greatest X-direction excursions for the Hybrid III head. V6 (no advanced restraints) produced the greatest X-direction excursions for the Hybrid

III shoulders and the THOR-50M head and shoulders. V15 (no advanced restraints) produced the greatest X-direction excursions for the Hybrid III hip and knees. V13 (no advanced restraints) produced the greatest X-direction excursions for the THOR hip and knees.

Similar results were observed for vehicle comparisons for the scaled/specific sled pulse compared to the generic sled pulse discussed above. The same vehicles produced the lowest excursions for each body region and ATD for the scaled/specific sled pulse as for the generic sled pulse. The same vehicles as in the generic pulse comparisons also produced the greatest excursions for each body region and ATD for the scaled/specific pulse with the exception of the Hybrid III head. Instead of V10, V19 (advanced restraints) produced the greatest X-direction excursion for the Hybrid III head.

Comparing between vehicles for NCAP85 pulses, V1 and V14 produced the lowest X-direction excursions, depending on the body region and ATD. V1 produced the lowest X-direction excursions for the Hybrid III knee and the THOR shoulder, hip, and knee. V14 produced the lowest X-direction excursions for the THOR head and the Hybrid III head, shoulder, and hip. For the greatest X-direction excursions, V19 produced the highest excursions for the head and shoulders for both ATDs. V13 produced the greatest excursions for the hips and knees for both ATDs.

Evaluation of the Effect of the Standard THOR Abdomen Versus the ABISUP Abdomen

To assess the effect of the ABISUP abdomen versus the standard THOR-50M abdomen on the response of the THOR-50M, matched tests were performed using the generic scaled sled pulse (tests FRS-V15-1 and FRS-V15-2). The time histories of the resultant accelerations (head and chest), upper neck and T12 forces and moments, ASIS forces, and chest deflections were compared (Figure 4-1 through Figure 4-6). It should be noted that the data for V15-2 was time shifted forward by 5 ms based on visual inspection to compensate for delay in the generation of sled acceleration for V15-2 compared to V15-1. This was done to more closely align the traces so that the peaks and shapes could be better compared. This minimizes the influence of the subtle differences between the test accelerations, particularly near the onset of acceleration. The original time histories are provided in Appendix BB. The time histories showed that there were no considerable differences in the magnitude, shape, polarity, or phasing for any of the variables compared. Peak signal values, peak injury metrics and probabilities, and peak excursions were compared also, as shown in Table KK 4 through Table KK 6. These comparisons illustrated that the ABISUP abdomen did not have a considerable effect on the response of the THOR-50M, and that both the THOR-50M and testing procedures were extremely repeatable. Similarly, the VICON data showed only slight differences in the THOR-50M excursions between the ABISUP and standard abdomen. The Hybrid III showed a similar degree of difference in excursions between tests, further suggesting minimal influence of the ABISUP in the THOR-50M.

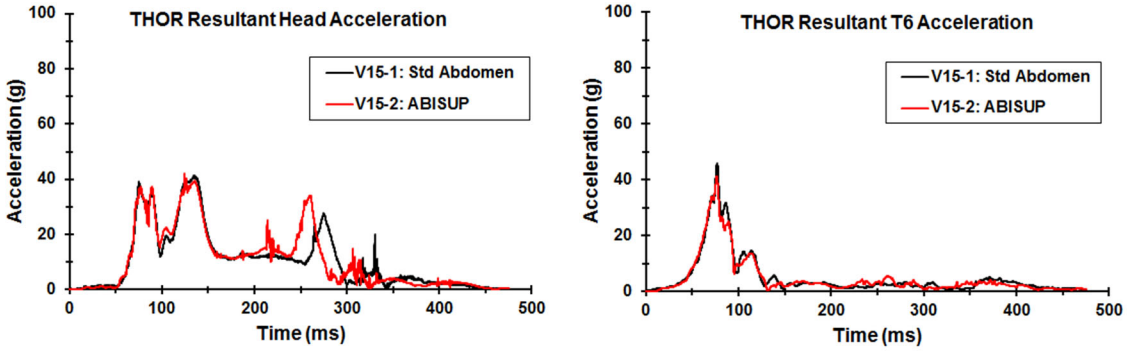

Figure 4-1. THOR Resultant Head (Left) and Chest Acceleration (Right) for V15-1 & V15-2

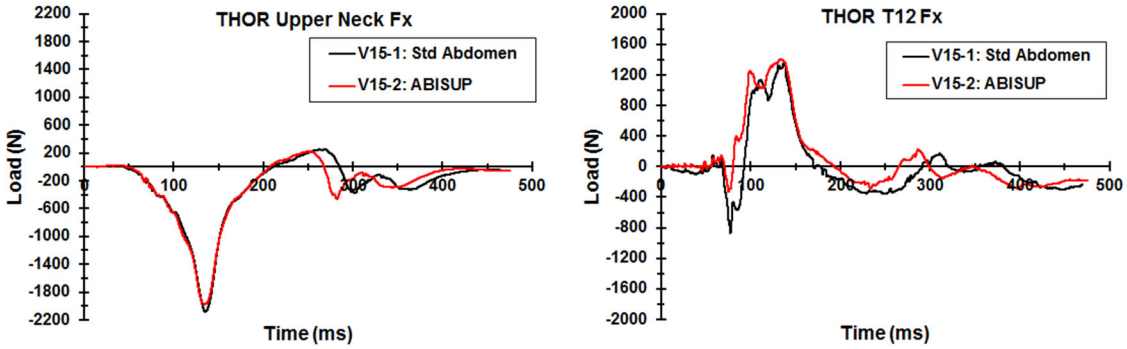

Figure 4-2. THOR Upper Neck (Left) and T12 (Right) Fx For V15-1 & V15-2

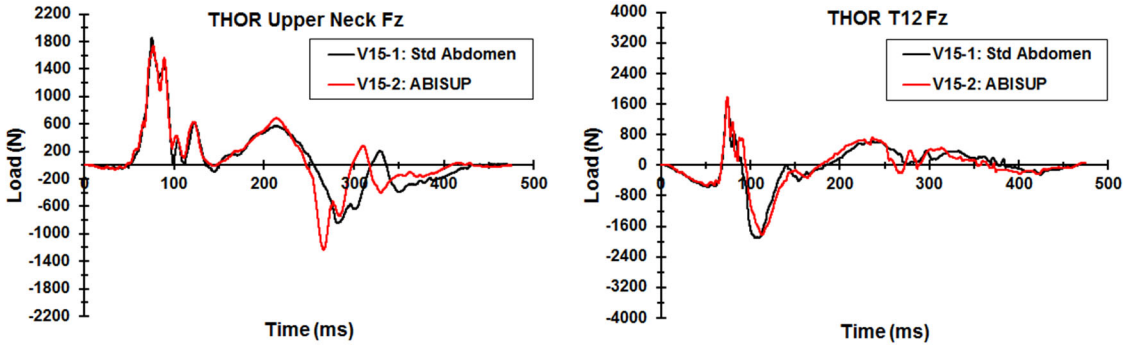

Figure 4-3. THOR Upper Neck (Left) and T12 (Right) Fz for V15-1 & V15-2

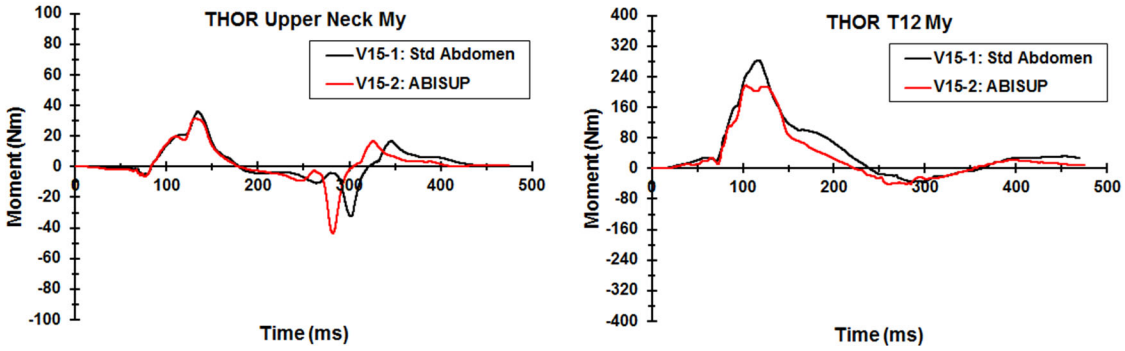

Figure 4-4. THOR Upper Neck (Left) and T12 (Right) My for V15-1 & V15-2

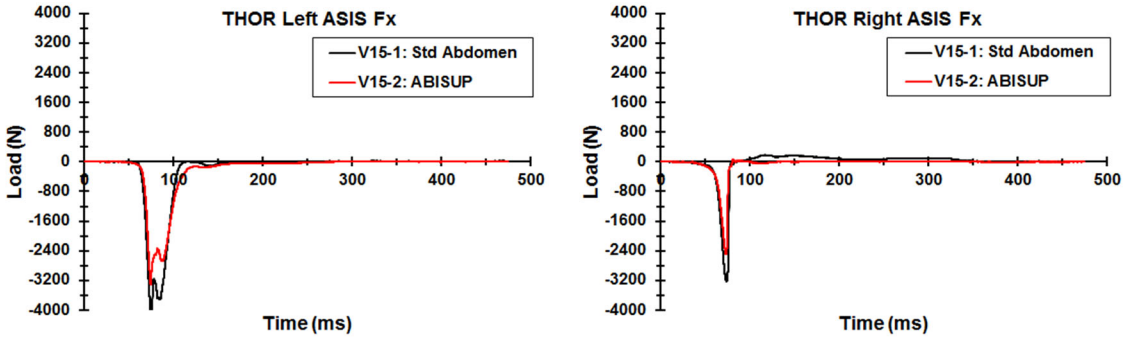

Figure 4-5. THOR Left (Left) and Right (Right) ASIS Fx for V15-1 & V15-2

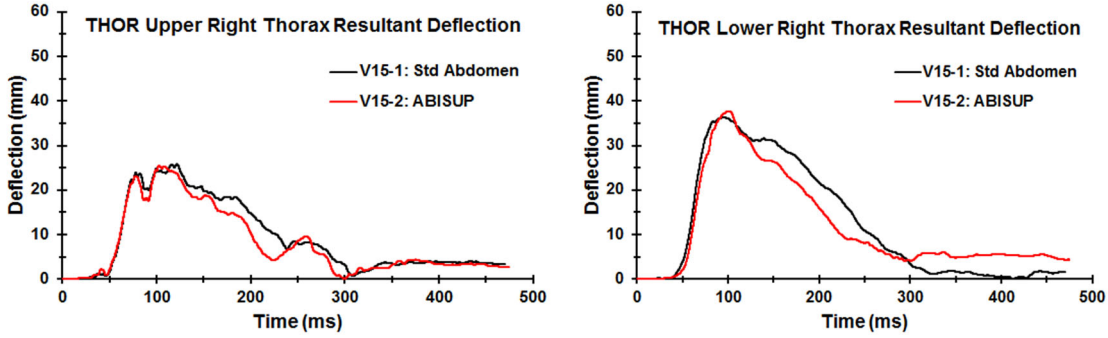

Figure 4-6. THOR UR (Left) and LR (Right) Resultant Chest Deflection for V15-1 & V19-2

Comparison of the THOR Response Before and After Retightening Spine Bolts

Following the first NCAP85 test on V19 (V19-3), the post-test damage inspection of the THOR revealed that several of the bolts in the spine were not fully tightened. The lower mounting bolts for the T12 load cell, which attach the load cell to the lumbar spine, were particularly loose. All of the bolts were then retightened and a second NCAP85 test was performed on V19 (V19-4) to assess the effect of the spine bolts not being fully tightened. The time histories of the resultant accelerations (head, chest, and pelvis), upper neck and T12 forces and moments, ASIS forces, chest deflections, and abdominal pressures were compared between the two tests (Figure 4-7

through Figure 4-14). The data for V19-4 was time shifted slightly for the sake of the comparison. The time histories showed that there were no considerable differences in the magnitude, shape, or phasing for any of the variables compared. This comparison illustrated that the bolts did not have a considerable effect on the response of the THOR, and that the THOR and testing procedures were very repeatable.

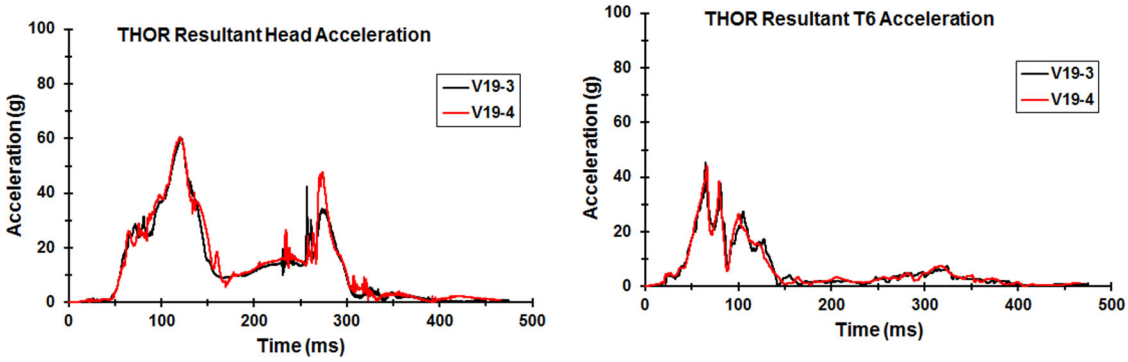

Figure 4-7. THOR Resultant Head (Left) and Chest Accelerations (Right) for V19-3 & V19-4

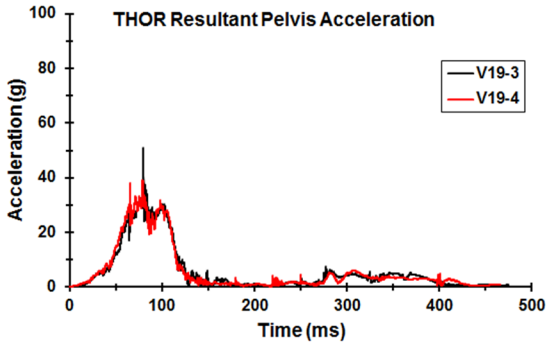

Figure 4-8. THOR Resultant Pelvis Accelerations for V19-3 & V19-4

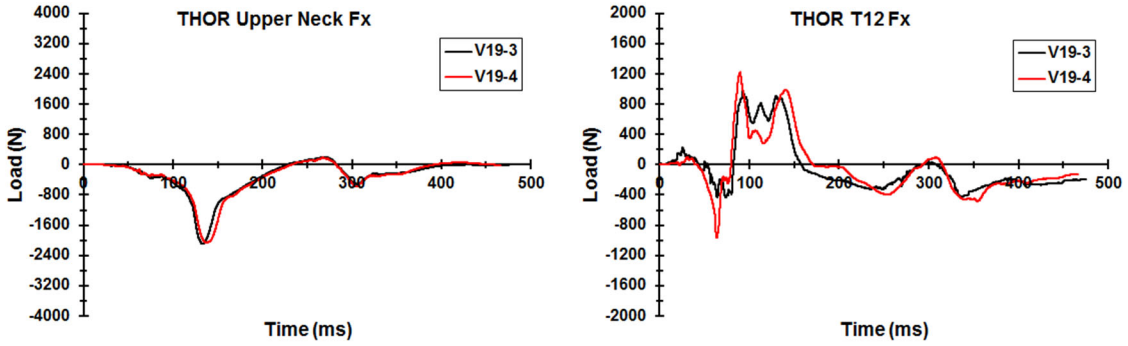

Figure 4-9. THOR Upper Neck (Left) and T12 (Right) Fx for V19-3 & V19-4

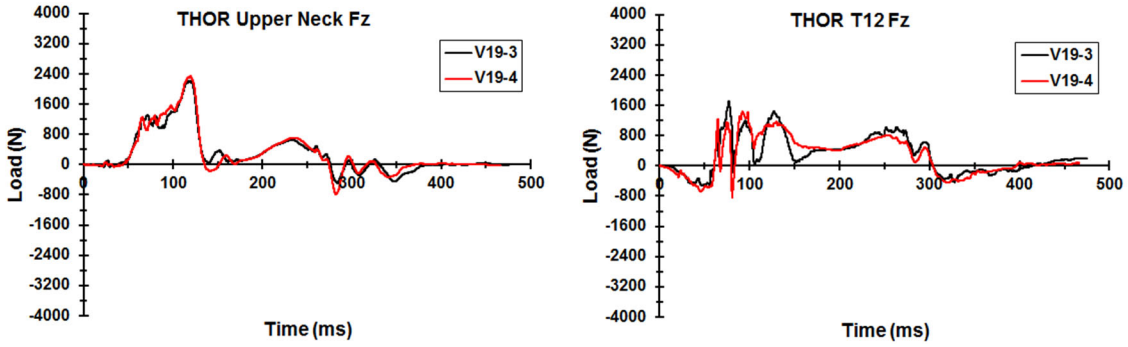

Figure 4-10. THOR Upper Neck (Left) and T12 (Right) Fz for V19-3 & V19-4

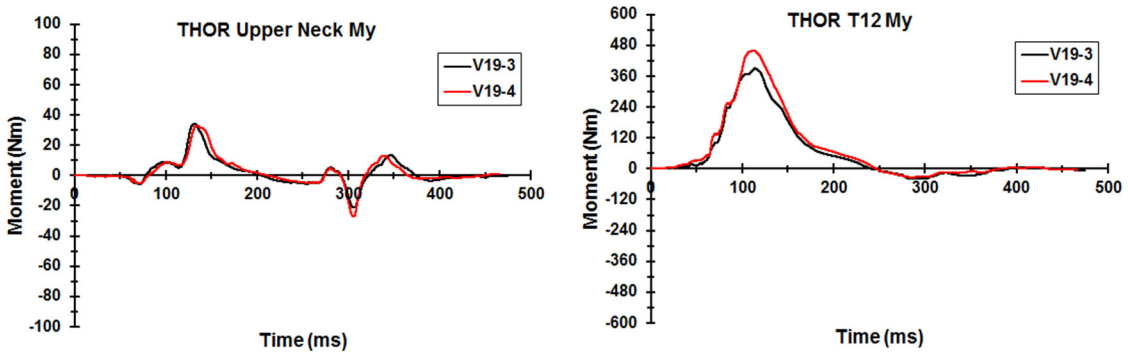

Figure 4-11. THOR Upper Neck (Left) and T12 (Right) My for V19-3 & V19-4

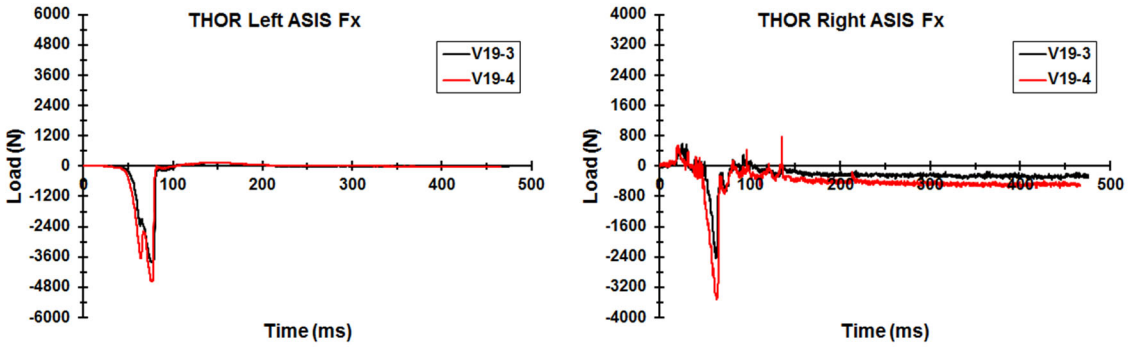

Figure 4-12. THOR Left (Left) and Right (Right) ASIS Fx for V19-3 & V19-4

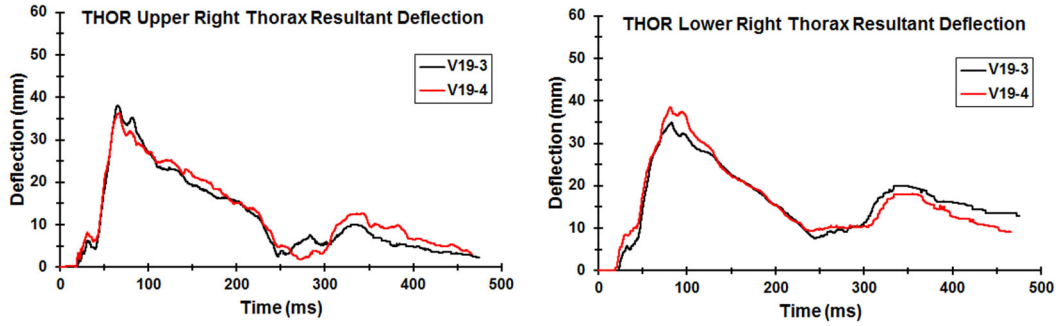

Figure 4-13. THOR UR (Left) and LR (Right) Resultant Chest Deflection for V19-3 & V19-4

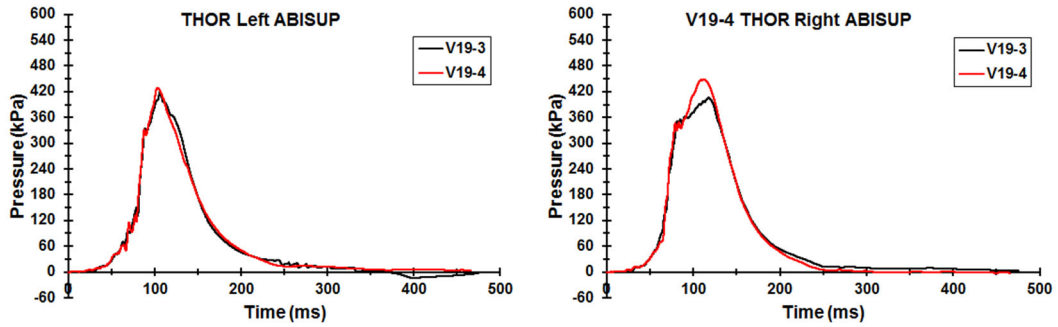

Figure 4-14. THOR Left (Left) and Right (Right) Abdominal Pressures for V19-3 & V19-4

Evaluation of Hybrid III Repeatability

Since the NCAP85 test for V19 was repeated (V19-3 and V19-4), the time histories of the resultant accelerations (head, chest, and pelvis), upper neck and lumbar forces and moments, and chest deflections for the Hybrid III were compared between these two tests to assess the repeatability of the Hybrid III (Figure 4-15 through Figure 4-20). It should be noted that the data for V19-4 was time shifted slightly for the sake of the comparison. Peak signal values, peak injury metrics and probabilities, and peak excursions were compared also, as shown in Table KK-7 through Table KK-9. The time histories showed that there were no considerable differences in the magnitude, shape, or phasing for any of the variables compared. This comparison illustrated that the Hybrid III and testing procedures were extremely repeatable.

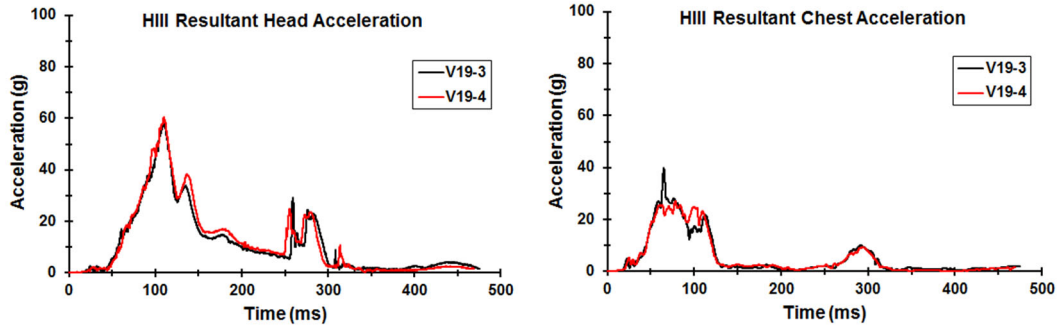

Figure 4-15. HIII Resultant Head (Left) and Chest Accelerations (Right) for V19-3 & V19-4

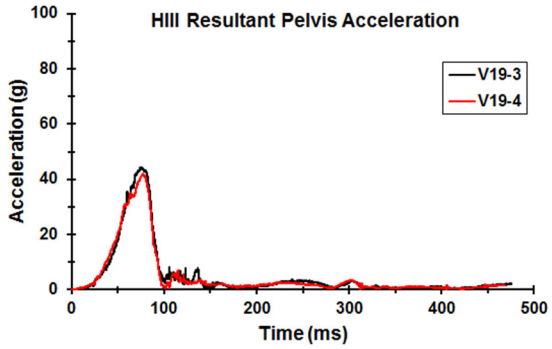

Figure 4-16. HIII Resultant Pelvis Accelerations for V19-3 & V19-4

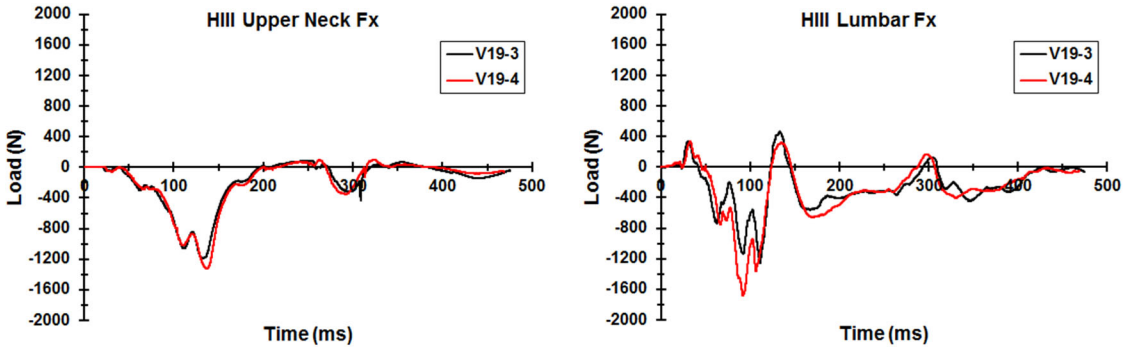

Figure 4-17. HIII Upper Neck (Left) and Lumbar (Right) Fx for V19-3 & V19-4

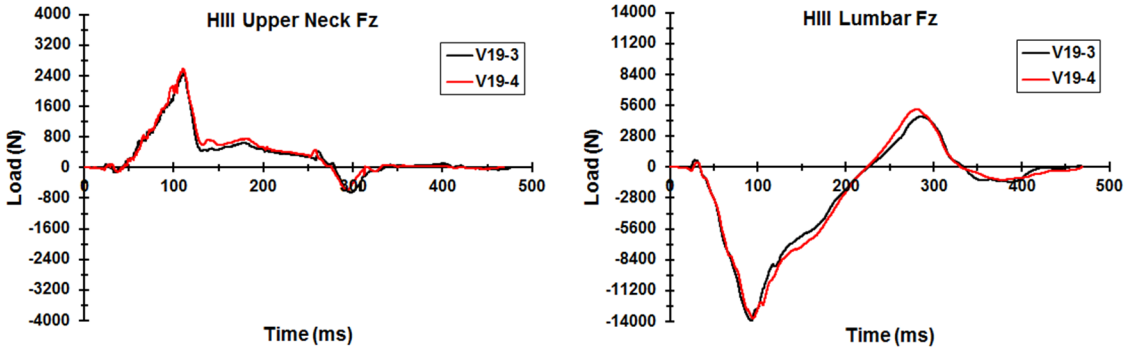

Figure 4-18. HIII Upper Neck (Left) and Lumbar (Right) Fz for V19-3 & V19-4

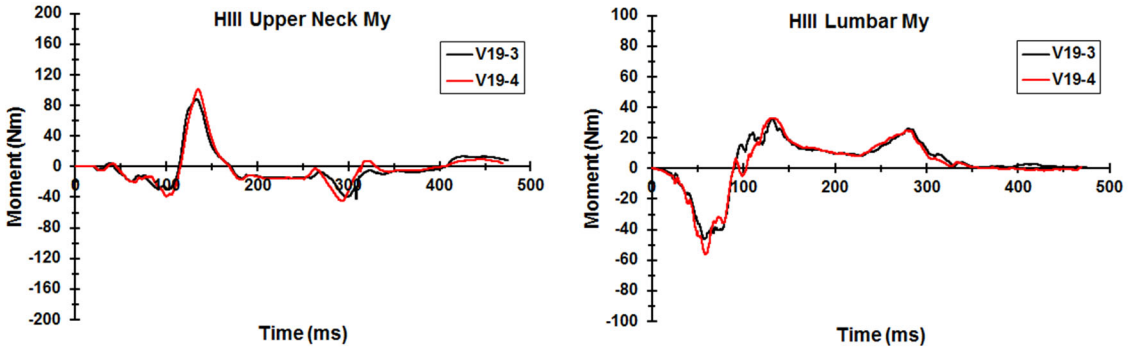

Figure 4-19. HIII Upper Neck (Left) and Lumbar (Right) My for V19-3 & V19-4

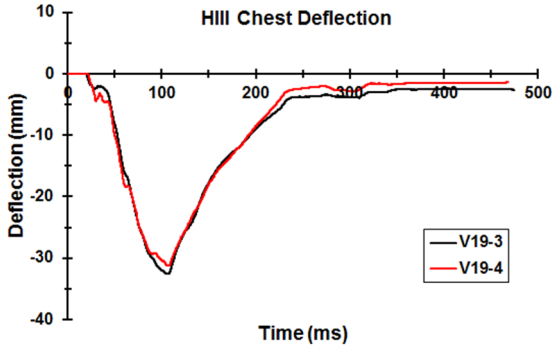

Figure 4-20. HIII Chest Deflection for V19-3 & V19-4

Comparison Between Hybrid III and THOR for a Vehicle With Good Occupant Protection

The time histories of the resultant accelerations (head, chest, and pelvis), upper neck and lumbar forces and moments, and shoulder belt forces were compared for an NCAP85 test that had good occupant protection performance and no submarining for either ATD (V14-4) (Figure 4-21 through Figure 4-26). The time histories showed that the shape, polarity, and phasing of the data were similar between the two ATDs. The polarity of the lower neck (Fx and Fz) forces differed between the two ATDs. In addition, the similarity/dissimilarity in the magnitudes of a given measurement between the two ATDs varied between variables. For example, the magnitudes of the resultant chest and pelvis accelerations were similar, while the first peak in the resultant head acceleration of the THOR was larger than the respective peak for the Hybrid III.

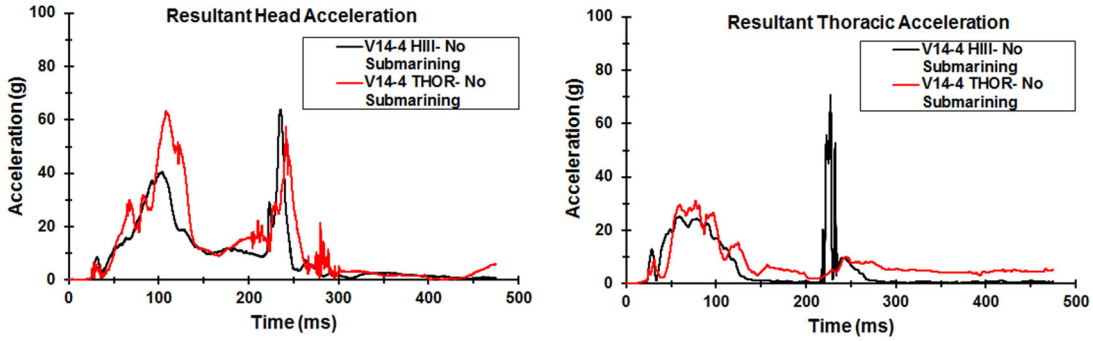

Figure 4-21. HIII Versus THOR Resultant Head (Left) and Chest (Right) Accelerations for V13-2

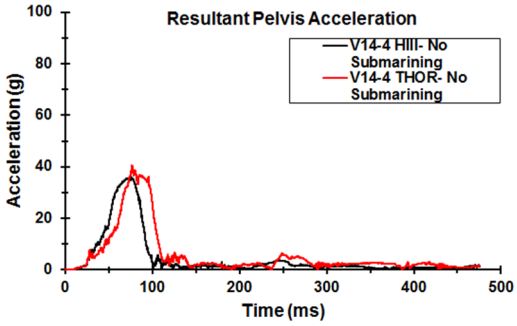

Figure 4-22. HIII Versus THOR Resultant Pelvis Accelerations for V13-2

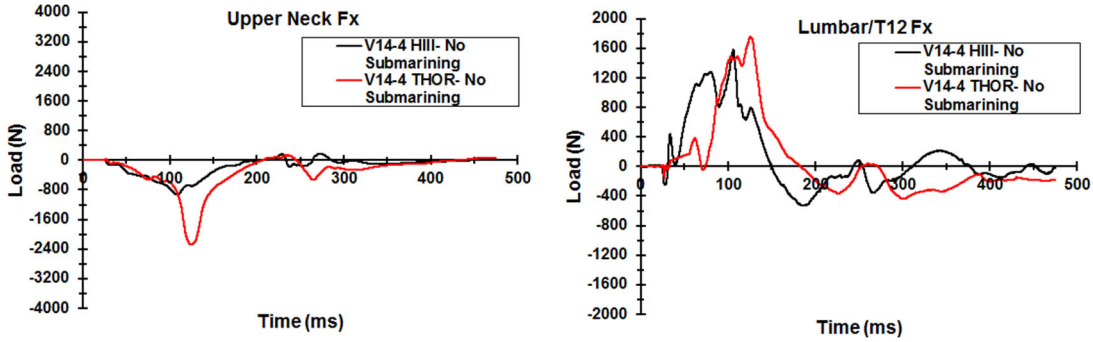

Figure 4-23. HIII Versus THOR Upper Neck (Left) and Lumbar (Right) Fx for V14-4

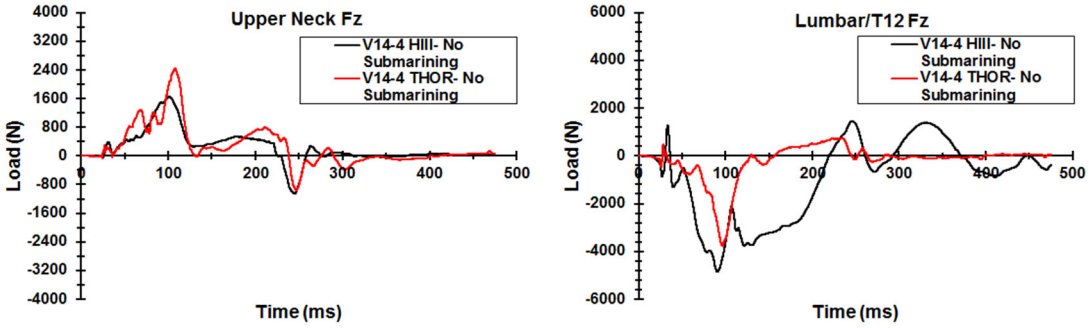

Figure 4-24. HIII Versus THOR Upper Neck (Left) and Lumbar (Right) Fz for V14-4

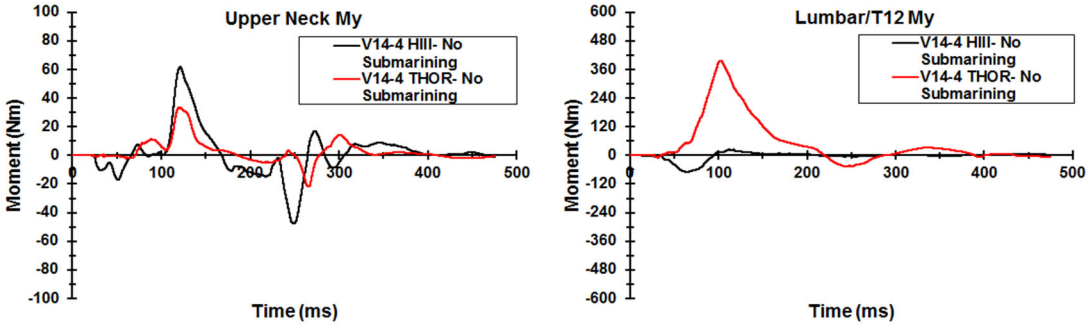

Figure 4-25. HIII Versus THOR Upper Neck (Left) and Lumbar (Right) My for V14-4

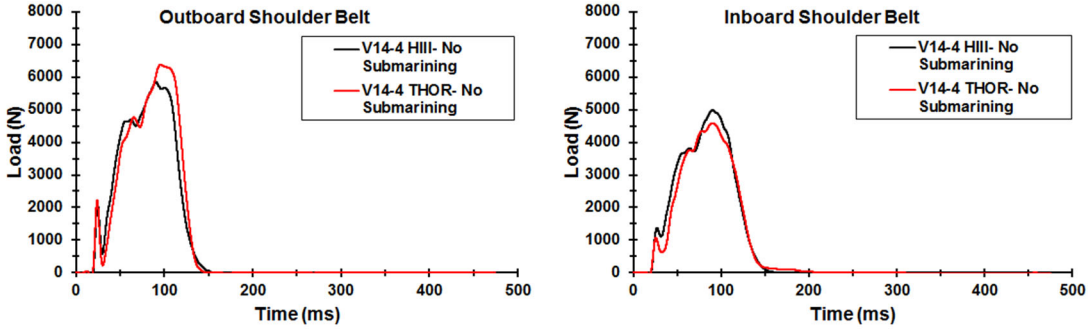

Figure 4-26. HIII Versus THOR Outer (Left) and Inner (Right) Shoulder Belt Forces for V14-4

Comparison Between Hybrid III and THOR for a Severe Submarining Case

The respective responses of the ATDs were compared for an NCAP85 test in which the THOR experienced severe submarining while the Hybrid III did not submarine (V13-2). The time histories of the resultant accelerations (head, chest, and pelvis), upper neck and lumbar forces and moments, and shoulder belt forces were compared between the ATDs (Figure 4-27 through Figure 4-32). The shape of the curves differed between ATDs for a number of variables. For example, resultant chest acceleration, resultant pelvis acceleration, and inboard shoulder belt force demonstrated a bimodal response for the THOR due to the occurrence of submarining, whereas the Hybrid III demonstrated a more parabolic response. In addition, the polarity of the

lower neck forces (Fx and Fz) and lumbar T12 axial force (Fz) differed between the ATDs. Although the peaks were similar between the ATDs for some variables, there were several variables for which the magnitudes differed between the ATDs, most notably the lumbar/T12 forces/moments and the upper neck My.

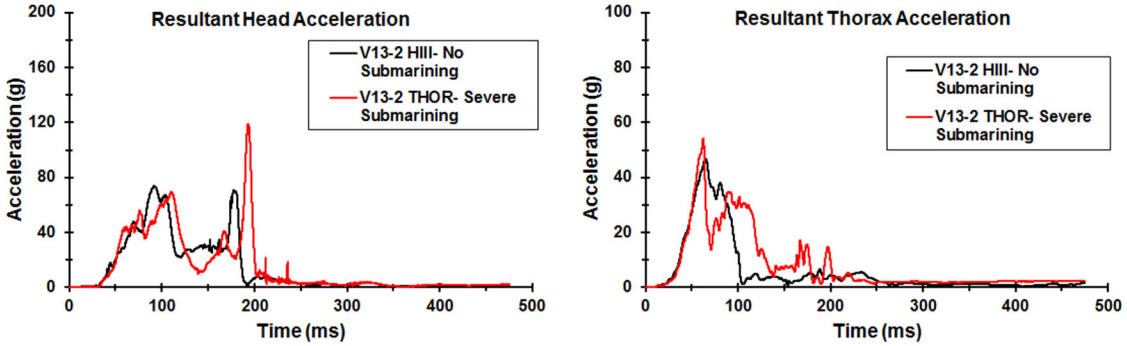

Figure 4-27. HIII Versus THOR Resultant Head (Left) and Chest (Right) Accelerations for V13-2

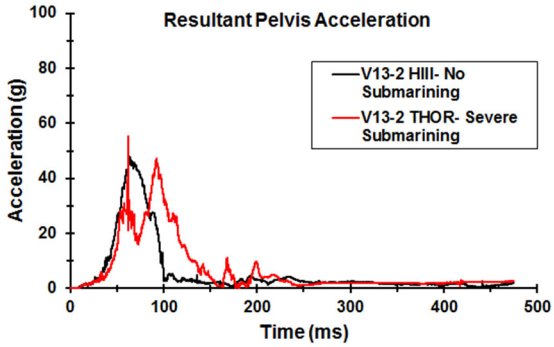

Figure 4-28. HIII Versus THOR Resultant Pelvis Accelerations for V13-2

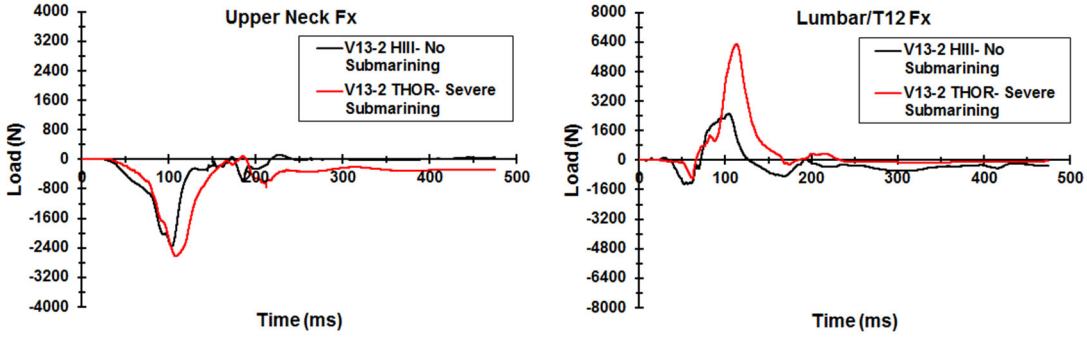

Figure 4-29. HIII Versus THOR Upper Neck (Left) and Lumbar (Right) Fx for V13-2

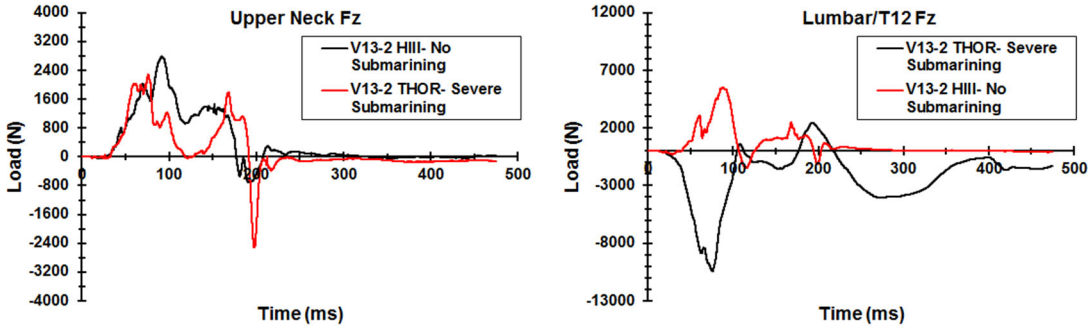

Figure 4-30. HIII Versus THOR Upper Neck (Left) and Lumbar/T12 (Right) Fz for V13-2

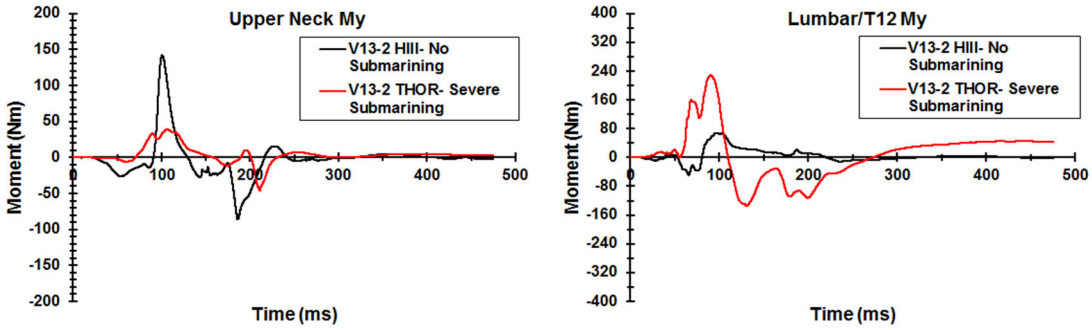

Figure 4-31. HIII Versus THOR Upper Neck (Left) and Lumbar (Right) My for V13-2

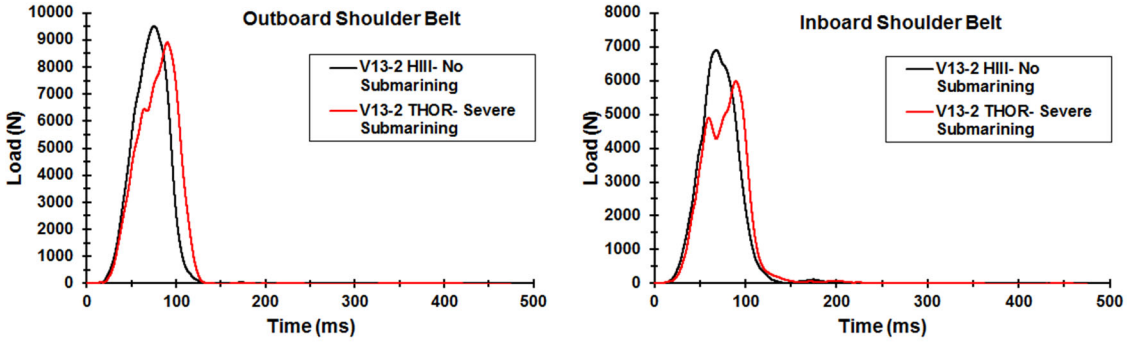

Figure 4-32. HIII Versus THOR Outer (Left) and Inner (Right) Shoulder Belt Forces for V13-2

Submarining Assessment

Accurate assessment of submarining occurrence is not always straightforward. A number of observations and measurements must be combined to reach a conclusion with confidence. Within these tests, high-speed video, post-test observations/photographs, seat belt loads, ABISUP pressure, and ASIS X-direction loads and moments about the Y-axis were used. Submarining is indicated by the presence of a steep drop in ASIS loads and moments, and a steep drop in seat belt loads, often followed by a plateau at a much lower load. Peak ABISUP pressure is considerably larger for submarining cases (typically above 200 kPa), accompanied by a rapid

transition to peak once the belt slips into the abdomen. None of these indicators is necessarily conclusive by itself, and in some cases these indicators do not agree. However, taken together, the presence of submarining can be determined reasonably well. Typically, if post-test photos do not show submarining, and seat belt load patterns are inconclusive, ASIS load and moments, along with test video, will show submarining. ABISUP pressure is particularly reliable for determining submarining. Occasionally, the relative extent of submarining could not be determined conclusively. Sixteen out of 25 tests resulted in some degree of submarining in the THOR dummy. The Hybrid III dummy did not submarine during any test.

Table 4-5 shows the results of the submarining assessment. Vehicles V1 and V14 had pretensioners and load limiters, and demonstrated no substantive submarining. Vehicle V1 exhibited minor submarining for the first two tests. This was related to the pretensioners lifting the belt on the inboard (right) side. Technically, these two responses are categorized as submarining, but more accurately they can be described as representing enhanced engagement of the abdomen by the belt on one side. Vehicle V19 also had pretensioners and load limiters but submarining was not eliminated in the THOR-50M. Similar to vehicle V1, the minor cases of submarining for vehicle V19 were related to pretensioner "belt lift." Typically for cases involving belt lift, the ASIS loads and moments exhibit a submarining signature (rapid drop in force or change in moment), but ABISUP pressure is only moderately elevated, and the rise in pressure is not characterized by a rapid transition. Post-test photos do not show penetration of the belt into the abdomen. Vehicle V6 had basic retractors and captain's chair style seats with basket style seat bottoms mounted to stow-and-go frames, and demonstrated no submarining. Vehicle V15 had basic retractors but had pronounced anti-submarining ramps under the seat bottom cushion, and produced some degree of submarining in the THOR-50M. Vehicle V13 had simple retractors and a relatively flat surface under the seat and was associated with the most pronounced submarining. Vehicle V10 had simple retractors and track mounted basket style seats with relatively weak metal brackets holding the metal frame, which deformed considerably during the tests. The deformation of the seat bottom brackets contributed to pronounced submarining.

The degrees of submarining were separated into three categories: minor, moderate, and severe. Minor submarining was associated with the belt encroaching upon the abdomen on one side, typically the right side (inboard for the THOR-50M), and was likely related to shoulder belt "lift." Moderate submarining was associated with bilateral encroachment of the lap belt upon the abdomen, without substantial penetration of the abdomen as indicated by the ABISUP pressure sensors. Test FRS-V19-2 involved bilateral departure slipping of the lap belt off the ASIS, but the extent of the interaction was small, so this occurrence was deemed minor as well. The two severe cases of submarining involved considerable penetration of the belt into the abdomen, very large ABISUP pressures, and substantial departure of the dummy pelvis from the seat.

Table 4-6 summarizes the interpretation of submarining evidence for these tests, in support of the findings shown in Table 4-5. Post-test pictures, seat belt loads, ASIS loads and/or moments, ABISUP pressure, and test video were examined to determine the presence of submarining. Again, 16 out of 25 tests demonstrated some degree of submarining for the THOR-50M. A plus sign (+) reflects a positive indication of submarining.

Figure 4-33 shows a case of moderate submarining (Test FRS-V13-1) in the THOR. These post-test pictures show the capture of the lap belt in the abdomen on both sides, which was accompanied by roping of the belt. They also show the slouched posture of the THOR.

Figure 4-34 illustrates one type of lap-belt loading profile that can be associated with submarining. The right-side (inboard) "lap belt" was placed low on the shoulder strap next to the ASIS. There was an initial peak followed by a rapid transition to a lower pressure plateau as the belt slipped over the ASIS and penetrated the abdomen. Often, the initial peak was less than what would be expected when the belt stayed below the ASIS. The ABISUP pressures were higher (~200 kPa) than what would register for non-submarining cases (~100 kPa) and were of a longer duration than when there was no submarining. Peak ABISUP pressures well over 300 kPa could be registered during severe submarining. The time associated with seat belt load reduction coincided with the time of more rapid increase in ABISUP pressure, particularly for the right side.

Figure 4-35 shows ASIS X-direction loads and moments about the Y-axis for Test FRS-V13-1. The steep reduction in load and moment magnitudes indicate that the the lap belt slips over the ASIS, and corresponds to the rapid reduction in lap belt load and rapid increase in ABISUP pressure.

Figure 4-36 shows a case of minor submarining (Test FRS-V15-2) in the THOR. There was some roping of the lap belt. The belt slipped into the abdomen on the right (inboard) side. The belt stayed below the ASIS on the left (outboard) side.

Table 4-5. Assessment of THOR-50M Submarining in FRS Series of Second-Row Sled Tests

Buck	Test #	Submarining	Degree	Description	Note
V1	1	Yes	Minor	Right Side	Pretensioner belt lift initiated
	2	Yes	Minor	Right Side	Pretensioner belt lift initiated
	3	No	na	na	
V6	1	No	na	na	
	2	No	na	na	
	3	No	na	na	
	4	No	na	na	
V10	1	Yes	Moderate	Bilateral	
	2	Yes	Moderate	Bilateral	
	3	Yes	Severe	Bilateral	Maximum ABISUP pressures
V13	1	Yes	Moderate	Bilateral	Seat departure. Slouch.
	2	Yes	Severe	Bilateral	Seat departure.
	3	Yes	Moderate	Bilateral	Seat departure.
V14	1	No	na	na	
	2	No	na	na	
	3	No	na	na	
	4	No	na	na	
V15	1	Yes	Minor	Right Side	Small slouch/rotation. Shoulder belt lift.
	2	Yes	Minor	Right Side	Small slouch/rotation. Shoulder belt lift.
	3	Yes	Minor	Right Side	Small slouch/rotation. Shoulder belt lift.
	4	Yes	Moderate	Bilateral	Slouch.

Buck	Test #	Submarining	Degree	Description	Note
V19	1	Yes	Minor	Right Side	Pretensioner belt lift contributed
	2	Yes	Minor	Right Side	Pretensioner belt lift contributed
	3	Yes	Moderate	Bilateral	Right side first. No slouch.
	4	Yes	Moderate	Bilateral	Right side first. No slouch.

Table 4-6. Sources of Submarining Evidence for the FRS Tests. A Plus Sign (+) Indicates a Positive Sign of Submarining.

Buck	Test #	Submarining		Post-Test Picture		Seat Belt Loads		ASIS Fx and/or My		ABISUP Pressure		Test Video	
		L	R	L	R	L	R	L	R	L	R	L	R
V1	1	No	Yes	-	-	-	-	-	?	-	+	-	+
	2	No	Yes	?	?	-	-	-	?	-	?	-	+
	3	No	No	-	-	-	-	-	-	-	-	-	-
V6	1	No	No	-	-	?	-	?	-	-	-	-	-
	2	No	No	-	-	-	-	-	-	-	-	-	-
	3	No	No	-	-							-	-
	4	No	No	?	?	-	-	-	-	-	-	-	-
V10	1	Yes	Yes	+	-	+	+	+	+	+	+	+	?
	2	Yes	Yes	+	?	+	+	+	+	+	+	+	?
	3	Yes	Yes	+	?	?	+	+	+	+	+	+	+
V13	1	Yes	Yes	+	+	+	+	+	+	+	+	+	+
	2	Yes	Yes	+	+	-	?	+	+	+	+	+	+
	3	Yes	Yes	+	+	+	+	+	+	+	+	+	+
V14	1	No	No	-	-	?	-	-	-	-	-	-	-
	2	No	No	?	?	+	-	-	?	-	-	-	-
	3	No	No	?	?	-	-	-	-	-	-	-	-
	4	No	No	-	-	?	-	-	-	-	-	-	-
V15	1	No	Yes	?	?	-	-	-	+			-	+
	2	No	Yes	?	+	-	-	-	+	-	+	-	+
	3	No	Yes	-	+	-	-	-	+	-	+	-	+
	4	Yes	Yes	+	+	?	-	+	+	+	+	+	+
V19	1	No	Yes	-	-	?	?	-	+	-	?	-	?
	2	No	Yes	-	?	-	?	-	+	-	+	-	?
	3	Yes	Yes	+	+	+	-	+	+	+	+	+	+
	4	Yes	Yes	+	?	+	-	+	+	+	+	+	+

Key: + evidence of submarining, - no evidence of submarining, ? inconclusive

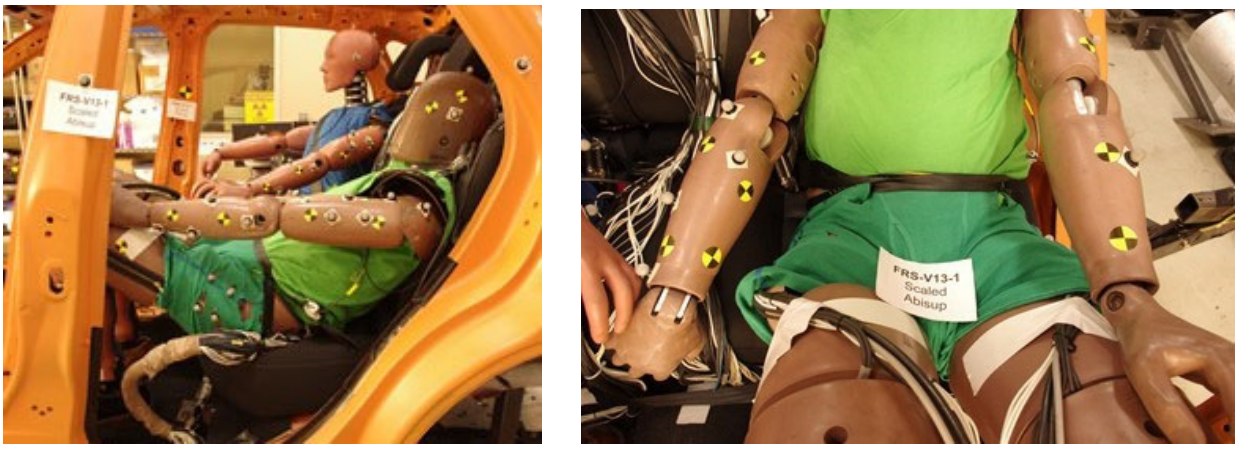

Figure 4-33. Post-Test Pictures of Test FRS-V13-1, Which Involved Moderate Submarining of the THOR Dummy, Partial Departure of the Pelvis From the Seat Bottom, and Slouching of the Dummy During/After Seat Belt Unloading

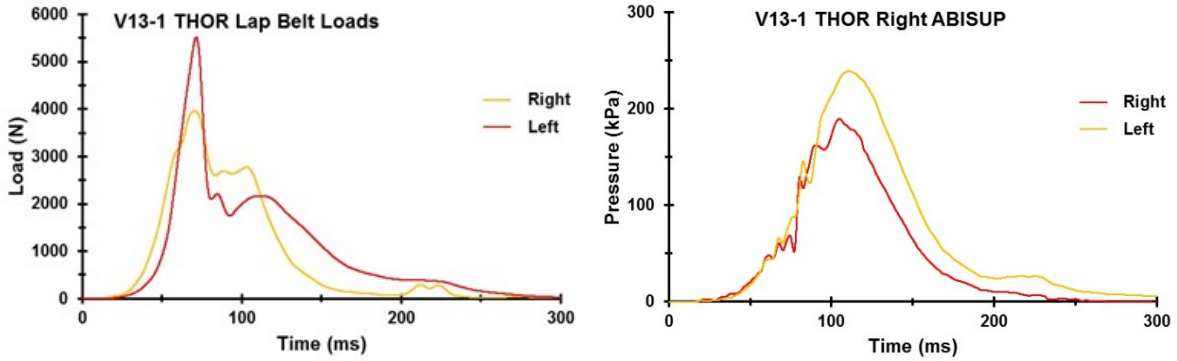

Figure 4-34. Lap Belt Loads (Left) From Test FRS-V13-1, Which Show the Rapid Drop in Seat Belt Tension When the Belt Slips off the ASIS Followed by a Lower Load Plateau as the Belt Loads the Abdomen, and Elevated and Extended ABISUP Pressures (Right)

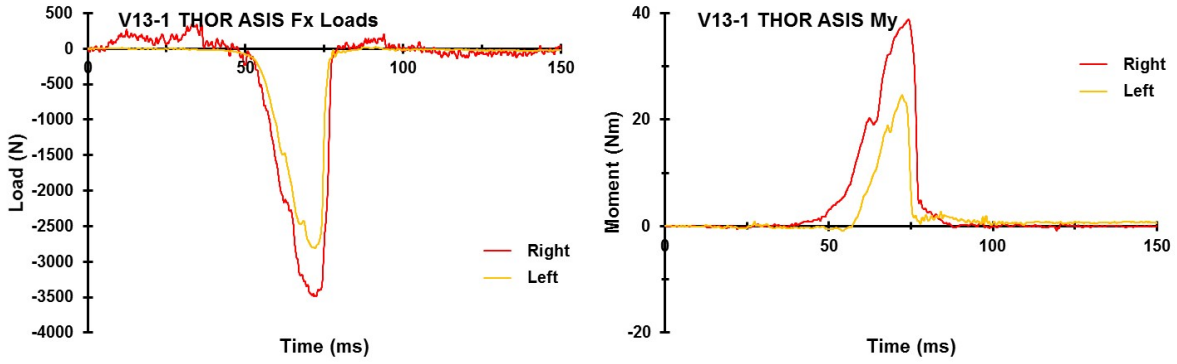

Figure 4-35. ASIS X-Direction Loads (Left) and Y-Axis Moments (Right) From Test FRS-V13-1, Which Show the Rapid Drop in Lap Belt Interaction With the ASIS When the Belt Slips off the ASIS and Into the Abdomen

Figure 4-36. Post-Test Pictures of Test FRS-V15-2, Which Involved Minor Submarining of the THOR Dummy With the Belt Penetrating the Abdomen on the Right (Inboard) Side

Figure 4-37 compares the lap belt loads from the right and left sides, and the ABISUP pressures from both sides. The right (submarined) side exhibited lower seat belt loads, and a local dip in load when the belt slips. Often, this local dip was quite pronounced. In this case, the lower peak load provided more of a clue as to what might be happening but was not conclusive by itself. The ABISUP pressure on the right side approached 300 kPa, which is in a range for which submarining would be strongly suspected. The left side registered less than 100 kPa, and the dummy did not submarine on this side.

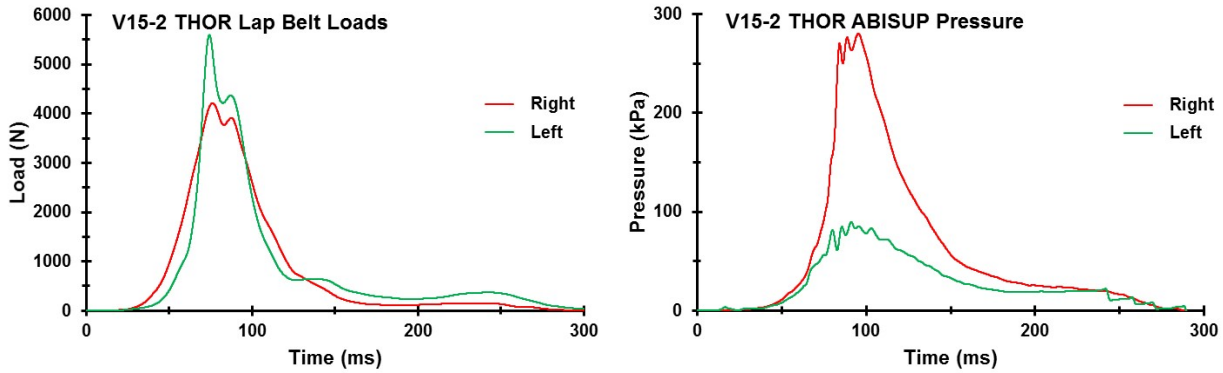

Figure 4-37. Lap Belt Loads (Left) From Test FRS-V15-2, Which Exhibit a Relative Low Peak Load for the Right (Submarined) Side, snd ABISUP Pressures (Right) Showing a Substantially Elevated Response on the Right Side

Figure 4-38 shows ASIS X-direction loads and moments about the Y-axis for Test FRS-V15-2. The steep reduction in load and moment magnitudes on the right side indicate that the the lap belt slipped over the ASIS and into the abdomen. The left-side loads and moments exhibit continued contact between the lap belt and the ASIS throughout the test.

As mentioned, all of the indicators described above do not always point toward the same conclusion. If multiple indicators provided clear indication of submarining, even if all did not, and if there was clear video evidence, then it was concluded that submaring had occurred. Within these tests, identification of submarining was usually uncomplicated.

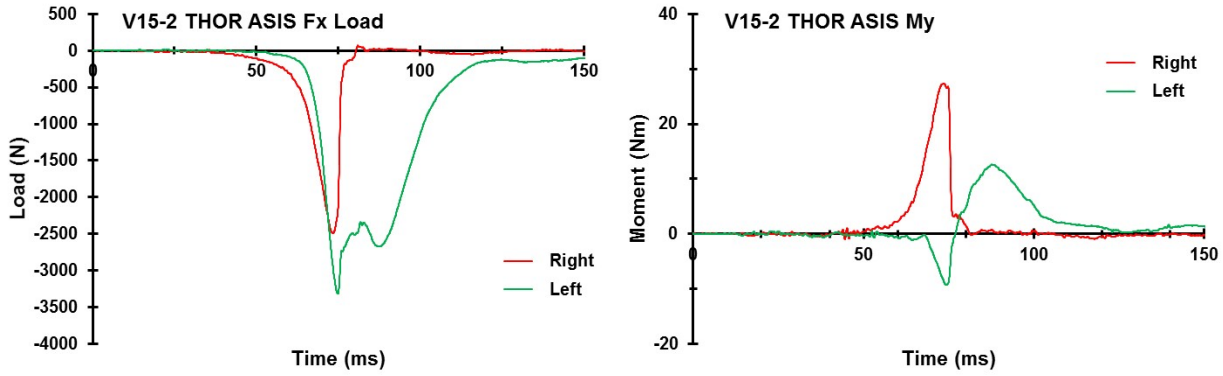

Figure 4-38. ASIS X-Direction Loads (Left) and Y-Axis Moments (Right) From Test FRS-V15-2, Which Show the Rapid Drop in Lap Belt Interaction With the ASIS When the Belt Slips off the Right ASIS, But Not the Left ASIS, and Into the Abdomen

Peak Resultant Head Acceleration and Injury Risk Comparison

The peak resultant head accelerations, HIC15 values, and BrIC injury risks were plotted for each vehicle and ATD (Figure 4-39 through Figure 4-42). When comparing between the scaled sled pulses for a given vehicle and ATD, there were no substantial differences in peak resultant head acceleration, HIC15, BrIC, or BrIC injury risk between the scaled generic pulse and scaled vehicle specific pulse except for the THOR-50M in test V13. However, the NCAP85 pulse resulted in considerably larger resultant head acceleration, HIC15, BrIC, and BrIC injury risk values than the scaled low-energy (generic and specific) pulses. The HIC15 values were well below the threshold for injury for all of the tests performed using the scaled low-energy pulses, whereas BrIC injury risk was relatively high for four vehicle specific scaled tests. For the NCAP85 pulses, the THOR-50M and Hybrid III generally showed the same trends in peak resultant head acceleration, HIC15, BrIC, and BrIC injury risk when comparing between vehicles. However, the magnitudes of each variable differed between ATDs for a given vehicle. The THOR-50M exceeded the HIC15 injury threshold (700) for two NCAP85 vehicle tests (V13 and V15), while the Hybrid III nearly exceeded the HIC15 injury threshold for four NCAP85 vehicle tests (V6, V10, V13, and V15), all of which did not have pretensioners or load limiters (Figure 4-40). In regard to BrIC injury risk, five vehicles (V6, V10, V13, V15, and V19) for the Hybrid III NCAP85 tests and three vehicles (V6, V10, and V15) for the NCAP85 THOR-50M tests exceeded the BrIC injury threshold (Figure 4-42). Peak values related to when the ATD's head made contact with the seat or returned to seat are denoted with an asterisk (*) in each table and bar chart.

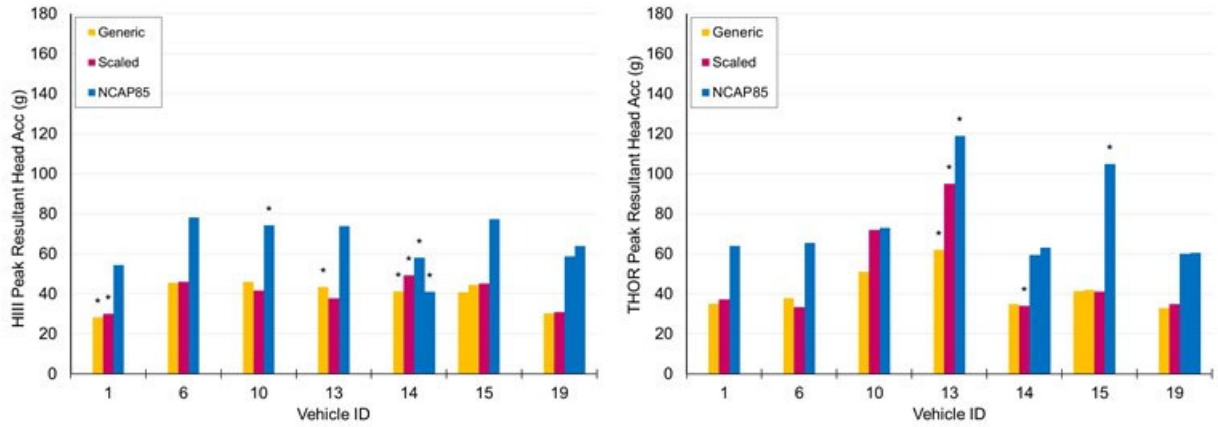

Figure 4-39. Peak Resultant Head Accelerations for HIII (Left) and THOR (Right)

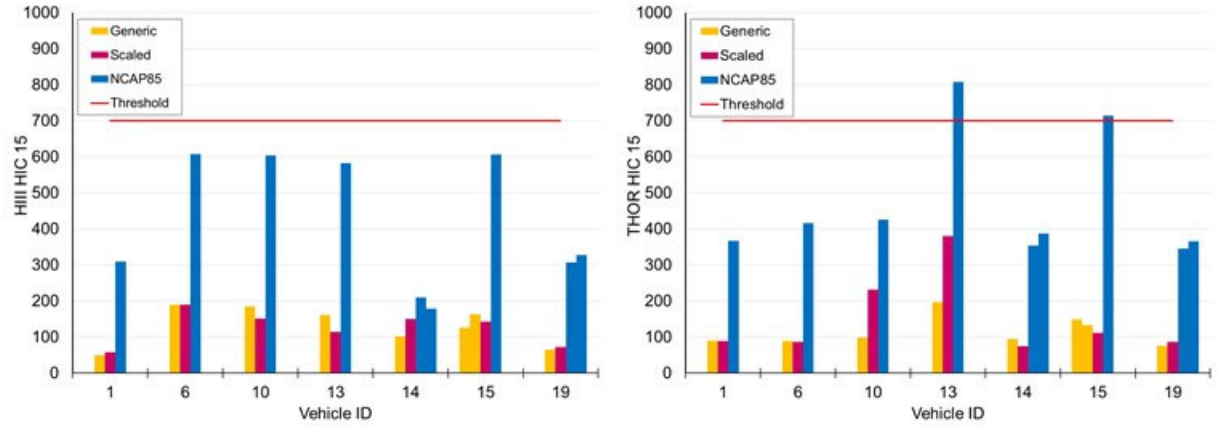

Figure 4-40. HIC15 for HIII (Left) and THOR (Right)

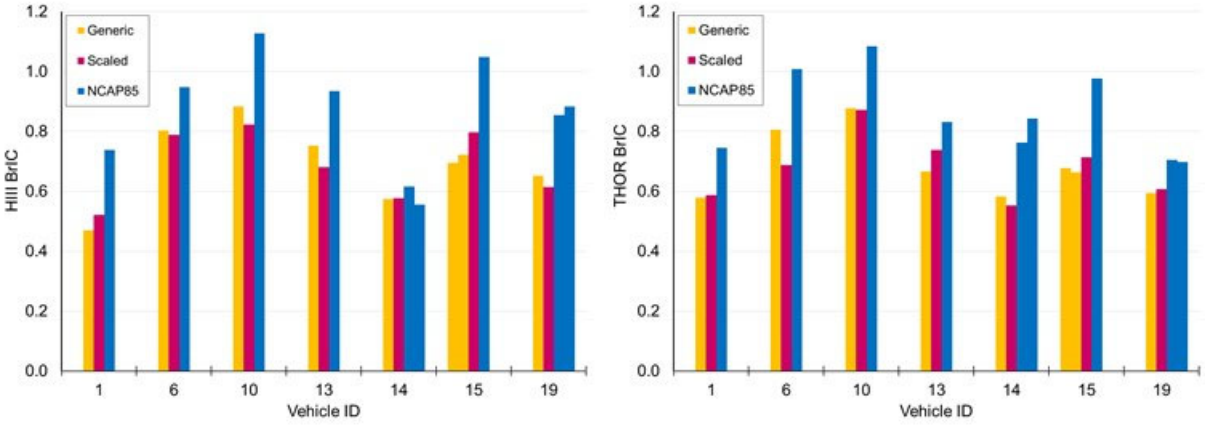

Figure 4-41. BrIC for HIII (Left) and THOR (Right)

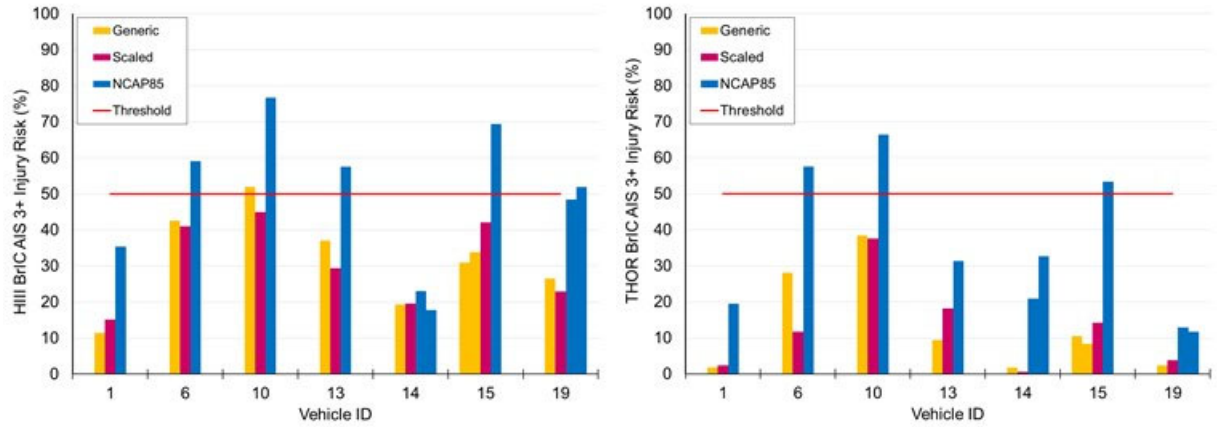

Figure 4-42. BrIC Injury Risk for HIII (Left) and THOR (Right)

Peak Neck Force and Moment Comparison

For the upper neck, the peak fore/aft forces (Fx), peak tension/compression forces (Fz), peak flexion/extension moments (My), Nij, and neck injury risks were plotted for each vehicle and ATD (Figure 4-43 through Figure 4-45 and Figure 4-49 through Figure 4-50). When comparing between the scaled sled pulses for a given vehicle and ATD, there were no substantial differences in peak fore/aft forces, peak tension/compression forces, peak flexion/extension moments, or neck injury risks between the scaled generic pulse and scaled vehicle specific pulse for the upper neck, except for the THOR upper neck compressive force for V10.

The Hybrid III and THOR had reasonably similar responses in regard to Fx and Fz (Figure 4-43 through Figure 4-44). However, the THOR demonstrated higher negative Fx forces (head rearward/chest forward) for the scaled low-energy pulses and substantially higher compressive forces for the V10, V13, and V15 NCAP85 pulses. Neither ATD exceed the maximum tension or compression thresholds for the upper neck. Although the upper neck flexion/extension moments were reasonably below the Nij critical values for the Hybrid III, the THOR flexion moment nearly exceeded the Nij critical value for the THOR for two NCAP85 tests (V10-3 and V15-4).

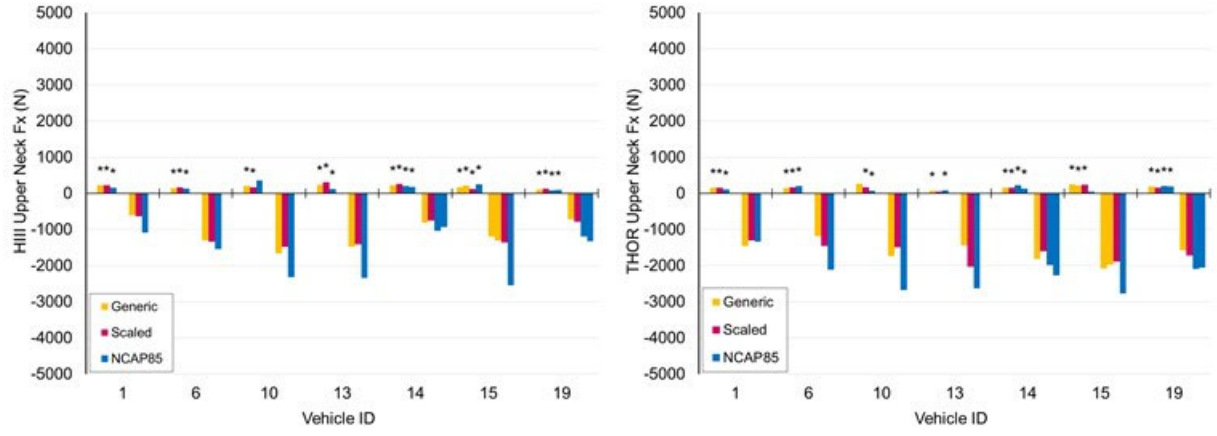

Figure 4-43. HIII (Left) and THOR (Right) Upper Neck Fore/Aft Load (Fx)

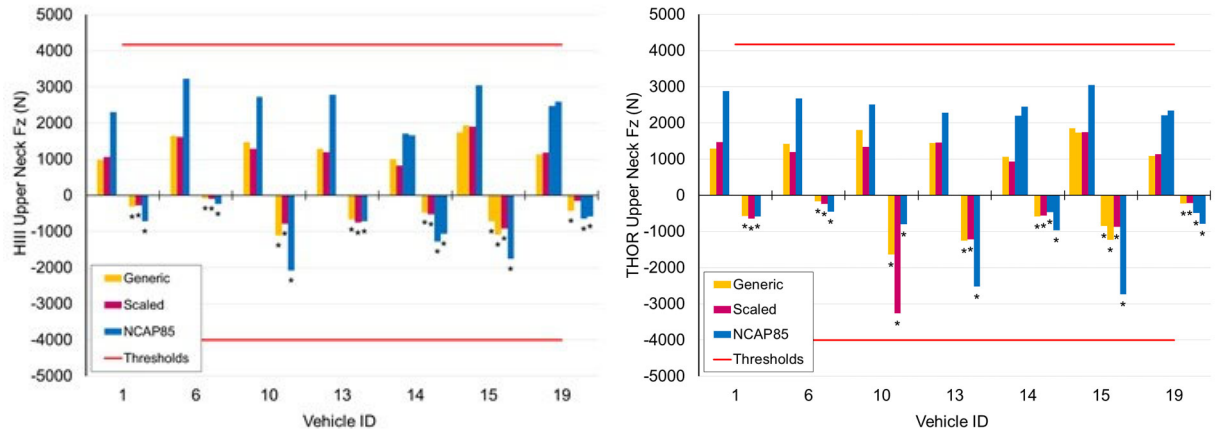

Figure 4-44. HIII (Left) and THOR (Right) Upper Neck Tension/Compression Load (Fz)

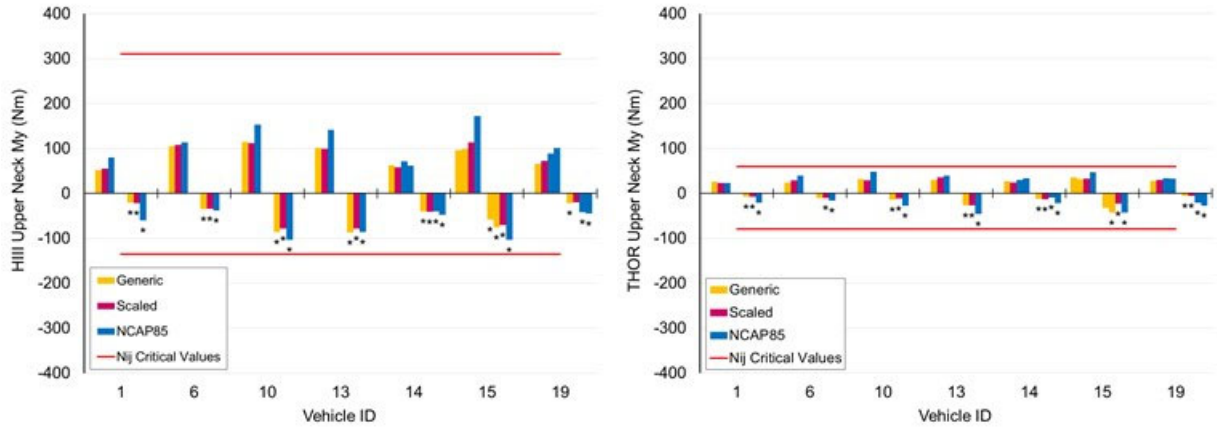

Figure 4-45. HIII (Left) and THOR (Right) Upper Neck Flexion/Extension Moment (My)

For the lower neck, the Hybrid III and THOR-50M had different responses in regard to peak fore/aft and peak tension/compression forces (Figure 4-46 and Figure 4-47). When comparing between the scaled sled pulses for a given vehicle and ATD, there were no substantial differences in peak fore/aft forces, peak tension/compression forces, peak flexion/extension moments, or neck injury risks between the scaled generic pulse and scaled vehicle specific pulse for either the lower neck. While the Hybrid III had larger negative loading for Fx (head rearward/chest forward), the THOR had larger positive loading for Fx (head forward/chest rearward). The Hybrid III had larger positive loading for Fz (tension), while the THOR had larger negative loading for Fz (compression). Lower neck flexion/extension moments for the Hybrid III were consistently considerably larger than those for the THOR-50M (Figure 4-48).

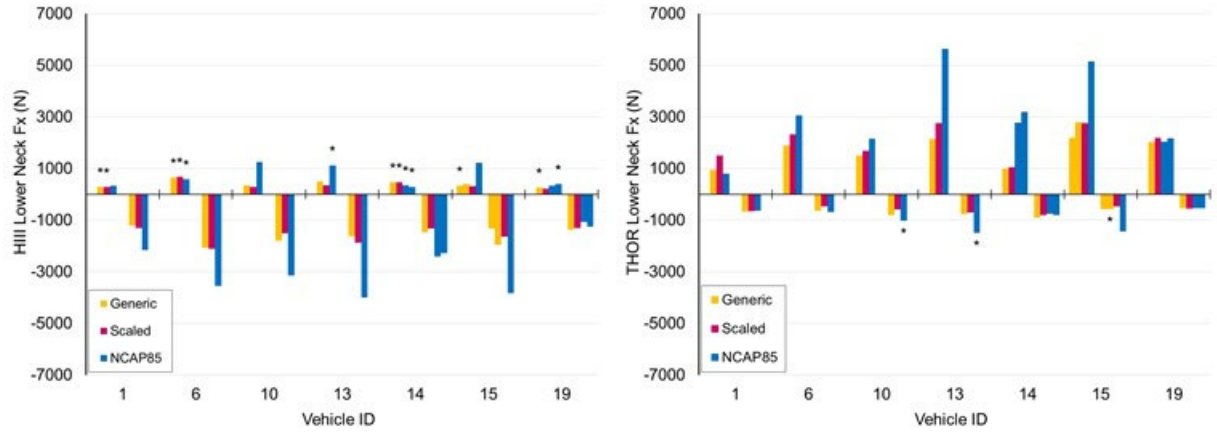

Figure 4-46. HIII (Left) and THOR (Right) Lower Neck Fore/Aft Load (Fx)

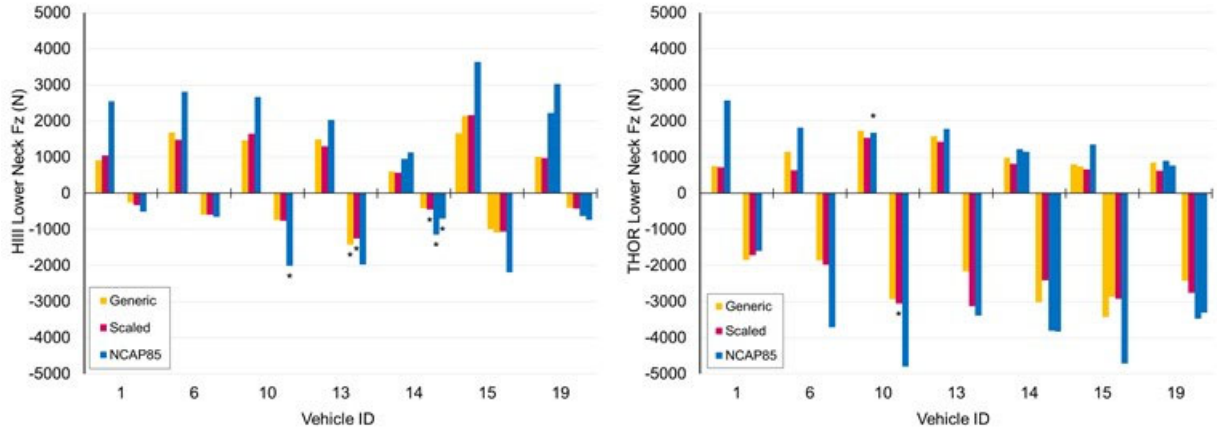

Figure 4-47. HIII (Left) and THOR (Right) Lower Neck Tension/Compression Load (Fz)

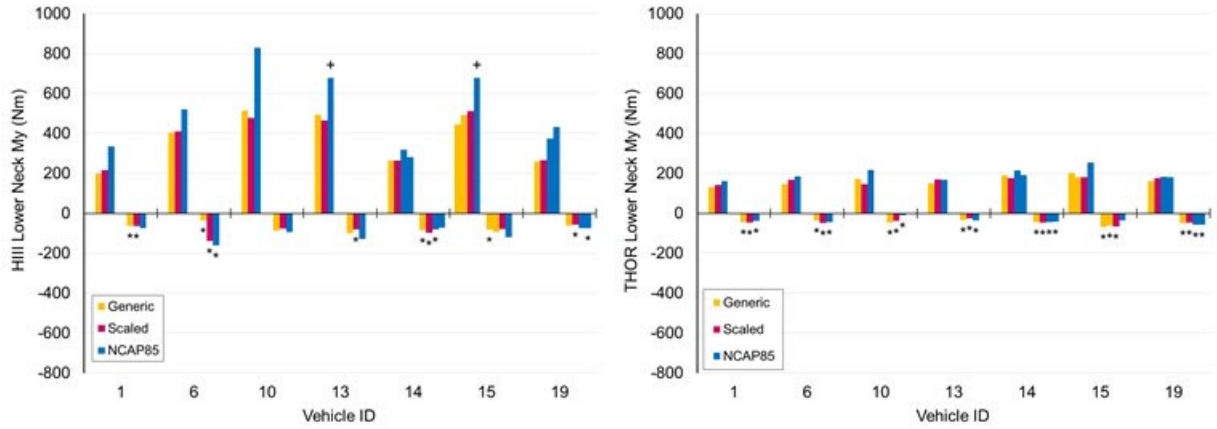

Note: + = The positive measurable range of the Hybrid III load cell was exceeded.

Figure 4-48. HIII (Left) and THOR (Right) Lower Neck Flexion/Extension Moment (My)

In regard to neck injury risk, there were NCAP85 tests that exceeded the injury thresholds for both ATDs (Figure 4-49). For the Hybrid III, two NCAP85 tests (V10 and V15) resulted in Nij values greater than 1, while a third NCAP85 test (V13) nearly exceeded the threshold. For the THOR, Nij values greater than 1 were observed for three NCAP85 tests (V14, V15, and V19), while a fourth NCAP 85 test (V10) nearly exceeded the threshold. Interestingly, Hybrid III Nij appeared to be sensitive to the presence of pretensioners and load limiters for the NCAP85 tests; vehicles without these devices (V6, V10, V13, and V15) had much higher Nij values than vehicles with these devices (V1, V14, and V19). Conversely, THOR Nij did not appear to be sensitive to the presence of pretensioners and load limiters for the NCAP85 tests. However, it was difficult to make any definitive conclusions in regard to the sensitivity of THOR Nij to these devices given that this comparison could potentially be confounded by the presence of submarining in this dataset.

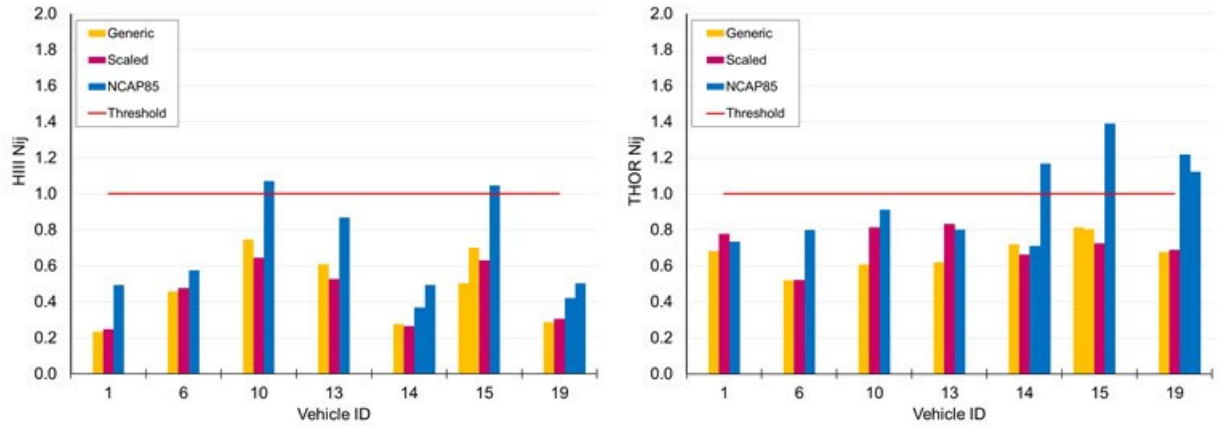

Figure 4-49. Nij for HIII (Left) and THOR (Right)

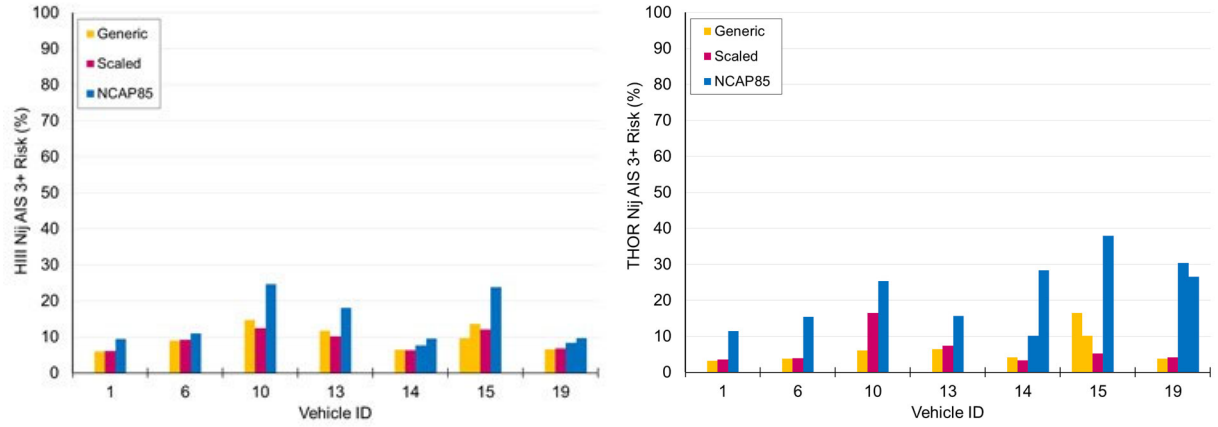

Note: Nij AIS3+ threshold based on Nij risk that corresponds to Nij=1.

Figure 4-50. Nij AIS 3+ Injury Risk for HIII (Left) and THOR (Right)

Peak Resultant Chest Acceleration, Deflection, and Injury Risk Comparison

The peak resultant chest accelerations, peak resultant chest acceleration 3ms clips, peak chest deflections, and chest injury risks were plotted for each vehicle and ATD (Figure 4-51 through Figure 4-57). When comparing between the scaled sled pulses for a given vehicle and ATD, there were no substantial differences in peak resultant chest acceleration, peak resultant chest acceleration 3ms clip, peak chest deflection, or chest injury risks between the scaled generic pulse and scaled vehicle specific pulse, except for V6 for the THOR-50M. The chest acceleration injury metrics were below the respective injury thresholds for all tests performed using the lower-energy pulses. For vehicle specific NCAP85 pulses, the Hybrid III exceeded the peak resultant chest acceleration 3 ms clip threshold for one vehicle (V15), which did not have pretensioners or load limiters; the THOR values (included for comparison) did not exceed this threshold (Figure 4-52). It should be noted that the THOR resultant chest acceleration could not be calculated for V15 due to a sensor malfunction.

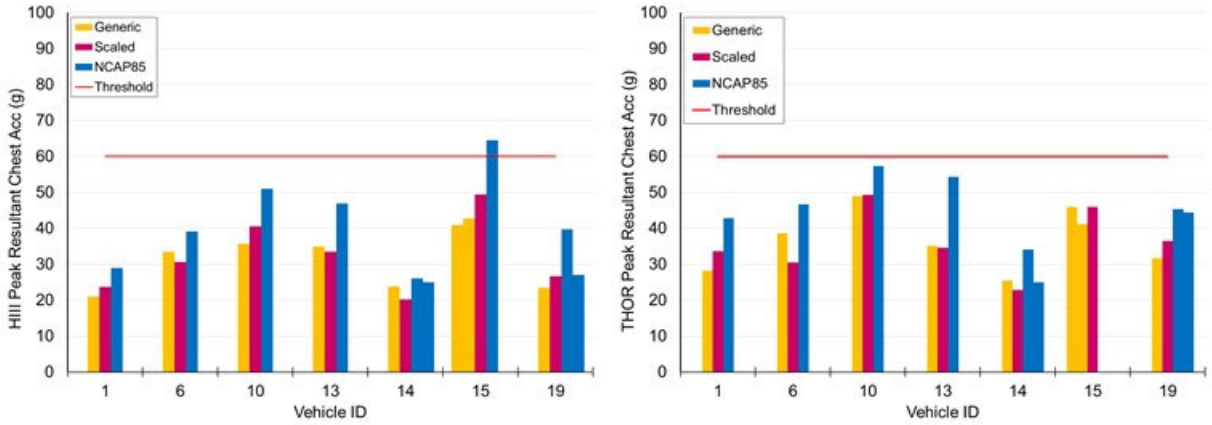

Figure 4-51. HIII (Left) and THOR (Right) Peak Resultant Chest Acceleration

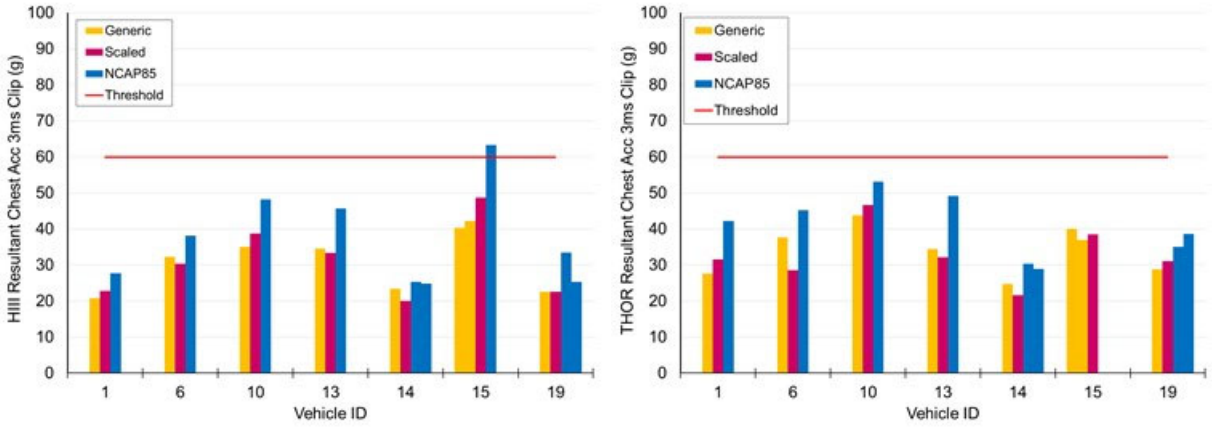

Figure 4-52. HIII (Left) and THOR (Right) Peak Resultant Chest Acceleration 3ms Clip

In regard to chest max deflection and thoracic injury risk, the Hybrid III and THOR showed different magnitudes and trends when comparing between vehicles for the NCAP85 tests. The max chest deflection and AIS3+ injury risk threshold for a 40-year-old were exceeded for the Hybrid III for three vehicles (V10, V13, and V15), none of which had pretensioners or load limiters (Figure 4-53 and Figure 4-54). For the THOR-50M, the Rmax AIS3+ injury risk threshold for a 40-year-old was exceeded in one NCAP85 test (V1), which had load limiters and pretensioners (Figure 4-54). It is important to note, however, that three other vehicles (V13, V15, and V19) had moderate to severe submarining for the THOR-50M, which could have resulted in a different load path between the belt and occupant. When considering AIS3+ injury risk for the 35-year-old (Figure 4-55), the Hybrid III results are consistent with those for the 40-year-old, and the THOR-50M generated no results that exceeded the Rmax threshold. The Rmax AIS3+ injury risk threshold for a 45-year-old was exceeded or nearly exceeded for the THOR for four vehicles (V1, V6, V14, and V15), two of which lacked pretensioners or load limiters (Figure 4-56). For a 55-year old, the Rmax AIS3+ injury risk threshold was exceeded for the THOR for five lower-energy tests and for all but two NCAP85 tests (both V19) (Figure 4-56). The PCA score AIS3+ injury risk threshold for a 35-year-old was not exceeded for any test, but was exceeded for a 40-year-old for the THOR for two vehicles (V14 and V15) (Figure 4-57).

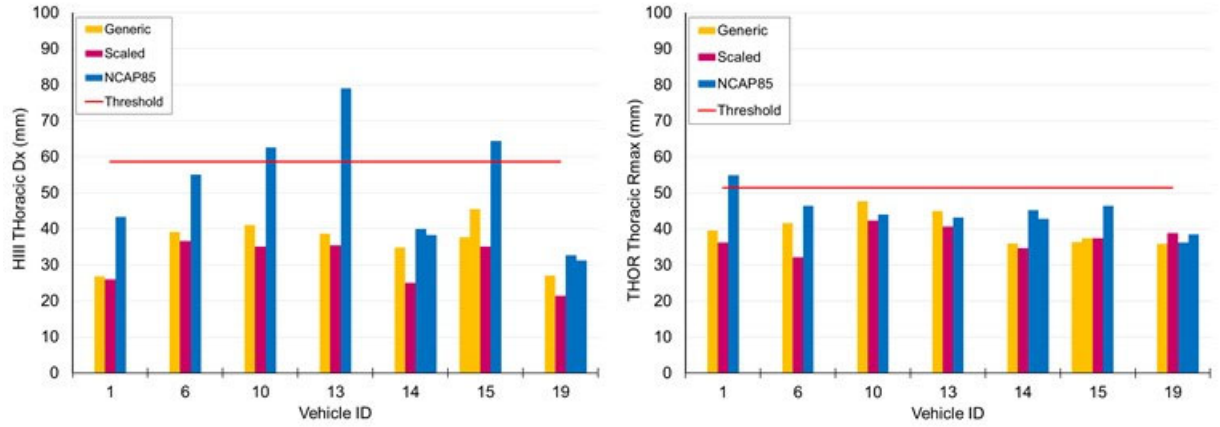

Note: The polarity of peak Hybrid III chest deflection was inverted for the sake of comparison. The threshold is based on 50% risk of AIS3+ for a 40-Year-Old.

Figure 4-53. Peak Chest Deflection for HIII (Left) and THOR (Right)

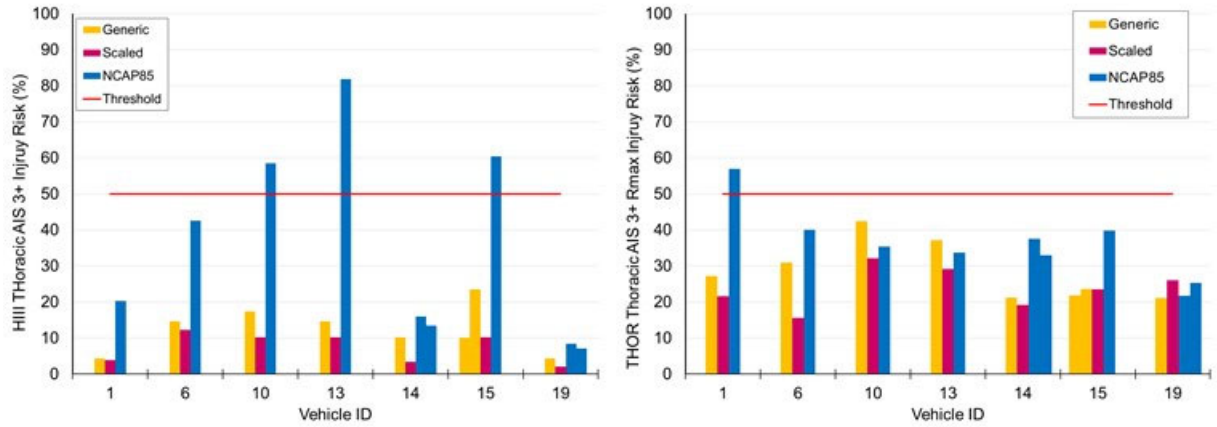

Figure 4-54. Thoracic AIS 3+ Injury Risk for a 40-Year-Old Based on HIII Max Deflection (Left) and Risk Functions From Craig et al. (2020)/Federal Register (2015) for THOR (Right)

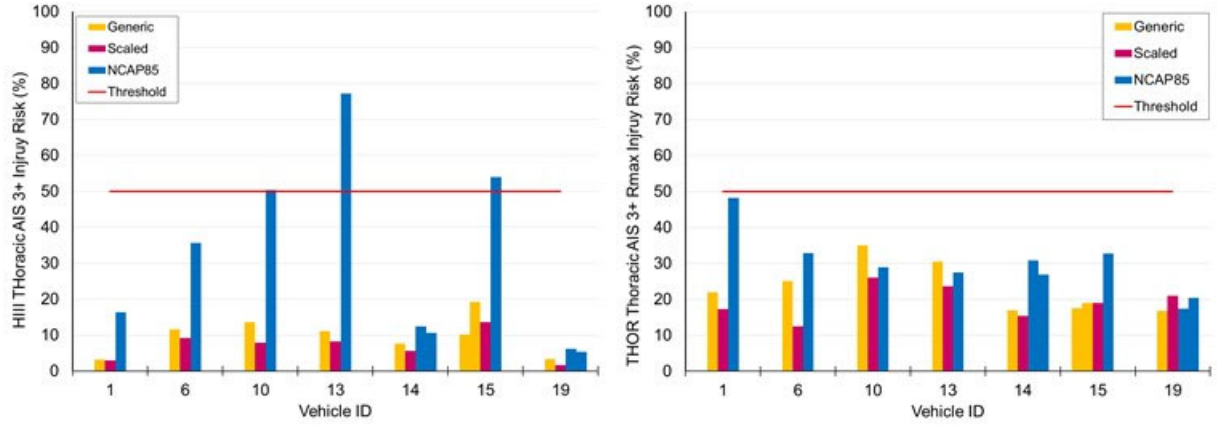

Figure 4-55. Thoracic AIS 3+ Injury Risk for a 35-Year-Old Based on HIII Max Deflection (Left) and Risk Functions From Craig et al. (2020)/Federal Register (2015) for THOR (Right)

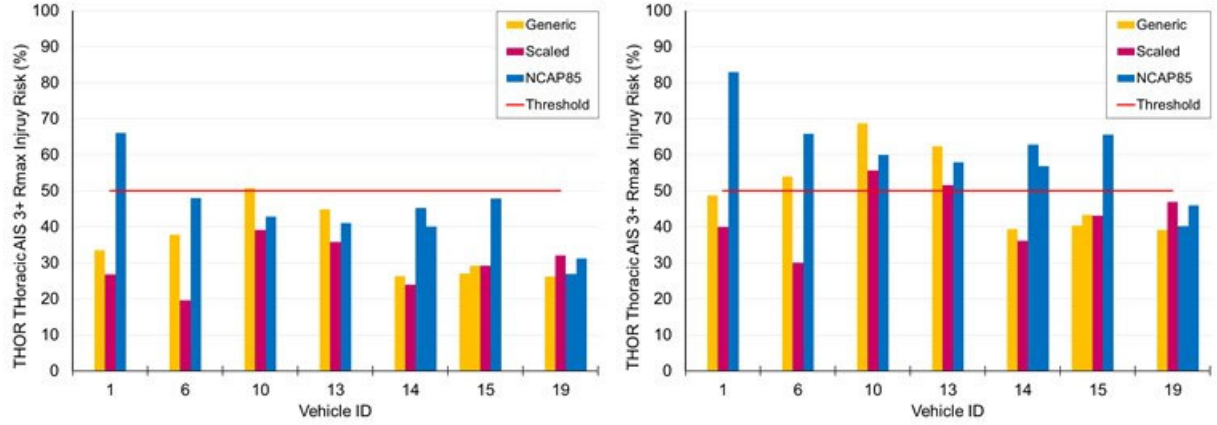

Figure 4-56. THOR Thoracic AIS 3+ Injury Risk for a 45-Year-Old (Left) and 55-Year-Old (Right) Based on Max Deflection Using the Risk Function From the Federal Register (2015)

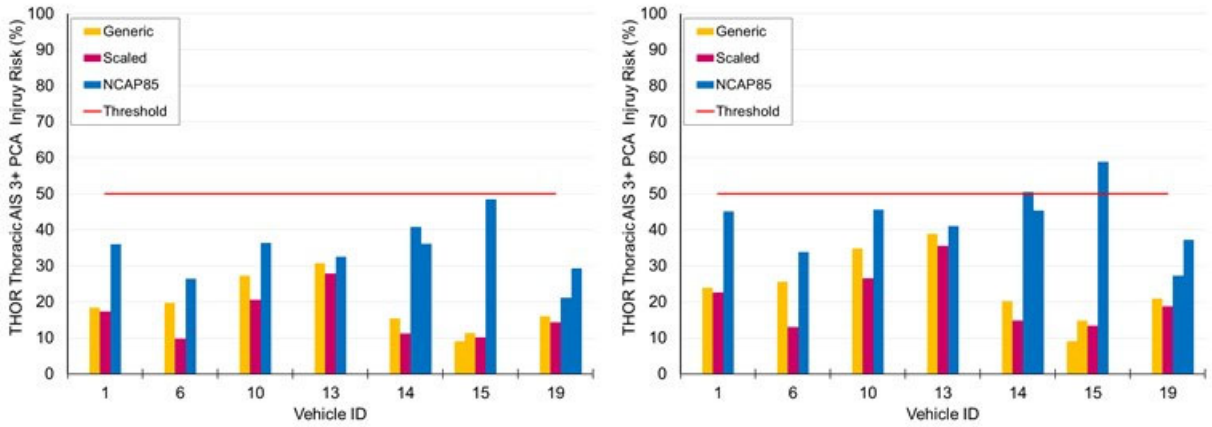

Figure 4-57. THOR Thoracic AIS 3+ Injury Risk for a 35-Year-Old (Left) and a 40-Year-Old (Right) Based on PCA Score

Peak Lumbar/T12 Force and Moment Comparison

For the lumbar/T12 load cells, the peak fore/aft forces (Fx), peak tension/compression forces (Fz), and peak flexion/extension moments (My) were plotted for each vehicle and ATD (Figure 4-58 through Figure 4-60). When comparing between the scaled sled pulses for a given vehicle and ATD, there were no substantial differences in peak fore/aft forces, peak tension/compression forces, or peak flexion/extension moments between the scaled generic pulse and scaled vehicle specific pulse, except for the Hybrid III compressive force and flexion moment for V13.

Overall, the Hybrid III lumbar load cell and THOR T12 load cell had considerably different peak fore/aft force, peak tension/compression force, and peak flexion/extension moment responses. In regard to the peak fore/aft loading (Fx), the Hybrid III had larger positive forces (chest rearward, pelvis forward) for most of the scaled low-energy pulses. However, the THOR had considerably larger positive forces for the V13 and V15 NCAP85 tests. Moderate to severe submarining was observed for the THOR for these two tests, which could explain the large T12 shear forces. It should be noted that these shear forces were considerably larger than the average shear failure force of lumbar spine functional spinal units — 1850 N and 2616 N for loading rates of 0.5 mm/s and 500 mm/s, respectively (Sundararajan, 2005). The Hybrid III had very large negative Fz loads (compression) for both the scaled and NCAP85 pulses, whereas the THOR had small compressive loads. This could be due to the difference in the inferior/superior locations of the two load cells. It is important to note that although there are no criteria for lumbar/thoracic axial loads (tension/compression), the compressive loads measured by the Hybrid III would likely result in moderate to severe spinal injuries. The average failure force for isolated lower thoracic and lumbar vertebral bodies in axial compression ranges from 3264 N to 8691 N, depending on the vertebral level and loading rate (Hansson et al., 1979; Hutton et al., 1979; Kazarian and Graves, 1977; Messerer, 1880; Pintar, 1986; Sonoda, 1962). The average failure force for lumbar spine functional spinal units in axial compression ranges from 5204 N to 12411 N, depending on the vertebral level, degree of disc degeneration, and loading rate (Brown et al., 1957; Perry, 1957; Yoganandan et al., 1989; Duma et al., 2006). This critical range (5204 N to 12411 N compressive force) is denoted in the lumbar Fz graphs as the shaded bar. In other words, the Hybrid III lumbar compressive loads for V13, V15, and V19 were 1.2 to 4.3 times higher than the average failure forces for isolated vertebral bodies, and 0.8 to 2.7 times higher than the

average failure forces for functional spinal units. In regard to the flexion/extension moments, the Hybrid III and THOR exhibited considerably different responses. Both ATDs measured low moment values in extension, which is to be expected for a frontal sled test. However, the Hybrid III measured very low flexion moments, while the THOR measured relatively large flexion moments for both the scaled and NCAP85 pulses.

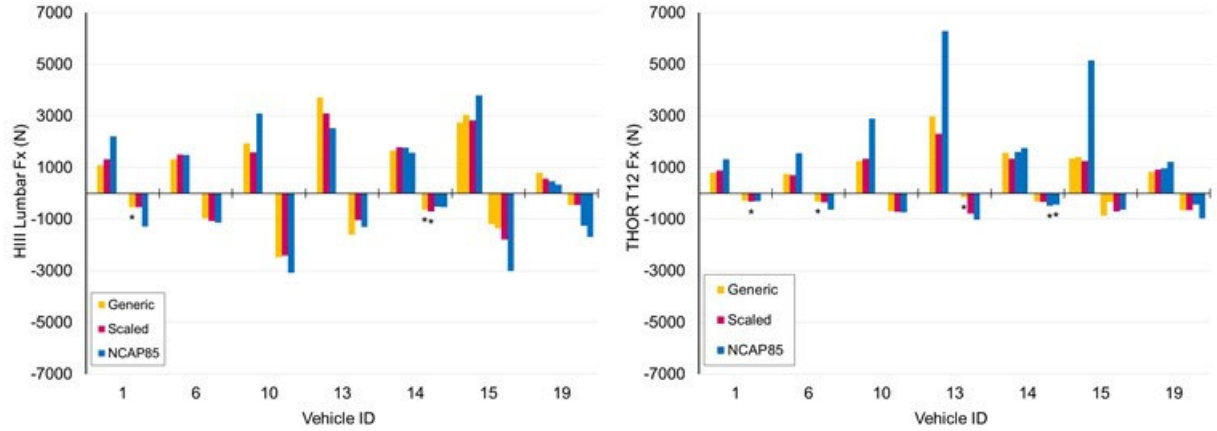

Figure 4-58. HIII Lumbar (Left) and THOR T12 (Right) Fore/Aft Load (Fx)

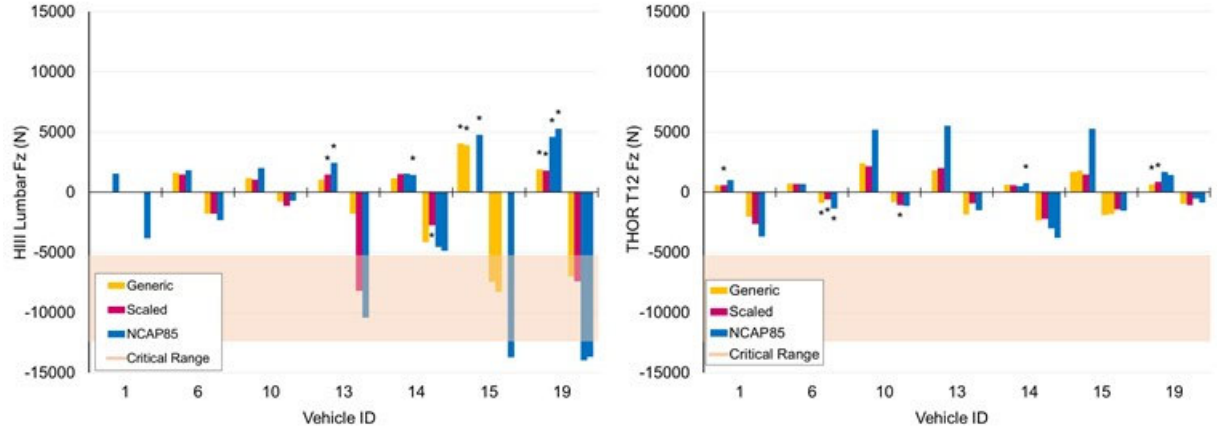

Figure 4-59. HIII Lumbar (Left) and THOR T12 (Right) Tension/Compression Load (Fz)

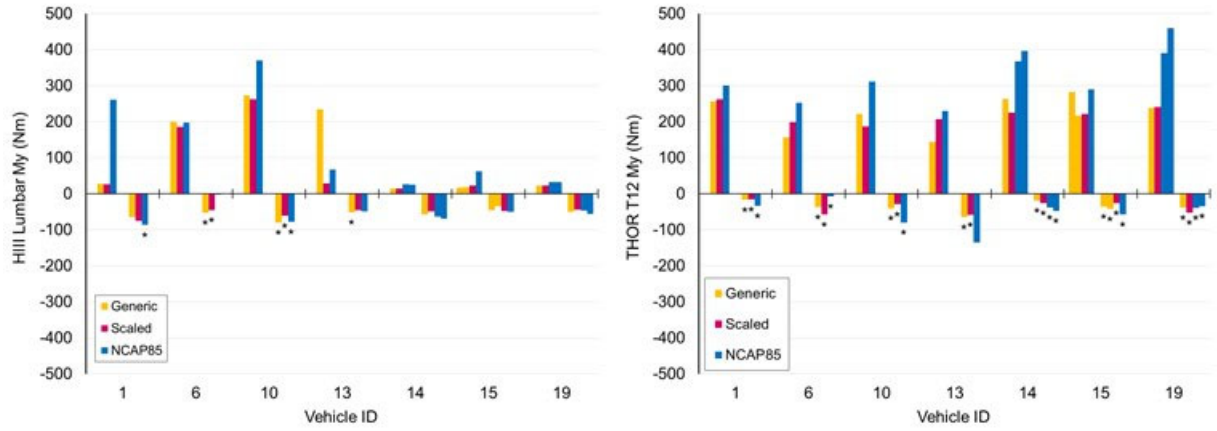

Figure 4-60. HIII Lumbar (Left) and THOR T12 (Right) Flexion/Extension Moment (My)

Peak Pelvis Acceleration Comparison

The peak resultant pelvis accelerations were plotted for each vehicle and ATD (Figure 4-61). When comparing between the scaled sled pulses for a given vehicle and ATD, there were no substantial differences in peak resultant pelvis acceleration. However, the NCAP85 pulse resulted in larger peak resultant pelvis accelerations than the scaled low-energy pulses. For the NCAP85 pulses, the THOR and Hybrid III generally showed the same trends in peak resultant pelvis acceleration when comparing between vehicles.

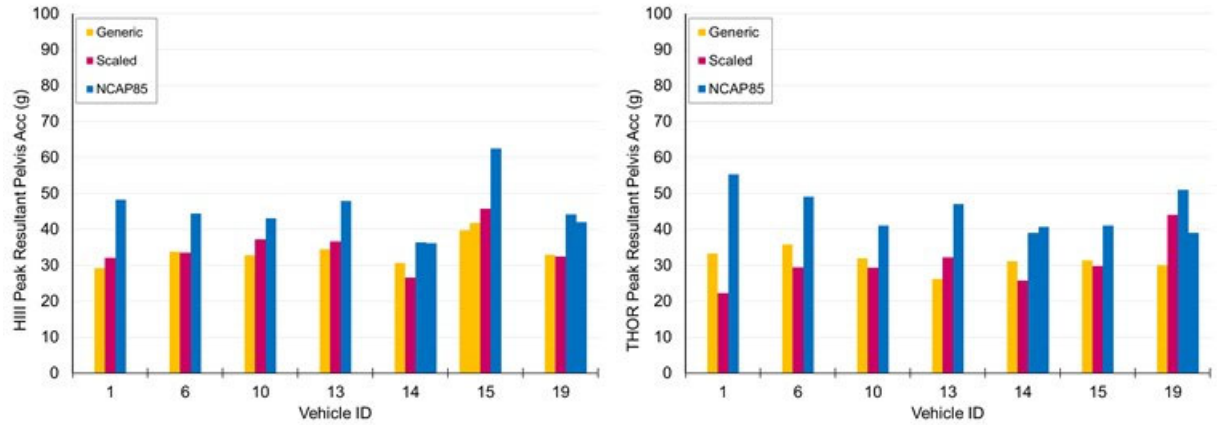

Figure 4-61. Peak Resultant Pelvis Accelerations for HIII (Left) and THOR (Right)

Peak Abdomen Pressure Comparison

The right and left abdominal pressures were plotted for each THOR test that incorporated the ABISUP abdomen (Figure 4-62). The low pressures for V1, V6, and V14 can be attributed to the lack of observable submarining for both the scaled and NCAP85 pulses. For the scaled low-energy pulses, minor (unilateral) to moderate (bilateral) submarining resulted in higher abdominal pressures for V10, V13, and V15, and potentially V19. For the NCAP85 tests, moderate (bilateral) to severe (bilateral with deep penetration and possible seat departure) submarining resulted in very high abdominal pressures (greater than 300 kPa) for V10, V13, V15, and V19 relative to other tests within this series.

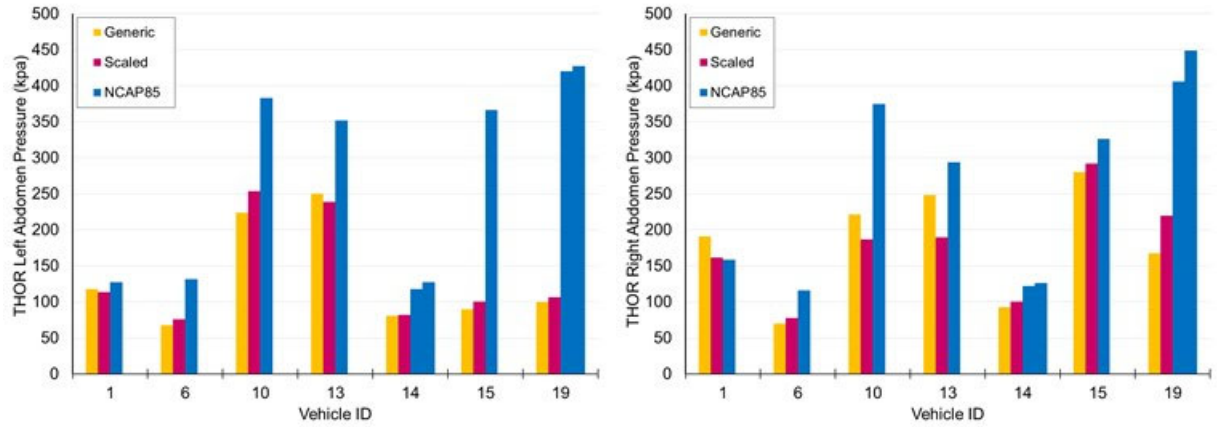

Figure 4-62. Peak Left/Right Abdominal Pressures for THOR Tests With the ABISUP

Summary Remarks

The first finding of the ATD sled testing was that the ABISUP abdomen did not have a considerable effect on the response of the THOR-50M. Another finding was that loosening of bolts in the THOR-50M did not have a considerable effect on its response. It was also found that the THOR-50M, Hybrid-III, and testing procedures were very repeatable. When comparing between the scaled generic and scaled vehicle-specific sled pulses for a given vehicle and ATD, there were no substantial differences in peak measurements nor injury risks found.

Comparison between the Hybrid III and THOR-50M responses for an NCAP85 test that had good occupant protection performance and no submarining for either ATD (V14-4) showed that the shape, polarity, and phasing of the data were similar between the two ATDs for the variables plotted. Comparison between the Hybrid III and THOR-50M responses for NCAP85 tests in which the THOR experienced severe submarining while the Hybrid III showed no submarining indicated that the shape of the curves differed between ATDs for a number of variables and that the polarity of the lower neck forces and lumbar T12 axial force differed between the ATDs. Some degree of submarining in the THOR-50M dummy was seen in 16 out of 25 tests. The Hybrid III dummy did not submarine during any test.

Vehicles without pretensioners or load limiters generally had higher peak resultant head acceleration, HIC15, and BrIC injury risk for the NCAP85 tests. Similarly, vehicles without pretensioners or load limiters generally produced higher peak upper neck Fx forces and My moments. The Hybrid III and THOR-50M had similar responses in regard to peak Fx and peak Fz upper neck forces, with the exception of the Fz compressive force for three vehicles. Neither ATD exceeded the maximum tension or the compression thresholds for the upper neck. However, the Hybrid III had a considerably higher flexion/extension moment (My) than the THOR-50M. The Hybrid III and THOR had different responses in terms of magnitude and/or polarity of the forces and moments for the lower neck.

For the chest, the Hybrid III exceeded the peak resultant chest acceleration 3ms clip threshold for one NCAP85 test, which did not have pretensioners or load limiters. The Hybrid III and THOR-50M exhibited different magnitudes and trends when comparing max chest deflection and thoracic injury risk between vehicles for the NCAP85 tests. The maximum chest deflection and AIS3+ injury risk thresholds were exceeded for the Hybrid III for three NCAP85 vehicle tests,

neither of which had pretensioners or load limiters. The PCA score AIS3+ injury risk threshold for a 35-year-old was exceeded for the THOR for two NCAP85 vehicle tests. Similarly, the Rmax AIS3+ injury risk threshold for a 40-year-old was exceeded in one THOR-50M NCAP85 test, which had load limiters and pretensioners. However, the Rmax AIS3+ injury risk threshold for a 45-year-old was exceeded or nearly exceeded for the THOR-50M for four vehicles, two of which lacked pretensioners or load limiters. In comparison, the Rmax AIS3+ injury risk threshold for a 55-year-old was exceeded for the THOR-50M for all but one vehicle. The interaction between the seat belt and chest is reduced in cases of submarining, for which the chest tends to slip under the belt instead of engaging it directly. This can result in reduced chest deflection.

The chest deflection results for the THOR-50M differed from those found by Hu et al. (2015, 2017). For many of Hu's tests, maximum chest deflection occurred in the lower quadrant nearest the buckle of the seat belt. Deflection of the upper chest was otherwise reduced when a pretensioner was used, but deflection near the buckle was not. For the current study, only 7 of the 24 tests resulted in Rmax being near the buckle (lower right). Rmax was found in the upper right quadrant, typically. In the tests involving pretensioners, 3 of the 11 resulted in Rmax being near the buckle. Of the 9 NCAP85 tests, 2 resulted in Rmax being near the buckle. However, for 10 of the 24 tests, the difference between Rmax and the next highest deflection was 3 mm or less, lessening the importance of these findings. In addition, there were differences in the restraint conditions used for these two test series. The Hu tests employed a pretensioner at the anchor location and a dynamic locking tongue, which locked the belt webbing for loads greater than 45 N, preventing any transition between the shoulder and lap belt portions once 45 N was reached. Some of Hu's tests employed an air bag as well, deployed from the back of the front seat. The current study employed a pretensioner at the retractor when one was used, and no front seats or dynamic locking tongues were present. Hu used a single vehicle buck, while the current study examined seven bucks. Given these differences in restraint features, it is difficult to directly compare these two studies and to draw any conclusions from such a comparison.

Overall, the Hybrid III lumbar load cell and THOR-50M T12 load cell registered considerably different peak fore/aft force, peak tension/compression force, and peak flexion/extension moment responses.

Moderate to severe submarining that was observed for two THOR-50M tests resulted in shear forces that were considerably larger than the average shear failure force of lumbar spine functional spinal units. On the other hand, the high compressive loads measured by the Hybrid III for both the scaled and NCAP85 pulses would likely result in moderate to severe spinal injuries, since they exceeded or nearly exceeded the average compressive failure force for isolated lumbar vertebral bodies and lumbar spine functional spinal units.

Table 4-6 shows that the ABISUP was able to disclose submarining in the THOR-50M for nearly all cases. The conclusions reached from examination of ABISUP pressures correspond to the overall assessments of submarining, with the exception of two inconclusive ABISUP data points. Other measures, such as ASIS load and moment and seat belt load, were used to corroborate the ABISUP results. Submarining ranged from minor unilateral impingement of the belt upon the abdomen, such as in cases of pretensioner belt lift, to full bilateral penetration of the belt. Advanced restraint systems could generate "belt lift," which would potentiate limited encroachment of the abdomen by the belt.

5. ATD FEM Verification and Validation

To assess the validity of the ATD models, the tests from six vehicles (V1, V6, V13, V14, V15, and V19) were modeled and then quantitatively compared to the test data and injury risks. The seventh vehicle (V10) was not modeled due to the complexities associated with modeling the metal seat bottom frame and bracket, which deformed considerably during the test. The methods for these simulations were similar to those used for the initial simulations. However, the positioning data and seat belt load cell data from the physical tests were used to update the simulations. To simulate the actual tests, the ATD models were positioned as in the simplified seat models based on FARO data. The seats were then deformed using the LS-PREPOST (LSTC, v. 4.3.14) seat deformer tool, allowing for exact positioning of the ATD FEMs rather than approximated positioning via settling simulations. The seat belts were routed as in the sled tests, with seat belt parameters such as pretensioner timing and stroke defined according to the sled test data and the high-speed video. Finally, the crash pulses were applied to each model.

The time histories of ATD FEM signals and belt loads were compared to the sled data using CORA (Gehre et al., 2009), an objective rating software. As interpretation is usually application specific; there is no standard that researchers use to assess CORA scores. However, for the purposes of this study, a CORA score of 0.7 and above was considered "good." This is similar to the typical interpretation of a correlation coefficient for which a value of 0.8 or greater is considered to reflect a "strong relationship." Specific signals for the Hybrid III included chest deflection, upper neck, lower neck, lumbar, femur, and belt loads, head, chest, and pelvis accelerations, and head, shoulder, hip, and knee excursions. The THOR signals included IR-TRACC deflections, upper neck, lower neck, thoracic spine, femur, ASIS, and belt loads, head, chest, and pelvis accelerations, and head, shoulder, hip, and knee excursions. The recorded data were used to calculate injury metrics (Equation 5-1 through Equation 5-10) and injury probabilities (Equation 5-11 through Equation 5-17). The critical values in Table 5-1 were used to evaluate Nij. For both dummies, HIC15, BrIC, Nij, chest 3ms clip, and max chest deflection were calculated. For the THOR-50M dummy, PCA scores were also calculated.

HIC15 Hybrid III & THOR-50M (Federal Register, 2015)	$HIC_{15} = \left\lvert (t_2 - t_1)\left[\frac{1}{(t_2-t_1)}\int_{t_1}^{t_2} a(t)dt\right]^{2.5}\right\rvert_{\max}$	Equation 5-1
BrIC HIII & THOR-50M (Federal Register, 2015; Takhounts et al., 2013)	$BrIC = \sqrt{\left(\frac{max(\lvert w_x\rvert)}{w_{xc}}\right)^2 + \left(\frac{max(\lvert w_y\rvert)}{w_{yc}}\right)^2 + \left(\frac{max(\lvert w_z\rvert)}{w_{zc}}\right)^2}$ Where: w_{xc}=66.25 rad/s, w_{yc}=56.45 rad/s, w_{zc}=42.87 rad/s.	Equation 5-2
Nij HIII & THOR-50M (Eppinger et al., 1999, 2000)	$N_{ij} = \left(\frac{F_z}{F_{zc}}\right) + \left(\frac{M_y}{M_{yc}}\right)$	Equation 5-3
Chest Deflection THOR-50M (Federal Register, 2015)	$R_{max} = \max(UL_{max}, UR_{max}, LL_{max}, LR_{max})$	Equation 5-4
	Where: $\{U/L\lvert R/L\}_{max} =$ $max\left(\sqrt{[L/R]X^2_{[U/L]S} + [L/R]Y^2_{[U/L]S} + [L/R]Z^2_{[U/L]S}}\right)$	Equation 5-5

THOR-50M (Federal Register, 2015)	$PCA\ Score = 0.485\left(\frac{up_{tot}}{17.509}\right) + 0.499\left(\frac{low_{tot}}{15.526}\right) + 0.493\left(\frac{up_{dif}}{10.479}\right) + 0.522\left(\frac{low_{dif}}{11.996}\right)$ **Where:** $up_{tot} = \lvert UL\rvert max + \lvert UR\rvert max$ $up_{dif} = \lvert UL - UR\rvert max$ $low_{tot} = \lvert LL\rvert max + \lvert LR\rvert max$ $low_{dif} = \lvert LL - LR\rvert max$	Equation 5-6 Equation 5-7 Equation 5-8 Equation 5-9 Equation 5-10

Table 5-1. Limits and Intercepts/Critical Values for Nij Calculations

ATD FEM	Criterion	Peak Limits		Nij Intercepts/Critical Values (F_{zc}, M_{yc})			
		F_{zc}		F_{zc}		M_{yc}	
	Nij	Tension	Comp	Tension	Comp	Flexion	Extension
		(N)	(N)	(N)	(N)	(Nm)	(Nm)
HIII 50th M	Nij	4170	-4000	6806	-6160	310	-135
THOR 50th M	Nij	4170	-4000	4200	-4520	60	-79.2

For the Hybrid III dummy, neck injury risk was also calculated based on axial tension and compression. For the THOR-50M dummy, chest injury risk was calculated based upon the PCA scores as well. The injury risks for individual body regions were calculated based on the published probabilities curves as indicated below.

HIC15 HIII & THOR-50M (Federal Register, 2015)	$p(AIS3+) = \Phi\left(\frac{ln(HIC) - 7.45231}{.73998}\right)$	Equation 5-11
BrIC HIII & THOR-50M (Federal Register, 2015; Takata, 2017)	$p(AIS3+) = 1 - e^{-\left[\frac{BrIC}{0.987}\right]^{2.84}}$	Equation 5-12
Nij HIII & THOR-50M (Federal Register, 2008)	$p(AIS3+) = \frac{1}{1 + e^{3.227 - 1.969 N_{ij}}}$	Equation 5-13
Neck tension/compression HIII (NHTSA NCAP, 2008)	$p(AIS3+) = \frac{1}{1 + e^{10.9745 - 2.375\mathrm{F}}}$	Equation 5-14
Chest Deflection HIII (Federal Register, 2008)	$p(AIS3+) = \frac{1}{1 + e^{10.5456 - 1.568 * (\delta_{max})^{0.4612}}}$	Equation 5-15
Chest Deflection THOR-50M (Poplin et al., 2017)	$p(AIS3+) = 1 - e^{-\left[\frac{R_{max}}{e^{4.7775 - 0.0171 * (age)}}\right]^{3.356}}$	Equation 5-16
THOR-50M (Federal Register, 2015)	$p(AIS3+) = 1 - e^{-\left[\frac{PCA\ Score}{e^{2.6092 - 0.0113 * (age)}}\right]^{4.4444}}$	Equation 5-17

Results

Kinematic responses of ATD models showed reasonable agreement to the test results (e.g., Figure 5-1, vehicle 14 under NCAP85 crash pulse). The average CORA scores for the Hybrid III and THOR simulations were 0.69 and 0.64, respectively (Table 5-2 and Table 5-3). Therefore, it can be concluded that the numerical simulations reasonably replicated the experimental data. Interpretation of CORA scores is usually application specific. Various studies have used different sets of coefficients, or modified CORA score expressions that make comparison between studies difficult. However, in previous studies (Iwamoto et al., 2015; Pietsch et al., 2016) CORA ratings of 0.86 to 1.0, 0.65 to 0.86, 0.44 to 0.65, 0.26 to 0.44, and 0.0 to 0.26 are evaluated as excellent, good, fair, marginal, and unacceptable, respectively. Overall, the scores were consistent from vehicle to vehicle and pulse to pulse except those from V6. This could be caused by the spring-type seat bottom, which increased the complexity of the seat model. Additionally, no pretensioner was used in V6, which made matching belt load curve and chest deflection curves during the impact challenging.

Table 5-2. CORA Scores for Generic (G), Scaled (S), and NCAP85 (N) Pulse Simulations With the HIII ATD FEM

Vehicle	**V14**			**V15**			**V13**		**V19**			**V1**			**V6**			**Average**
Pulse	**G**	**S**	**N**	**G**	**S**	**N**	**S**	**N**	**G**	**S**	**N**	**G**	**S**	**N**	**G**	**S**	**N**	
Head Acceleration	0.78	0.84	0.87	0.75	0.79	0.83	0.74	0.62	0.75	0.79	0.82	0.85	0.90	0.87	0.61	0.64	0.64	0.77
Chest Acceleration	0.54	0.62	0.78	0.78	0.82	0.86	0.74	0.80	0.77	0.82	0.77	0.73	0.73	0.78	0.92	0.83	0.87	0.77
Pelvis Acceleration	0.93	0.89	0.88	0.86	0.90	0.84	0.81	0.81	0.73	0.75	0.76	0.77	0.80	0.63	0.90	0.79	0.74	0.81
Upper Neck Fx	0.61	0.68	0.80	0.86	0.85	0.89	0.75	0.71	0.66	0.68	0.74	0.71	0.74	0.72	0.61	0.70	0.59	0.72
Upper Neck Fz	0.83	0.84	0.95	0.81	0.75	0.76	0.72	0.72	0.78	0.80	0.79	0.81	0.85	0.85	0.63	0.62	0.70	0.78
Upper Neck My	0.74	0.76	0.67	0.82	0.79	0.79	0.84	0.74	0.69	0.73	0.62	0.77	0.77	0.66	0.57	0.62	0.49	0.71
Lower Neck Fx	0.86	0.83	0.92	0.88	0.81	0.94	0.86	0.79	0.80	0.77	0.45	0.76	0.70	0.77	0.38	0.36	0.33	0.72
Lower Neck Fz	0.59	0.56	0.81	0.83	0.87	0.82	0.65	0.53	0.57	0.63	0.78	0.66	0.67	0.83	0.56	0.57	0.35	0.66
Lower Neck My	0.82	0.82	0.89	0.77	0.74	0.79	0.87	0.70	0.81	0.84	0.68	0.81	0.77	0.83	0.69	0.71	0.54	0.77
Lumbar Fx	0.62	0.75	0.49	0.32	0.32	0.51	0.77	0.72	0.44	0.41	0.69	0.54	0.55	0.61	0.35	0.40	0.45	0.53
Lumbar Fz	0.69	0.63	0.34	0.58		0.50	0.31	0.52	0.25	0.24	0.15			0.42	0.60	0.59	0.47	0.45
Lumbar My	0.14	0.18	0.21	0.24	0.17	0.15	0.12	0.17	0.10	0.10	0.11	0.13	0.13	0.68	0.81	0.75	0.82	0.29
Chest Deflection	0.84	0.91	0.96	0.97	0.93	0.75	0.93	0.90	0.64	0.82	0.75	0.66	0.68	0.91	0.18	0.19	0.16	0.72
Inboard Lap Belt	0.76	0.79	0.56	0.95	0.95	0.84	0.69	0.72	0.67	0.68	0.48	0.74	0.74	0.57	0.41	0.38	0.41	0.67
Outboard Lap Belt	0.72	0.74	0.71	0.73	0.65	0.80	0.66	0.70	0.85	0.82	0.83	0.79	0.87	0.89	0.56	0.46	0.53	0.72
Shoulder Belt	0.77	0.77	0.89	0.88	0.87	0.90	0.95	0.95	0.84	0.89	0.93	0.88	0.84		0.63	0.61	0.66	0.83
Total	0.70	0.72	0.73	0.75	0.75	0.75	0.71	0.69	0.65	0.67	0.65	0.71	0.72	0.74	0.59	0.58	0.55	0.69

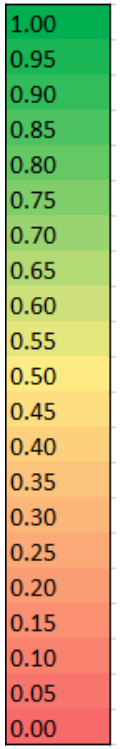

Note: Gray box denotes missing/corrupted data.

Table 5-3. CORA Scores for Generic (G), Scaled (S), and NCAP85 (N) Pulse Simulations With the THOR Dummy

Vehicle	**V14**			**V15**			**V13**		**V19**			**V1**			**V6**			**Average**
Pulse	**G**	**S**	**N**	**G**	**S**	**N**	**S**	**N**	**G**	**S**	**N**	**G**	**S**	**N**	**G**	**S**	**N**	
Head Acceleration	0.78	0.81	0.85	0.78	0.66	0.70	0.83	0.65	0.75	0.78	0.89	0.73	0.81	0.93	0.77	0.56	0.67	0.76
Chest Acceleration	0.66	0.60	0.66	0.77	0.75		0.73	0.72	0.94	0.95	0.86	0.81	0.69	0.86	0.80	0.55	0.60	0.75
Pelvis Acceleration	0.91	0.83	0.72	0.89	0.88	0.78	0.53	0.82	0.88	0.85	0.74	0.64	0.59	0.92	0.90	0.52	0.59	0.77
Upper Neck Fx	0.95	0.96	0.80	0.54	0.51	0.76	0.70	0.61	0.81	0.79	0.74	0.88	0.94	0.92	0.54	0.47	0.80	0.75
Upper Neck Fz	0.47	0.54	0.53	0.68	0.57	0.39	0.53	0.20	0.40	0.44	0.67	0.76	0.72	0.88	0.66	0.41	0.69	0.56
Upper Neck My	0.69	0.69	0.83	0.67	0.46	0.67	0.48	0.58	0.70	0.66	0.66	0.75	0.77	0.89	0.58	0.44	0.83	0.67
Lower Neck Fx	0.67	0.63	0.56	0.50	0.47	0.78	0.55	0.83	0.54	0.57	0.63	0.27	0.35	0.25	0.36	0.36	0.17	0.50
Lower Neck Fz	0.49	0.57	0.48	0.66	0.41	0.71	0.67	0.46	0.51	0.58	0.37	0.45	0.56	0.76	0.60	0.58	0.34	0.54
Lower Neck My	0.81	0.82	0.74	0.59	0.43	0.68	0.67	0.54	0.86	0.94	0.81	0.66	0.72	0.92	0.55	0.45	0.82	0.70
T12 Fx	0.74	0.74	0.76	0.50	0.37	0.48	0.43	0.60	0.67	0.67	0.35	0.58	0.50	0.42	0.66	0.44	0.43	0.55
T12 Fz	0.49	0.51	0.58	0.41	0.38	0.41	0.43	0.53	0.33	0.36	0.38	0.33	0.41	0.40	0.22	0.17	0.27	0.39
T12 My	0.77	0.72	0.85	0.86	0.86	0.64	0.74	0.59	0.96	0.98	0.59	0.85	0.85	0.83	0.88	0.51	0.81	0.78
Chest Deflection – Upper Right	0.34	0.14	0.75	0.49	0.50	0.76	0.81	0.73	0.87	0.85	0.94	0.76	0.85	0.81	0.68	0.52	0.66	0.67
Chest Deflection – Upper Left	0.85	0.91	0.68	0.29	0.20	0.63	0.74	0.68	0.85	0.81		0.44	0.46	0.23	0.59	0.54	0.40	0.58
Chest Deflection – Lower Right	0.45	0.53	0.76	0.52	0.51	0.73	0.63	0.45	0.71	0.78	0.84	0.56	0.52	0.51	0.72	0.54	0.47	0.60
Chest Deflection – Lower Right	0.59	0.72	0.41	0.83	0.80	0.55	0.64	0.73	0.49	0.35	0.34	0.50	0.51	0.34	0.55	0.88	0.49	0.57
Left ASIS Fx	0.47	0.46	0.81	0.35	0.33	0.47	0.43	0.53	0.85	0.74	0.50	0.57	0.52	0.89	0.45	0.26	0.41	0.53
Right ASIS Fx	0.76	0.74	0.74	0.70	0.73	0.45	0.66	0.68	0.83	0.70	0.56	0.73	0.81	0.71	0.42	0.25	0.36	0.64
Inboard Lap Belt	0.71	0.80	0.61	0.93	0.94	0.99	0.78	0.83	0.72	0.74	0.45	0.60	0.69	0.52	0.39	0.32	0.42	0.67
Outboard Lap Belt	0.66	0.61	0.81	0.70	0.72	0.76	0.58		0.88	0.89	0.68	0.76	0.74	0.86	0.55	0.34	0.50	0.69
Shoulder Belt	0.87	0.90	0.90	0.78	0.66	0.89	0.64	0.88	0.87	0.87	0.96	0.81	0.82	0.89	0.47	0.39	0.64	0.78
Total	0.67	0.68	0.71	0.64	0.58	0.66	0.63	0.63	0.73	0.73	0.65	0.64	0.66	0.70	0.59	0.45	0.54	0.64

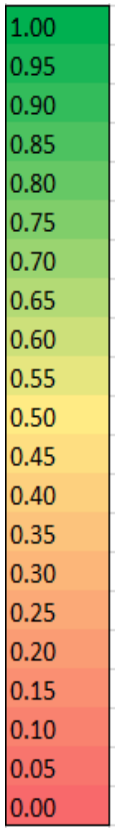

Note: Gray box denotes missing/corrupted data.

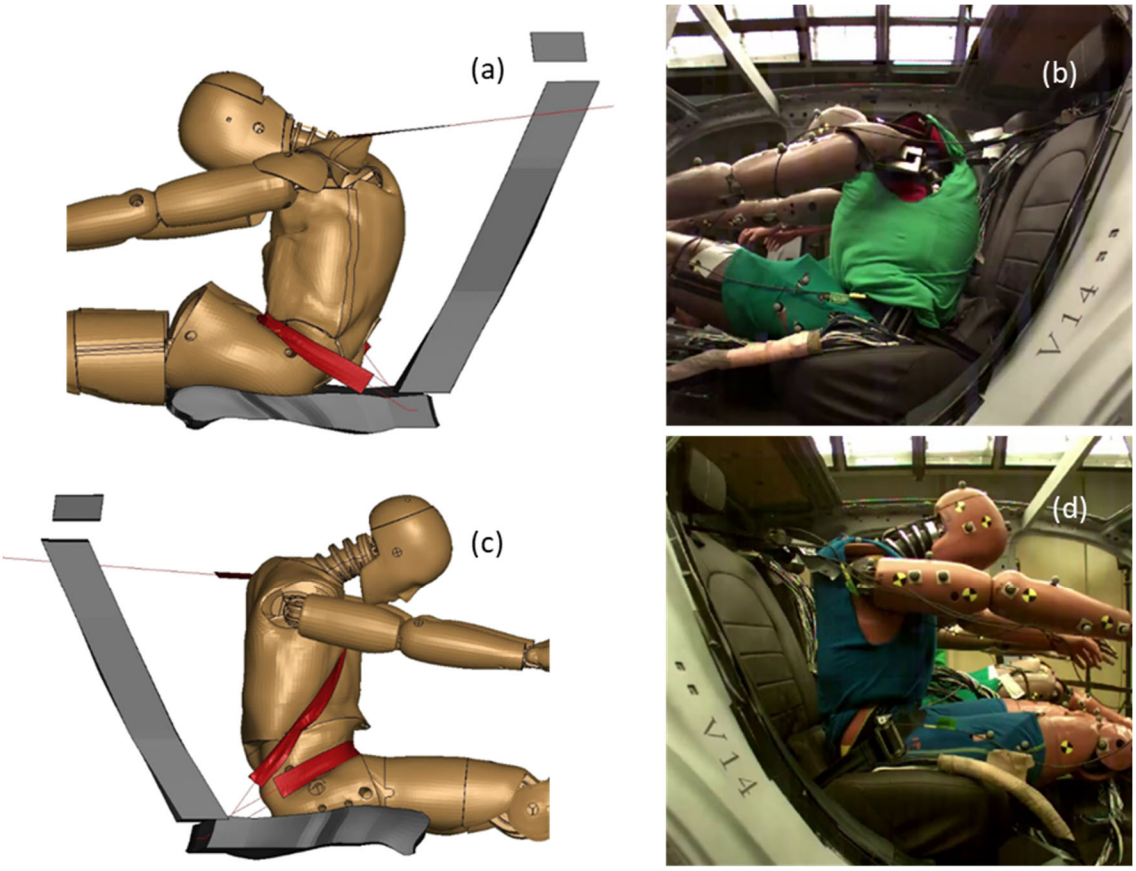

Figure 5-1. THOR (a,b) and HIII (c,d) in the Vehicle 14 NCAP85 Sled Test at 100 ms

When the ATD FEM excursions were investigated, the cases could be roughly divided into types with submarining and types without submarining. In cases where submarining did not occur, the simulation excursions better fit the test data (Figure 5-2) than in the cases where the ATD FEM submarined (Figure 5-3). In other words, it was challenging to match submarining with the ATD models.

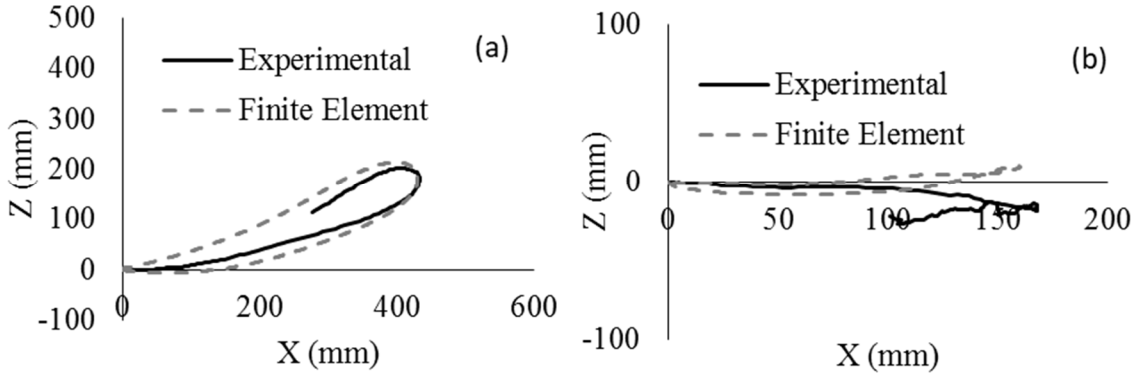

Figure 5-2. Head (a) and Hip (b) Excursion for a Non-Submarining Case With the HIII ATD FEM (V14 NCAP85)

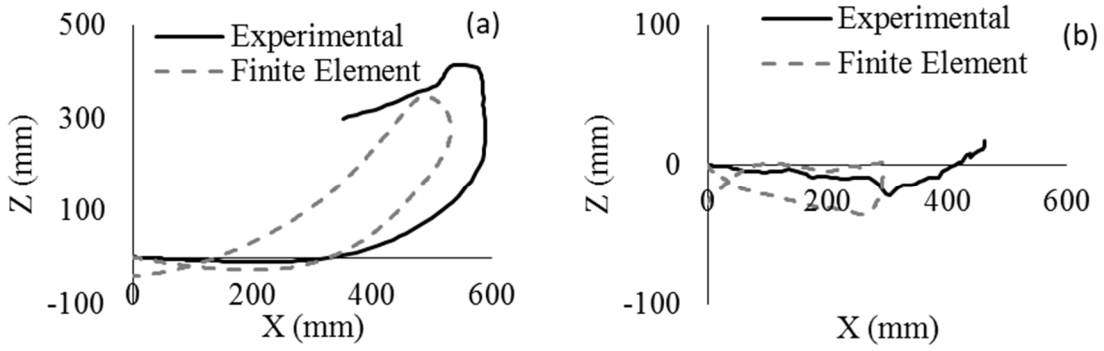

Figure 5-3. Head (a) and Hip (b) Excursion for a Submarining Case With the THOR ATD FEM (V13 NCAP85)

Injury Metrics and Assessed Injury Probabilities From FE Simulations

Injury risks were calculated based on the recorded data (Table 5-4 through Table 5-7). The injury metrics varied over a wide range. For example, two simulations with the Hybrid III had an HIC15 value larger than the threshold (700) while all the other simulations had a much lower HIC15 value (Table 5-4). The head and chest injuries were observed to be the most common source of serious injury in the rear seat during this type of impact. In terms of injury predictions, the dummy models usually overpredicted the test data (except V6). The error was calculated as the differences between simulation results and test data divided by the test data. The lowest errors were observed in generic tests and the highest errors were observed in NCAP85 tests. The average error for each injury metric between simulation results and test data was consistent (0.01–0.3) except the max Nij for THOR (0.5) (Table 5-8).

Table 5-4. Injury Metrics for Generic, Scaled, and NCAP85 Pulse Simulations With the HIII ATD FEM

Pulse	Injury Metric	V1			V6			V13			V14			V15			V19		
		Model	**Test**	**Error**	**Model**	**Test**	**Error**	**Model**	**Test**	**Error**	**Model**	**Test**	**Error**	**Model**	**Test**	**Error**	**Model**	**Test**	**Error**
Generic	HIC15	74.2	48.5	0.53	104.8	190.0	-0.45	184.5	161.5	0.14	138.7	102.3	0.36	211.6	163.9	0.29	153.4	67.9	1.26
	BrIC	0.7	0.5	0.49	0.82	0.80	0.02	0.83	0.75	0.10	0.8	0.6	0.39	1.01	0.72	0.40	0.84	0.65	0.29
	Max Nij	0.54	0.23	1.32	0.34	0.46	-0.26	0.43	0.61	-0.29	0.38	0.28	0.38	0.5	0.7	-0.29	0.74	0.29	1.57
	Chest Dmax (mm)	37	27	0.38	10	39	-0.74	38	39	-0.02	34	34.8	-0.02	41	45	-0.10	22	27	-0.19
	Chest 3ms Clip (g)	34	20.8	0.64	34	32	0.05	42	34	0.22	30	23.4	0.28	45	42	0.07	39	23	0.73
Scaled	HIC15	72.7	58.04	0.25	83	189.47	-0.56	247.6	114.87	1.16	106.3	150.49	-0.29	211.2	143.24	0.47	150.5	73.06	1.06
	BrIC	0.72	0.52	0.38	0.73	41	-0.98	0.89	0.68	0.31	0.69	0.58	0.19	1.07	0.8	0.34	0.8	0.61	0.31
	Max Nij	0.51	0.25	1.04	0.3	0.48	-0.38	0.48	0.53	-0.09	0.33	0.27	0.22	0.57	0.63	-0.10	0.7	0.31	1.26
	Chest Dmax (mm)	35	26	0.35	9	37	-0.76	38	35	0.09	32	32	0.00	42	41	0.02	21	21	0.00
	Chest 3ms Clip (g)	33	23	0.43	27	30	-0.10	42	33	0.27	27	20	0.35	48	49	-0.02	38	23	0.65
NCAP85	HIC15	375.9	309.08	0.22	334.6	607.34	-0.45	1196.4	583.15	1.05	220.8	179.19	0.23	783.6	609.0	0.29	400.8	328.51	0.22
	BrIC	0.9	0.74	0.22	0.99	0.95	0.04	1.35	0.93	0.45	0.78	0.56	0.39	1.27	1.05	0.21	0.98	0.88	0.11
	Max Nij	0.76	0.49	0.55	0.51	0.57	-0.11	1.43	0.87	0.64	0.38	0.49	-0.22	0.87	1.05	-0.17	0.78	0.5	0.56
	Chest Dmax (mm)	47	43	0.09	12	55	-0.78	54	79	-0.32	42	38	0.11	52	64	-0.19	25	31	-0.19
	Chest 3ms Clip (g)	46	28	0.64	38	38	0.00	57	46	0.24	32	45	-0.29	56	63	-0.11	42	25	0.68

Table 5-5. Injury Risks for Generic, Scaled, and NCAP85 Pulse Simulations With the HIII ATD FEM

Pulse	Injury Risk %	V1			V6			V13			V14			V15			V19		
		Model	Test	Error	Model	Test	Error	Model	Test	Error	Model	Test	Error	Model	Test	Error	Model	Test	Error
Generic	HIC	0.0	0.0	0.00	0.0	0.1	-1.00	0.1	0.1	0.45	0.0	0.0	0.00	0.2	0.1	1.71	0.1	0.0	0.00
	BrIC	31.4	11.42	1.75	44.4	42.58	0.04	45.9	37.04	0.24	42.8	19.3	1.22	65.8	33.82	0.95	47.3	26.5	0.78
	Nij	10.4	5.9	0.76	7.2	8.91	-0.19	8.5	11.64	-0.27	7.7	6.4	0.20	9.6	13.6	-0.29	14.7	6.53	1.25
	Neck Tension	0	0	0.00	0	0	0.00	0.1	0	0.00	0	0	0.00	0.1	0	0.00	0.1	0	0.00
	Neck Comp.	0	0.02	-1.00	0	0.09	-1.00	0	0.04	-1.00	0	0.02	-1.00	0	0.17	-1.00	0	0.03	-1.00
	Chest Dmax	9.49	3.21	1.96	0.24	11.57	-0.98	10.41	11.07	-0.06	7.10	7.68	-0.08	13.55	19.26	-0.30	1.76	3.32	-0.47
Scaled	HIC	0.0	0.0	0.00	0.0	0.1	-1.0	0.4	0.0	30.75	0.0	0.05	-1.00	0.2	0.0	4.18	0.0	0.0	-1.00
	BrIC	33.3	15.09	1.21	34.4	41	-0.16	53.1	29.38	0.81	30.7	19.54	0.57	71.3	42.05	0.70	42.9	22.9	0.87
	Nij	9.8	6.07	0.61	6.7	9.2	-0.27	9.2	10.08	-0.09	7.1	6.28	0.13	10.9	12.08	-0.10	13.6	6.75	1.01
	Neck Tension	0	0	0.00	0	0	0.00	0.1	0	0.00	0	0	0.00	0.1	0	0.00	0.1	0	0.00
	Neck Comp.	0	0.02	-1.00	0	0.08	-1.00	0	0.03	-1.00	0	0.01	-1.00	0	0.16	-1.00	0	0.03	-1.00
	Chest Dmax	7.84	2.9	1.70	0.20	9.16	-0.98	10.41	8.18	0.27	5.78	5.55	0.04	14.73	13.59	0.08	1.54	1.63	-0.06
NCAP85	HIC	2.1	1.0	1.1	1.3	7.9	-0.8	31.1	5.8	4.38	0.3	0.1	1.71	14.3	8.0	0.79	2.4	1.3	0.91
	BrIC	53.3	35.43	0.50	63.9	59.08	0.08	91.3	57.57	0.59	40.3	17.75	1.27	87.1	69.45	0.25	62.2	51.86	0.20
	Nij	15	9.47	0.58	9.8	10.95	-0.11	40.1	17.99	1.23	7.7	9.46	-0.19	18	23.78	-0.24	15.7	9.66	0.63
	Neck Tension	0.7	0	0.00	0.3	0	0.00	56.6	0	0.00	0.1	0	0.00	8	0	0.00	0.6	0	0.00
	Neck Comp.	0	0.41	-1.00	0	3.55	-1.00	0	1.26	-1.00	0	0.09	-1.00	0	2.3	-1.00	0	0.81	-1.00
	Chest Dmax	21.63	16.32	0.33	0.36	35.67	-0.99	33.73	77.2	-0.56	14.73	10.66	0.38	30.03	53.98	-0.44	2.59	5.35	-0.52

Table 5-6. Injury Metrics for Generic, Scaled, and NCAP85 Pulse Simulations With the THOR ATD FEM

Pulse	Injury Metric	V1			V6			V13			V14			V15			V19		
		Model	**Test**	**Error**	**Model**	**Test**	**Error**	**Model**	**Test**	**Error**	**Model**	**Test**	**Error**	**Model**	**Test**	**Error**	**Model**	**Test**	**Error**
Generic	HIC15	55.6	90.26	-0.38	62.2	88.97	-0.30	124.7	197.37	-0.37	66	96.01	-0.31	126.6	129.86	-0.03	96.7	76.09	0.27
	BrIC	0.7	0.58	0.21	0.7	0.81	-0.14	0.7	0.67	0.04	0.8	0.58	0.38	0.9	0.66	0.36	0.9	0.59	0.53
	Max Nij	0.43	0.48	-0.11	0.46	0.52	-0.12	0.79	0.62	0.27	0.63	0.53	0.18	0.67	0.71	-0.06	0.58	0.52	0.12
	Max Rmax (mm)	42.9	39.62	0.08	42.1	41.67	0.01	54	45	0.20	52.5	35.95	0.46	53.3	37.48	0.42	44	35.86	0.23
	PCA Score	5.5	5.96	-0.08	6	6.07	-0.01	9	6.81	0.32	7.6	5.71	0.33	7.9	5.29	0.49	6.6	5.76	0.15
	Chest 3ms Clip (g)	24.9	27.61	-0.10	28.6	37.7	-0.24	36.5	34.39	0.06	38.9	24.75	0.57	32.4	36.97	-0.12	35.3	28.86	0.22
Scaled	HIC15	54.3	89.63	-0.39	53.7	87.19	-0.38	131.2	381	-0.66	44.7	73.14	-0.39	140.6	112.43	0.25	83.7	86.97	-0.04
	BrIC	0.7	0.59	0.19	0.7	0.69	0.01	0.7	0.74	-0.05	0.7	0.55	0.27	0.9	0.71	0.27	0.9	0.61	0.48
	Max Nij	0.45	0.51	-0.12	0.48	0.52	-0.08	0.76	0.65	0.17	0.51	0.49	0.04	0.73	0.58	0.26	0.60	0.54	0.11
	Max Rmax (mm)	41.9	36.19	0.16	37.6	32.1	0.17	53.7	40.17	0.34	48	34.62	0.39	56.3	37.43	0.50	43.6	38.89	0.12
	PCA Score	5.4	5.87	-0.08	5.4	5.12	0.05	9	6.63	0.36	6.9	5.29	0.30	8.2	5.15	0.59	6.7	5.6	0.20
	Chest 3ms Clip (g)	25.6	31.58	-0.19	24.5	28.58	-0.14	36.5	32.2	0.13	33.8	21.6	0.56	37.9	38.47	-0.01	34.4	31.02	0.11
NCAP85	HIC15	281.7	367.56	-0.23	132.2	416.4	-0.68	131.2	807.66	-0.84	305.8	387.37	-0.21	565.9	707.25	-0.20	190.5	357.71	-0.47
	BrIC	0.8	0.75	0.07	0.7	1.01	-0.31	0.7	0.83	-0.16	0.9	0.84	0.07	1.3	0.98	0.33	1	0.7	0.43
	Max Nij	0.67	0.73	-0.08	0.63	0.80	-0.21	0.76	0.80	-0.05	0.96	0.81	0.18	1.41	0.93	0.52	0.69	0.73	-0.06
	Max Rmax (mm)	59.9	54.95	0.09	39.9	46.44	-0.14	53.7	43.19	0.24	54.5	42.77	0.27	74.3	46.35	0.60	44.7	38.51	0.16
	PCA Score	7.2	7.12	0.01	6.1	6.54	-0.07	9	6.92	0.30	8.5	7.12	0.19	10.8	7.77	0.39	7	6.72	0.04
	Chest 3ms Clip (g)	33.3	42.27	-0.21	30.5	45.2	-0.33	36.5	49.18	-0.26	41.5	28.9	0.44	52.6	25.6	1.05	48.3	38.63	0.25

Table 5-7. Injury Risks for Generic, Scaled, and NCAP85 Pulse Simulations With the THOR ATD FEM

Pulse	Injury Risk %	V1			V6			V13			V14			V15			V19		
		Model	Test	Error	Model	Test	Error	Model	Test	Error	Model	Test	Error	Model	Test	Error	Model	Test	Error
Generic	HIC	0	0.003	-1.00	0	0.0031	-1.00	0	0.1703	-1.00	0	0.0048	-1.00	0	0.0238	-1.00	0	0.0012	-1.00
	BrIC	9.4	1.71	4.50	13.4	27.5	-0.51	16.7	9.04	0.85	29.3	1.92	14.26	36.1	8.67	3.16	35	2.69	12.01
	Nij	2.34	3.15	-0.26	2.79	3.83	-0.27	14.47	6.45	1.24	6.62	4.41	0.50	8.26	10.09	-0.18	5.27	3.8	0.39
	Chest Rmax	33.3	24.28	0.37	31.6	30.94	0.02	55.1	37.22	0.48	52.2	21.21	1.46	53.7	23.67	1.27	35.3	21.07	0.68
	PCA score	15.6	23.91	-0.35	20.8	25.62	-0.19	58.3	38.94	0.50	38.9	20.14	0.93	43.5	14.87	1.93	26.5	20.9	0.27
Scaled	HIC	0	0.003	-1.00	0	0.0028	-1.00	0	2.0678	-1.00	0	0.001	-1.00	0	0.0112	-1.00	0	0.0027	-1.00
	BrIC	41.8	2.19	18.09	7.7	11.43	-0.33	16.4	17.85	-0.08	10.7	0.57	17.77	15.1	14.6	0.03	42.4	3.62	10.71
	Nij	2.63	3.57	-0.26	3.07	3.86	-0.20	12.82	7.33	0.75	3.61	3.37	0.07	11.29	5.24	1.15	5.8	4.19	0.38
	Chest Rmax	34.5	21.59	0.60	23.8	15.66	0.52	43.1	29.2	0.48	31.3	19.2	0.63	54.5	23.58	1.31	59.6	26.02	1.29
	PCA score	28.2	22.54	0.25	14.5	12.99	0.12	29.9	35.52	-0.16	15.1	14.83	0.02	58.6	13.34	3.39	47.7	18.7	1.55
NCAP85	HIC	0.7	1.8	-0.62	0	2.7	-1.00	0	15.2796	-1.00	0.1	2.1826	-0.95	6.6	11.4316	-0.42	0.1	1.6784	-0.94
	BrIC	32.5	18.88	0.72	11.4	57.2	-0.80	15.1	31.31	-0.52	36.7	33.04	0.11	83.2	52.82	0.58	54.8	12.62	3.34
	Nij	8.37	11.42	-0.27	6.83	15.42	-0.56	15.17	15.6	-0.03	30.36	15.91	0.91	83.54	26.97	2.10	9.05	11.09	-0.18
	Chest Rmax	66.4	56.99	0.17	27.7	40.01	-0.31	54.5	33.76	0.61	56	32.96	0.70	87.4	39.85	1.19	36.6	25.37	0.44
	PCA score	34.1	45.12	-0.24	21.1	33.85	-0.38	58.6	41.09	0.43	51.6	45.31	0.14	80.1	58.91	0.36	32.2	37.15	-0.13

Table 5-8. Average Error for Each Injury Metrics

Injury metrics	HIII	THOR
HIC15	0.32	-0.30
BrIC	0.20	0.17
Max Nij	0.31	0.05
Chest Dmax (mm)	-0.13	/
Chest 3ms Clip (g)	0.26	0.10
Max Rmax (mm)	/	0.24

Summary Remarks

The numerical simulations reasonably replicated the experimental data with average CORA scores of 0.69 and 0.64 for the Hybrid III and THOR-50M, respectively. The highest scores were usually recorded in head/chest/pelvis acceleration, while the lowest were recorded in vertical forces of lumbar/T12. The scores were consistent between vehicles and pulses, except for cases having a spring-type seat bottom. The simulation excursions fitted the test data better for cases without submarining.

In terms of injury prediction, the dummy models typically overpredicted the test data (except for V6), with the lowest errors found for the generic tests and the highest errors found for the NCAP85 tests. The error between simulation injury metrics and test data were consistent (0.01–0.3), except for the peak Nij for THOR-50M (0.5). The ATD models were deemed to represent the performance of the ATDs well enough for them to be useful in parametric studies.

Concluding Remarks

This study had five specific goals that were developed in collaboration with NHTSA. Evaluation of the expected incidences and outcomes of rear-seat occupants in forward-facing seats found that there is increased risk for those seated in the rear compared to those seated in the front row. This is more pronounced for older occupants and for new vehicles. The assessment of ATD performance for rear-seat occupants for frontal crash testing has been supported by 25 sled tests using the Hybrid III and THOR-50M ATDs. Positioning procedures for rear-seat ATDs for frontal crash testing were developed as part of this effort. Matched PMHS testing is now needed to further support this assessment, as well as to assess candidate injury criteria for rear-seat occupants for frontal crash testing. The future PMHS testing will enable the assessment of ATD FEM and human body model (HBM) performance for prediction of injury in the rear seat.

This study provides the foundational work required to prepare for PMHS testing, which is critical for evaluating the efficacy of the candidate ATDs, ATD FEMs, and their respective injury criteria. Future work will include testing of PMHS using four of the vehicle bucks employed for the ATD testing. Three PMHS will be tested for each buck. The impact and injury responses obtained during the PMHS tests will be compared to ATD performance and injury prediction for both the Hybrid III and THOR-50M. This comparison will facilitate evaluation of the ATDs' ability to predict injury for rear-seat occupants involved in a frontal crash and will determine the efficacy of using these dummies for this crash scenario. Finally, simulations of the PMHS sled tests will be conducted using a human body model. This will help in the assessment of the appropriateness of such a model for examining this crash scenario in the virtual world.

The findings of this research further support the importance of examining rear-seat occupant safety in both standard vehicles and ADS-DVs, and provide a wealth of critical information that will inform the consideration of translating FMVSS No. 208 to extend elements of the standard to occupants behind the front row.

References

Beck, B., Brown, J., & Bilston, L. (2014). Assessment of vehicle and restraint design changes for mitigating rear seat occupant injuries. *Traffic Injury Prevention, 15*(7), 711–719.

Bilston, L., Du, W., & Brown, J. (2010). A matched-cohort analysis of belted front and rear seat occupants in newer and older model vehicles shows that gains in front occupant safety have outpaced gains for rear seat occupants. *Accident Analysis and Prevention*, *42*, 1974–1977.

Blanco, M., Chaka, M., Stowe, L., Gabler, H. C., Weinstein, K., Gibbons, R. B., Neurauter, L., McNeil, J., Fitzgerald, K. E., Tatem, W., & Fitchett, V. L. (2020, April). *FMVSS considerations for vehicles with automated driving systems: Volume 1* (Report No. DOT HS 812 796). National Highway Traffic Safety Administration. www.nhtsa.gov/sites/nhtsa.gov/files/documents/ads-dv_fmvss_vol1-042320-v8-tag.pdf

Bose, D., Crandall, J., Forman, J., Longhitano, D., & Arregui-Dalmases, C. (2017). Epidemiology of injuries sustained by rear-seat passengers in frontal motor vehicle crashes. *Journal of Transport & Health*, 4, 132–139.

Brown, T., Hansen, R., & Yora, A. (1957). Some mechanical tests on the lumbosacral spine with particular reference to the intervertebral disks. *Journal of Bone and Joint Surgery*, *39-A*(5), 1135-1164.

Chaka, M., Blanco, M., Stowe, L., McNeil, J., Kefauver, K., Fitchett, V. L., Fitzgerald, K. E., Trimble, T. E., Kizyma, D., Neurauter, L., Hardy, W. N., Anderson, G. T., Schultz, J., Thorn, E., Harper, C., & Weinstein, K. (2021, January). *FMVSS considerations for vehicles with automated driving systems: Volume 2* (Report No. DOT HS 813 024). National Highway Traffic Safety Administration. https://rosap.ntl.bts.gov/view/dot/54442/dot_54442_DS1.pdf

Craig, M., Parent, D., Lee, E., Rudd, R., Takhounts, E., & Hasija, V. (2020). *Injury criteria for the THOR 50th male ATD* (Docket No. NHTSA-2019-0106-0008). National Highway Traffic Safety Administration. https://downloads.regulations.gov/NHTSA-2019-0106-0008/attachment_1.pdf

Crandall, J. (2013). *Injury Criteria Development – THOR Metric SD3 Shoulder Advanced Frontal Crash Test Dummy* (NHTSA-DTNH22-09-H-00247). Center for Applied Biomechanics, Automobile Safety Laboratory, University of Virginia.

Duma, S., Kemper, A., McNeely, D., Brolinson, G., & Matsuoka, F. (2006). Biomechanical response of the lumbar spine in dynamic compression. *Biomedical Sciences Instrumentation Symposium*, *42*, 476-481.

Durbin, D., Jermakian, J., Kallan, M., McCartt, A., Arbogast, K., Zonfrillo, M., & Myers, R. (2015). Rear seat safety: Variation in protection by occupant, crash and vehicle characteristics. *Accident Analysis and Prevention*, *80*, 185–192.

Eppinger, R., Sun, E., Kuppa, S., & Saul, R. (2000, March). *Supplement: Development of improved injury criteria for the assessment of advanced automotive restraint systems – II*. National Highway Traffic Safety Administration. www.nhtsa.gov/sites/nhtsa.gov/files/finalrule_all_0.pdf

Federal Register. *Part V. National Highway Traffic Safety Administration Consumer Information: New Car Assessment Program*. U.S. Department of Transportation, Vol. 80, No. 241 /Wednesday, December 16, 2015.

Federal Register. *Part II. National Highway Traffic Safety Administration Consumer Information: New Car Assessment Program*. U.S. Department of Transportation, Vol. 73, No. 134 / Friday, July 11, 2008.

Forman, J., Michaelson, J., Kent, R., Kuppa, S., & Bostrom, O. (2008). Occupant restraint in the rear seat: ATD responses to standard and pre-tensioning, force-limiting belt restraints. *Annals of Advances in Automotive Medicine*, *52*, 141–154.

Forman, J., Lopez-Valdes, F., Kindig, M., Kent, R., Ridella, S., & Bostrom, O. (2009). Rear seat occupant safety: An investigation of a progressive force-limiting, pretensioning 3-point belt system using adult PMHS in frontal sled tests. *Stapp Car Crash Journal, 53*, 49–74.

Forman, J., Lopez-Valdes, F., Dennis, N., Kent, R., Tanji, H., & Higuchi, K. (2010). An inflatable belt system in the rear seat occupant environment: Investigating feasibility and benefit in frontal impact sled tests with a 50th percentile male ATD. *Annals of Advances in Automotive Medicine*, *54*, 111–126.

Fulton, W. (2015, April). *The future of parking in an era of car-sharing: Services like Uber and Zipcar could radically change city streets*. Governing. www.governing.com/archive/gov-drive-less-park-less.html

Gehre, C., Gades, H., & Wernicke, P. (2009, June 15-18). *Objective rating of signals using test and simulation responses*. 21st International Technical Conference on the Enhanced Safety of Vehicles, Stuttgart, Germany.

Humanetics Innovative Solutions. (2018). THOR-50M US NCAP Dummy LS-DYNA Model.

Hansson, T., Roos, B., & Nachemson, A. (1979). The bone mineral content and ultimate compressive strength of lumbar vertebrae. *Spine 5*(1), 46–55.

Hughes, T. (2017, July). *The effect of ride-sharing on the auto industry*. Moddy's Analytics Risk Perspectives: Managing Disruption, IX. www.moodysanalytics.com/risk-perspectives-magazine/managing-disruption/op-ed/the-effect-of-ride-sharing-on-the-auto-industry

Hu, J., Fischer, K., Lange, P., & Adler, A. (2015, April 21-23). *Effects of crash pulse, impact angle, occupant size, front seat location, and restraint system on rear seat occupant protection* (Paper No. SAE-2015-01-1453). SAE 2015 World Congress, Detroit, MI.

Hu, J., Reed, M., Rupp, J., Fischer, K., Lange, P., & Adler, A. (2017). Optimizing seat belt and airbag designs for rear seat occupant protection in frontal crashes. *Stapp Car Crash Journal*, *61*, 67–100.

Hutton, W., Cyron, B., & Stott, J. (1979). The compressive strength of lumbar vertebrae. *Journal of Anatomy, 129*(4), 753–758.

Iwamoto, M., Nakahira, Y., & Kimpara, H. (2015). Development and validation of the total HUman Model for Safety (THUMS) toward further understanding of occupant injury mechanisms in precrash and during crash. *Traffic Injury Prevention, 16* (Suppl 1), S36-48.

Kazarian, L., & Graves, G. (1977). Compressive strength characteristics of the human vertebrae centrum. *Spine 2*(1), 1–14.

Kleinberger, M., Sun, E., Eppinger, R., Kuppa, S., & Saul, R. (1998). *Development of improved injury criteria for the assessment of advanced automotive restraint systems* (NHTSA Docket, 4405(9), 12–17). National Highway Traffic Safety Administration.

Koppel, S., Jiménez Octavio, J., Bohman, K., Logan, D., Raphael, W., Quintana Jimenez, L., & Lopez-Valdes, F. (2019). Seating configuration and position preferences in fully automated vehicles. *Traffic Injury Prevention*, *20*(sup2), S103-S109.

Kuppa, S., Saunders, J., & Fessahaie, O. (2005). Rear seat occupant protection in frontal crashes. *Proceeding of the Enhanced Safety of Vehicle Conference* (05-0212).

Laituri, T. R., Prasad, P., Sullivan, K., Frankstein, M., & Thomas, R. S. (2005). *Derivation and evaluation of a provisional, age-dependent, AIS3+ thoracic risk curve for belted adults in frontal impacts* (SAE Technical Paper. No. 0148-7191).

Luet, C., Trosseille, X., Drazétic, P., Potier, P., & Vallancien, G. (2012). Kinematics and Dynamics of the pelvis in the process of submarining using PMHS sled tests. *Stapp Car Crash Journal*, *56*, 411–442.

Messerer, O. (1880). *Uber elasticitat and festigkeit der meuschlichen knochen*. Stutgrat, J.G. Cottaschen Buchhandeling.

Michaelson, J., Forman, J., Kent, R., & Kuppa, S. (2008). Rear seat occupant safety: Kinematics and injury of PMHS restrained by a standard 3-point belt in frontal crashes. *Stapp Car Crash Journal*, *52*, 295–325.

Mitchell, R., Bambach, M., & Toson, B. (2015). Injury risk for matched front and rear seat car passengers by injury severity and crash type: An exploratory study. *Accident Analysis and Prevention*, *82*, 171–179.

National Center for Statistics and Analysis. (2020, November). *Traffic safety facts 2018 annual report: A compilation of motor vehicle crash data* (Report No. DOT HS 812 981). National Highway Traffic Safety Administration. https://crashstats.nhtsa.dot.gov/Api/Public/ViewPublication/812981

National Highway Traffic Safety Administration. (2005, July 27). *Laboratory test procedure for: FMVSS 208, Occupant Crash Protection FMVSS 212, windshield mounting FMVSS 219, windshield zone intrusion FMVSS 301F, fuel system integrity – frontal, TP208-13*.

National Traffic Highway Safety Administration. (2018). *Procedures for Assembly, Disassembly, and Inspection for the THOR-50M ATD (PADI).*

Nemire, K. (2017). *Seat belt use by adult rear seat passengers in private passenger, taxi, and rideshare vehicles*. Proceedings of the Human Factors and Ergonomics Society Annual Meeting, 61(1), 1644-1648. DOI: 10.1177/1541931213601896

Nie, B., Gan, S., Chen, W., and Zhou, Q. (2020) Seating preferences in highly automated vehicles and occupant safety awareness: A national survey of Chinese perceptions. *Traffic Injury and Prevention, 21(4)*, 247–253.

Perry, O. (1957). Fracture of the vertebral end-plate in the lumbar spine. *Acta Orthopaedica Scandinavica, 25* (suppl.), 2-101.

Pietsch, H., Bosch, K., Weyland, D., Spratley, E., Henderson, K., Salzar, R., Smith, T., Sagara, B., Demetropoulos, C., Dooley, C., & Merkle, A. (2016). Evaluation of WIAMan technology demonstrator biofidelity relative to sub-injurious PMHS response in simulated under-body blast events. *Stapp Car Crash Journal, 60*, 199.

Pintar, F. (1986). *The biomechanics of spinal elements* [Doctoral dissertation]. Marquette University Graduate School. Milwaukee, WI.

Poplin, G., McMurry, T., Forman, J., Ash, J., Parent, D., Craig, M., Song, E., Kent, R., Shaw, G., & Crandall, J. (2017). Development of thoracic injury risk functions for the THOR ATD. *Accident Analysis & Prevention*, *106*, 122–130.

Rouhana, S. Jedrzejczak, E., & McCleary J. (1990) Assessing submarining and abdominal injury risk in the Hybrid III family of dummies: Part II – development of the small female frangible abdomen. *Proceeding of the 34th Stapp Car Crash Conference (*SAE paper no. 902317*)*.

Rouhana, S., Viano, D., Jedrzejczak, E., & McCleary, J. (1989) Assessing submarining and abdominal injury risk in the Hybrid III family of dummies. *Proceeding of the 33rd Stapp Car Crash Conference* (SAE paper no. 892440).

Shoup, D. (2017). *The high cost of free parking: Updated edition*. Routledge

Sonoda, T. (1962). Studies on the strength for compression, tension, and torsion of human vertebrae column. *Journal of Kyoto Prefectural University of Medicine*, *71*, 659–702.

Sundararajan, S. (2005). Characteristics of PMHS lumbar motion segments in lateral shear. In *Proceedings of the 49th Stapp Car Crash Conference* (pp. 367–379).

Sundararajan, S., Rouhana, S., Board, D., DeSmet, E., Prasad, P., Rupp, J., Miller, C., & Schneider, L. (2011). Biomechanical assessment of a rear-seat inflatable seat belt in frontal impacts. *Stapp Car Crash Journal*, *55*.

Tavakoli, M., & Brelin-Fornari, J. (2015). *Effects of pretensioners and load limiters on 50th male and 5th female seated in rear seat during a frontal collision* (SAE paper no. 2015-01-1460).). SAE 2015 World Congress, Detroit, MI. DOI: 10.4271/2015-01-1460

Takata Corporation. (2017). *Advanced adaptive restraint systems.* (Report No. DOT HS 812 432). National Highway Traffic Safety Administration.

Takhounts, E. G., Craig, M., Moorhouse, K., McFadden, J., & Hasija, V. (2013). *Development of brain injury criteria (BrIC)* (No. 2013-22-0010, SAE Technical Paper). Also published in *Stapp Car Crash Journal, Vol. 57* (November 2013), pp. 243-266

Trowbridge, M., & Kent, R. (2009). Rear-seat motor vehicle travel in the U.S.: Using national data to define a population at risk. *American Journal of Preventive Medicine*, *37*(4), 321–323.

Uriot, J., Potier, P., Baudrit, P., Trosseille, X., Petit, P., Richard, O., Compigne, S., Masuda, M., & Douard, R. (2015). Reference PMHS sled tests to assess submarining. *Stapp Car Crash Journal*, *59*, 203–223.

Wietholter, K., Louden, A., Sullivan, L., & Burton, R. (2016, June; revised 2021, September). *Evaluation of seat foams for the FMVSS No. 213 test bench*. (Report No. DOT HS 813 099). National Highway Traffic Safety Administration.. https://rosap.ntl.bts.gov/view/dot/57336/dot_57336_DS1.pdf

Yoganandan, N., Ray, G., Pintar, F., Myklebust, J., & Sances, A. (1989). Stiffness and strain energy criteria to evaluate the threshold of injury to an intervertebral joint. *Journal of Biomechanics*, *22*, 135–142.

Appendix A. V1 Buck Development

Figure A-1. The Completed V1 Buck on Casters

Figure A-2. Frontal View of the V1 Buck

Figure A-3. Anchor Point Reinforcement Detail on the V1 Buck

Figure A-4. Underside of the V1 Buck Showing Detachable Seat Track and Frame Support

Figure A-5. The Seat Track and Frame Reinforcement

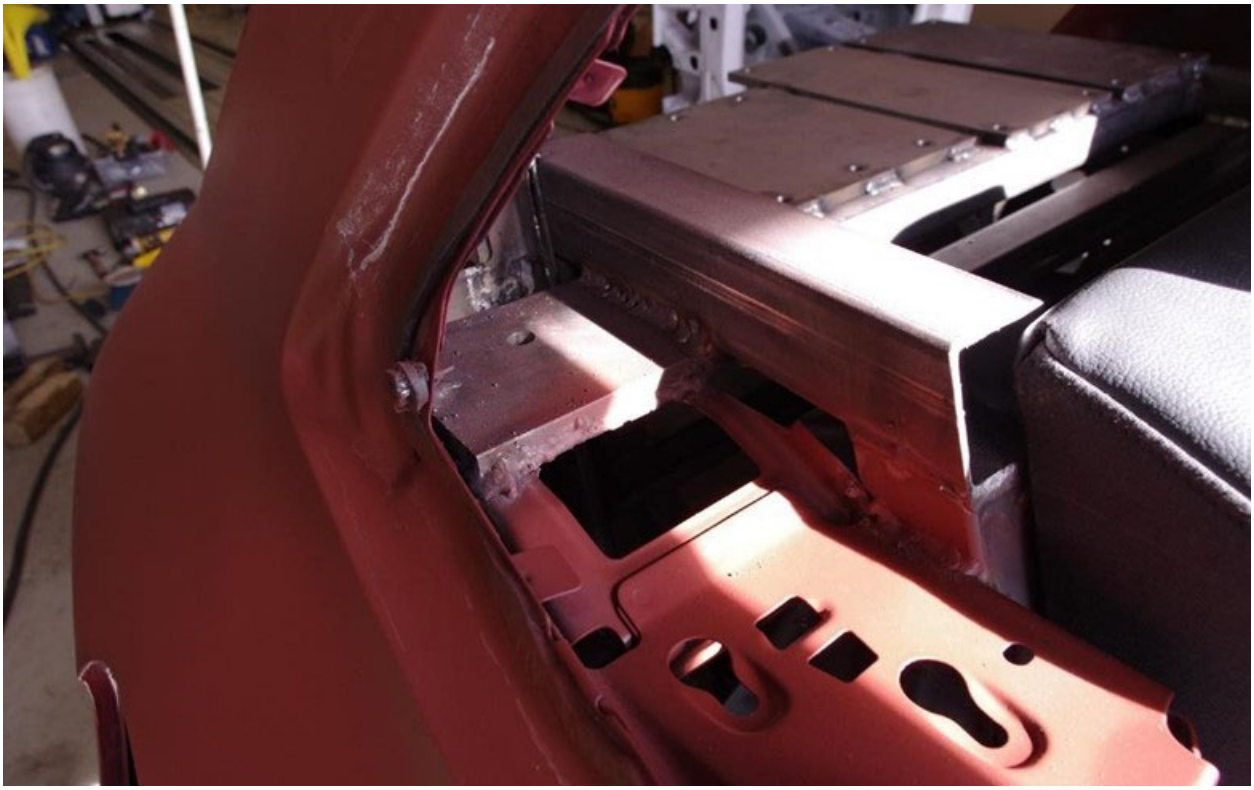

Figure A-6. Retractor Location Reinforcement on the V1 Buck

Figure A-7. Rear Seat and Retractor Reinforcement of the V1 Buck

Figure A-8. Rear Seat Reinforcement of the V1 Buck

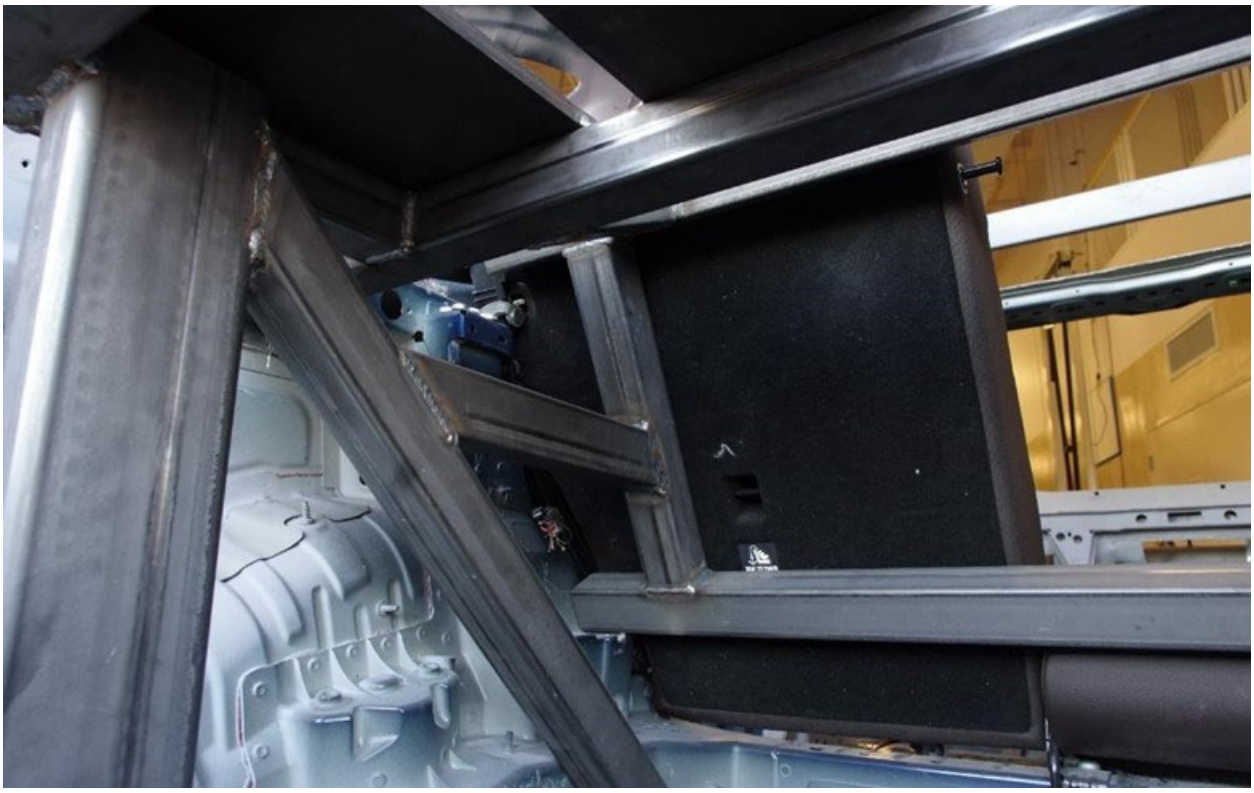

Figure A-9. Rear Seat Reinforcement Structure Beneath the DAS Plates of the V1 Buck

Figure A-10. Reinforcement of the Interior Front of the V1 Buck.

Appendix B. V6 Buck Development

Figure B-1. The Completed V6 Buck on Casters

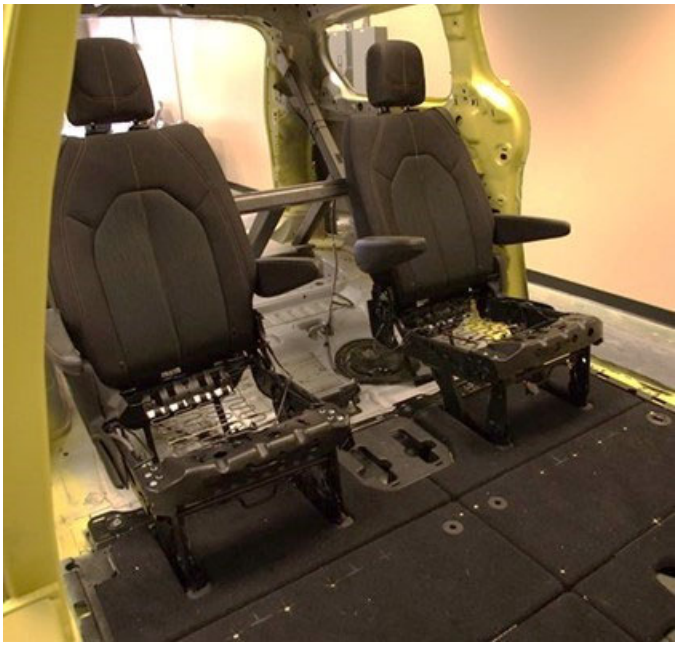

Figure B-2. Front V6 Buck Detail (Left) and Second Row Seating and Floor Detail (Right)

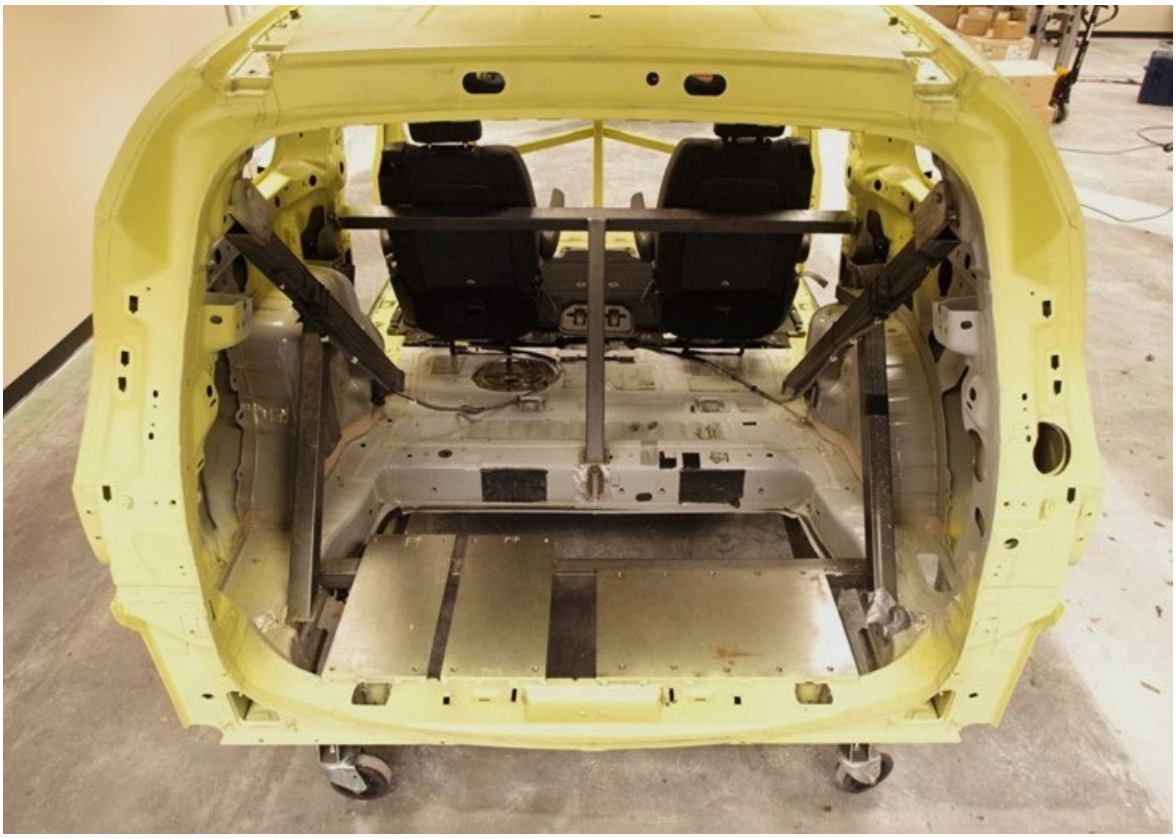

Figure B-3. Rear of V6 Buck Showing Seat and Structural Supports

Figure B-4. Internal V6 Buck Rear Structural Detail

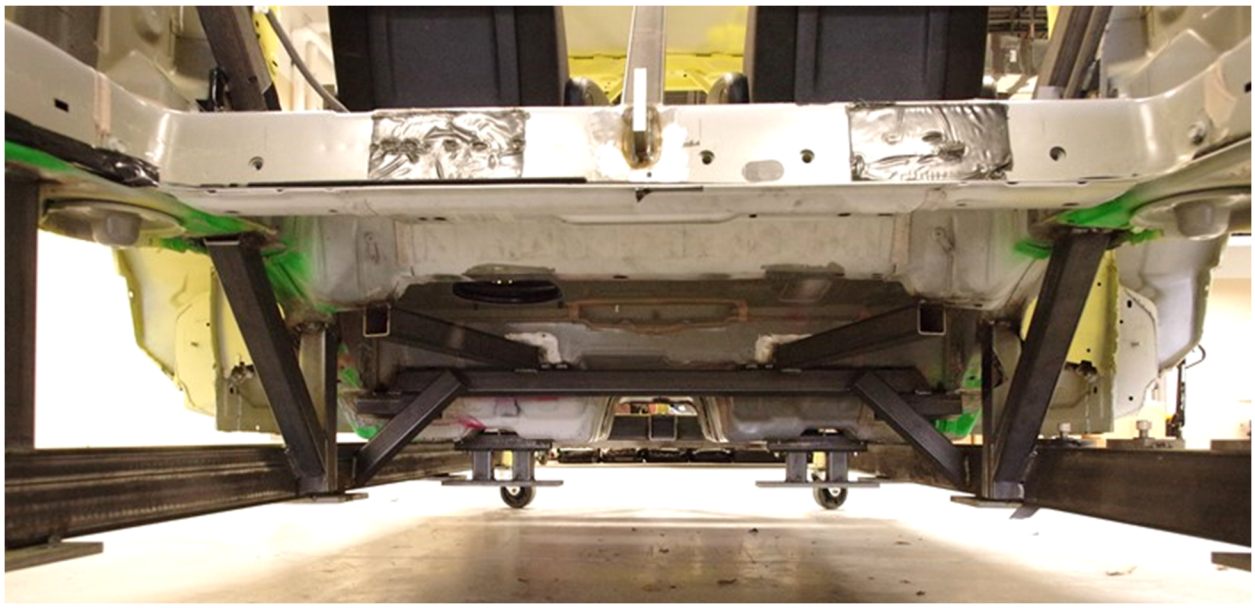

Figure B-5. Underneath V6 Buck Rear Seat and Anchor Reinforcements

Figure B-6. Underneath V6 Buck Rear Reinforcement Details

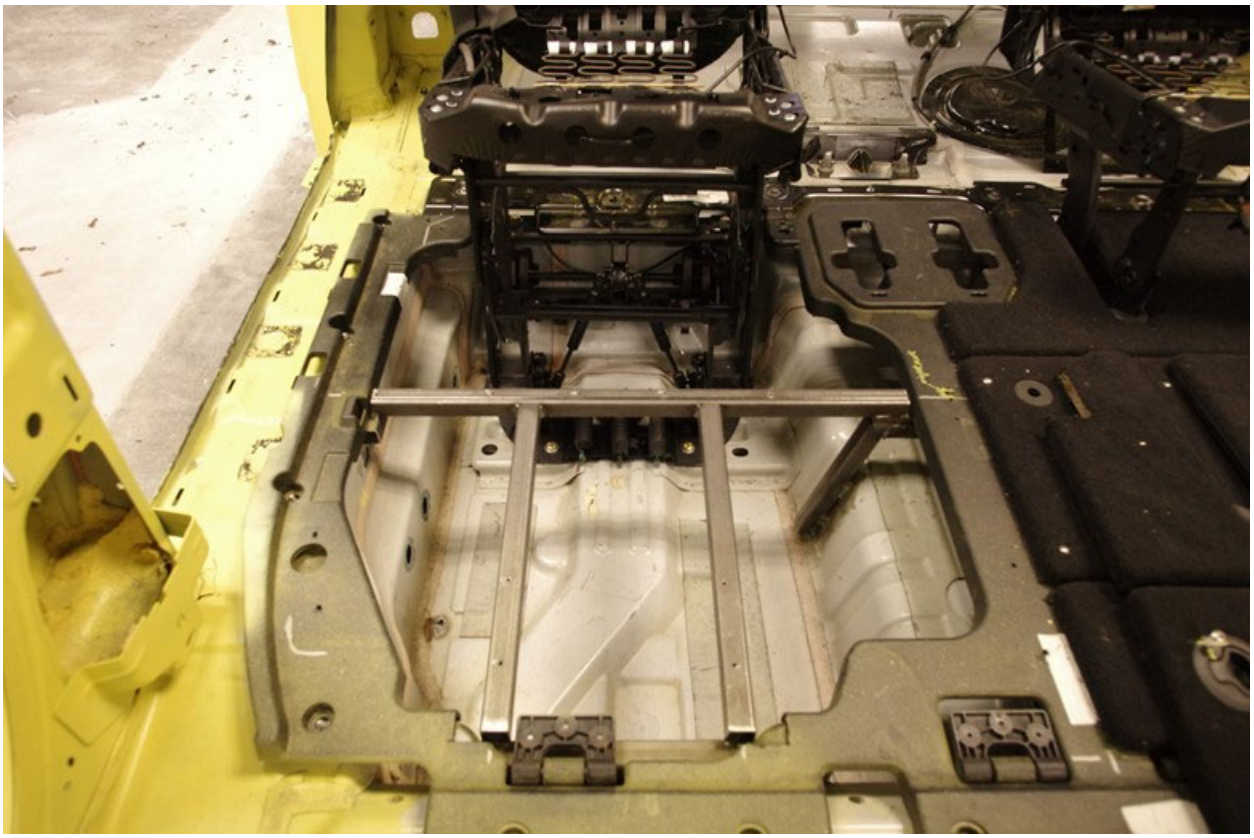

Figure B-7. Reinforcement Over the "Stow-And-Go" Recess in the V6 Buck

Appendix C. V10 Buck Development

Figure C-1. The Completed V10 Buck Mounted to the Deck of the Servosled

Figure C-2. Front Reinforcement Structure Detail of the V10 Buck

Figure C-3. Rear Reinforcement Structure and Seat Support in the V10 Buck

Figure C-4. Interior Detail of Rear Structural Reinforcement and Restraint Support

Figure C-5. Exterior Detail of Rear Structural Reinforcement and Restraint Support

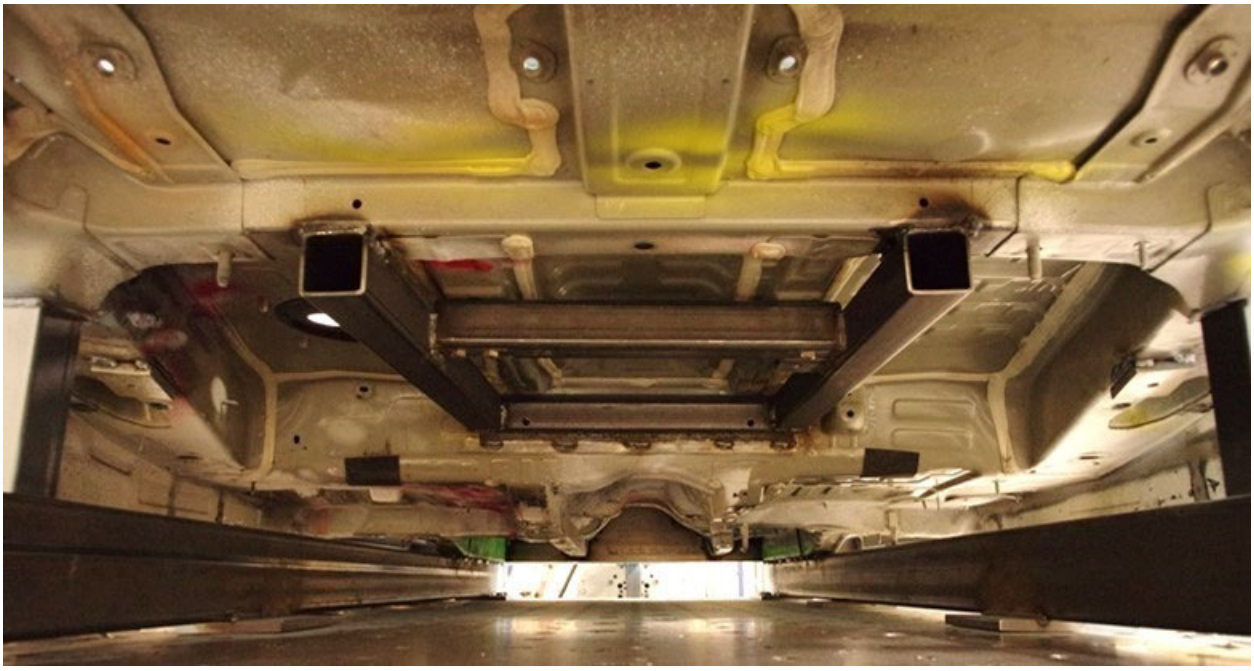

Figure C-6. Underneath V10 Buck Rear Seat and Anchor Reinforcements

Appendix D. V13 Buck Development

Figure D-1. Lateral Perspective of the V13 Buck on the Sled

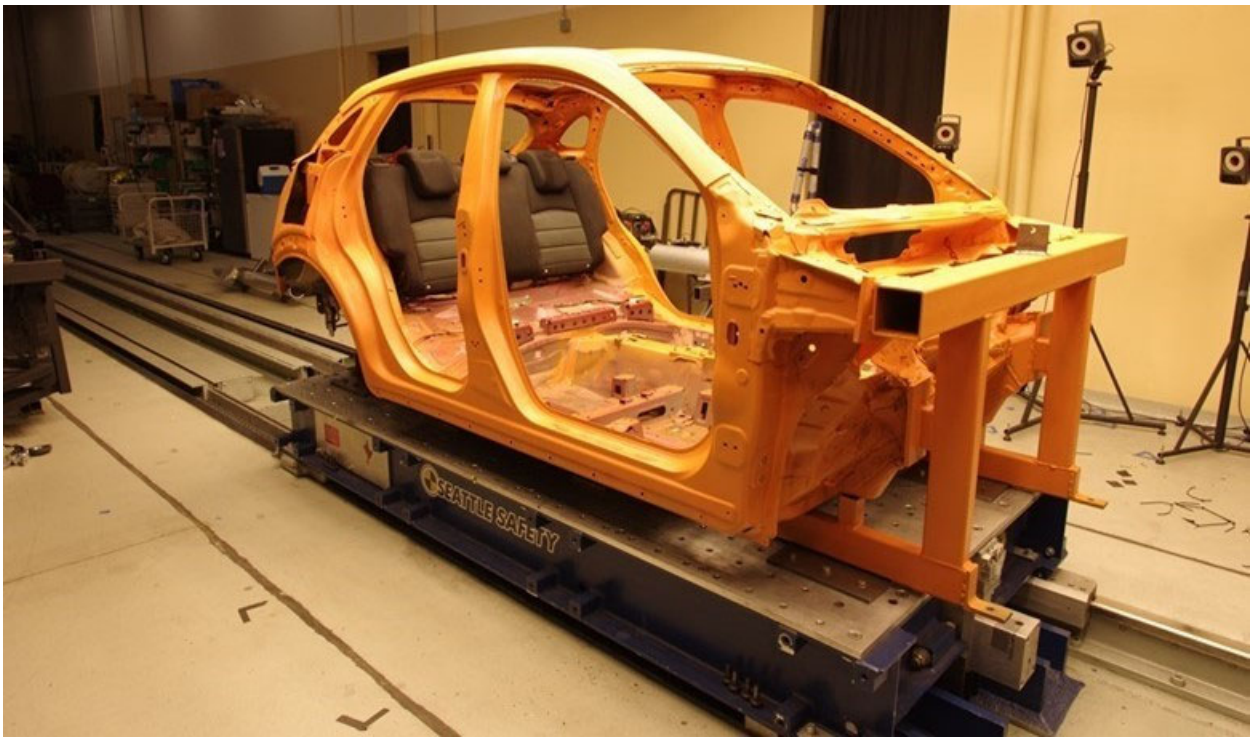

Figure D-2. Oblique Perspective of the V13 Buck on the Sled

Figure D-3. Frontal Perspective of the V13 Buck on the Sled

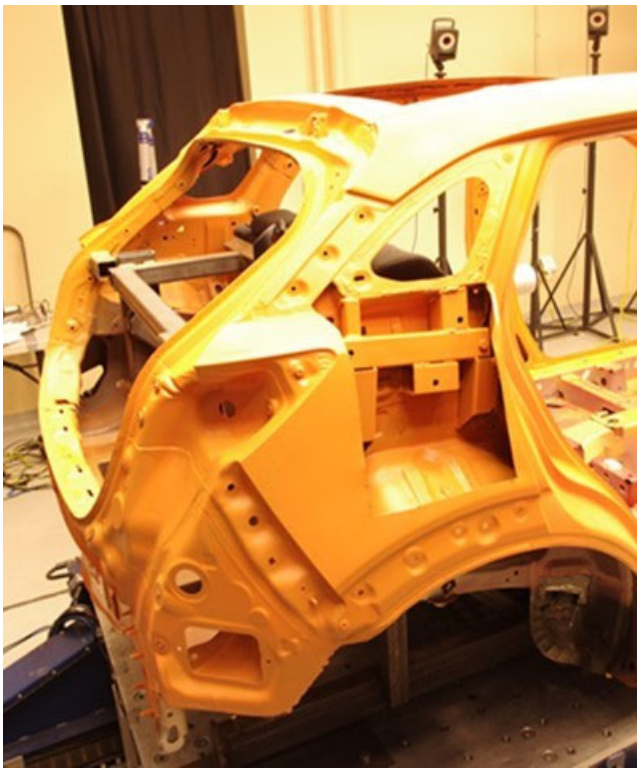

Figure D-4. Detail of the Rear Seat and Retractor Reinforcement on the V13 Buck

Appendix E. V14 Buck Development

Figure E-1. The Completed V14 Buck on Casters

Figure E-2. Frontal View of the V14 Buck

Figure E-3. Front Reinforcement Detail of the V14 Buck

Figure E-4. Underside of the V14 Buck Anchor Point and Seat Pan Reinforcements

Figure E-5. Detail of the V14 Buck Seat Pan Reinforcement From Below

Figure E-6. Detail of the V14 Buck Seat Pan Reinforcement From Above

Figure E-7. Retractor Location Reinforcement on the V14 Buck

Figure E-8. Posterior View of the V14 Buck Showing Seatback Reinforcement

Appendix F. V15 Buck Development

Figure F-1. The Completed V15 Buck on the Sled

Figure F-2. Lateral View of the V15 Buck on the Sled Under the Lights

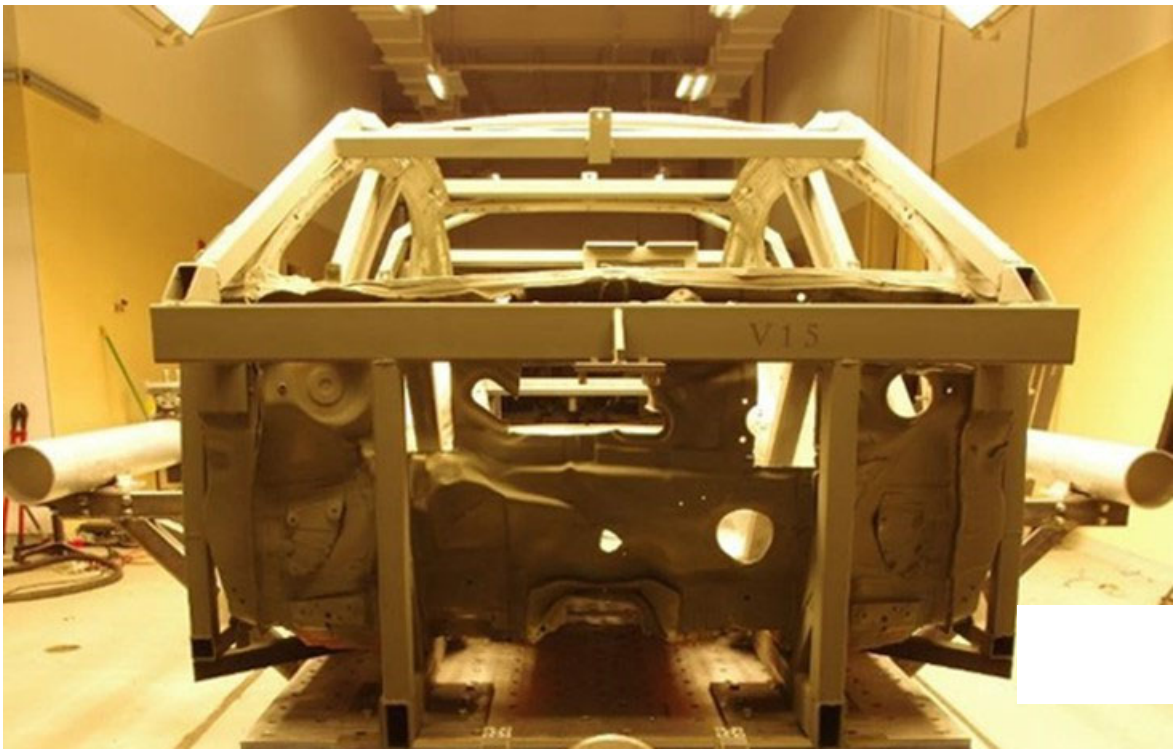

Figure F-3. Frontal View of the V15 Buck on the Sled Under the Lights

Figure F-4. Posterior Oblique View of the V15 Buck on the Sled Showing Seatback Reinforcement and DAS Mounting Plates

Figure F-5. Underside of the V15 Buck on the Sled

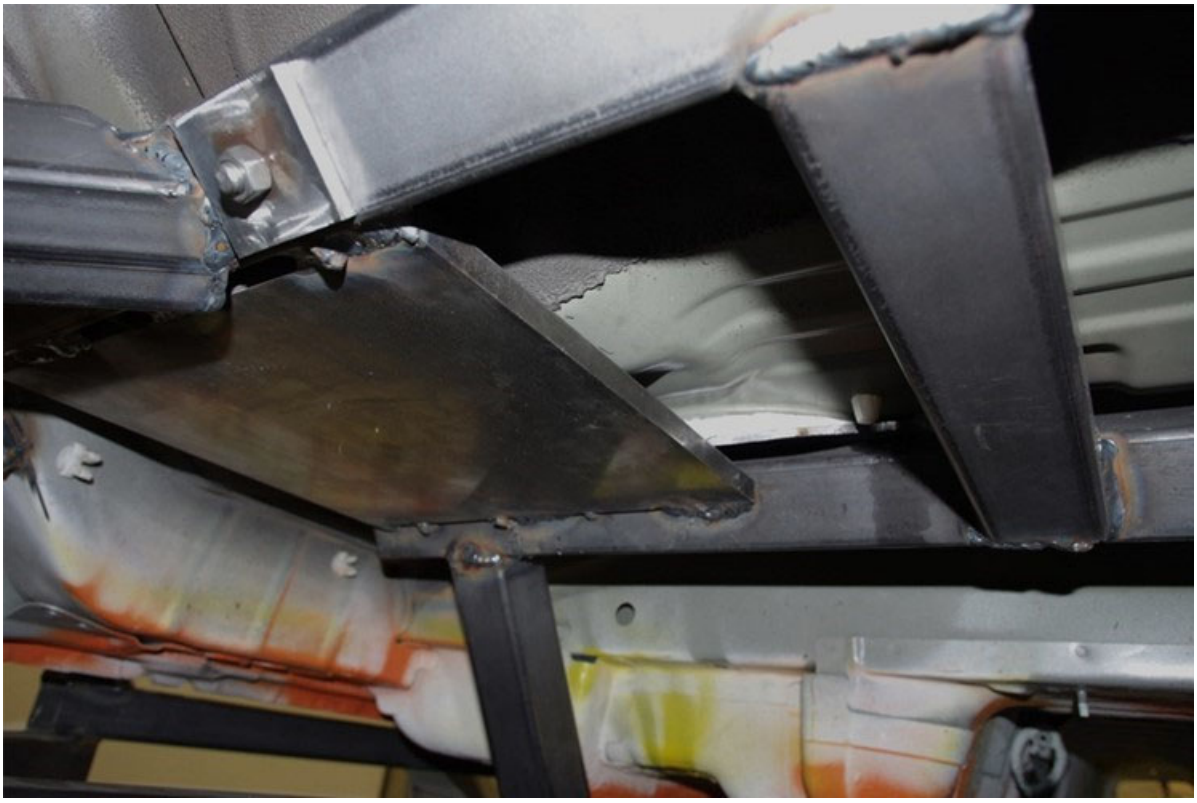

Figure F-6. Seat Pan Reinforcement of the V15 Buck

Figure F-7. Fuel Tank Access Structural Reinforcement on the V15 Buck

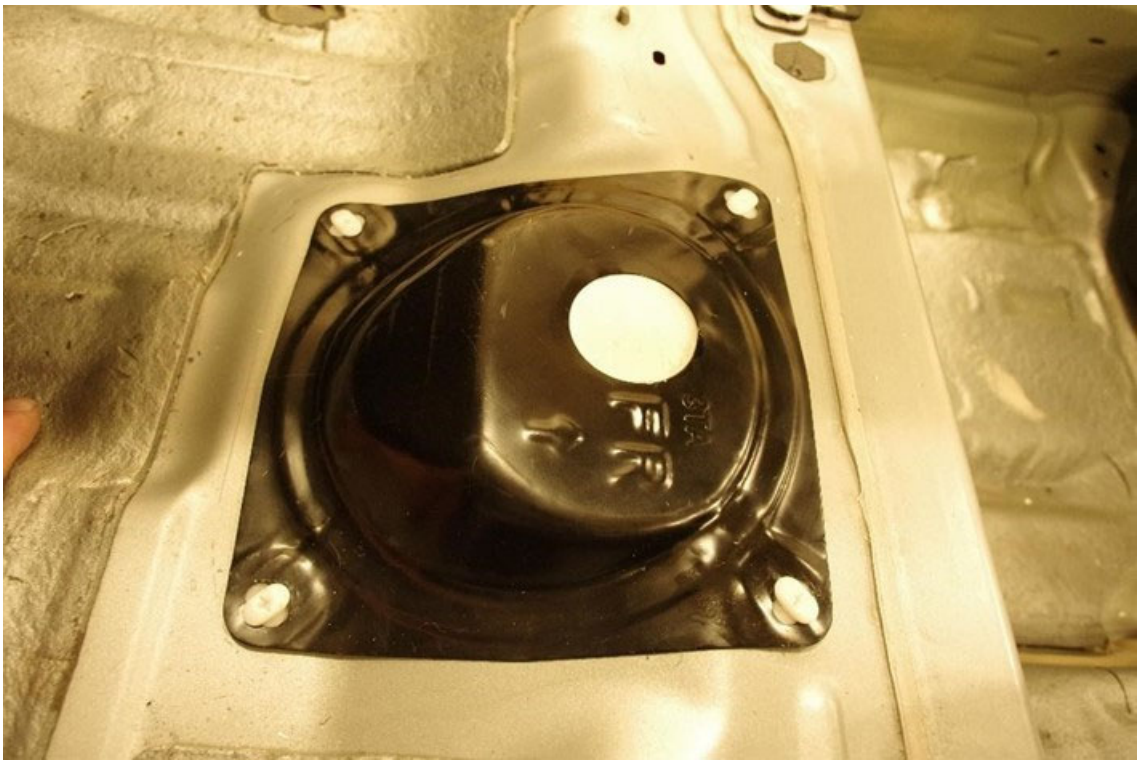

Figure F-8. Urethane Foam Support of the Fuel Tank Access Cover

Appendix G. V19 Buck Development

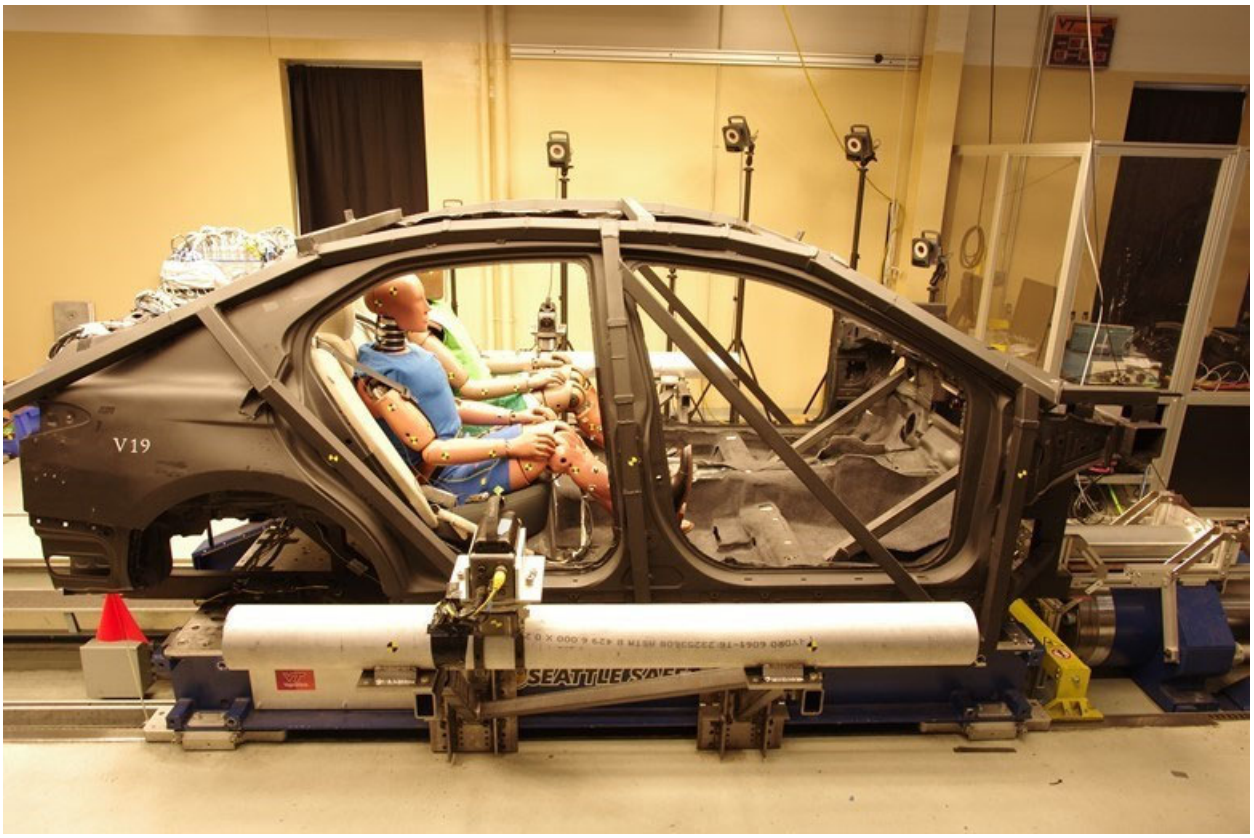

Figure G-1. Lateral Perspective of the V19 Buck on the Sled With ATDs Installed

Figure G-2. Frontal Aspect of the V19 Buck

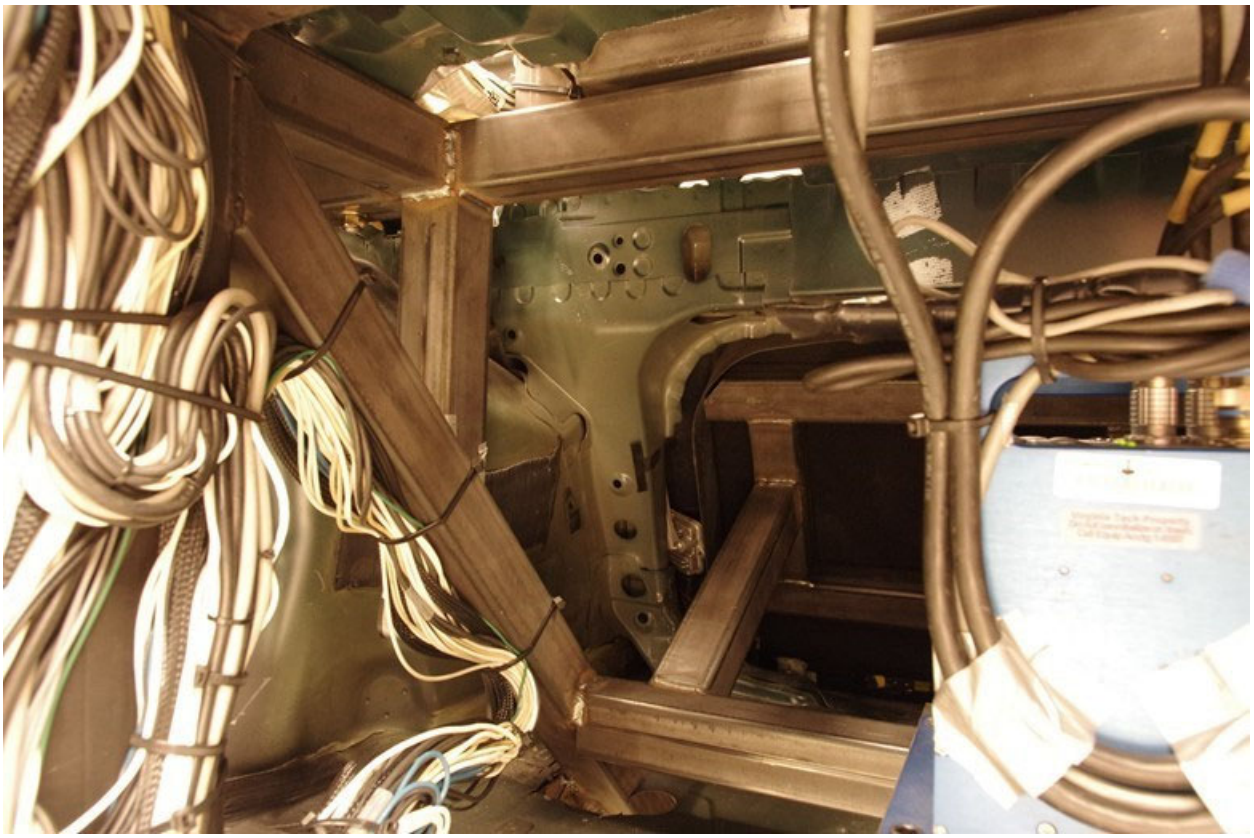

Figure G-3. Rear of V19 Buck Showing Seat Back Reinforcement

Figure G-4. Underside of the V19 Buck Showing Rear Supports

Figure G-5. Rear Seat and Anchor Reinforcement on the V19 Buck

Figure G-6. Detail of Rear Anchor and Seat Support Structure on the V19 Buck

Appendix H. Sled Acceleration Pulses for All Tests

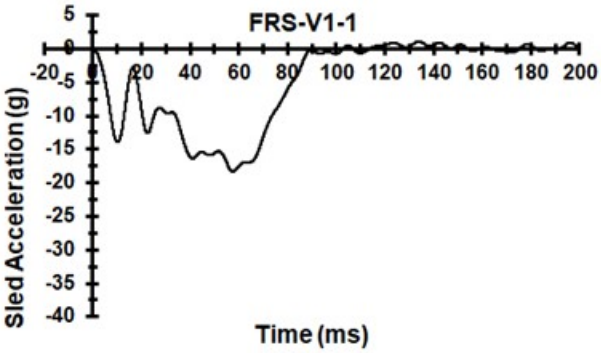
FRS-V1-1
Sled Acceleration (g)
Time (ms)

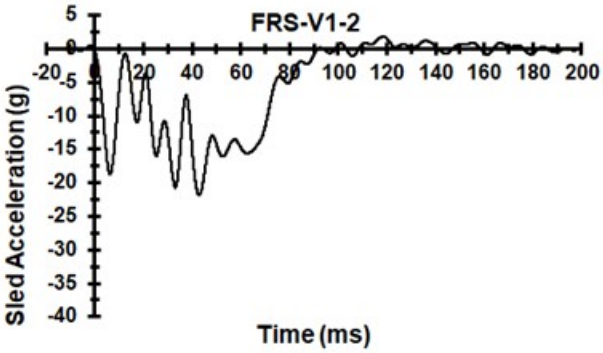
FRS-V1-2
Sled Acceleration (g)
Time (ms)

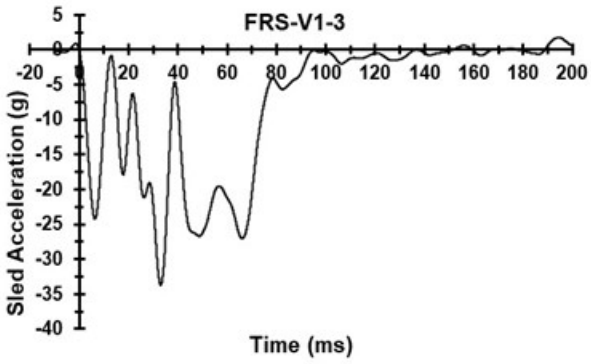
FRS-V1-3
Sled Acceleration (g)
Time (ms)

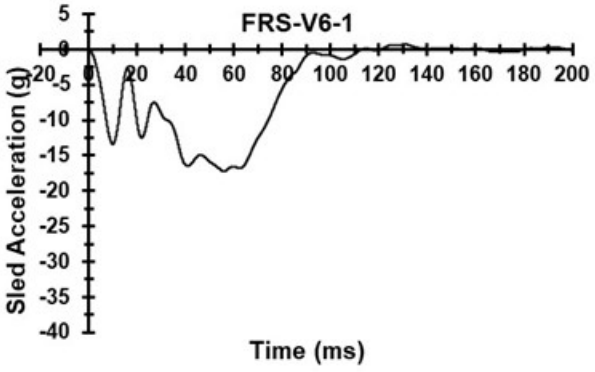
FRS-V6-1
Sled Acceleration (g)
Time (ms)

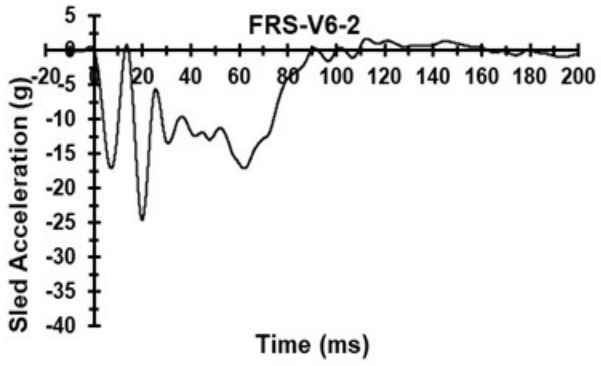
FRS-V6-2
Sled Acceleration (g)
Time (ms)

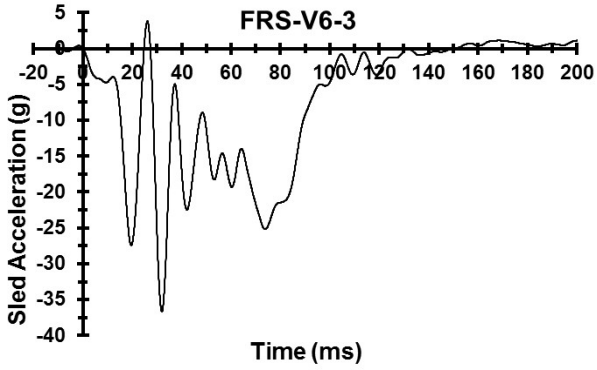
FRS-V6-3
Sled Acceleration (g)
Time (ms)

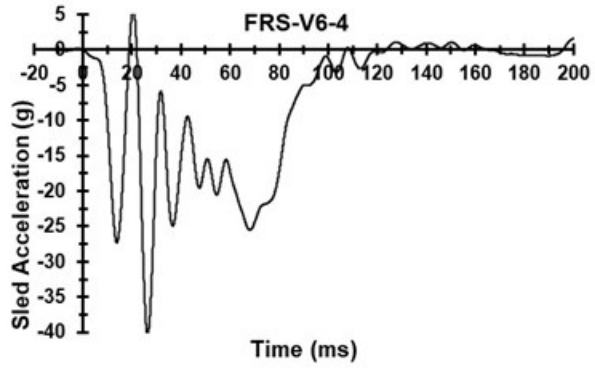
FRS-V6-4
Sled Acceleration (g)
Time (ms)

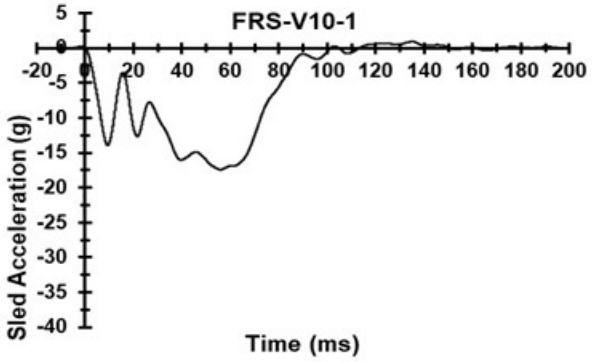
FRS-V10-1
Sled Acceleration (g)
Time (ms)

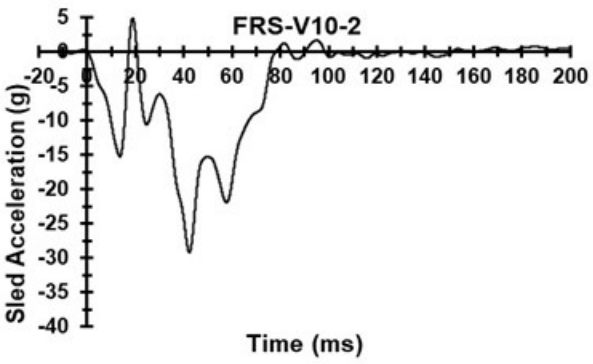
FRS-V10-2
Sled Acceleration (g)
Time (ms)

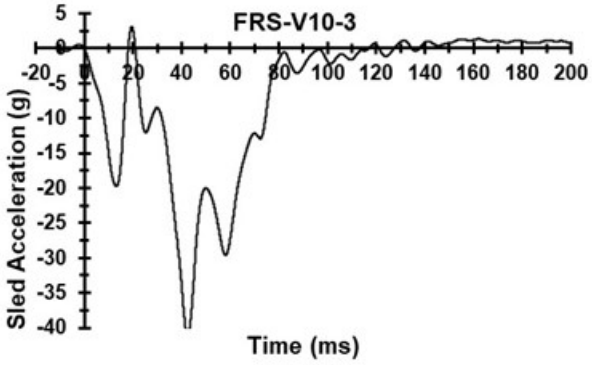
FRS-V10-3
Sled Acceleration (g)
Time (ms)

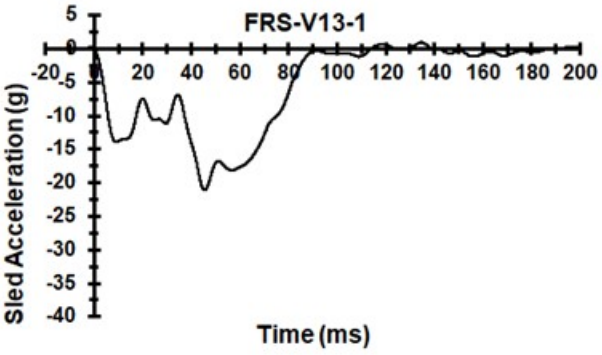
FRS-V13-1
Sled Acceleration (g)
Time (ms)

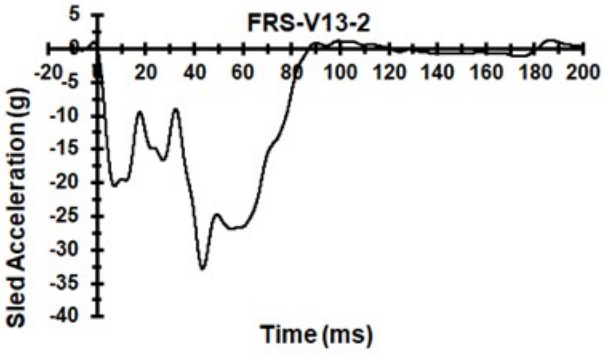
FRS-V13-2
Sled Acceleration (g)
Time (ms)

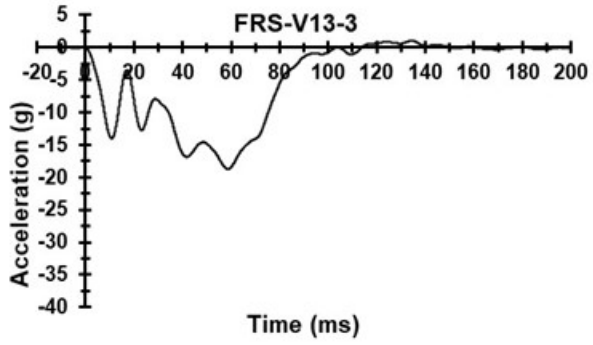
FRS-V13-3
Acceleration (g)
Time (ms)

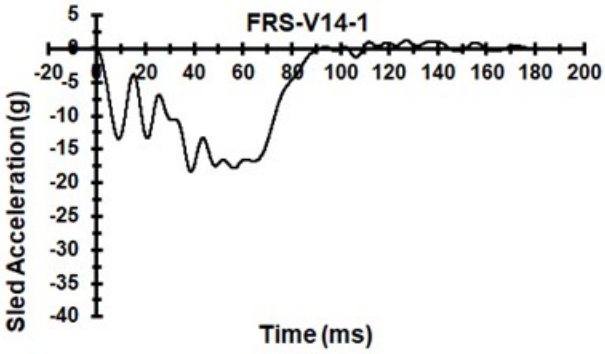
FRS-V14-1
Sled Acceleration (g)
Time (ms)

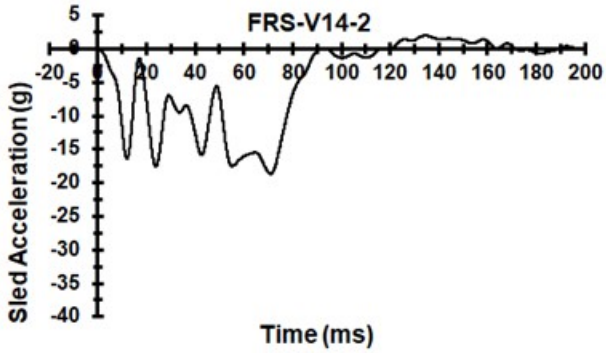
FRS-V14-2
Sled Acceleration (g)
Time (ms)

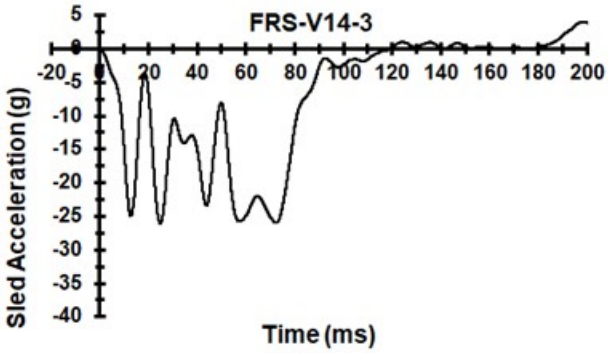
FRS-V14-3
Sled Acceleration (g)
Time (ms)

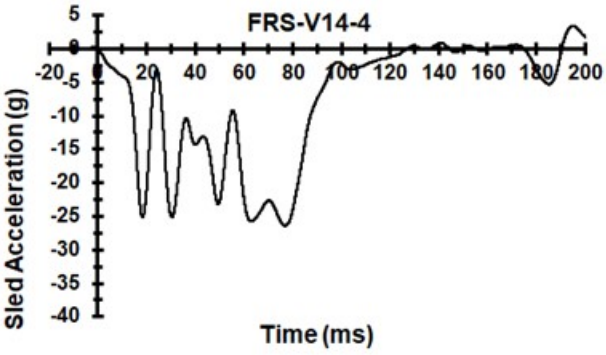
FRS-V14-4
Sled Acceleration (g)
Time (ms)

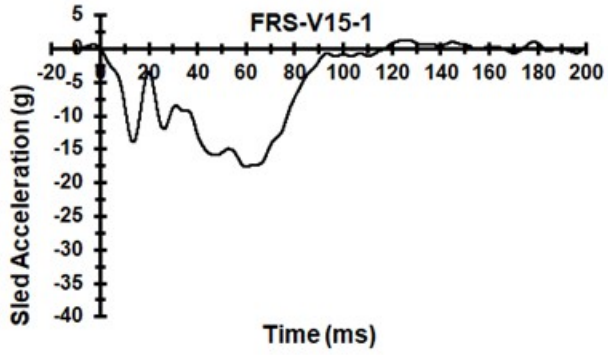
FRS-V15-1
Sled Acceleration (g)
Time (ms)

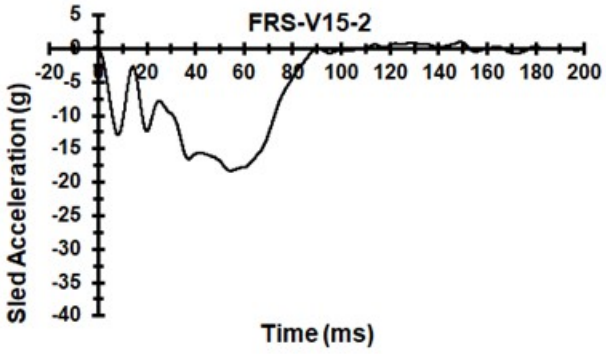
FRS-V15-2
Sled Acceleration (g)
Time (ms)

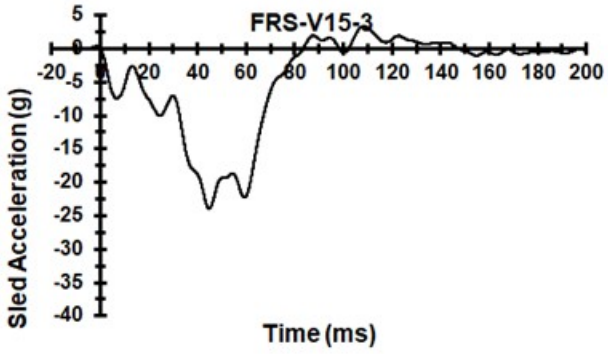
FRS-V15-3
Sled Acceleration (g)
Time (ms)

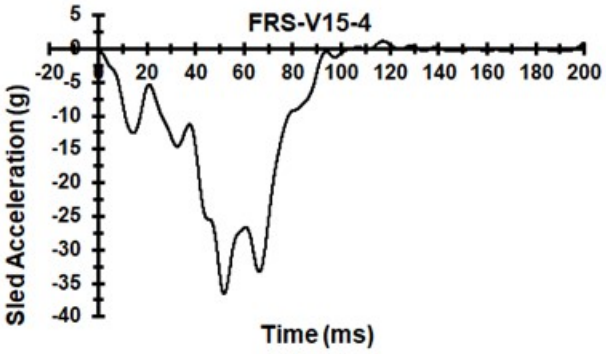
FRS-V15-4
Sled Acceleration (g)
Time (ms)

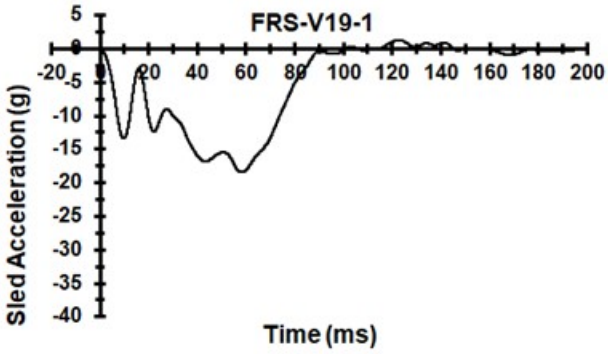
FRS-V19-1
Sled Acceleration (g)
Time (ms)

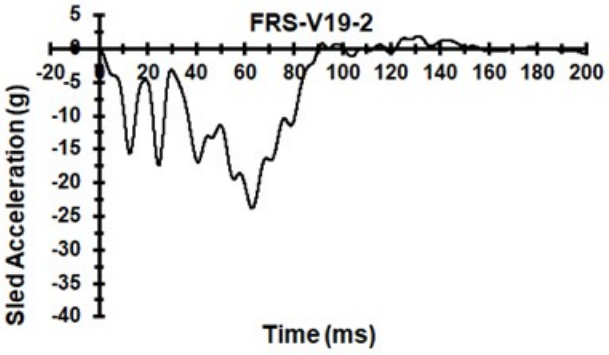
FRS-V19-2
Sled Acceleration (g)
Time (ms)
5
0
-5
-10
-15
-20
-25
-30
-35
-40
-20
0
20
40
60
80
100
120
140
160
180
200

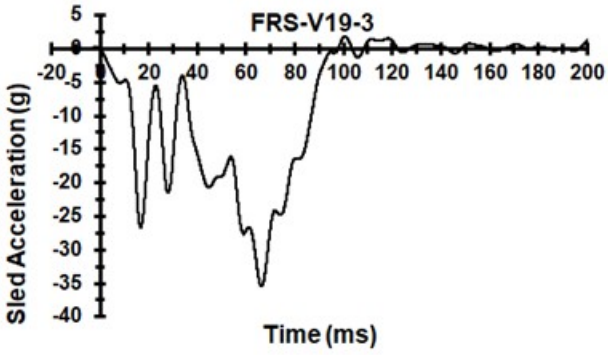
FRS-V19-3
Sled Acceleration (g)
Time (ms)
5
0
-5
-10
-15
-20
-25
-30
-35
-40
-20
0
20
40
60
80
100
120
140
160
180
200

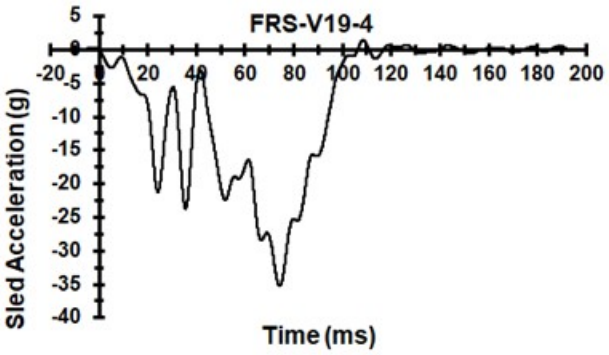
FRS-V19-4
Sled Acceleration (g)
Time (ms)
5
0
-5
-10
-15
-20
-25
-30
-35
-40
-20
0
20
40
60
80
100
120
140
160
180
200

Appendix I. Test-Specific Issues

This appendix catalogs the major issues encountered and resolved while conducting sled tests using the THOR-50M and Hybrid III 50th percentile male ATDs. The issues range from a torn THOR-50M pelvis, ABISUP, and collar flesh to dummy bolts coming loose, DAS failures, and torn shoulder belts. Some issues caused tests to be repeated. Presentation of these issues is ordered by vehicle buck and test number rather than the order in which testing was conducted. Tests for which there were no issues of concern are not listed.

Test FRS-V1-3

For Tests V1-1 and V1-2 the seat bottom structure was heavily reinforced so that support shape but not support deformation would contribute to the measured responses. This reinforcement allowed the seat bottom structure to be used for more than one test. However, there was concern that the reinforcement might have produced an artificial situation that could have negatively impacted the measured responses, or could do so for the final high-energy test. Therefore, it was decided to reinstall the original equipment structure for the last test, V1-3, which used an NCAP85 pulse. Figure I-1 shows the reinforced structure on the left, and the original structure on the right. The structure did not deform appreciably during the NCAP85 test, providing confidence in the earlier results.

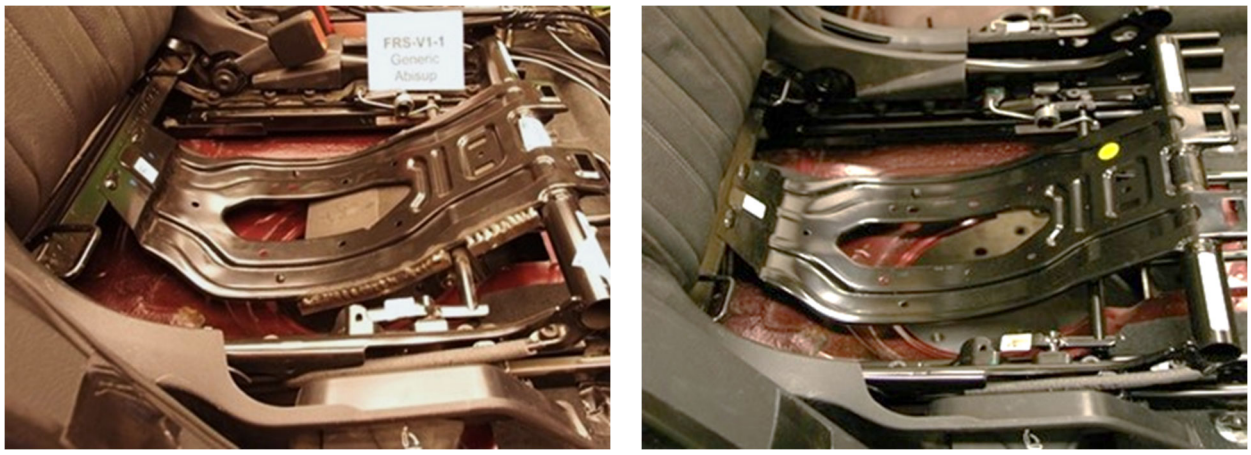

Figure I-1. The Reinforced Seat Bottom Structure Used for Tests V1-1 and V1-2 (Left): An Original Equipment Frame Was Used for Test V1-3 (Right), Which Was an NCAP85 Test

Test FRS-V6-1

Test V6-1 provides an example of the de-spiking techniques applied to some of the signals throughout this test series. No spikes were removed that were deemed to be useful data. Spikes that were removed resulted from cable pulls, faulty wiring, or mechanical noise (loose transducer mounting, metal-to-metal contact, spring snapping, etc.). No spikes that were removed would have contributed to the accurate calculation of an injury metric or probability but might otherwise have provided an erroneous peak value (i.e., a peak at a point for which there should not be a peak). Therefore, this process did not influence the results; it only provided data that are more easily viewed using an appropriate scale. This process was applied very conservatively, to only a few signals for each test. Signals associated with the THOR-50M lower extremities were predominantly involved. These signals were not used for analysis in this study. Also, a full-processed dataset, minus any de-spiking applied, is provided.

Figure I-1 shows an example original data trace. Figure I-3 shows the de-spiked version of these data. The onset of a spike was identified by the presence of an unrealistic change in signal value from one time step to the next. Typically, the threshold for this change was considered to be 15 percent or greater for signals not neighboring zero. Once the threshold was applied, the result was assessed to see if the threshold should be adjusted. This technique essentially provided a check on spikes that could be located by inspection. This process was applied prior to any other processing steps. Two sections of spike are reduced for this case. The important peaks of the real data are not changed. The spikes were reduced by interpolating over the affected time window. The interpolation takes the form of cubic spline or linear, or a combination of the two, approximations to the data within the identified window.

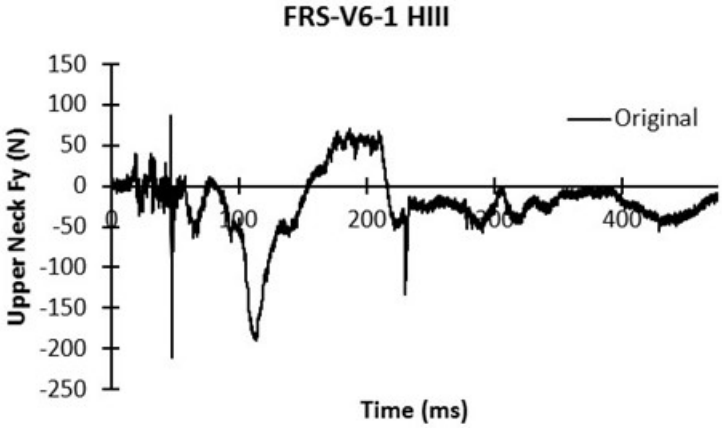

Figure I-2. Test V6-2 THOR-50M Seat Pedestal Mounting Bracket Separated and Deformed: The Pedestals for Both ATDs Were Realigned and Reinforced for Test V6-3

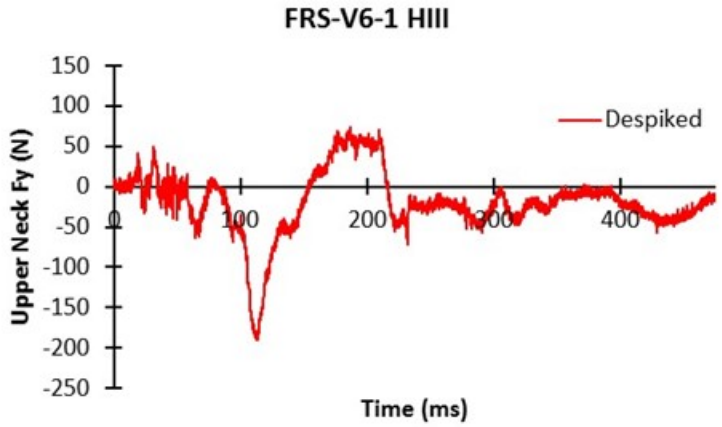

Figure I-3. Test V6-2 THOR-50M Seat Pedestal Mounting Bracket Separated and Deformed: The Pedestals for Both ATDs Were Realigned and Reinforced for Test V6-3

Test FRS-V6-2

Test V6-2 used a scaled vehicle-specific pulse. The inboard rear anchor for the seat pedestal occupied by the THOR-50M was damaged during the test. The large mounting holes in the pedestal brackets allowed the retaining washer to be folded on itself, and the bracket impacted the retaining bolt. The bolt was bent, and the bracket escaped the bolt. This is shown in Figure I-4. In turn, this allowed components of the pedestal bracket to separate and deform (Figure I-5).

The pedestal brackets were returned to their original shape and welded together for reinforcement prior to Test V6-3. This damage occurred last in the event, and was not deemed to influence the results enough to merit repeating Test V6-2, as evidenced by the results of Test V6-2 comparing well to test V6-1.

Figure I-4. Test V6-2, THOR-50M Inboard Rear-Seat Pedestal Anchor Pulled Through Bracket (Left), Deformed Anchor Bolt and Washer in Pedestal Riser (Middle), and Deformed Anchor Bolt and Washer in Pedestal Riser (Right): A Grade 9 Bolt Was Used for Test V6-3, and a Small Plate Was Used Instead of a Washer

Figure I-5. Test V6-2 THOR-50M Seat Pedestal Mounting Bracket Separated and Deformed: The Pedestals for Both ATDs Were Realigned and Reinforced by Welding for Test V6-3

Test FRS-V6-3

Test V6-3 provided several challenges that resulted in the test being repeated as Test V6-4. Both tests used the NCAP85 pulse. The first issue was an unusual response of the sled itself. The sled erroneously introduced an initial 5-g acceleration segment to the acquired pulse. The remainder of the acquired pulse matched the target pulse after this 10-ms anomaly subsided. Comparison between the acquired acceleration to the target acceleration and the target shifted by 10 ms as shown in Figure I-6.

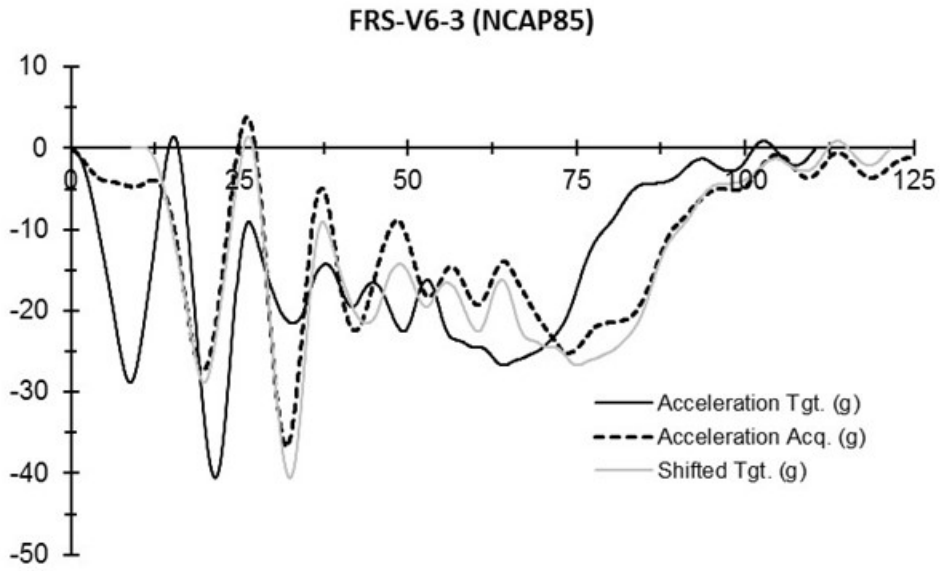

Figure I-6. Test V6-3 Target (Tgt.) and Acquired (Acq.) Sled Pulses: There Is a 5-g Anomaly at the Start of the Pulse, Approximately 10 ms in Duration. When Compared to a Time-Shifted Target, the Remainder of the Acquired Pulse Aligns

The shoulder belt for the THOR-50M embedded itself between the neck and shoulder of the dummy during Test V6-3. This allowed the shoulder belt to interact with the T1 accelerometer mounting block positioned at the top of the dummy spine box on the left side. This resulted in the shoulder belt being cut at the time of what would otherwise have been close to peak dummy excursion. Figure I-7 shows both sides of the cut shoulder belt. Fortunately, the belt webbing melted slightly as it was being cut. It melted enough for the webbing to get caught in the ring for the tongue at the buckle on the inboard, or right, side. This kept the dummy from escaping the buck. The final position and posture of the THOR-50M are shown in Figure I-8 for this test. Aside from invalidating the results of this test, the shoulder belt failure caused damage to the dummy.

The left knee clevis of the THOR-50M broke during Test V6-3 (Figure I-9). In addition, the mountings for the knee slider potentiometers were damaged for both knees (Figure I-10). These brackets, which provide over-rotation stops for the knee, were removed for subsequent tests (Test V6-4 and all V10 tests). Accordingly, the string pots were nested within the cable bundles for the lower extremities. The T1 Z-direction accelerometer was damaged during this test also. It was replaced.

Figure I-7. Test V6-3 Torn Shoulder Belt (Both Sides Shown) for the THOR-50M: The Belt Was Torn During Interaction With the T1 Accelerometer Mount and the Z-Direction Accelerometer Was Damaged

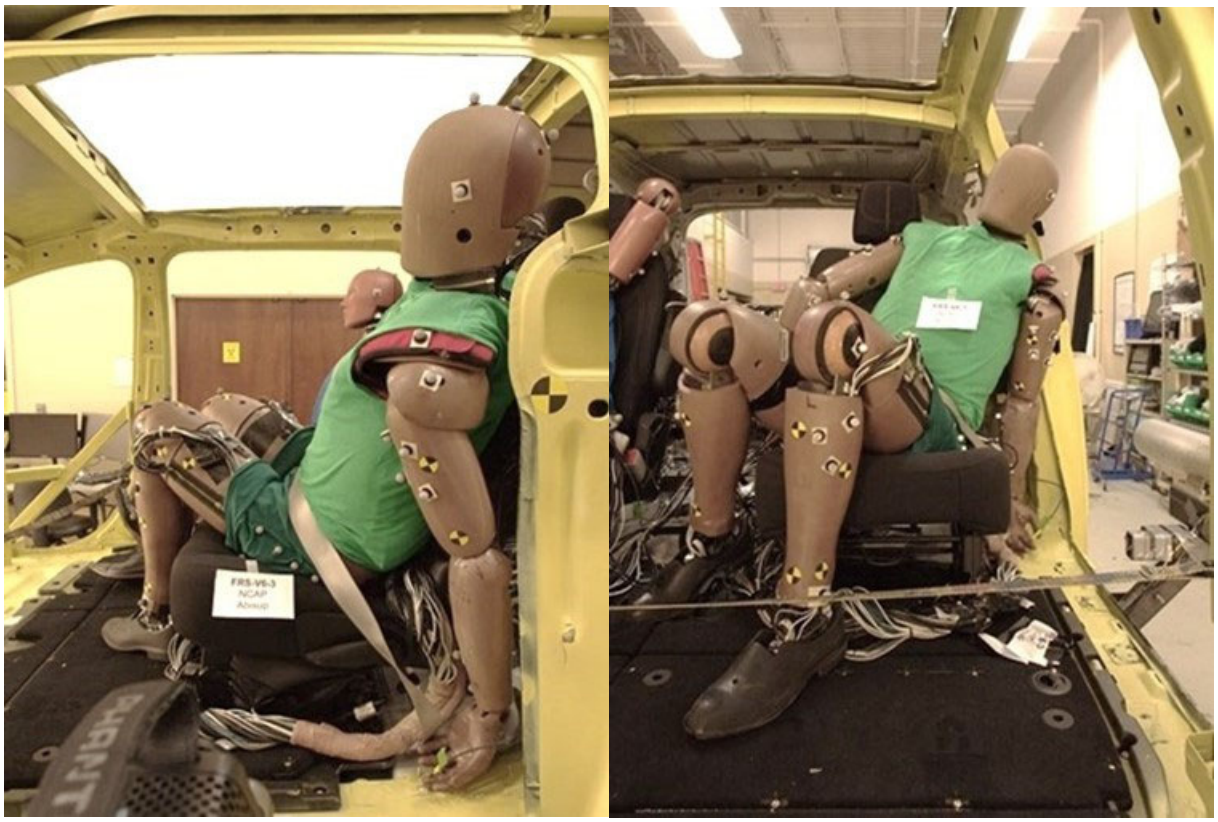

Figure I-8. Post Test V6-3 THOR-50M Final Posture Without the Shoulder Belt

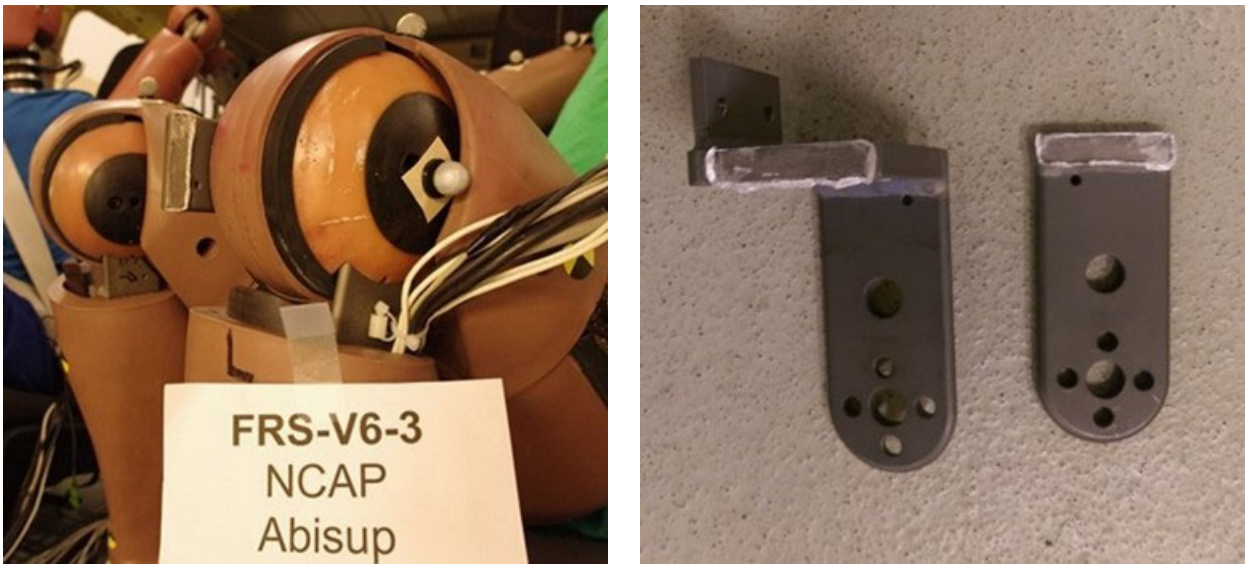

Figure I-9. Test V6-3 Broken THOR-50M Left Knee Clevis, in (Left) and out (Right) of the ATD

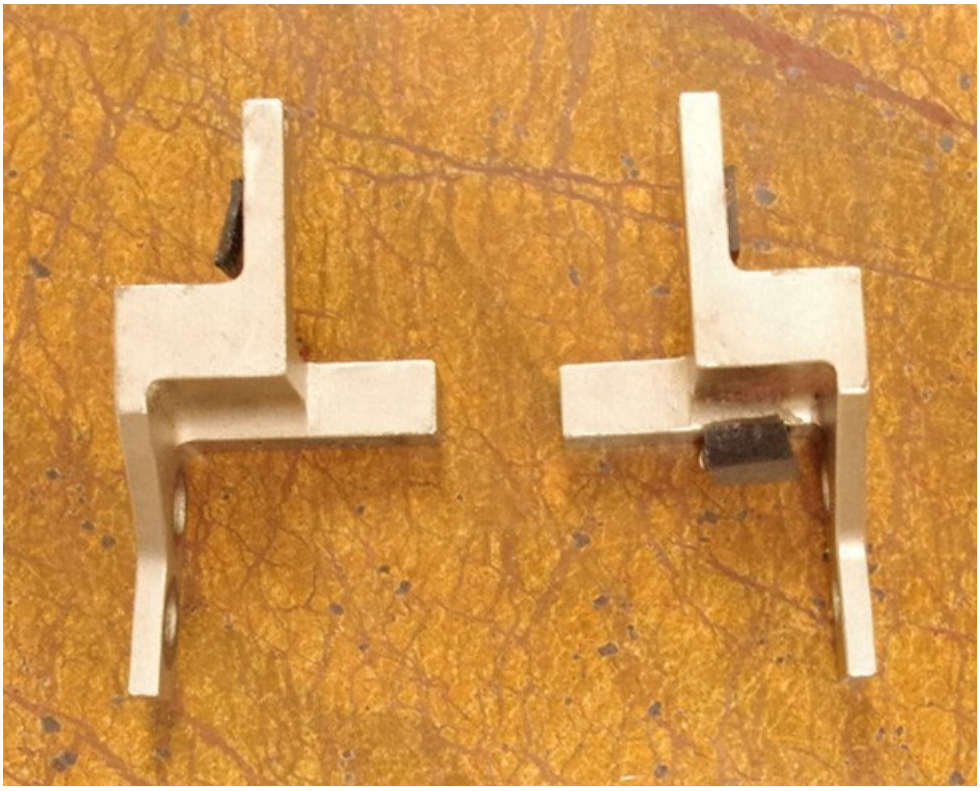

Figure I-10. Post Test V6-3 THOR-50M Damaged Knee Slider Potentiometer Mounting Brackets (Both Knees), Which Were Removed for Subsequent Tests

Test FRS-V6-4

New seat pedestals were installed for both ATDs for Test V6-4. However, based upon the experience gained during Test V6-2, components of the mounting brackets were welded together prior to installation of the seats to reinforce the structures. A new pedestal and its reinforced sections are shown in Figure I-11.

Similarly, the grade 9 bolts and distribution plates (these replaced the washer) that were used at the rear inboard seat anchor position for both dummies for test V6-3 were used for test V6-4. A new, reinforced, seat pedestal is shown in Figure I-12 as is a bolt/plate combination.

To prevent the shoulder belt from being cut by the T1 accelerometer mount, a plastic shroud was designed and fabricated. This shroud was intended to better fill the space between the neck and shoulder assemblies in the THOR-50M, and to provide a smooth surface for belt engagement if the webbing slipped past the dummy collar. Various perspectives of this shroud are shown in Figure I-13.

Figure I-11. New Seat Pedestals and Reinforcing Weldments Used for Test V6-4 for Both ATDs

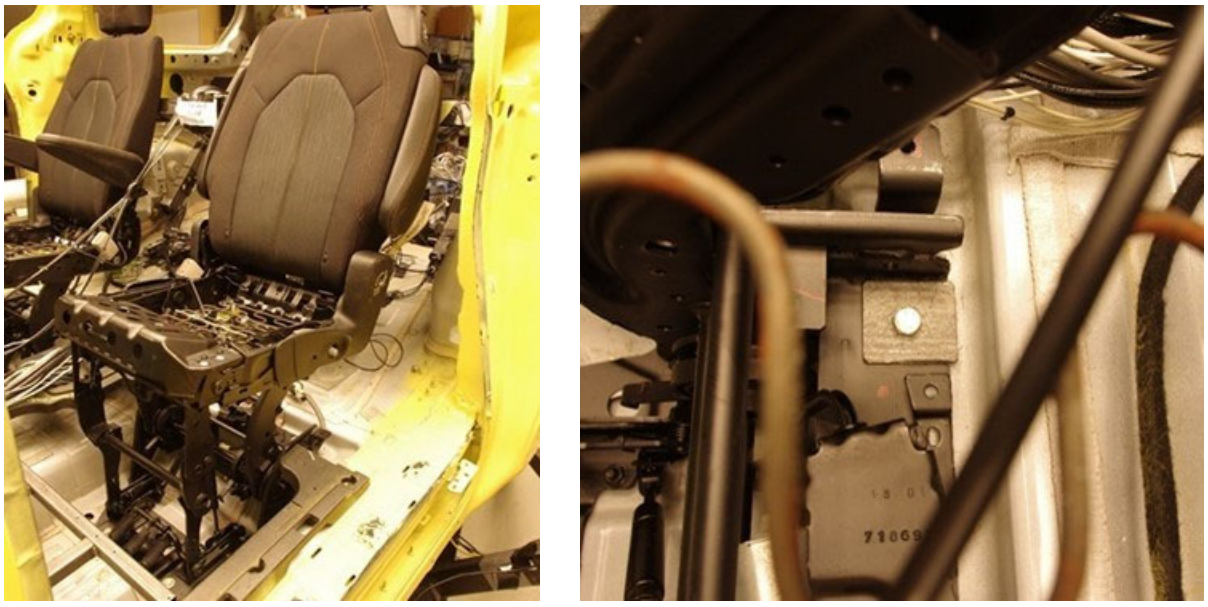

Figure I-12. New Reinforced Pedestals Installed for Test V6-4 (Left), Inboard Rear Grade 9 Anchor Bolt and Load-Distribution Plate Used for Both ATDs for Tests V6-3 and V6-4

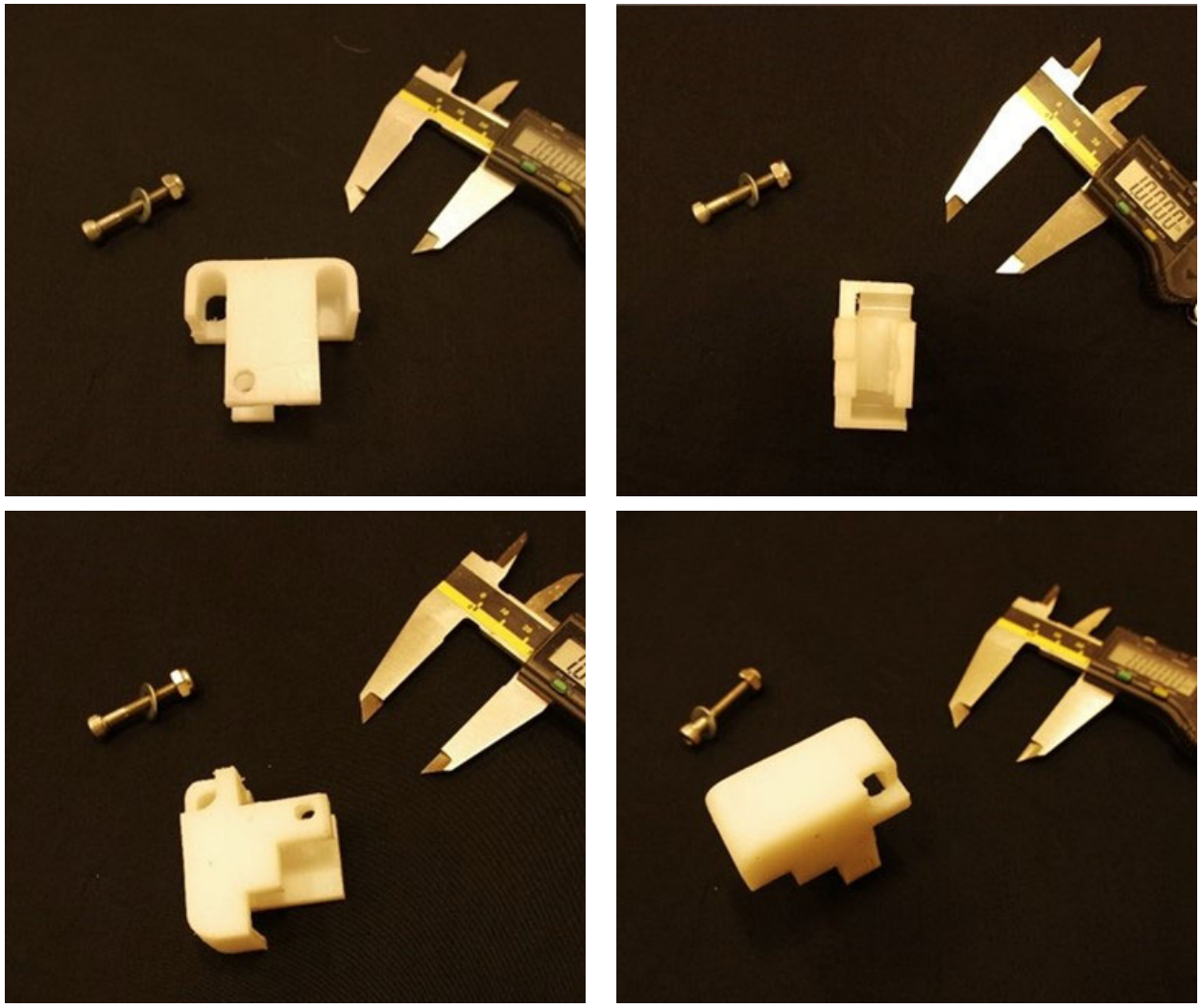

Figure I-13. Various Perspectives of the T1 Accelerometer Mount Shroud Implemented for THOR-50M for Use in Test V6-4

The T1 shroud was designed to bolt to the dummy spine box, covering the T1 mount and accelerometers, as shown in Figure I-14 and Figure I-15. It also served to fill some of the gap between the neck and shoulder of the dummy. However, while this shroud could protect the webbing from being cut, it could not inhibit penetration of the space between the neck and shoulder by the belt.

To help reduce the probability and extent of penetration by the belt, a supplemental bib was fashioned from leather. This bib rested above the shoulder assembly and the T1 shroud, beneath the dummy jacket and collar. It was thought that even if this bib did not keep the belt from slipping between the neck and shoulder, it would further protect the webbing from being cut. This bib is shown installed on the left side of the THOR-50M in Figure I-16.

Figure I-14. THOR-50M T1 Accelerometer Mount Shroud Installed for Test V-4: It Was Designed to Keep the T1 Mount From Cutting the Shoulder Belt

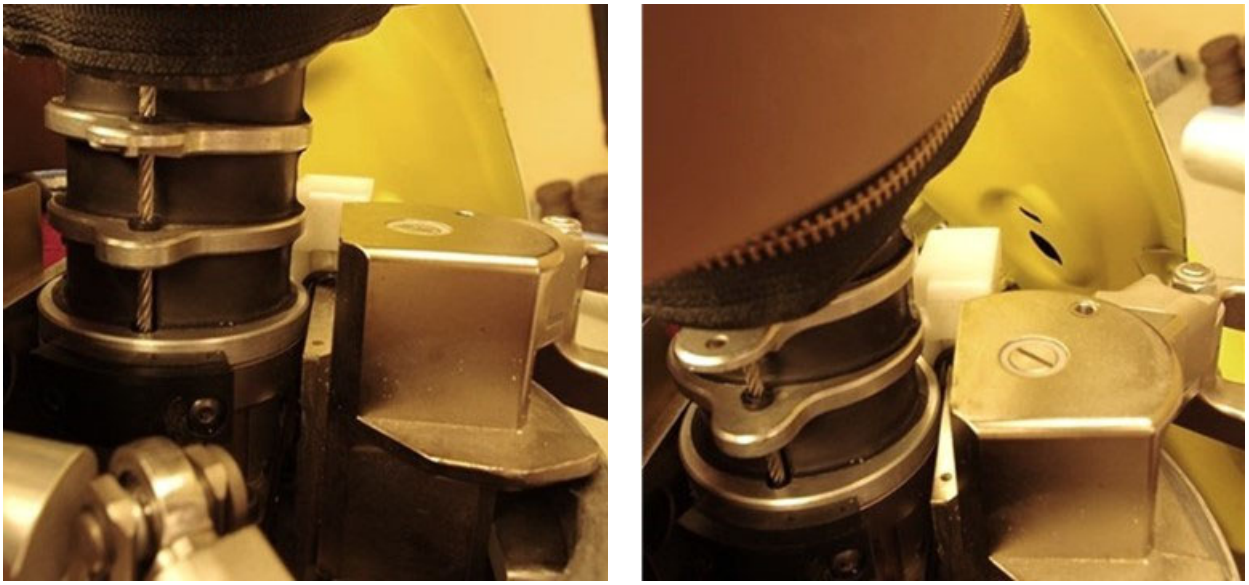

Figure I-15. The THOR-50M T1 Accelerometer Mount Shroud Protects the Shoulder Belt When It Slips Between the Neck and Shoulder

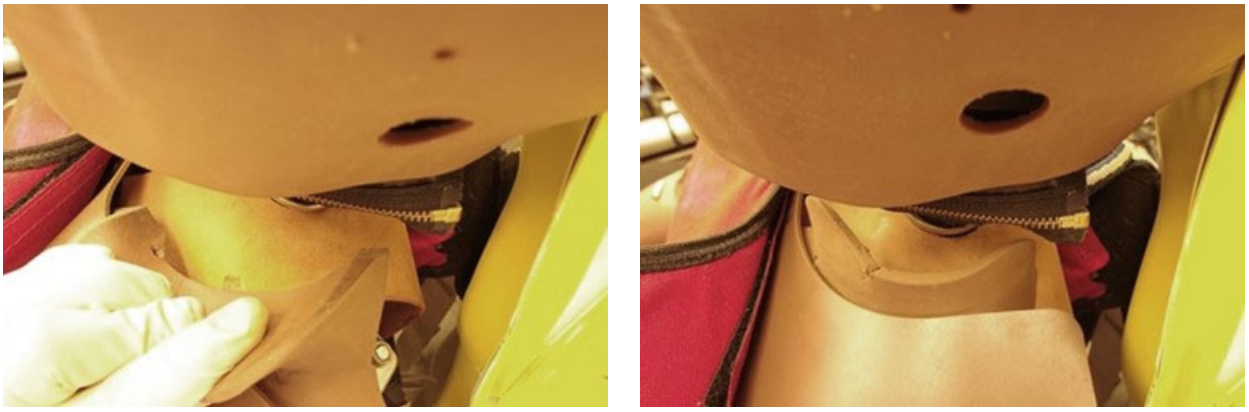

Figure I-16. THOR-50M Left Shoulder Supplemental Bib (Leather) Installed to Help Keep the Shoulder Belt From Slipping Between the Neck and Shoulder During Test V6-4

The D-ring sliders for both dummies had been set to the top-most position for previous tests using buck V6. This was because the THOR-50M dummy sat fairly high in the seat, and this position provided the best shoulder belt routing. This also kept the load applied to the slider as close as possible to an anchor for the slider. However, in an effort to route the shoulder belt more laterally over the dummy's shoulder and to keep it farther from the neck and collar, the D-ring was positioned at the second-from-top detent for Test V6-4. This position was 2 inches (50.8 mm) from the top position. This pre-test position is shown in Figure I-17 on the left. This resulted in deformation of the D-ring slider track. This post-test result is shown in Figure I-17 on the right.

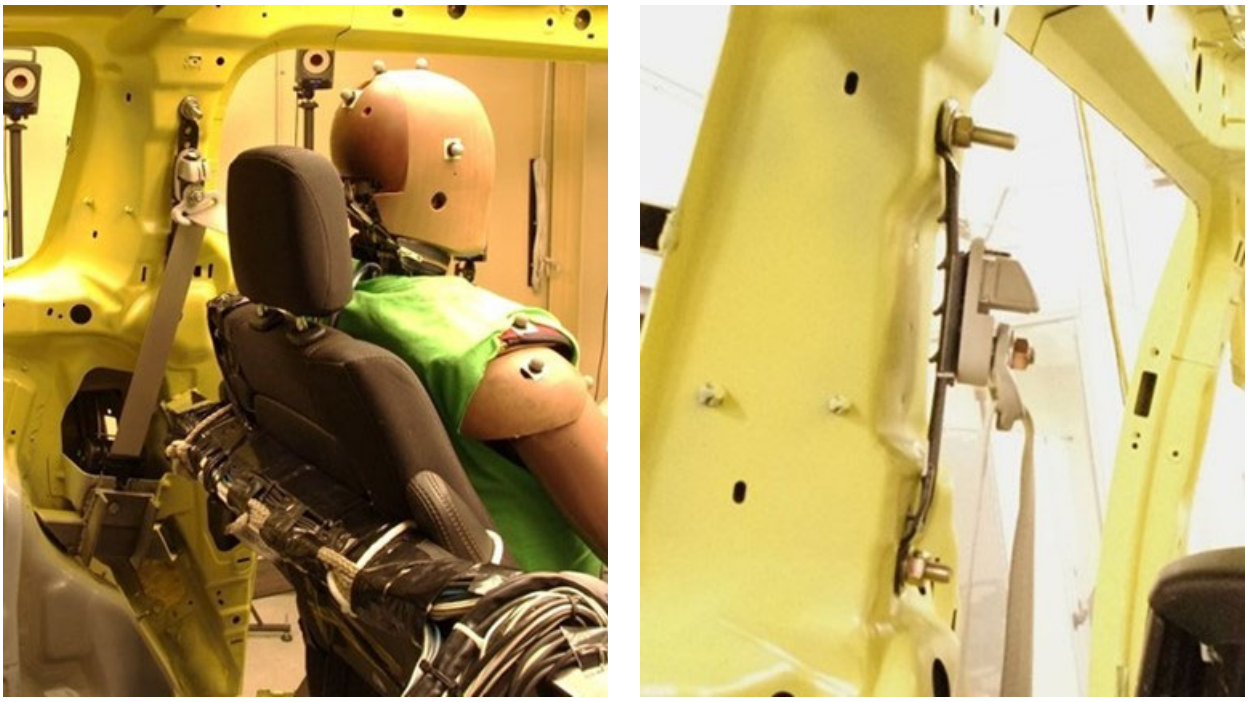

Figure I-17. Revised D-Ring Slider Position Used for the THOR-50M and HIII for Test V6-4: The Slider Is Two Positions (2 Inches) From the Top Location, Which Was Used for the Previous Three V6 Tests

Figure I-18 shows the post-test position and posture for the THOR-50M for Test V6-4. Importantly, the shoulder belt did not tear. The knees rotated past 180 degrees, but the knee slider mechanisms were neither contacted nor damaged. Figure I-19 shows that while the shoulder belt was not cut, it still penetrated the space between the neck and shoulder, having worked its way past the collar flesh. The webbing was trapped, and kept compression on the dummy thorax after the test. Figure I-20 shows the extricated webbing, illustrating the folding of the shoulder belt that occurred when it got trapped.

Figure I-21shows that the shoulder belt became trapped between the T1 accelerometer mount shroud and the shoulder assembly of the THOR-50M for Test V6-4. This resulted in damage to the retaining bolt for the T1 mount, and shearing of the one remaining locating pin (between the mount and spine box). The shroud was deformed slightly, and the X- and Y-direction accelerometers were damaged. Both accelerometers were subsequently replaced.

Figure I-22 shows the damage to the THOR-50M collar flesh as a result of Text V5-4. This damage indicates that the shoulder belt webbing did not slip past the collar, but cut its way through the collar instead. Fortunately, the supplemental leather bib and T1 accelerometer mount shroud protected the webbing from being cut, and the belt only folded over on itself.

Figure I-18. Post Test V6-4 THOR-50M Posture: The Shoulder Belt Slipped Between the Neck and Shoulder but Did Not Get Cut, and the Knees Did Not Over-Rotate Appreciably

Figure I-19. During Test V6-4 the Shoulder Belt Slipped Past the Collar and Leather Bib Installed on the THOR-50M and Was Trapped Between the T1 Accelerometer Mount Shroud and the Shoulder

Figure I-20. During Test V6-4 the Shoulder Belt Folded Over on Itself as It Was Trapped by the Shoulder of THOR-50M

Figure I-21. The THOR-50M T1 Accelerometer Mount and Shroud Were Damaged During Test V6-4: The Mount Locating Pin and Retaining Bolt Were Compromised

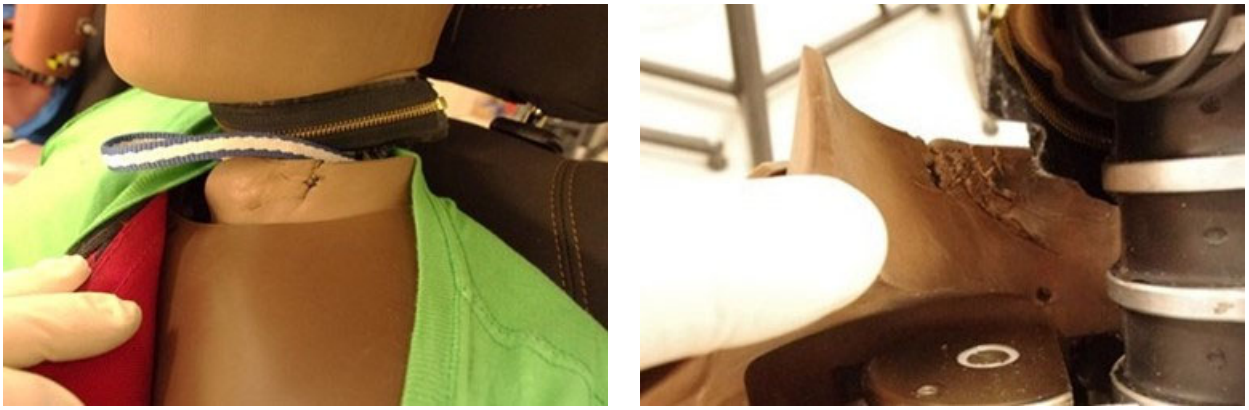

Figure I-22. THOR-50M Collar Damage From Test V6-4

Test FRS-V10-1

A new locating block was designed and implemented so that THOR-50M T1 accelerations could continue to be recorded after damage to the mount occurred during Test V6-4, without risk of losing accelerometer and data due to possible interaction with the shoulder belt. This locating block facilitated relocation of the T1 accelerometer mount to the right side of the dummy spine box, in the absence of any locating pins (a pin sheared during Test V6-4, and there was no provision for locating pins on the right side of the spine box). Various perspectives of the locating block are shown in Figure I-23. The locating block restricts rotation of the T1 accelerometer mount when the mount is otherwise attached by a single retaining bolt. A new retaining bolt and new accelerometers were installed. Figure I-24 shows the T1 accelerometer mount locating block installed on top of the right side of the THOR-50M spine box, with and without accelerometers installed.Figure I-25 shows the repair of the THOR-50M collar on the left side.

Figure I-23. Different Perspectives of the Locating Block Used to Position the T1 Accelerometer Mount on the Right Side of the THOR-50M Without Any Pins: This Block Was Used for All V10 Tests

Figure I-24. The T1 Accelerometer Mount Locating Block Installed on the Right Side of the THOR-50M Spine Box, Both Without and With Accelerometers

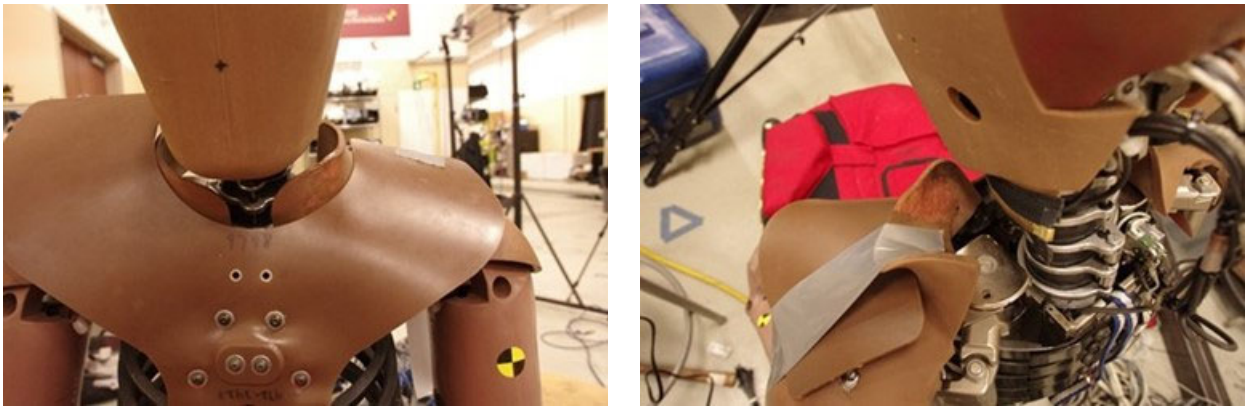

Figure I-25. Repair of the THOR-50M Collar Prior to Test V10-1

Test V10-1 (generic pulse) was executed with only one issue of consequence: the seat bottom support structures (hinges, basket, and lower frames) were damaged beyond repair. Figure I-26 shows the collection of damage to the seat bottom support structures. Essentially, the seat bottoms deformed until contact with the buck deck occurred. Components bent and twisted in multiple directions and planes. This necessitated acquisition of replacement parts for both of the remaining tests. This damage also illustrated that it was not possible to construct accurate FE representations of these seats, meaning that numerical simulation of these tests was not possible.

Test FRS-V10-2

Test V10-2 (scaled specific pulse) produced identical damage to the seat bottom support structures (not shown). These structures were again replaced prior to the next test. However, this test disclosed another issue: The toes of the THOR-50M contacted the riser for the front seat anchor points. This is shown in Figure I-27. On the left side of the figure is part of a frame from the onboard frontal video sequence. It shows contact between the dummy's toes and the riser. This contact was minimal, of short duration, and coincident with peak dummy excursion. Therefore, this contact was deemed inconsequential to the results. However, it did suggest that a much worse condition could develop during the NCAP85 test.

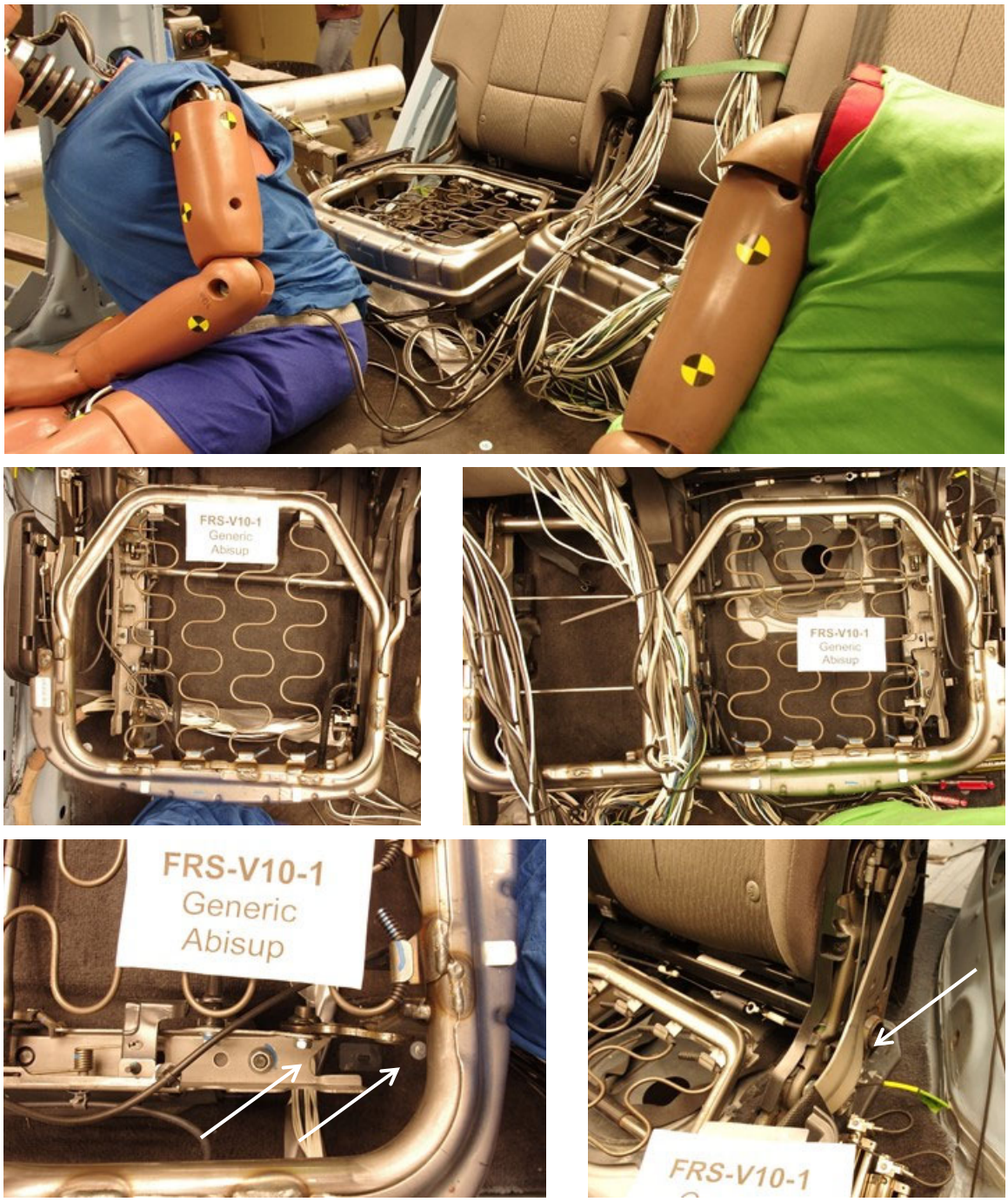

Figure I-26. Damage to Seat Bottom Structures During Test V10-1

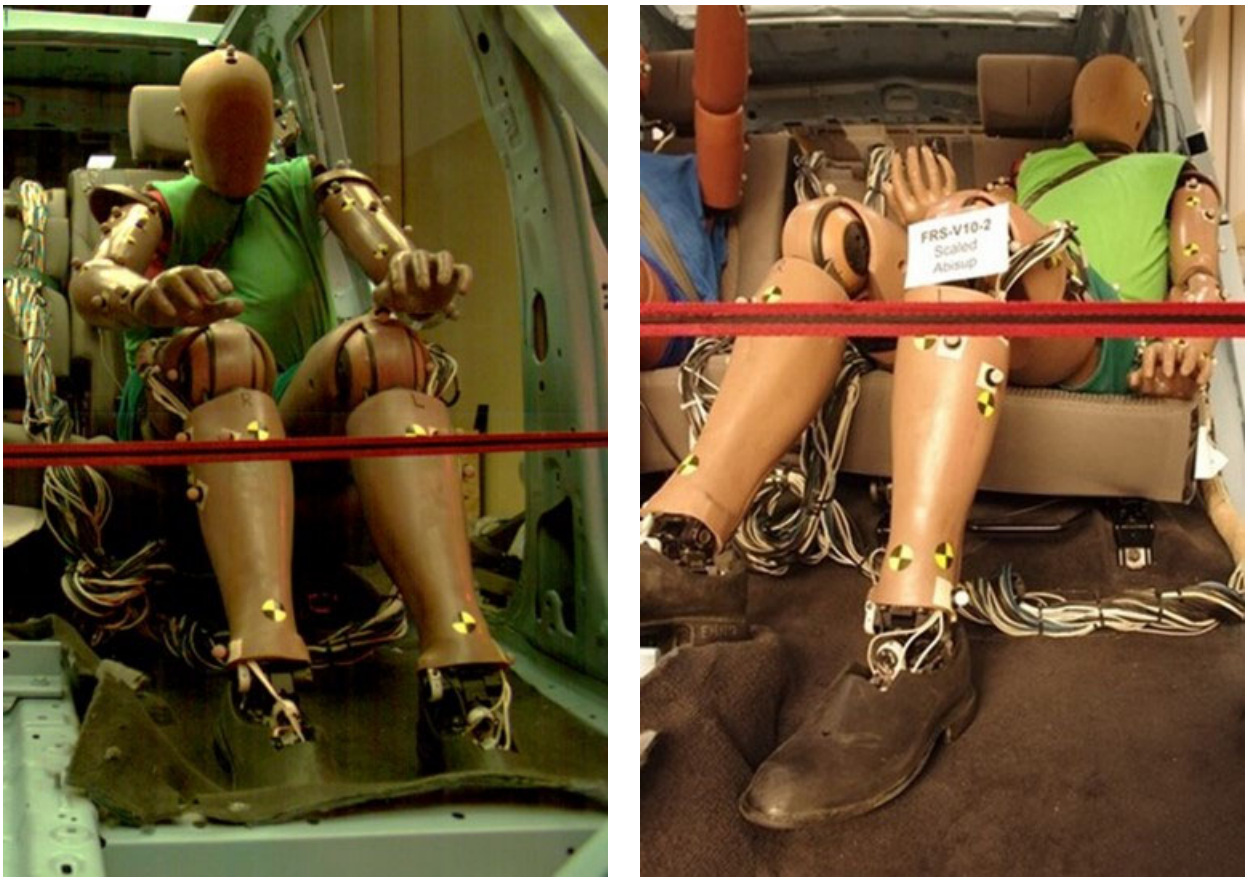

Figure I-27. The Toes of the THOR-50M Contacted the Riser for the Front Seat During Test V10-2: Video Frame at Contact (Left) and Finale Posture (Right). This Minor Contact Did Not Affect the Test Results

Test FRS-V10-3

The primary change for Test V10-3 (NCAP85) was further reduction of the sled pulse. The pulse was scaled by an additional 93 percent to reduce the energy to the maximum level the ServoSled could achieve.

Another change for Test V10-3 was the implementation of ramps to fill the front portion of the rear seat foot wells. These ramps were designed to keep the ATD toes from contacting the front seat risers. The ramps were fixed beneath the carpeting. The ramp on the Hybrid III side is shown in Figure I-28. The ramps were successful in eliminating toe contact.

Figure I-29 shows an expanded leather bib designed to help prevent shoulder belt penetration between the neck and shoulder assemblies of the THOR-50M and subsequent damage to the belt. This bib encompasses the neck and covers more of the shoulder. Figure I-29 also shows the T1 accelerometer mount shroud installed on the top of the left side of the spine box. The T1 mount is positioned on the right side. Although there was not an accelerometer mounting block on the left side, the shroud was installed to help fill the gap between the spine and shoulder and better prevent belt penetration of the space. This approach was successful in preventing the shoulder belt from getting trapped between the neck and shoulder assemblies during Test V10-3.

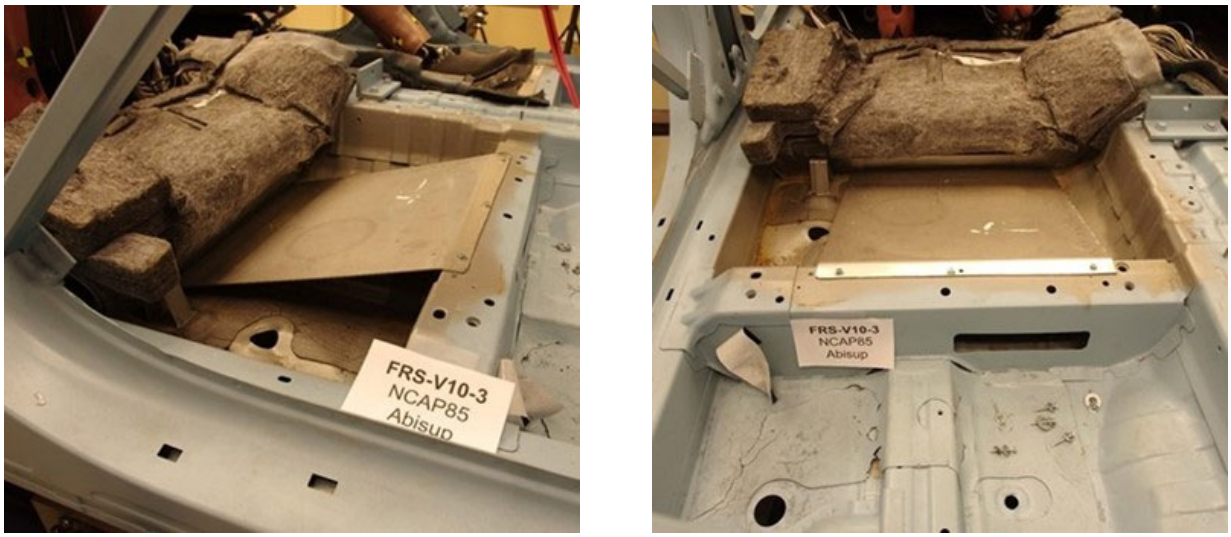

Figure I-28. Ramps Installed for Both ATDs in Buck V10 Prior to Test V10-3: These Ramps Were Designed to Prevent Contact Between the Dummy Toes and the Front Seat Riser

Figure I-29. The Expanded Bib Covering the Shoulder of the THOR-50M for Test V10-3 (Left), and the T1 Shroud Used to Fill the Space on the Left Side of the Dummy (Right)

Figure I-30 shows the damage to the repair of the THOR-50M neck collar flesh. The repair largely remained intact even for this higher-energy test. Figure I-31 shows the minor damage to the ABISUP abdomen for this higher-energy test. This was the final ATD sled test.

Figure I-32 shows the overall seat bottom damage from Test V10-3. Although this was an NCAP85 test, most damage was commensurate with the previous lower-energy tests, as the seat support structures had largely deflected and deformed as much as possible before contacting the buck deck. This is shown in Figure I-33, which catalogs the detailed damage to the seat bottom support structures (hinges, baskets, and lower frames). Minor differences compared to the lower-energy tests were the puckering of the seat track rail around the inboard rear-seat anchor point for Hybrid III, and minor deformation of this rail (bottom of Figure I-33).

Figure I-30. Damage to the THOR-50M Collar Repair From Test V10-3

Figure I-31. Damage to the THOR-50M ABISUP Abdomen During Test V10-3: All Damage Was Minor, and Was Related to Seams and Corners of the ABISU

Figure I-32. Seat Bottom Damage From Test V10-3

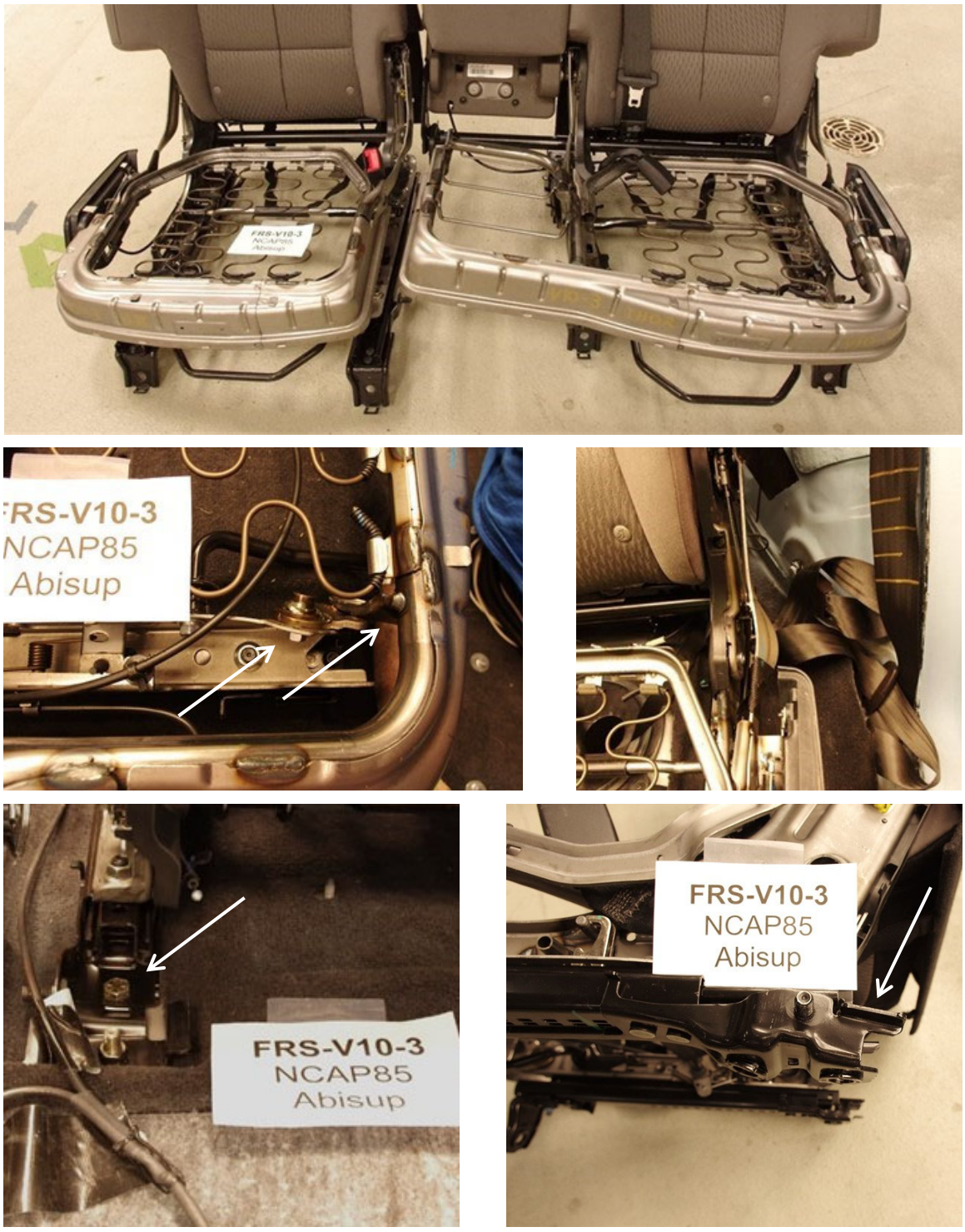

Figure I-33. Details of Seat Bottom Damage From Test V10-3

Test FRS-V13-2

Test V13-2 (NCAP85) resulted in damage to the outboard seat bottom supports on the buck for both ATD locations, as shown in Figure 34. This minor damage to sheet metal structures was repaired prior to Test V13-3.

Figure I-34. Damage to Seat Bottom Supports From Test V13-2 (Left and Right Outboard)

Tests FRS-V14-3 and FRS-V14-4

The TDAS Pro DAS used for these tests experienced failures for two tests: Test V14-3 and V14-4. Test V14-4 was conducted as a repeat of Test V14-3 because of the DAS glitches. However, the DAS largely repeated its behavior for Test V14-4. After detailed debugging efforts and consultation with DTS (the manufacturer of the TDAS Pro), it was established that the source of the problems was one of the racks that housed eight, eight-channel modules. The same 36 data channels were affected for both tests. The system and buck-mounting schemes were reconfigured to use two 4-module racks instead. This solved the problem for subsequent tests. It was also possible to reconstitute the scrambled data collected during Test V14-3 and V14-4.

There were several steps taken to reconstitute the data. Typically, the DAS would "collect" data from a transducer configured for one channel in a different channel. This would make the data appear in the incorrect location, with the wrong scale factor (sensitivity) applied. Further, this swap would occur sometime after the start of acquisition, instead of at the start (time zero). Finally, there would be a gap in data collection, usually lasting for 10–20 ms. Therefore, data channels had to be combined using the correct beginning data points and the subsequent points from the channel into which the data were swapped. An adjusted scale (taking into account the transducer sensitivities, excitation voltages, and channel gains) was applied to correct the values of the data points recovered from the swapped channel. Then, the data gaps were bridged by a combination of interpolation techniques and splicing of exemplar data. As these gaps occurred near the start of the responses, this approach did not affect any peak values or injury metric calculations. Additionally, datasets not having these gaps bridged are provided.

Figure I-35 shows an example of the effects associated with the data confusion. The incorrect data appearing in a DAS channel are shown as the "Data Channel" (black trace) and the correct signal having an incorrect scale factor applied are shown as the "Swapped Channel" (red trace). The bracket symbol indicates a gap (flat line) in the data. Prior to the start of this bracket the Data Channel points are correct. After the start of the bracket, the Data Channel points are incorrect. For the duration of this bracket, the Swapped Channel points are zero. After the end of

this bracket, the Swapped Channel points require adjustment. No processing has been applied to these traces. Figure I-36 shows the completely corrected, spliced, and processed data (red trace) compared to a version of the data manipulated using the same techniques, with the exception of bridging the zero-data gap (black trace). Table I-1 provides a compilation of the channels affected by this DAS data scrambling phenomenon. Those marked with an asterisk were not swapped with another channel but did suffer a dropout in data.

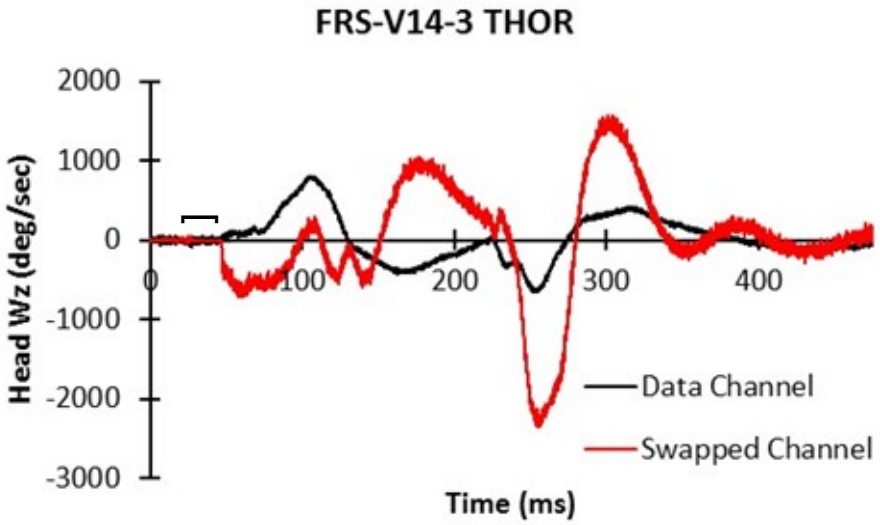

Figure I-35. Incorrect Data Appearing in a DAS "Data Channel" (Black Trace) and the Correct Signal Having an Incorrect Scale Factor Applied Appearing in the "Swapped Channel" (Red Trace)

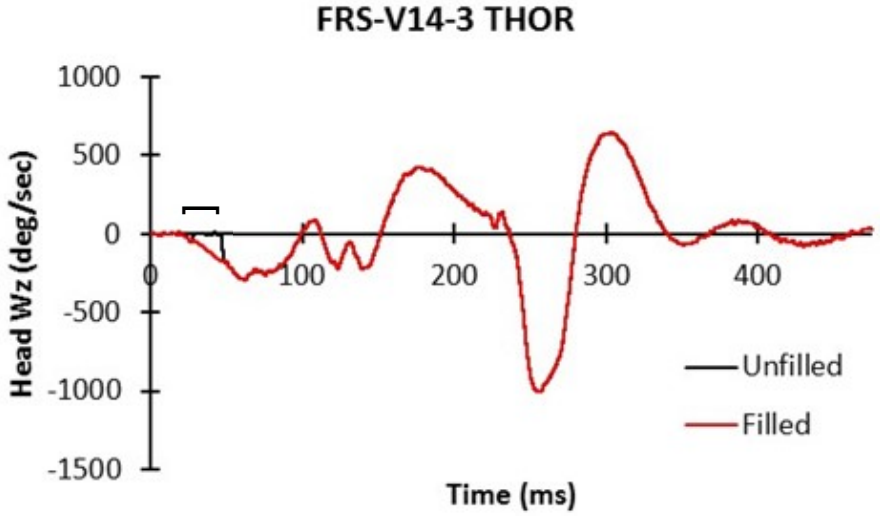

Figure I-36. An Example of Completely Corrected, Spliced, and Processed Data Recovered after A DAS Failure (the "Filled" Red Trace). the Effect of Filling the Data Gap Can be Seen by Comparing to the Red Trace to the Black ("Unfilled") Trace

Table I-1. List of Signals Affected by DAS Channel Scrambling and Data Dropouts

Test V14-3	**Test V14-4**
Head Acceleration X	Head Acceleration X
Head Acceleration Y	Head Acceleration Y
Head Acceleration Z	Head Acceleration Z
Head Angular Velocity X	Head Angular Velocity X
Head Angular Velocity Y	Head Angular Velocity Y
Head Angular Velocity Z	Head Angular Velocity Z
Front Neck Spring Force Z	Front Neck Spring Force Z
Rear Neck Spring Force Z	Rear Neck Spring Force Z
Lower Neck Force Y	Lower Neck Force Y
Lower Neck Force Z	Lower Neck Force Z
Lower Neck Moment X	Lower Neck Moment X
Lower Neck Moment Y	Lower Neck Moment Y
Lower Neck Moment Z	Lower Neck Moment Z
T1 Acceleration X	T1 Acceleration X
T1 Acceleration Y	T1 Acceleration Y
T1 Acceleration Z	T1 Acceleration Z
Upper Left Thorax IR-TRACC	Upper Left Thorax IR-TRACC*
Upper Left Thorax Y-axis Rotation	Upper Left Thorax Y-axis Rotation*
Upper Left Thorax Z-axis Rotation	Upper Left Thorax Z-axis Rotation*
Upper Right Thorax IR-TRACC	Upper Right Thorax IR-TRACC*
Upper Right Thorax Y-axis Rotation	Upper Right Thorax Y-axis Rotation*
Upper Right Thorax Z-axis Rotation	Upper Right Thorax Z-axis Rotation*
Lower Left Thorax IR-TRACC	Lower Left Thorax IR-TRACC*
Lower Left Thorax Y-axis Rotation	Lower Left Thorax Y-axis Rotation*
Lower Left Thorax Z-axis Rotation*	Lower Left Thorax Z-axis Rotation
Lower Right Thorax IR-TRACC*	Lower Right Thorax IR-TRACC
Lower Right Thorax Y-axis Rotation*	Lower Right Thorax Y-axis Rotation
Lower Right Thorax Z-axis Rotation*	Lower Right Thorax Z-axis Rotation
T6 Acceleration X*	T6 Acceleration X
T6 Acceleration Y*	T6 Acceleration Y
T6 Acceleration Z*	T6 Acceleration Z
T12 Force X*	T12 Force X
Right ABISUP Pressure	Right ABISUP Pressure
Left ASIS Force X	Left ASIS Force X
Left ASIS Moment Y	Left ASIS Moment Y
Right ASIS Force X	Right ASIS Force X

*Data did not scramble, but data was still lost for these channels during time windows similar to the other channels.

Test FRS-V15-4

Figure I-37 (left side) shows example minor damage to the THOR-50M pelvis flesh that resulted from interaction with the lap belt. Figure I-37 (right side) also shows the repair that was performed. This repair proved to be robust throughout testing.

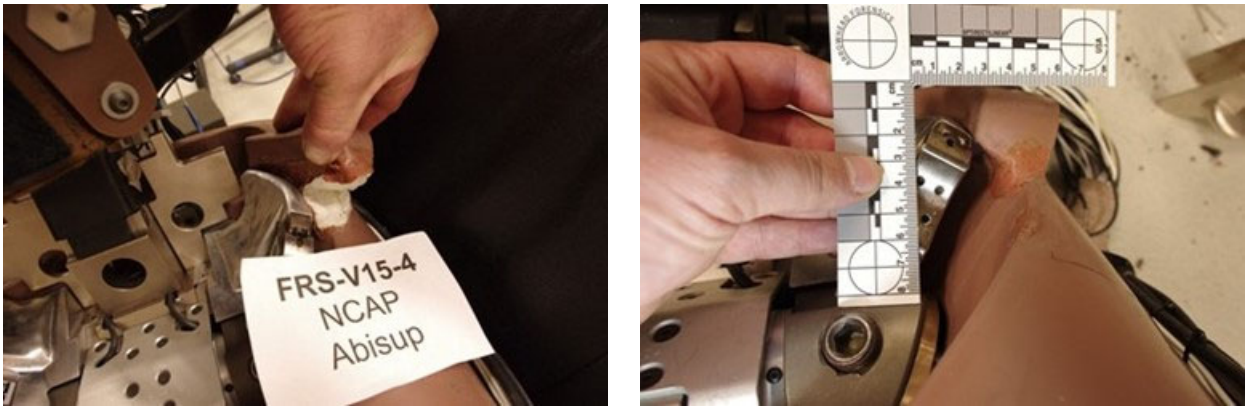

Figure I-37. Damage to the Pelvis Flesh of the THOR-50M From Test 15-4 (Left), and Subsequent Repair (Right)

Test FRS-V19-3

When extricating the THOR-50M from the buck after Test V19-3, it was determined that some of the fasteners in the dummy had loosened. Figure I-38 shows some of the bolts in the thorax that had come loose over the course of testing. Figure I-39 shows the loose bolts within the thoracoabdominal junction of the THOR-50M. Both dummies were inspected thoroughly. Only the THOR-50M was found to have issues. All fasteners were tightened to specification, with the addition of thread-locking compound. Consultation with the Vehicle Research and Test Center determined that the fasteners that were adjusted would not require recertification of the dummy. Discovery of the loose fasteners resulted in more thorough inspections of the dummies being conducted between tests. It is not known the extent to which these fasteners had loosened during previous tests. Test V19-3 was repeated as Test V19-4 to ascertain the integrity of the data conducted during Test V19-3 and for previous tests. The great similarity between the THOR-50M results for Test V19-3 and Test V19-4 suggested that there was not cause for concern regarding earlier data, and reinforced the confidence in those data.

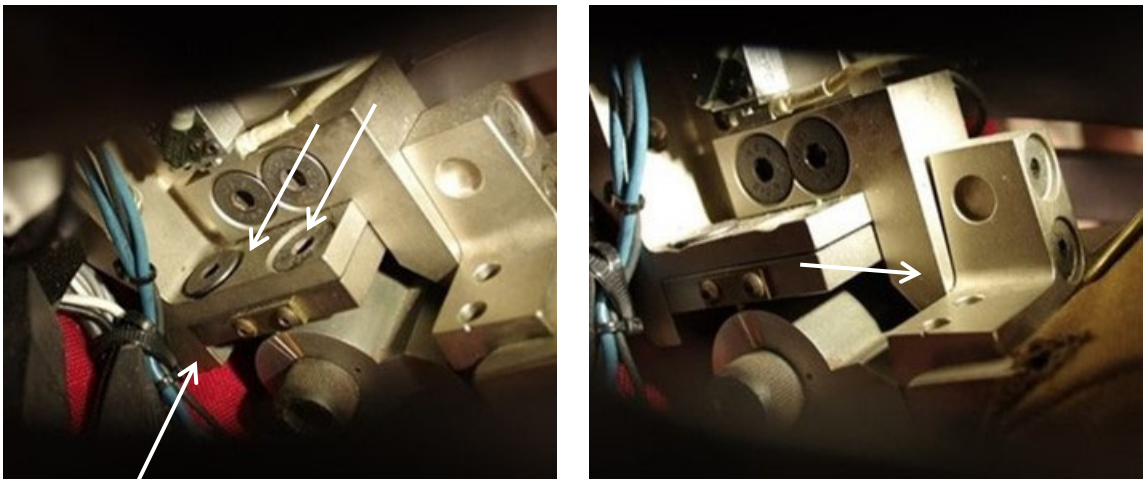

Figure I-38. Loose Bolts in the Thorax of the THOR-50M Discovered After Test V19-

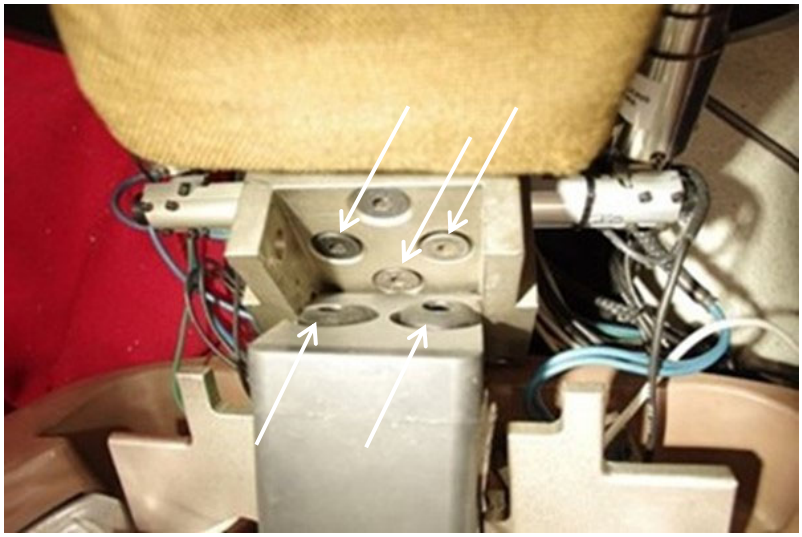

Figure I-39. Loose Bolts at the Thoracoabdominal Junction of the THOR-50M Discovered After Test V19-3

Test FRS-V19-4

Test V19-4 provides an example of the damage and repairs to the ABISUP (Figure I-40). Typically, the ABISUP was damaged at transitions in geometry, skin seams, regions that interface with the pelvis of the THOR-50M. Small strips of reinforced flexible plastic were bonded to the skin of the ABISUP at damage locations. The strips were kept small so that repairs could conform to the geometry of the ABISUP, and so that repairs could be adjusted or improved easily. While the ABISUP accumulated damage throughout testing, the repairs proved to be robust, needing to be redone rarely, and were applied to regions of the ABISUP thought to have little influence on the response of the device.

Figure I-40. Collection of Robust Repairs Made to the THOR-50M ABISUP Between Tests: Damage Typically Occurred at the Seams and Corners of the ABISUP

Appendix J. Pre- and Post-Test Images

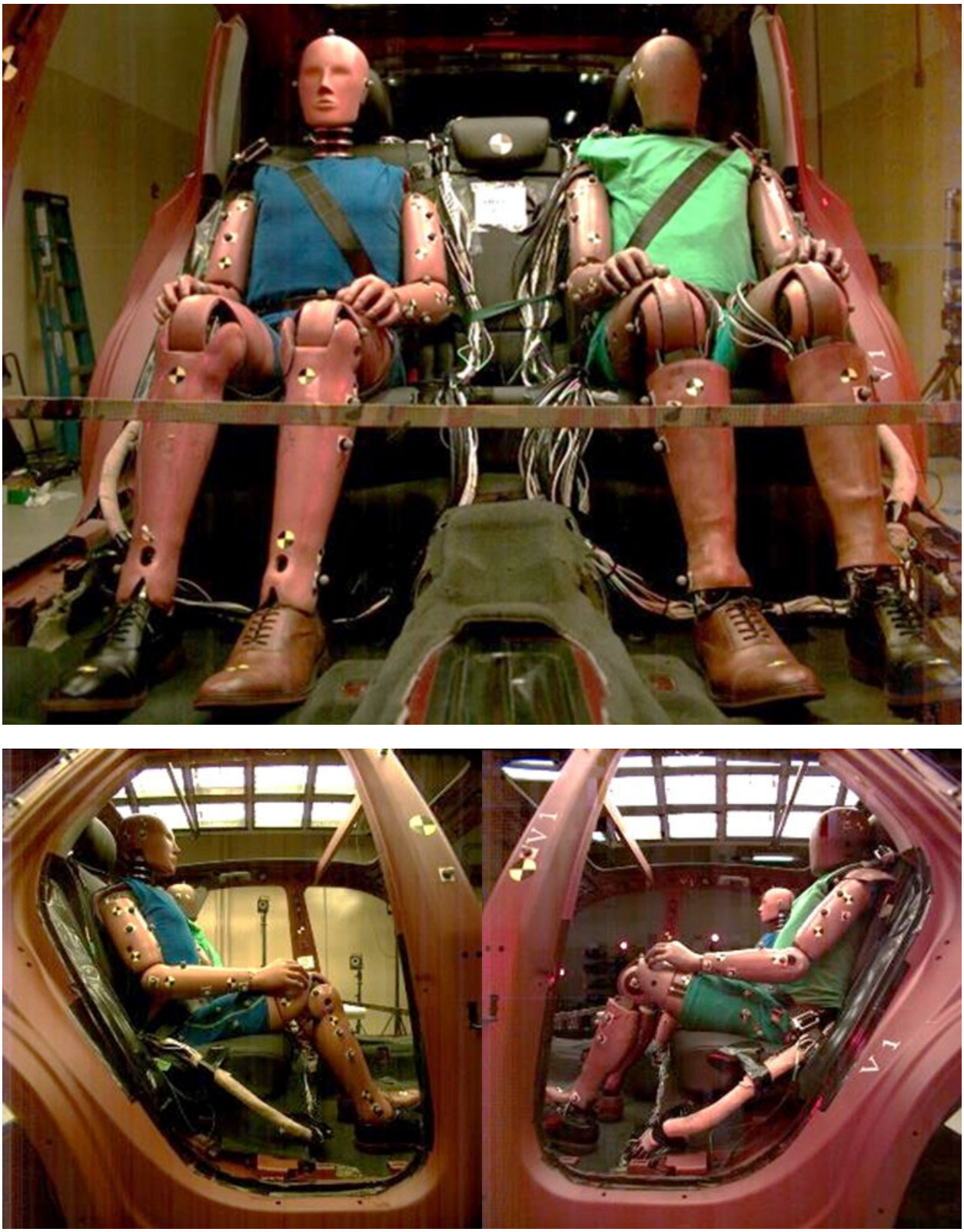

Figure J-1. Pre-Test Images for Vehicle V1, Test 1 (Generic Pulse)

Figure J-2. Post-Test Images for Vehicle V1, Test 1 (Generic Pulse)

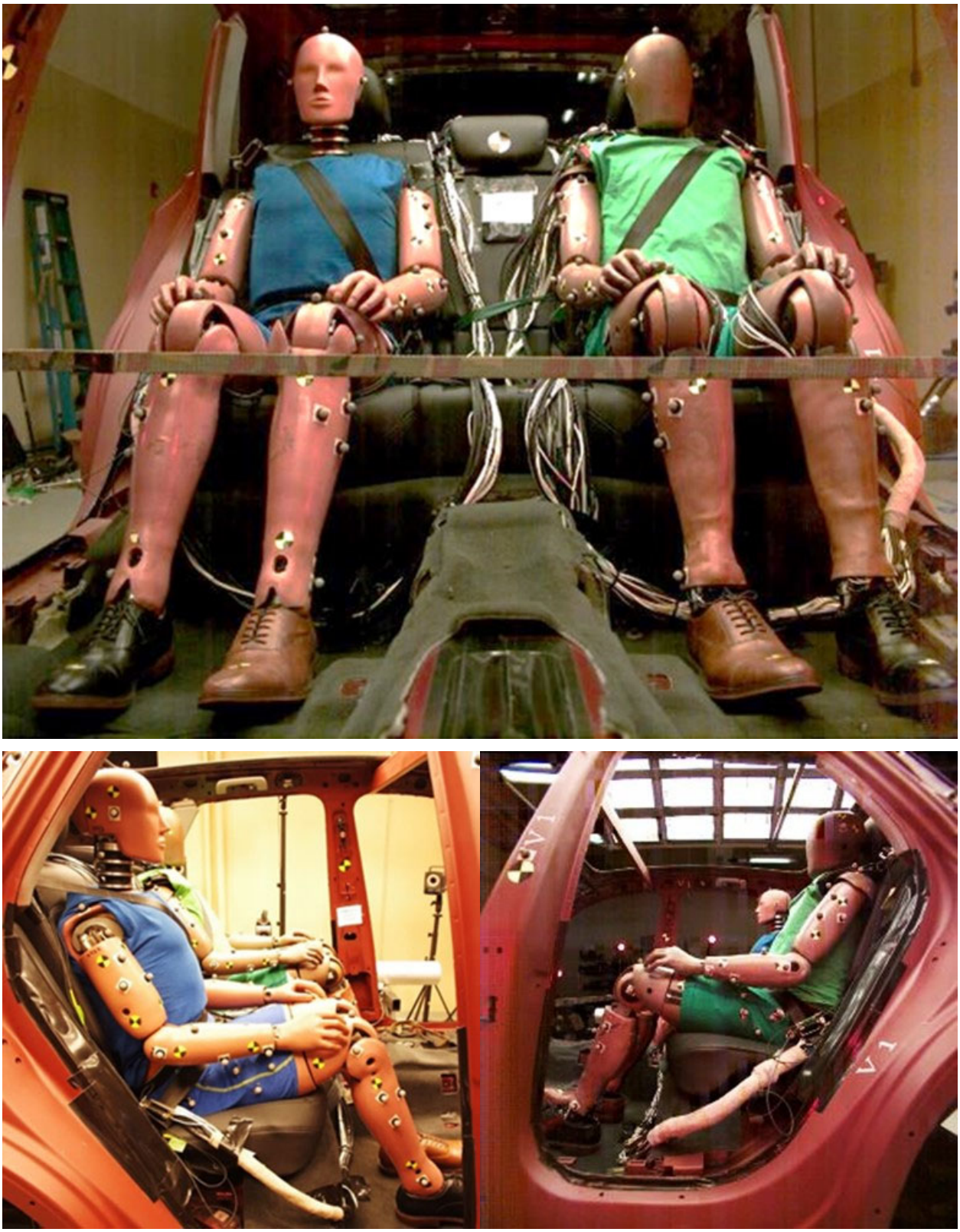

Figure J-3. Pre-Test Images for Vehicle V1, Test 2 (Specific/Scaled Pulse)

Figure J-4. Post-Test Images for Vehicle V1, Test 2 (Specific/Scaled Pulse)

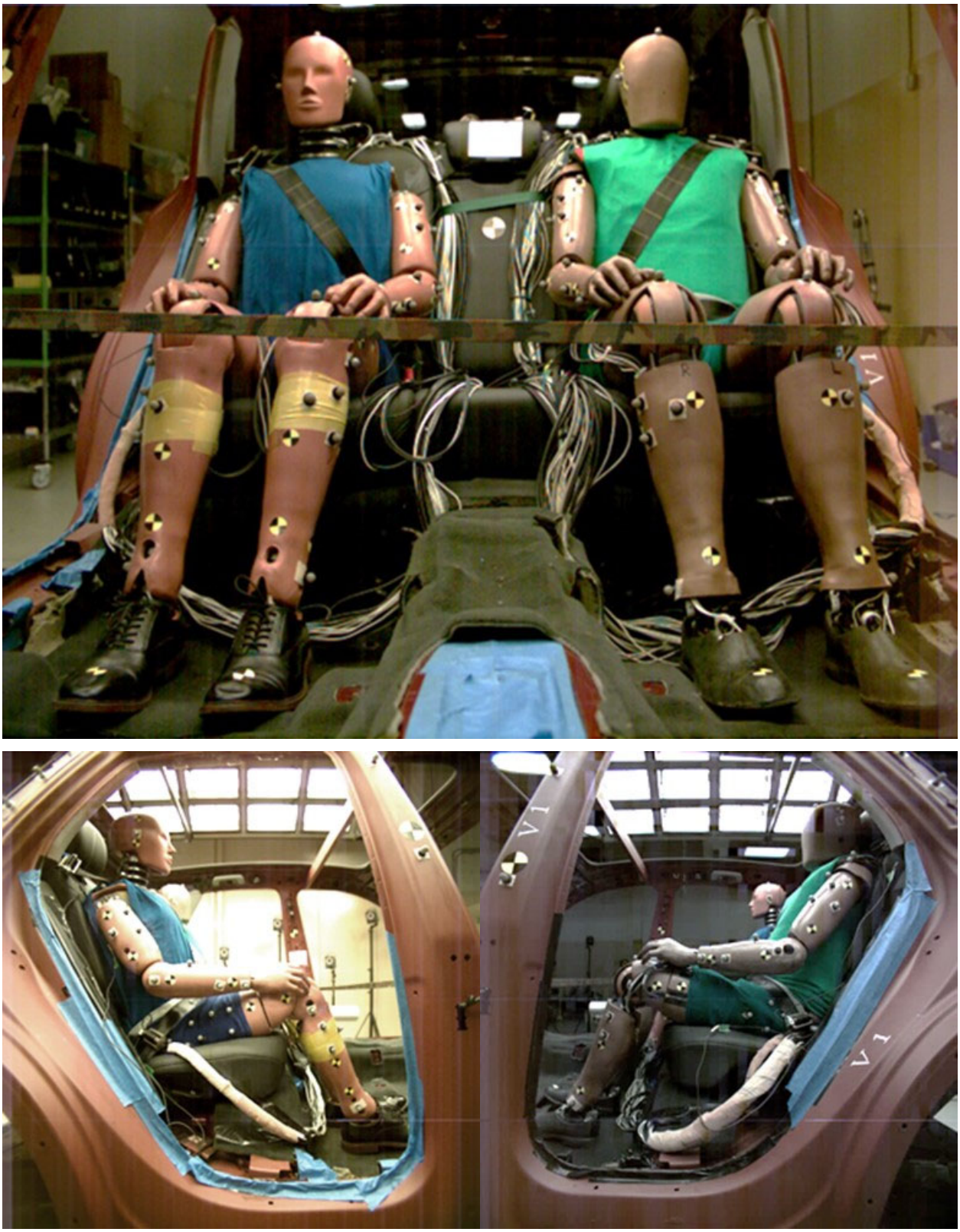

Figure J-5. Pre-Test Images for Vehicle V1, Test 3 (NCAP85 Pulse

Figure J-6. Post-Test Images for Vehicle V1, Test 3 (NCAP85 Pulse)

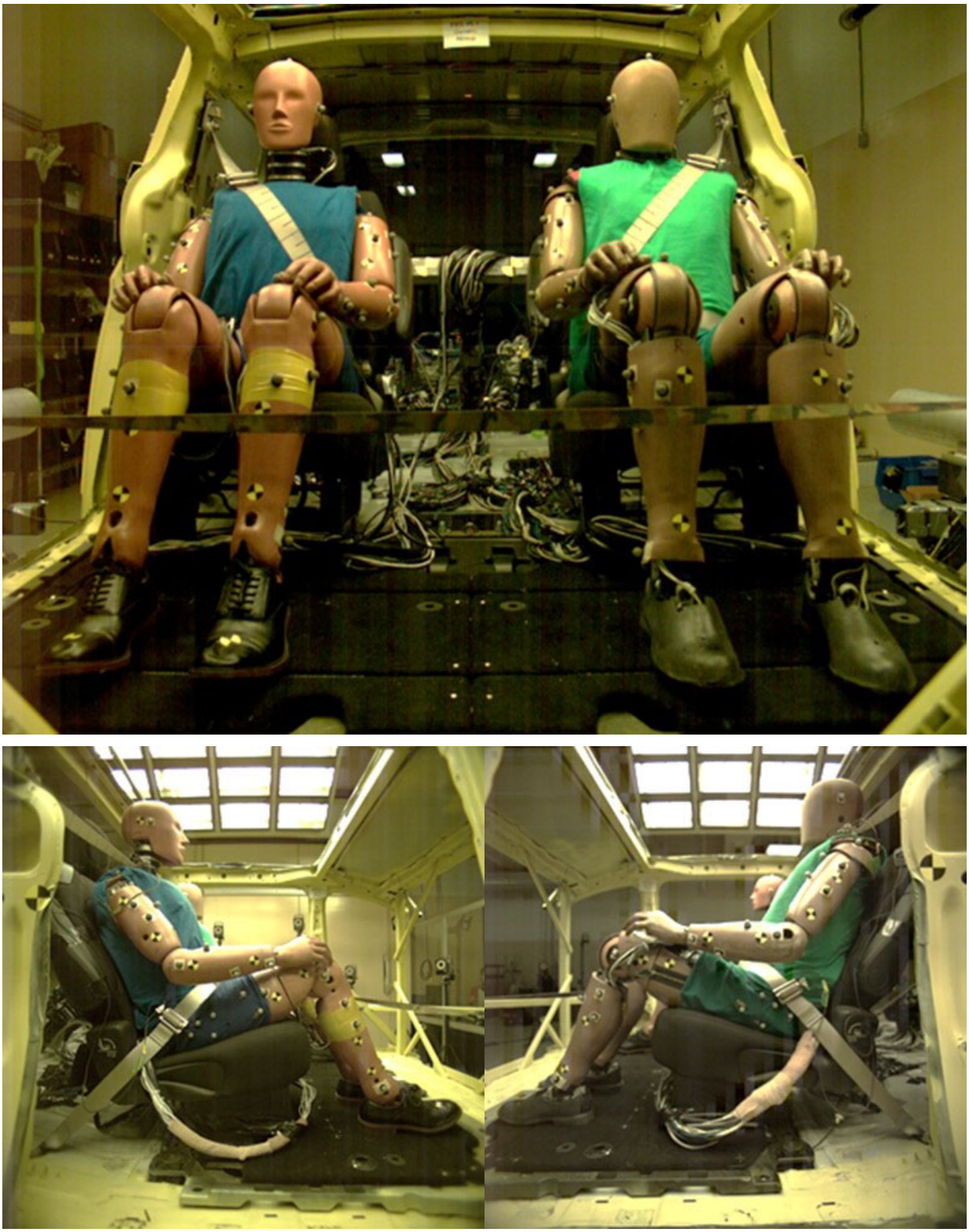

Figure J-7. Pre-Test Images for Vehicle V6, Test 1 (Generic Pulse)

Figure J-8. Post-Test Images for Vehicle V6, Test 1 (Generic Pulse)

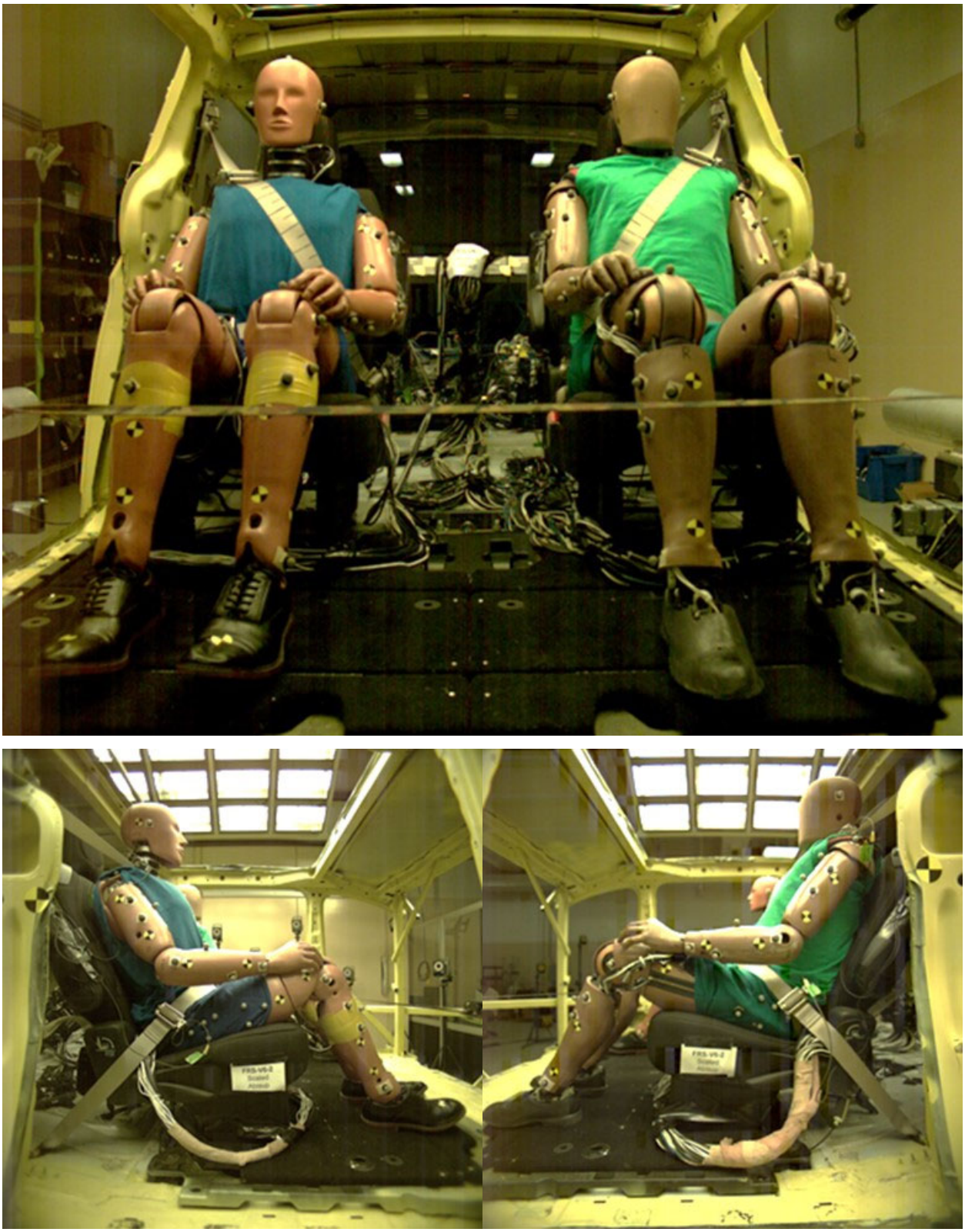

Figure J-9. Pre-Test Images for Vehicle V6, Test 2 (Specific/Scaled)

Figure J-10. Post-Test Images for Vehicle V6, Test 2 (Specific/Scaled)

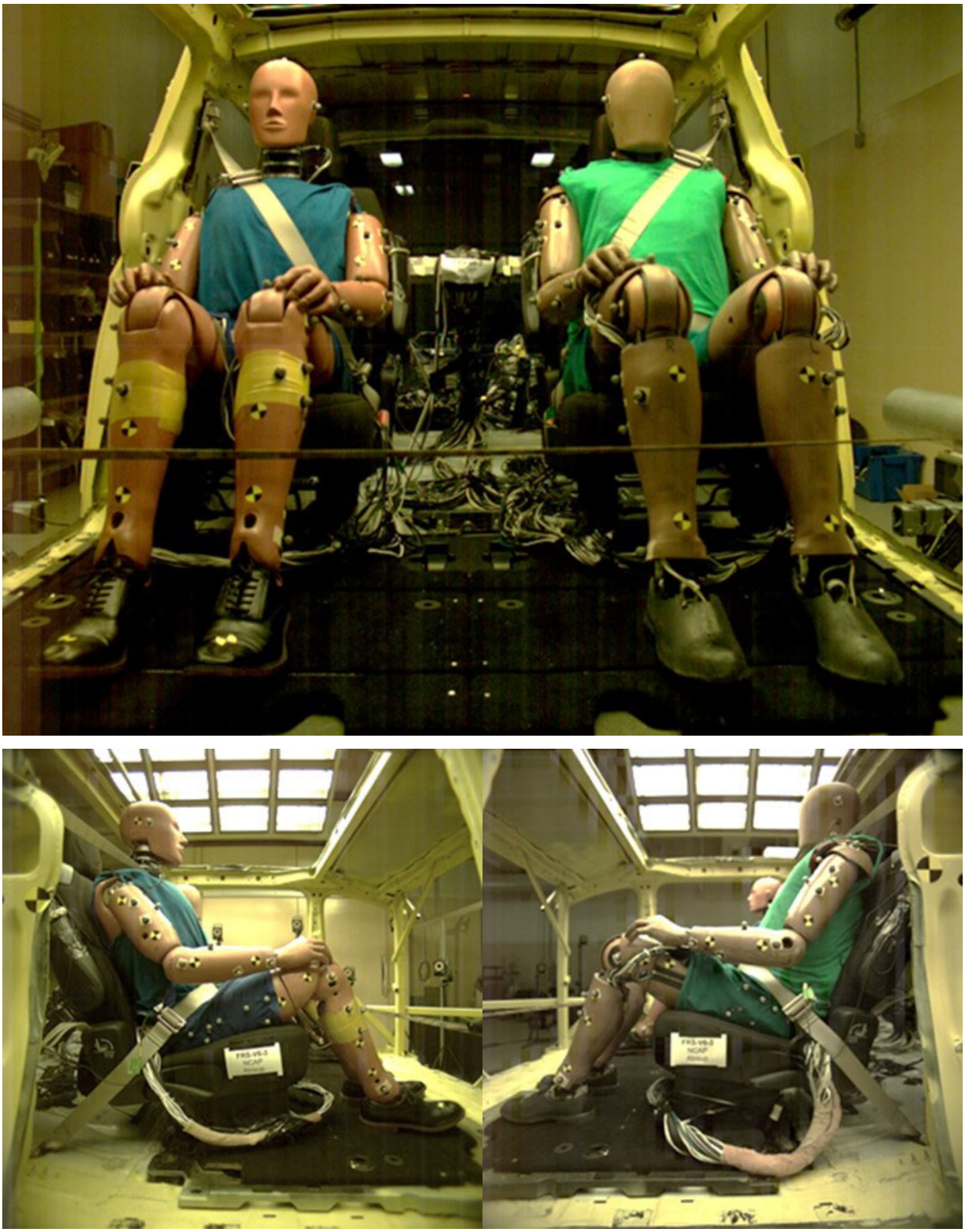

Figure J-11. Pre-Test Images for Vehicle V6, Test 3 (NCAP85)

Figure J-12. Post-Test Images for Vehicle V6, Test 3 (NCAP85)

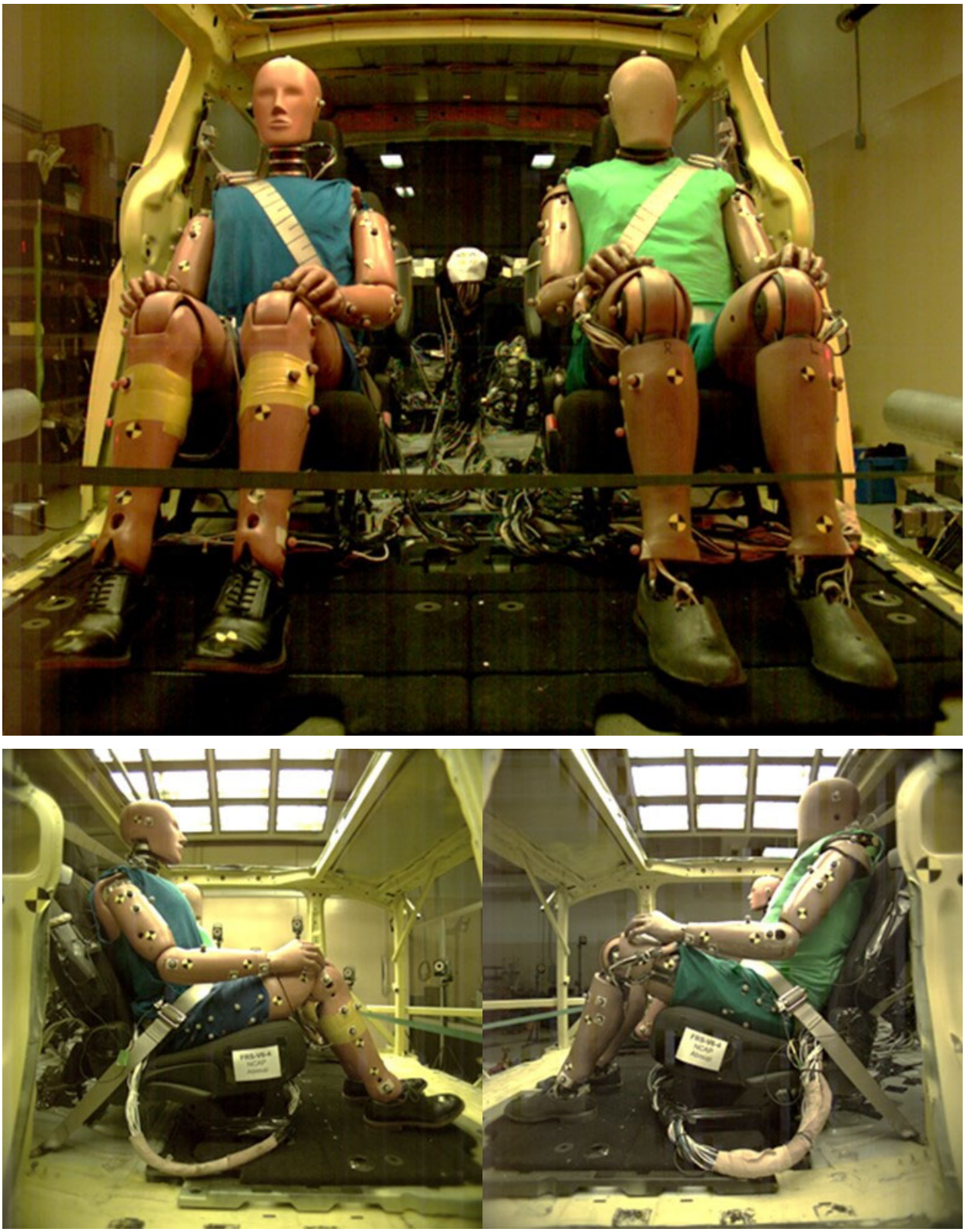

Figure J-13 Pre-Test Images for Vehicle V6, Test 4 (NCAP85 Repeat)

Figure J-14. Post-Test Images for Vehicle V6, Test 4 (NCAP85 Repeat)

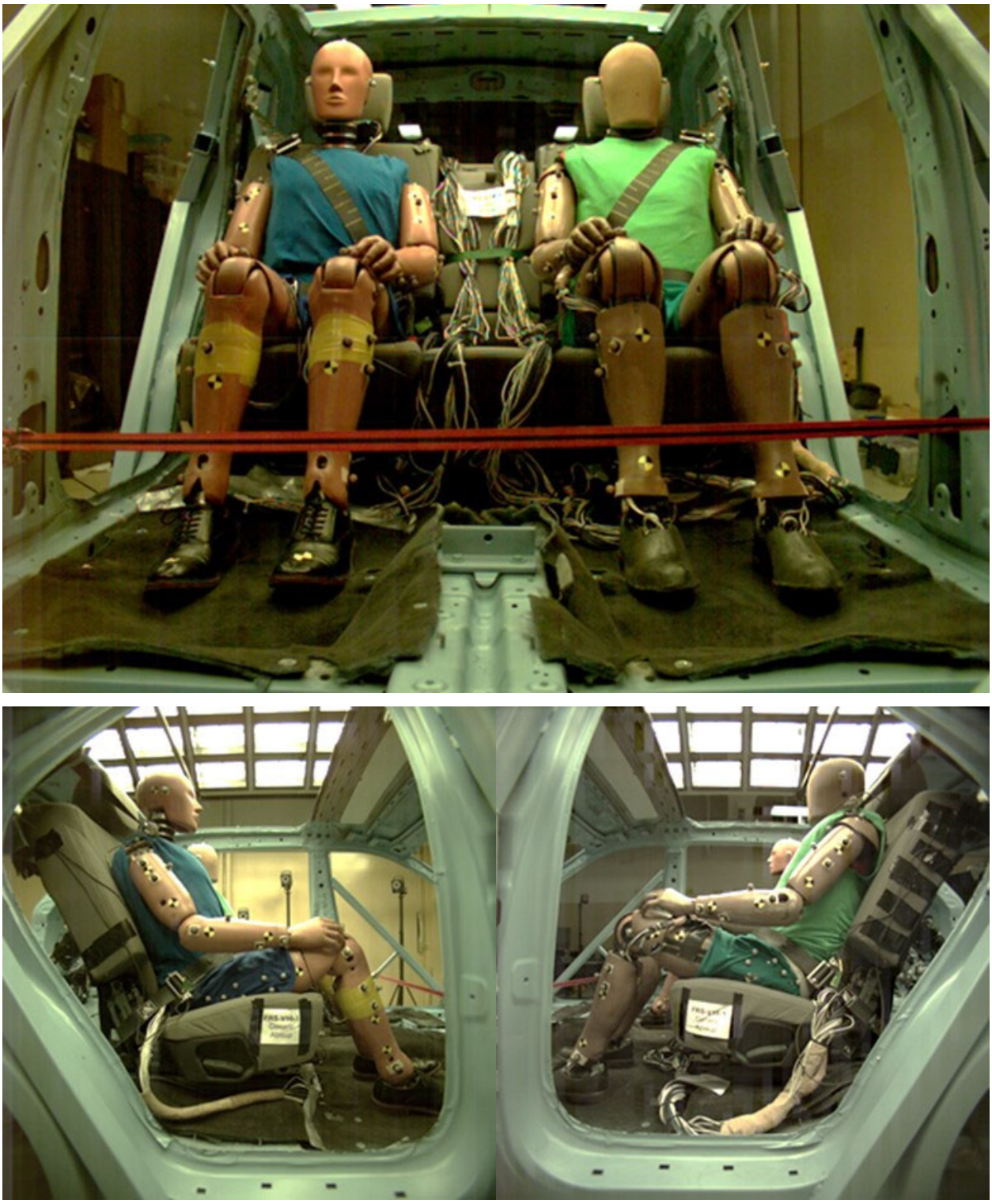

Figure J-15. Pre-Test Images for Vehicle V10, Test 1 (Generic Pulse)

Figure J-16. Post-Test Images for Vehicle V10, Test 1 (Generic Pulse)

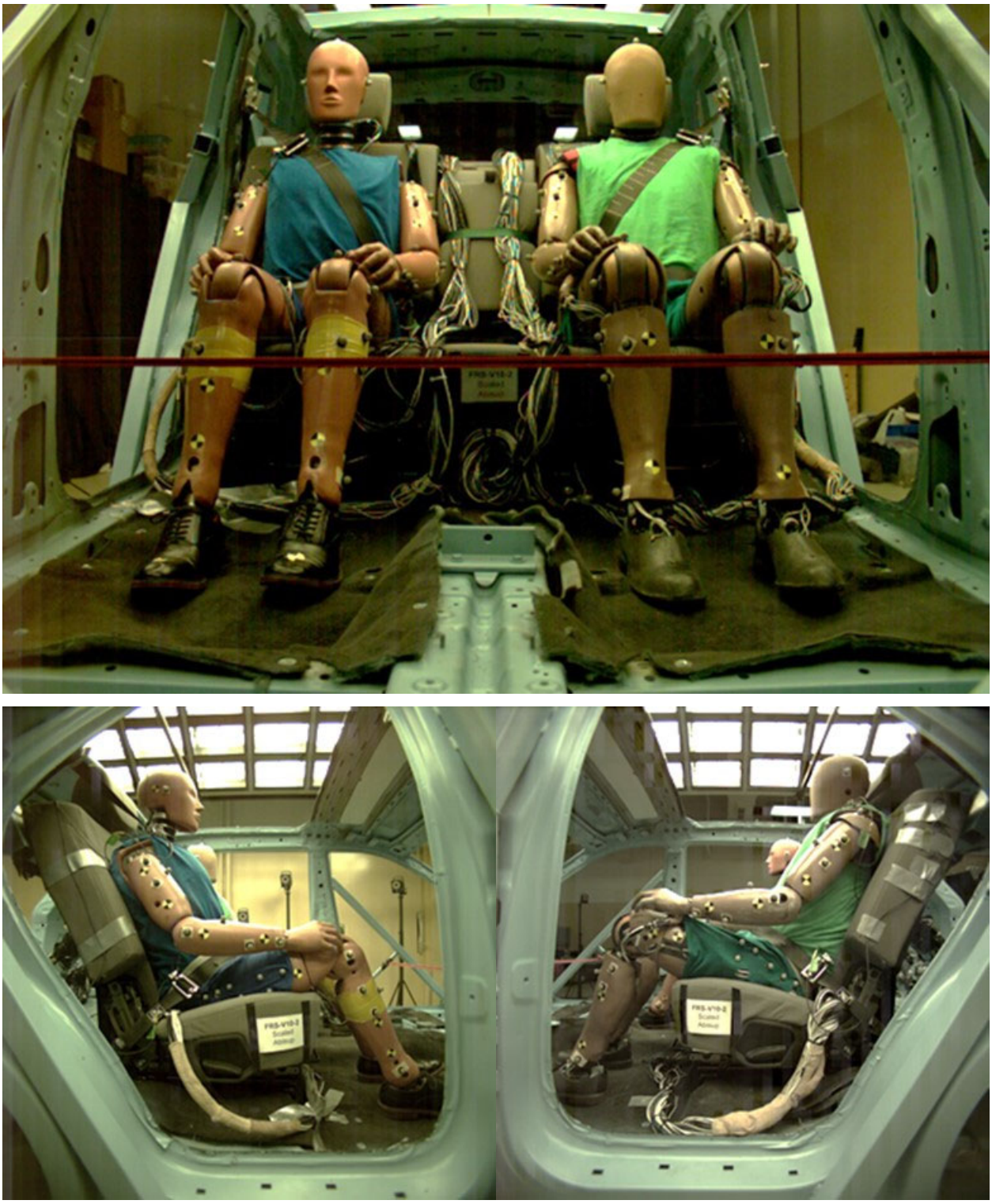

Figure J-17. Pre-Test Images for Vehicle V10, Test 2 (Specific/Scaled)

Figure J-18. Post-Test Images for Vehicle V10, Test 2 (Specific/Scaled)

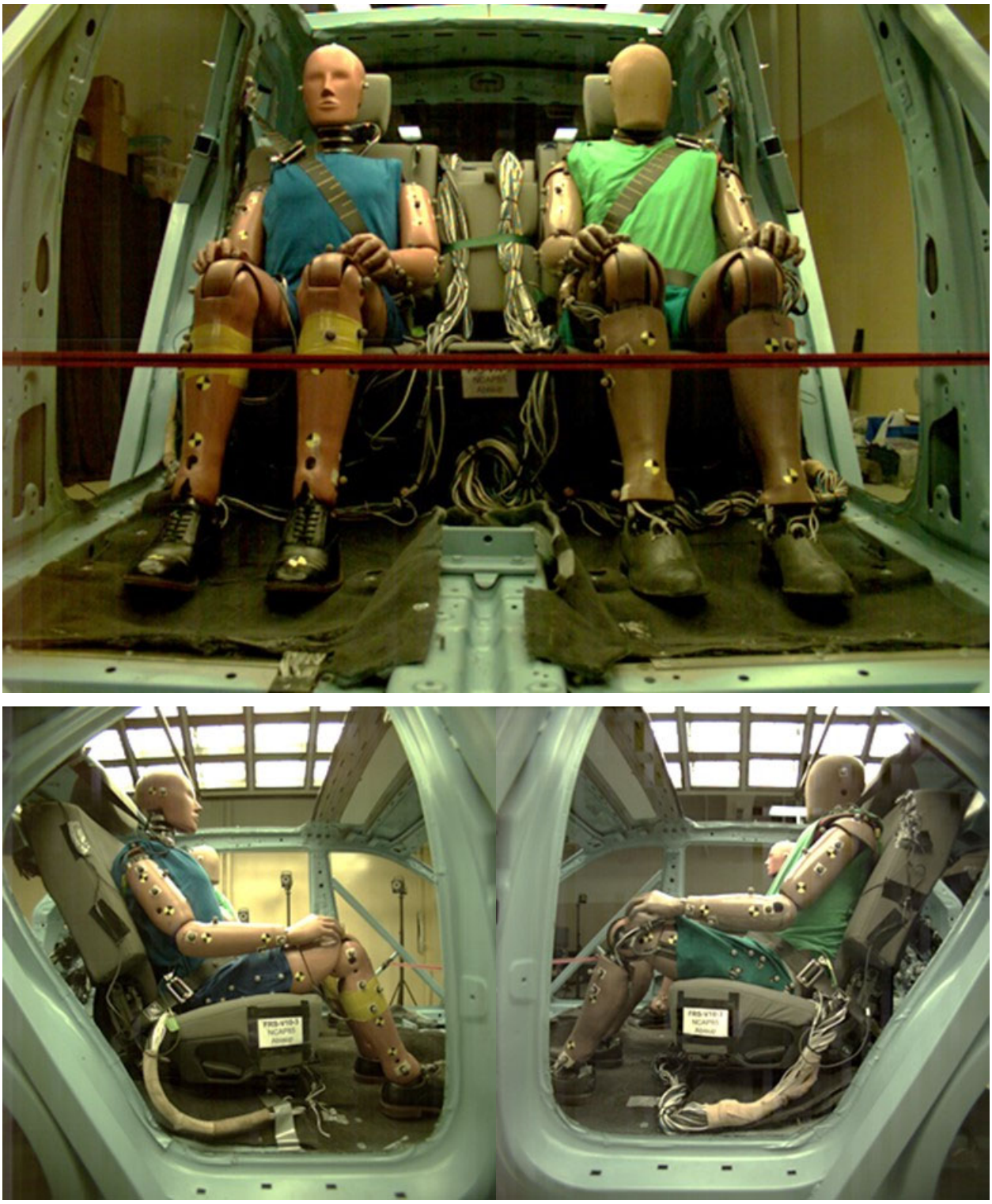

Figure J-19. Pre-Test Images for Vehicle V10, Test 3 (NCAP85)

Figure J-20. Post-Test Images for Vehicle V10, Test 3 (NCAP85)

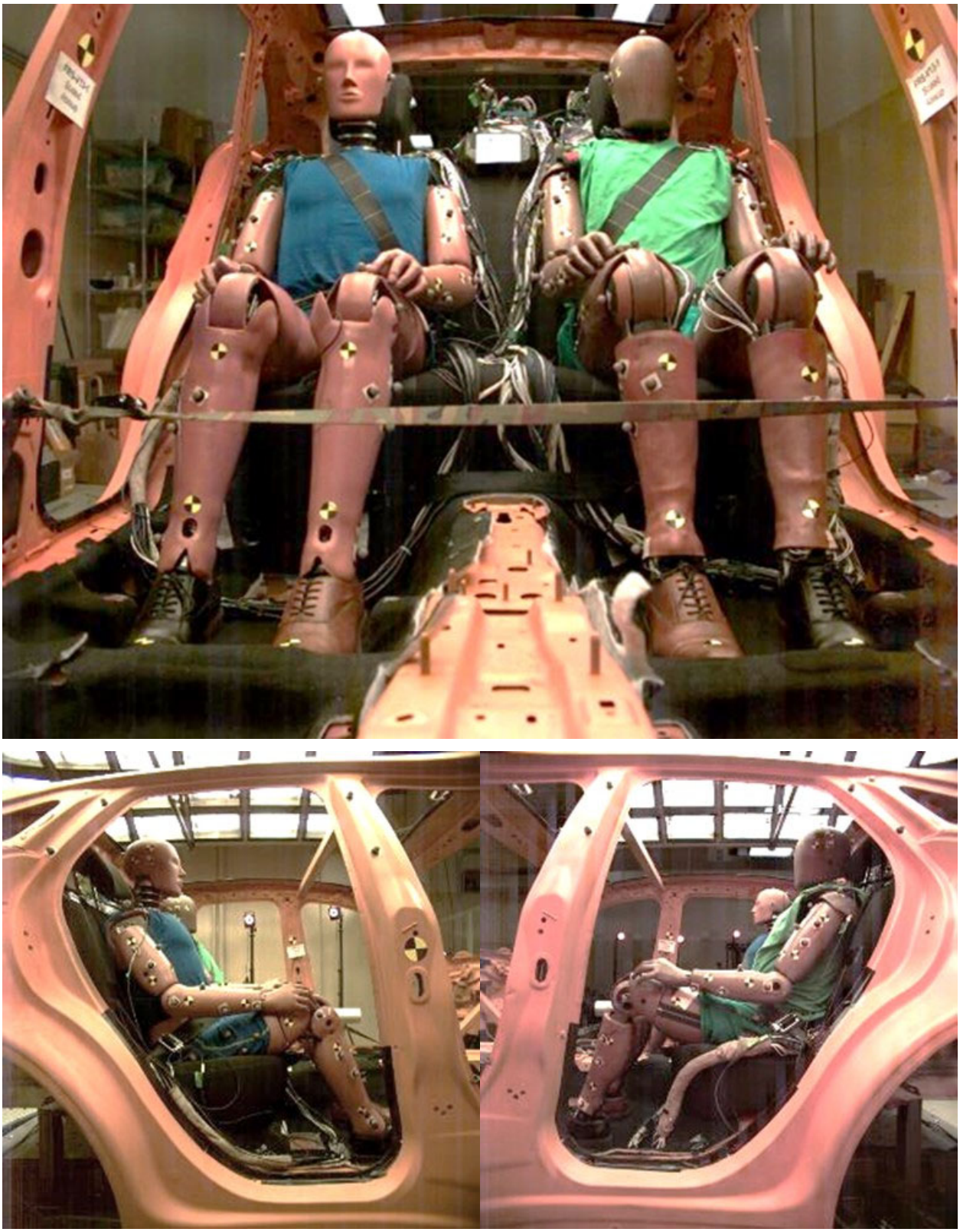

Figure J-21. Pre-Test Images for Vehicle V13, Test 1 (Specific/Scaled Pulse)

Figure J-22. Post-Test Images for Vehicle V13, Test 1 (Specific/Scaled Pulse)

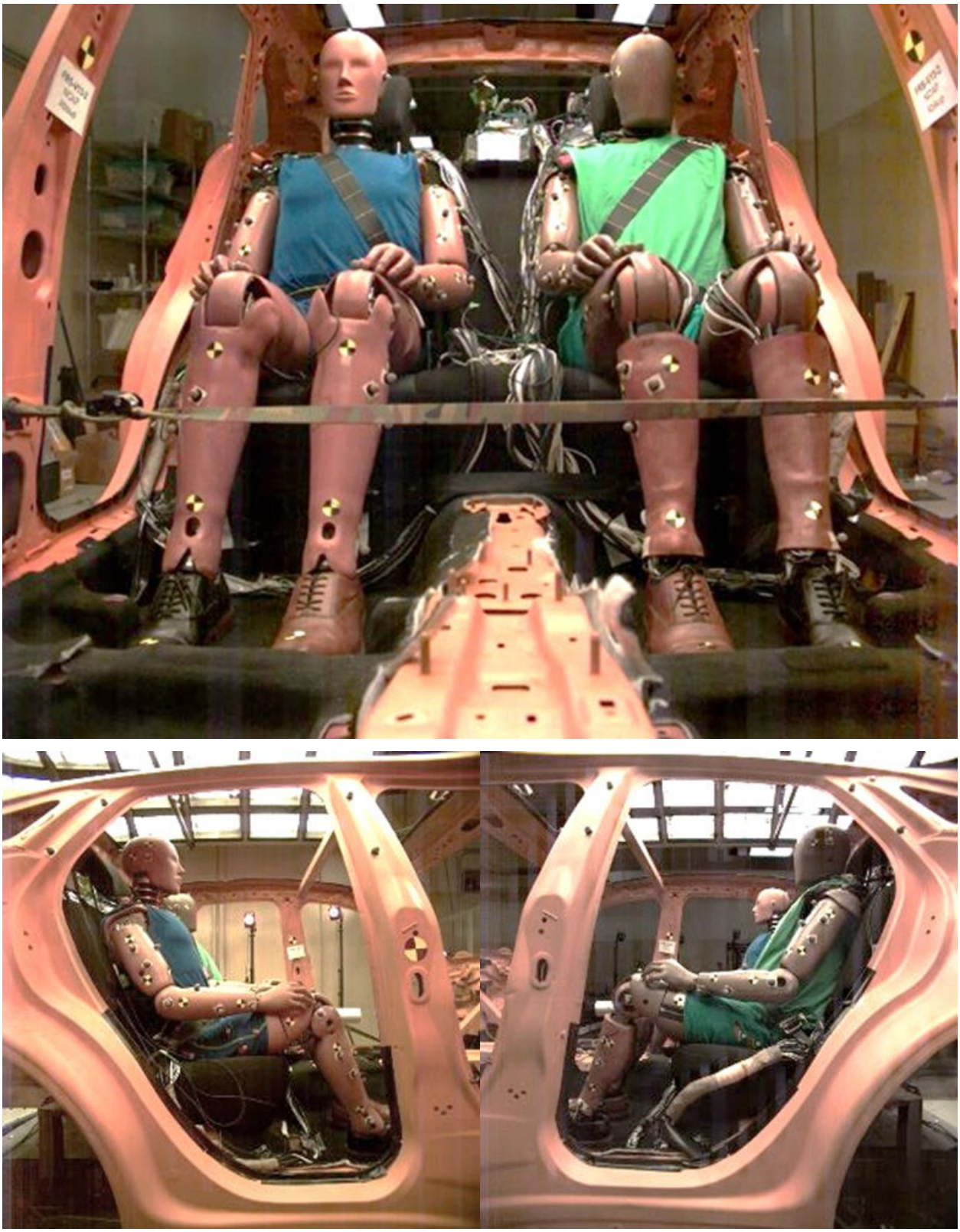

Figure J-23. Pre-Test Images for Vehicle V13, Test 2 (NCAP85 Pulse)

Figure J-24. Post-Test Images for Vehicle V13, Test 2 (NCAP85 Pulse)

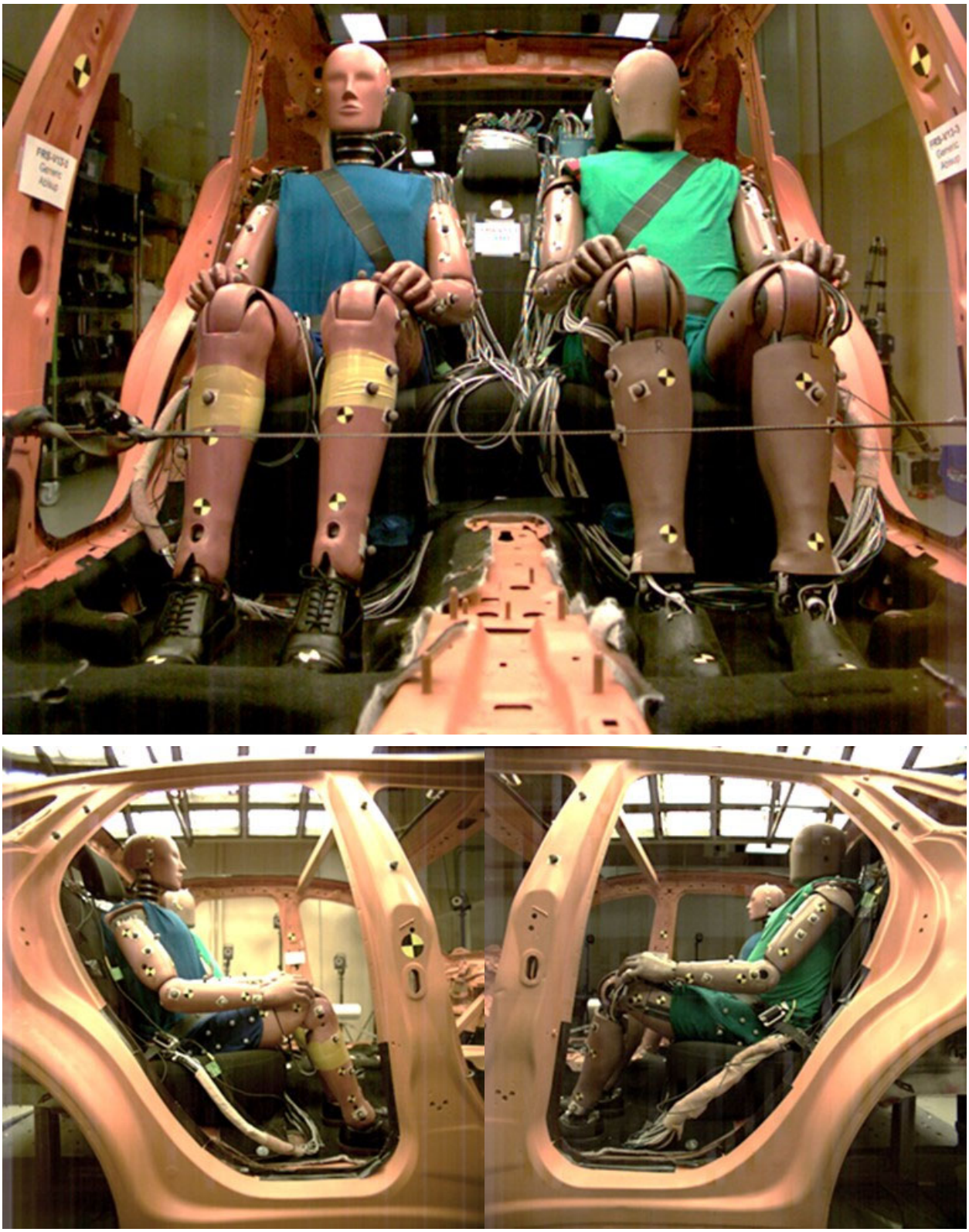

Figure J-25. Pre-Test Images for Vehicle V13, Test 3 (Generic Pulse)

Figure J-26. Pre-Test Images for Vehicle V13, Test 3 (Generic Pulse)

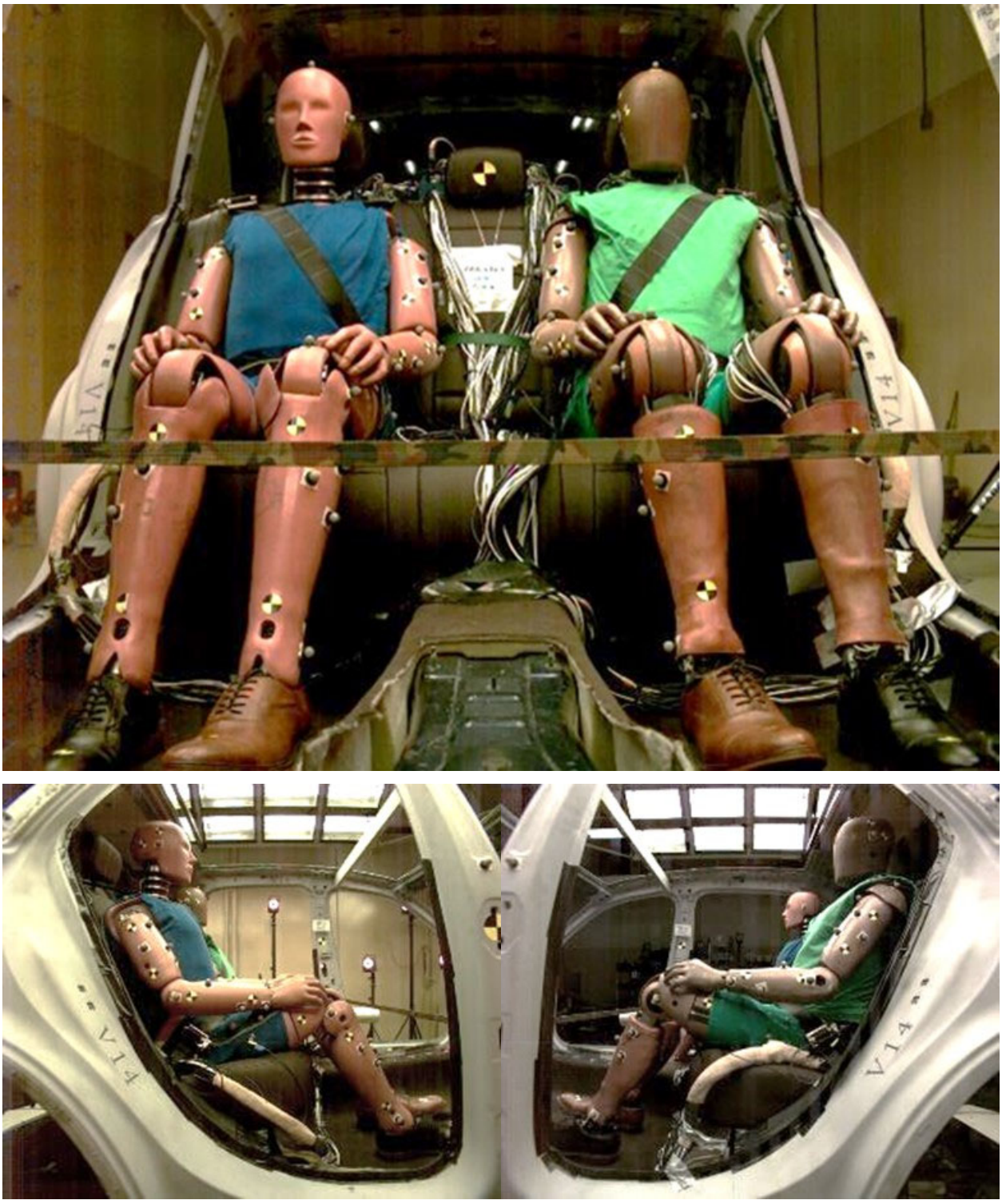

Figure J-27. Pre-Test Images for Vehicle V14, Test 1 (Generic Pulse)

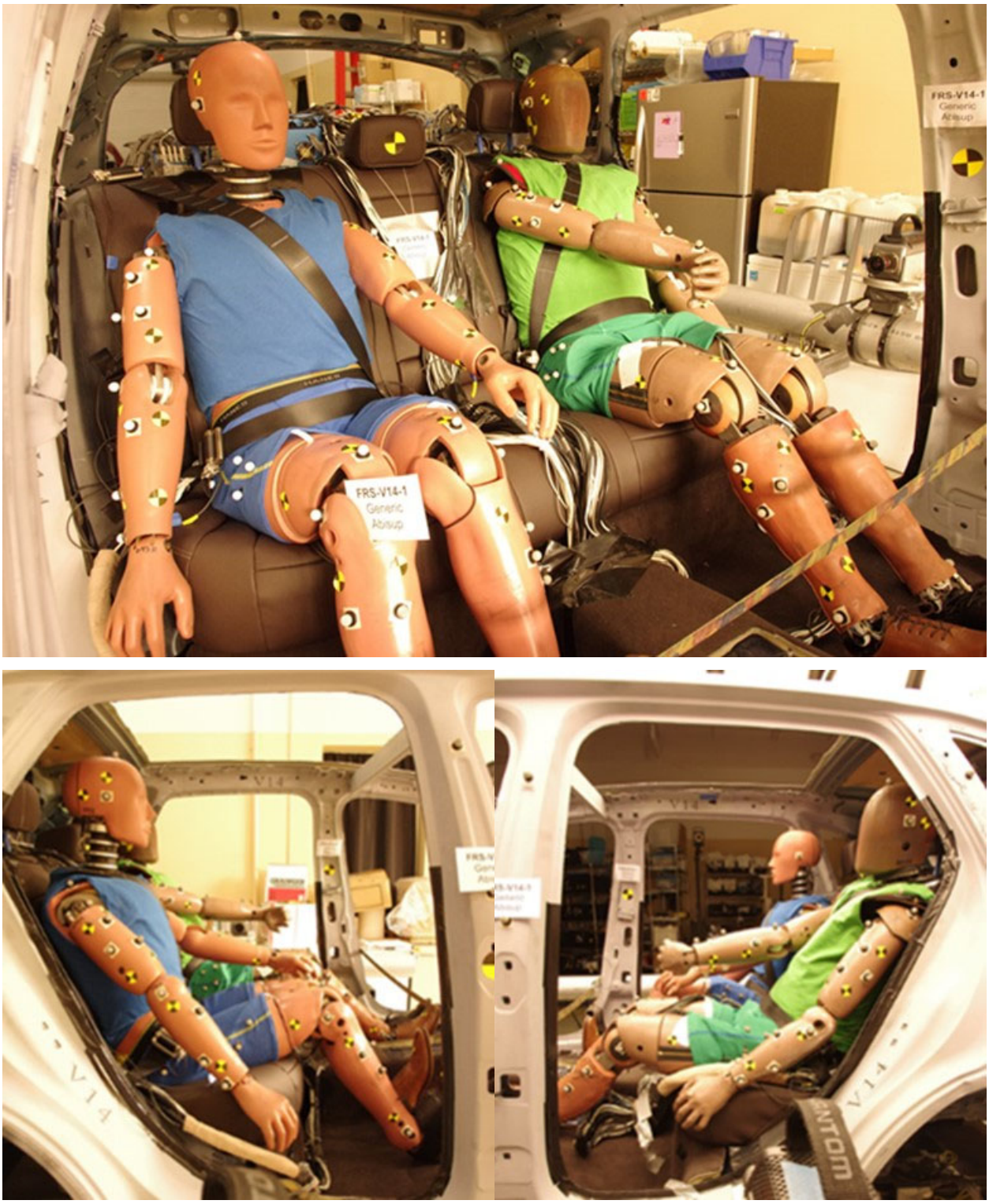

Figure J-28. Post-Test Images for Vehicle V14, Test 1 (Generic Pulse)

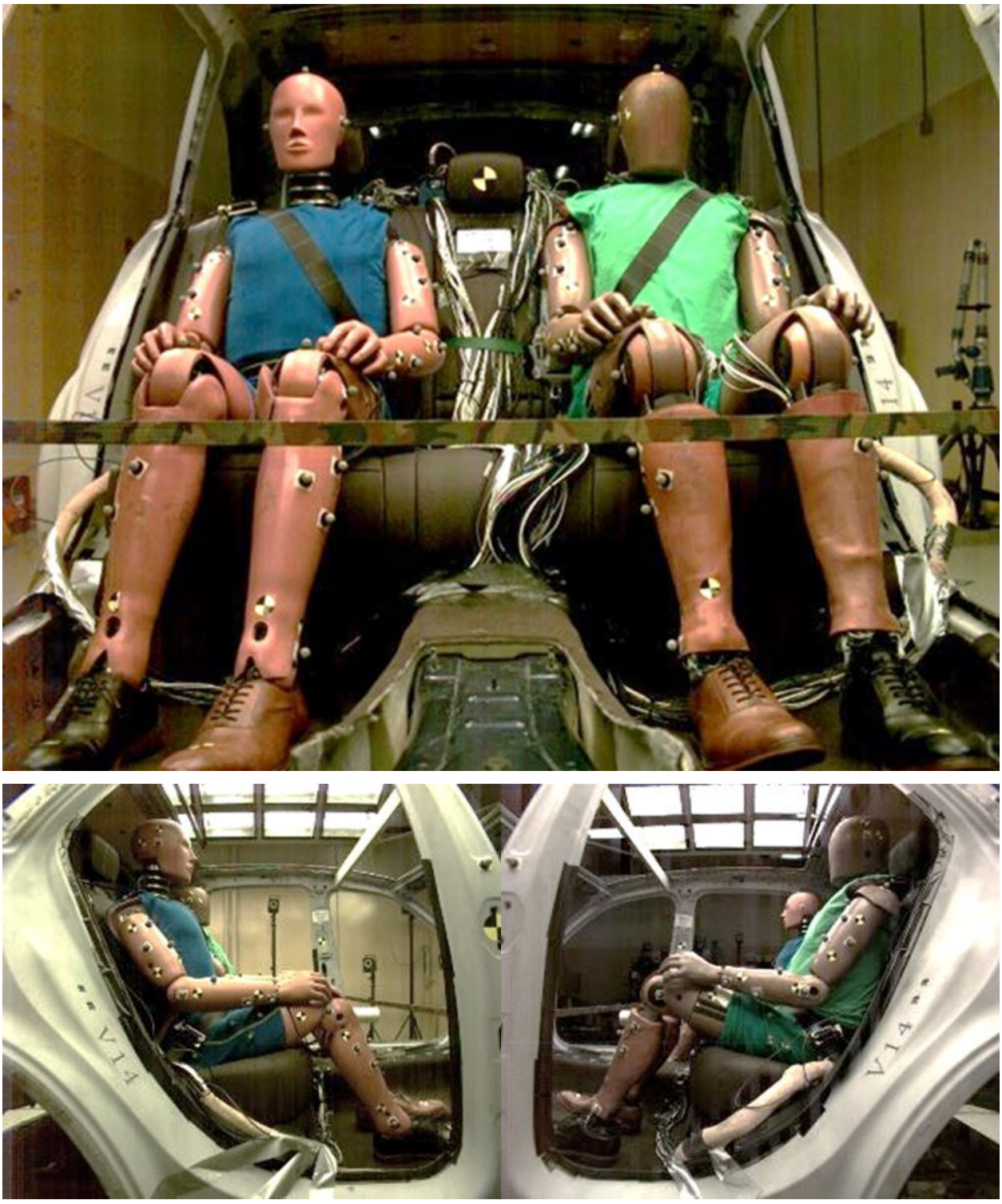

Figure J-29. Pre-Test Images for Vehicle V14, Test 2 (Specific/Scaled Pulse)

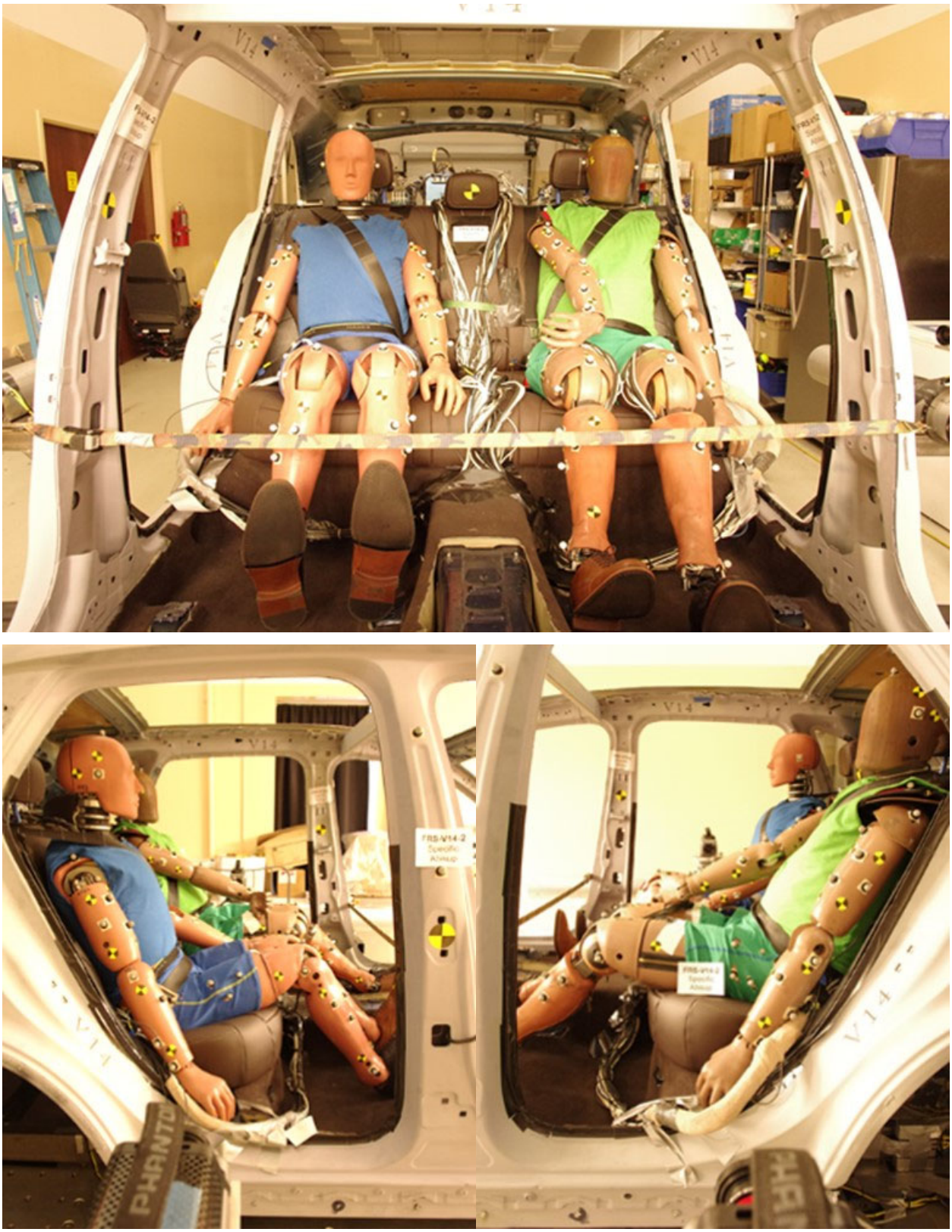

Figure J-30. Post-Test Images for Vehicle V14, Test 2 (Specific/Scaled Pulse)

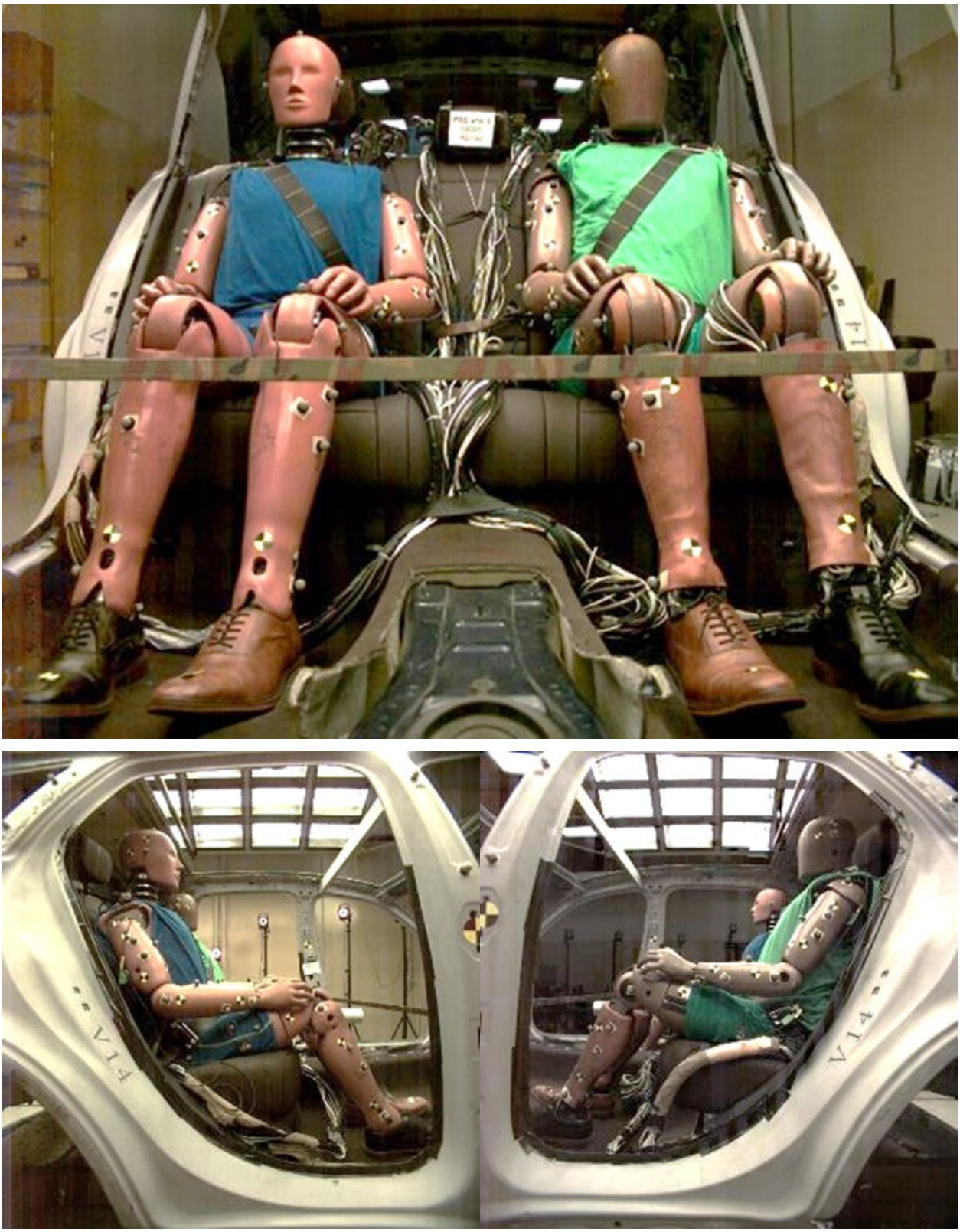

Figure J-31. Pre-Test Images for Vehicle V14, Test 3 (NCAP85 Pulse)

Figure J-32. Post-Test Images for Vehicle V14, Test 3 (NCAP85 Pulse)

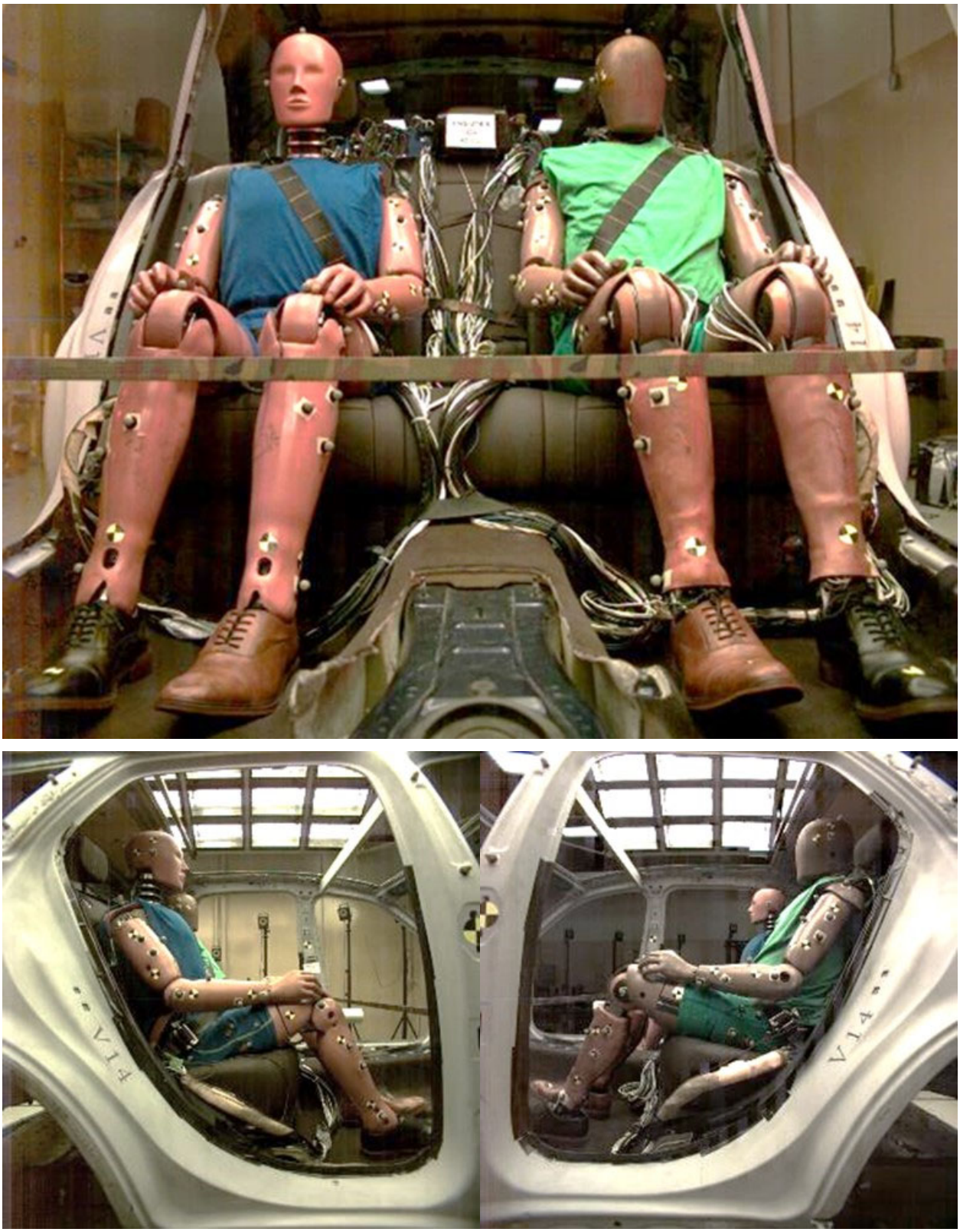

Figure J-33. Pre-Test Images for Vehicle V14, Test 4 (NCAP85 Pulse), Repeat

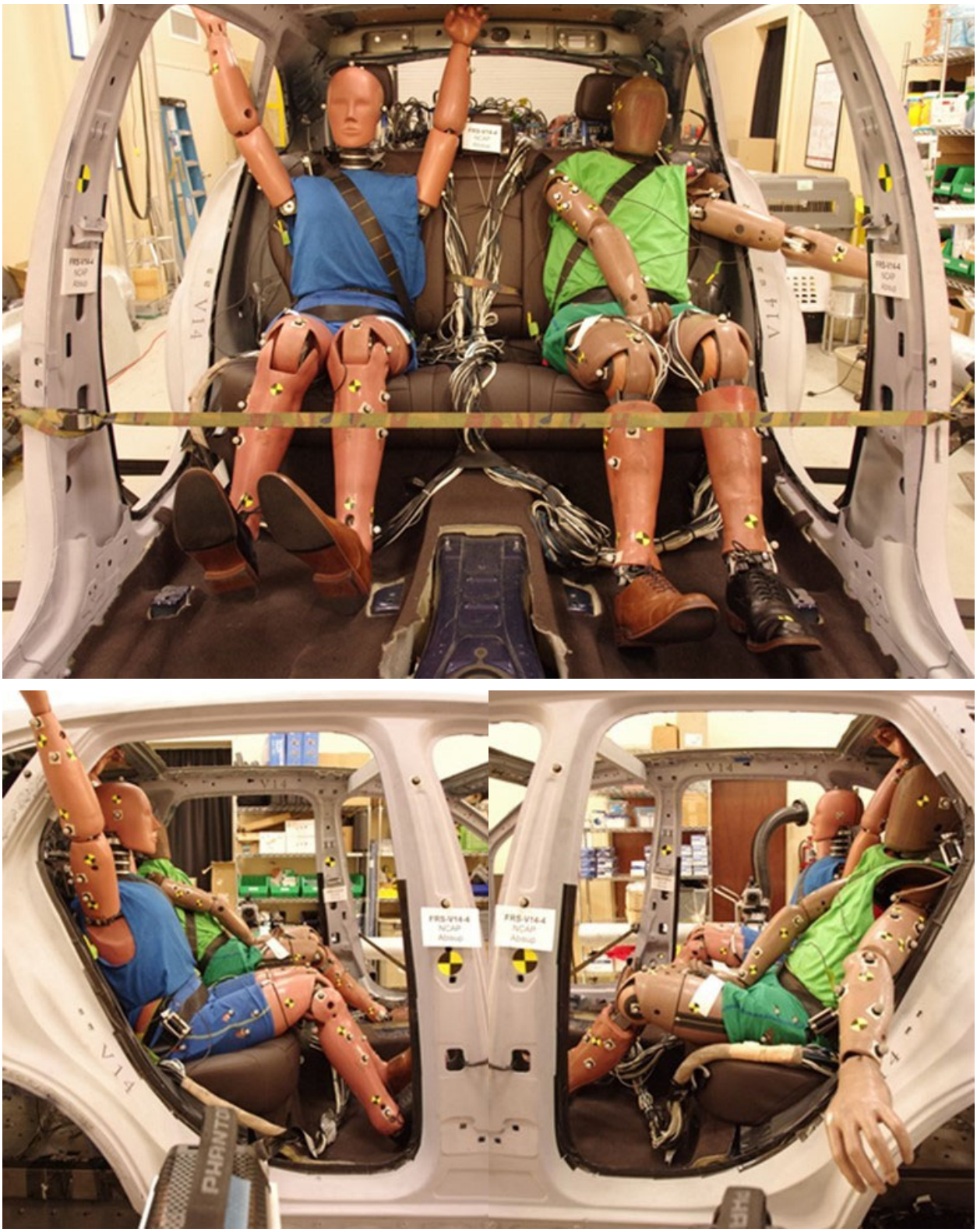

Figure J-34. Post-Test Images for Vehicle V14, Test 4 (NCAP85 Pulse), Repeat

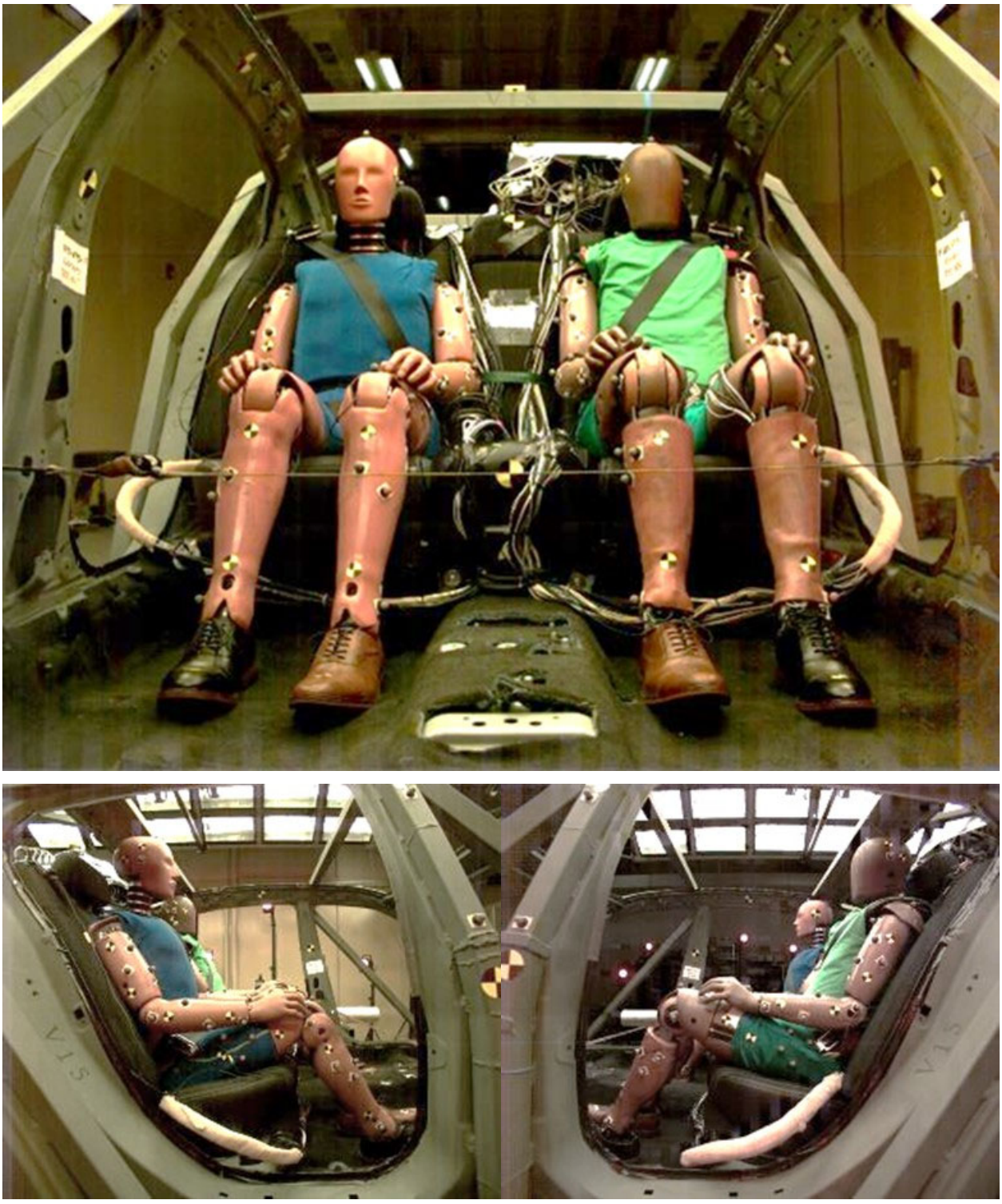

Figure J-35. Pre-Test Images for Vehicle V15, Test 1 (Generic Pulse and THOR Standard Abdomen)

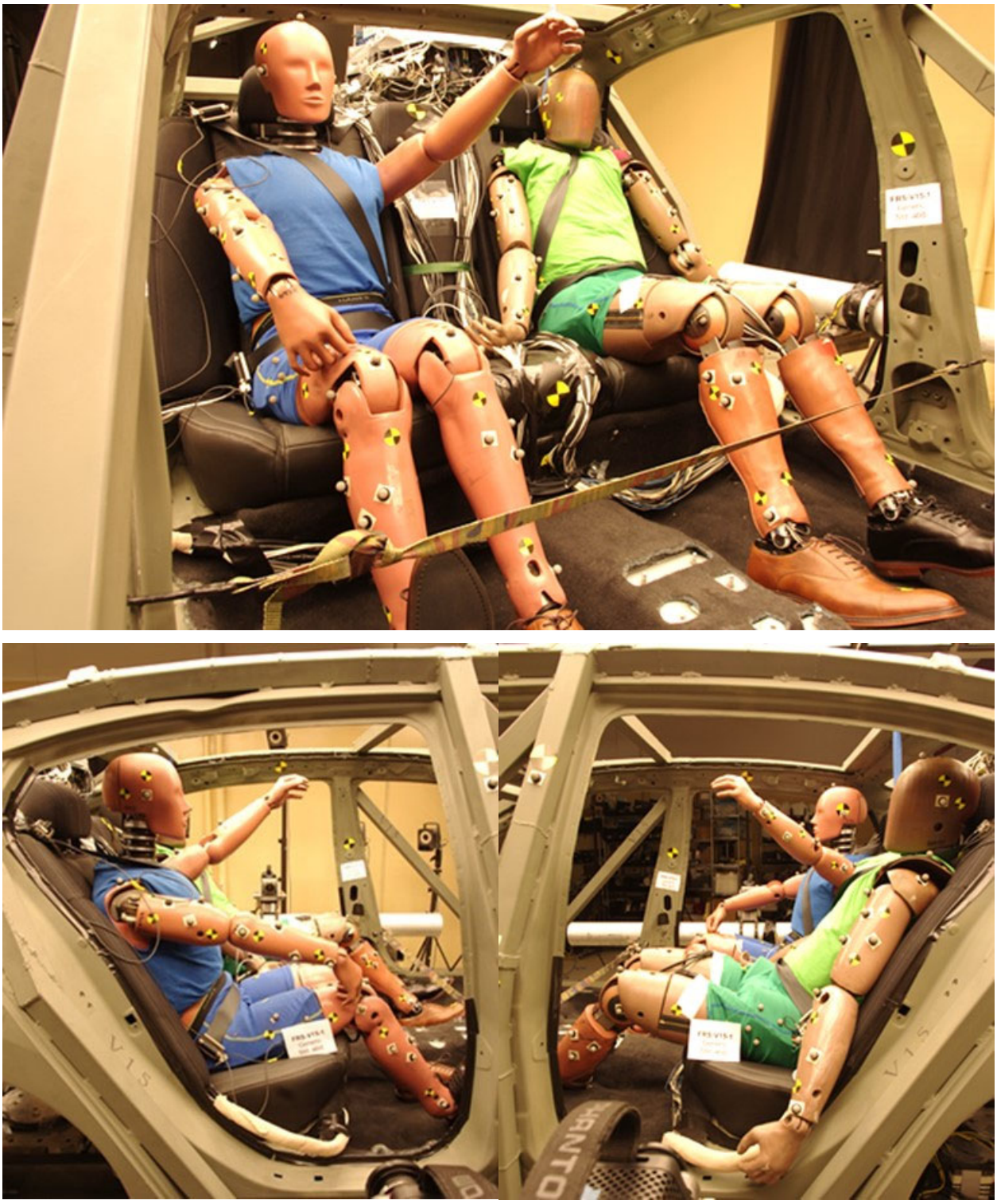

Figure J-36. Post-Test Images for Vehicle V15, Test 1 (Generic Pulse and THOR Standard Abdomen)

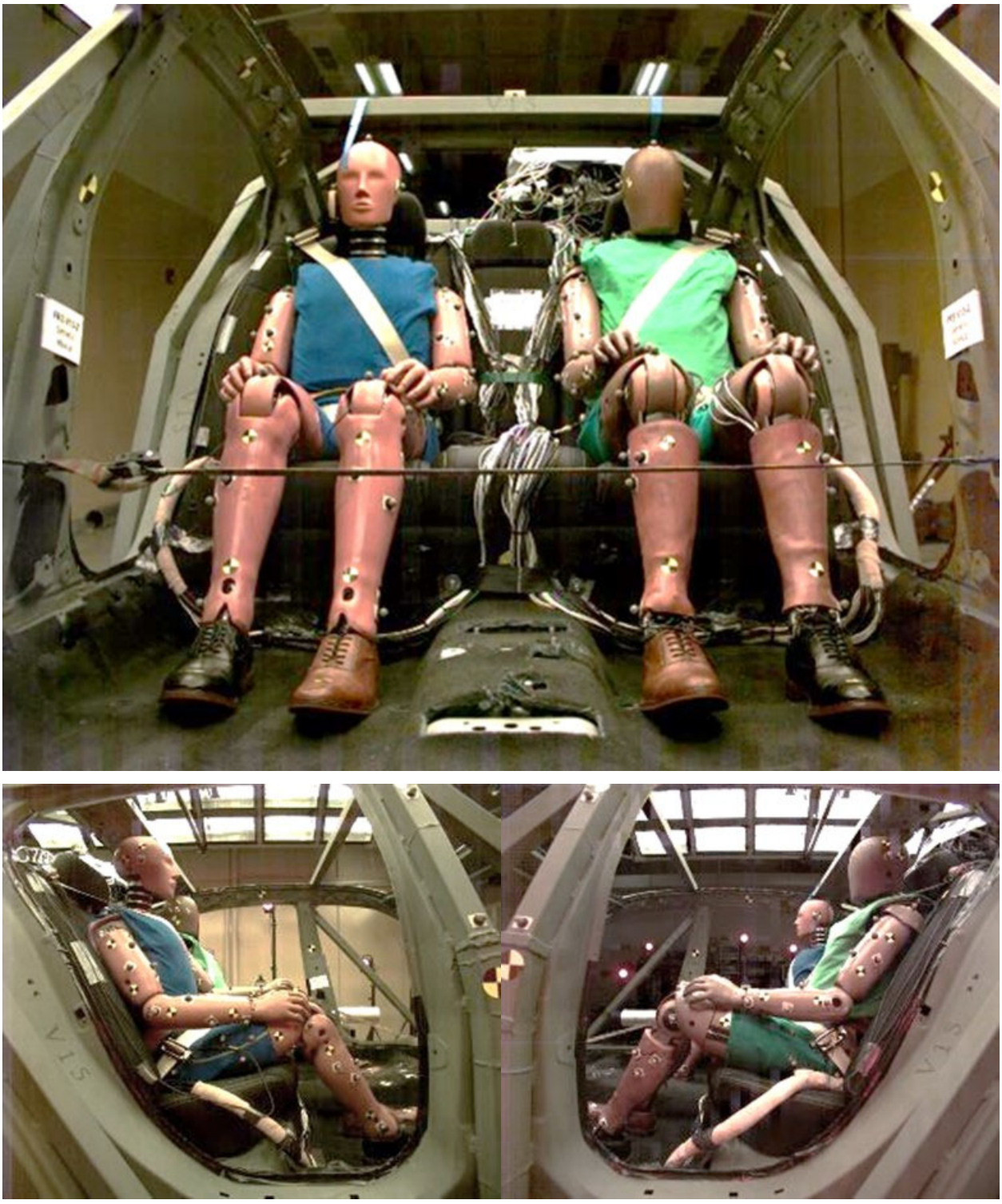

Figure J-37. Pre-Test Images for Vehicle V15, Test 2 (Specific/Scaled Pulse)

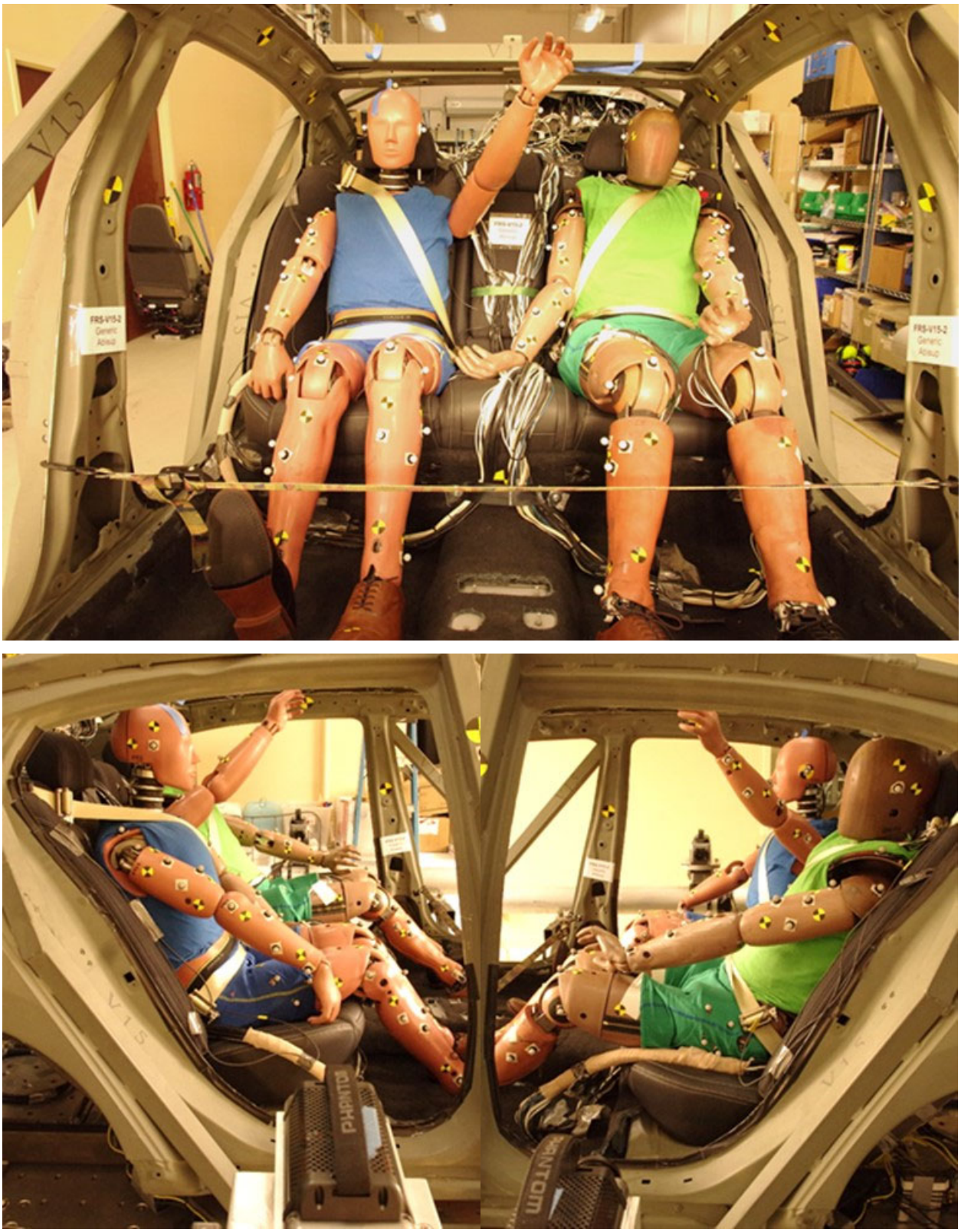

Figure J-38. Post-Test Images for Vehicle V15, Test 2 (Specific/Scaled Pulse)

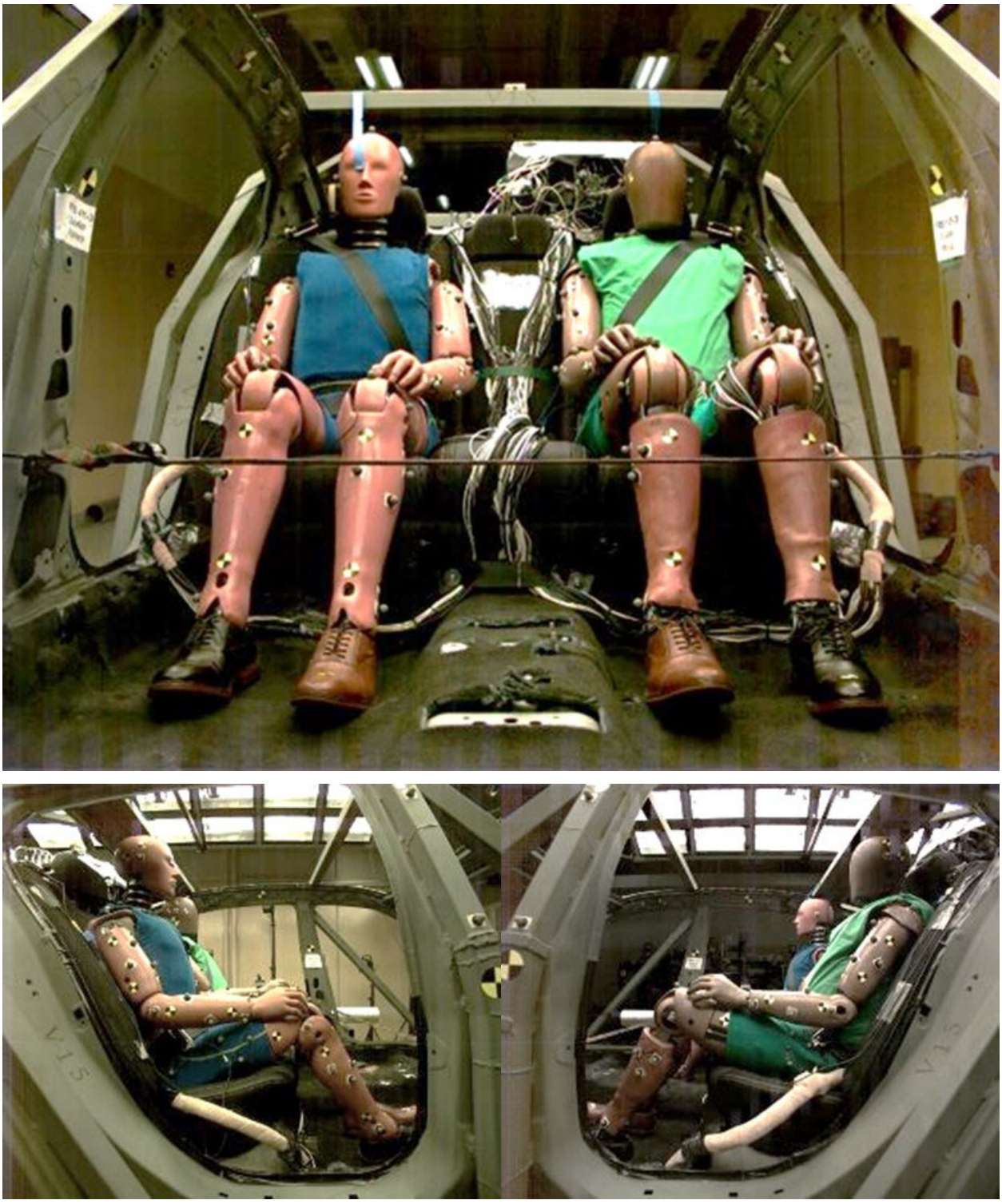

Figure J-39. Pre-Test Images for Vehicle V15, Test 3 (NCAP85 Pulse)

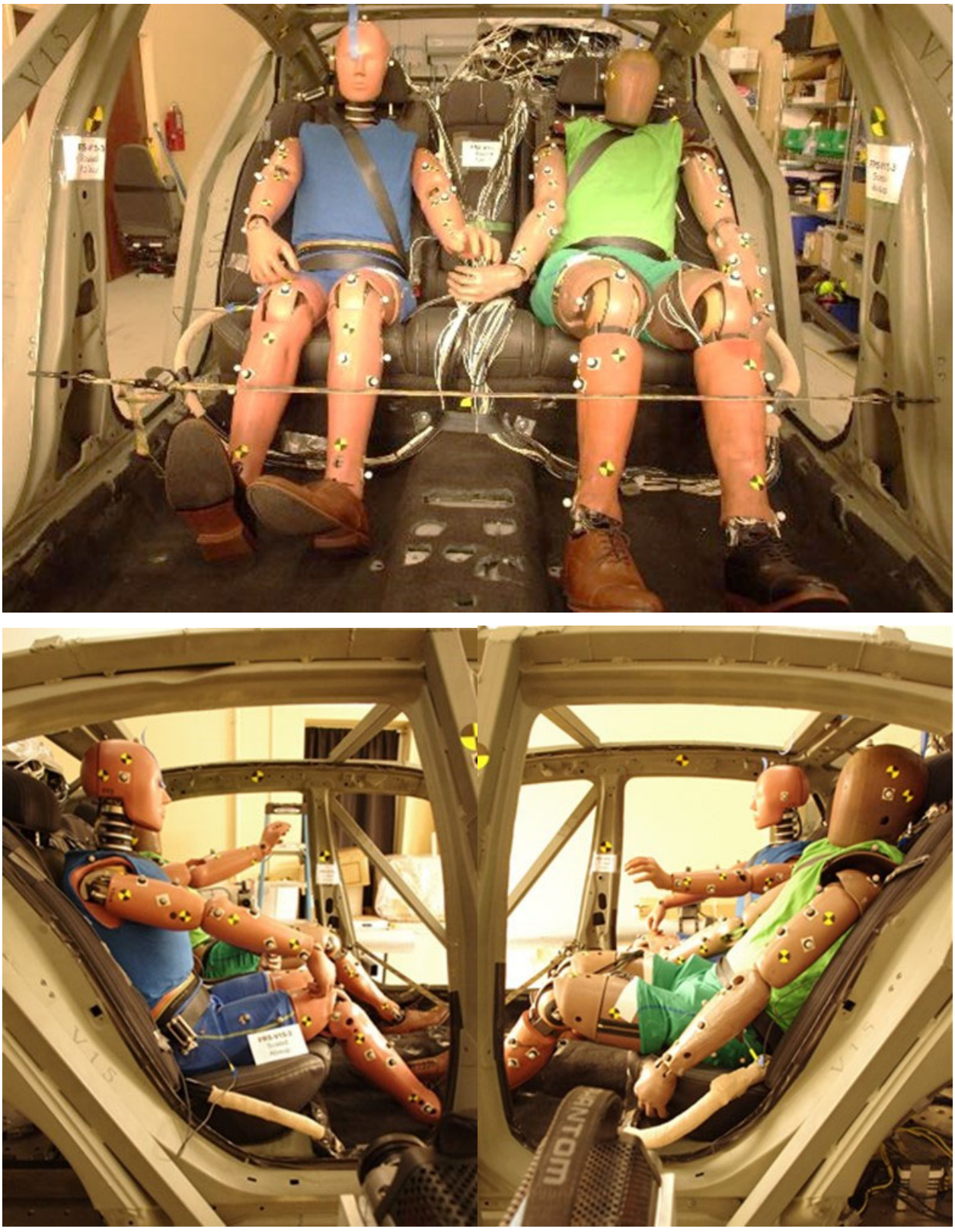

Figure J-40. Post-Test Images for Vehicle V15, Test 3 (NCAP85 Pulse), Repeat

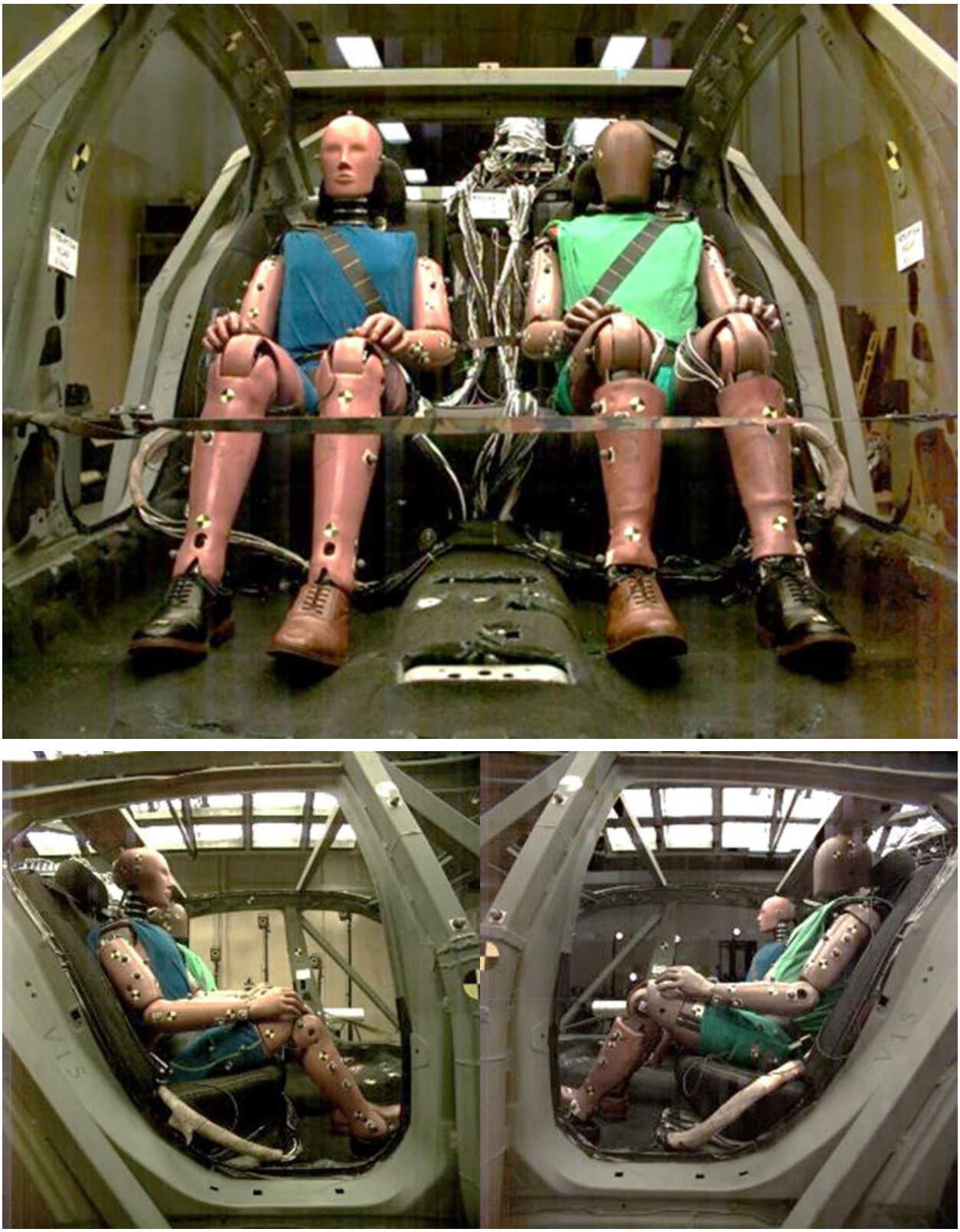

Figure J-41. Pre-Test Images for Vehicle V15, Test 4 (NCAP85 Pulse), Repeat

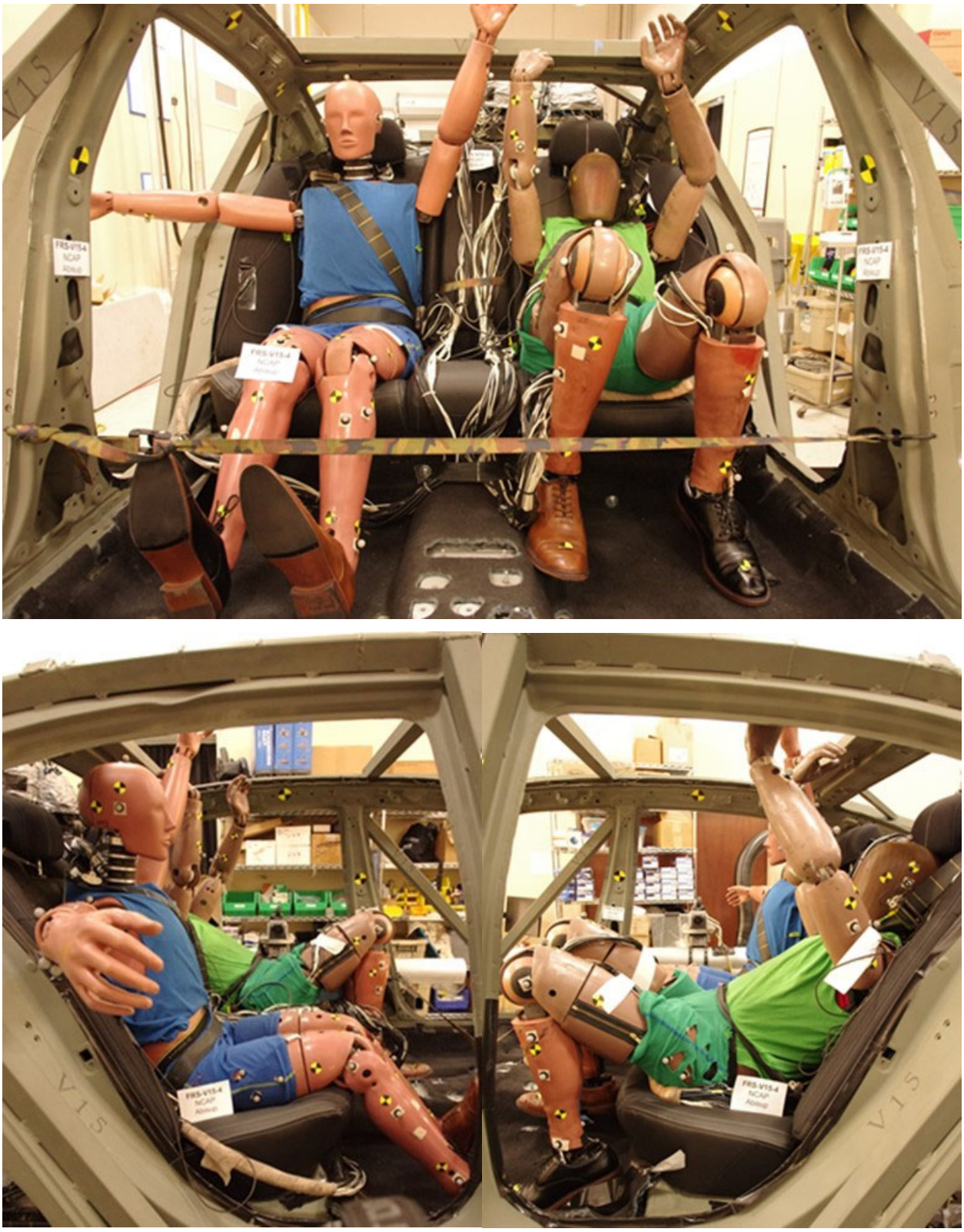

Figure J-42. Post-Test Images for Vehicle V15, Test 4 (Generic Pulse), Repeat

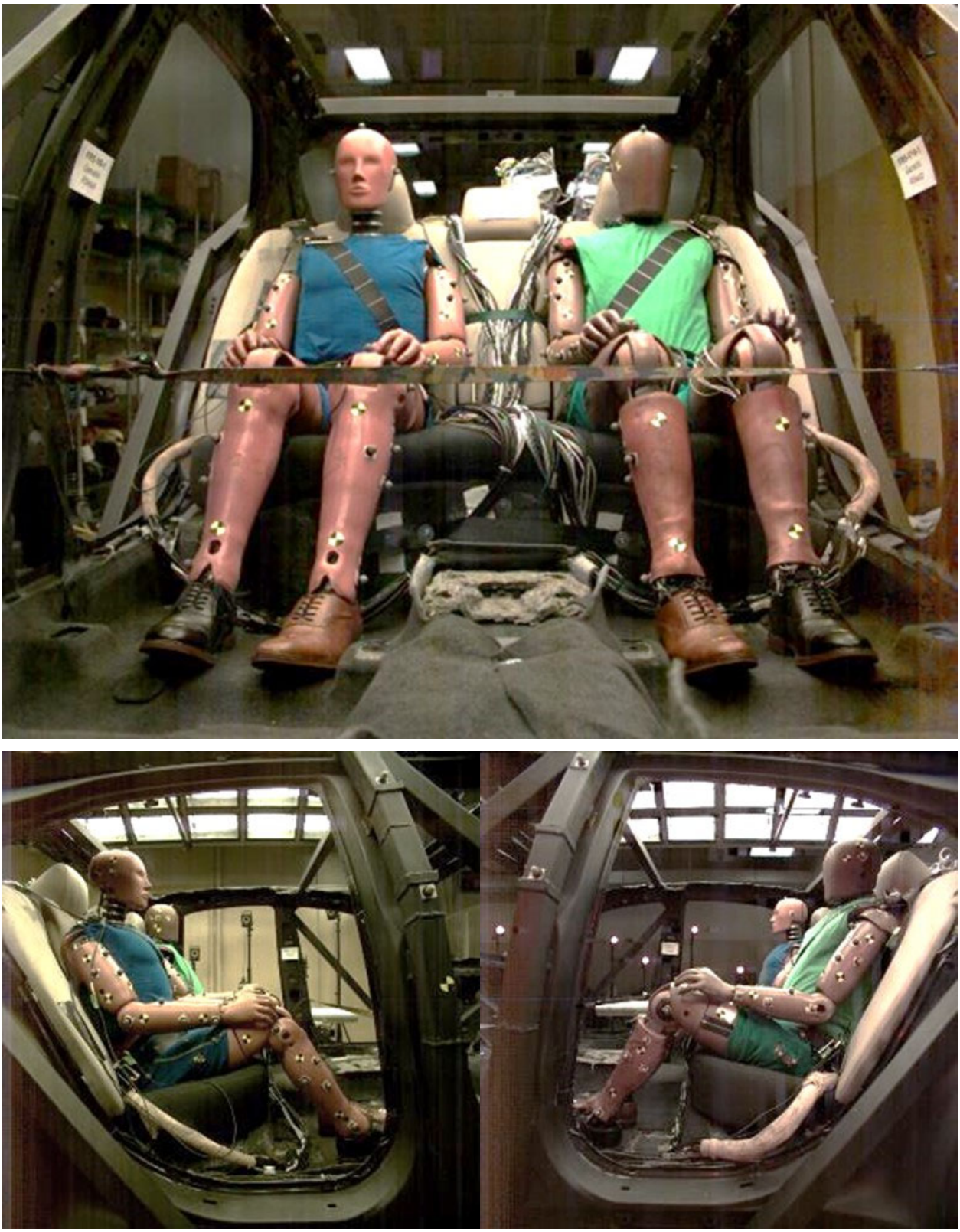

Figure J-43 Pre-Test Images for Vehicle V19, Test 1 (Generic Pulse)

Figure J-44. Post-Test Images for Vehicle V19, Test 1 (Generic Pulse)

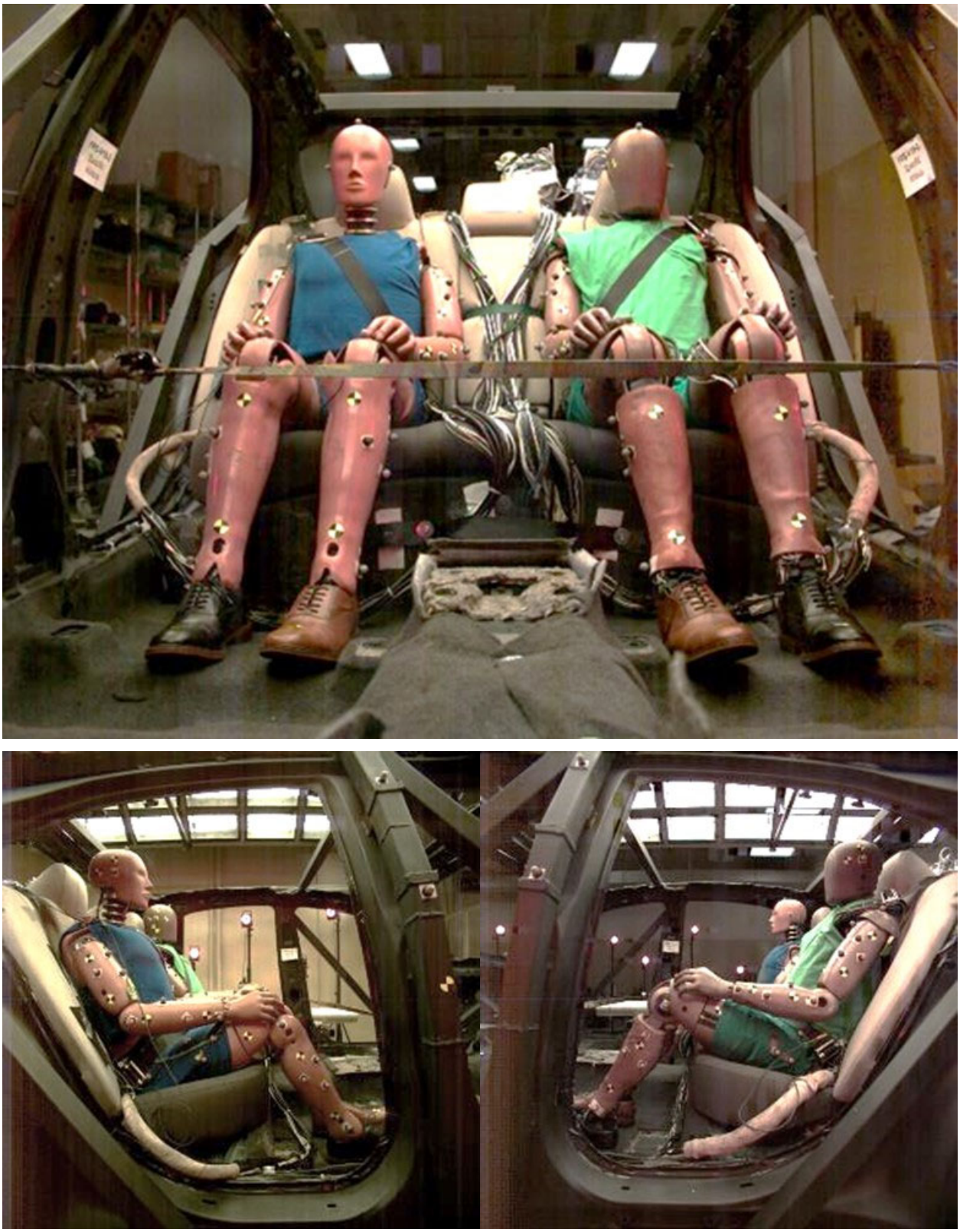

Figure J-45. Pre-Test Images for Vehicle V19, Test 2 (Specific/Scaled Pulse)

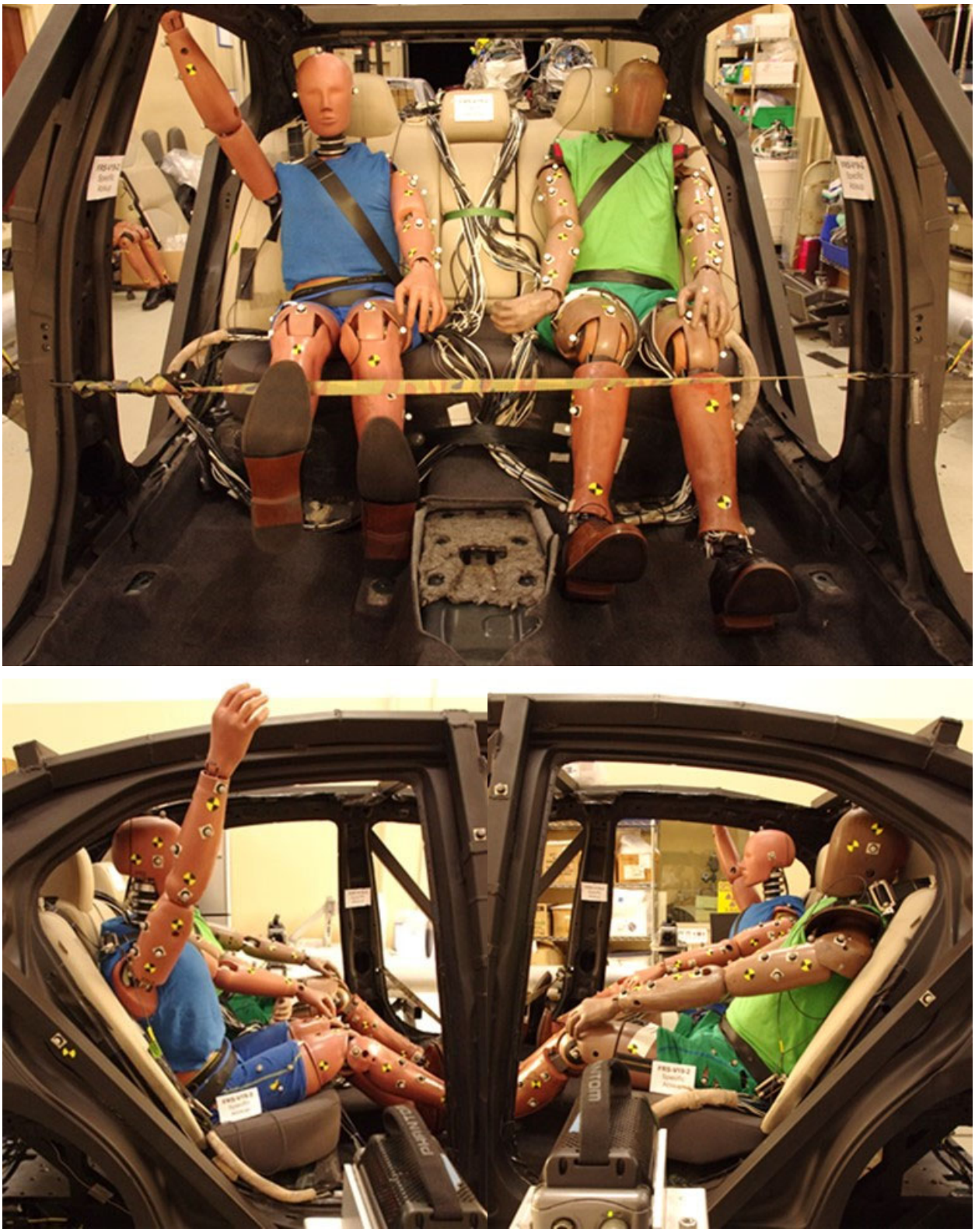

Figure J-46. Post-Test Images for Vehicle V19, Test 2 (Specific/Scaled Pulse)

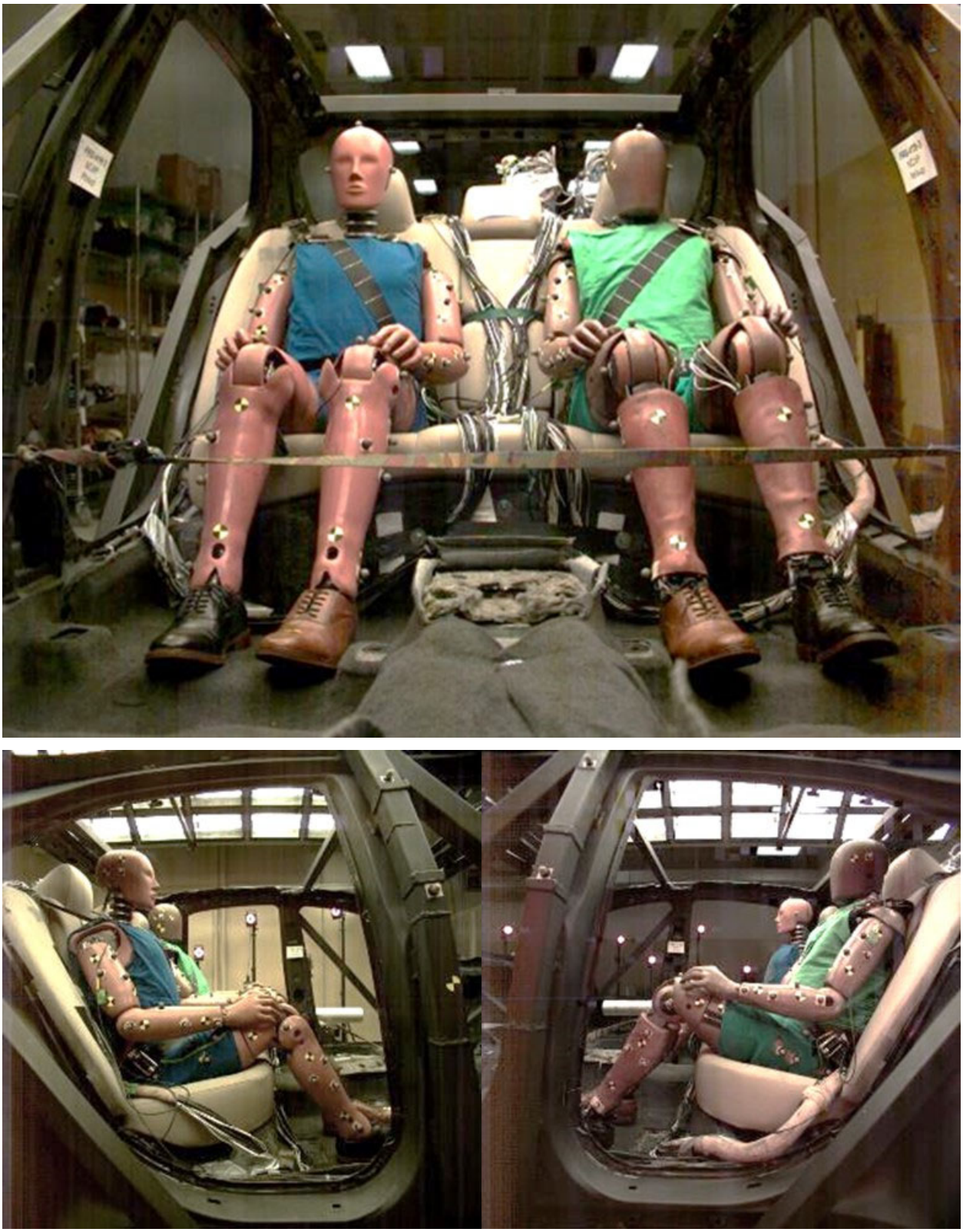

Figure J-47. Pre-Test Images for Vehicle V19, Test 3 (NCAP Pulse)

Figure J-48. Post-Test Images for Vehicle V19, Test 3 (NCAP Pulse)

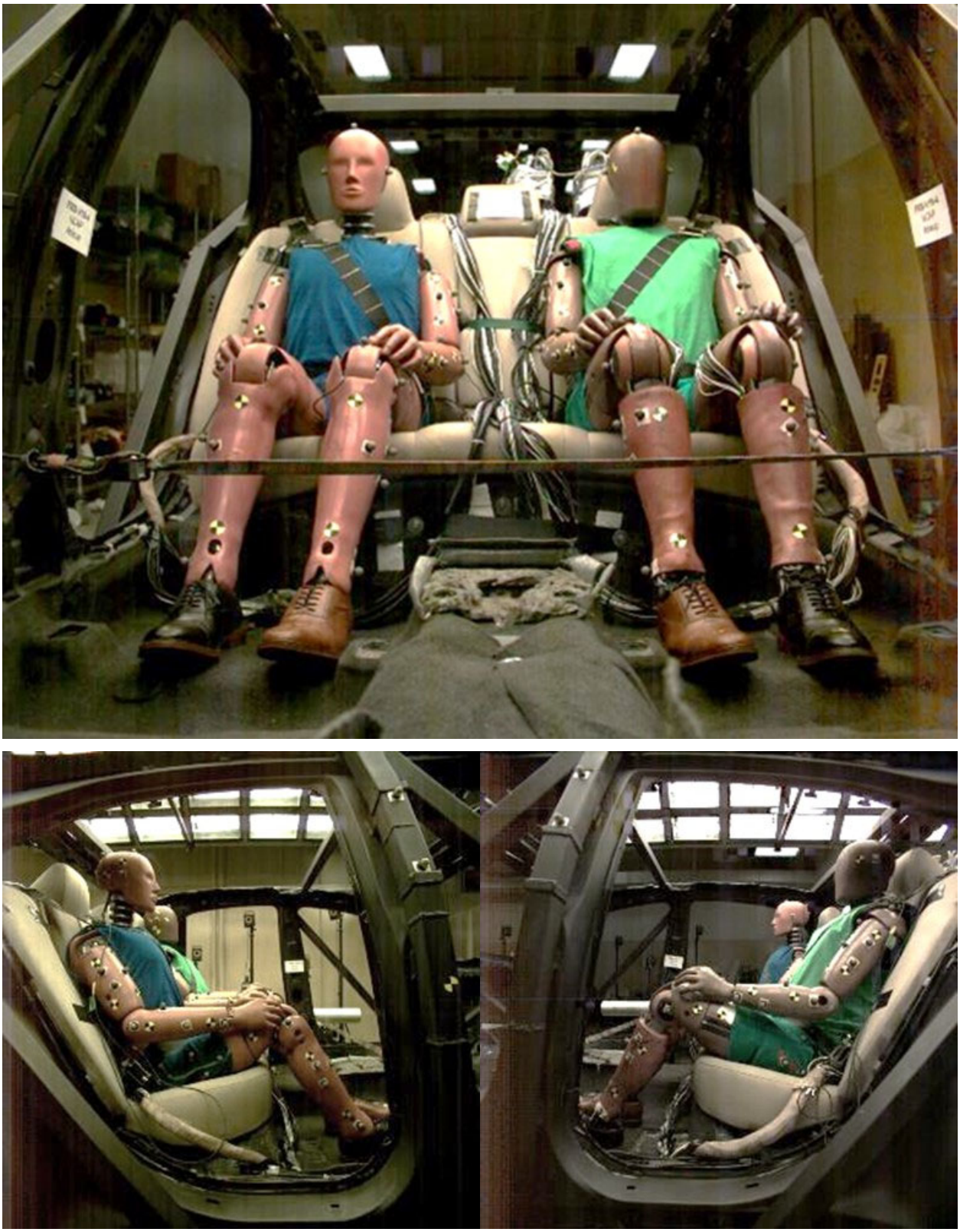

Figure J-49. Pre-Test Images for Vehicle V19, Test 4 (NCAP Pulse), Repeat

Figure J-50. Post-Test Images for Vehicle V19, Test 4 (NCAP Pulse), Repeat

Appendix K. Select Data Traces From Test FRS-V1-1

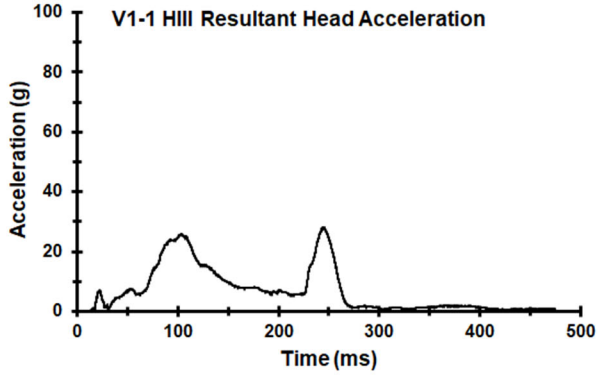
V1-1 HIII Resultant Head Acceleration
Acceleration (g)
Time (ms)

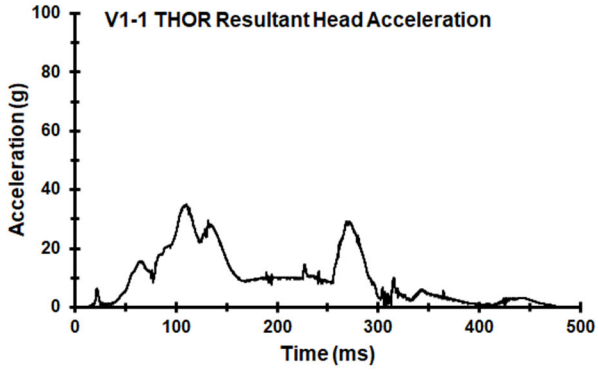
V1-1 THOR Resultant Head Acceleration
Acceleration (g)
Time (ms)

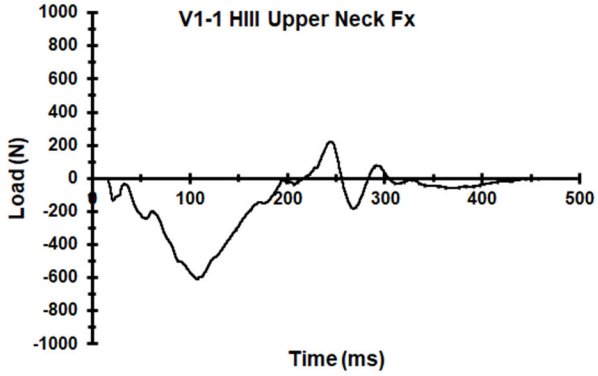
V1-1 HIII Upper Neck Fx
Load (N)
Time (ms)

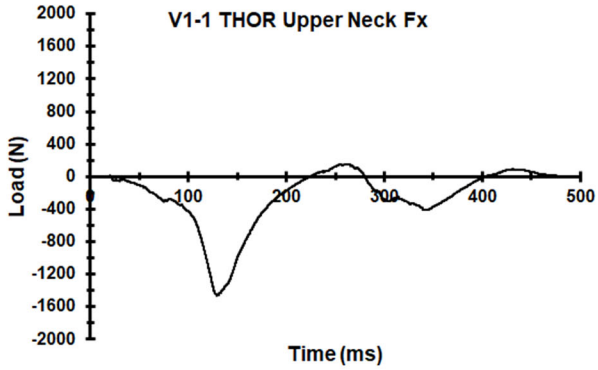
V1-1 THOR Upper Neck Fx
Load (N)
Time (ms)

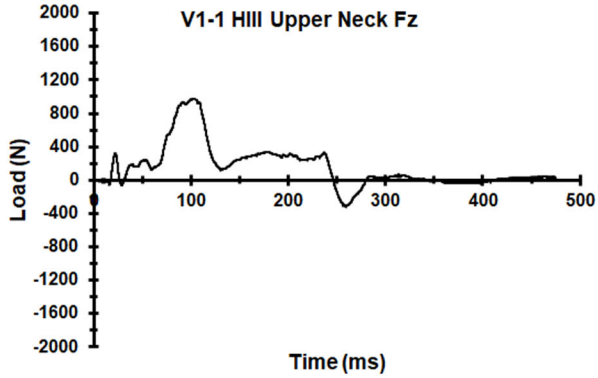
V1-1 HIII Upper Neck Fz
Load (N)
Time (ms)

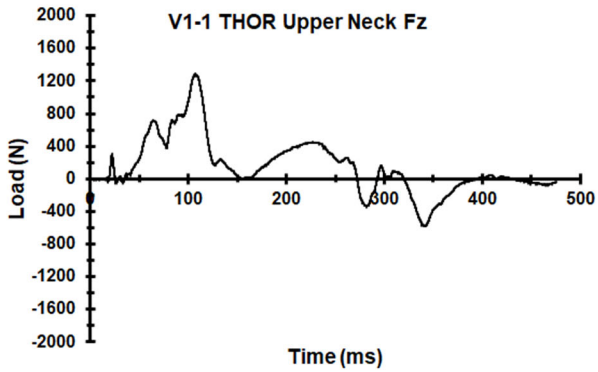
V1-1 THOR Upper Neck Fz
Load (N)
Time (ms)

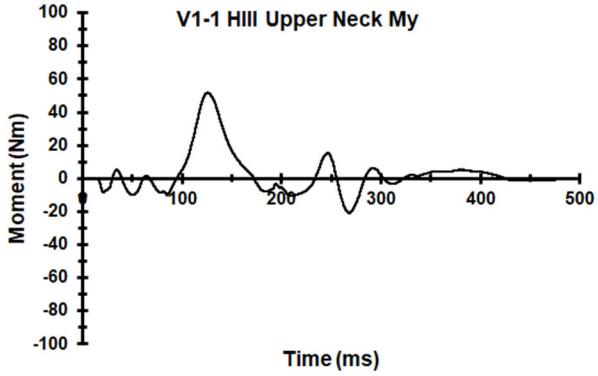
V1-1 HIII Upper Neck My
Moment (Nm)
Time (ms)

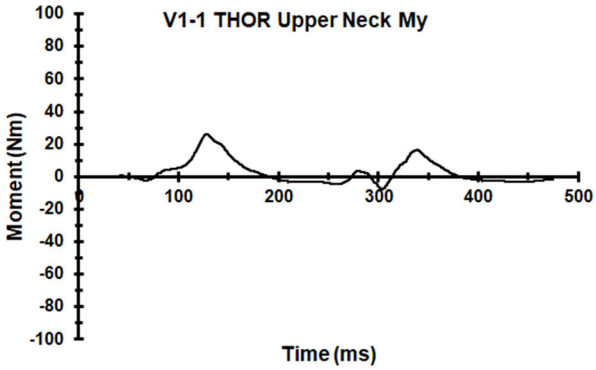
V1-1 THOR Upper Neck My
Moment (Nm)
Time (ms)

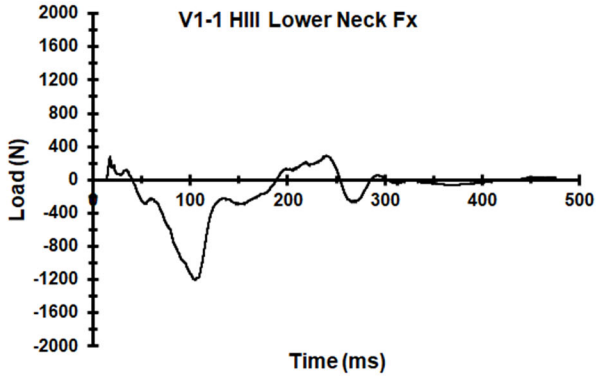
V1-1 HIII Lower Neck Fx
Load (N)
Time (ms)

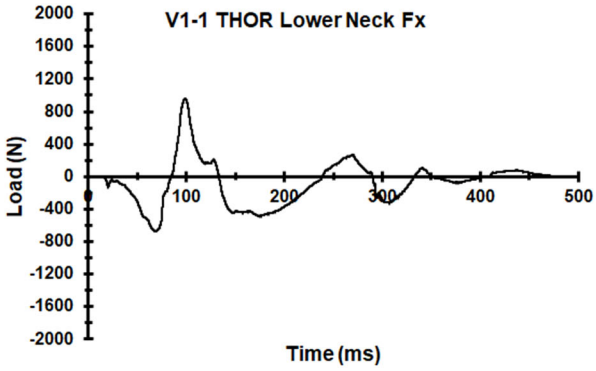
V1-1 THOR Lower Neck Fx
Load (N)
Time (ms)

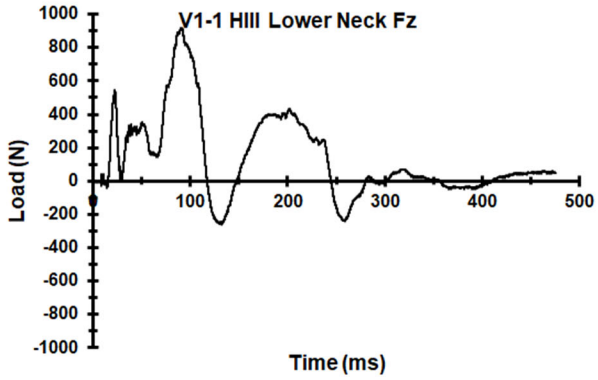
V1-1 HIII Lower Neck Fz
Load (N)
Time (ms)

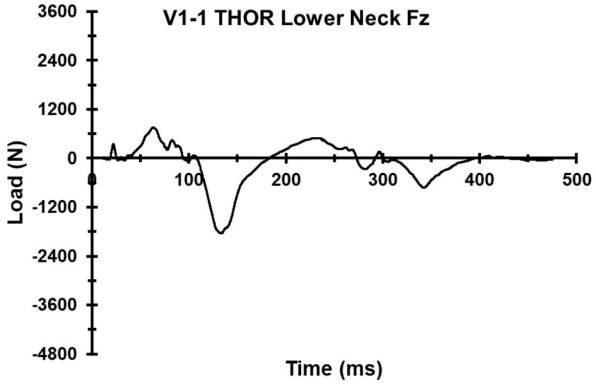
V1-1 THOR Lower Neck Fz
Load (N)
Time (ms)

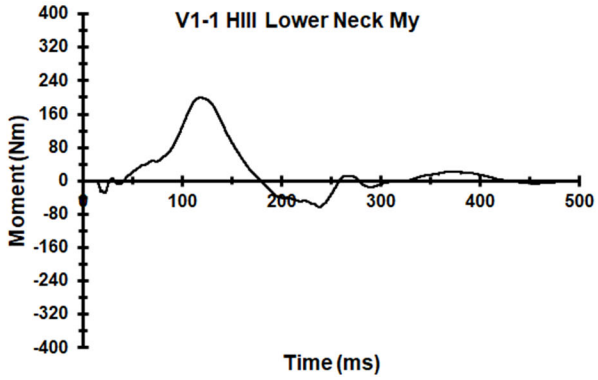
V1-1 HIII Lower Neck My
Moment (Nm)
400
320
240
160
80
0
-80
-160
-240
-320
-400
0
100
200
300
400
500
Time (ms)

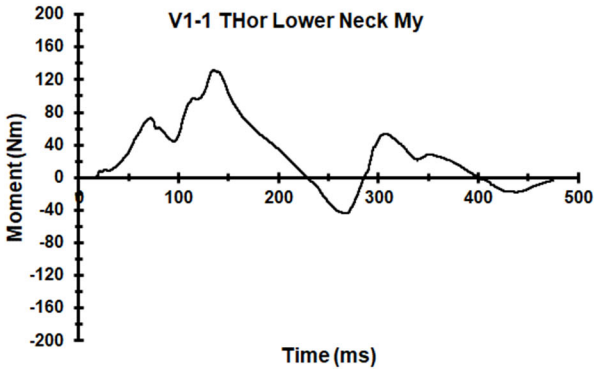
V1-1 THor Lower Neck My
Moment (Nm)
200
160
120
80
40
0
-40
-80
-120
-160
-200
0
100
200
300
400
500
Time (ms)

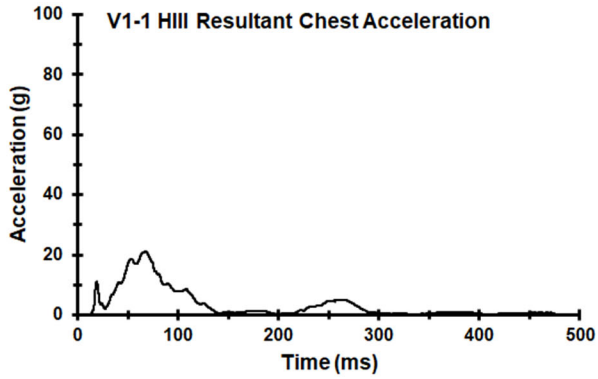
V1-1 HIII Resultant Chest Acceleration
Acceleration (g)
100
80
60
40
20
0
0
100
200
300
400
500
Time (ms)

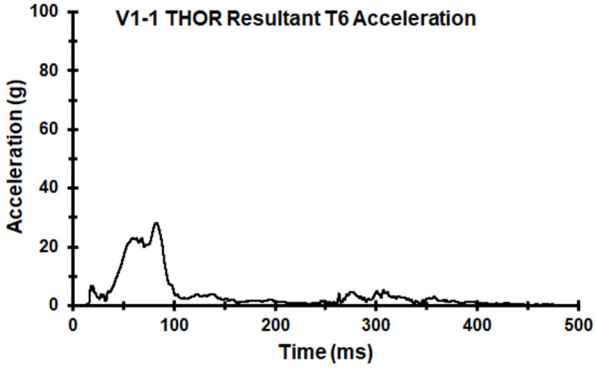
V1-1 THOR Resultant T6 Acceleration
Acceleration (g)
100
80
60
40
20
0
0
100
200
300
400
500
Time (ms)

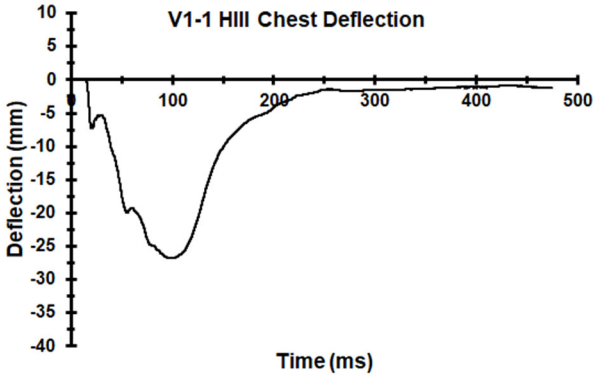
V1-1 HIII Chest Deflection
Deflection (mm)
Time (ms)

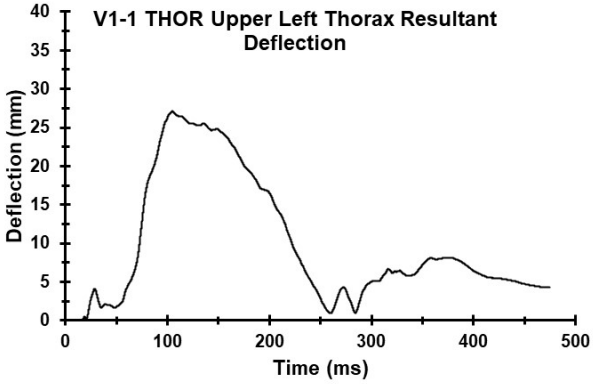
V1-1 THOR Upper Left Thorax Resultant Deflection
Deflection (mm)
Time (ms)

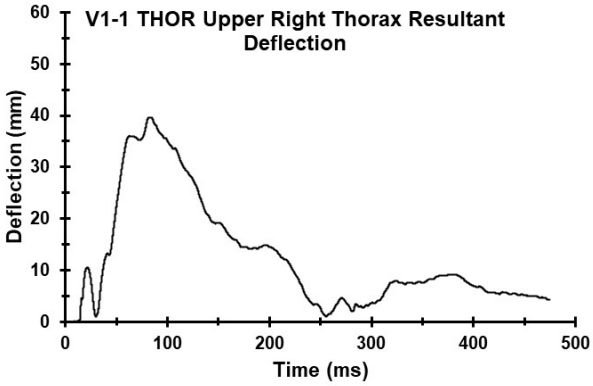
V1-1 THOR Upper Right Thorax Resultant Deflection
Deflection (mm)
Time (ms)

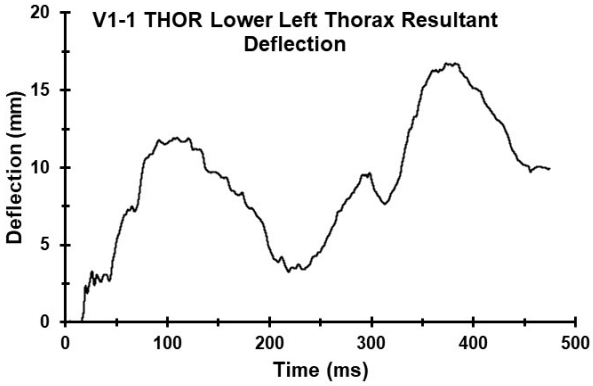
V1-1 THOR Lower Left Thorax Resultant Deflection
Deflection (mm)
Time (ms)

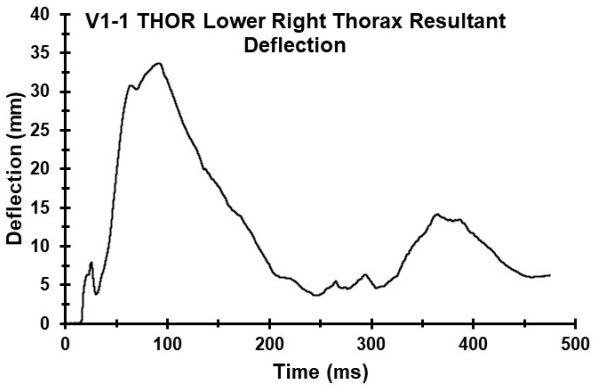
V1-1 THOR Lower Right Thorax Resultant Deflection
Deflection (mm)
Time (ms)

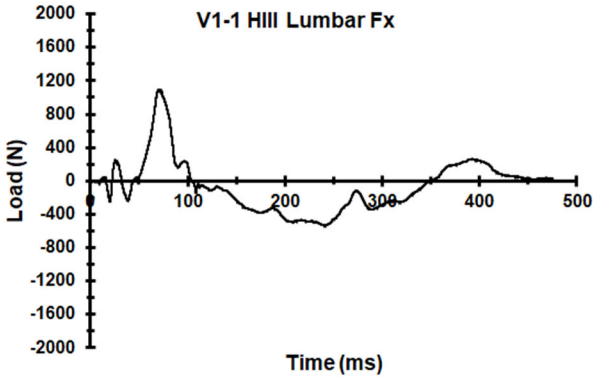
V1-1 HIII Lumbar Fx
Load (N)
Time (ms)

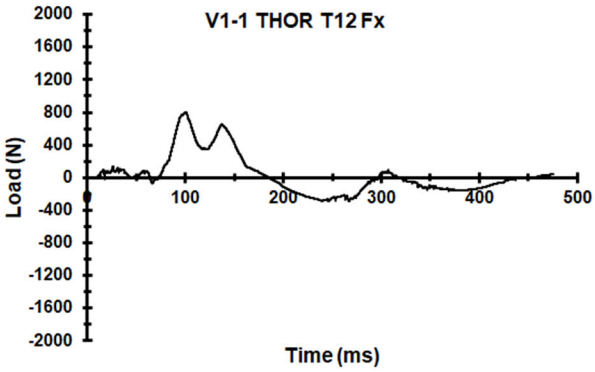
V1-1 THOR T12 Fx
Load (N)
Time (ms)

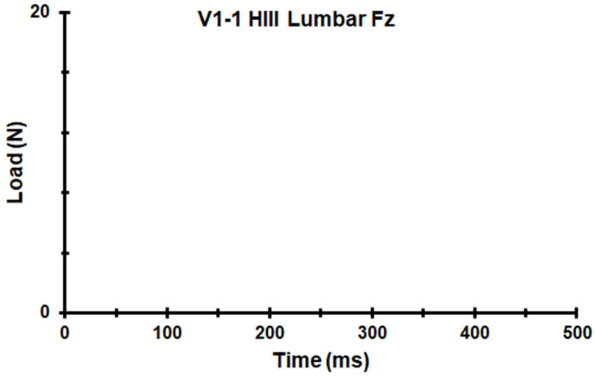
V1-1 HIII Lumbar Fz
Load (N)
Time (ms)

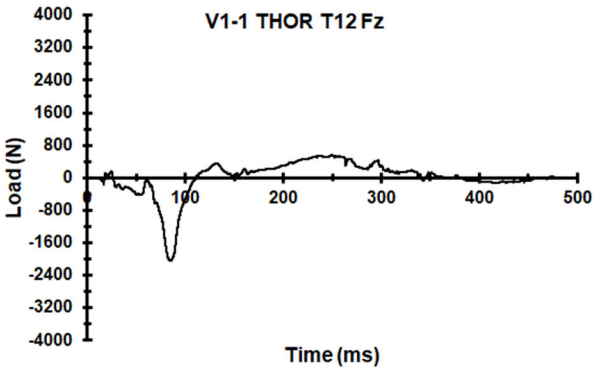
V1-1 THOR T12 Fz
Load (N)
Time (ms)

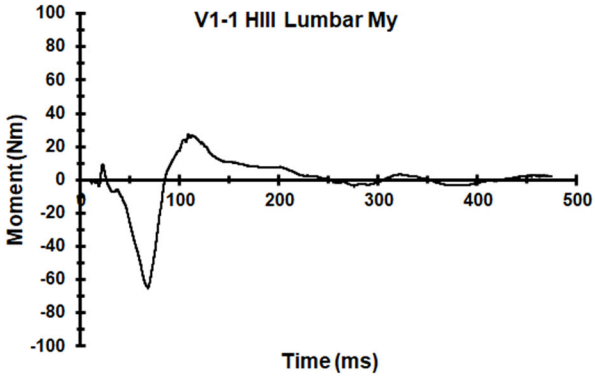
V1-1 HIII Lumbar My
Moment (Nm)
Time (ms)

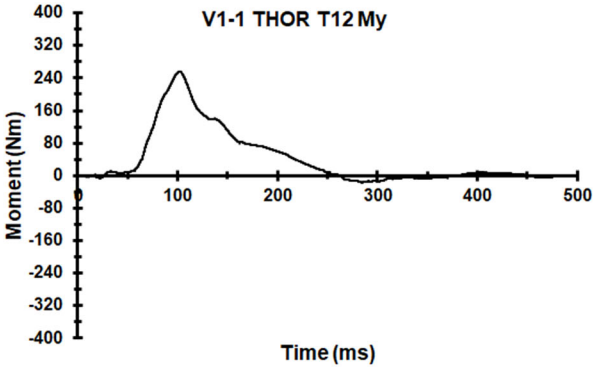
V1-1 THOR T12 My
Moment (Nm)
Time (ms)

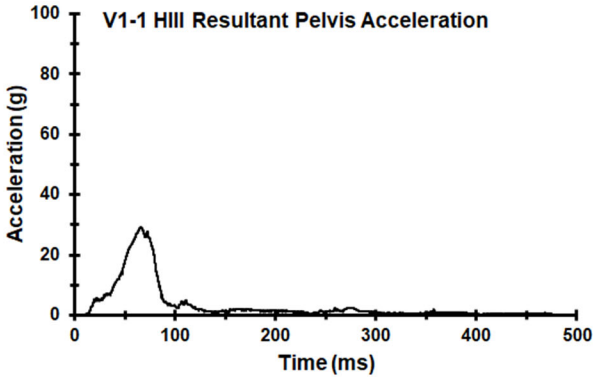
V1-1 HIII Resultant Pelvis Acceleration
Acceleration (g)
Time (ms)

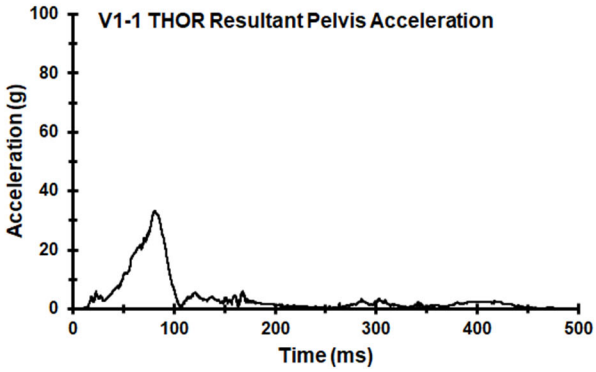
V1-1 THOR Resultant Pelvis Acceleration
Acceleration (g)
Time (ms)

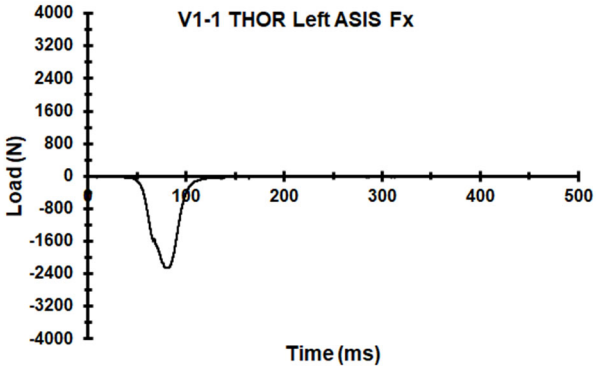
V1-1 THOR Left ASIS Fx
Load (N)
Time (ms)

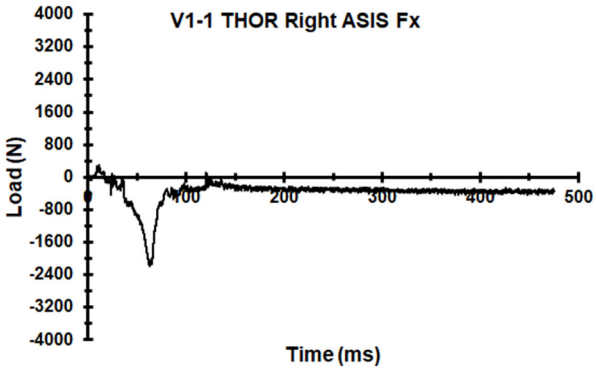
V1-1 THOR Right ASIS Fx
Load (N)
Time (ms)

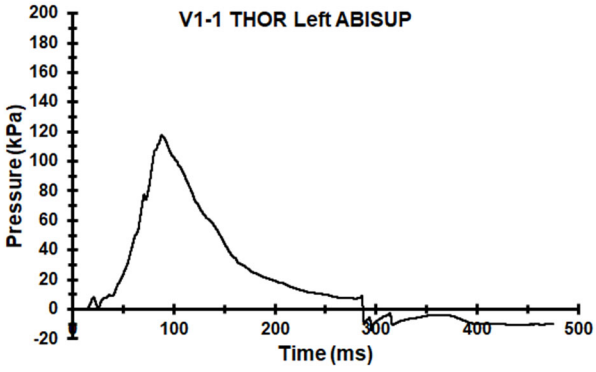
V1-1 THOR Left ABISUP
Pressure (kPa)
Time (ms)

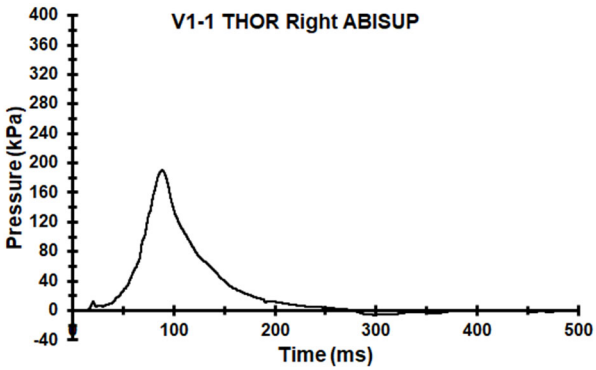
V1-1 THOR Right ABISUP
Pressure (kPa)
400
360
320
280
240
200
160
120
80
40
0
-40
100
200
300
400
500
Time (ms)

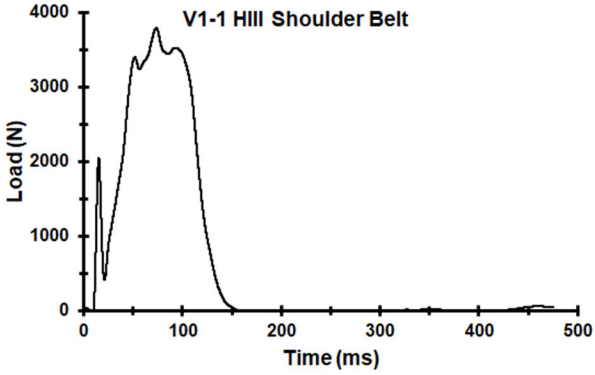
V1-1 HIII Shoulder Belt
Load (N)
4000
3000
2000
1000
0
0
100
200
300
400
500
Time (ms)

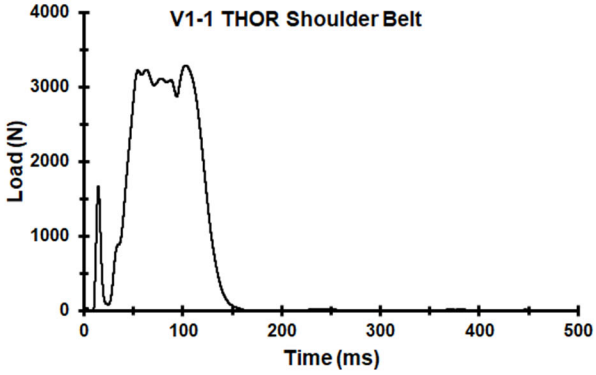
V1-1 THOR Shoulder Belt
Load (N)
4000
3000
2000
1000
0
0
100
200
300
400
500
Time (ms)

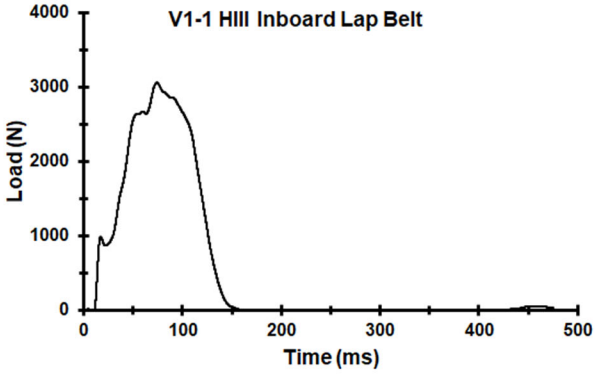
V1-1 HIII Inboard Lap Belt
Load (N)
4000
3000
2000
1000
0
0
100
200
300
400
500
Time (ms)

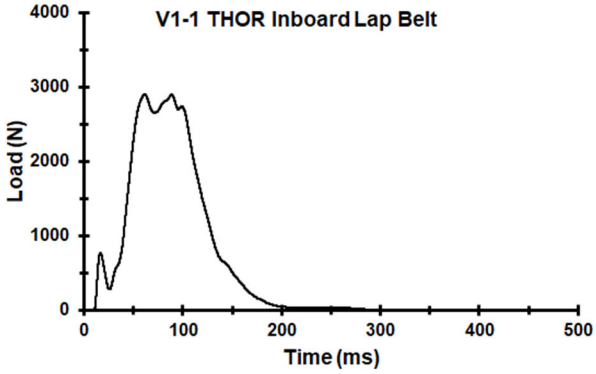
V1-1 THOR Inboard Lap Belt
Load (N)
4000
3000
2000
1000
0
0
100
200
300
400
500
Time (ms)

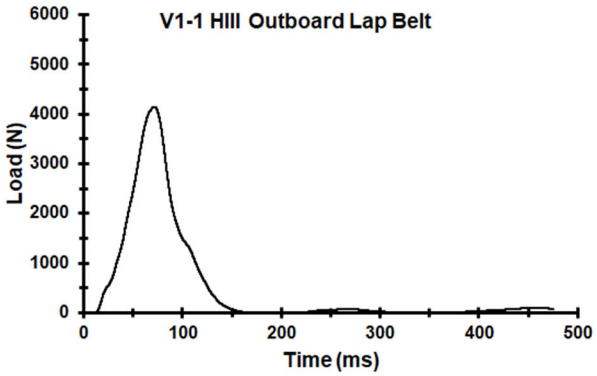
V1-1 HIII Outboard Lap Belt
Load (N)
6000
5000
4000
3000
2000
1000
0
0
100
200
300
400
500
Time (ms)

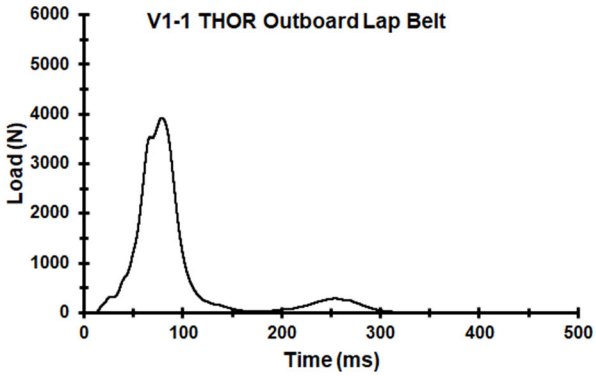
V1-1 THOR Outboard Lap Belt
Load (N)
6000
5000
4000
3000
2000
1000
0
0
100
200
300
400
500
Time (ms)

Appendix L. Select Data Traces From Test FRS-V1-2

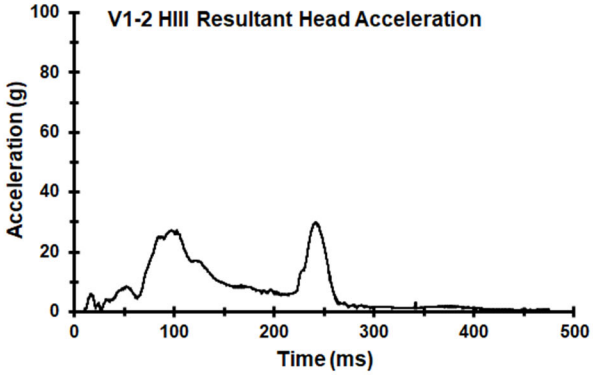
V1-2 HIII Resultant Head Acceleration
Acceleration (g)
Time (ms)

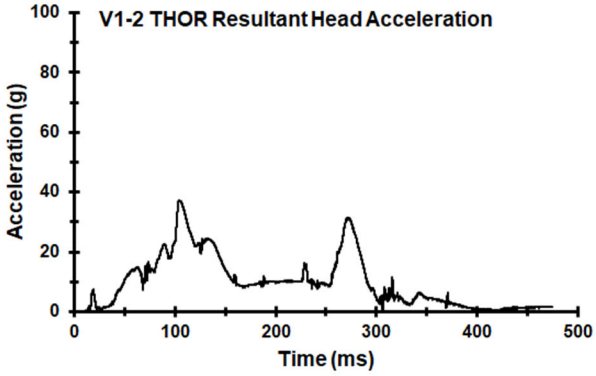
V1-2 THOR Resultant Head Acceleration
Acceleration (g)
Time (ms)

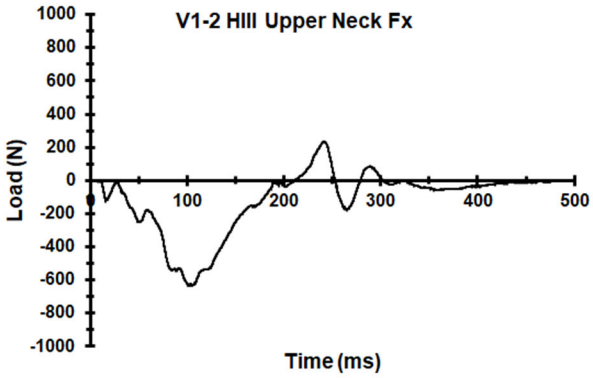
V1-2 HIII Upper Neck Fx
Load (N)
Time (ms)

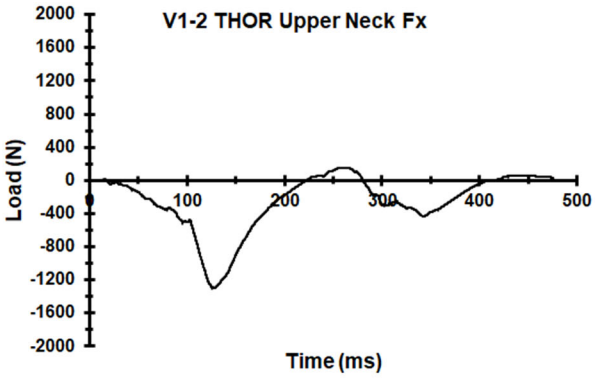
V1-2 THOR Upper Neck Fx
Load (N)
Time (ms)

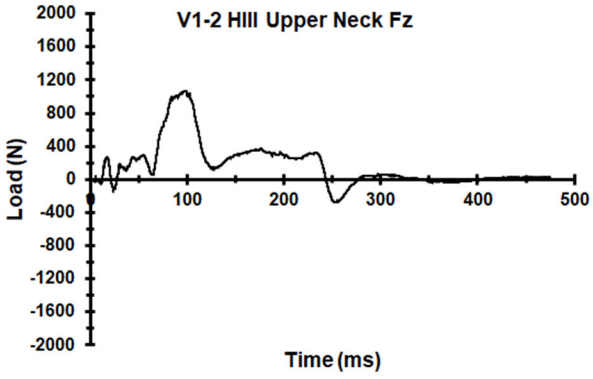
V1-2 HIII Upper Neck Fz
Load (N)
Time (ms)

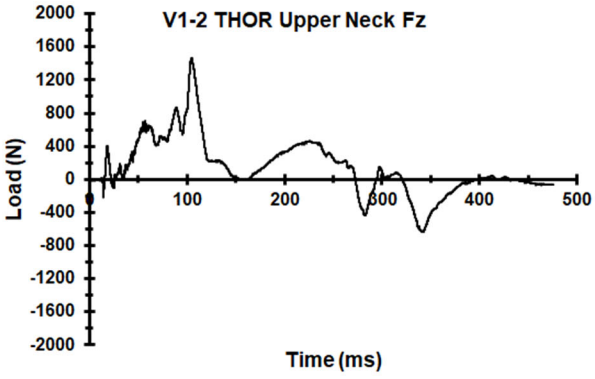
V1-2 THOR Upper Neck Fz
Load (N)
Time (ms)

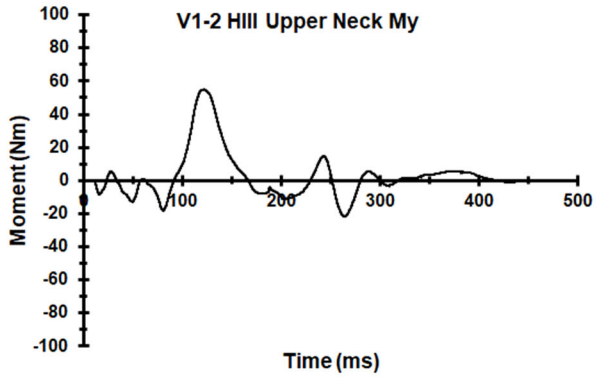
V1-2 HIII Upper Neck My
Moment (Nm)
Time (ms)

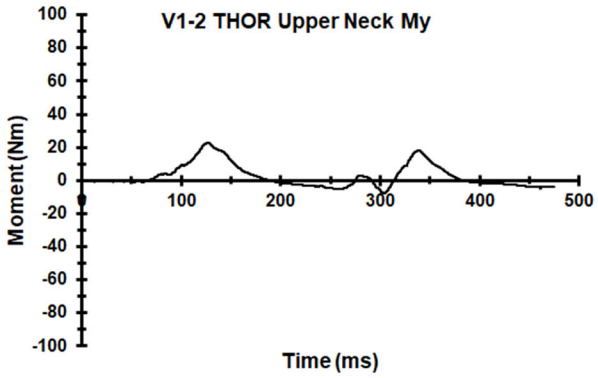
V1-2 THOR Upper Neck My
Moment (Nm)
Time (ms)

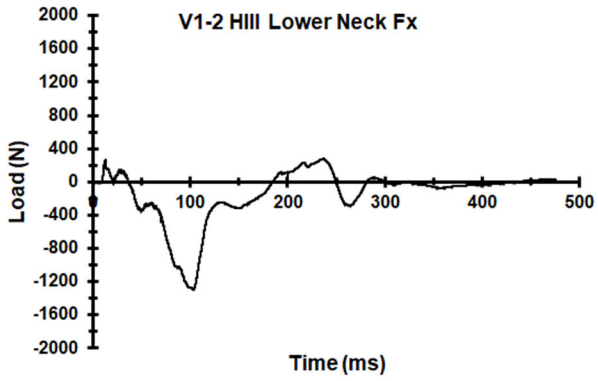
V1-2 HIII Lower Neck Fx
Load (N)
Time (ms)

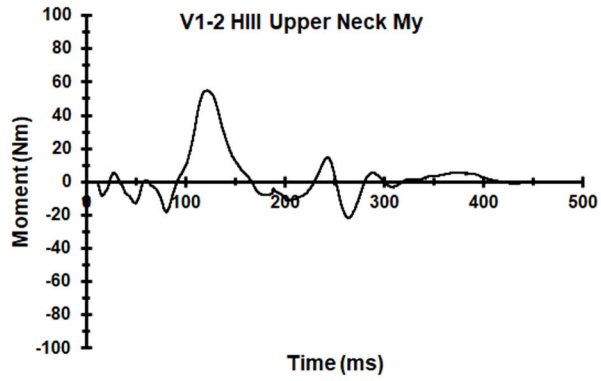
V1-2 HIII Upper Neck My
Moment (Nm)
Time (ms)

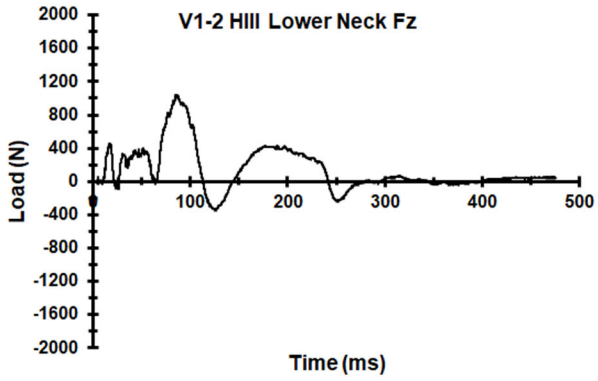
V1-2 HIII Lower Neck Fz
Load (N)
Time (ms)

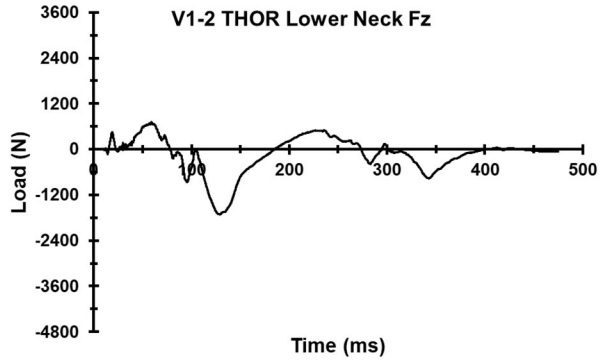
V1-2 THOR Lower Neck Fz
Load (N)
Time (ms)

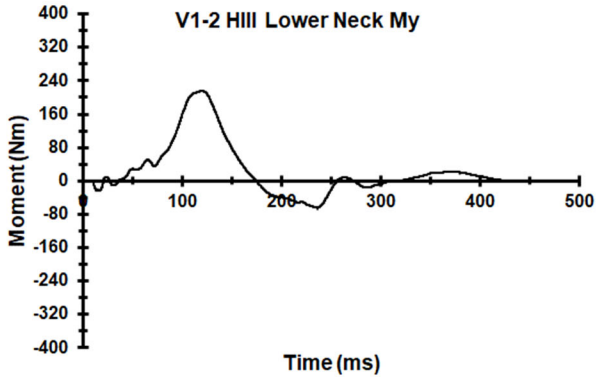
V1-2 HIII Lower Neck My
Moment (Nm)
400
320
240
160
80
0
-80
-160
-240
-320
-400
100
200
300
400
500
Time (ms)

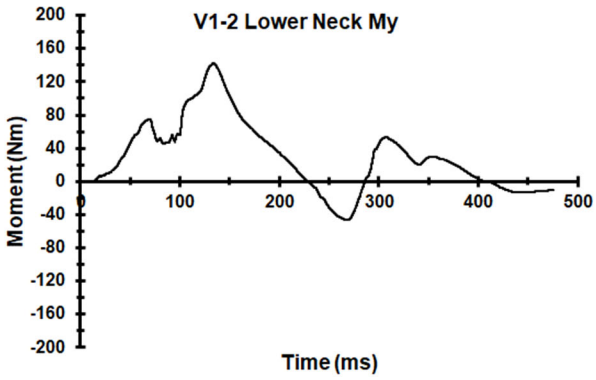
V1-2 Lower Neck My
Moment (Nm)
200
160
120
80
40
0
-40
-80
-120
-160
-200
100
200
300
400
500
Time (ms)

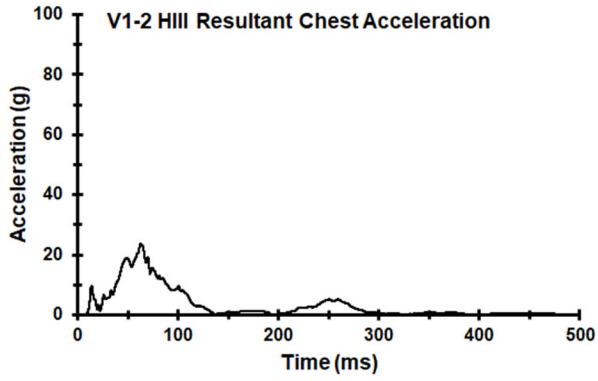
V1-2 HIII Resultant Chest Acceleration
Acceleration (g)
100
80
60
40
20
0
0
100
200
300
400
500
Time (ms)

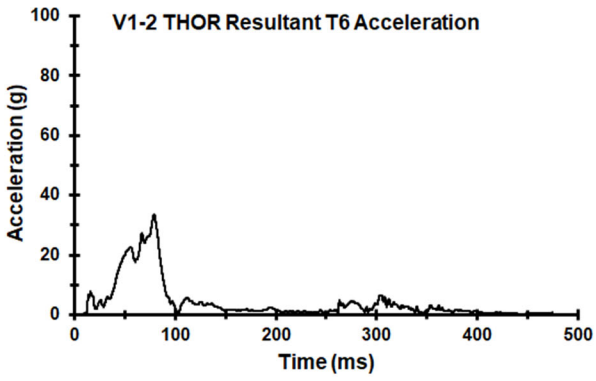
V1-2 THOR Resultant T6 Acceleration
Acceleration (g)
100
80
60
40
20
0
0
100
200
300
400
500
Time (ms)

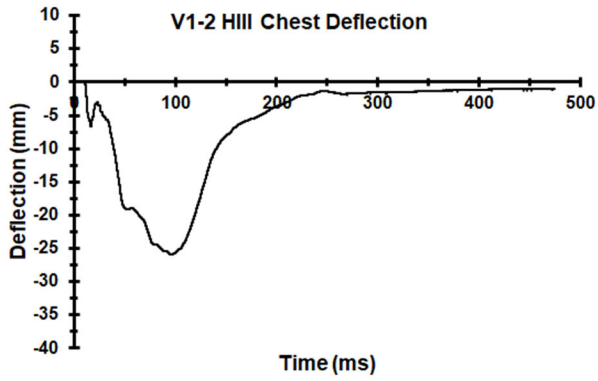
V1-2 HIII Chest Deflection
Deflection (mm)
10
5
0
-5
-10
-15
-20
-25
-30
-35
-40
100
200
300
400
500
Time (ms)

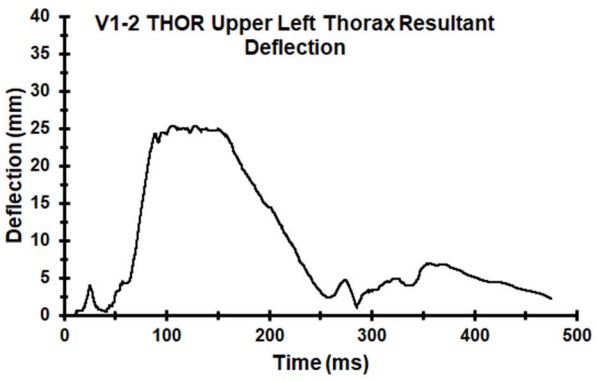
V1-2 THOR Upper Left Thorax Resultant Deflection
Deflection (mm)
40
35
30
25
20
15
10
5
0
0
100
200
300
400
500
Time (ms)

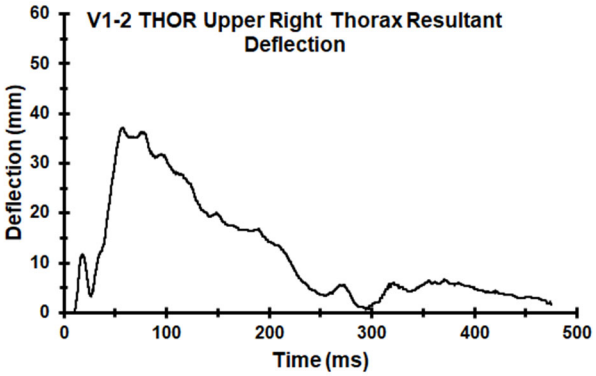
V1-2 THOR Upper Right Thorax Resultant Deflection
Deflection (mm)
60
50
40
30
20
10
0
0
100
200
300
400
500
Time (ms)

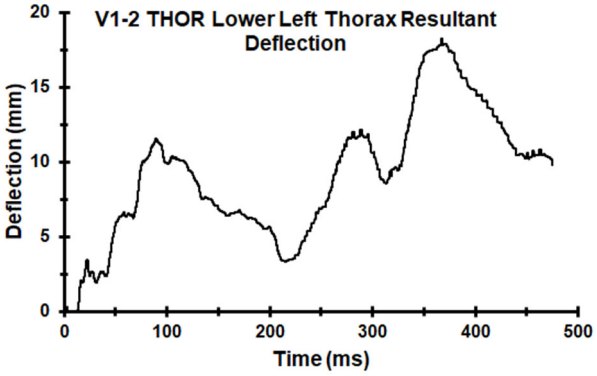
V1-2 THOR Lower Left Thorax Resultant Deflection
Deflection (mm)
Time (ms)

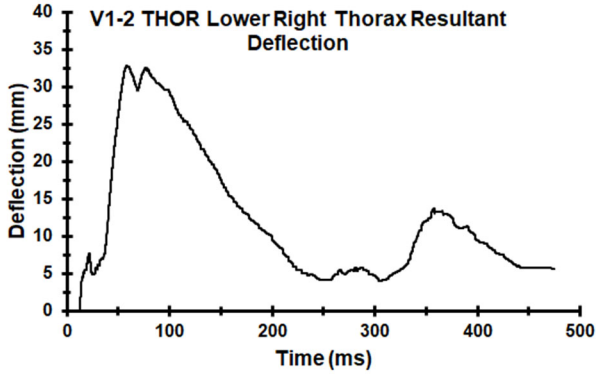
V1-2 THOR Lower Right Thorax Resultant Deflection
Deflection (mm)
Time (ms)

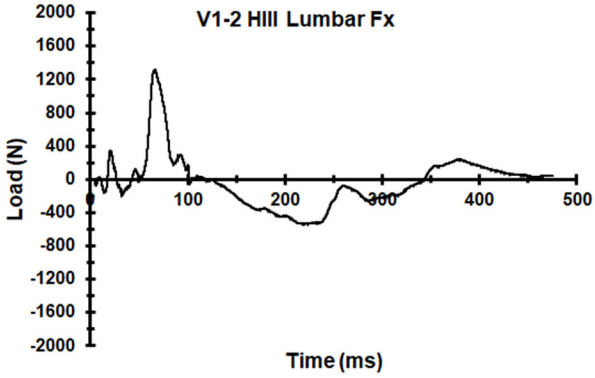
V1-2 HIII Lumbar Fx
Load (N)
Time (ms)

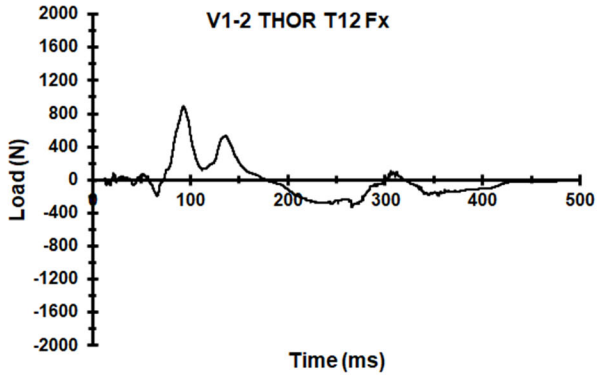
V1-2 THOR T12 Fx
Load (N)
Time (ms)

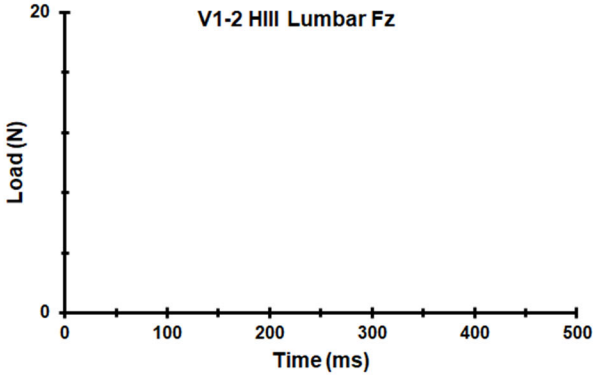
V1-2 HIII Lumbar Fz
Load (N)
Time (ms)

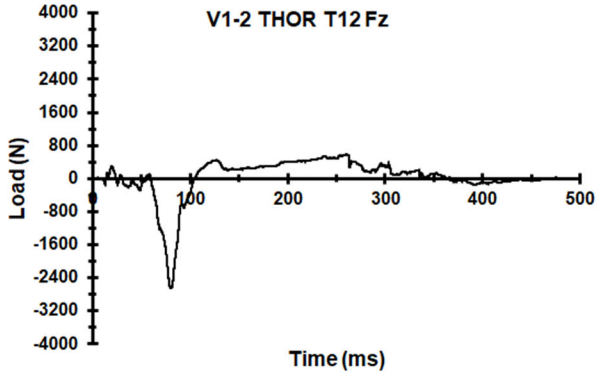
V1-2 THOR T12 Fz
Load (N)
Time (ms)

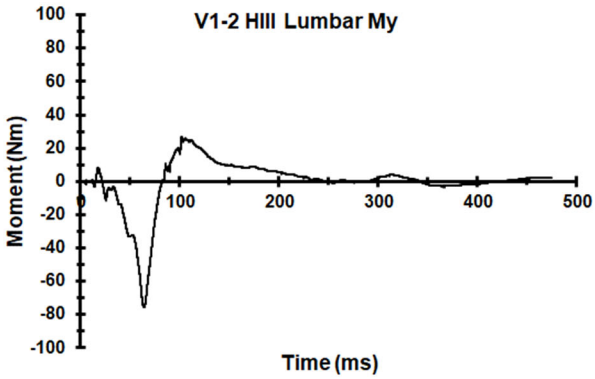
V1-2 HIII Lumbar My
Moment (Nm)
100
80
60
40
20
0
-20
-40
-60
-80
-100
0
100
200
300
400
500
Time (ms)

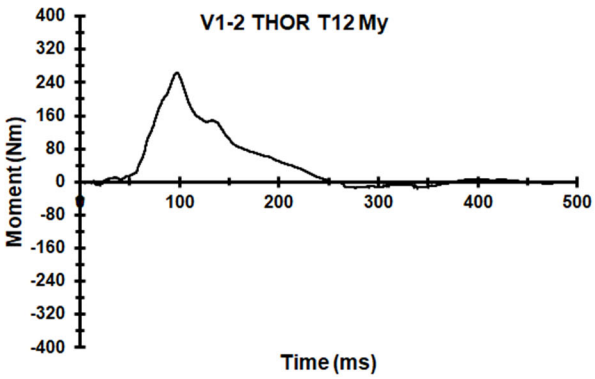
V1-2 THOR T12 My
Moment (Nm)
400
320
240
160
80
0
-80
-160
-240
-320
-400
0
100
200
300
400
500
Time (ms)

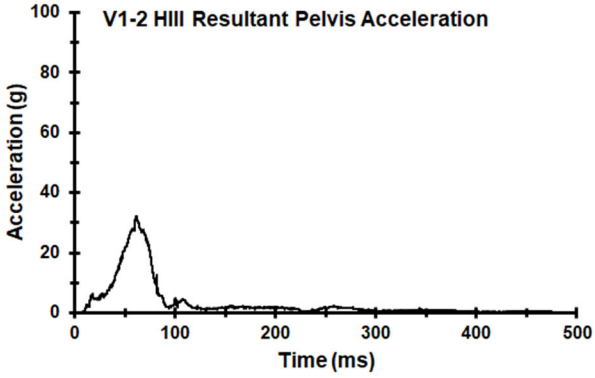
V1-2 HIII Resultant Pelvis Acceleration
Acceleration (g)
100
80
60
40
20
0
0
100
200
300
400
500
Time (ms)

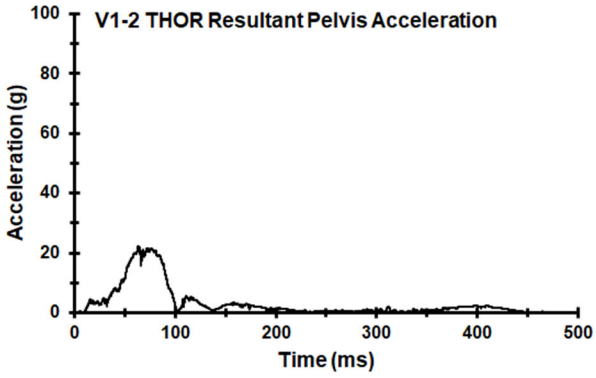
V1-2 THOR Resultant Pelvis Acceleration
Acceleration (g)
100
80
60
40
20
0
0
100
200
300
400
500
Time (ms)

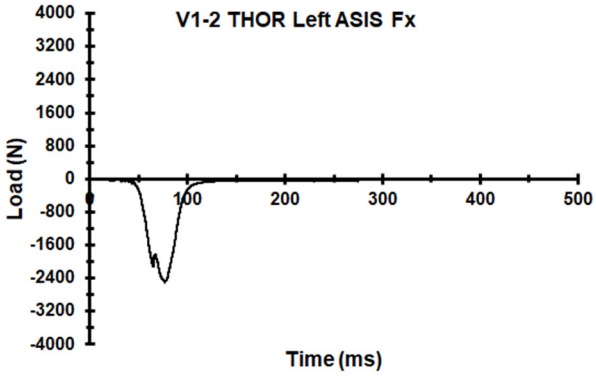
V1-2 THOR Left ASIS Fx
Load (N)
4000
3200
2400
1600
800
0
-800
-1600
-2400
-3200
-4000
0
100
200
300
400
500
Time (ms)

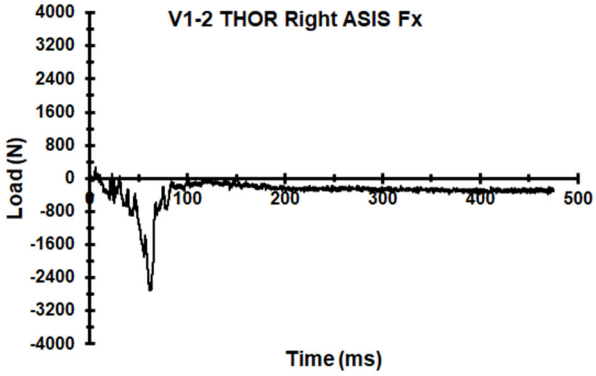
V1-2 THOR Right ASIS Fx
Load (N)
4000
3200
2400
1600
800
0
-800
-1600
-2400
-3200
-4000
0
100
200
300
400
500
Time (ms)

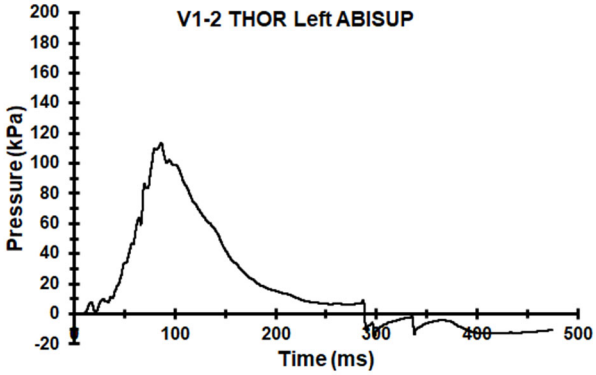
V1-2 THOR Left ABISUP
Pressure (kPa)
200
180
160
140
120
100
80
60
40
20
0
-20
100
200
300
400
500
Time (ms)

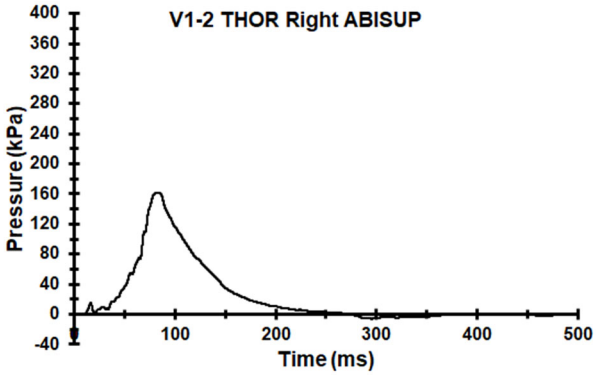
V1-2 THOR Right ABISUP
Pressure (kPa)
400
360
320
280
240
200
160
120
80
40
0
-40
100
200
300
400
500
Time (ms)

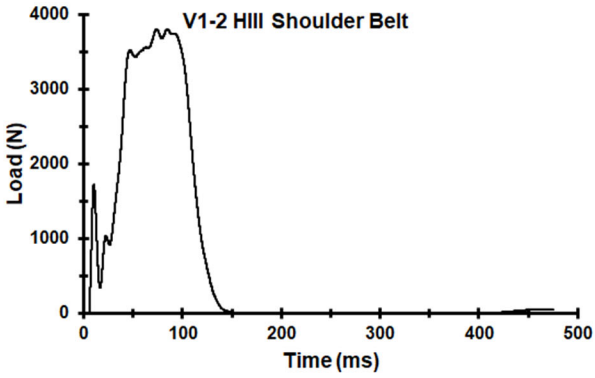
V1-2 HIII Shoulder Belt
Load (N)
4000
3000
2000
1000
0
0
100
200
300
400
500
Time (ms)

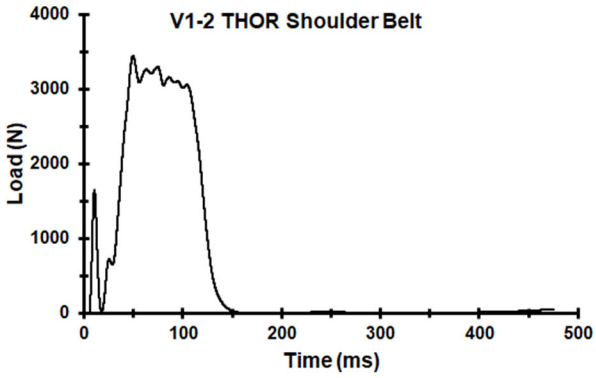
V1-2 THOR Shoulder Belt
Load (N)
4000
3000
2000
1000
0
0
100
200
300
400
500
Time (ms)

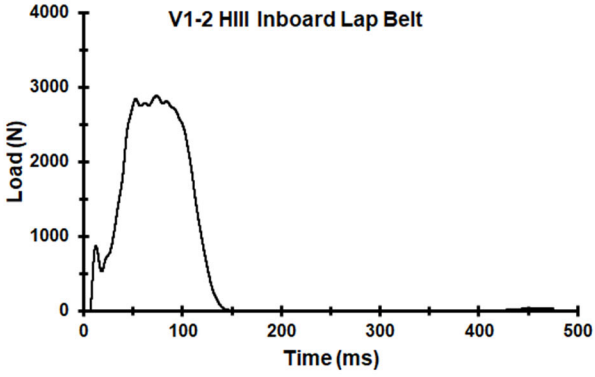
V1-2 HIII Inboard Lap Belt
Load (N)
4000
3000
2000
1000
0
0
100
200
300
400
500
Time (ms)

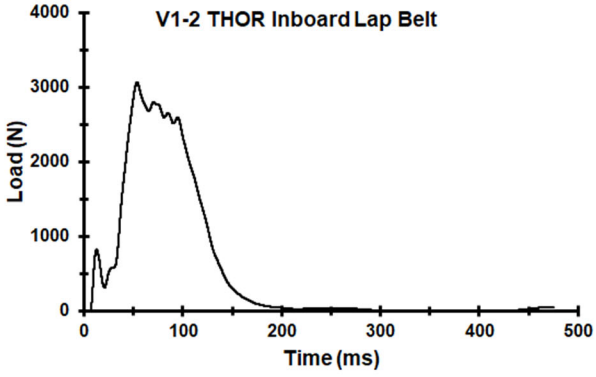
V1-2 THOR Inboard Lap Belt
Load (N)
4000
3000
2000
1000
0
0
100
200
300
400
500
Time (ms)

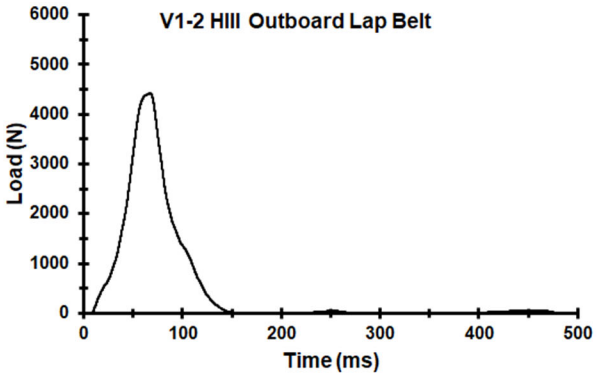
V1-2 HIII Outboard Lap Belt
Load (N)
6000
5000
4000
3000
2000
1000
0
0
100
200
300
400
500
Time (ms)

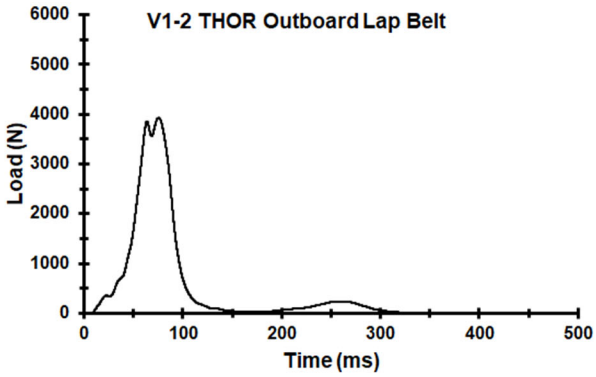
V1-2 THOR Outboard Lap Belt
Load (N)
6000
5000
4000
3000
2000
1000
0
0
100
200
300
400
500
Time (ms)

Appendix M. Select Data Traces From Test FRS-V1-3

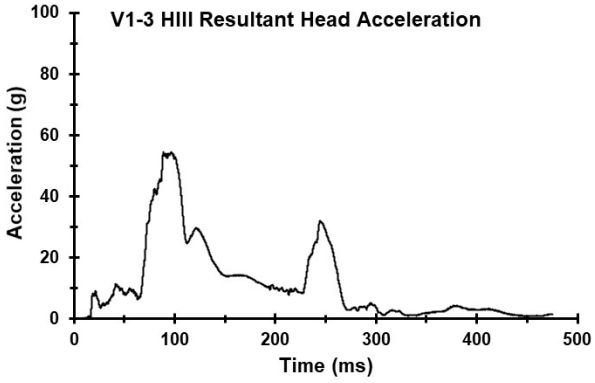
V1-3 HIII Resultant Head Acceleration
Acceleration (g)
Time (ms)

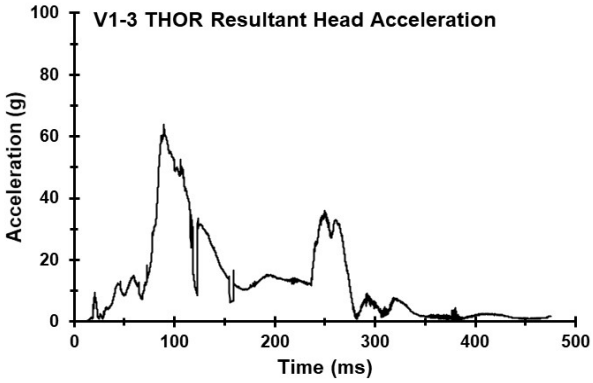
V1-3 THOR Resultant Head Acceleration
Acceleration (g)
Time (ms)

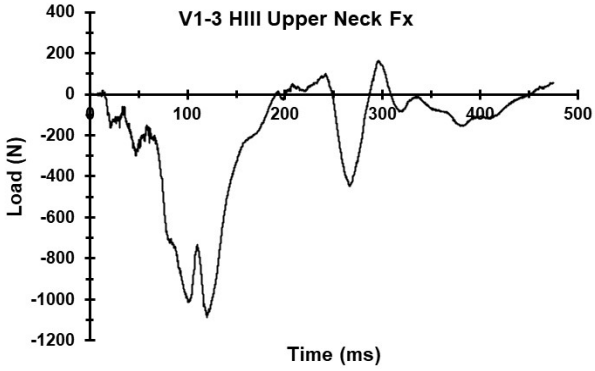
V1-3 HIII Upper Neck Fx
Load (N)
Time (ms)

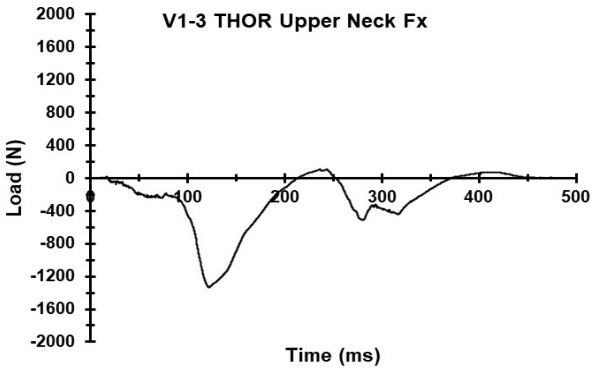
V1-3 THOR Upper Neck Fx
Load (N)
Time (ms)

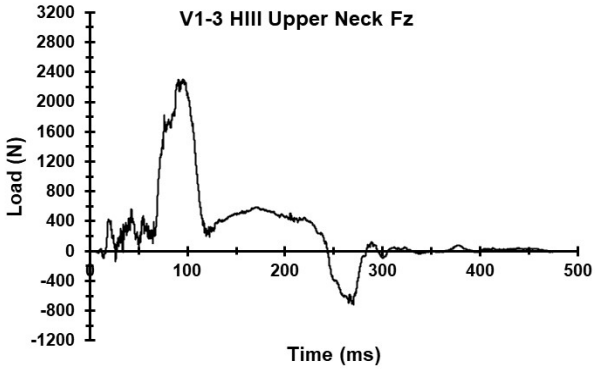
V1-3 HIII Upper Neck Fz
Load (N)
Time (ms)

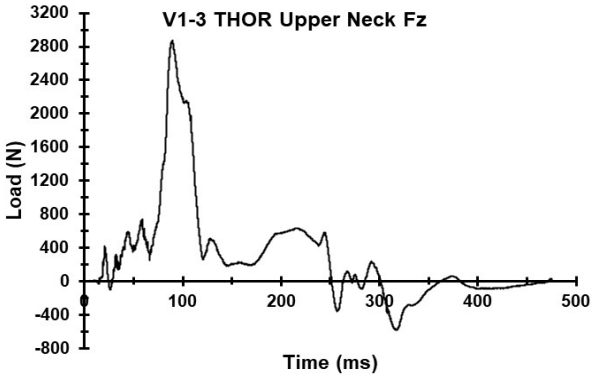
V1-3 THOR Upper Neck Fz
Load (N)
Time (ms)

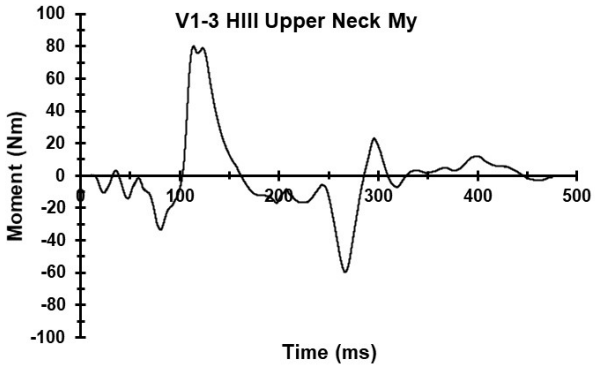
V1-3 HIII Upper Neck My
Moment (Nm)
Time (ms)

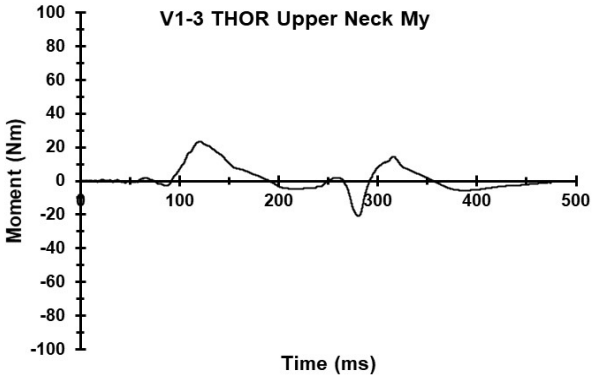
V1-3 THOR Upper Neck My
Moment (Nm)
Time (ms)

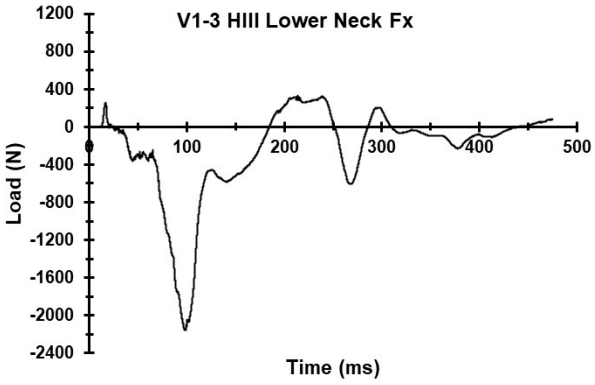
V1-3 HIII Lower Neck Fx
Load (N)
Time (ms)

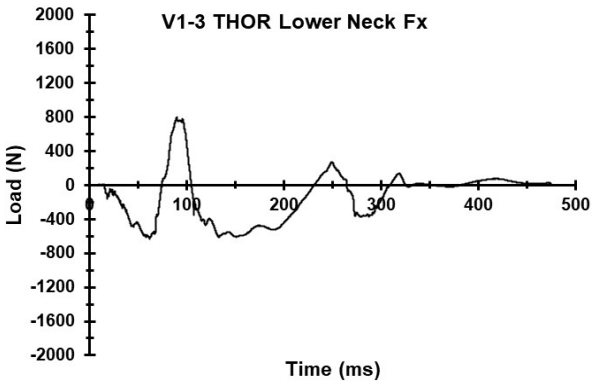
V1-3 THOR Lower Neck Fx
Load (N)
Time (ms)

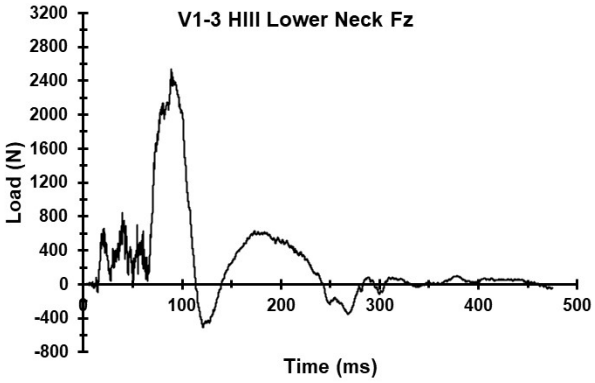
V1-3 HIII Lower Neck Fz
Load (N)
Time (ms)

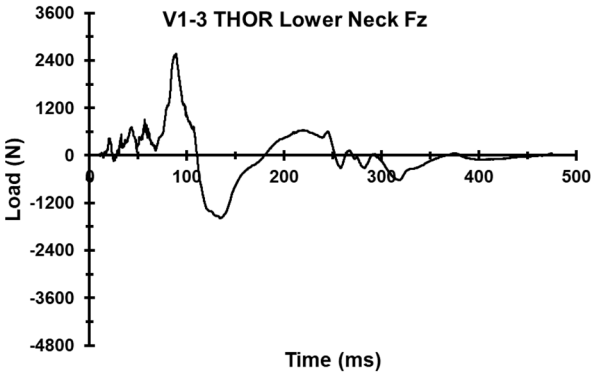
V1-3 THOR Lower Neck Fz
Load (N)
Time (ms)

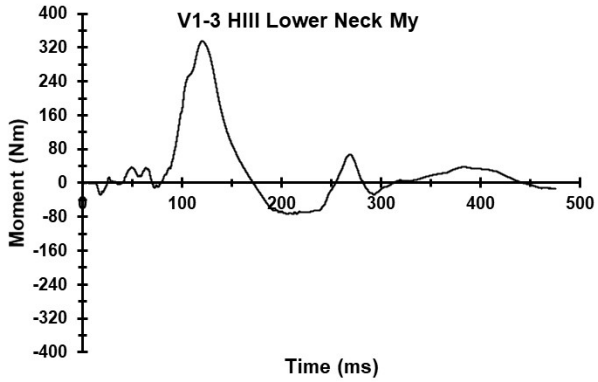
V1-3 HIII Lower Neck My
Moment (Nm)
Time (ms)

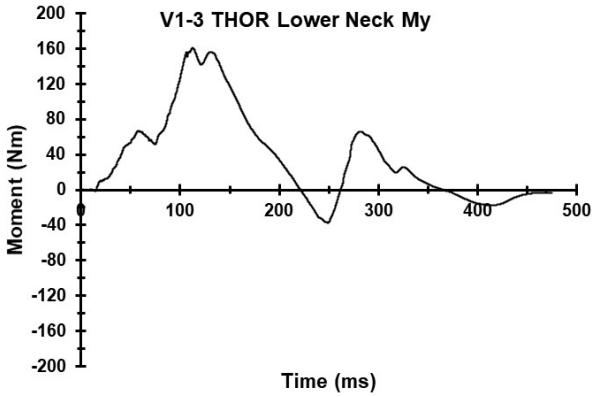
V1-3 THOR Lower Neck My
Moment (Nm)
Time (ms)

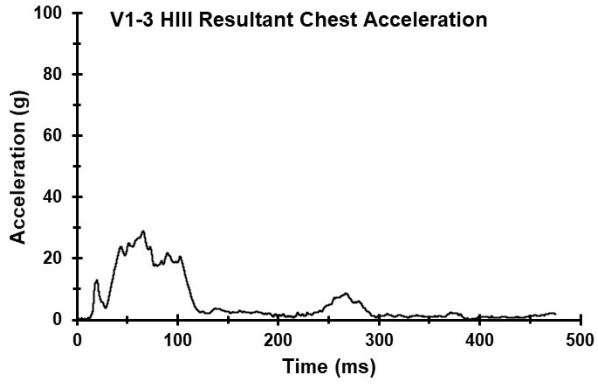
V1-3 HIII Resultant Chest Acceleration
Acceleration (g)
Time (ms)

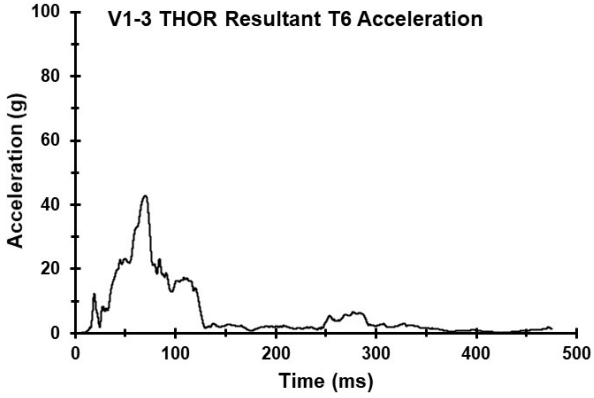
V1-3 THOR Resultant T6 Acceleration
Acceleration (g)
Time (ms)

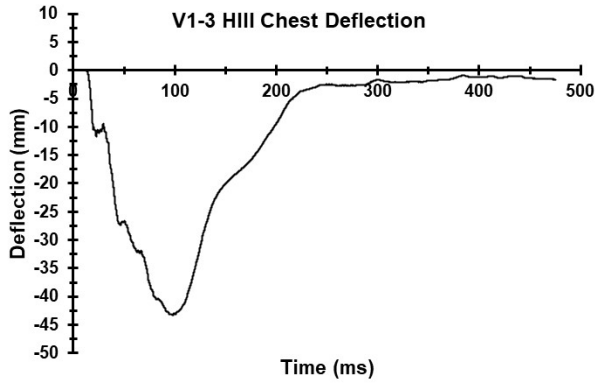
V1-3 HIII Chest Deflection
Deflection (mm)
Time (ms)

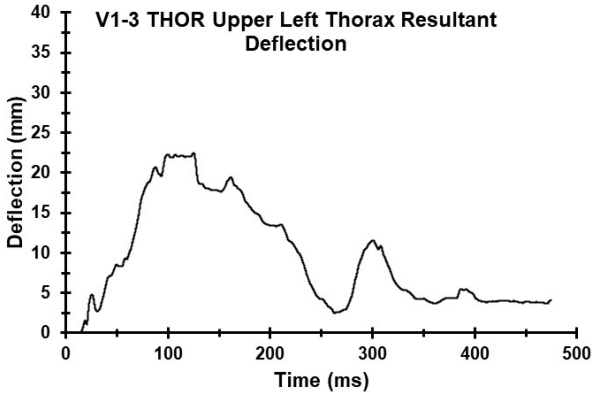
V1-3 THOR Upper Left Thorax Resultant Deflection
Deflection (mm)
Time (ms)

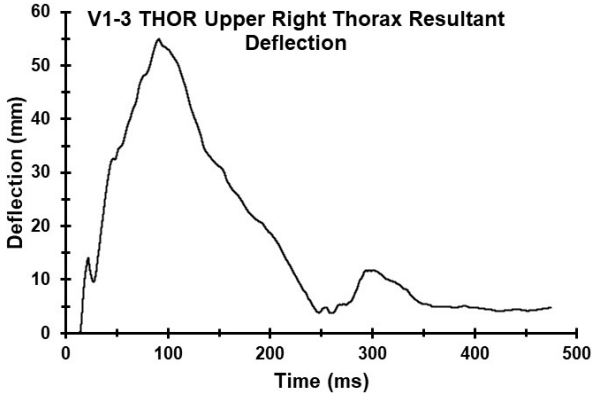
V1-3 THOR Upper Right Thorax Resultant Deflection
Deflection (mm)
Time (ms)
0
10
20
30
40
50
60
0
100
200
300
400
500

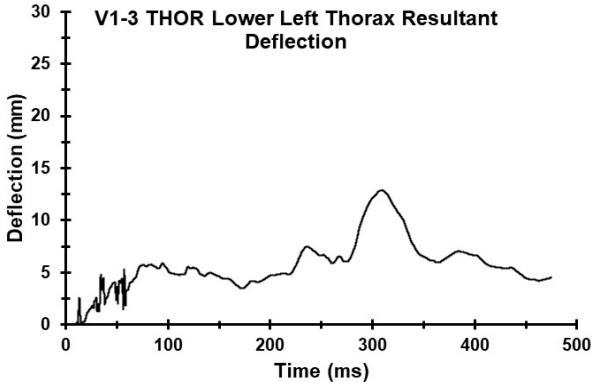
V1-3 THOR Lower Left Thorax Resultant Deflection
Deflection (mm)
Time (ms)
0
5
10
15
20
25
30
0
100
200
300
400
500

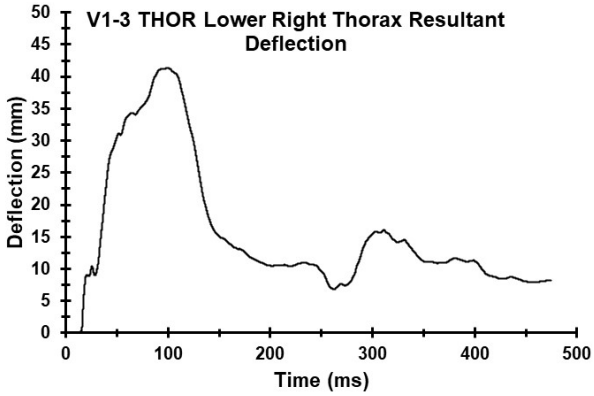
V1-3 THOR Lower Right Thorax Resultant Deflection
Deflection (mm)
Time (ms)
0
5
10
15
20
25
30
35
40
45
50
0
100
200
300
400
500

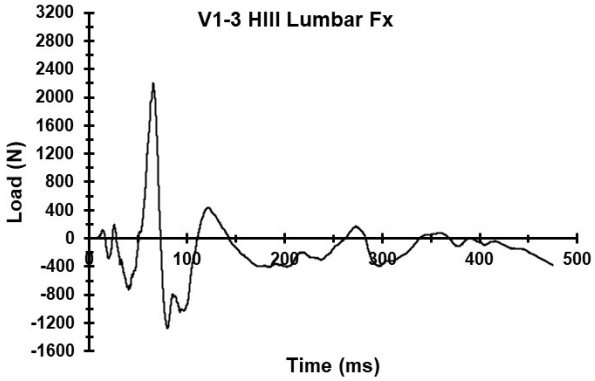
V1-3 HIII Lumbar Fx
Load (N)
Time (ms)

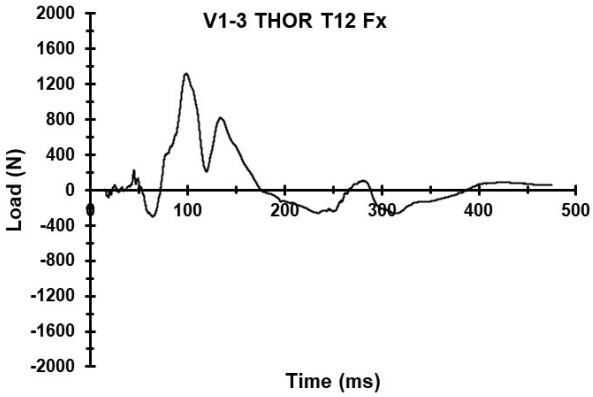
V1-3 THOR T12 Fx
Load (N)
Time (ms)

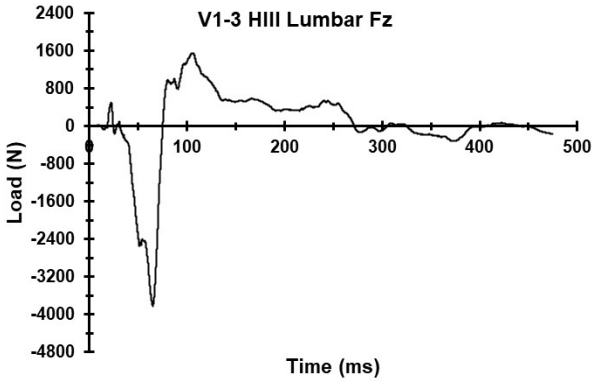
V1-3 HIII Lumbar Fz
Load (N)
Time (ms)

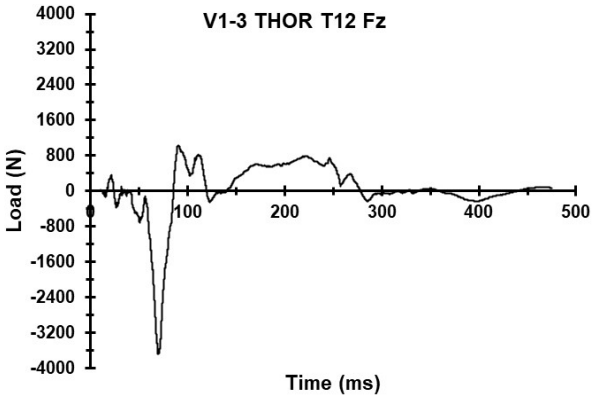
V1-3 THOR T12 Fz
Load (N)
Time (ms)

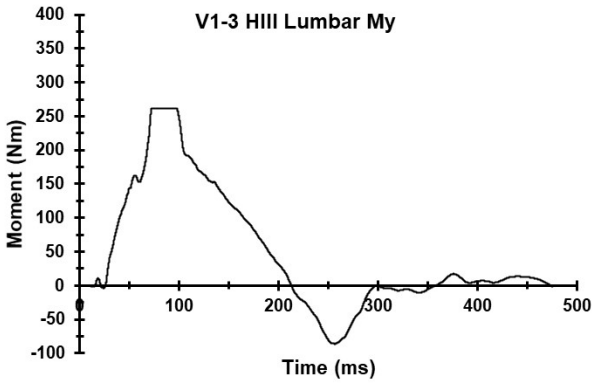
V1-3 HIII Lumbar My
Moment (Nm)
Time (ms)

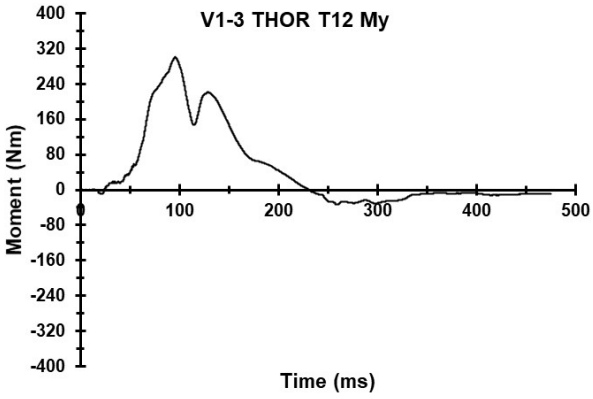
V1-3 THOR T12 My
Moment (Nm)
Time (ms)

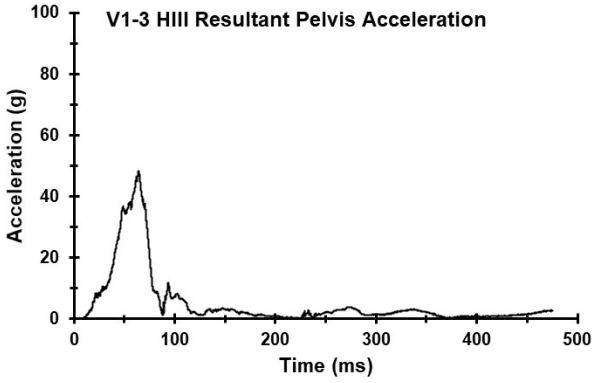
V1-3 HIII Resultant Pelvis Acceleration
Acceleration (g)
Time (ms)
100
80
60
40
20
0
0
100
200
300
400
500

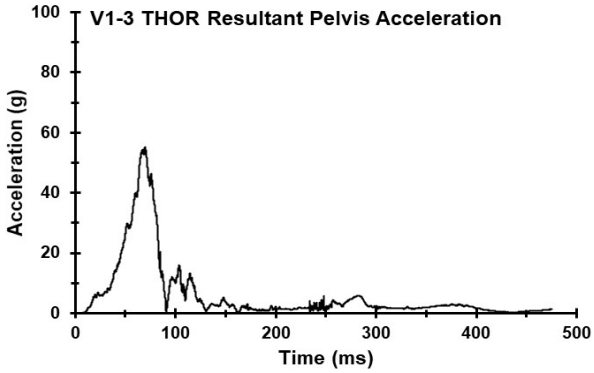
V1-3 THOR Resultant Pelvis Acceleration
Acceleration (g)
Time (ms)
100
80
60
40
20
0
0
100
200
300
400
500

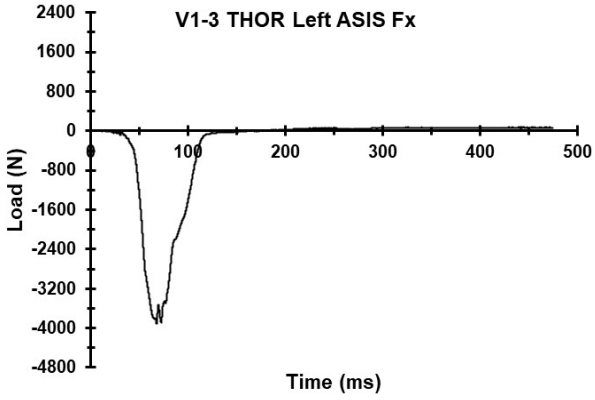
V1-3 THOR Left ASIS Fx
Load (N)
Time (ms)
2400
1600
800
0
-800
-1600
-2400
-3200
-4000
-4800
0
100
200
300
400
500

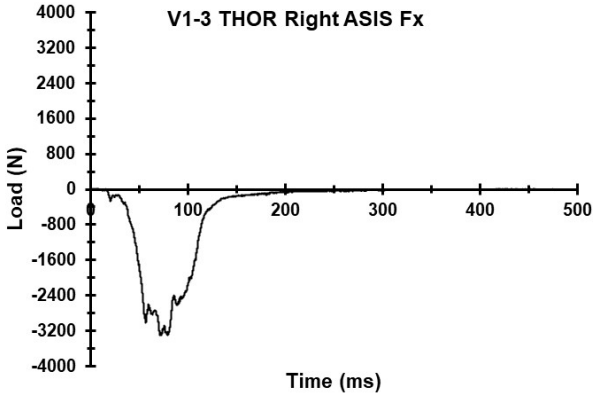
V1-3 THOR Right ASIS Fx
Load (N)
Time (ms)
4000
3200
2400
1600
800
0
-800
-1600
-2400
-3200
-4000
0
100
200
300
400
500

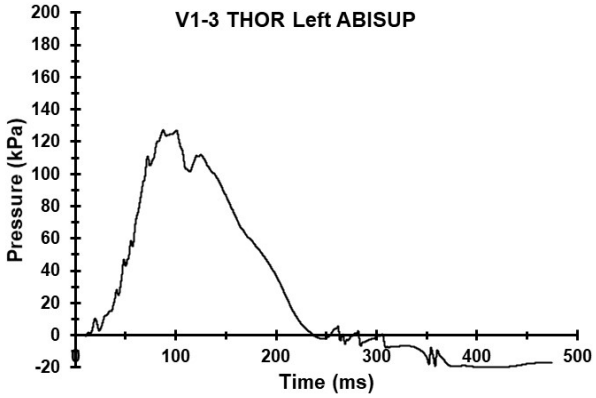
V1-3 THOR Left ABISUP
Pressure (kPa)
200
180
160
140
120
100
80
60
40
20
0
-20
0
100
200
300
400
500
Time (ms)

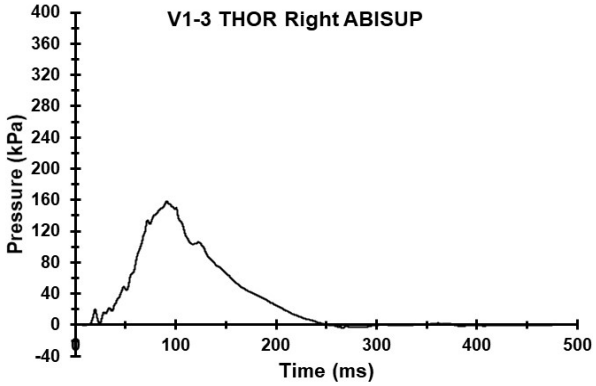
V1-3 THOR Right ABISUP
Pressure (kPa)
400
360
320
280
240
200
160
120
80
40
0
-40
0
100
200
300
400
500
Time (ms)

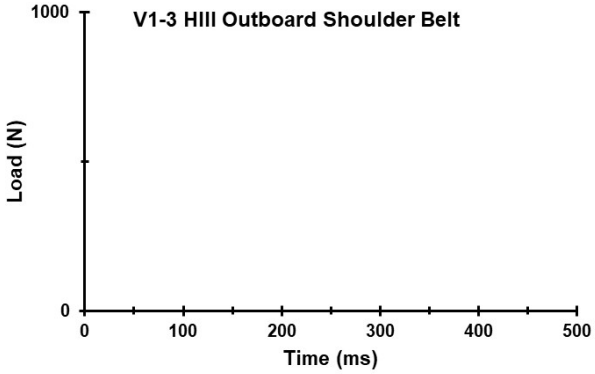
V1-3 HIII Outboard Shoulder Belt
Load (N)
1000
0
0
100
200
300
400
500
Time (ms)

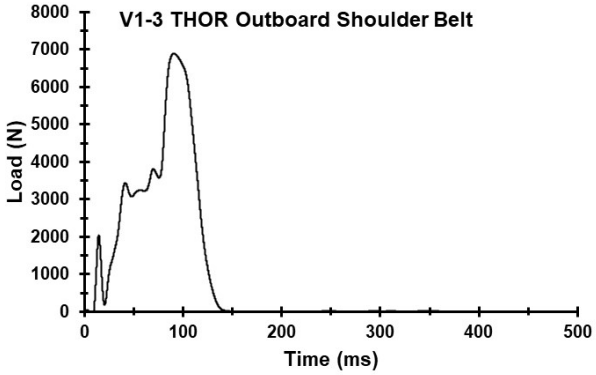
V1-3 THOR Outboard Shoulder Belt
Load (N)
8000
7000
6000
5000
4000
3000
2000
1000
0
0
100
200
300
400
500
Time (ms)

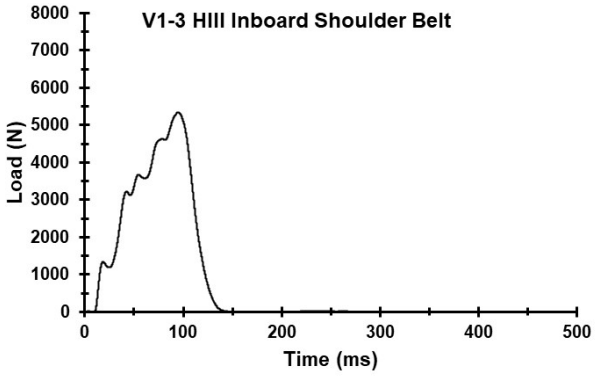
V1-3 HIII Inboard Shoulder Belt
Load (N)
8000
7000
6000
5000
4000
3000
2000
1000
0
0
100
200
300
400
500
Time (ms)

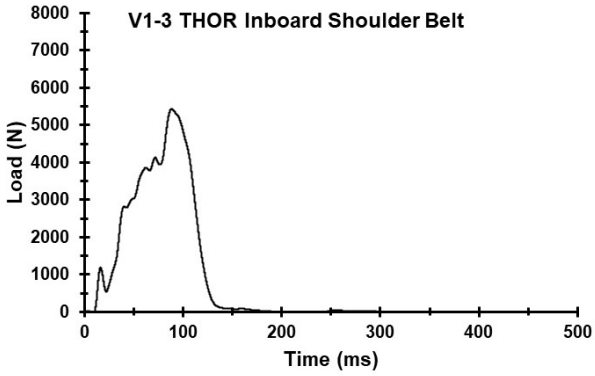
V1-3 THOR Inboard Shoulder Belt
Load (N)
8000
7000
6000
5000
4000
3000
2000
1000
0
0
100
200
300
400
500
Time (ms)

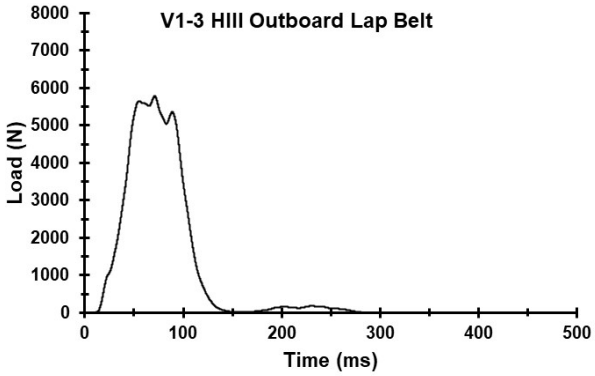
V1-3 HIII Outboard Lap Belt
Load (N)
8000
7000
6000
5000
4000
3000
2000
1000
0
0
100
200
300
400
500
Time (ms)

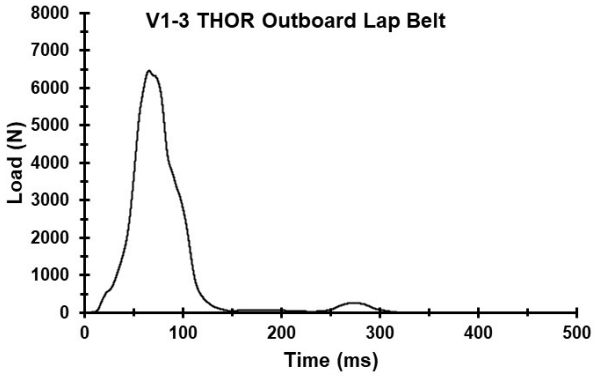
V1-3 THOR Outboard Lap Belt
Load (N)
8000
7000
6000
5000
4000
3000
2000
1000
0
0
100
200
300
400
500
Time (ms)

Appendix N. Select Data Traces From Test FRS-V6-1

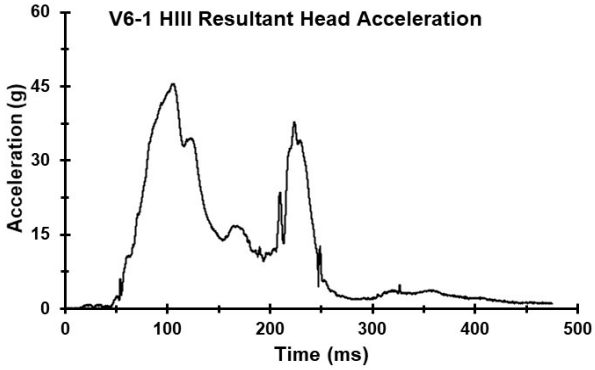
V6-1 HIII Resultant Head Acceleration
Acceleration (g)
60
45
30
15
0
0
100
200
300
400
500
Time (ms)

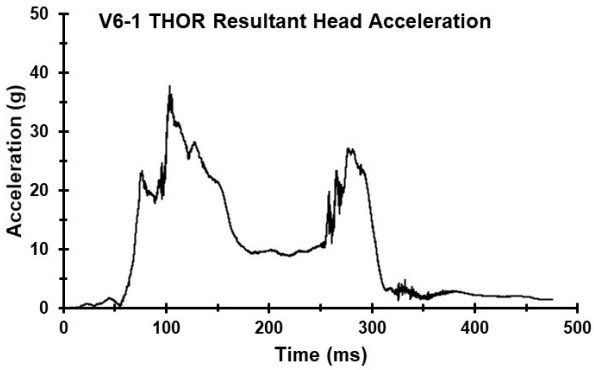
V6-1 THOR Resultant Head Acceleration
Acceleration (g)
50
40
30
20
10
0
0
100
200
300
400
500
Time (ms)

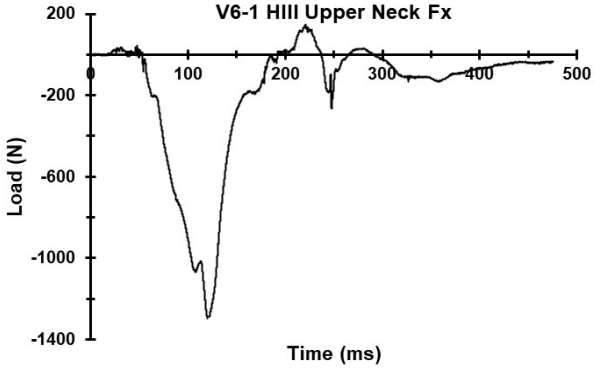
V6-1 HIII Upper Neck Fx
Load (N)
200
-200
-600
-1000
-1400
0
100
200
300
400
500
Time (ms)

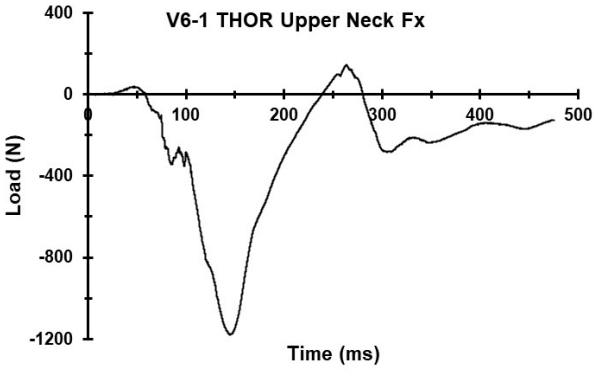
V6-1 THOR Upper Neck Fx
Load (N)
400
0
-400
-800
-1200
0
100
200
300
400
500
Time (ms)

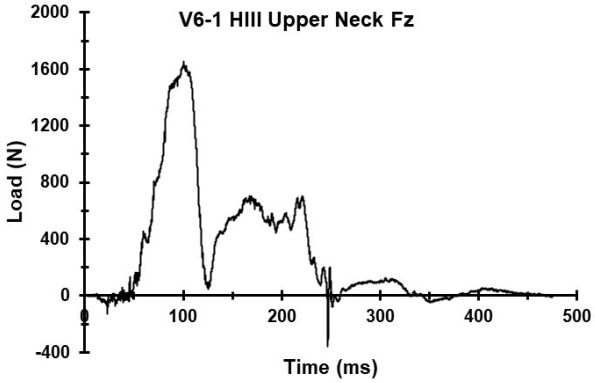
V6-1 HIII Upper Neck Fz
Load (N)
2000
1600
1200
800
400
0
-400
0
100
200
300
400
500
Time (ms)

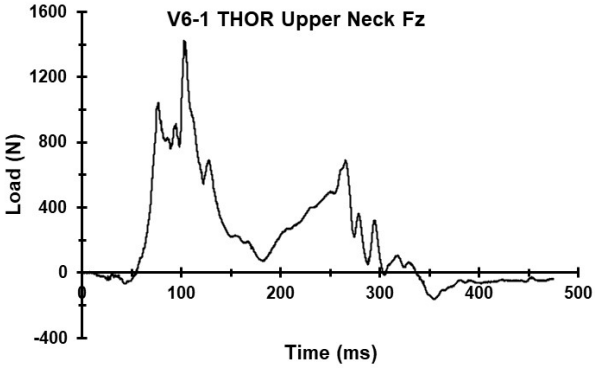
V6-1 THOR Upper Neck Fz
Load (N)
1600
1200
800
400
0
-400
0
100
200
300
400
500
Time (ms)

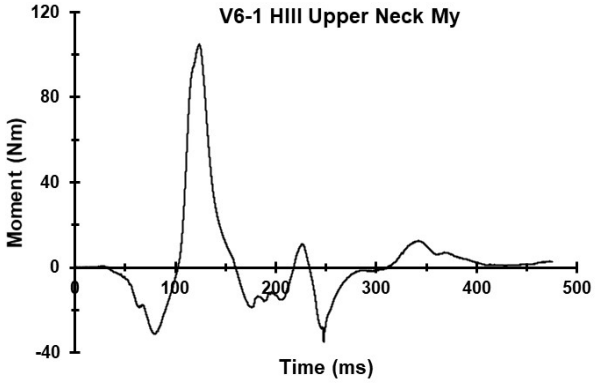
V6-1 HIII Upper Neck My
Moment (Nm)
120
80
40
0
-40
0
100
200
300
400
500
Time (ms)

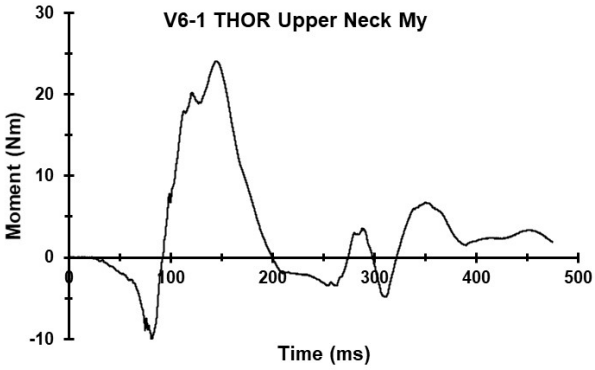
V6-1 THOR Upper Neck My
Moment (Nm)
30
20
10
0
-10
0
100
200
300
400
500
Time (ms)

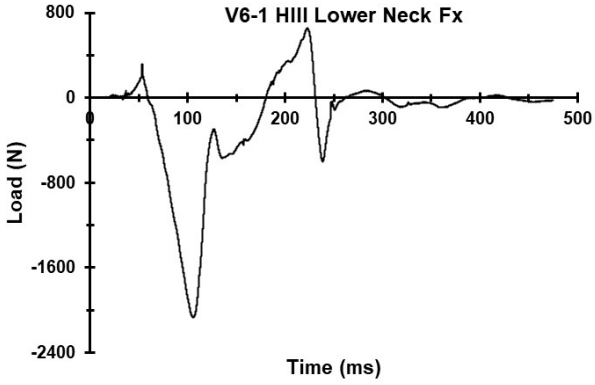
V6-1 HIII Lower Neck Fx
Load (N)
800
0
-800
-1600
-2400
0
100
200
300
400
500
Time (ms)

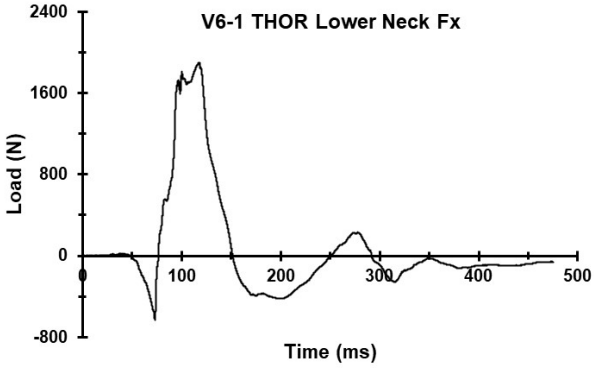
V6-1 THOR Lower Neck Fx
Load (N)
2400
1600
800
0
-800
0
100
200
300
400
500
Time (ms)

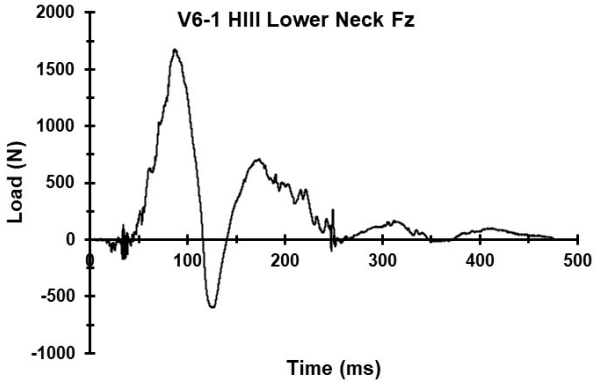
V6-1 HIII Lower Neck Fz
Load (N)
2000
1500
1000
500
0
-500
-1000
0
100
200
300
400
500
Time (ms)

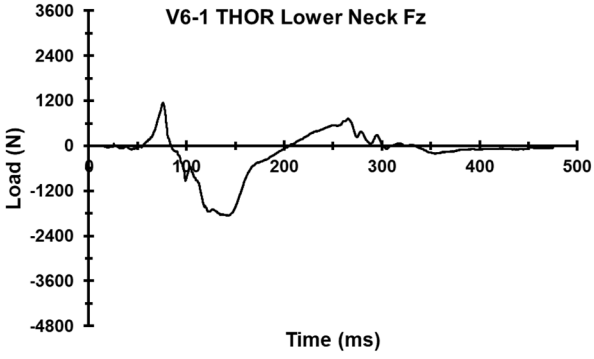
V6-1 THOR Lower Neck Fz
Load (N)
3600
2400
1200
0
-1200
-2400
-3600
-4800
0
100
200
300
400
500
Time (ms)

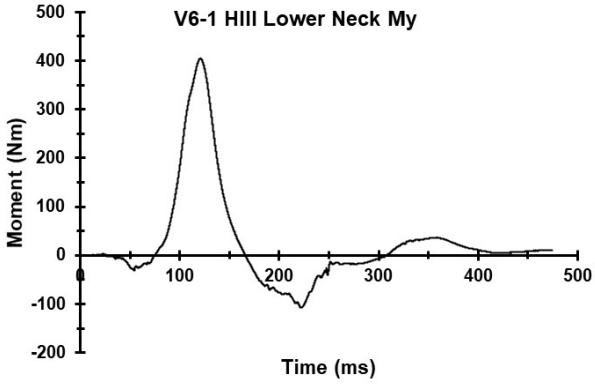
V6-1 HIII Lower Neck My
Moment (Nm)
500
400
300
200
100
0
-100
-200
0
100
200
300
400
500
Time (ms)

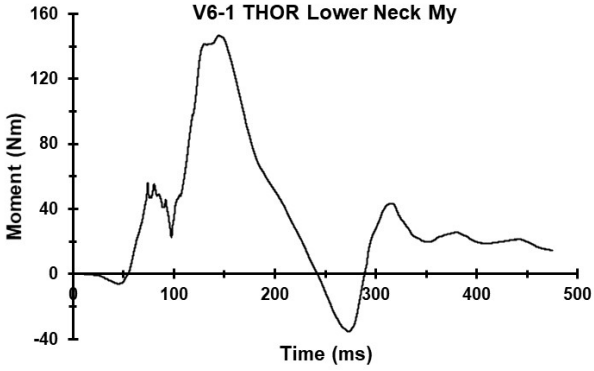
V6-1 THOR Lower Neck My
Moment (Nm)
160
120
80
40
0
-40
0
100
200
300
400
500
Time (ms)

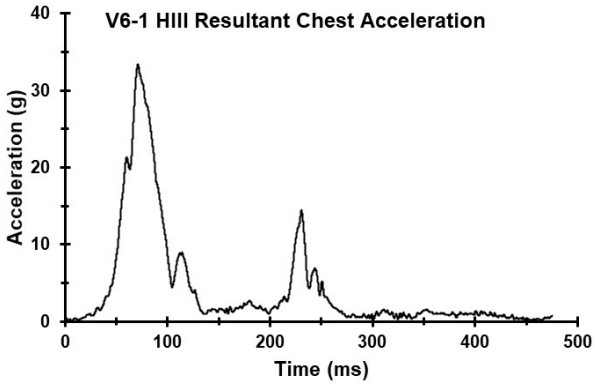
V6-1 HIII Resultant Chest Acceleration
Acceleration (g)
Time (ms)

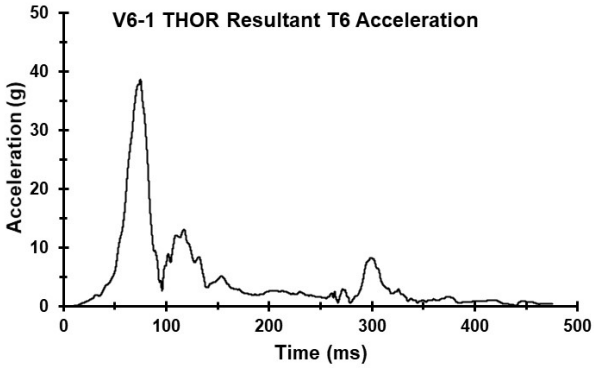
V6-1 THOR Resultant T6 Acceleration
Acceleration (g)
Time (ms)

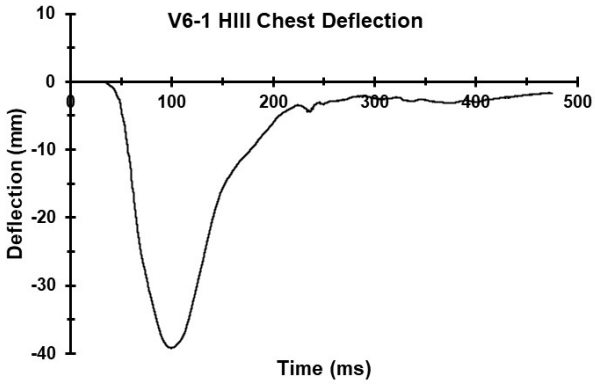
V6-1 HIII Chest Deflection
Deflection (mm)
Time (ms)

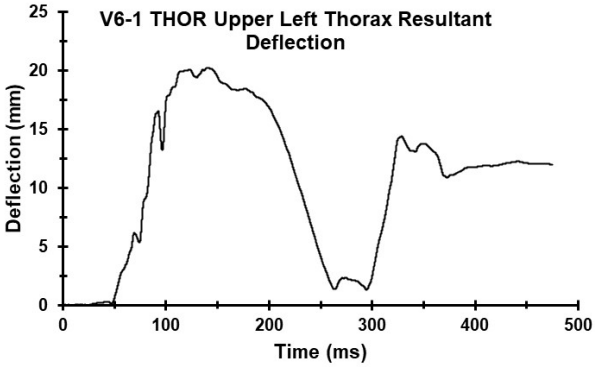
V6-1 THOR Upper Left Thorax Resultant Deflection
Deflection (mm)
Time (ms)

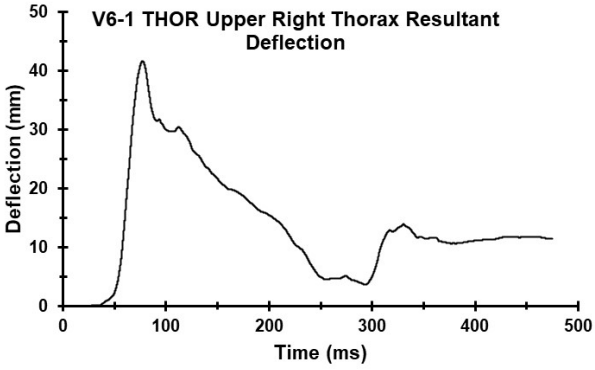
V6-1 THOR Upper Right Thorax Resultant Deflection
Deflection (mm)
Time (ms)

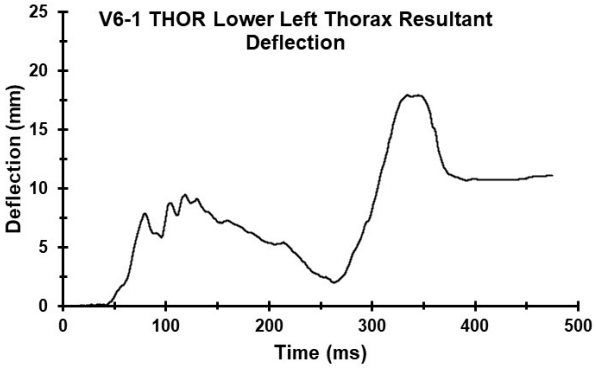
V6-1 THOR Lower Left Thorax Resultant Deflection
Deflection (mm)
25
20
15
10
5
0
0
100
200
300
400
500
Time (ms)

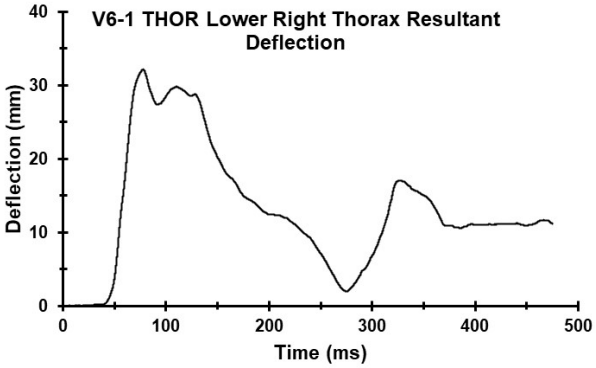
V6-1 THOR Lower Right Thorax Resultant Deflection
Deflection (mm)
40
30
20
10
0
0
100
200
300
400
500
Time (ms)

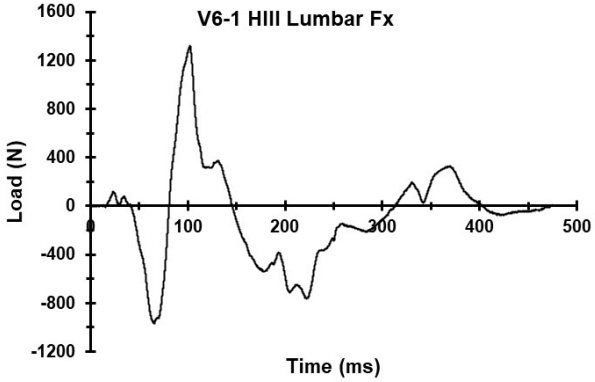
V6-1 HIII Lumbar Fx
Load (N)
1600
1200
800
400
0
-400
-800
-1200
0
100
200
300
400
500
Time (ms)

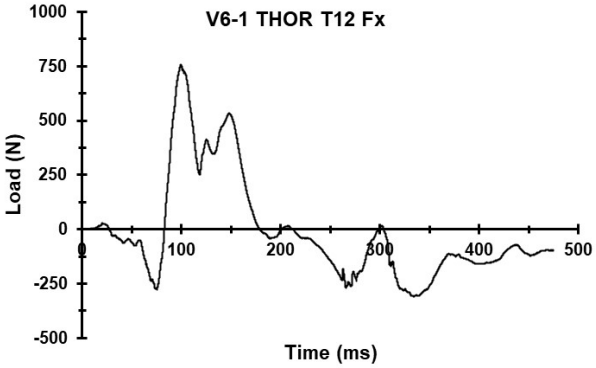
V6-1 THOR T12 Fx
Load (N)
1000
750
500
250
0
-250
-500
0
100
200
300
400
500
Time (ms)

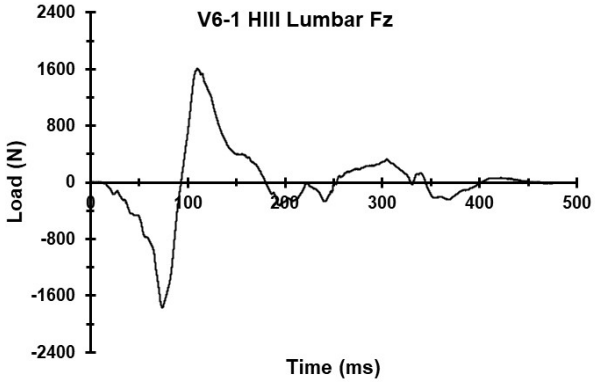
V6-1 HIII Lumbar Fz
Load (N)
2400
1600
800
0
-800
-1600
-2400
0
100
200
300
400
500
Time (ms)

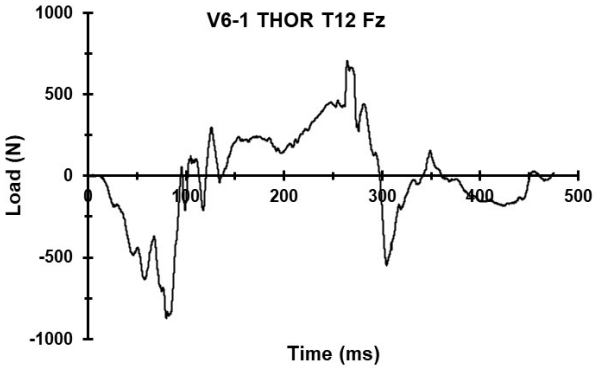
V6-1 THOR T12 Fz
Load (N)
1000
500
0
-500
-1000
0
100
200
300
400
500
Time (ms)

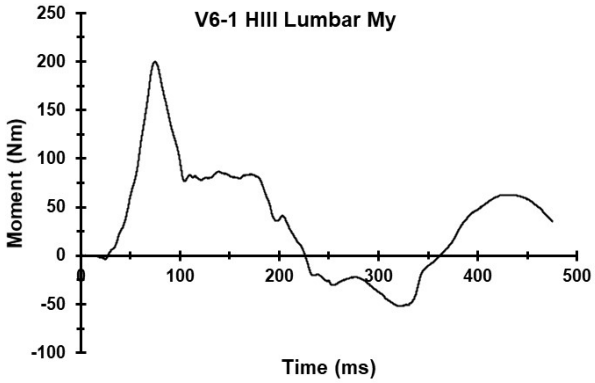
V6-1 HIII Lumbar My
Moment (Nm)
250
200
150
100
50
0
-50
-100
0
100
200
300
400
500
Time (ms)

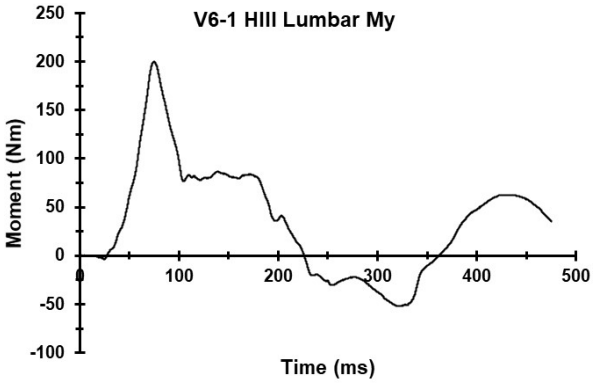
V6-1 HIII Lumbar My
Moment (Nm)
250
200
150
100
50
0
-50
-100
0
100
200
300
400
500
Time (ms)

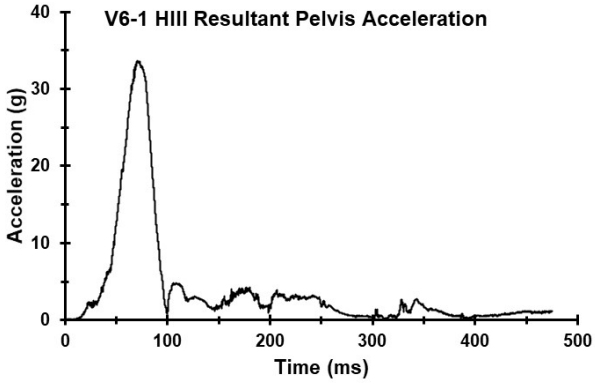
V6-1 HIII Resultant Pelvis Acceleration
Acceleration (g)
40
30
20
10
0
0
100
200
300
400
500
Time (ms)

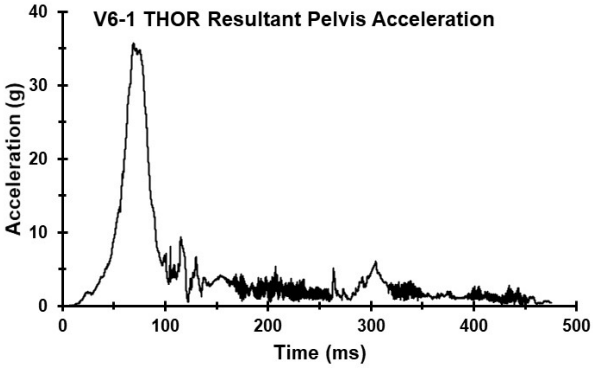
V6-1 THOR Resultant Pelvis Acceleration
Acceleration (g)
40
30
20
10
0
0
100
200
300
400
500
Time (ms)

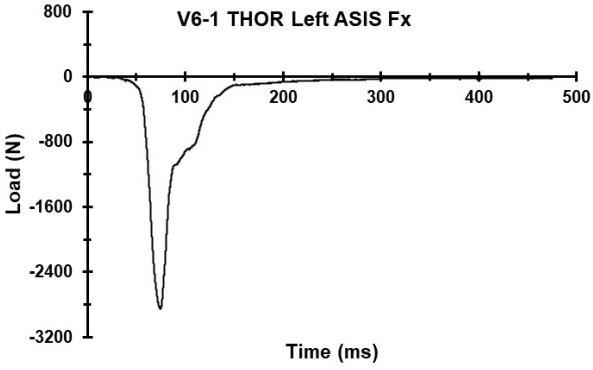
V6-1 THOR Left ASIS Fx
Load (N)
800
0
-800
-1600
-2400
-3200
0
100
200
300
400
500
Time (ms)

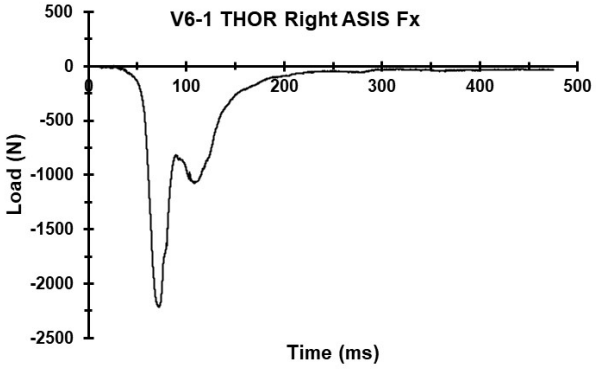
V6-1 THOR Right ASIS Fx
Load (N)
Time (ms)
500
0
-500
-1000
-1500
-2000
-2500
0
100
200
300
400
500

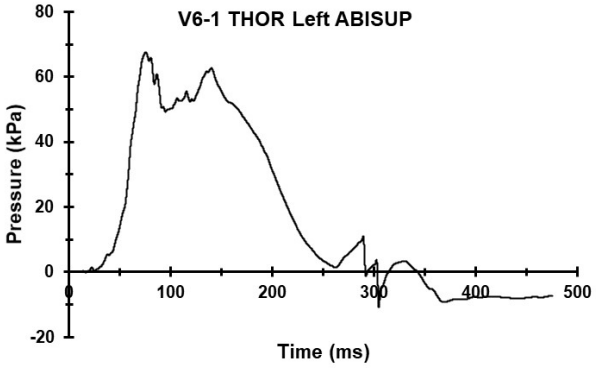
V6-1 THOR Left ABISUP
Pressure (kPa)
Time (ms)
80
60
40
20
0
-20
0
100
200
300
400
500

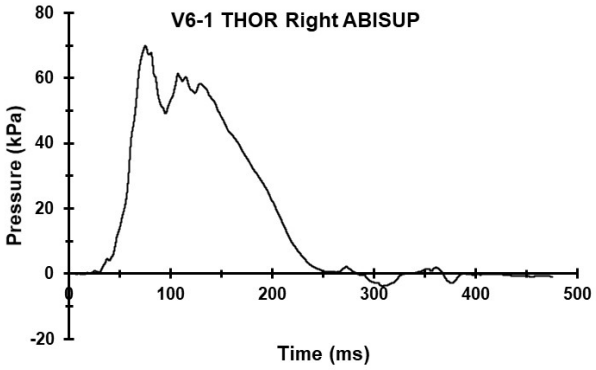
V6-1 THOR Right ABISUP
Pressure (kPa)
Time (ms)
80
60
40
20
0
-20
0
100
200
300
400
500

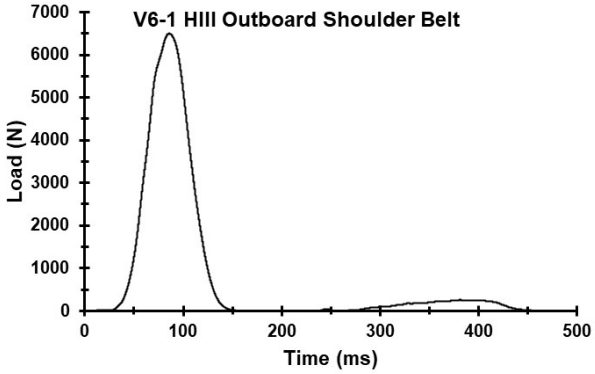
V6-1 HIII Outboard Shoulder Belt
Load (N)
Time (ms)
7000
6000
5000
4000
3000
2000
1000
0
0
100
200
300
400
500

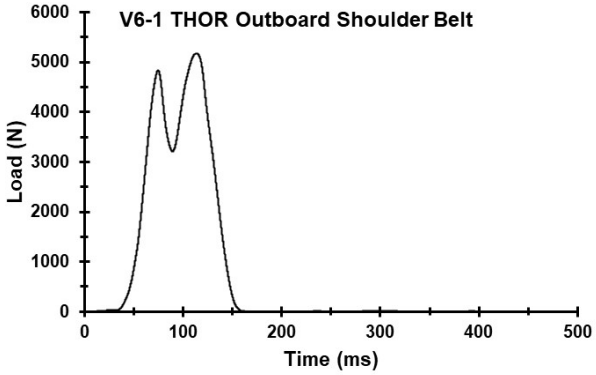
V6-1 THOR Outboard Shoulder Belt
Load (N)
Time (ms)
6000
5000
4000
3000
2000
1000
0
0
100
200
300
400
500

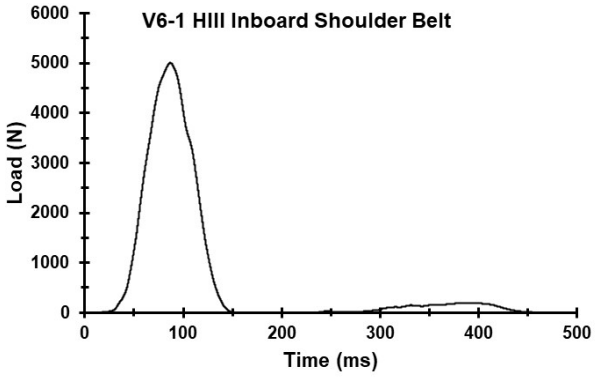
V6-1 HIII Inboard Shoulder Belt
Load (N)
6000
5000
4000
3000
2000
1000
0
0
100
200
300
400
500
Time (ms)

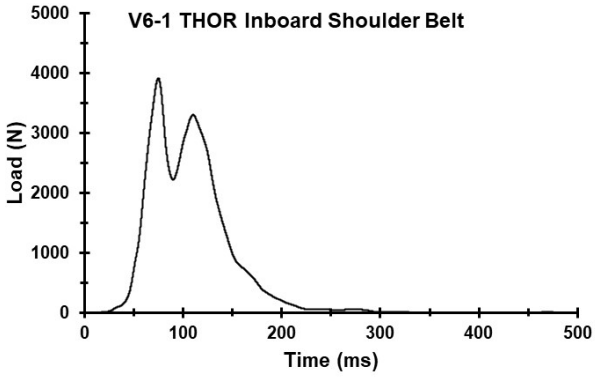
V6-1 THOR Inboard Shoulder Belt
Load (N)
5000
4000
3000
2000
1000
0
0
100
200
300
400
500
Time (ms)

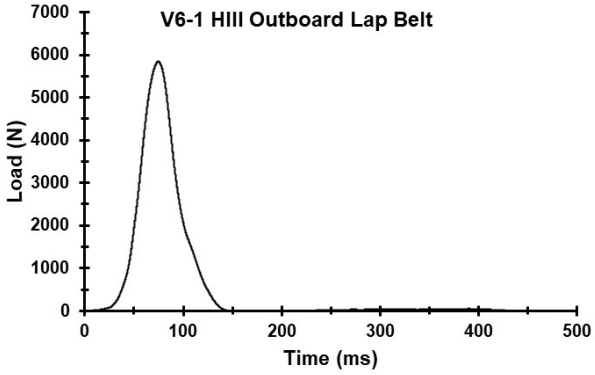
V6-1 HIII Outboard Lap Belt
Load (N)
7000
6000
5000
4000
3000
2000
1000
0
0
100
200
300
400
500
Time (ms)

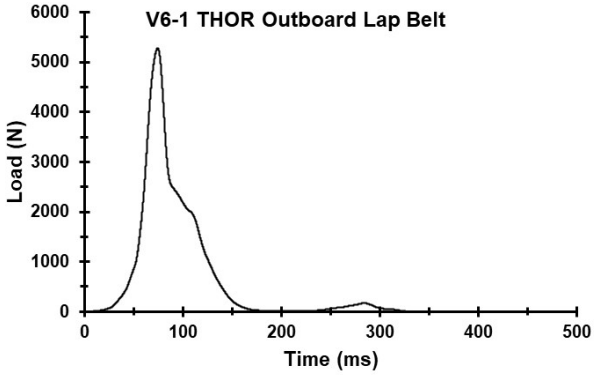
V6-1 THOR Outboard Lap Belt
Load (N)
6000
5000
4000
3000
2000
1000
0
0
100
200
300
400
500
Time (ms)

Appendix O. Select Data Traces From Test FRS-V6-2

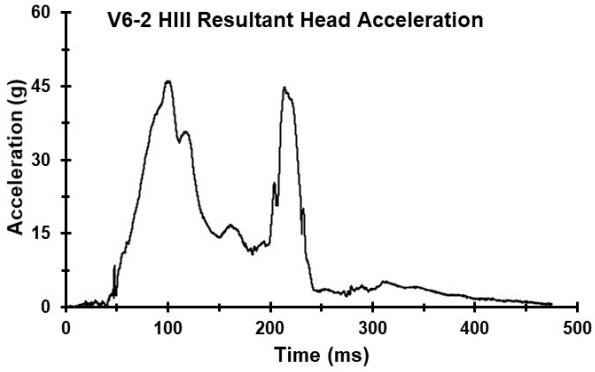
V6-2 HIII Resultant Head Acceleration
Acceleration (g)
60
45
30
15
0
0
100
200
300
400
500
Time (ms)

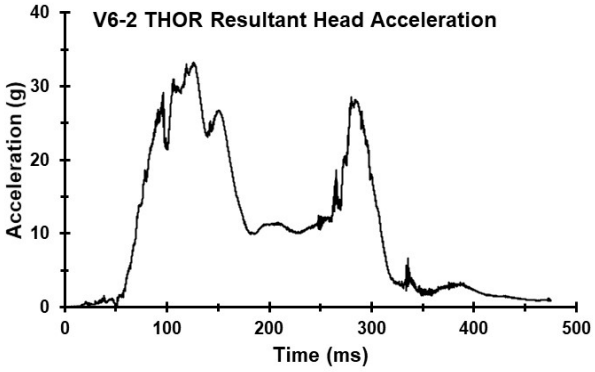
V6-2 THOR Resultant Head Acceleration
Acceleration (g)
40
30
20
10
0
0
100
200
300
400
500
Time (ms)

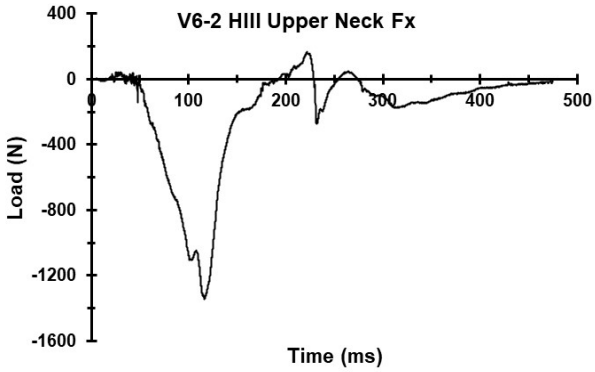
V6-2 HIII Upper Neck Fx
Load (N)
400
0
-400
-800
-1200
-1600
0
100
200
300
400
500
Time (ms)

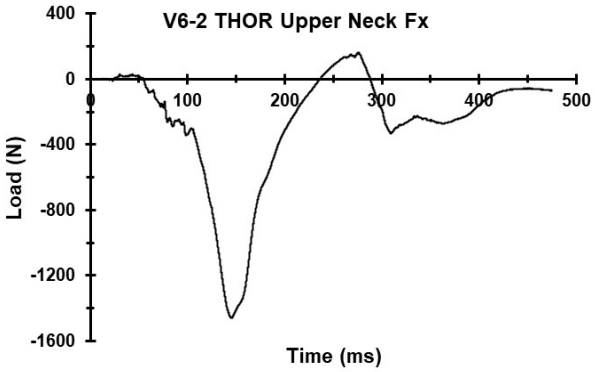
V6-2 THOR Upper Neck Fx
Load (N)
400
0
-400
-800
-1200
-1600
0
100
200
300
400
500
Time (ms)

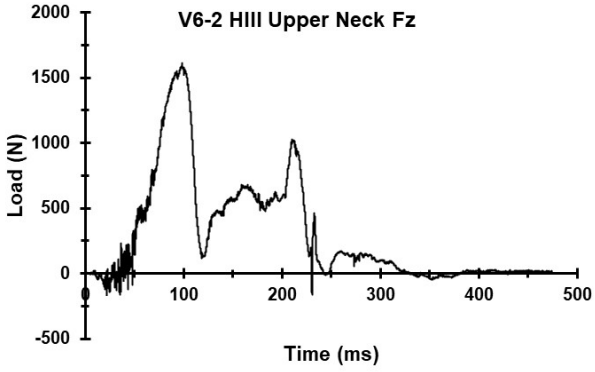
V6-2 HIII Upper Neck Fz
Load (N)
2000
1500
1000
500
0
-500
0
100
200
300
400
500
Time (ms)

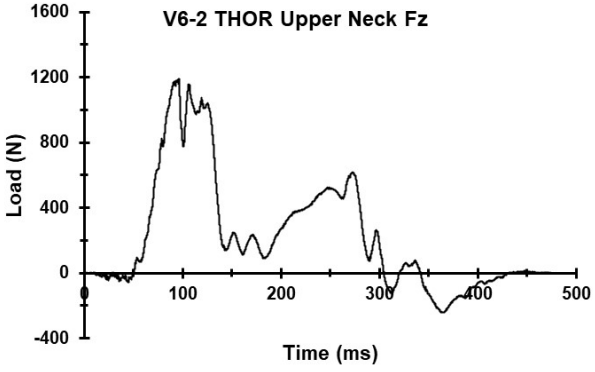
V6-2 THOR Upper Neck Fz
Load (N)
1600
1200
800
400
0
-400
0
100
200
300
400
500
Time (ms)

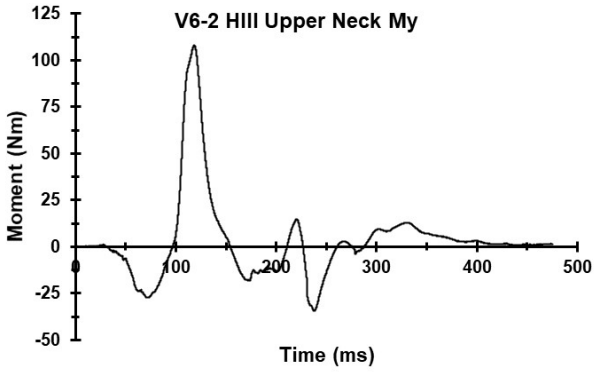
V6-2 HIII Upper Neck My
Moment (Nm)
125
100
75
50
25
0
-25
-50
100
200
300
400
500
Time (ms)

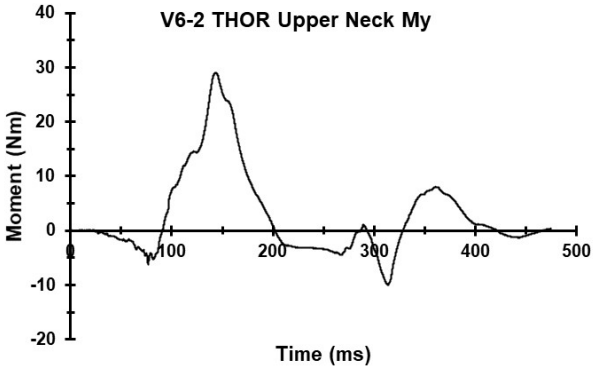
V6-2 THOR Upper Neck My
Moment (Nm)
40
30
20
10
0
-10
-20
100
200
300
400
500
Time (ms)

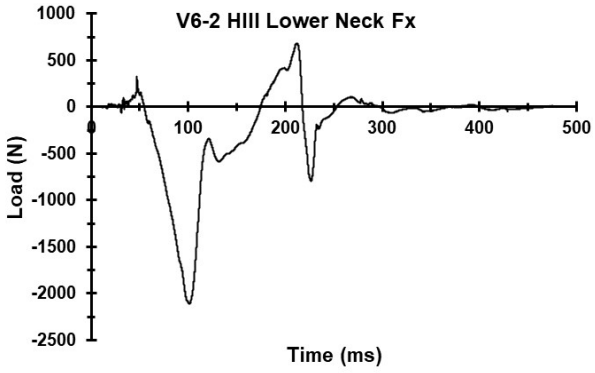
V6-2 HIII Lower Neck Fx
Load (N)
1000
500
0
-500
-1000
-1500
-2000
-2500
100
200
300
400
500
Time (ms)

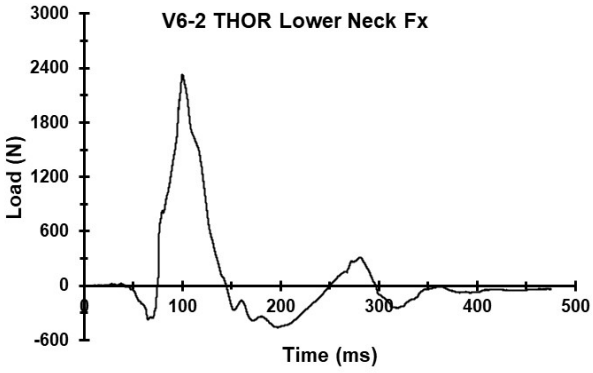
V6-2 THOR Lower Neck Fx
Load (N)
3000
2400
1800
1200
600
0
-600
100
200
300
400
500
Time (ms)

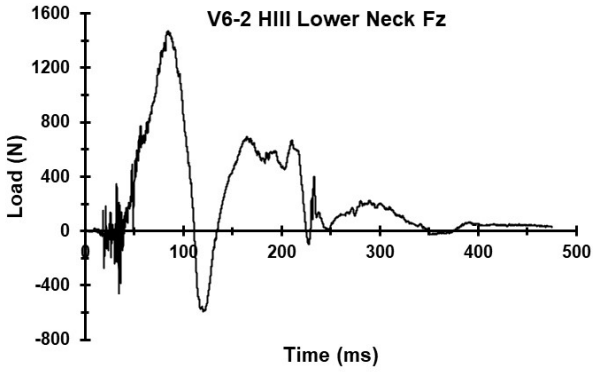
V6-2 HIII Lower Neck Fz
Load (N)
1600
1200
800
400
0
-400
-800
100
200
300
400
500
Time (ms)

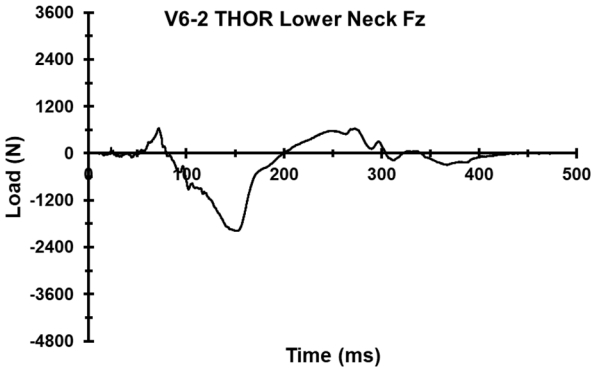
V6-2 THOR Lower Neck Fz
Load (N)
3600
2400
1200
0
-1200
-2400
-3600
-4800
100
200
300
400
500
Time (ms)

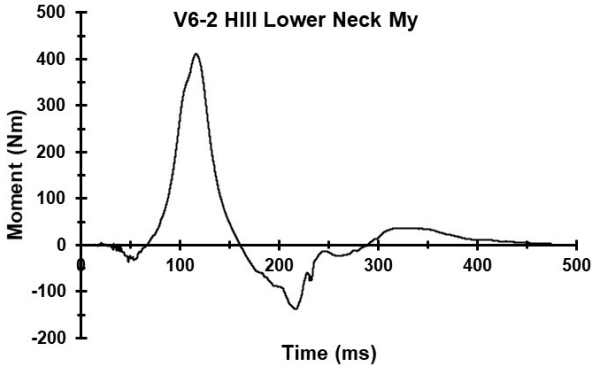
V6-2 HIII Lower Neck My
Moment (Nm)
500
400
300
200
100
0
-100
-200
100
200
300
400
500
Time (ms)

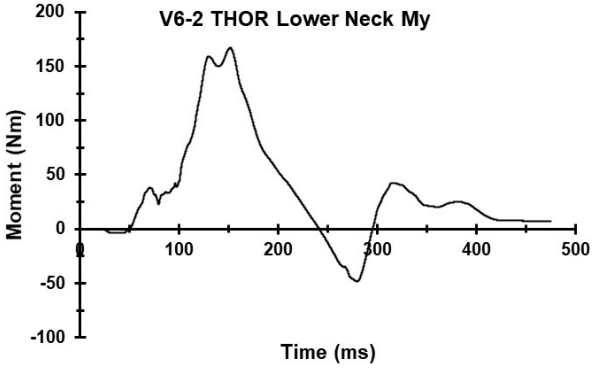
V6-2 THOR Lower Neck My
Moment (Nm)
200
150
100
50
0
-50
-100
100
200
300
400
500
Time (ms)

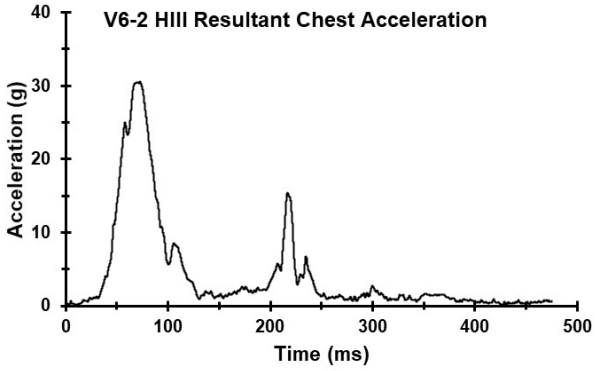
V6-2 HIII Resultant Chest Acceleration
Acceleration (g)
Time (ms)

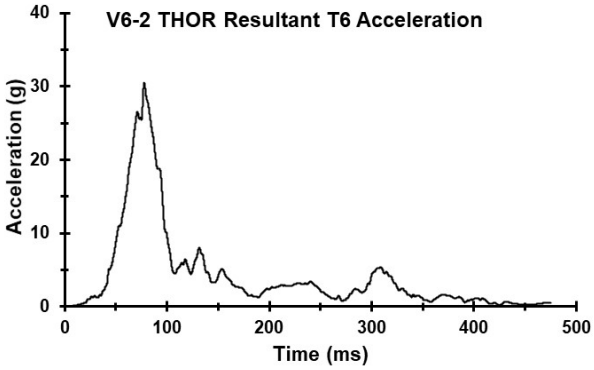
V6-2 THOR Resultant T6 Acceleration
Acceleration (g)
Time (ms)

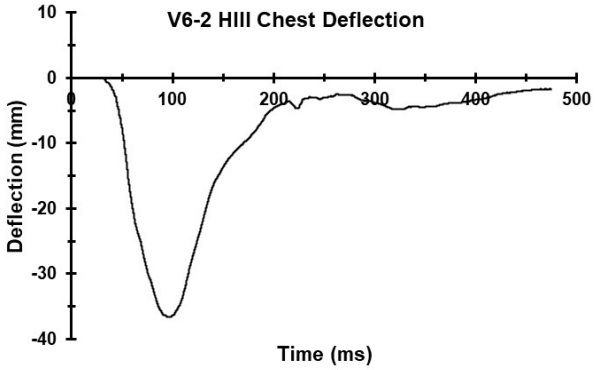
V6-2 HIII Chest Deflection
Deflection (mm)
Time (ms)

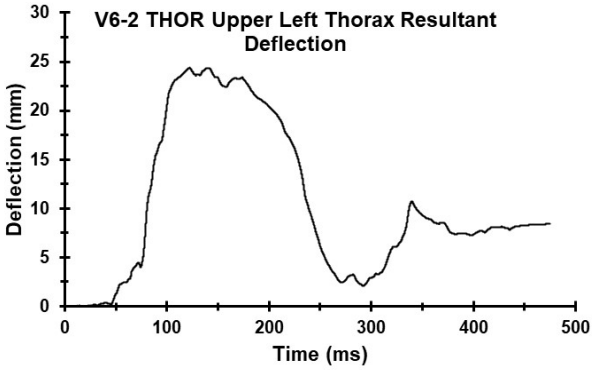
V6-2 THOR Upper Left Thorax Resultant Deflection
Deflection (mm)
Time (ms)

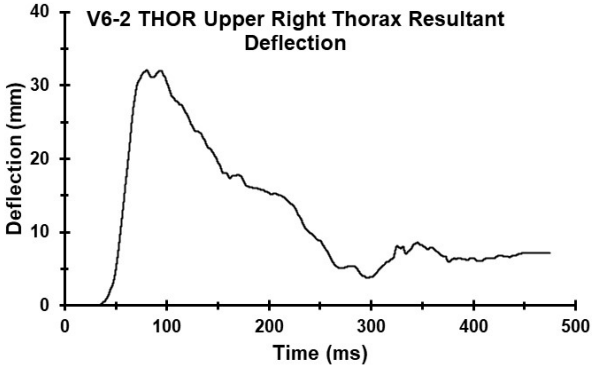
V6-2 THOR Upper Right Thorax Resultant Deflection
Deflection (mm)
Time (ms)

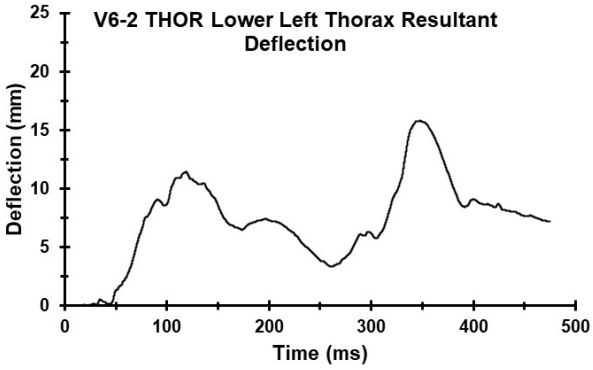
V6-2 THOR Lower Left Thorax Resultant Deflection
Deflection (mm)
Time (ms)

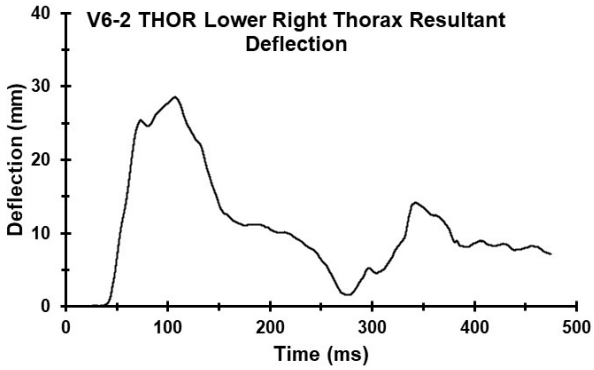
V6-2 THOR Lower Right Thorax Resultant Deflection
Deflection (mm)
40
30
20
10
0
0
100
200
300
400
500
Time (ms)

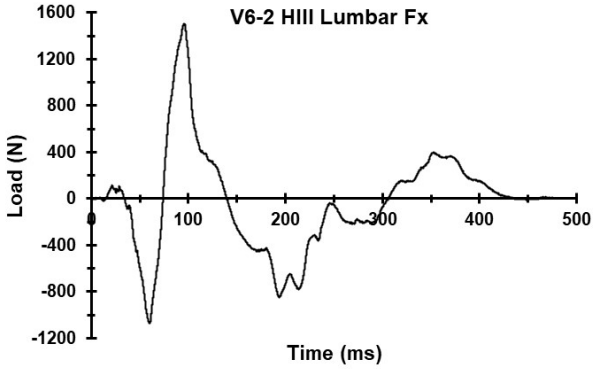
V6-2 HIII Lumbar Fx
Load (N)
1600
1200
800
400
0
-400
-800
-1200
0
100
200
300
400
500
Time (ms)

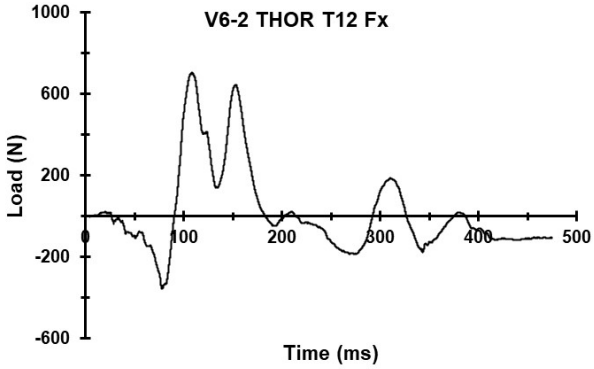
V6-2 THOR T12 Fx
Load (N)
1000
600
200
-200
-600
0
100
200
300
400
500
Time (ms)

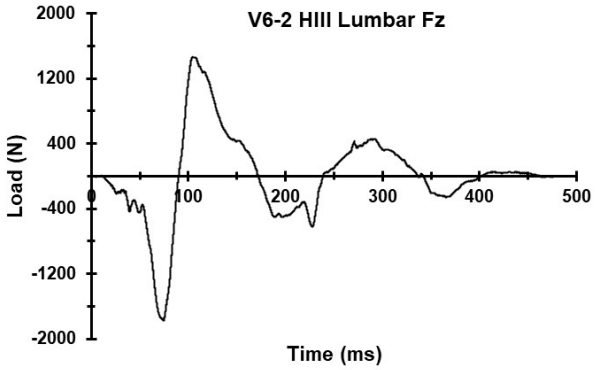
V6-2 HIII Lumbar Fz
Load (N)
2000
1200
400
-400
-1200
-2000
0
100
200
300
400
500
Time (ms)

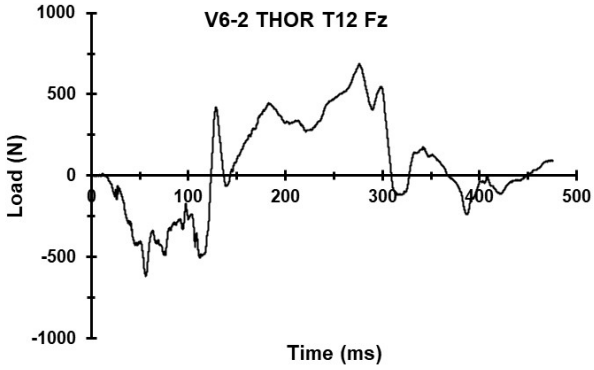
V6-2 THOR T12 Fz
Load (N)
1000
500
0
-500
-1000
0
100
200
300
400
500
Time (ms)

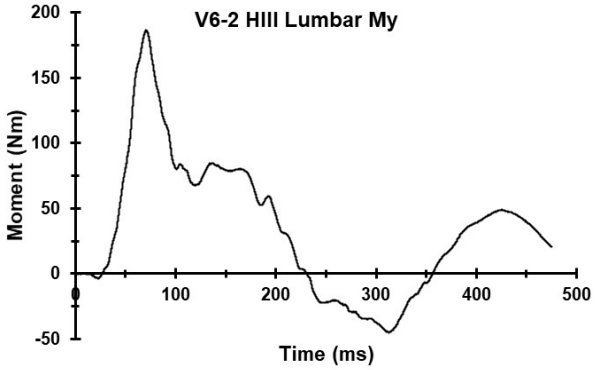
V6-2 HIII Lumbar My
Moment (Nm)
200
150
100
50
0
-50
0
100
200
300
400
500
Time (ms)

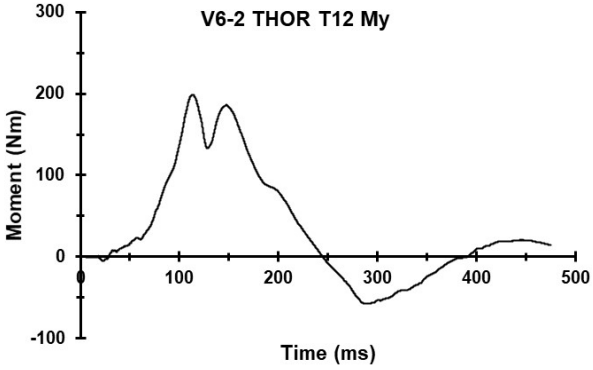
V6-2 THOR T12 My
Moment (Nm)
300
200
100
0
-100
0
100
200
300
400
500
Time (ms)

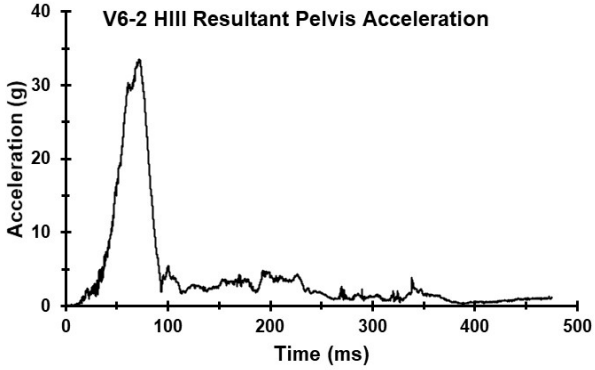
V6-2 HIII Resultant Pelvis Acceleration
Acceleration (g)
40
30
20
10
0
0
100
200
300
400
500
Time (ms)

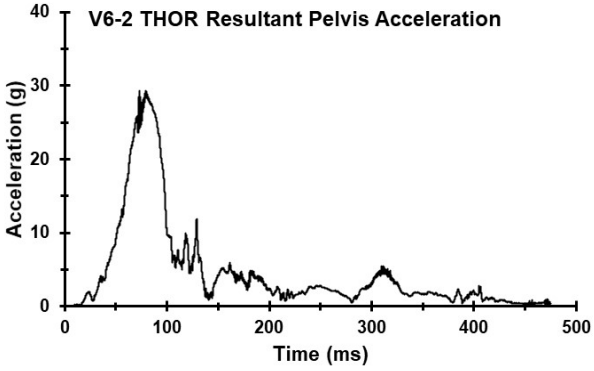
V6-2 THOR Resultant Pelvis Acceleration
Acceleration (g)
40
30
20
10
0
0
100
200
300
400
500
Time (ms)

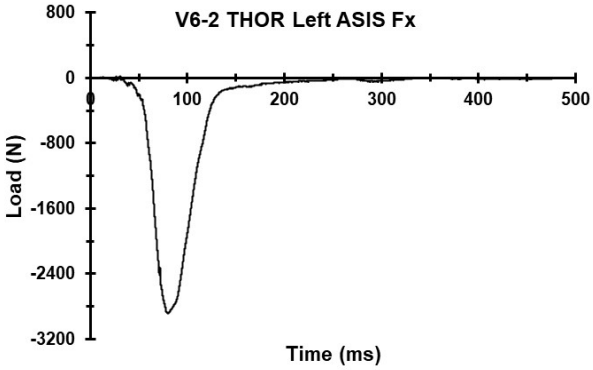
V6-2 THOR Left ASIS Fx
Load (N)
800
0
-800
-1600
-2400
-3200
0
100
200
300
400
500
Time (ms)

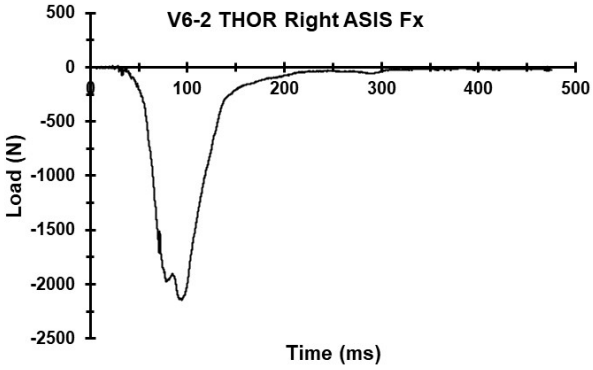
V6-2 THOR Right ASIS Fx
Load (N)
500
0
-500
-1000
-1500
-2000
-2500
0
100
200
300
400
500
Time (ms)

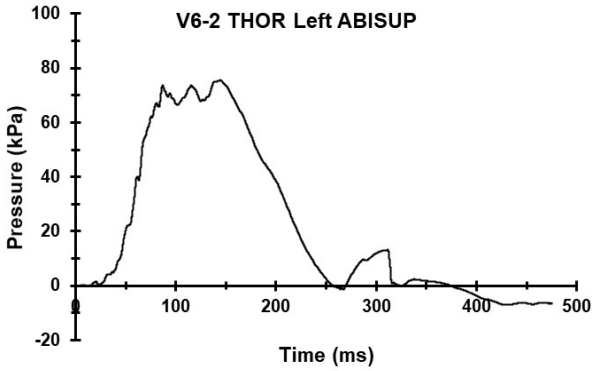
V6-2 THOR Left ABISUP
Pressure (kPa)
100
80
60
40
20
0
-20
0
100
200
300
400
500
Time (ms)

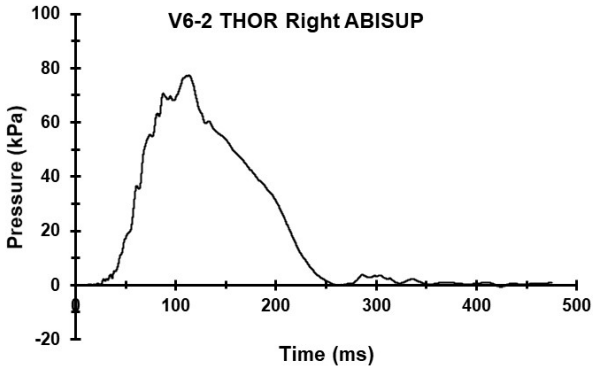
V6-2 THOR Right ABISUP
Pressure (kPa)
100
80
60
40
20
0
-20
0
100
200
300
400
500
Time (ms)

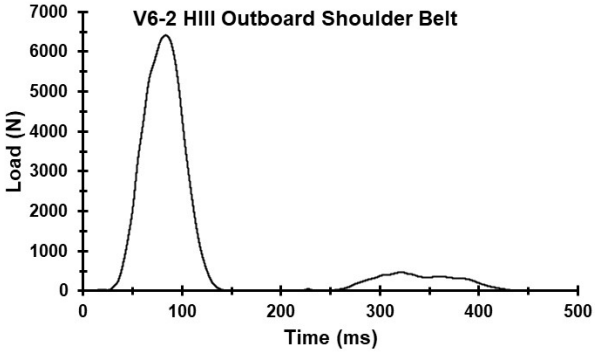
V6-2 HIII Outboard Shoulder Belt
Load (N)
7000
6000
5000
4000
3000
2000
1000
0
0
100
200
300
400
500
Time (ms)

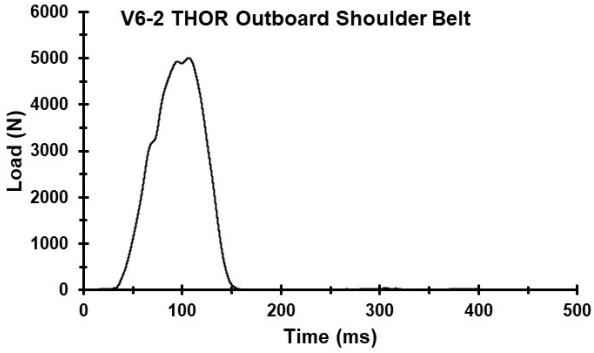
V6-2 THOR Outboard Shoulder Belt
Load (N)
6000
5000
4000
3000
2000
1000
0
0
100
200
300
400
500
Time (ms)

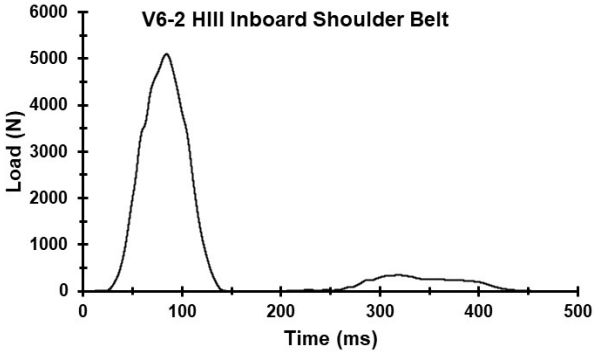
V6-2 HIII Inboard Shoulder Belt
Load (N)
6000
5000
4000
3000
2000
1000
0
0
100
200
300
400
500
Time (ms)

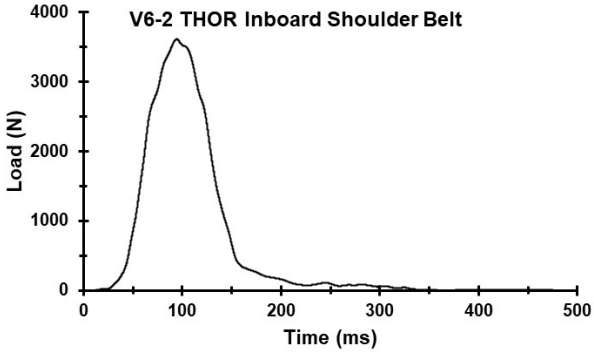
V6-2 THOR Inboard Shoulder Belt
Load (N)
4000
3000
2000
1000
0
0
100
200
300
400
500
Time (ms)

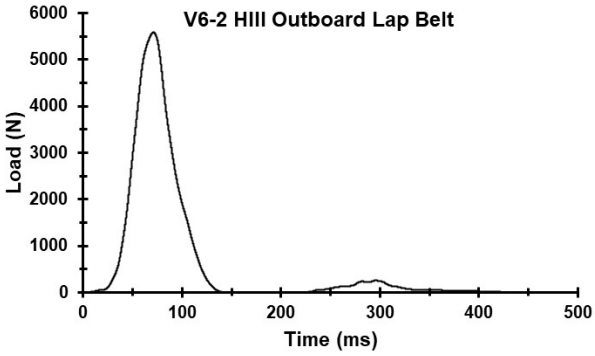
V6-2 HIII Outboard Lap Belt
Load (N)
6000
5000
4000
3000
2000
1000
0
0
100
200
300
400
500
Time (ms)

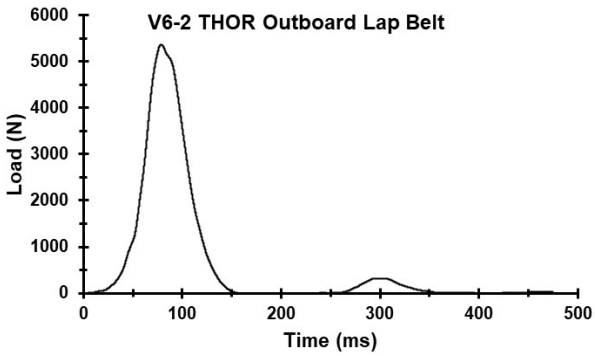
V6-2 THOR Outboard Lap Belt
Load (N)
6000
5000
4000
3000
2000
1000
0
0
100
200
300
400
500
Time (ms)

Appendix P. Select Data Traces From Test FRS-V6-4

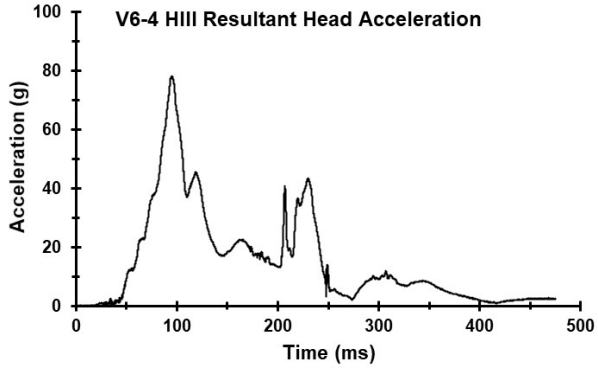
V6-4 HIII Resultant Head Acceleration
Acceleration (g)
Time (ms)

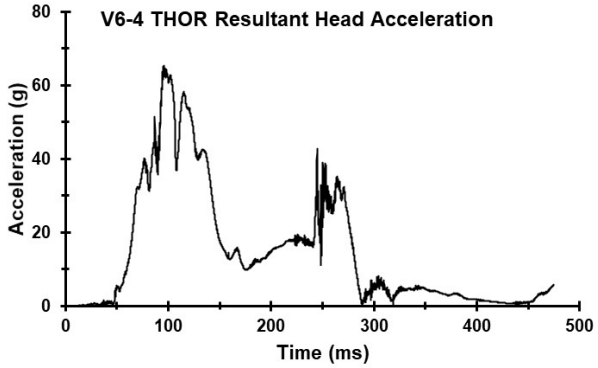
V6-4 THOR Resultant Head Acceleration
Acceleration (g)
Time (ms)

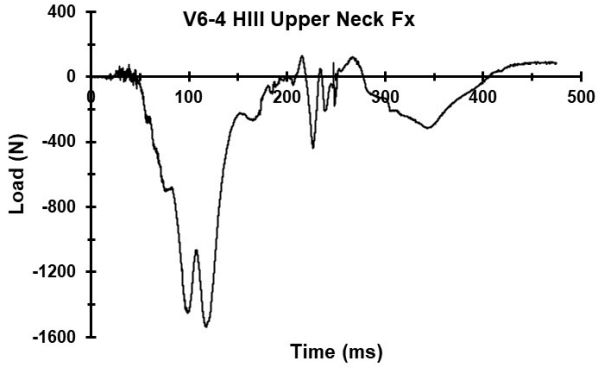
V6-4 HIII Upper Neck Fx
Load (N)
Time (ms)

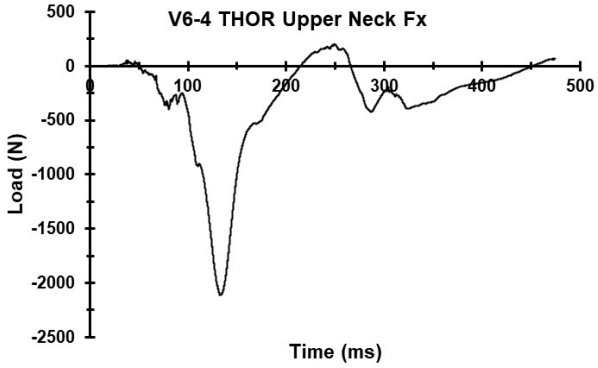
V6-4 THOR Upper Neck Fx
Load (N)
Time (ms)

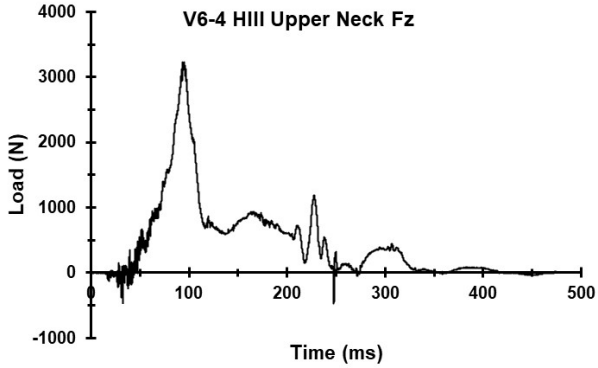
V6-4 HIII Upper Neck Fz
Load (N)
Time (ms)

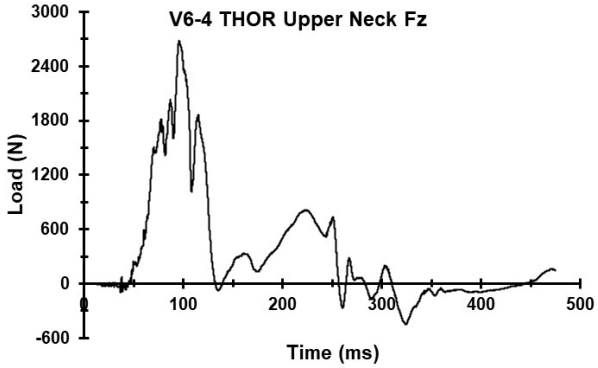
V6-4 THOR Upper Neck Fz
Load (N)
Time (ms)

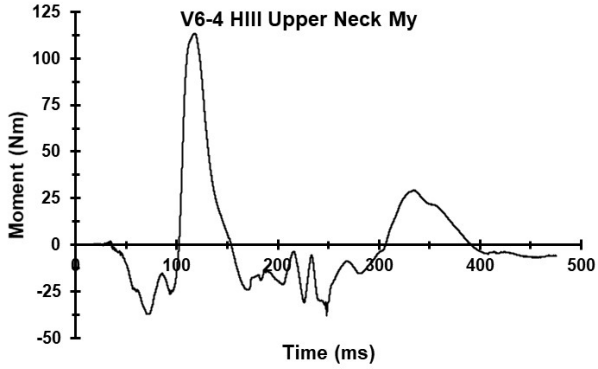
V6-4 HIII Upper Neck My
Moment (Nm)
Time (ms)

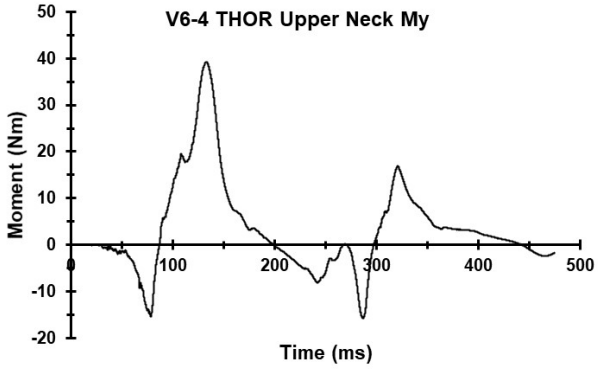
V6-4 THOR Upper Neck My
Moment (Nm)
Time (ms)

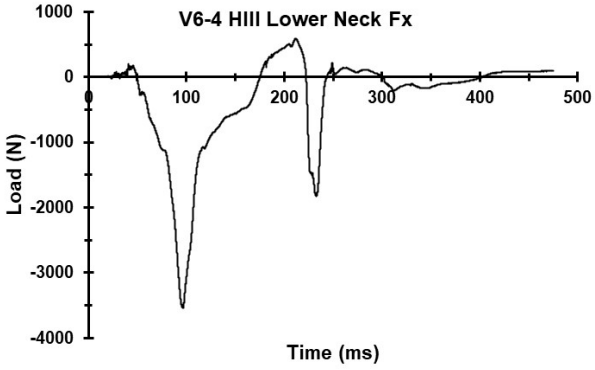
V6-4 HIII Lower Neck Fx
Load (N)
1000
0
-1000
-2000
-3000
-4000
100
200
300
400
500
Time (ms)

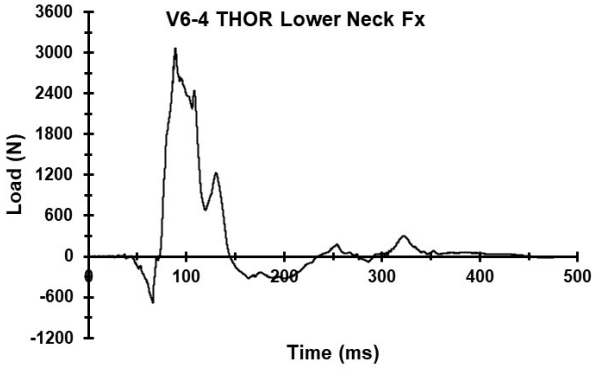
V6-4 THOR Lower Neck Fx
Load (N)
3600
3000
2400
1800
1200
600
0
-600
-1200
100
200
300
400
500
Time (ms)

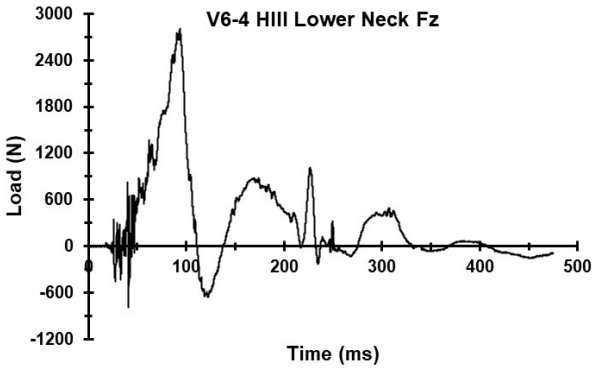
V6-4 HIII Lower Neck Fz
Load (N)
3000
2400
1800
1200
600
0
-600
-1200
100
200
300
400
500
Time (ms)

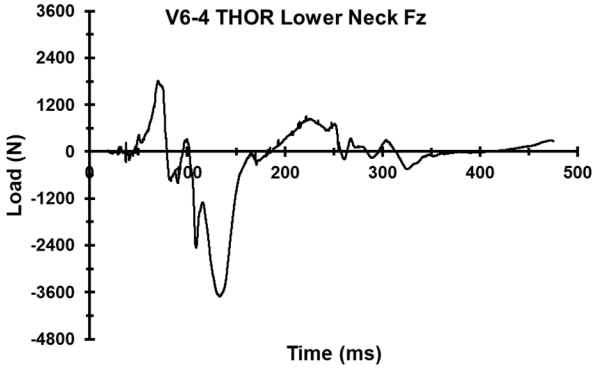
V6-4 THOR Lower Neck Fz
Load (N)
3600
2400
1200
0
-1200
-2400
-3600
-4800
100
200
300
400
500
Time (ms)

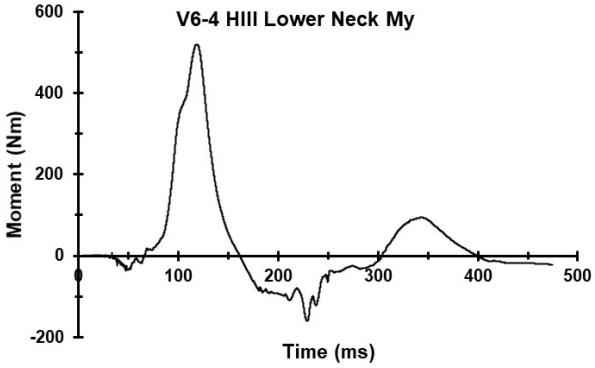
V6-4 HIII Lower Neck My
Moment (Nm)
600
400
200
0
-200
100
200
300
400
500
Time (ms)

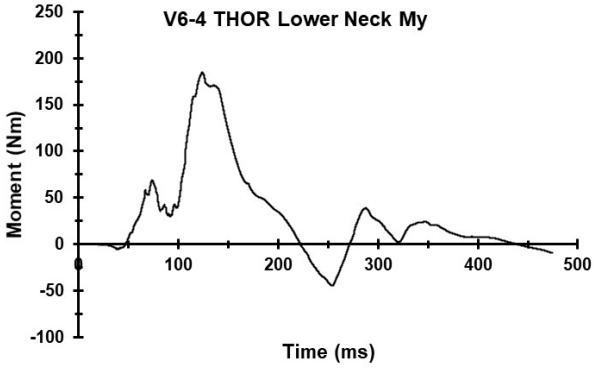
V6-4 THOR Lower Neck My
Moment (Nm)
250
200
150
100
50
0
-50
-100
100
200
300
400
500
Time (ms)

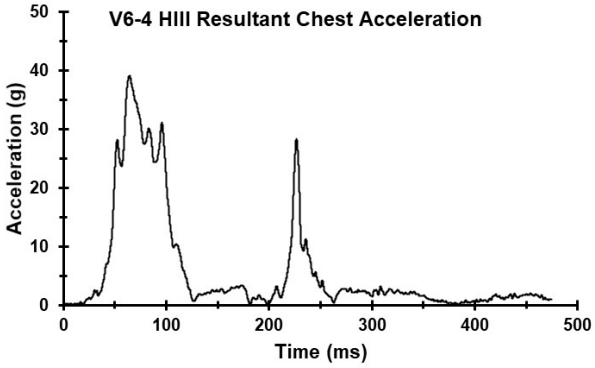
V6-4 HIII Resultant Chest Acceleration
Acceleration (g)
50
40
30
20
10
0
0
100
200
300
400
500
Time (ms)

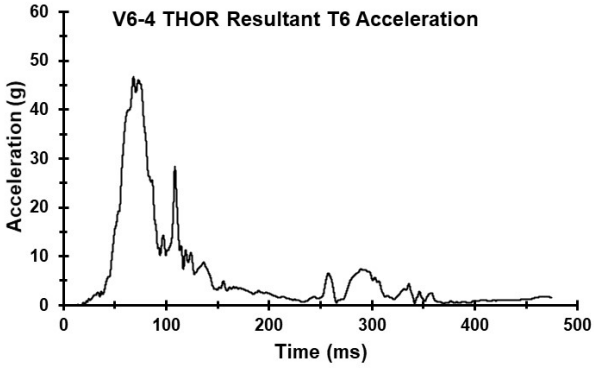
V6-4 THOR Resultant T6 Acceleration
Acceleration (g)
60
50
40
30
20
10
0
0
100
200
300
400
500
Time (ms)

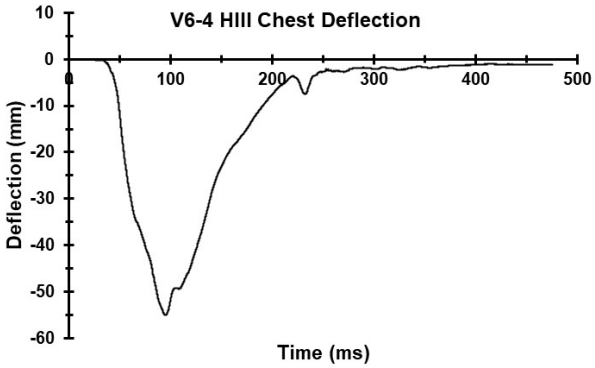
V6-4 HIII Chest Deflection
Deflection (mm)
Time (ms)
10
0
-10
-20
-30
-40
-50
-60
100
200
300
400
500

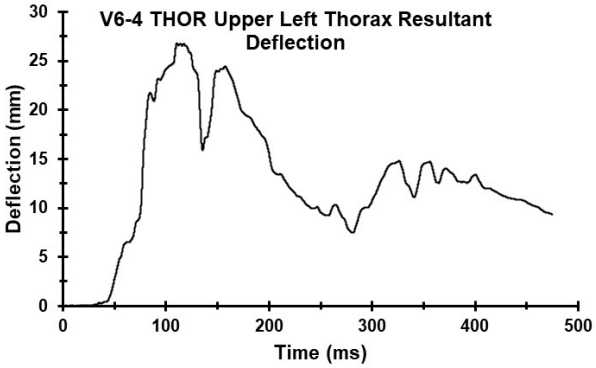
V6-4 THOR Upper Left Thorax Resultant Deflection
Deflection (mm)
Time (ms)
30
25
20
15
10
5
0
100
200
300
400
500

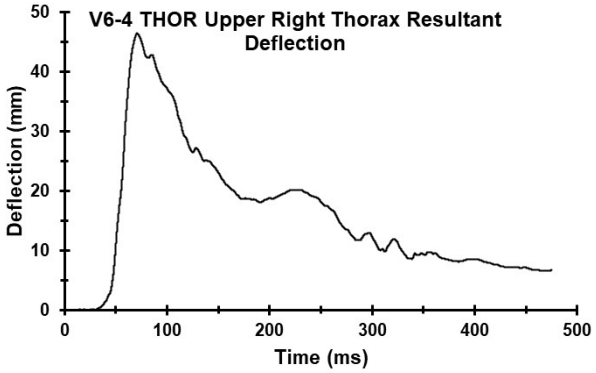
V6-4 THOR Upper Right Thorax Resultant Deflection
Deflection (mm)
Time (ms)
50
40
30
20
10
0
100
200
300
400
500

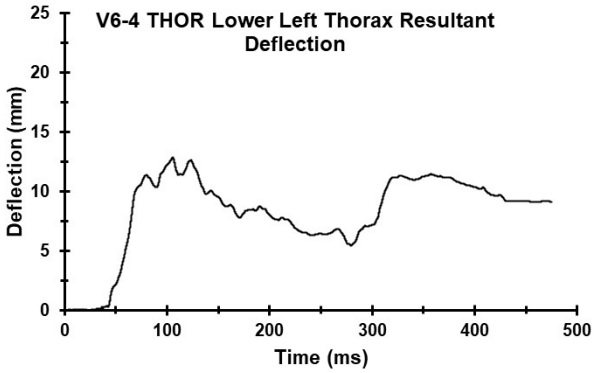
V6-4 THOR Lower Left Thorax Resultant Deflection
Deflection (mm)
Time (ms)
25
20
15
10
5
0
100
200
300
400
500

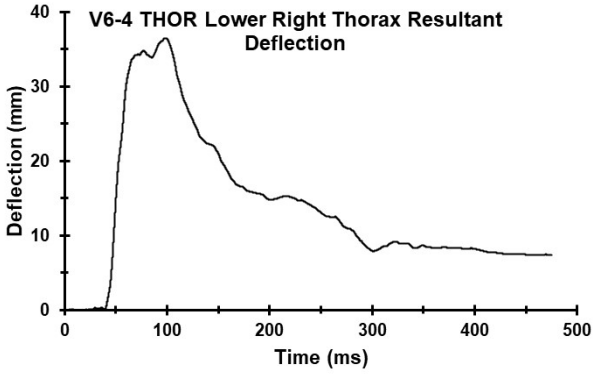
V6-4 THOR Lower Right Thorax Resultant Deflection
Deflection (mm)
Time (ms)

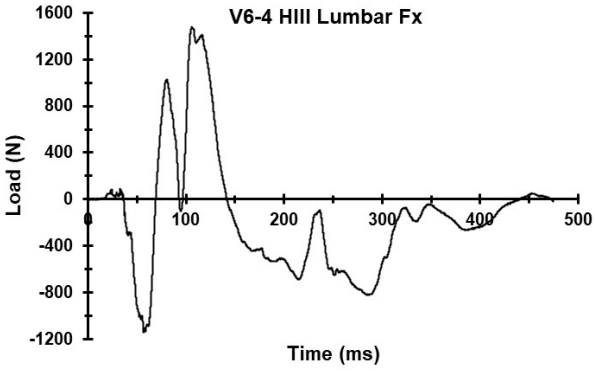
V6-4 HIII Lumbar Fx
Load (N)
Time (ms)

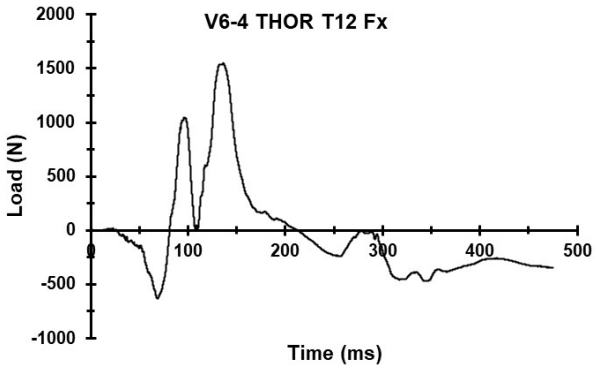
V6-4 THOR T12 Fx
Load (N)
Time (ms)

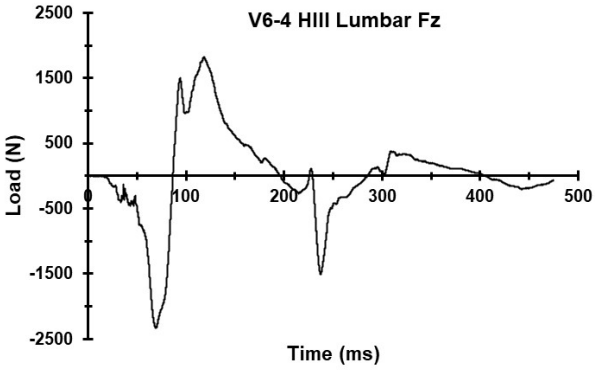
V6-4 HIII Lumbar Fz
Load (N)
Time (ms)

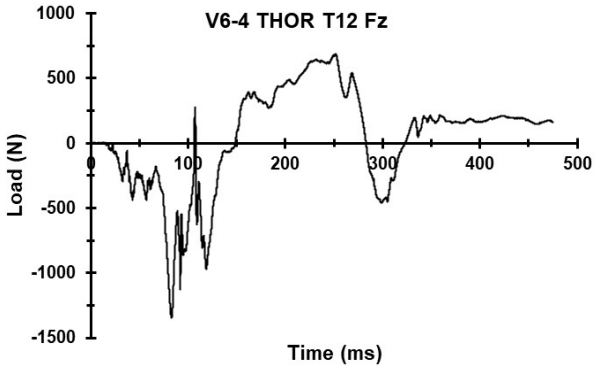
V6-4 THOR T12 Fz
Load (N)
Time (ms)

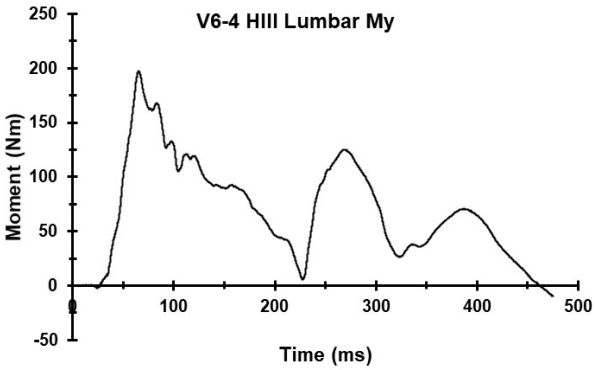
V6-4 HIII Lumbar My
Moment (Nm)
Time (ms)

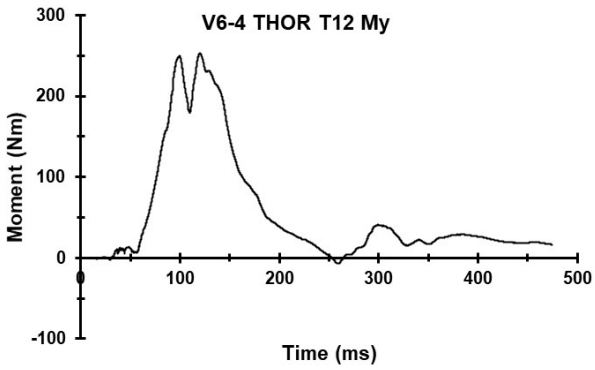
V6-4 THOR T12 My
Moment (Nm)
Time (ms)

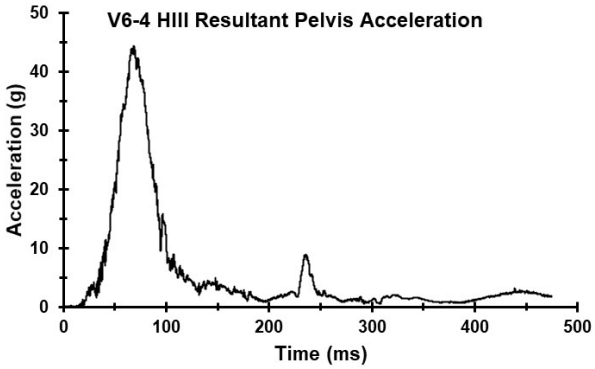
V6-4 HIII Resultant Pelvis Acceleration
Acceleration (g)
Time (ms)
50
40
30
20
10
0
0
100
200
300
400
500

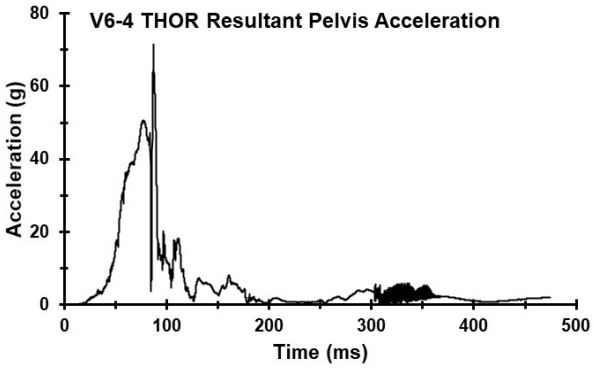
V6-4 THOR Resultant Pelvis Acceleration
Acceleration (g)
Time (ms)
80
60
40
20
0
0
100
200
300
400
500

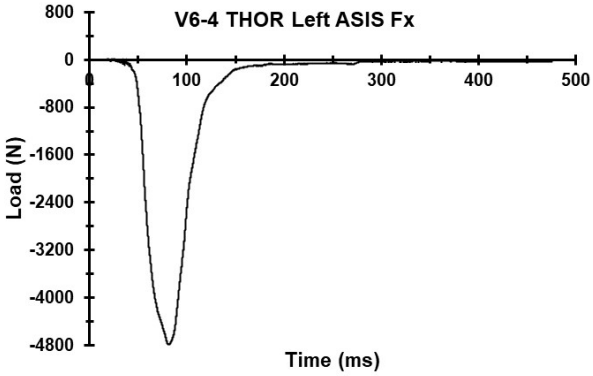
V6-4 THOR Left ASIS Fx
Load (N)
Time (ms)
800
0
-800
-1600
-2400
-3200
-4000
-4800
0
100
200
300
400
500

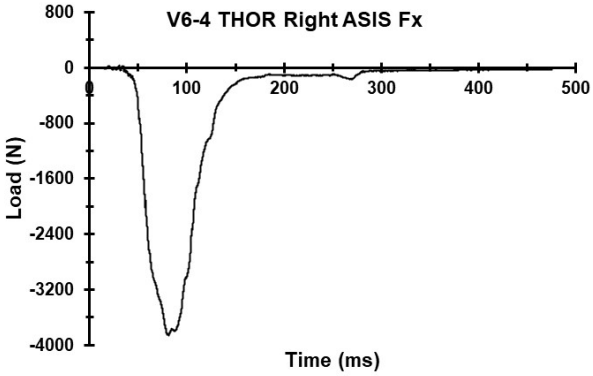
V6-4 THOR Right ASIS Fx
Load (N)
Time (ms)
800
0
-800
-1600
-2400
-3200
-4000
0
100
200
300
400
500

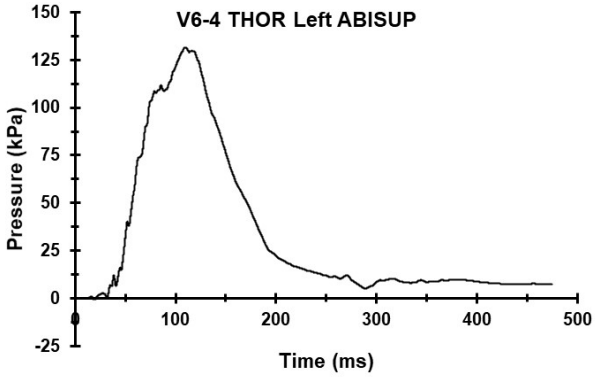
V6-4 THOR Left ABISUP
Pressure (kPa)
150
125
100
75
50
25
0
-25
0
100
200
300
400
500
Time (ms)

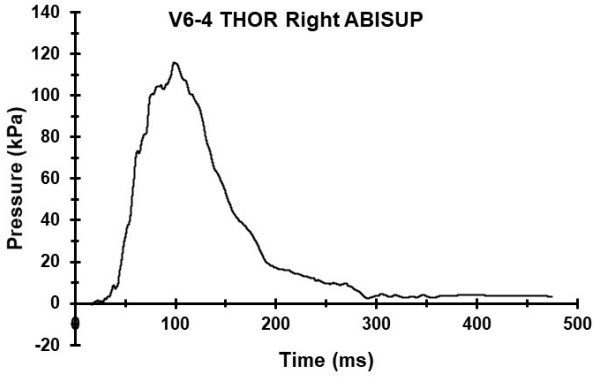
V6-4 THOR Right ABISUP
Pressure (kPa)
140
120
100
80
60
40
20
0
-20
0
100
200
300
400
500
Time (ms)

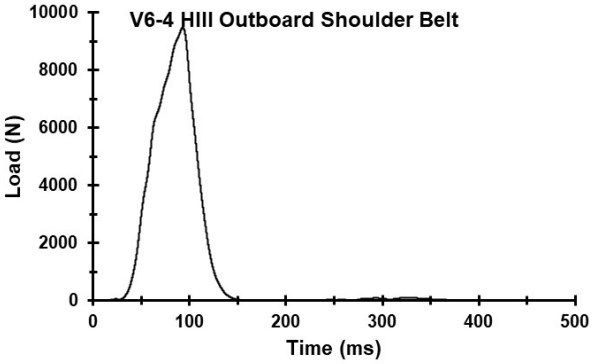
V6-4 HIII Outboard Shoulder Belt
Load (N)
10000
8000
6000
4000
2000
0
0
100
200
300
400
500
Time (ms)

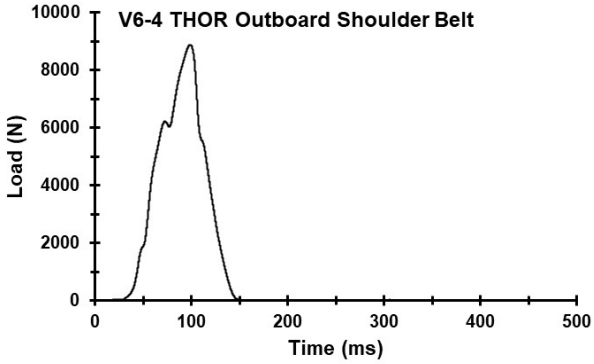
V6-4 THOR Outboard Shoulder Belt
Load (N)
10000
8000
6000
4000
2000
0
0
100
200
300
400
500
Time (ms)

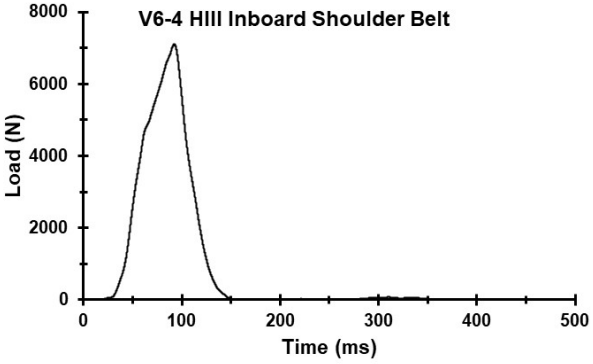
V6-4 HIII Inboard Shoulder Belt
Load (N)
8000
6000
4000
2000
0
0
100
200
300
400
500
Time (ms)

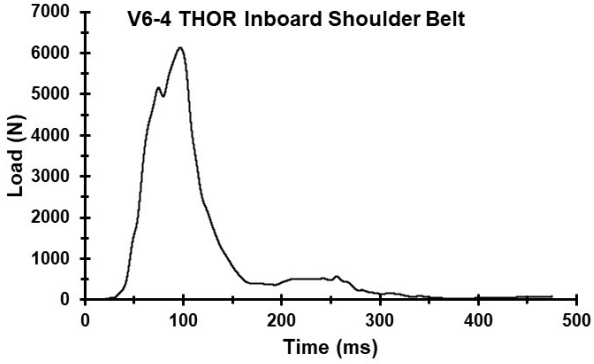
V6-4 THOR Inboard Shoulder Belt
Load (N)
7000
6000
5000
4000
3000
2000
1000
0
0
100
200
300
400
500
Time (ms)

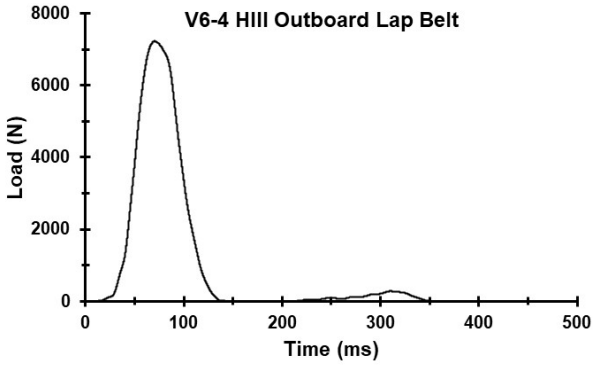
V6-4 HIII Outboard Lap Belt
Load (N)
8000
6000
4000
2000
0
0
100
200
300
400
500
Time (ms)

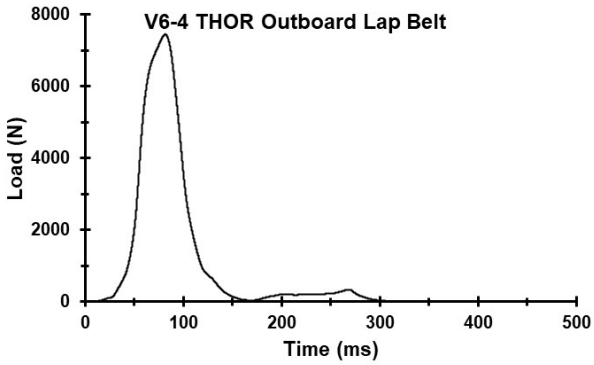
V6-4 THOR Outboard Lap Belt
Load (N)
8000
6000
4000
2000
0
0
100
200
300
400
500
Time (ms)

Appendix Q. Select Data Traces From Test FRS-V10-1

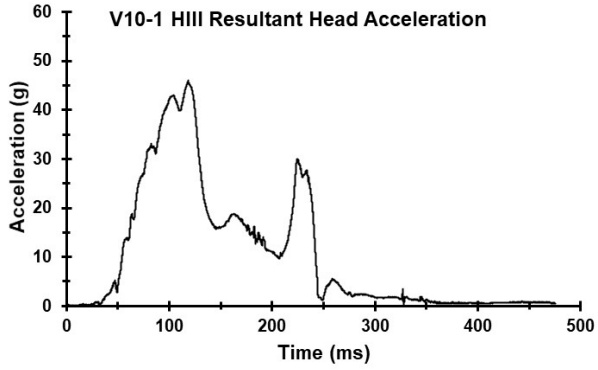
V10-1 HIII Resultant Head Acceleration
Acceleration (g)
Time (ms)

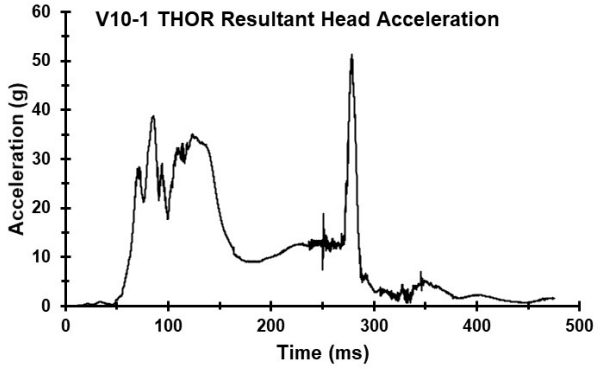
V10-1 THOR Resultant Head Acceleration
Acceleration (g)
Time (ms)

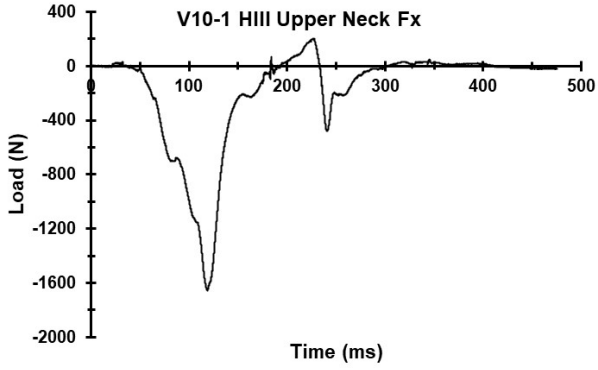
V10-1 HIII Upper Neck Fx
Load (N)
Time (ms)

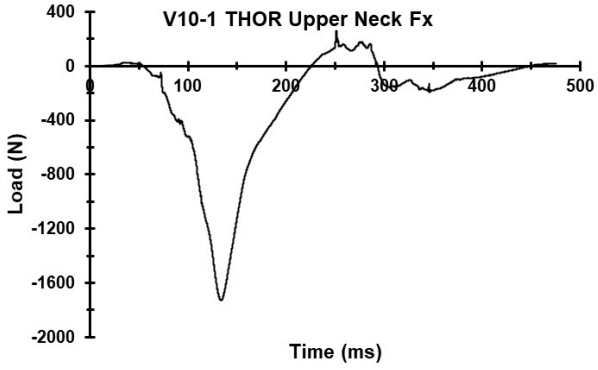
V10-1 THOR Upper Neck Fx
Load (N)
Time (ms)

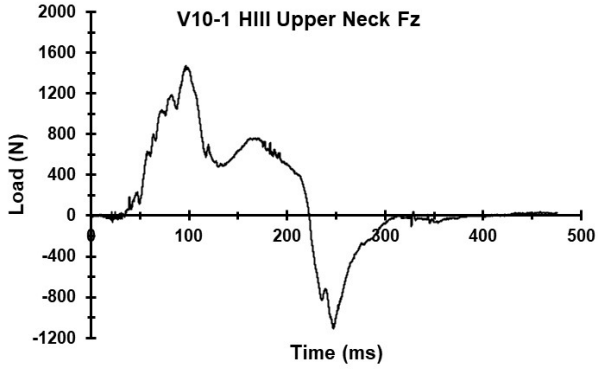
V10-1 HIII Upper Neck Fz
Load (N)
Time (ms)

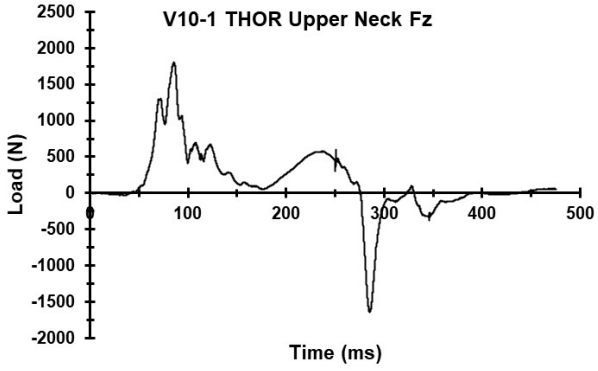
V10-1 THOR Upper Neck Fz
Load (N)
Time (ms)

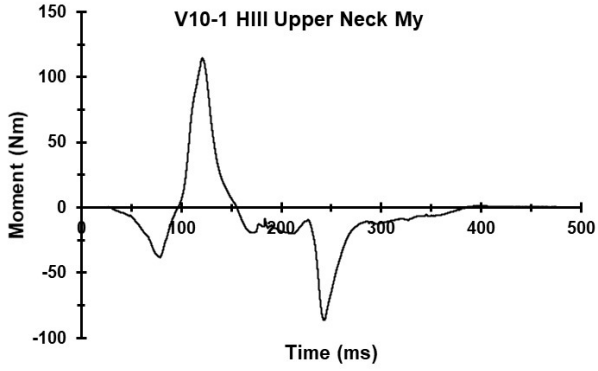
V10-1 HIII Upper Neck My
Moment (Nm)
Time (ms)

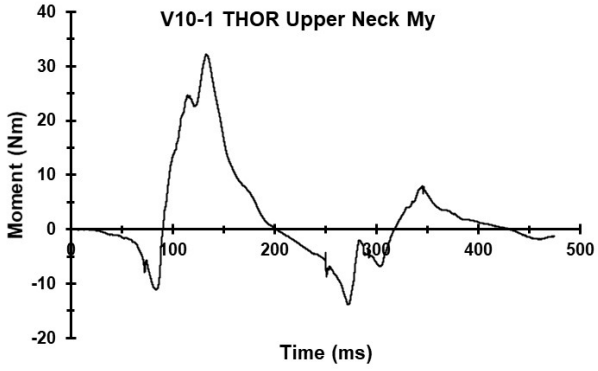
V10-1 THOR Upper Neck My
Moment (Nm)
Time (ms)

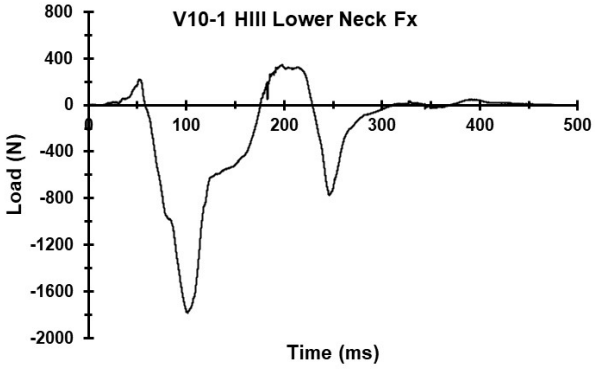
V10-1 HIII Lower Neck Fx
Load (N)
Time (ms)

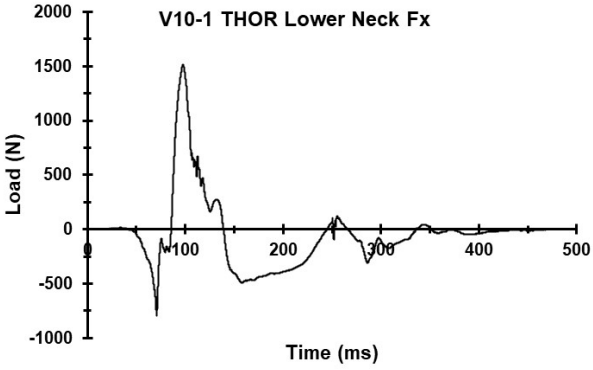
V10-1 THOR Lower Neck Fx
Load (N)
Time (ms)

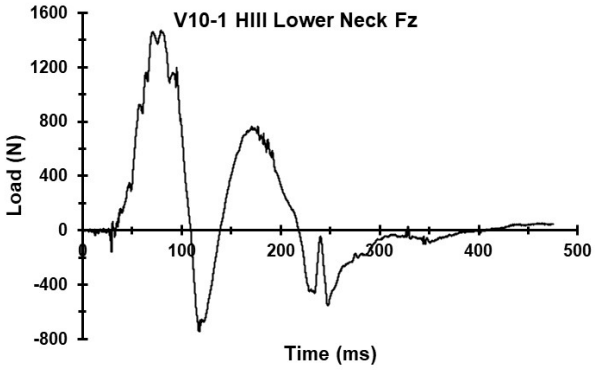
V10-1 HIII Lower Neck Fz
Load (N)
Time (ms)

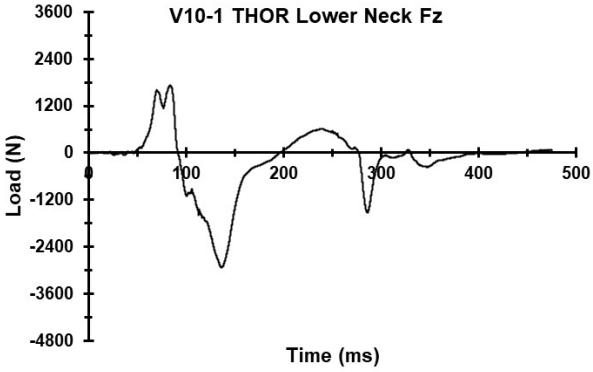
V10-1 THOR Lower Neck Fz
Load (N)
Time (ms)

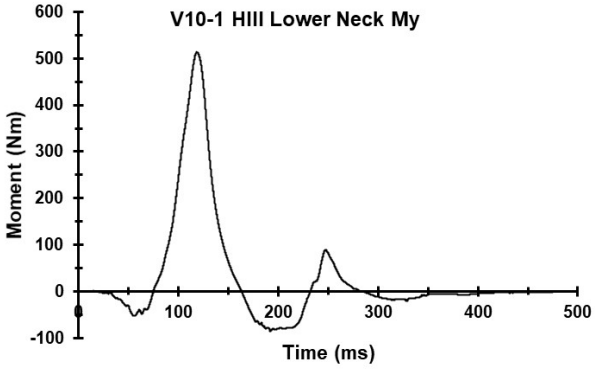
V10-1 HIII Lower Neck My
Moment (Nm)
Time (ms)

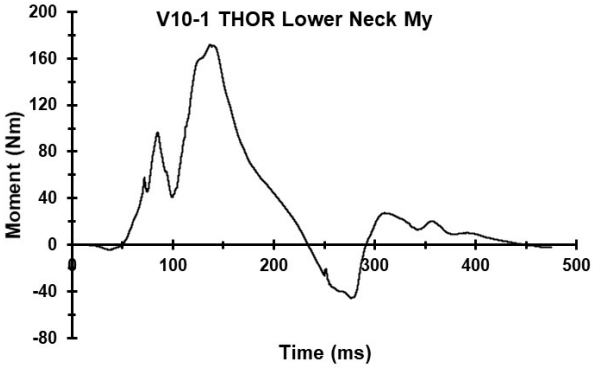
V10-1 THOR Lower Neck My
Moment (Nm)
Time (ms)

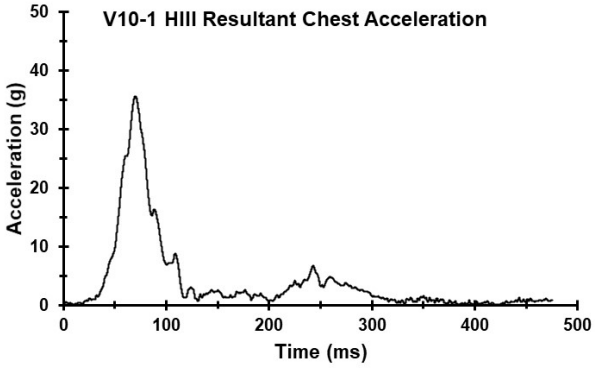
V10-1 HIII Resultant Chest Acceleration
Acceleration (g)
Time (ms)

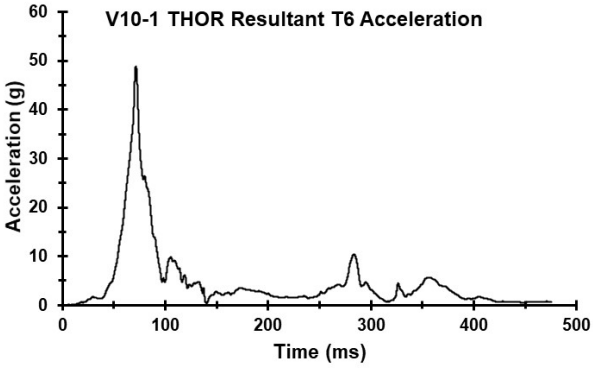
V10-1 THOR Resultant T6 Acceleration
Acceleration (g)
Time (ms)

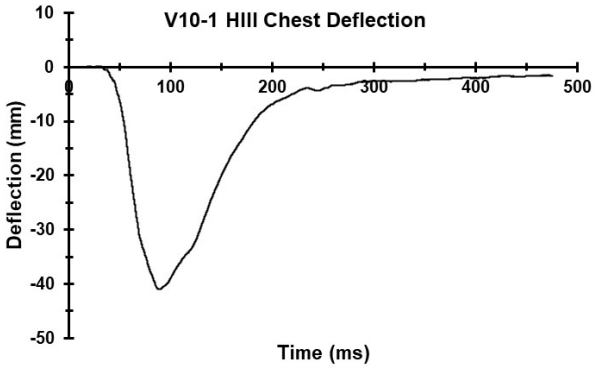
V10-1 HIII Chest Deflection
Deflection (mm)
Time (ms)
10
0
-10
-20
-30
-40
-50
0
100
200
300
400
500

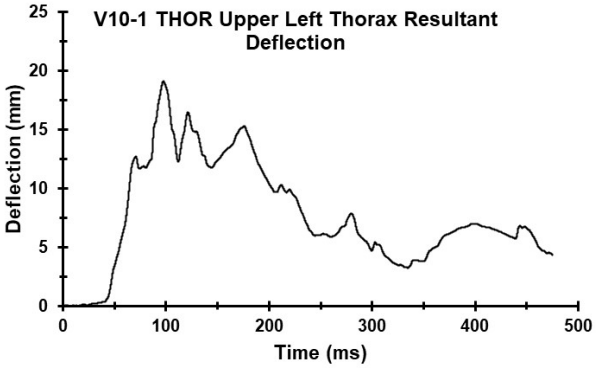
V10-1 THOR Upper Left Thorax Resultant Deflection
Deflection (mm)
Time (ms)
25
20
15
10
5
0
0
100
200
300
400
500

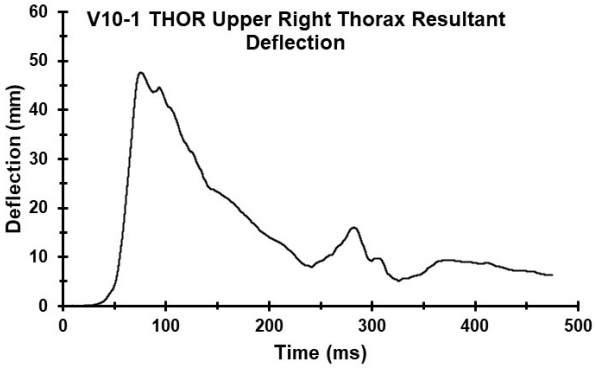
V10-1 THOR Upper Right Thorax Resultant Deflection
Deflection (mm)
Time (ms)
60
50
40
30
20
10
0
0
100
200
300
400
500

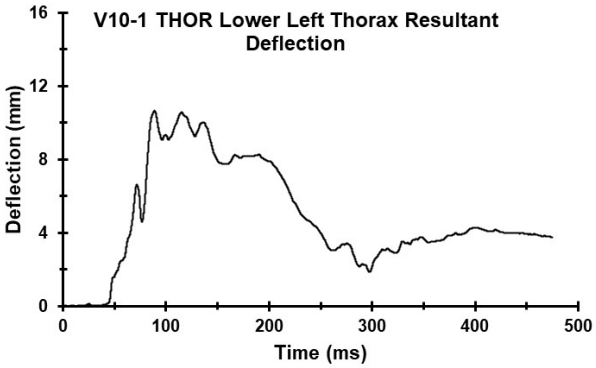
V10-1 THOR Lower Left Thorax Resultant Deflection
Deflection (mm)
Time (ms)
16
12
8
4
0
0
100
200
300
400
500

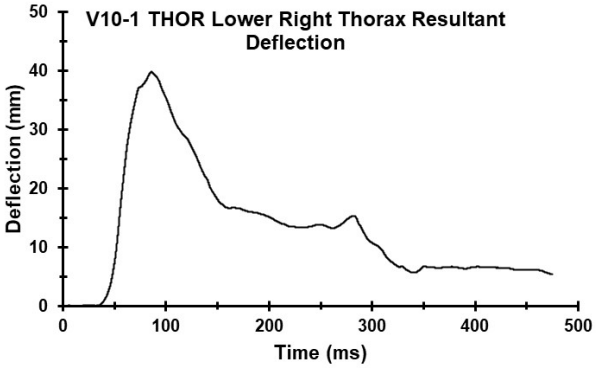
V10-1 THOR Lower Right Thorax Resultant Deflection
Deflection (mm)
Time (ms)
50
40
30
20
10
0
0
100
200
300
400
500

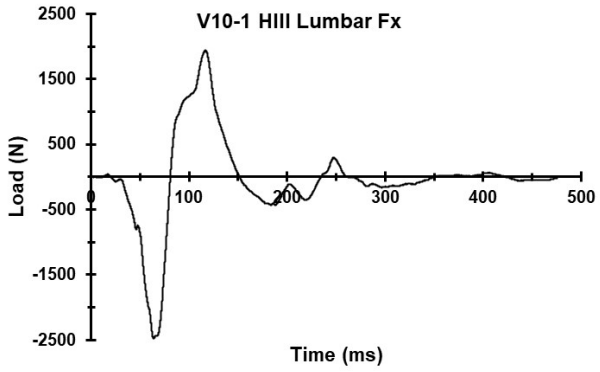
V10-1 HIII Lumbar Fx
Load (N)
2500
1500
500
-500
-1500
-2500
0
100
200
300
400
500
Time (ms)

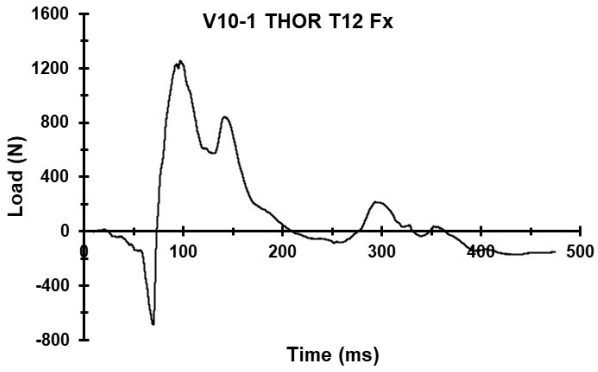
V10-1 THOR T12 Fx
Load (N)
1600
1200
800
400
0
-400
-800
0
100
200
300
400
500
Time (ms)

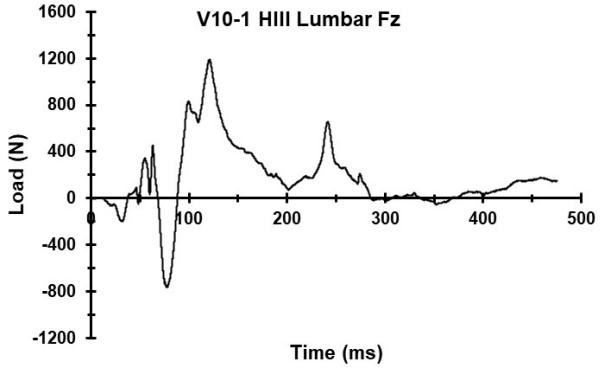
V10-1 HIII Lumbar Fz
Load (N)
1600
1200
800
400
0
-400
-800
-1200
0
100
200
300
400
500
Time (ms)

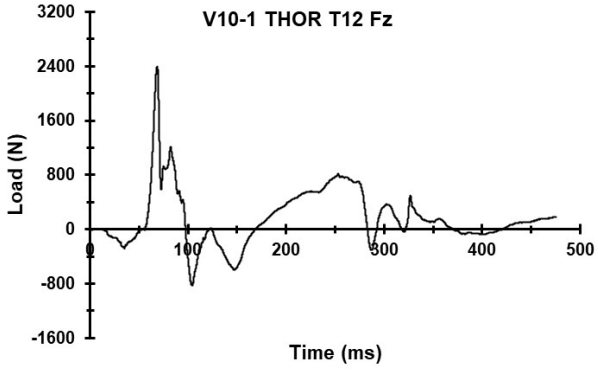
V10-1 THOR T12 Fz
Load (N)
3200
2400
1600
800
0
-800
-1600
0
100
200
300
400
500
Time (ms)

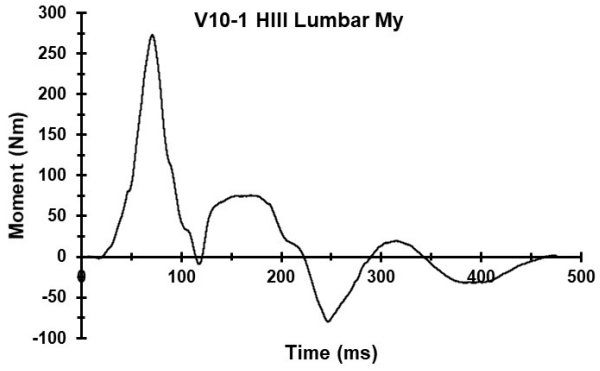
V10-1 HIII Lumbar My
Moment (Nm)
300
250
200
150
100
50
0
-50
-100
0
100
200
300
400
500
Time (ms)

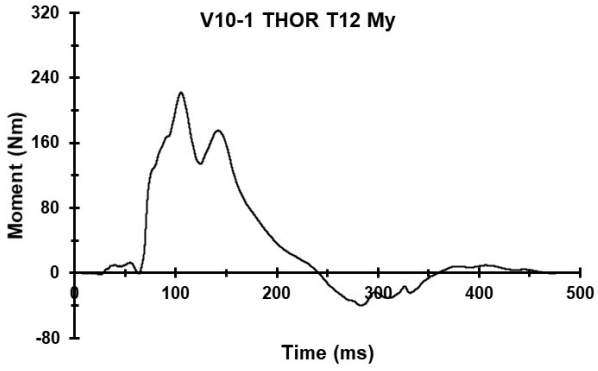
V10-1 THOR T12 My
Moment (Nm)
320
240
160
80
0
-80
0
100
200
300
400
500
Time (ms)

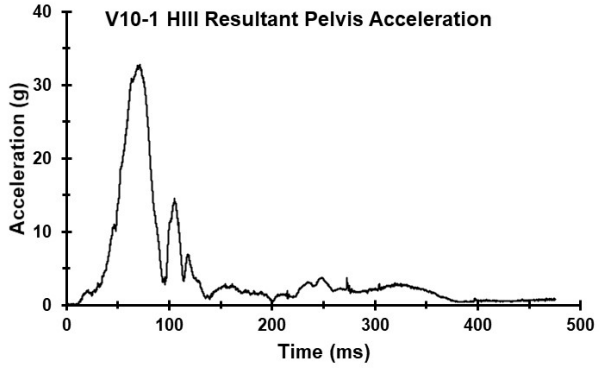
V10-1 HIII Resultant Pelvis Acceleration
Acceleration (g)
40
30
20
10
0
0
100
200
300
400
500
Time (ms)

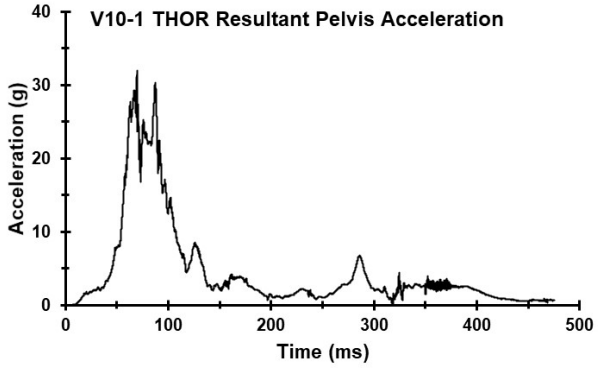
V10-1 THOR Resultant Pelvis Acceleration
Acceleration (g)
40
30
20
10
0
0
100
200
300
400
500
Time (ms)

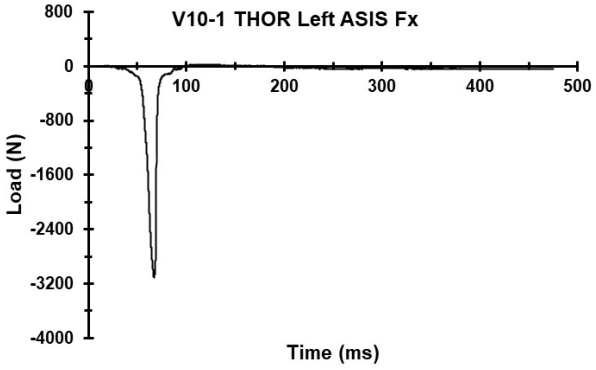
V10-1 THOR Left ASIS Fx
800
0
-800
-1600
-2400
-3200
-4000
Load (N)
0
100
200
300
400
500
Time (ms)

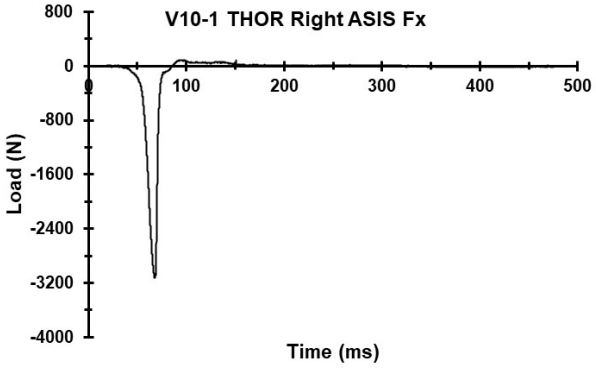
V10-1 THOR Right ASIS Fx
800
0
-800
-1600
-2400
-3200
-4000
Load (N)
0
100
200
300
400
500
Time (ms)

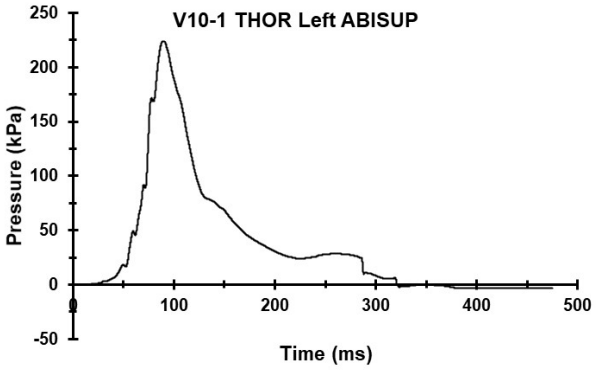
V10-1 THOR Left ABISUP
250
200
150
100
50
0
-50
Pressure (kPa)
0
100
200
300
400
500
Time (ms)

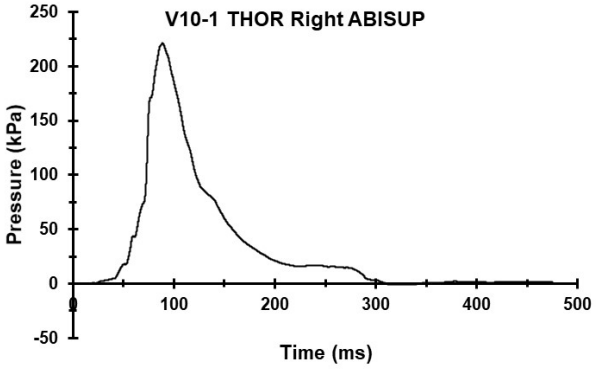
V10-1 THOR Right ABISUP
250
200
150
100
50
0
-50
Pressure (kPa)
0
100
200
300
400
500
Time (ms)

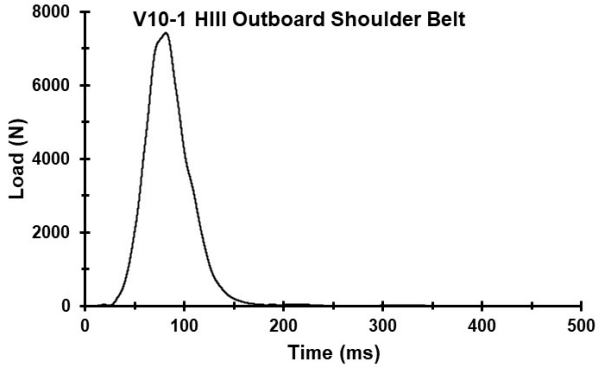
V10-1 HIII Outboard Shoulder Belt
Load (N)
8000
6000
4000
2000
0
0
100
200
300
400
500
Time (ms)

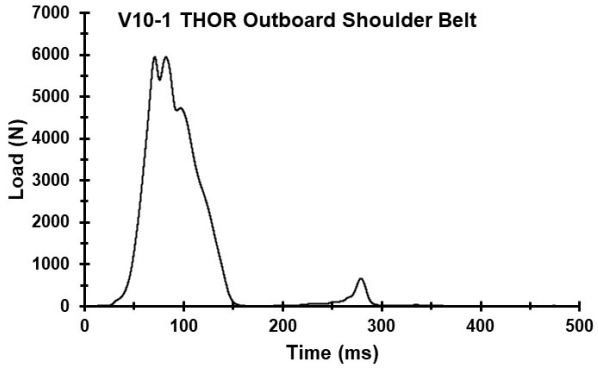
V10-1 THOR Outboard Shoulder Belt
Load (N)
7000
6000
5000
4000
3000
2000
1000
0
0
100
200
300
400
500
Time (ms)

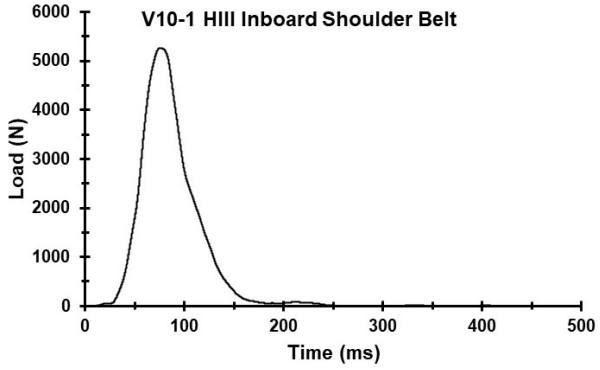
V10-1 HIII Inboard Shoulder Belt
Load (N)
6000
5000
4000
3000
2000
1000
0
0
100
200
300
400
500
Time (ms)

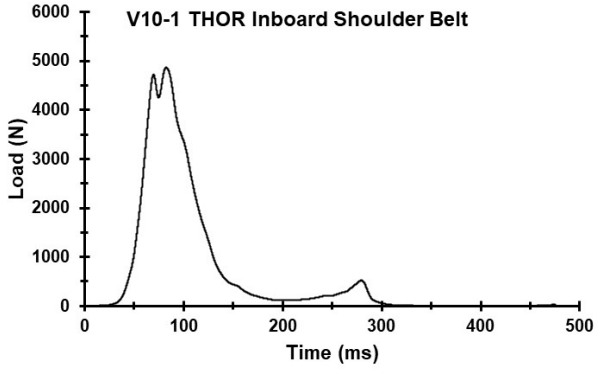
V10-1 THOR Inboard Shoulder Belt
Load (N)
6000
5000
4000
3000
2000
1000
0
0
100
200
300
400
500
Time (ms)

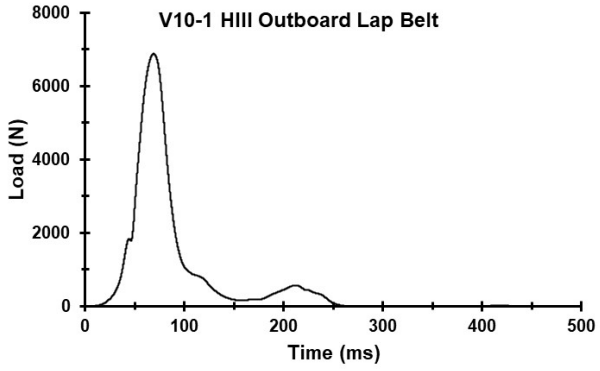
V10-1 HIII Outboard Lap Belt
Load (N)
8000
6000
4000
2000
0
0
100
200
300
400
500
Time (ms)

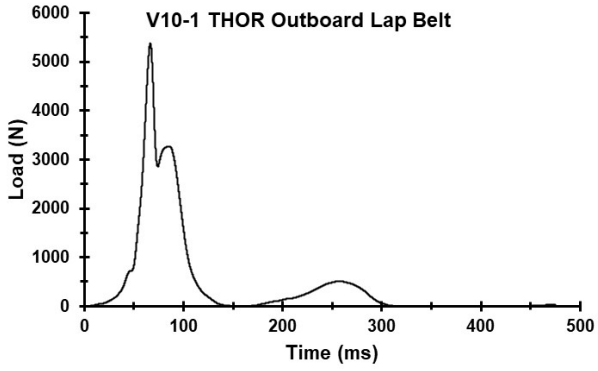
V10-1 THOR Outboard Lap Belt
Load (N)
6000
5000
4000
3000
2000
1000
0
0
100
200
300
400
500
Time (ms)

Appendix R. Select Data Traces From Test FRS-V10-2

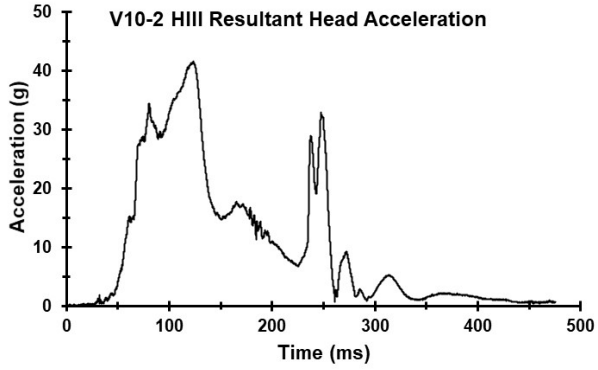
V10-2 HIII Resultant Head Acceleration
Acceleration (g)
Time (ms)

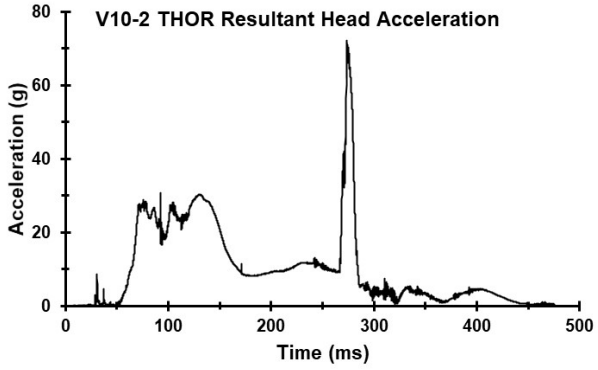
V10-2 THOR Resultant Head Acceleration
Acceleration (g)
Time (ms)

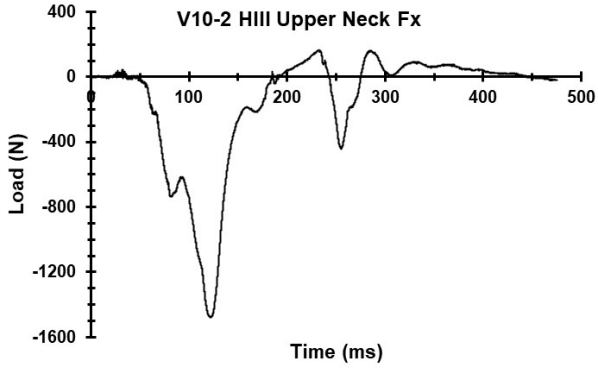
V10-2 HIII Upper Neck Fx
Load (N)
Time (ms)

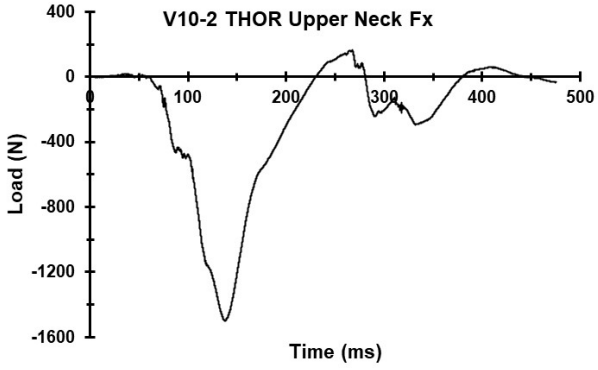
V10-2 THOR Upper Neck Fx
Load (N)
Time (ms)

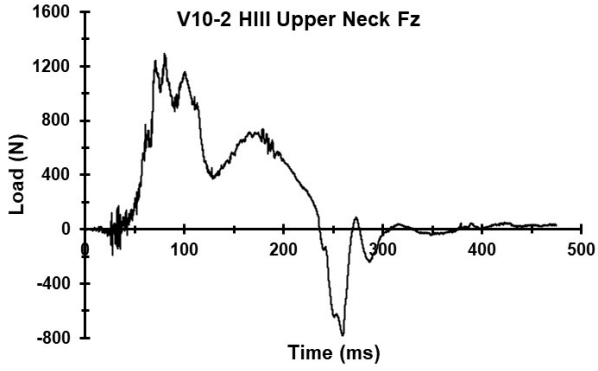
V10-2 HIII Upper Neck Fz
Load (N)
Time (ms)

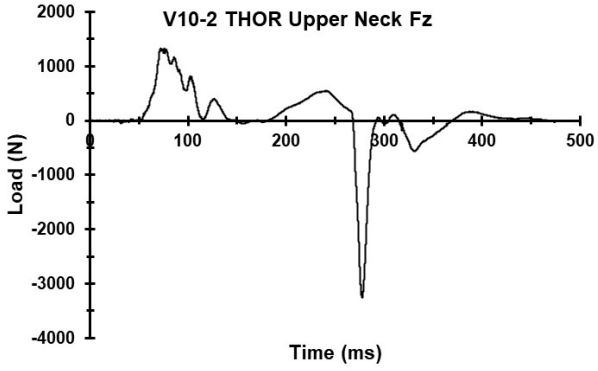
V10-2 THOR Upper Neck Fz
Load (N)
Time (ms)

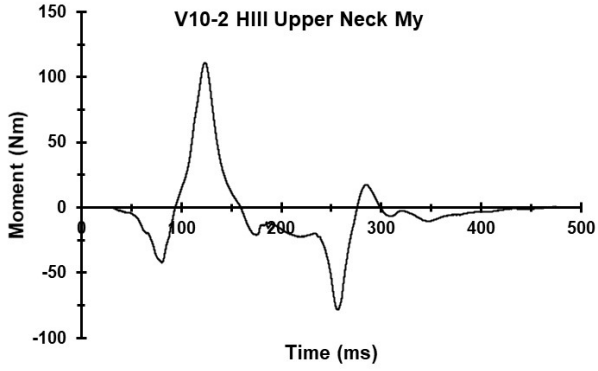
V10-2 HIII Upper Neck My
Moment (Nm)
Time (ms)

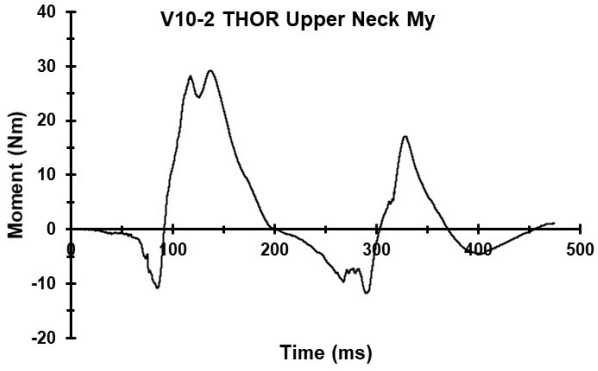
V10-2 THOR Upper Neck My
Moment (Nm)
Time (ms)

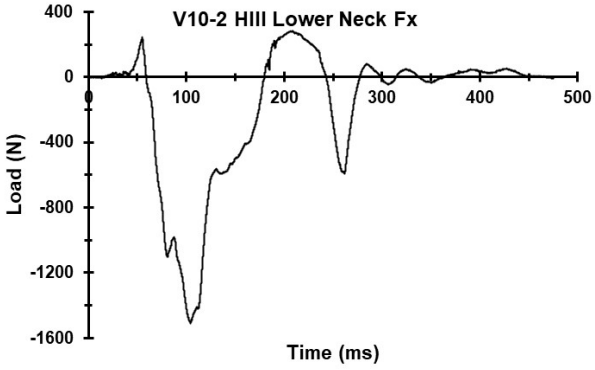
V10-2 HIII Lower Neck Fx
Load (N)
Time (ms)

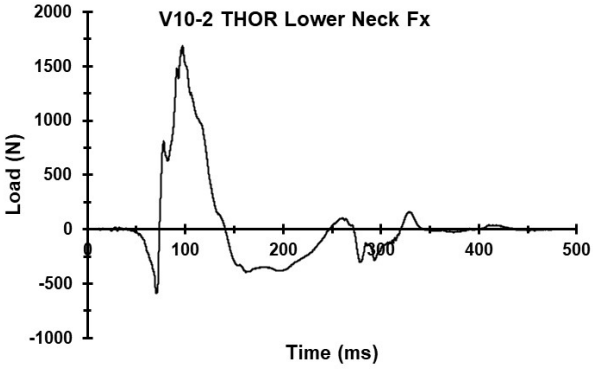
V10-2 THOR Lower Neck Fx
Load (N)
Time (ms)

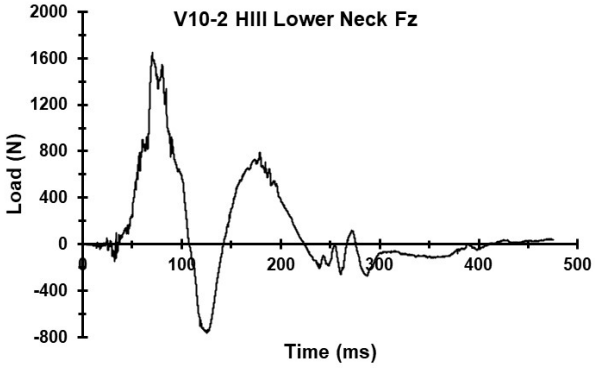
V10-2 HIII Lower Neck Fz
Load (N)
Time (ms)

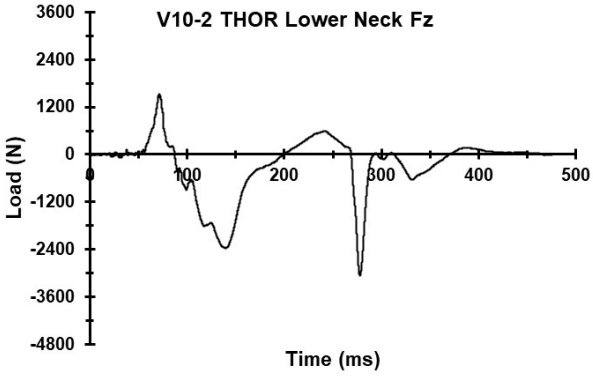
V10-2 THOR Lower Neck Fz
Load (N)
Time (ms)

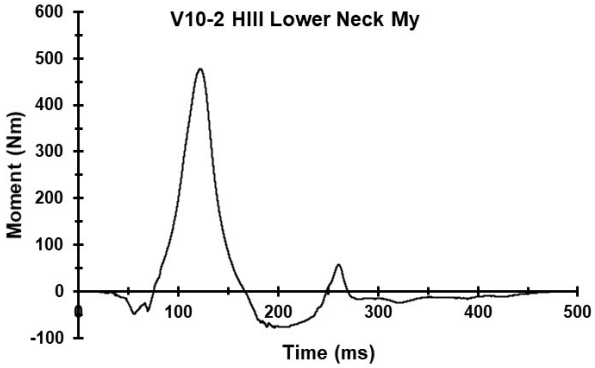
V10-2 HIII Lower Neck My
Moment (Nm)
Time (ms)

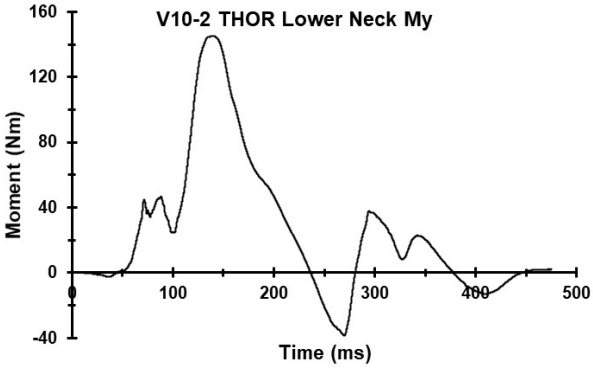
V10-2 THOR Lower Neck My
Moment (Nm)
Time (ms)

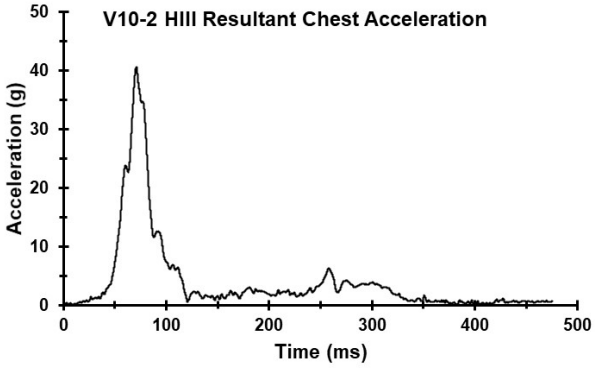
V10-2 HIII Resultant Chest Acceleration
Acceleration (g)
Time (ms)

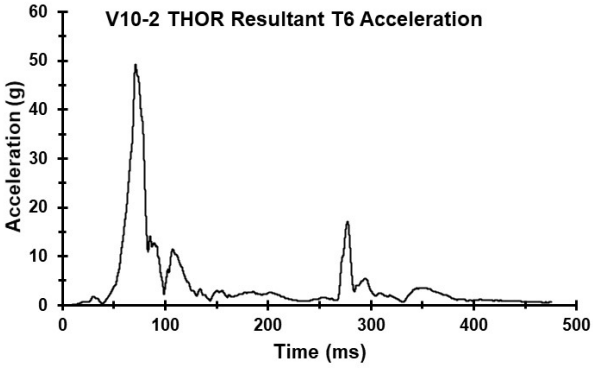
V10-2 THOR Resultant T6 Acceleration
Acceleration (g)
Time (ms)

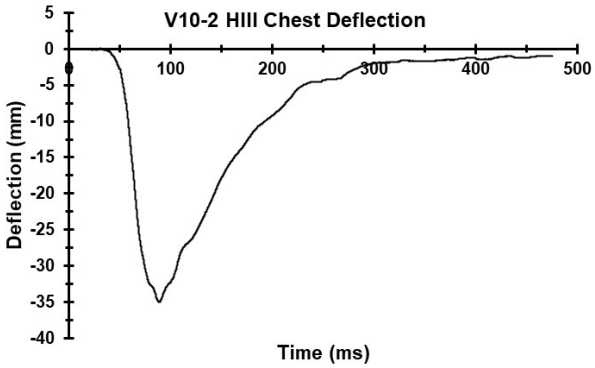
V10-2 HIII Chest Deflection
Deflection (mm)
Time (ms)
5
0
-5
-10
-15
-20
-25
-30
-35
-40
0
100
200
300
400
500

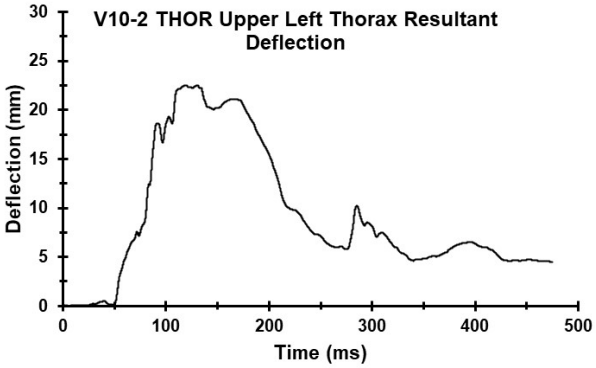
V10-2 THOR Upper Left Thorax Resultant Deflection
Deflection (mm)
Time (ms)
30
25
20
15
10
5
0
0
100
200
300
400
500

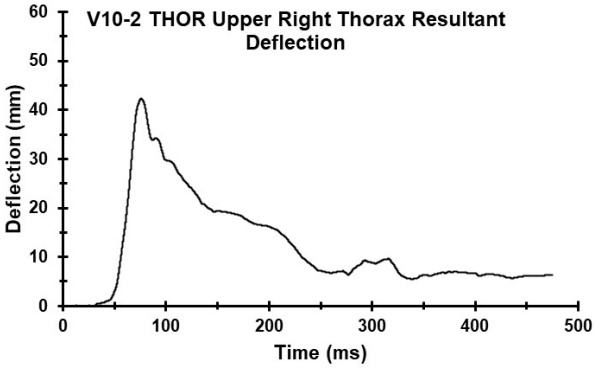
V10-2 THOR Upper Right Thorax Resultant Deflection
Deflection (mm)
Time (ms)
60
50
40
30
20
10
0
0
100
200
300
400
500

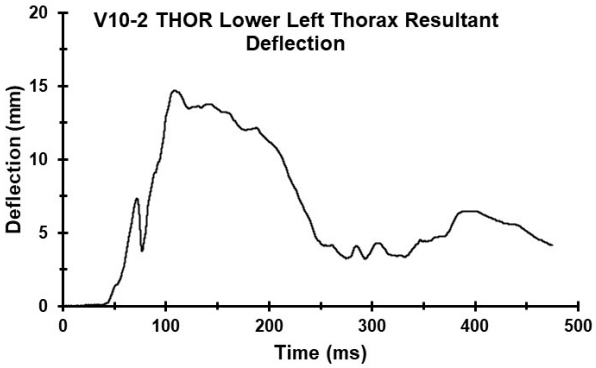
V10-2 THOR Lower Left Thorax Resultant Deflection
Deflection (mm)
Time (ms)
20
15
10
5
0
0
100
200
300
400
500

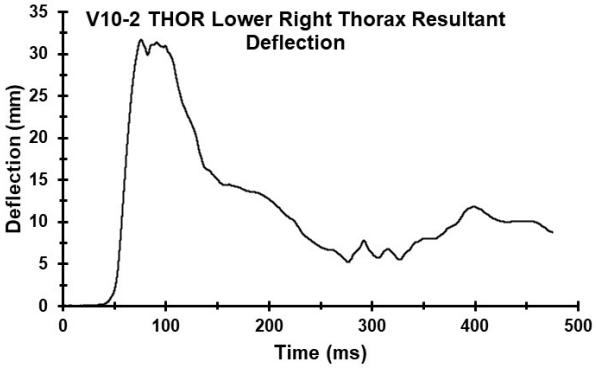
V10-2 THOR Lower Right Thorax Resultant Deflection
Deflection (mm)
Time (ms)
35
30
25
20
15
10
5
0
0
100
200
300
400
500

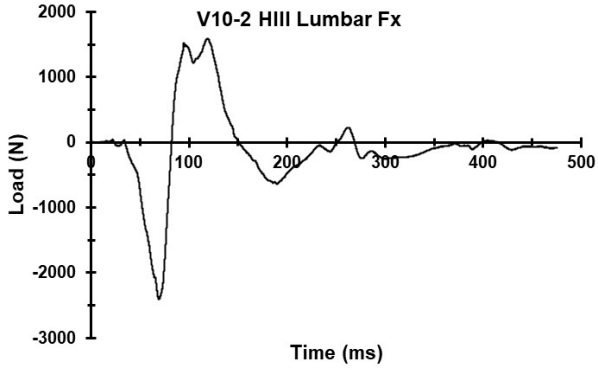
V10-2 HIII Lumbar Fx
Load (N)
Time (ms)

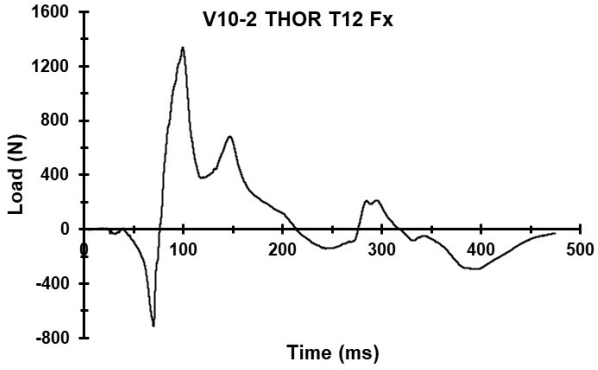
V10-2 THOR T12 Fx
Load (N)
Time (ms)

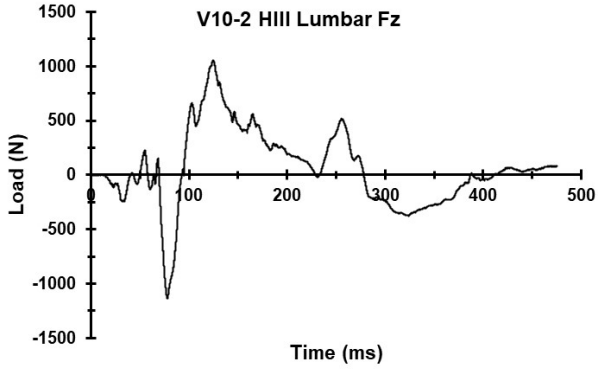
V10-2 HIII Lumbar Fz
Load (N)
Time (ms)

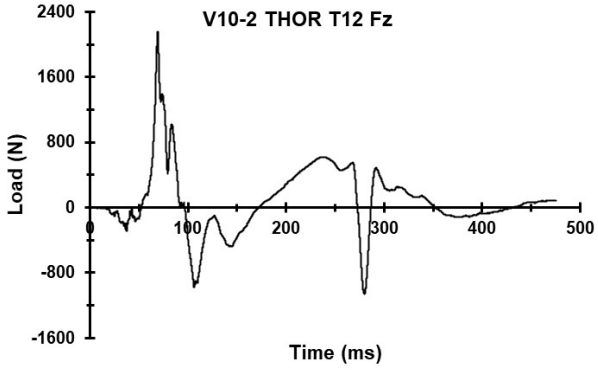
V10-2 THOR T12 Fz
Load (N)
Time (ms)

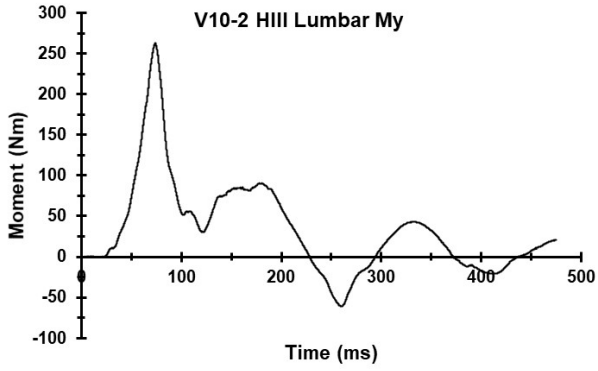
V10-2 HIII Lumbar My
Moment (Nm)
Time (ms)

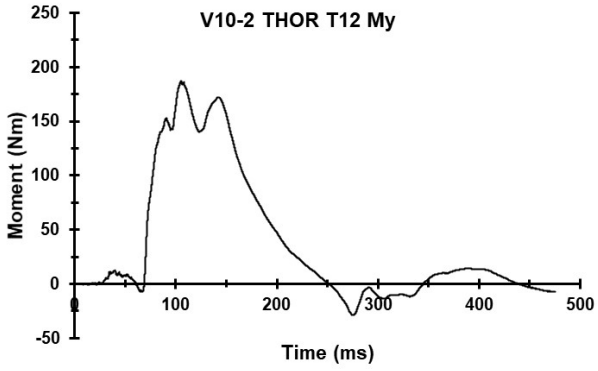
V10-2 THOR T12 My
Moment (Nm)
Time (ms)

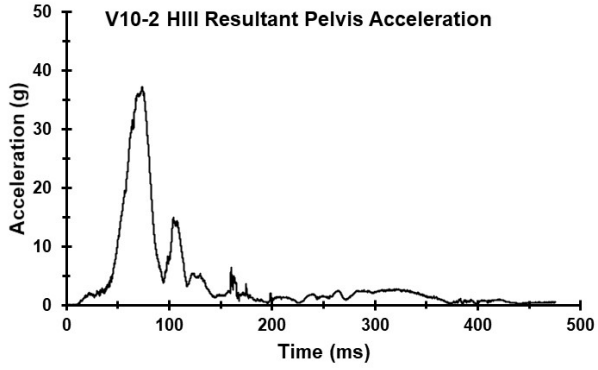
V10-2 HIII Resultant Pelvis Acceleration
Acceleration (g)
Time (ms)

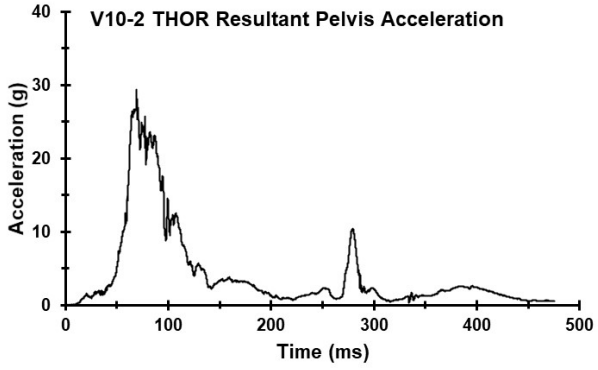
V10-2 THOR Resultant Pelvis Acceleration
Acceleration (g)
Time (ms)

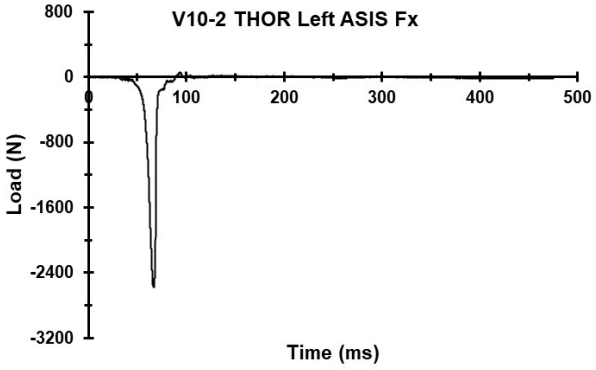
V10-2 THOR Left ASIS Fx
800
0
-800
-1600
-2400
-3200
Load (N)
0
100
200
300
400
500
Time (ms)

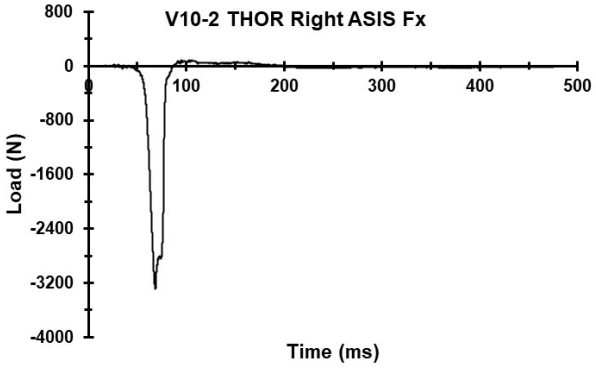
V10-2 THOR Right ASIS Fx
800
0
-800
-1600
-2400
-3200
-4000
Load (N)
0
100
200
300
400
500
Time (ms)

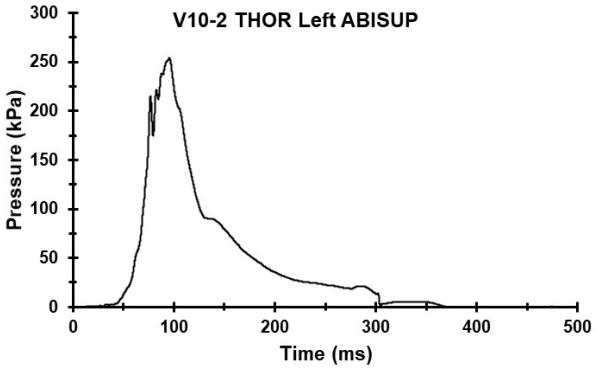
V10-2 THOR Left ABISUP
300
250
200
150
100
50
0
Pressure (kPa)
0
100
200
300
400
500
Time (ms)

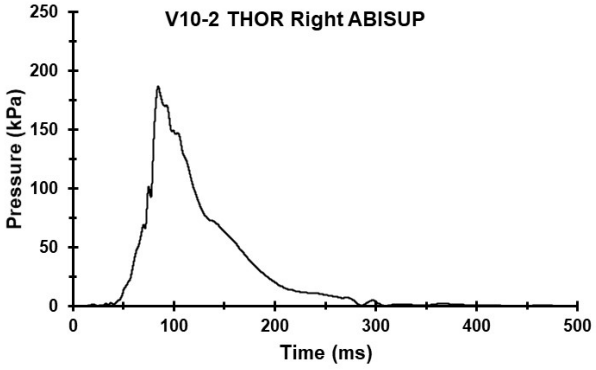
V10-2 THOR Right ABISUP
250
200
150
100
50
0
Pressure (kPa)
0
100
200
300
400
500
Time (ms)

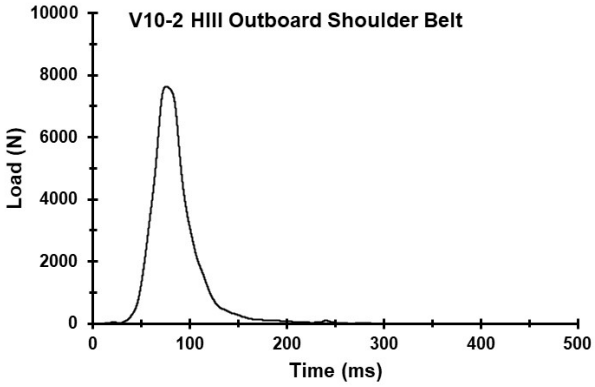
V10-2 HIII Outboard Shoulder Belt
Load (N)
Time (ms)

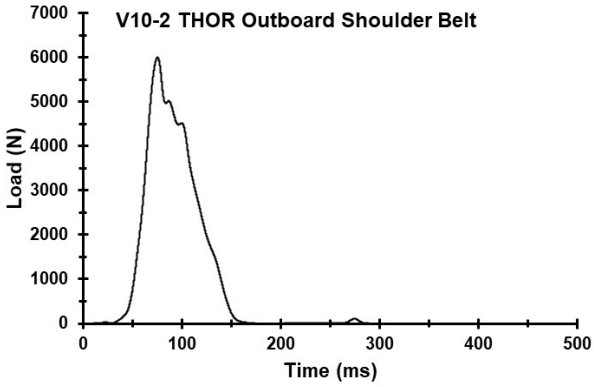
V10-2 THOR Outboard Shoulder Belt
Load (N)
Time (ms)

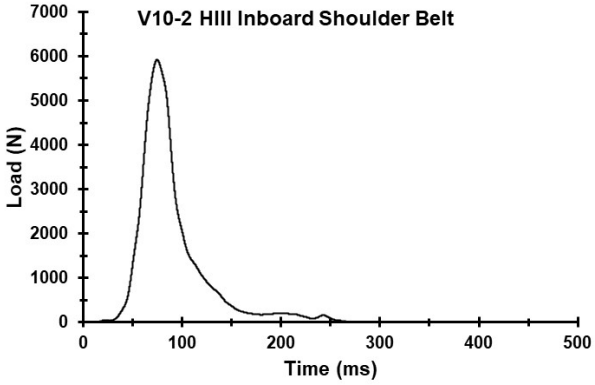
V10-2 HIII Inboard Shoulder Belt
Load (N)
Time (ms)

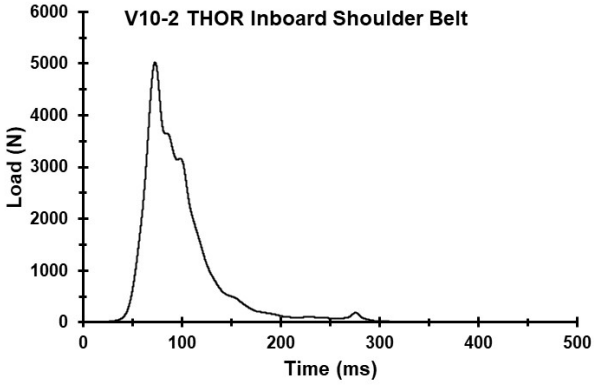
V10-2 THOR Inboard Shoulder Belt
Load (N)
Time (ms)

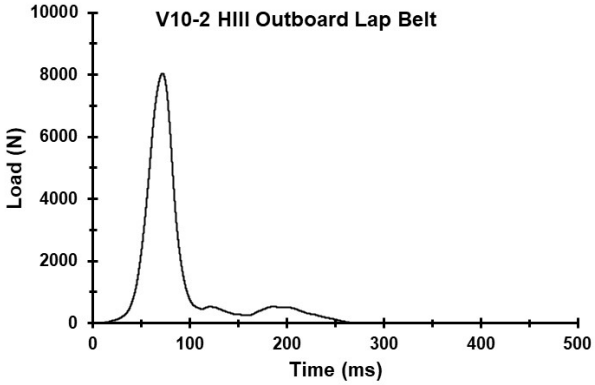
V10-2 HIII Outboard Lap Belt
Load (N)
Time (ms)

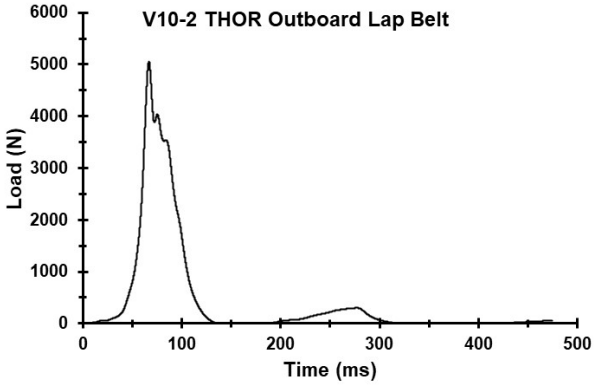
V10-2 THOR Outboard Lap Belt
Load (N)
Time (ms)

Appendix S. Select Data Traces From Test FRS-V10-3

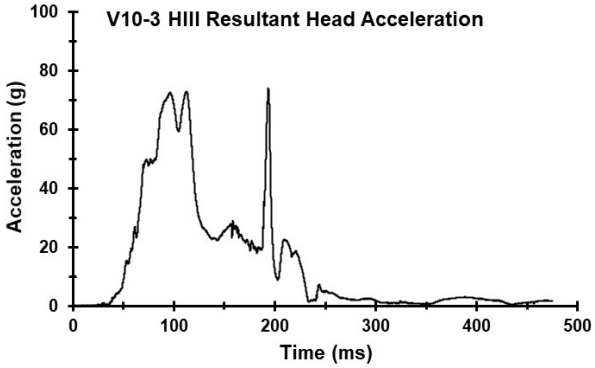
V10-3 HIII Resultant Head Acceleration
Acceleration (g)
Time (ms)

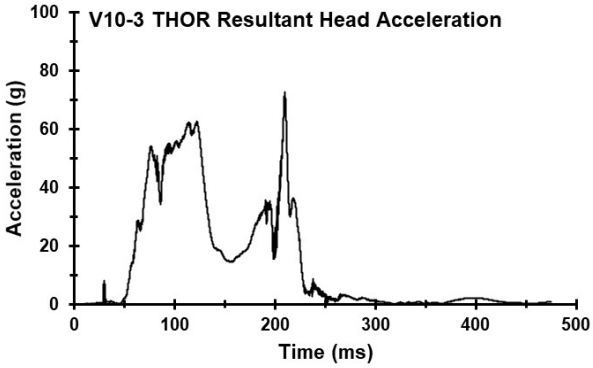
V10-3 THOR Resultant Head Acceleration
Acceleration (g)
Time (ms)

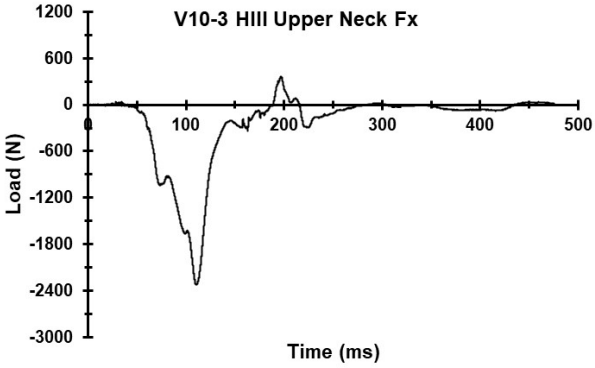
V10-3 HIII Upper Neck Fx
Load (N)
Time (ms)

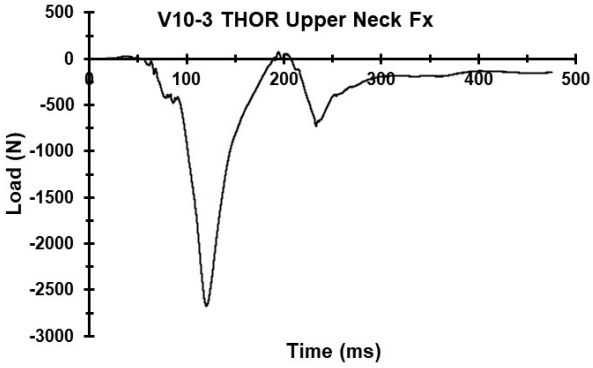
V10-3 THOR Upper Neck Fx
Load (N)
Time (ms)

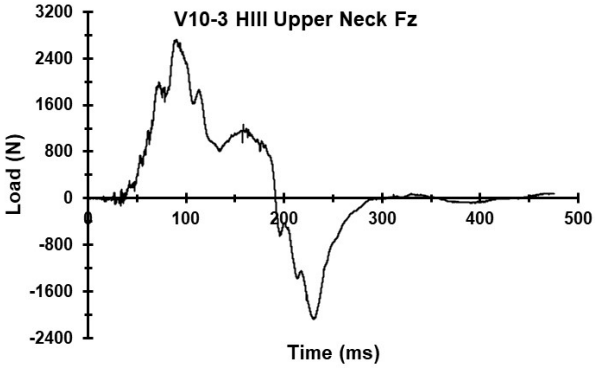
V10-3 HIII Upper Neck Fz
Load (N)
Time (ms)

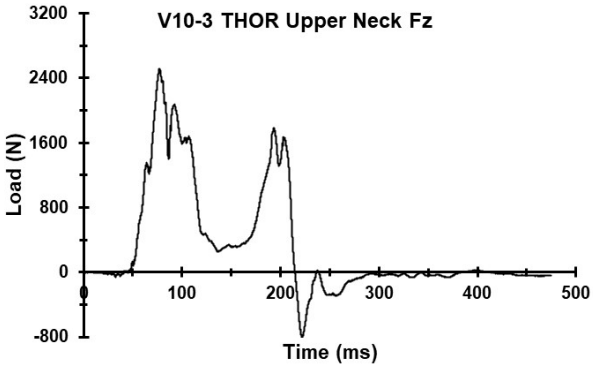
V10-3 THOR Upper Neck Fz
Load (N)
Time (ms)

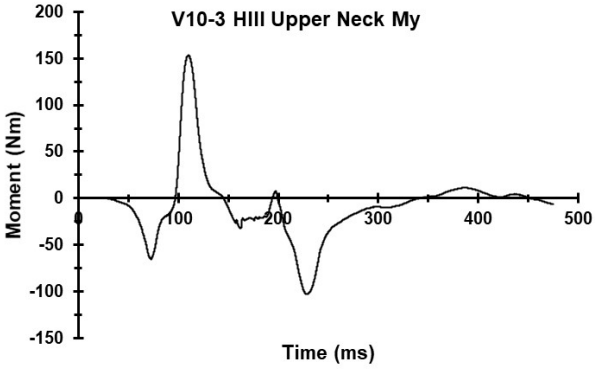
V10-3 HIII Upper Neck My
Moment (Nm)
Time (ms)

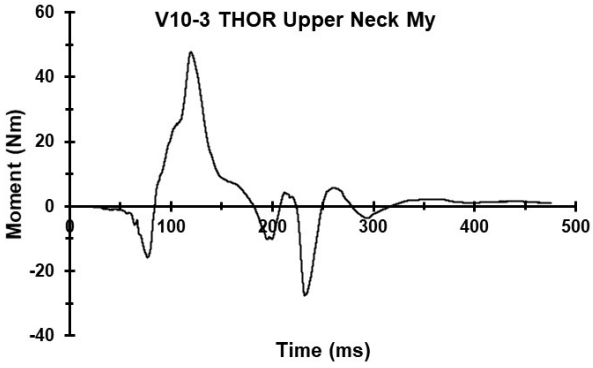
V10-3 THOR Upper Neck My
Moment (Nm)
Time (ms)

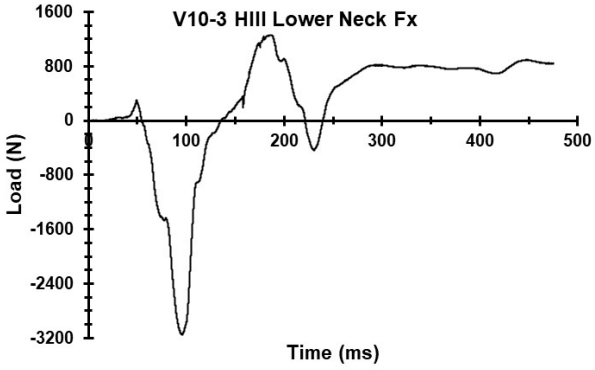
V10-3 HIII Lower Neck Fx
Load (N)
1600
800
0
-800
-1600
-2400
-3200
0
100
200
300
400
500
Time (ms)

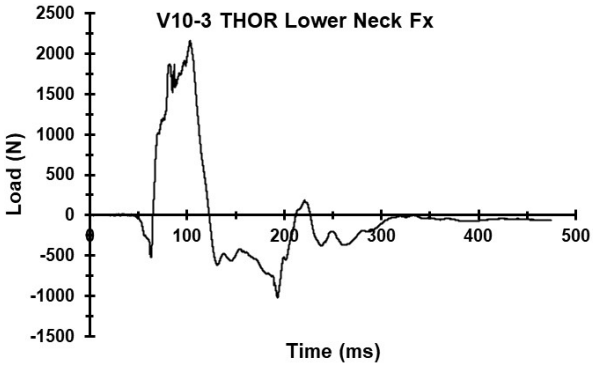
V10-3 THOR Lower Neck Fx
Load (N)
2500
2000
1500
1000
500
0
-500
-1000
-1500
0
100
200
300
400
500
Time (ms)

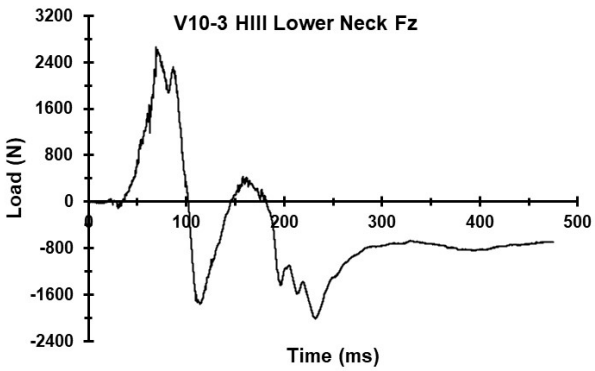
V10-3 HIII Lower Neck Fz
Load (N)
3200
2400
1600
800
0
-800
-1600
-2400
0
100
200
300
400
500
Time (ms)

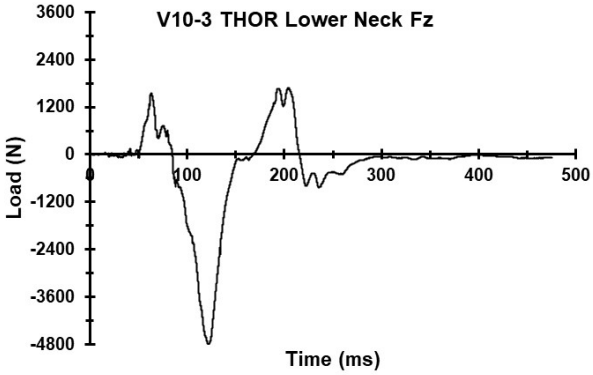
V10-3 THOR Lower Neck Fz
Load (N)
3600
2400
1200
0
-1200
-2400
-3600
-4800
0
100
200
300
400
500
Time (ms)

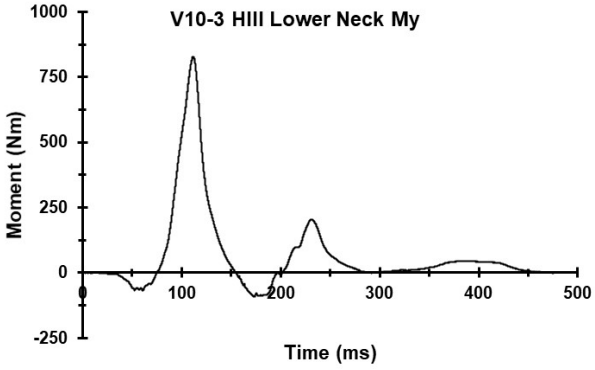
V10-3 HIII Lower Neck My
Moment (Nm)
1000
750
500
250
0
-250
0
100
200
300
400
500
Time (ms)

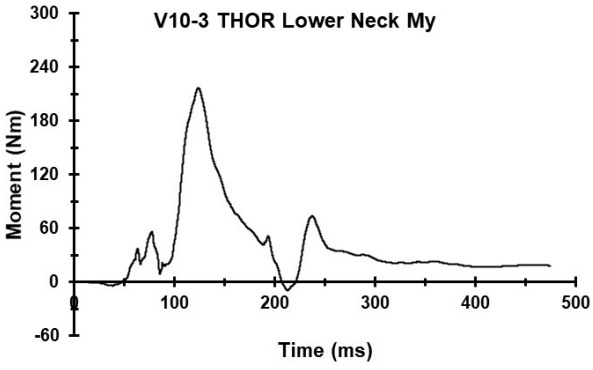
V10-3 THOR Lower Neck My
Moment (Nm)
300
240
180
120
60
0
-60
0
100
200
300
400
500
Time (ms)

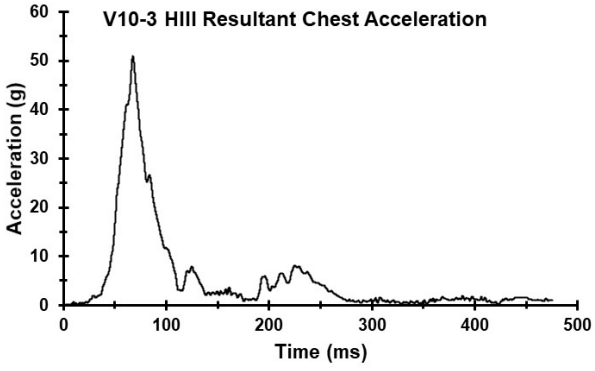
V10-3 HIII Resultant Chest Acceleration
Acceleration (g)
60
50
40
30
20
10
0
0
100
200
300
400
500
Time (ms)

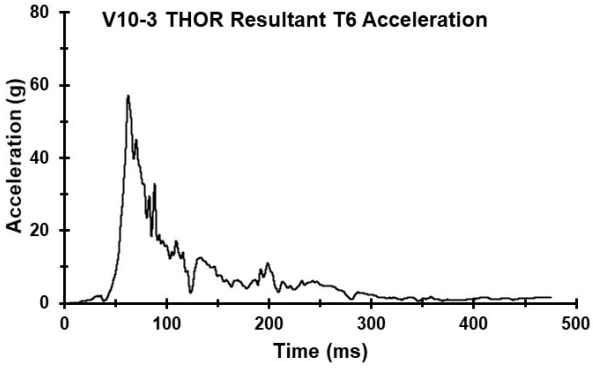
V10-3 THOR Resultant T6 Acceleration
Acceleration (g)
80
60
40
20
0
0
100
200
300
400
500
Time (ms)

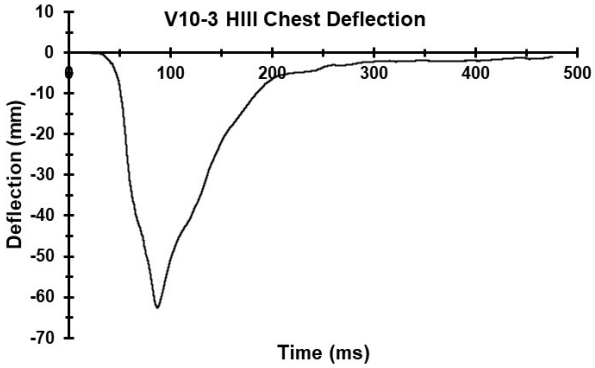
V10-3 HIII Chest Deflection
Deflection (mm)
Time (ms)

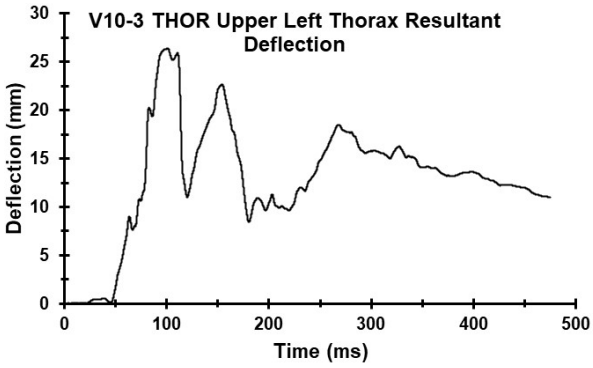
V10-3 THOR Upper Left Thorax Resultant Deflection
Deflection (mm)
Time (ms)

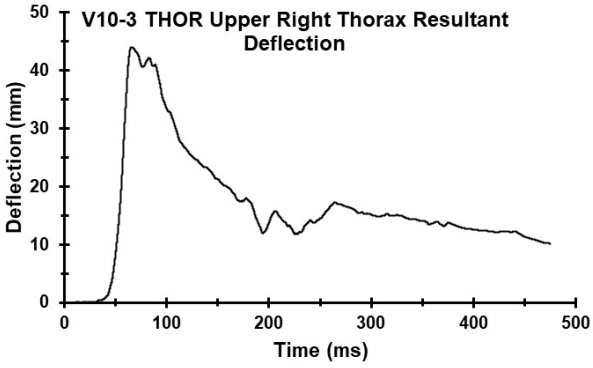
V10-3 THOR Upper Right Thorax Resultant Deflection
Deflection (mm)
Time (ms)

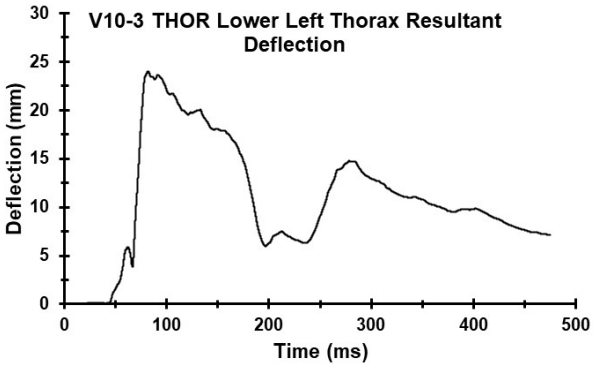
V10-3 THOR Lower Left Thorax Resultant Deflection
Deflection (mm)
Time (ms)

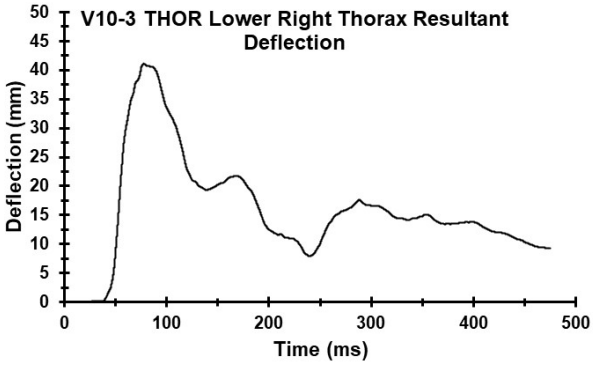
V10-3 THOR Lower Right Thorax Resultant Deflection
Deflection (mm)
Time (ms)

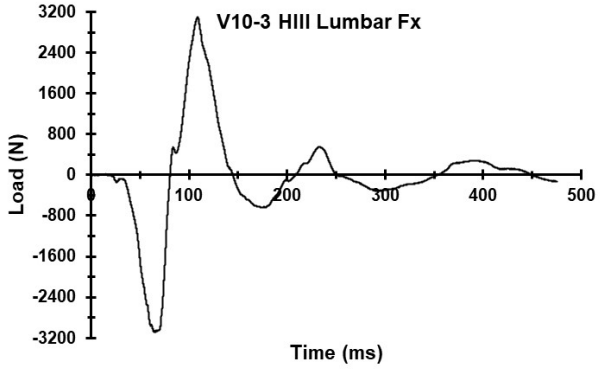
V10-3 HIII Lumbar Fx
Load (N)
Time (ms)

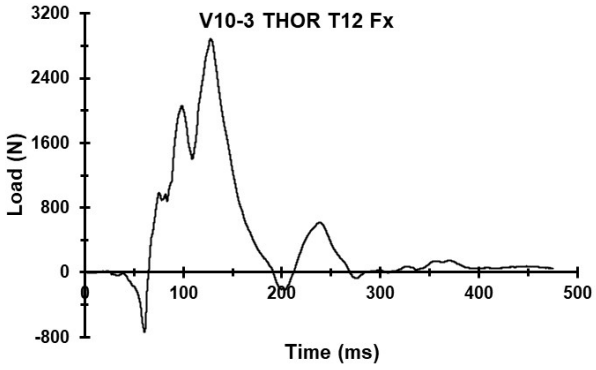
V10-3 THOR T12 Fx
Load (N)
Time (ms)

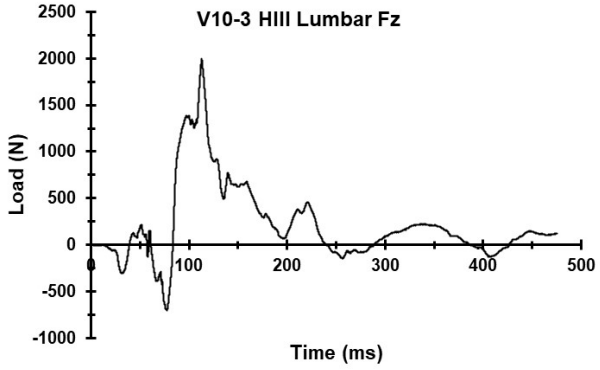
V10-3 HIII Lumbar Fz
Load (N)
Time (ms)

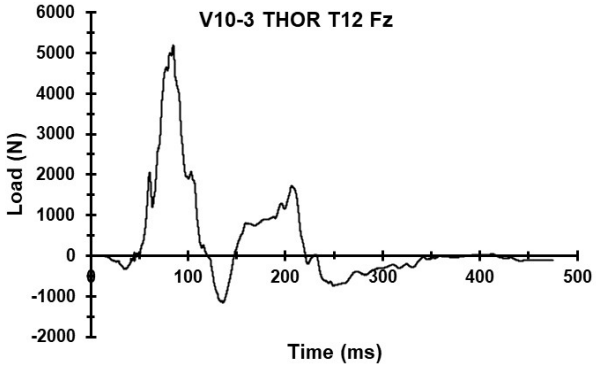
V10-3 THOR T12 Fz
Load (N)
Time (ms)

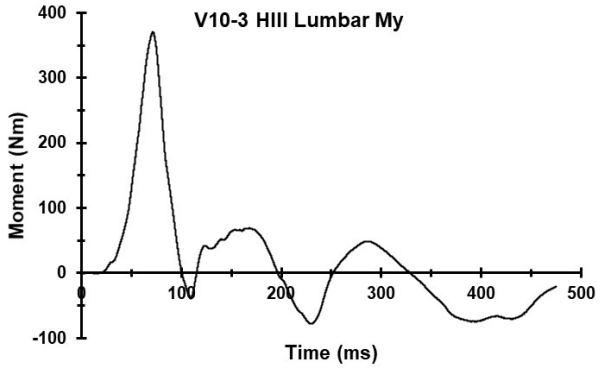
V10-3 HIII Lumbar My
Moment (Nm)
Time (ms)

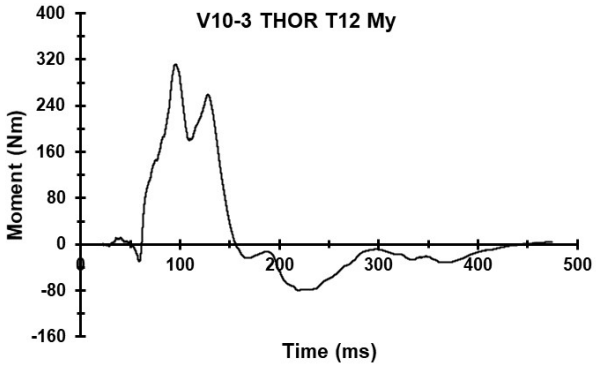
V10-3 THOR T12 My
Moment (Nm)
Time (ms)

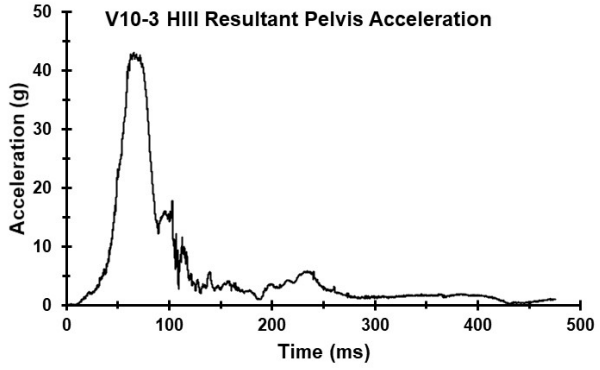
V10-3 HIII Resultant Pelvis Acceleration
Acceleration (g)
Time (ms)

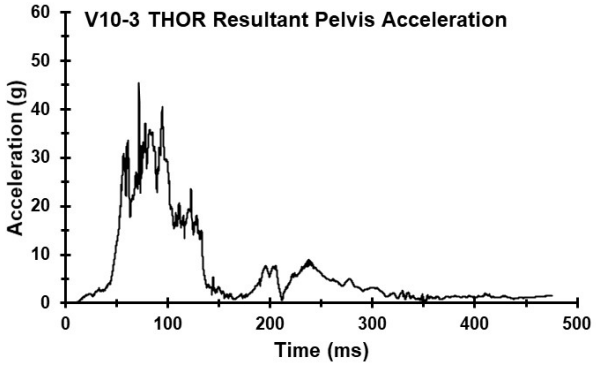
V10-3 THOR Resultant Pelvis Acceleration
Acceleration (g)
Time (ms)

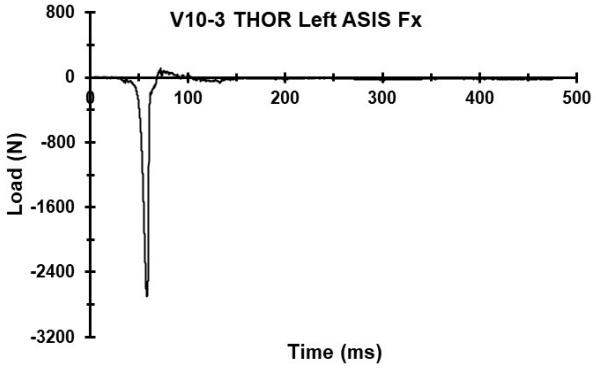
V10-3 THOR Left ASIS Fx
800
0
-800
-1600
-2400
-3200
Load (N)
0
100
200
300
400
500
Time (ms)

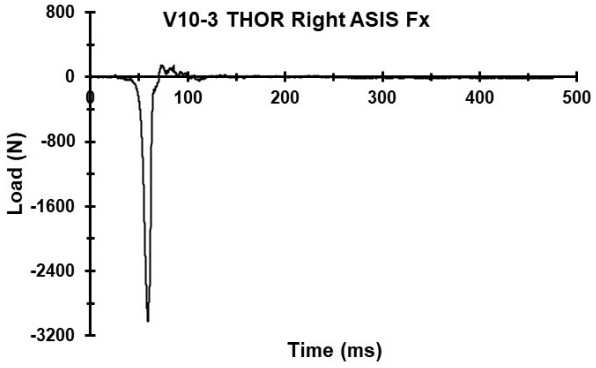
V10-3 THOR Right ASIS Fx
800
0
-800
-1600
-2400
-3200
Load (N)
0
100
200
300
400
500
Time (ms)

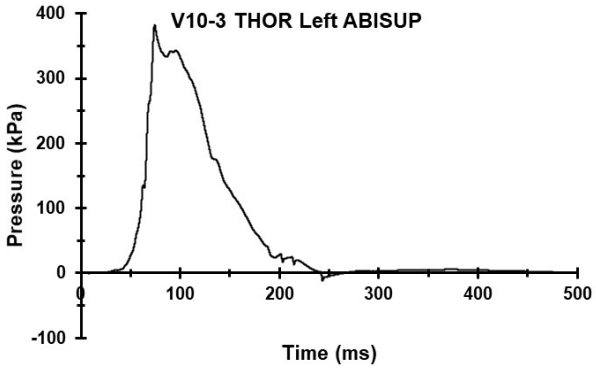
V10-3 THOR Left ABISUP
400
300
200
100
0
-100
Pressure (kPa)
0
100
200
300
400
500
Time (ms)

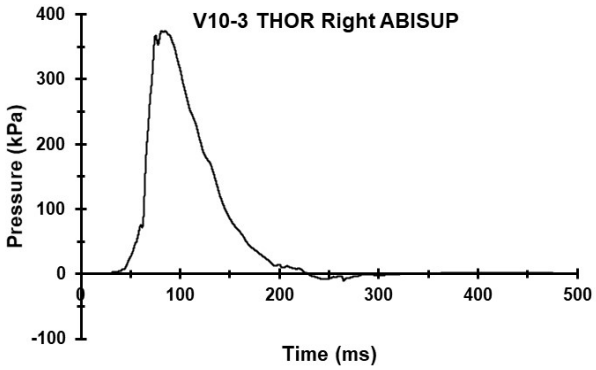
V10-3 THOR Right ABISUP
400
300
200
100
0
-100
Pressure (kPa)
0
100
200
300
400
500
Time (ms)

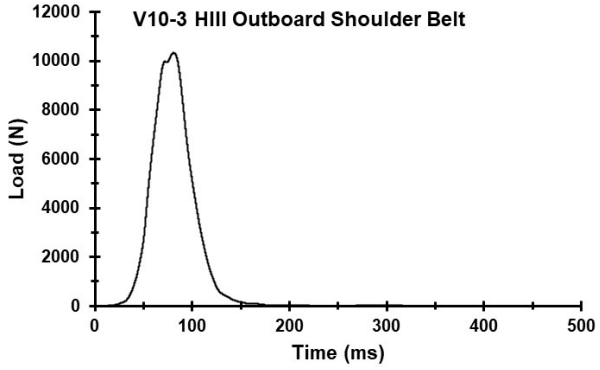
V10-3 HIII Outboard Shoulder Belt
Load (N)
Time (ms)
0
2000
4000
6000
8000
10000
12000
0
100
200
300
400
500

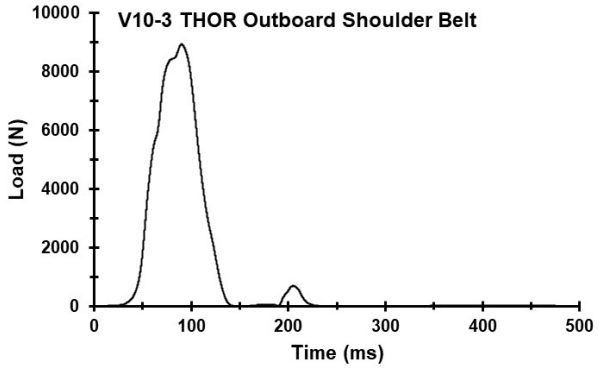
V10-3 THOR Outboard Shoulder Belt
Load (N)
Time (ms)
0
2000
4000
6000
8000
10000
0
100
200
300
400
500

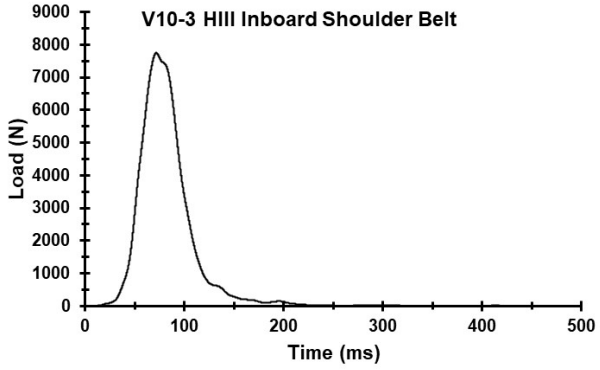
V10-3 HIII Inboard Shoulder Belt
Load (N)
Time (ms)
0
1000
2000
3000
4000
5000
6000
7000
8000
9000
0
100
200
300
400
500

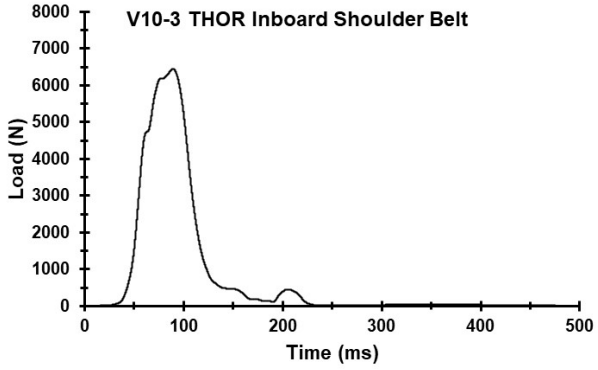
V10-3 THOR Inboard Shoulder Belt
Load (N)
Time (ms)
0
1000
2000
3000
4000
5000
6000
7000
8000
0
100
200
300
400
500

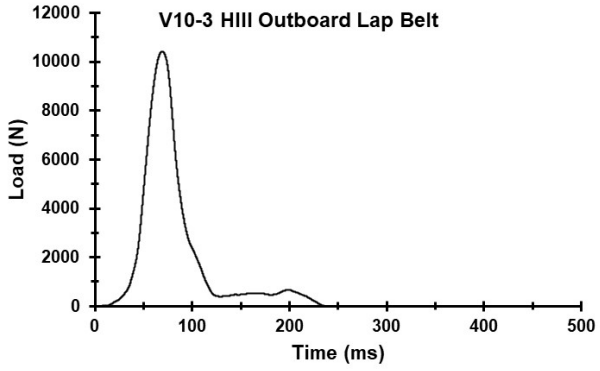
V10-3 HIII Outboard Lap Belt
Load (N)
Time (ms)
0
2000
4000
6000
8000
10000
12000
0
100
200
300
400
500

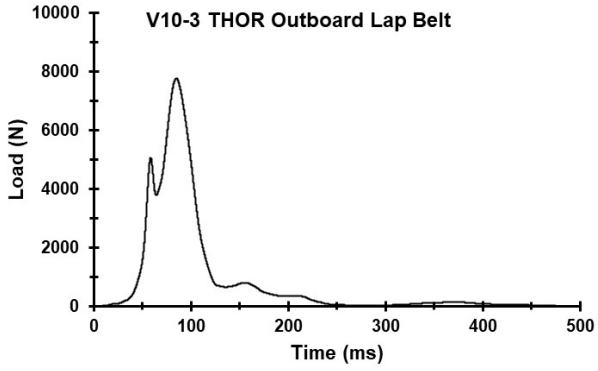
V10-3 THOR Outboard Lap Belt
Load (N)
Time (ms)
0
2000
4000
6000
8000
10000
0
100
200
300
400
500

Appendix T. Select Data Traces From Test FRS-V13-1

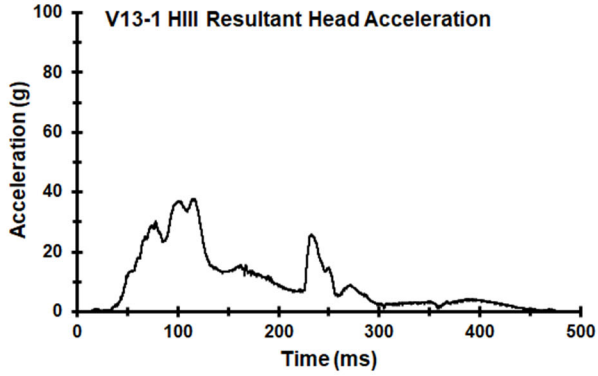
V13-1 HIII Resultant Head Acceleration
Acceleration (g)
Time (ms)

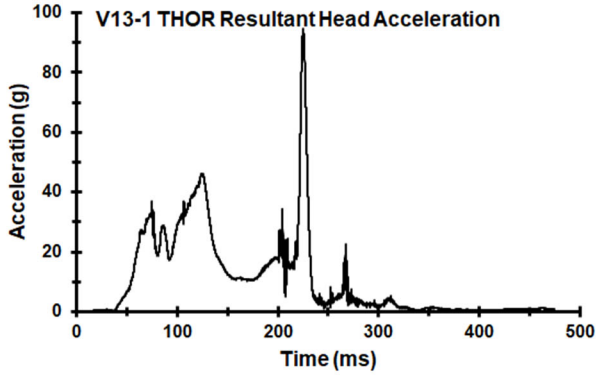
V13-1 THOR Resultant Head Acceleration
Acceleration (g)
Time (ms)

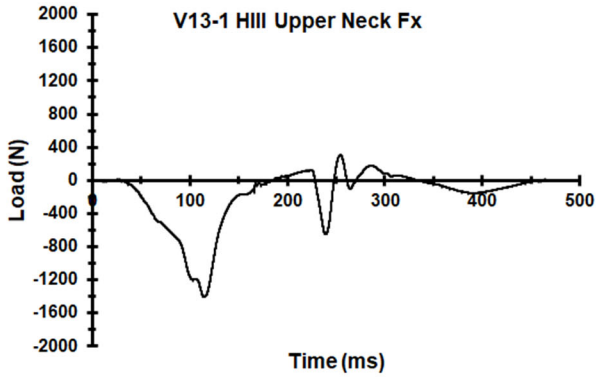
V13-1 HIII Upper Neck Fx
Load (N)
Time (ms)

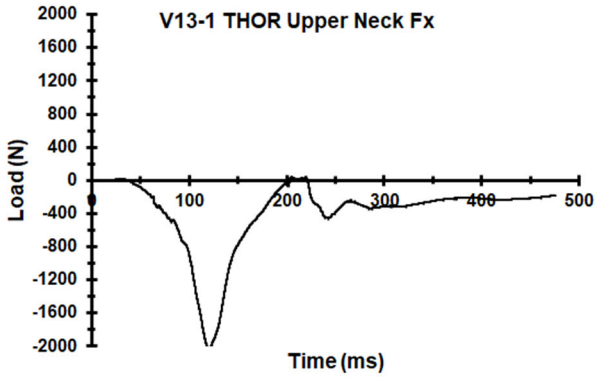
V13-1 THOR Upper Neck Fx
Load (N)
Time (ms)

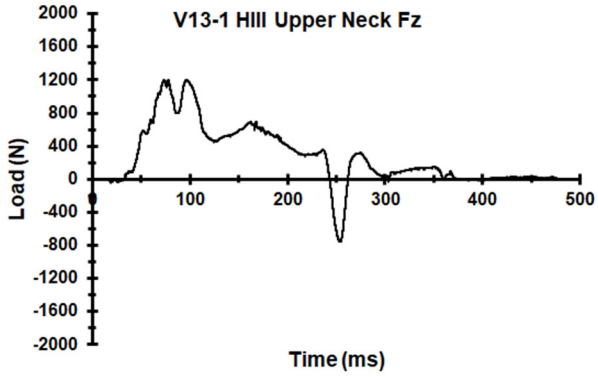
V13-1 HIII Upper Neck Fz
Load (N)
Time (ms)

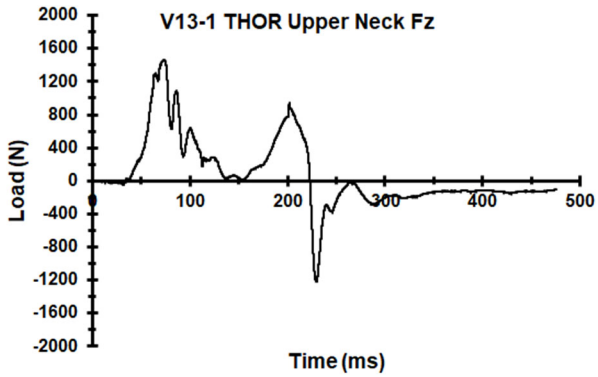
V13-1 THOR Upper Neck Fz
Load (N)
Time (ms)

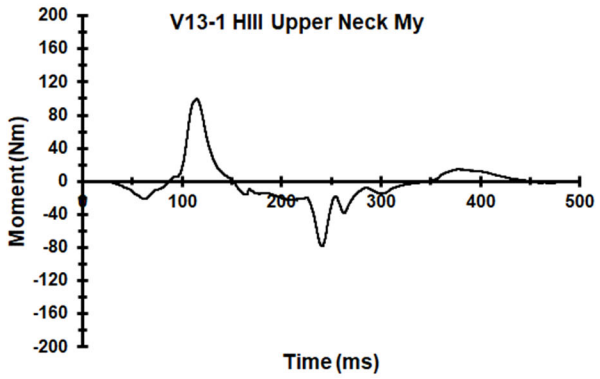
V13-1 HIII Upper Neck My
Moment (Nm)
200
160
120
80
40
0
-40
-80
-120
-160
-200
0
100
200
300
400
500
Time (ms)

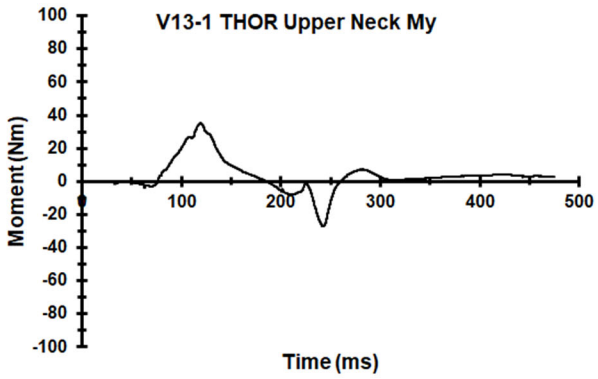
V13-1 THOR Upper Neck My
Moment (Nm)
100
80
60
40
20
0
-20
-40
-60
-80
-100
0
100
200
300
400
500
Time (ms)

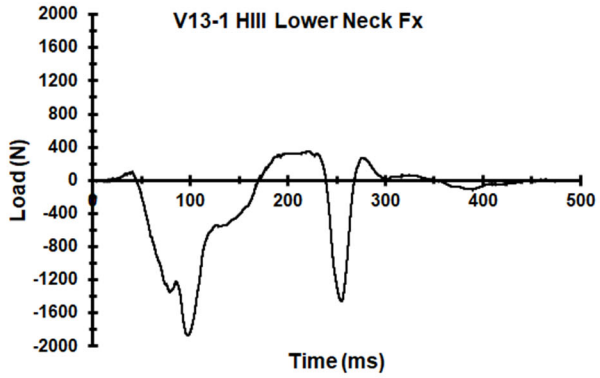
V13-1 HIII Lower Neck Fx
Load (N)
2000
1600
1200
800
400
0
-400
-800
-1200
-1600
-2000
0
100
200
300
400
500
Time (ms)

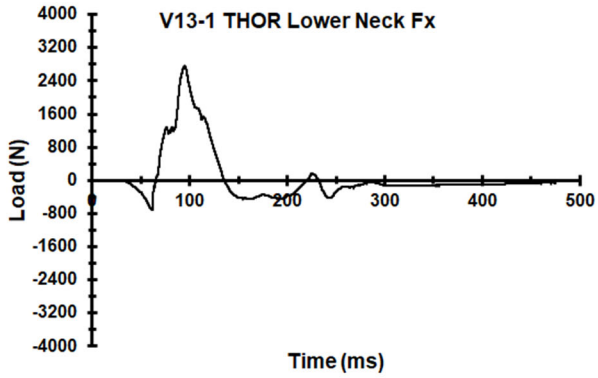
V13-1 THOR Lower Neck Fx
Load (N)
4000
3200
2400
1600
800
0
-800
-1600
-2400
-3200
-4000
0
100
200
300
400
500
Time (ms)

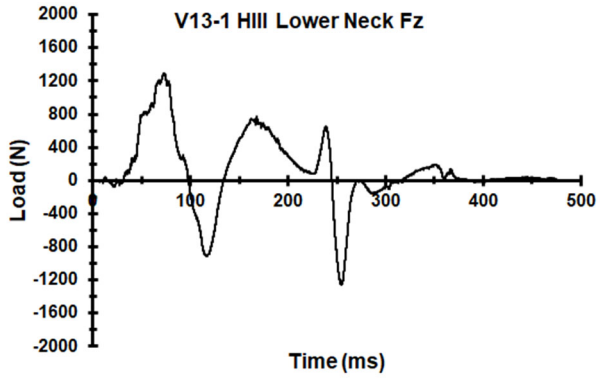
V13-1 HIII Lower Neck Fz
Load (N)
2000
1600
1200
800
400
0
-400
-800
-1200
-1600
-2000
0
100
200
300
400
500
Time (ms)

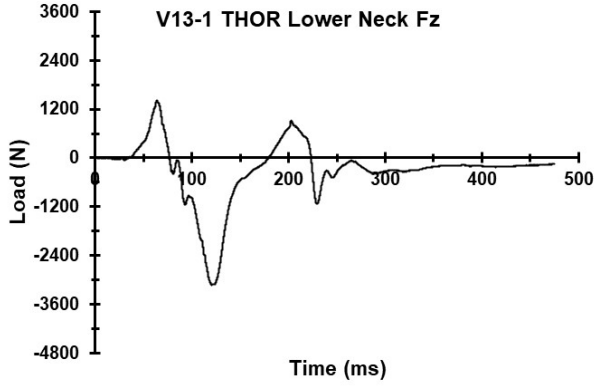
V13-1 THOR Lower Neck Fz
Load (N)
3600
2400
1200
0
-1200
-2400
-3600
-4800
0
100
200
300
400
500
Time (ms)

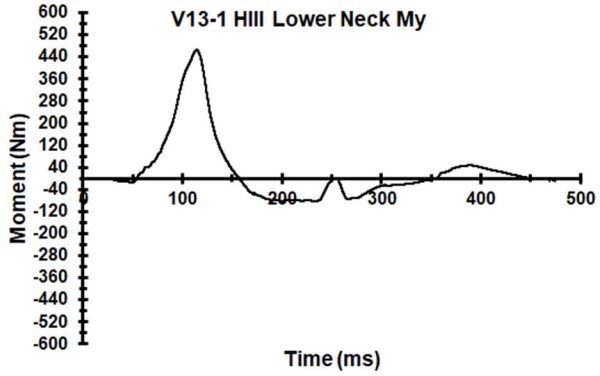
V13-1 HIII Lower Neck My
Moment (Nm)
600
520
440
360
280
200
120
40
-40
-120
-200
-280
-360
-440
-520
-600
0
100
200
300
400
500
Time (ms)

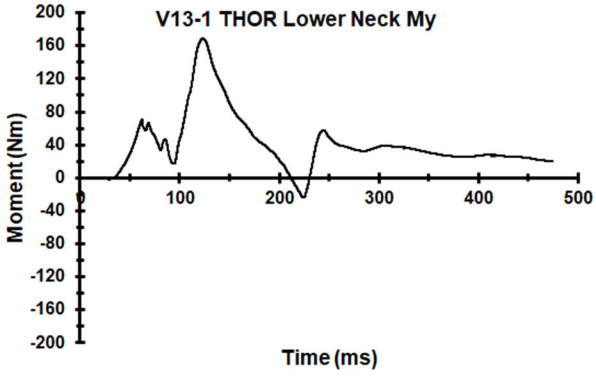
V13-1 THOR Lower Neck My
Moment (Nm)
200
160
120
80
40
0
-40
-80
-120
-160
-200
0
100
200
300
400
500
Time (ms)

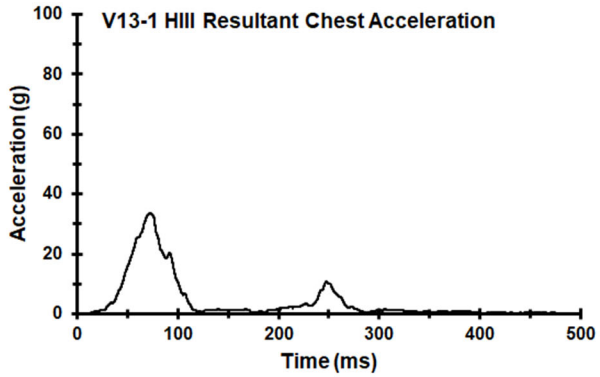
V13-1 HIII Resultant Chest Acceleration
Acceleration (g)
100
80
60
40
20
0
0
100
200
300
400
500
Time (ms)

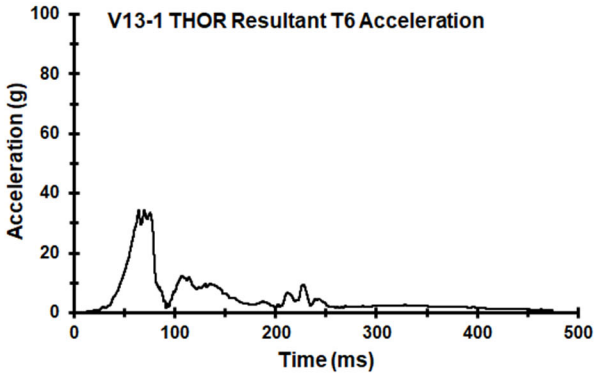
V13-1 THOR Resultant T6 Acceleration
Acceleration (g)
100
80
60
40
20
0
0
100
200
300
400
500
Time (ms)

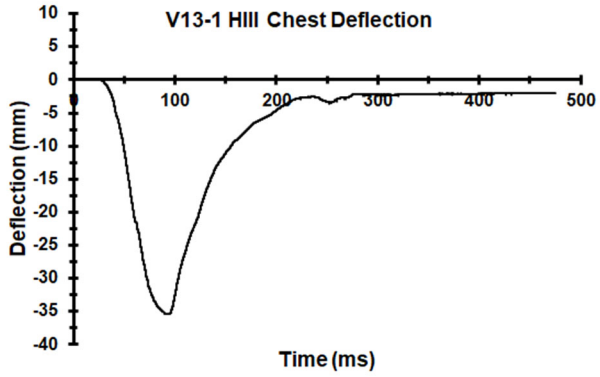
V13-1 HIII Chest Deflection
Deflection (mm)
10
5
0
-5
-10
-15
-20
-25
-30
-35
-40
0
100
200
300
400
500
Time (ms)

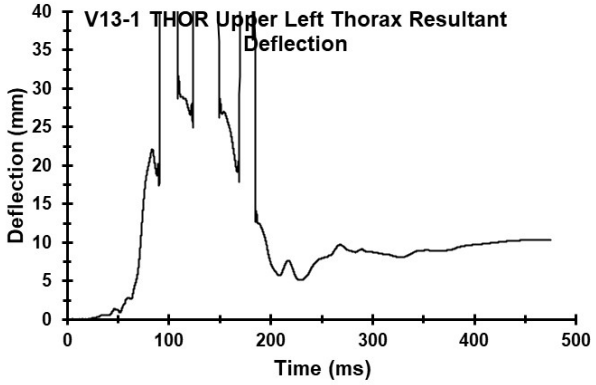
V13-1 THOR Upper Left Thorax Resultant Deflection
Deflection (mm)
40
35
30
25
20
15
10
5
0
0
100
200
300
400
500
Time (ms)

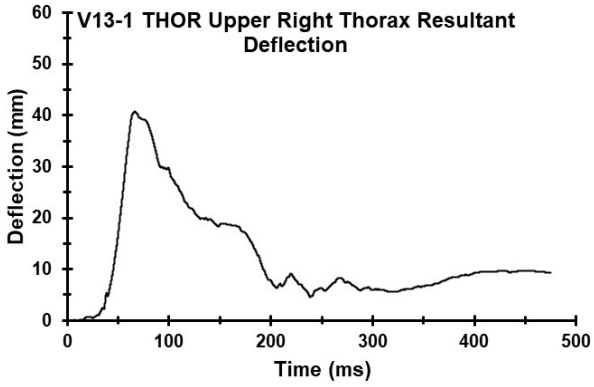
V13-1 THOR Upper Right Thorax Resultant Deflection
Deflection (mm)
Time (ms)

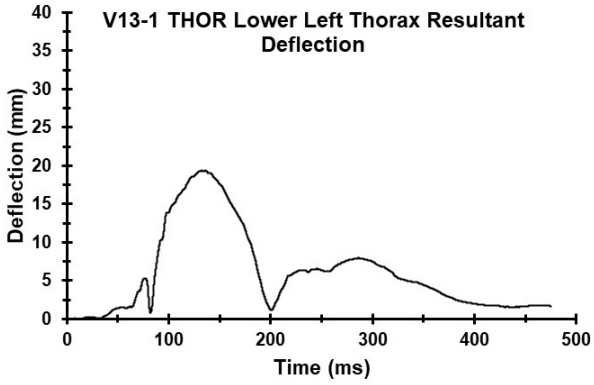
V13-1 THOR Lower Left Thorax Resultant Deflection
Deflection (mm)
Time (ms)

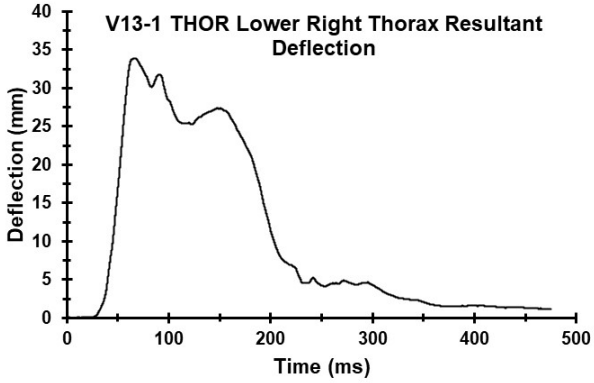
V13-1 THOR Lower Right Thorax Resultant Deflection
Deflection (mm)
Time (ms)

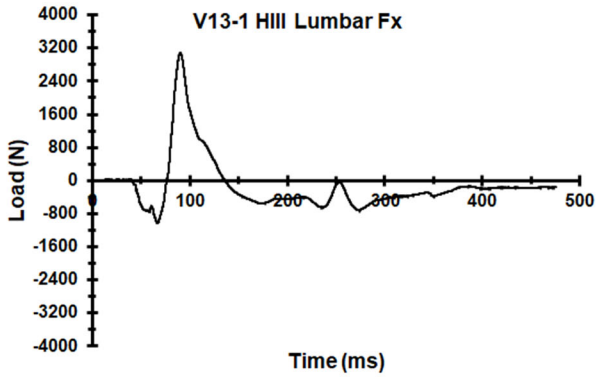
V13-1 HIII Lumbar Fx
Load (N)
Time (ms)

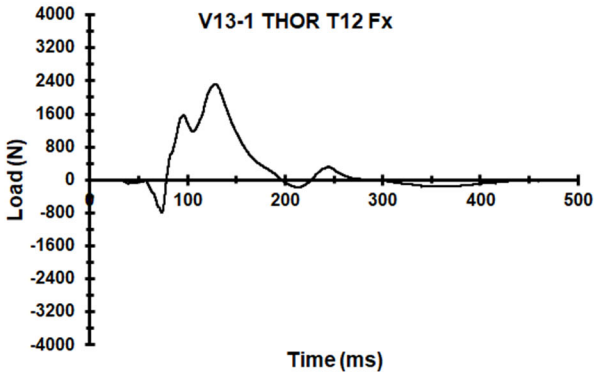
V13-1 THOR T12 Fx
Load (N)
Time (ms)

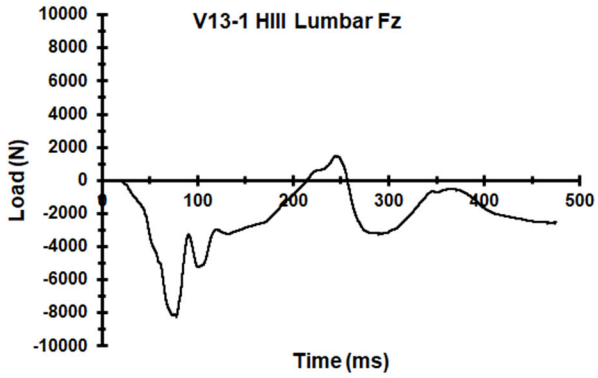
V13-1 HIII Lumbar Fz
Load (N)
Time (ms)

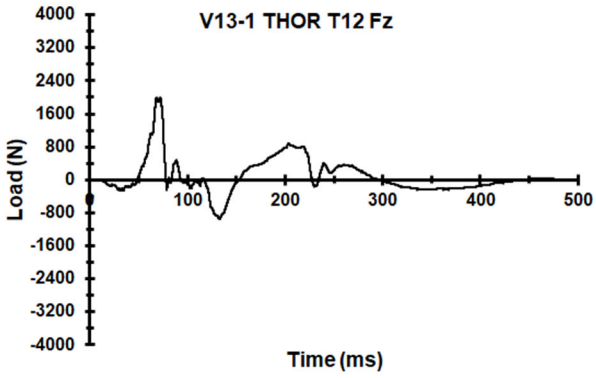
V13-1 THOR T12 Fz
Load (N)
Time (ms)

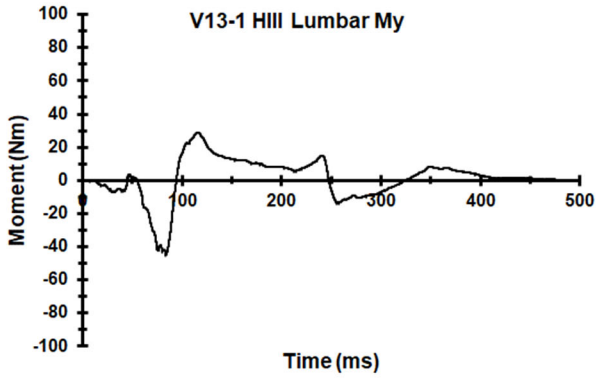
V13-1 HIII Lumbar My
Moment (Nm)
Time (ms)

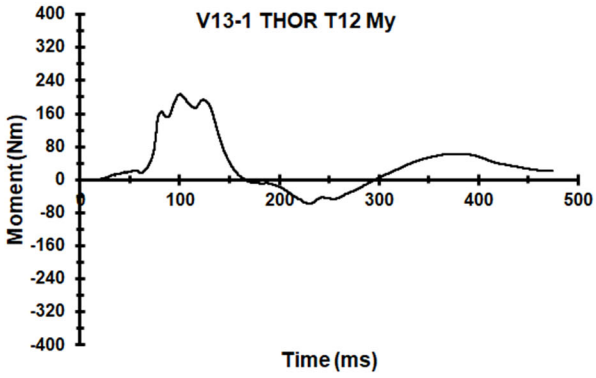
V13-1 THOR T12 My
Moment (Nm)
Time (ms)

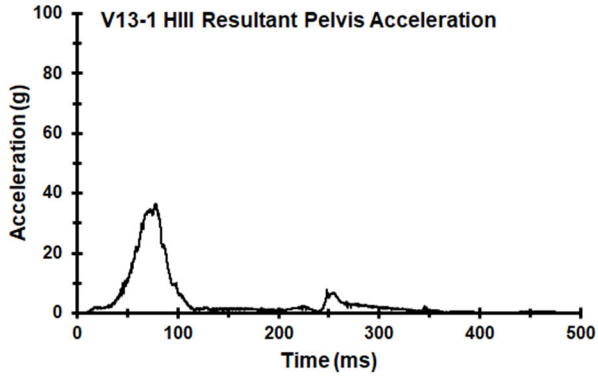
V13-1 HIII Resultant Pelvis Acceleration
Acceleration (g)
Time (ms)

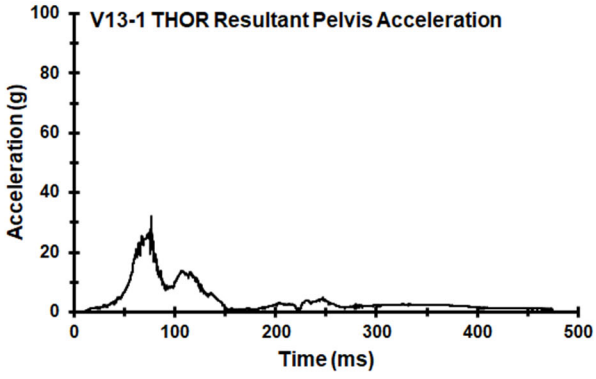
V13-1 THOR Resultant Pelvis Acceleration
Acceleration (g)
Time (ms)

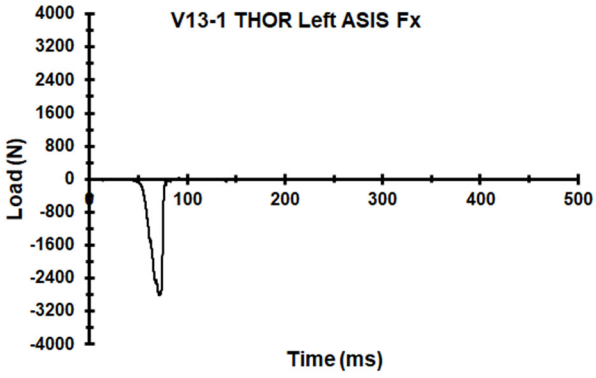
V13-1 THOR Left ASIS Fx
Load (N)
Time (ms)

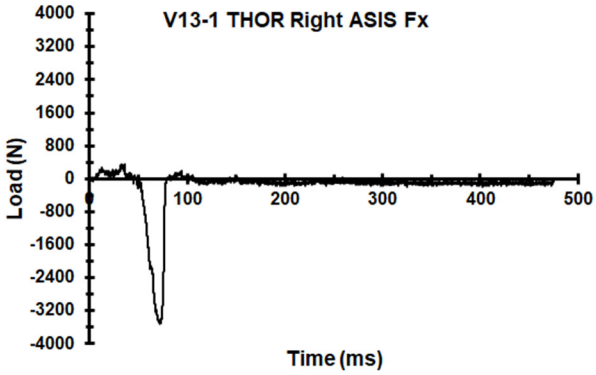
V13-1 THOR Right ASIS Fx
Load (N)
4000
3200
2400
1600
800
0
-800
-1600
-2400
-3200
-4000
100
200
300
400
500
Time (ms)

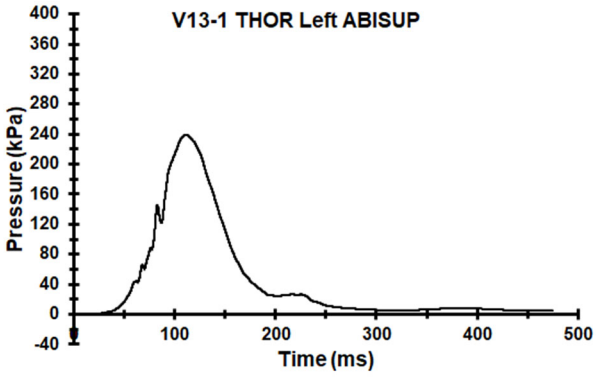
V13-1 THOR Left ABISUP
Pressure (kPa)
400
360
320
280
240
200
160
120
80
40
0
-40
100
200
300
400
500
Time (ms)

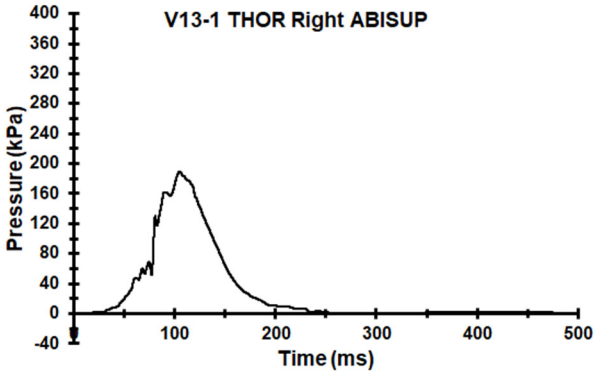
V13-1 THOR Right ABISUP
Pressure (kPa)
400
360
320
280
240
200
160
120
80
40
0
-40
100
200
300
400
500
Time (ms)

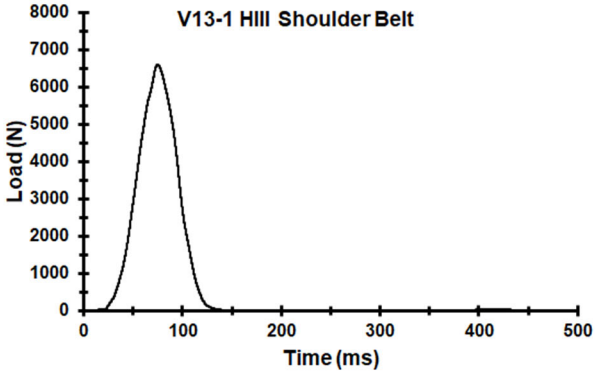
V13-1 HIII Shoulder Belt
Load (N)
Time (ms)
0
1000
2000
3000
4000
5000
6000
7000
8000
0
100
200
300
400
500

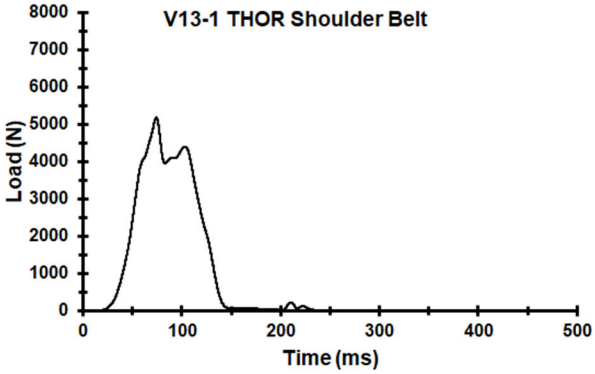
V13-1 THOR Shoulder Belt
Load (N)
Time (ms)
0
1000
2000
3000
4000
5000
6000
7000
8000
0
100
200
300
400
500

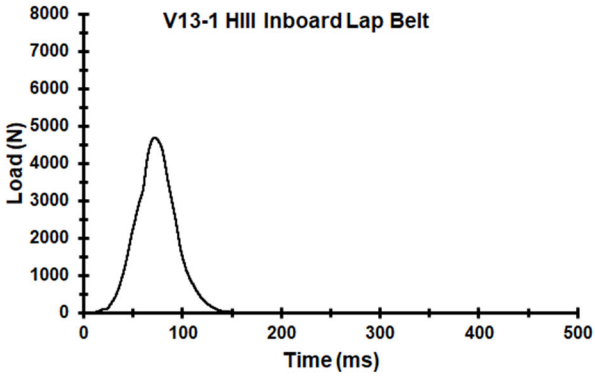
V13-1 HIII Inboard Lap Belt
Load (N)
Time (ms)
0
1000
2000
3000
4000
5000
6000
7000
8000
0
100
200
300
400
500

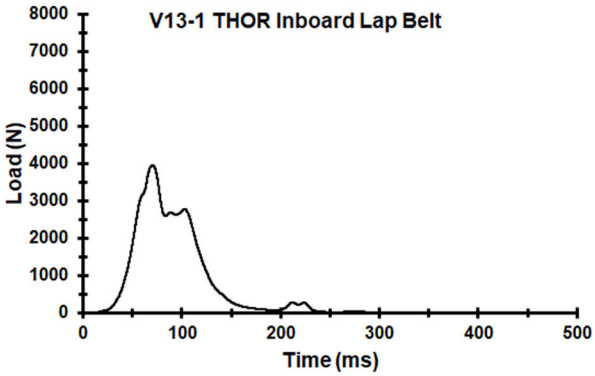
V13-1 THOR Inboard Lap Belt
Load (N)
Time (ms)
0
1000
2000
3000
4000
5000
6000
7000
8000
0
100
200
300
400
500

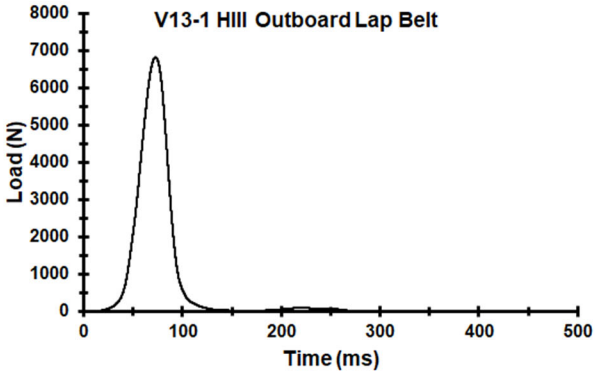
V13-1 HIII Outboard Lap Belt
Load (N)
Time (ms)
0
1000
2000
3000
4000
5000
6000
7000
8000
0
100
200
300
400
500

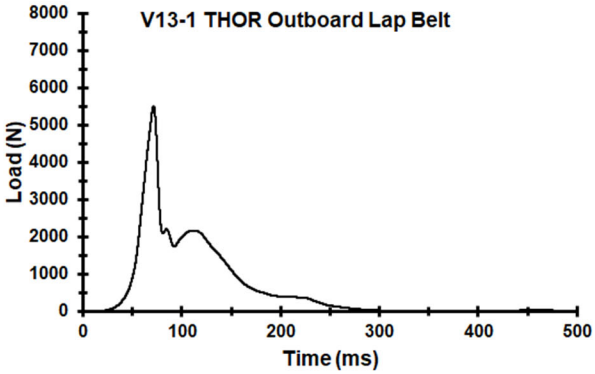
V13-1 THOR Outboard Lap Belt
Load (N)
Time (ms)
0
1000
2000
3000
4000
5000
6000
7000
8000
0
100
200
300
400
500

Appendix U. Select Data Traces From Test FRS-V13-2

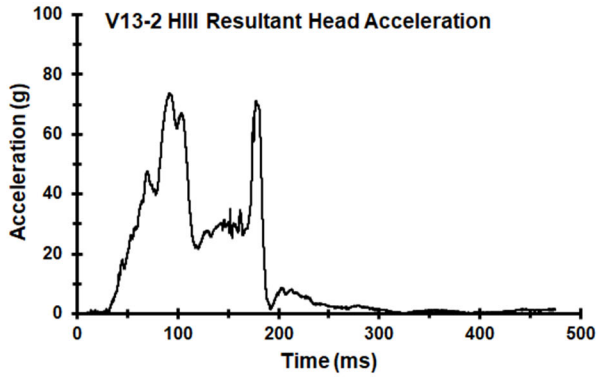
V13-2 HIII Resultant Head Acceleration
Acceleration (g)
Time (ms)

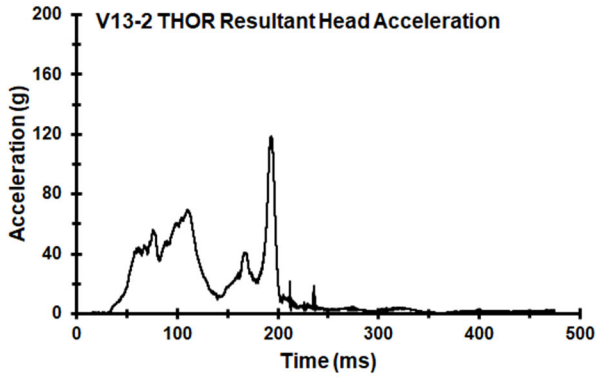
V13-2 THOR Resultant Head Acceleration
Acceleration (g)
Time (ms)

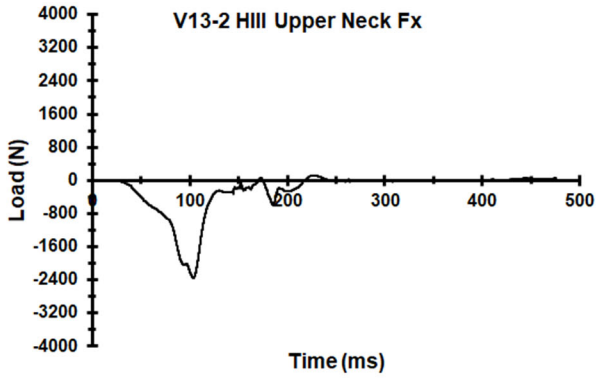
V13-2 HIII Upper Neck Fx
Load (N)
Time (ms)

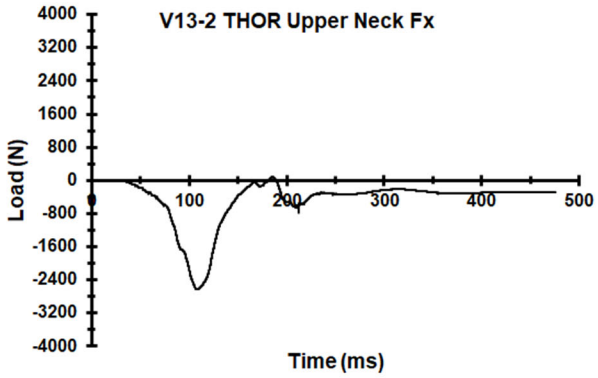
V13-2 THOR Upper Neck Fx
Load (N)
Time (ms)

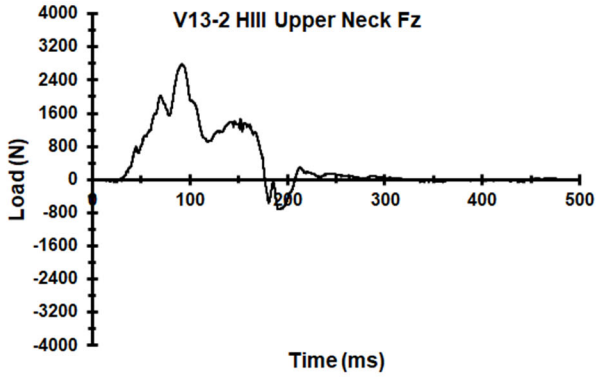
V13-2 HIII Upper Neck Fz
Load (N)
Time (ms)

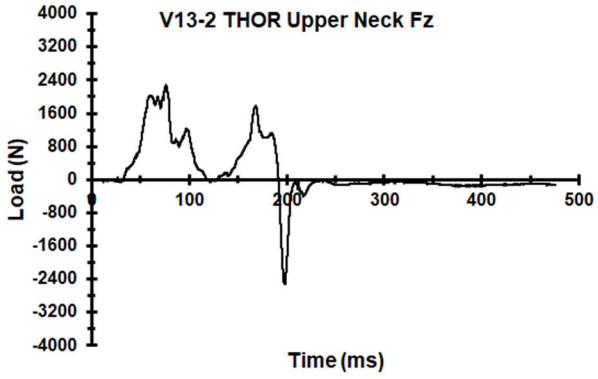
V13-2 THOR Upper Neck Fz
Load (N)
Time (ms)

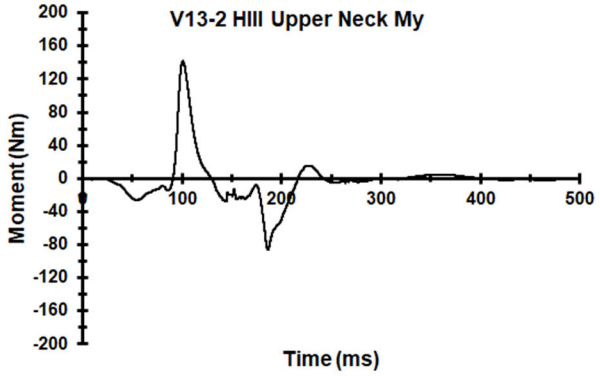
V13-2 HIII Upper Neck My
Moment (Nm)
Time (ms)

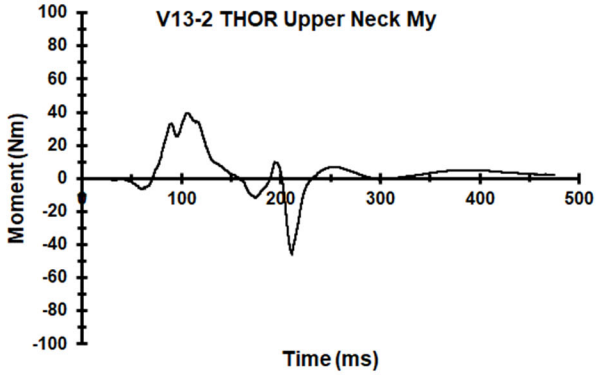
V13-2 THOR Upper Neck My
Moment (Nm)
Time (ms)

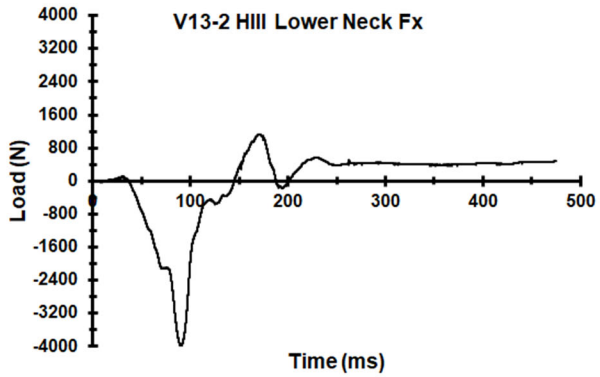
V13-2 HIII Lower Neck Fx
Load (N)
Time (ms)

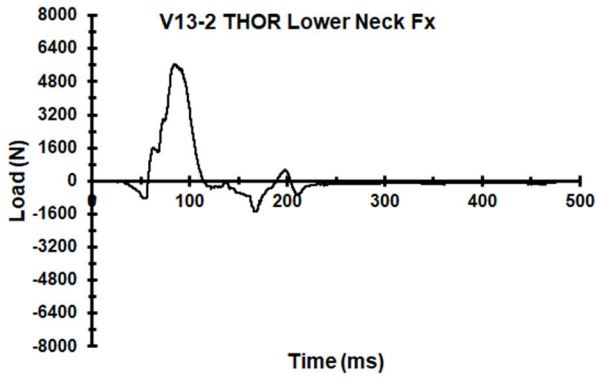
V13-2 THOR Lower Neck Fx
Load (N)
Time (ms)

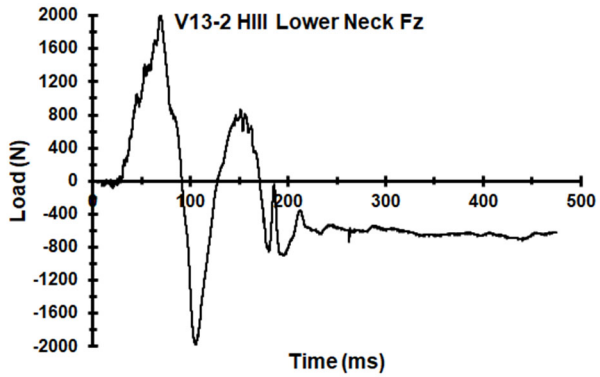
V13-2 HIII Lower Neck Fz
Load (N)
Time (ms)

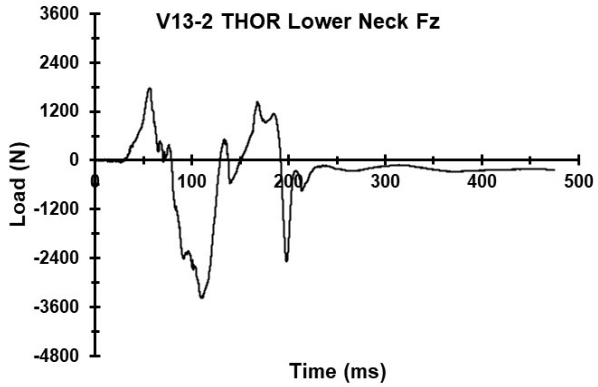
V13-2 THOR Lower Neck Fz
Load (N)
Time (ms)

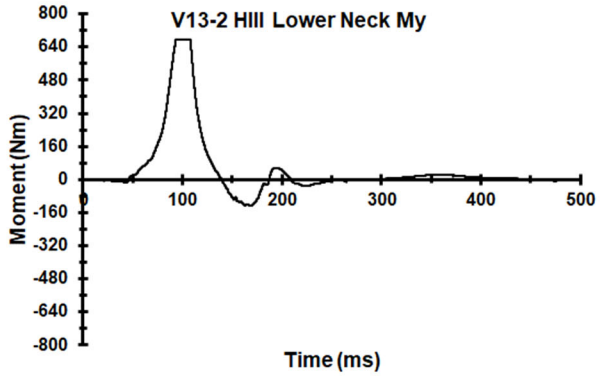
V13-2 HIII Lower Neck My
Moment (Nm)
Time (ms)

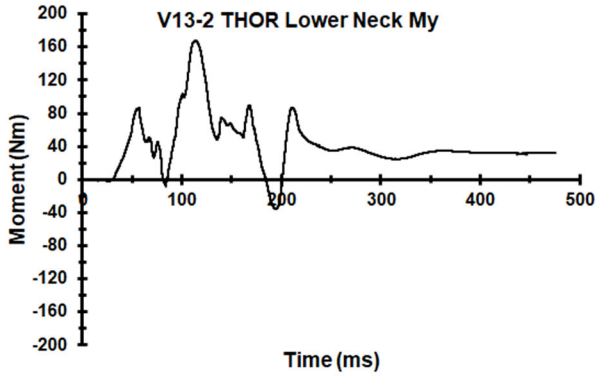
V13-2 THOR Lower Neck My
Moment (Nm)
Time (ms)

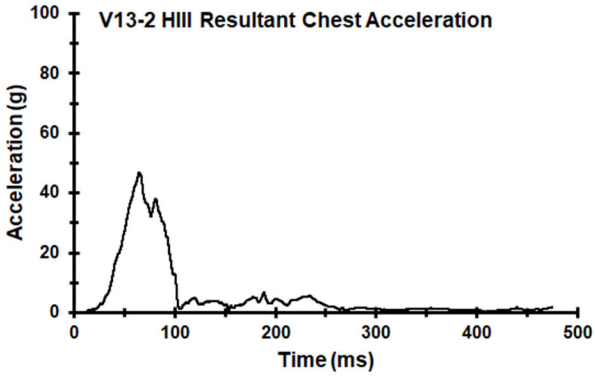
V13-2 HIII Resultant Chest Acceleration
Acceleration (g)
Time (ms)

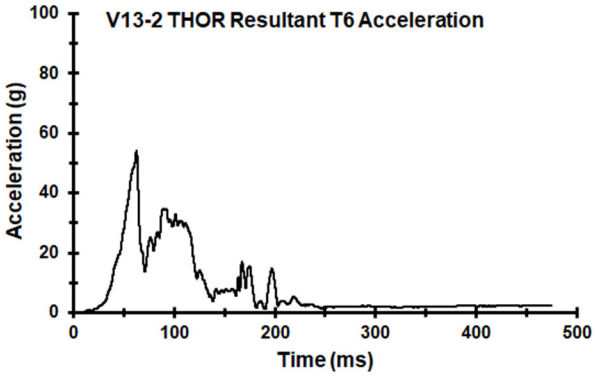
V13-2 THOR Resultant T6 Acceleration
Acceleration (g)
Time (ms)

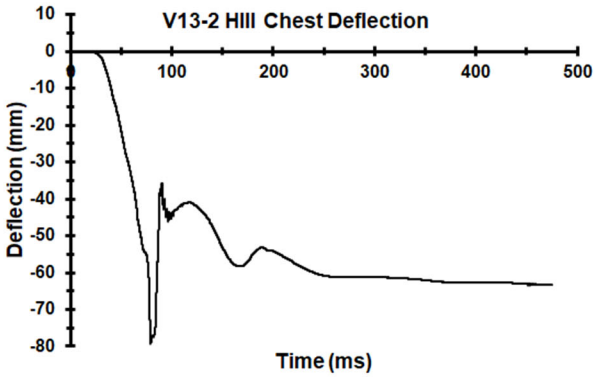
V13-2 HIII Chest Deflection
Deflection (mm)
Time (ms)

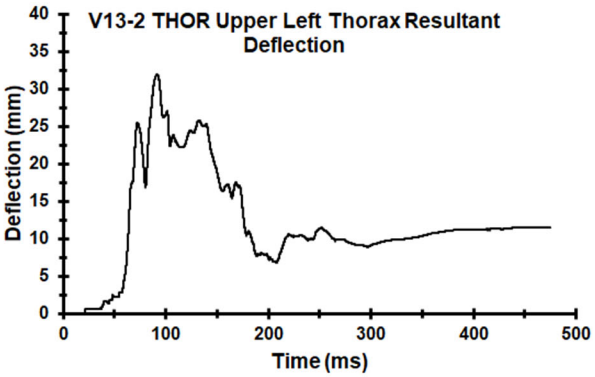
V13-2 THOR Upper Left Thorax Resultant Deflection
Deflection (mm)
Time (ms)

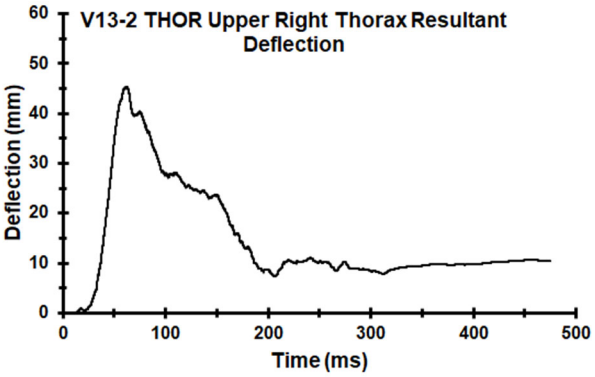
V13-2 THOR Upper Right Thorax Resultant Deflection
Deflection (mm)
Time (ms)

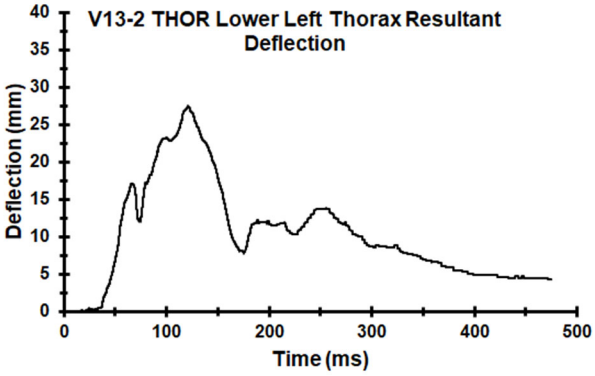
V13-2 THOR Lower Left Thorax Resultant Deflection
Deflection (mm)
Time (ms)

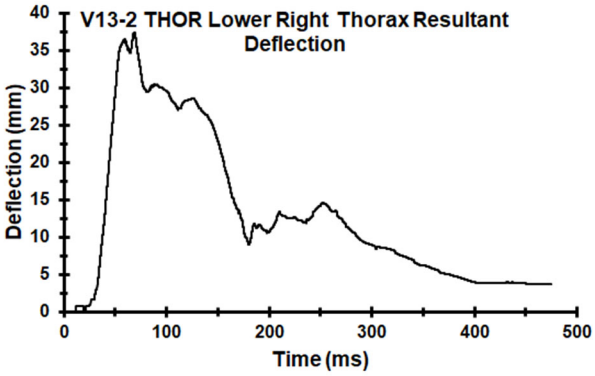
V13-2 THOR Lower Right Thorax Resultant Deflection
Deflection (mm)
Time (ms)

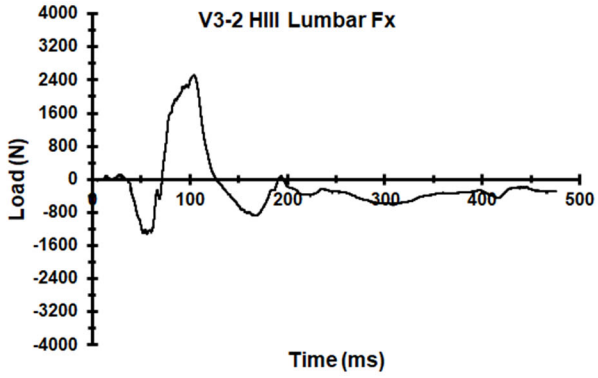
V3-2 HIII Lumbar Fx
Load (N)
Time (ms)

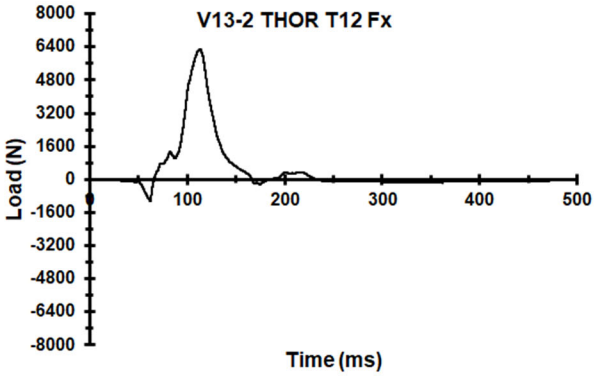
V13-2 THOR T12 Fx
Load (N)
Time (ms)

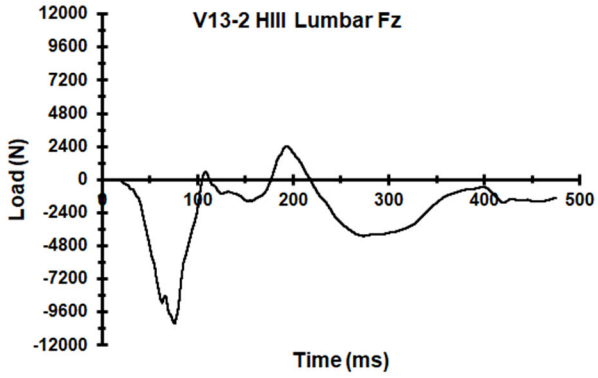
V13-2 HIII Lumbar Fz
Load (N)
Time (ms)

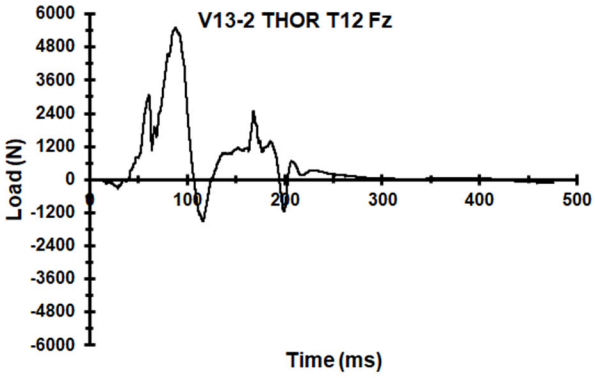
V13-2 THOR T12 Fz
Load (N)
Time (ms)

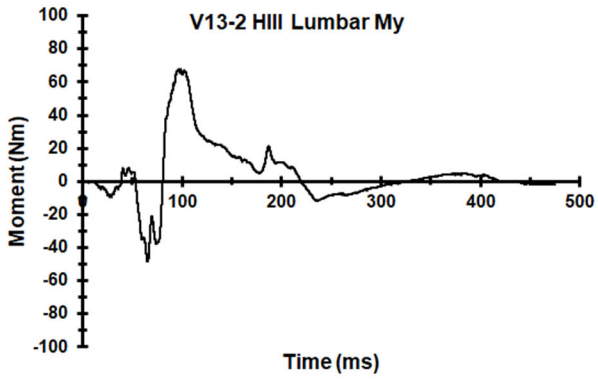
V13-2 HIII Lumbar My
Moment (Nm)
Time (ms)

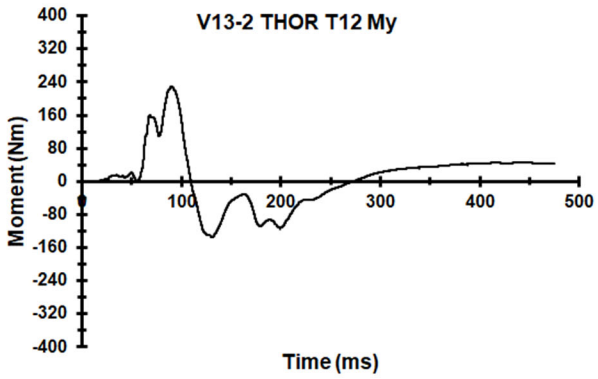
V13-2 THOR T12 My
Moment (Nm)
Time (ms)

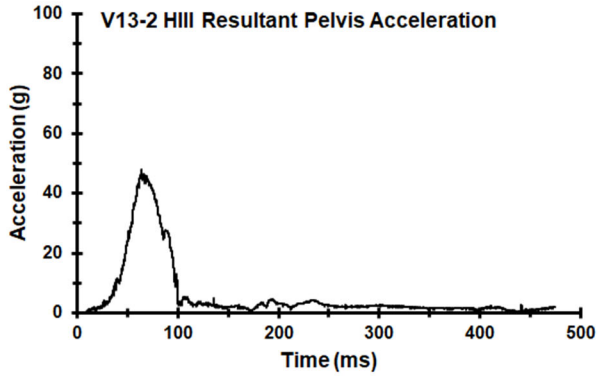
V13-2 HIII Resultant Pelvis Acceleration
Acceleration (g)
Time (ms)

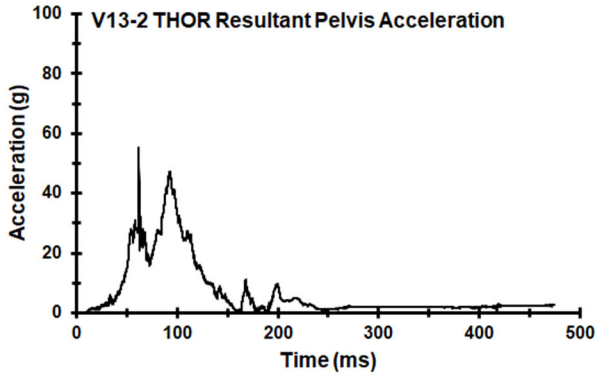
V13-2 THOR Resultant Pelvis Acceleration
Acceleration (g)
Time (ms)

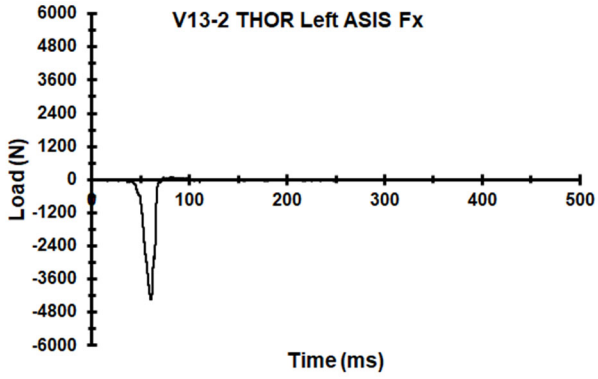
V13-2 THOR Left ASIS Fx
Load (N)
Time (ms)

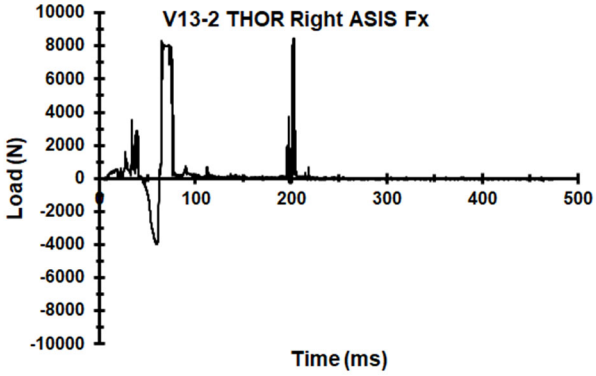
V13-2 THOR Right ASIS Fx
Load (N)
Time (ms)

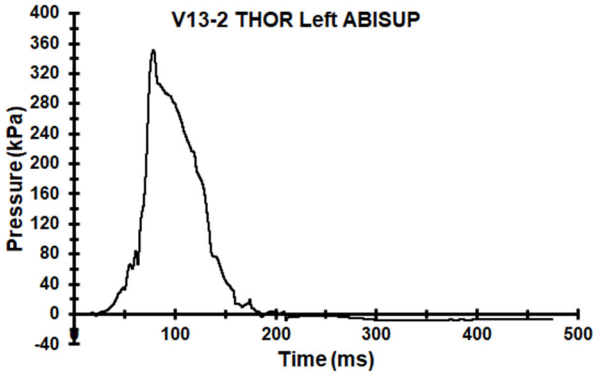
V13-2 THOR Left ABISUP
Pressure (kPa)
Time (ms)

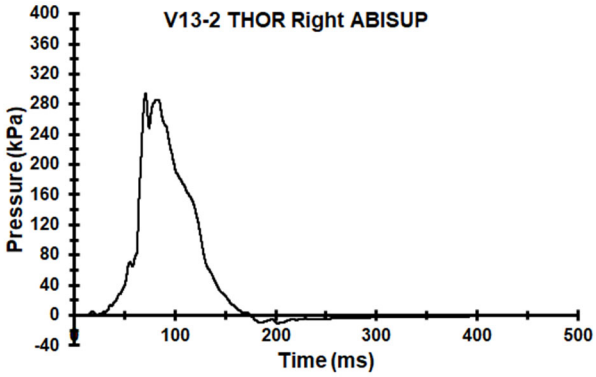
V13-2 THOR Right ABISUP
Pressure (kPa)
Time (ms)

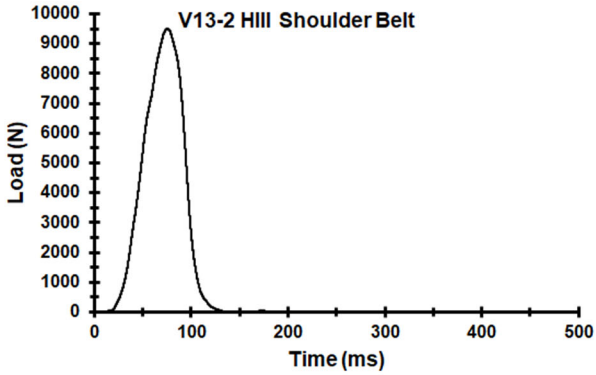
V13-2 HIII Shoulder Belt
Load (N)
Time (ms)

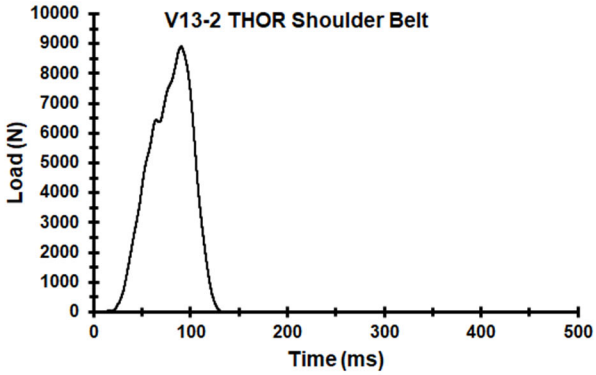
V13-2 THOR Shoulder Belt
Load (N)
Time (ms)

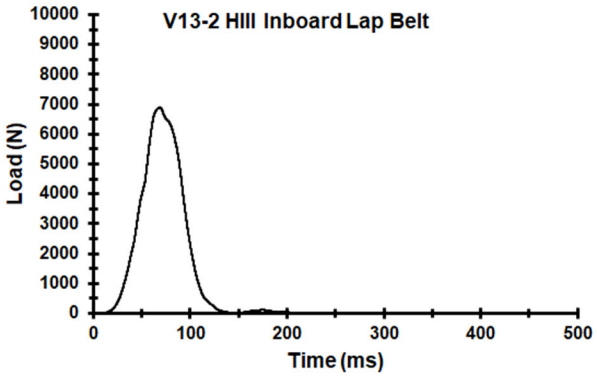
V13-2 HIII Inboard Lap Belt
Load (N)
Time (ms)
0
1000
2000
3000
4000
5000
6000
7000
8000
9000
10000
0
100
200
300
400
500

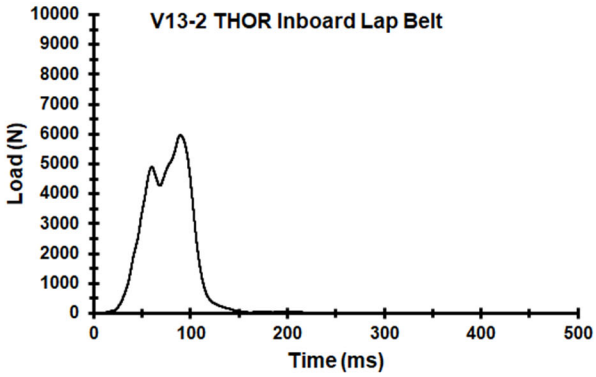
V13-2 THOR Inboard Lap Belt
Load (N)
Time (ms)
0
1000
2000
3000
4000
5000
6000
7000
8000
9000
10000
0
100
200
300
400
500

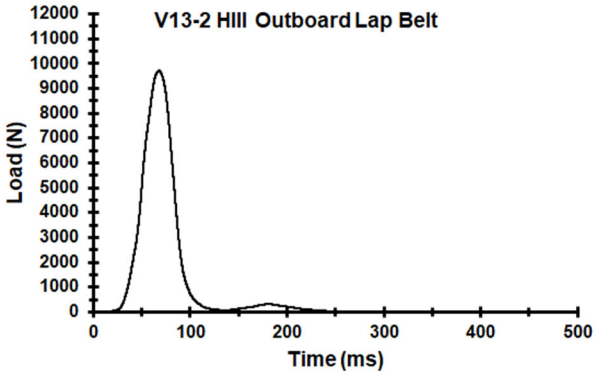
V13-2 HIII Outboard Lap Belt
Load (N)
Time (ms)
0
1000
2000
3000
4000
5000
6000
7000
8000
9000
10000
11000
12000
0
100
200
300
400
500

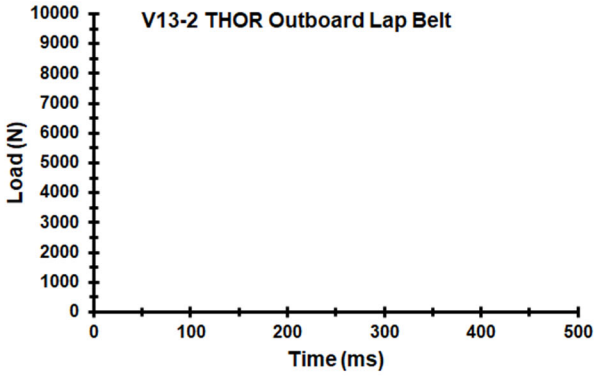
V13-2 THOR Outboard Lap Belt
Load (N)
Time (ms)
0
1000
2000
3000
4000
5000
6000
7000
8000
9000
10000
0
100
200
300
400
500

Appendix V. Select Data Traces From Test FRS-V13-3

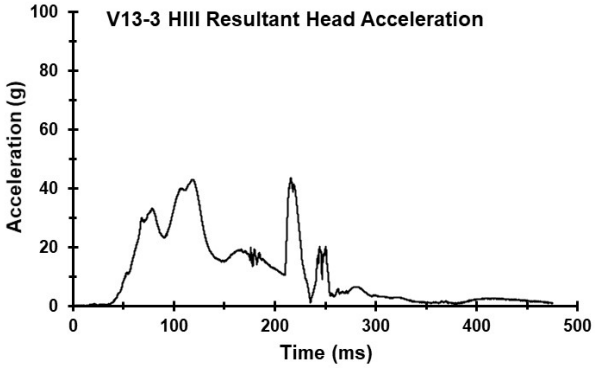
V13-3 HIII Resultant Head Acceleration
Acceleration (g)
Time (ms)

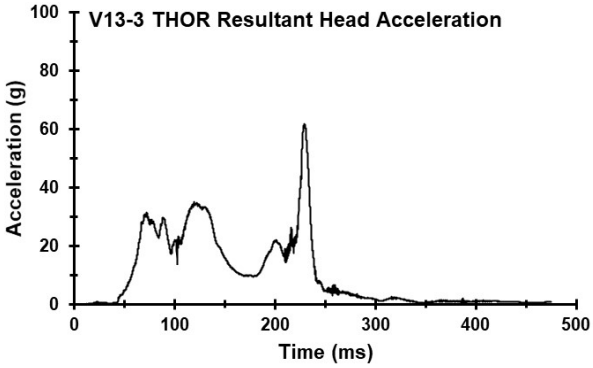
V13-3 THOR Resultant Head Acceleration
Acceleration (g)
Time (ms)

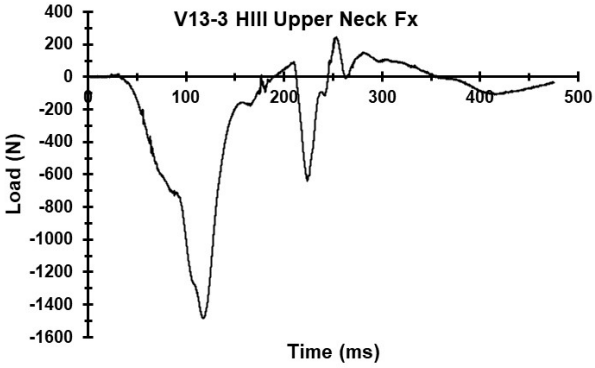
V13-3 HIII Upper Neck Fx
Load (N)
Time (ms)

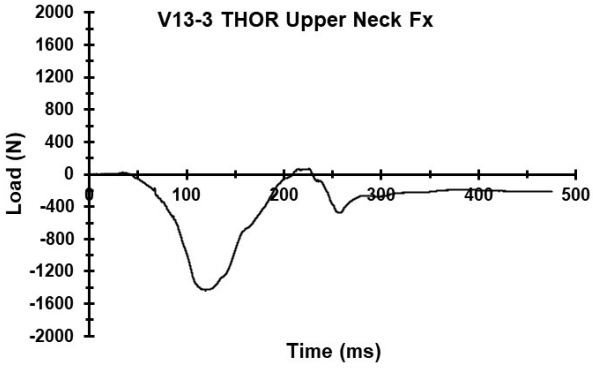
V13-3 THOR Upper Neck Fx
Load (N)
Time (ms)

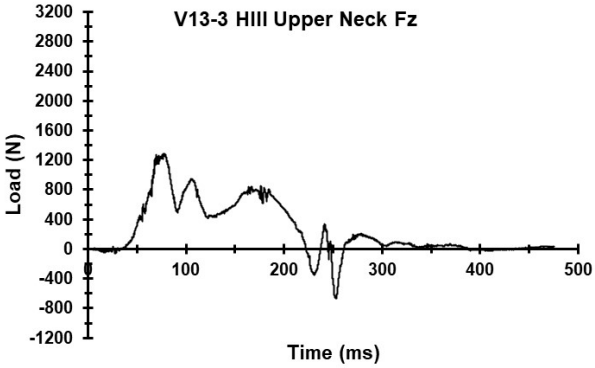
V13-3 HIII Upper Neck Fz
Load (N)
Time (ms)

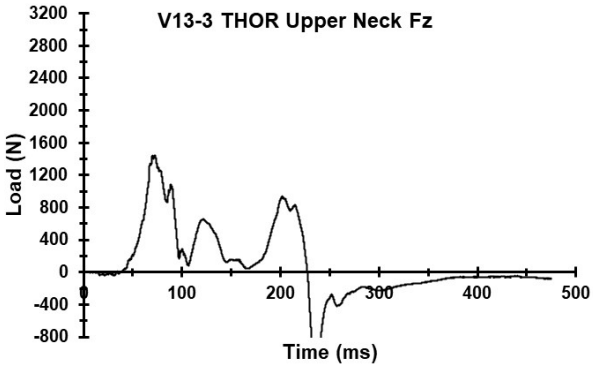
V13-3 THOR Upper Neck Fz
Load (N)
Time (ms)

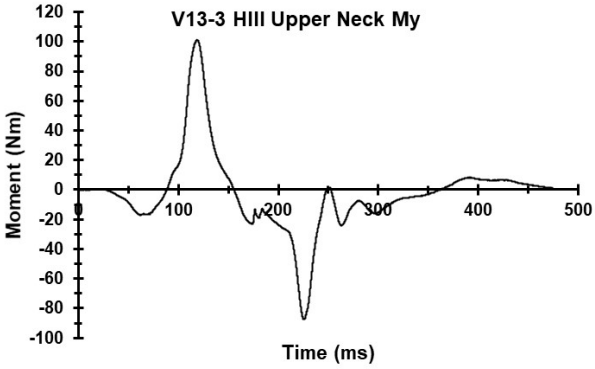
V13-3 HIII Upper Neck My
Moment (Nm)
Time (ms)

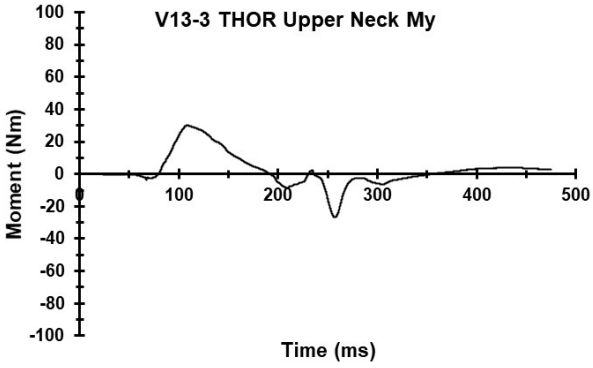
V13-3 THOR Upper Neck My
Moment (Nm)
Time (ms)

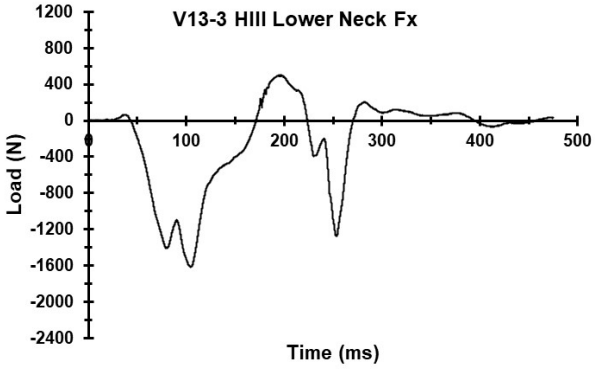
V13-3 HIII Lower Neck Fx
Load (N)
Time (ms)

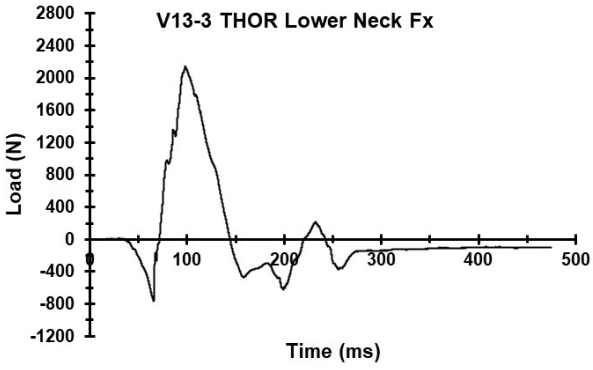
V13-3 THOR Lower Neck Fx
Load (N)
Time (ms)

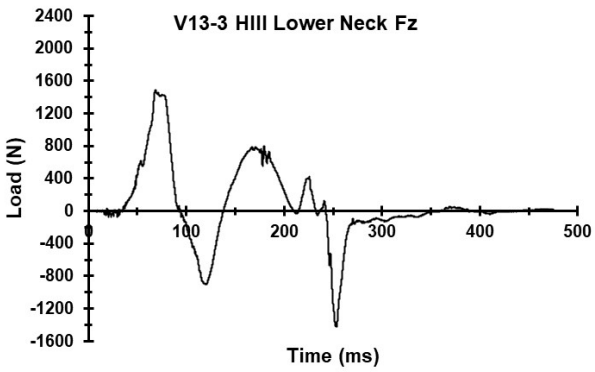
V13-3 HIII Lower Neck Fz
Load (N)
Time (ms)

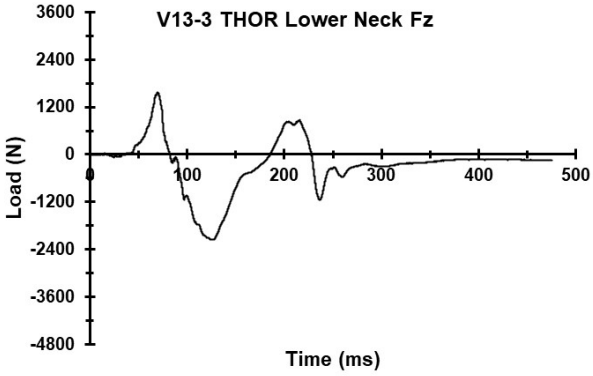
V13-3 THOR Lower Neck Fz
Load (N)
Time (ms)

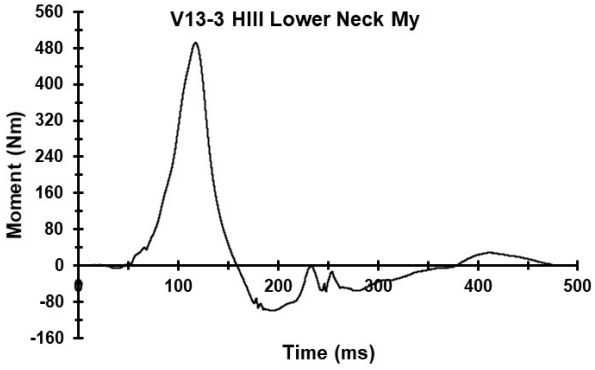
V13-3 HIII Lower Neck My
Moment (Nm)
Time (ms)

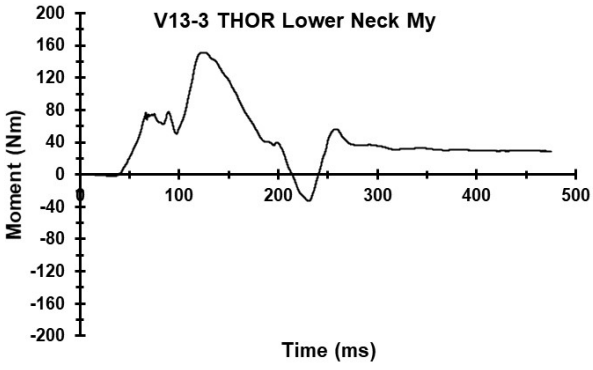
V13-3 THOR Lower Neck My
Moment (Nm)
Time (ms)

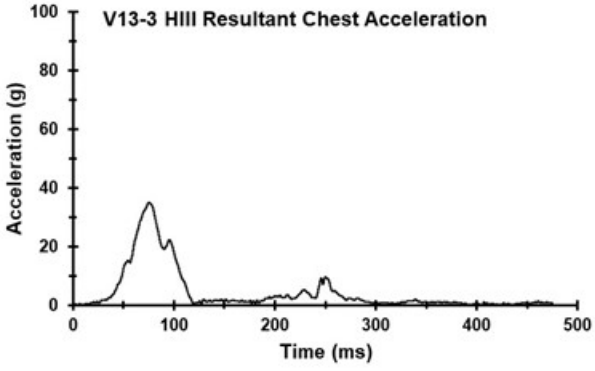
V13-3 HIII Resultant Chest Acceleration
Acceleration (g)
Time (ms)

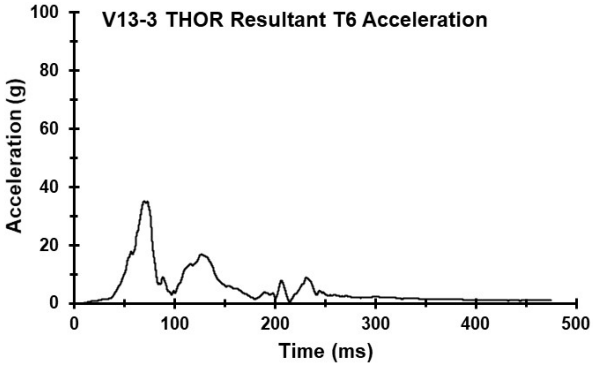
V13-3 THOR Resultant T6 Acceleration
Acceleration (g)
Time (ms)

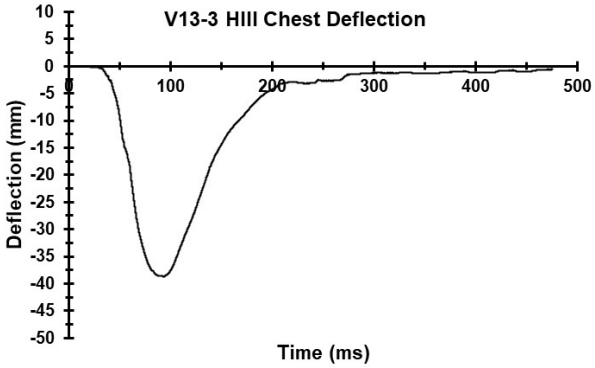
V13-3 HIII Chest Deflection
Deflection (mm)
Time (ms)

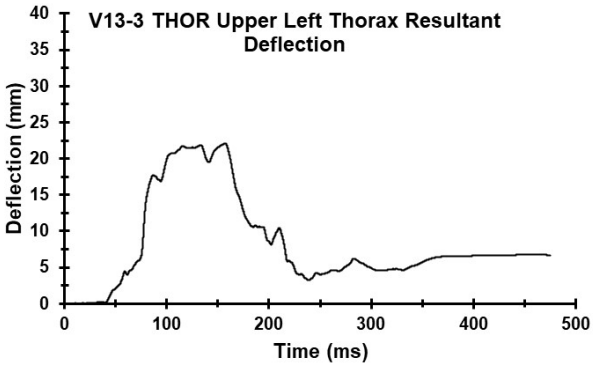
V13-3 THOR Upper Left Thorax Resultant Deflection
Deflection (mm)
Time (ms)

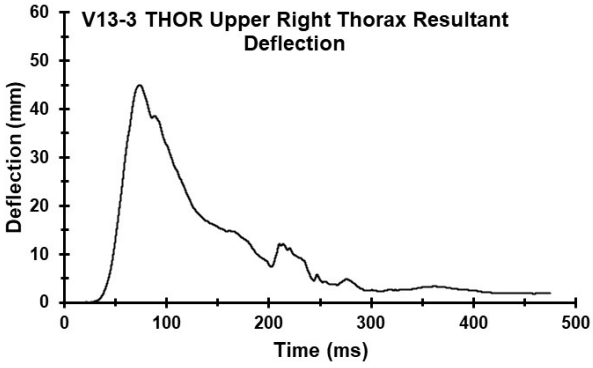
V13-3 THOR Upper Right Thorax Resultant Deflection
Deflection (mm)
Time (ms)

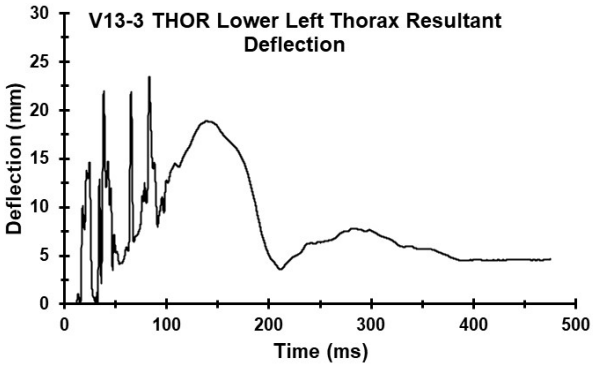
V13-3 THOR Lower Left Thorax Resultant Deflection
Deflection (mm)
Time (ms)

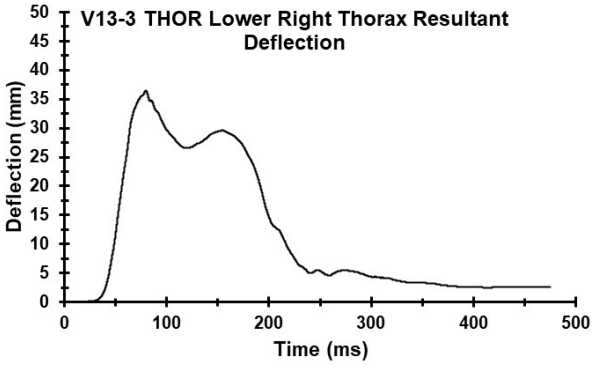
V13-3 THOR Lower Right Thorax Resultant Deflection
Deflection (mm)
Time (ms)

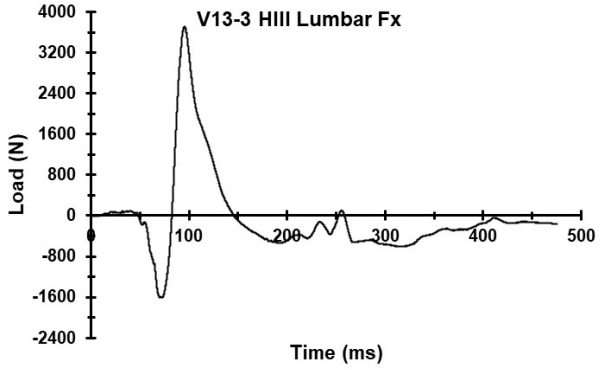
V13-3 HIII Lumbar Fx
Load (N)
Time (ms)

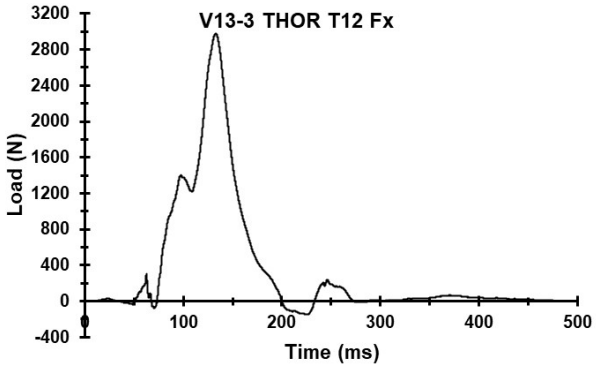
V13-3 THOR T12 Fx
Load (N)
Time (ms)

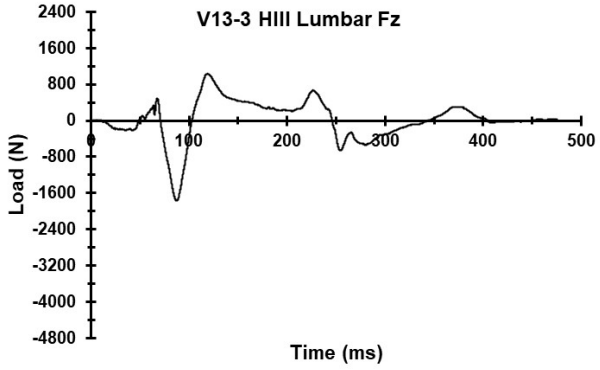
V13-3 HIII Lumbar Fz
Load (N)
Time (ms)

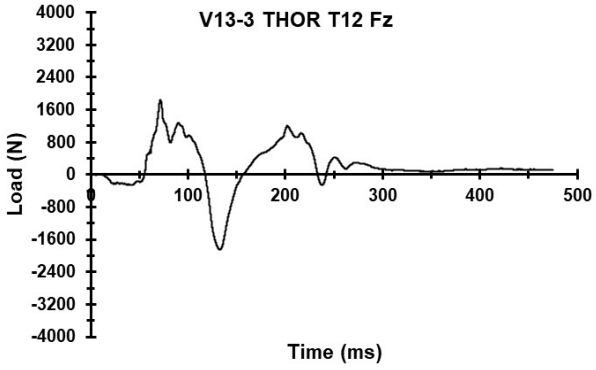
V13-3 THOR T12 Fz
Load (N)
Time (ms)

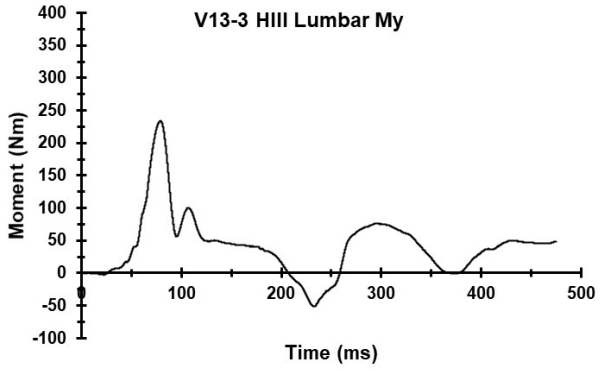
V13-3 HIII Lumbar My
Moment (Nm)
Time (ms)

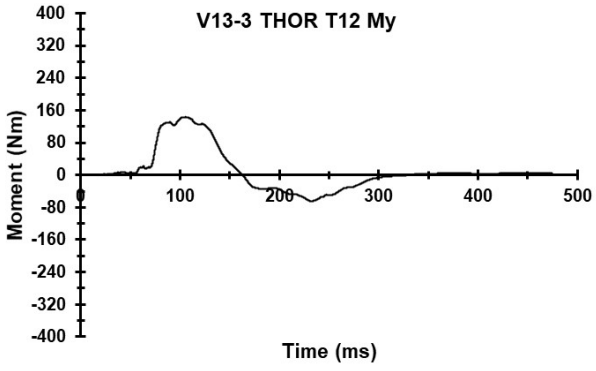
V13-3 THOR T12 My
Moment (Nm)
Time (ms)

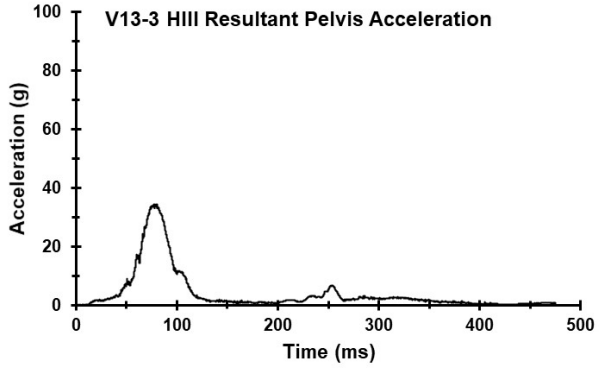
V13-3 HIII Resultant Pelvis Acceleration
Acceleration (g)
Time (ms)

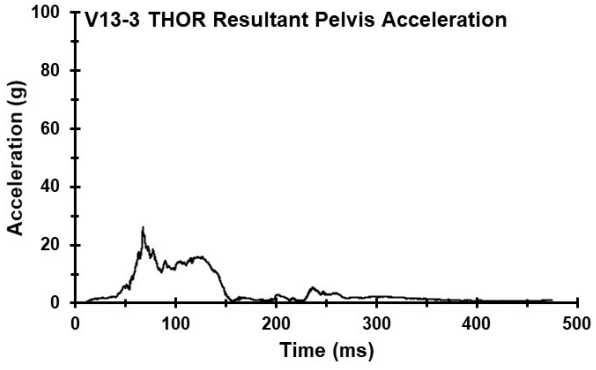
V13-3 THOR Resultant Pelvis Acceleration
Acceleration (g)
Time (ms)

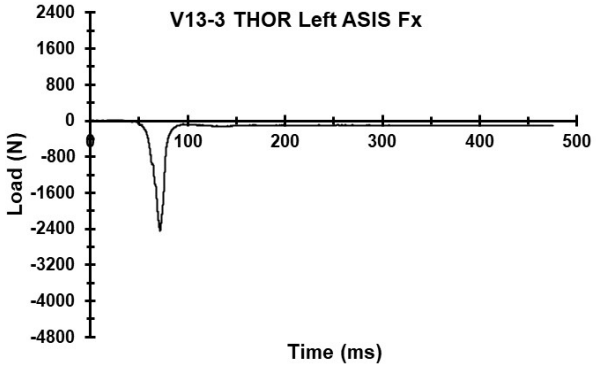
V13-3 THOR Left ASIS Fx
Load (N)
2400
1600
800
0
-800
-1600
-2400
-3200
-4000
-4800
100
200
300
400
500
Time (ms)

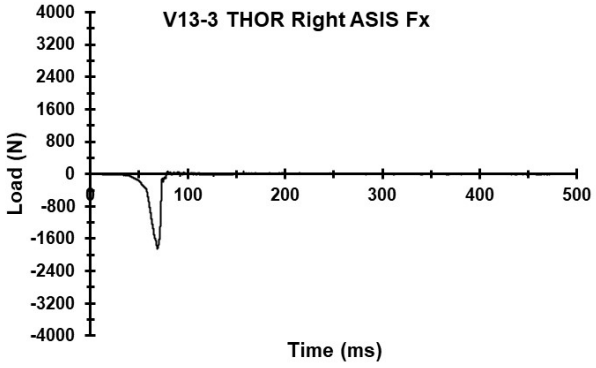
V13-3 THOR Right ASIS Fx
Load (N)
4000
3200
2400
1600
800
0
-800
-1600
-2400
-3200
-4000
100
200
300
400
500
Time (ms)

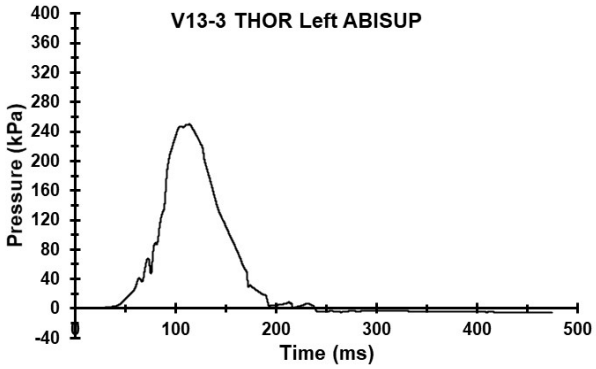
V13-3 THOR Left ABISUP
Pressure (kPa)
400
360
320
280
240
200
160
120
80
40
0
-40
100
200
300
400
500
Time (ms)

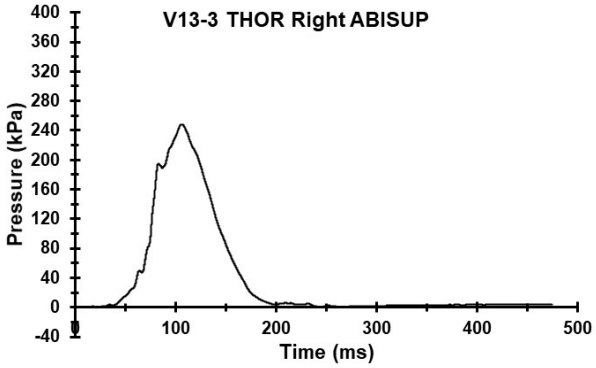
V13-3 THOR Right ABISUP
Pressure (kPa)
400
360
320
280
240
200
160
120
80
40
0
-40
100
200
300
400
500
Time (ms)

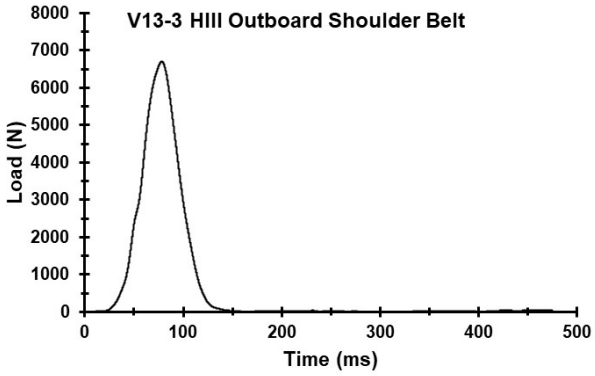
V13-3 HIII Outboard Shoulder Belt
Load (N)
Time (ms)

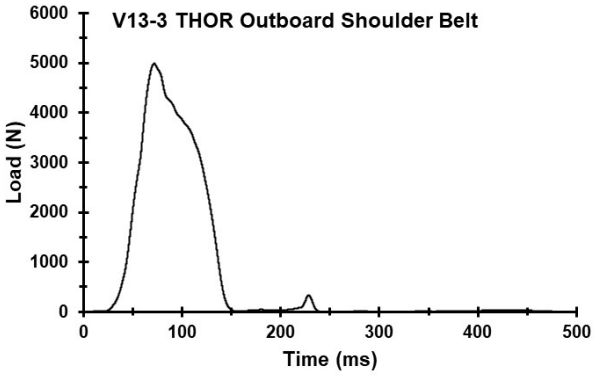
V13-3 THOR Outboard Shoulder Belt
Load (N)
Time (ms)

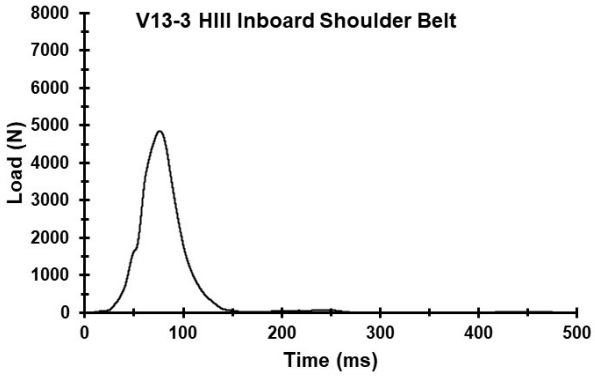
V13-3 HIII Inboard Shoulder Belt
Load (N)
Time (ms)

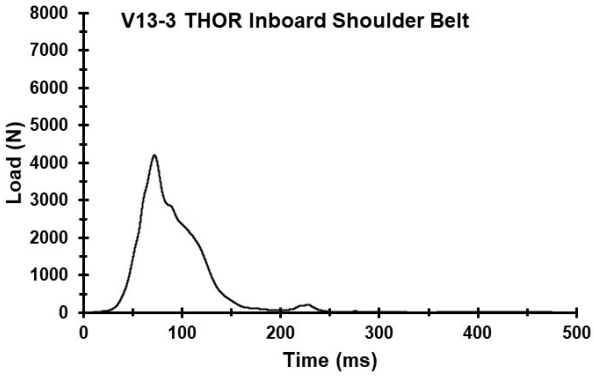
V13-3 THOR Inboard Shoulder Belt
Load (N)
Time (ms)

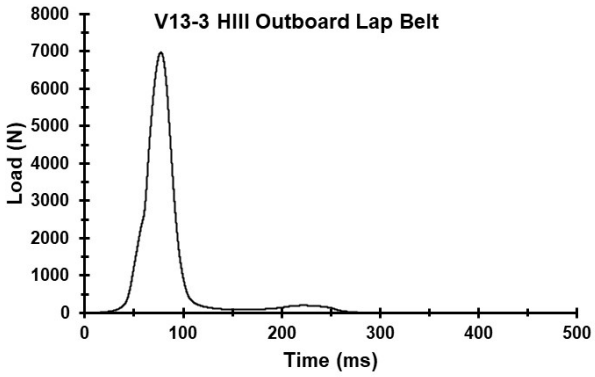
V13-3 HIII Outboard Lap Belt
Load (N)
Time (ms)

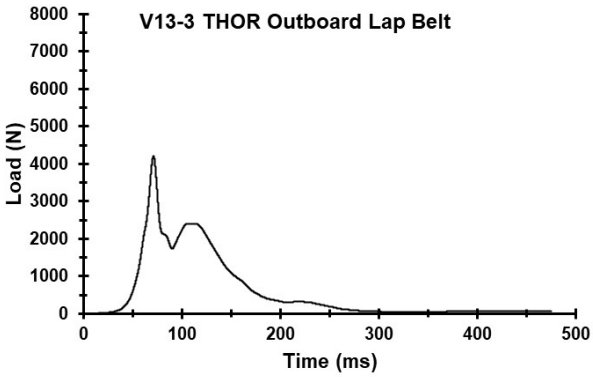
V13-3 THOR Outboard Lap Belt
Load (N)
Time (ms)

Appendix W. Select Data Traces From Test FRS-V14-1

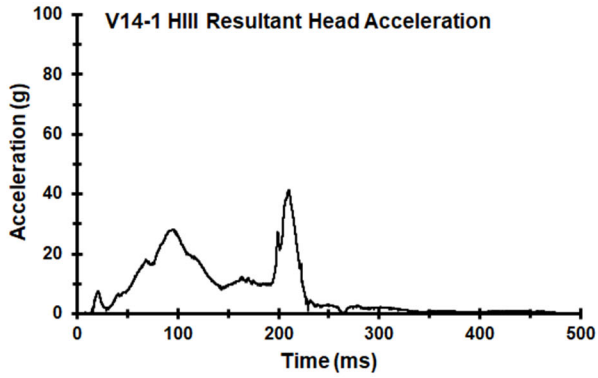
V14-1 HIII Resultant Head Acceleration
Acceleration (g)
Time (ms)

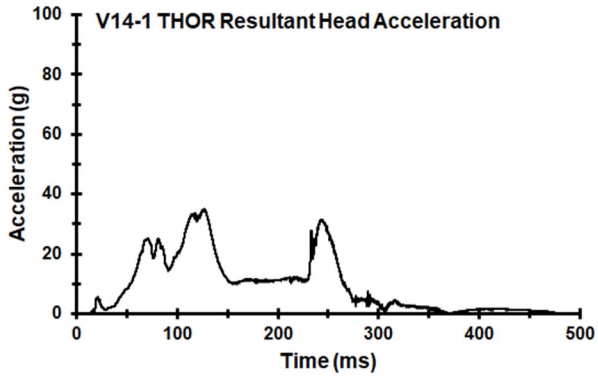
V14-1 THOR Resultant Head Acceleration
Acceleration (g)
Time (ms)

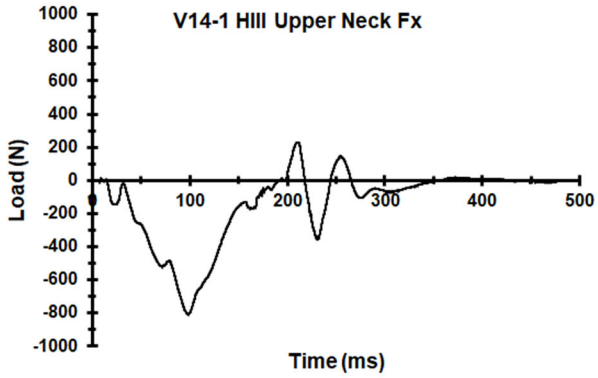
V14-1 HIII Upper Neck Fx
Load (N)
Time (ms)

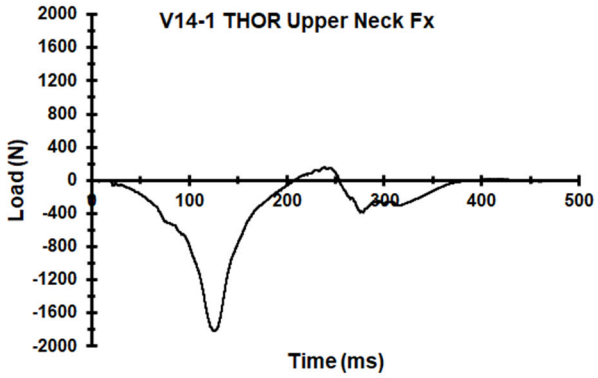
V14-1 THOR Upper Neck Fx
Load (N)
Time (ms)

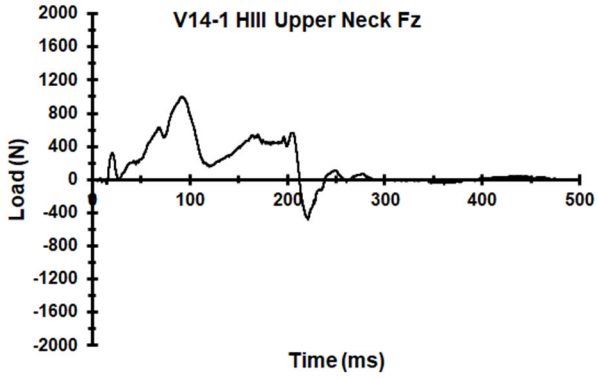
V14-1 HIII Upper Neck Fz
Load (N)
Time (ms)

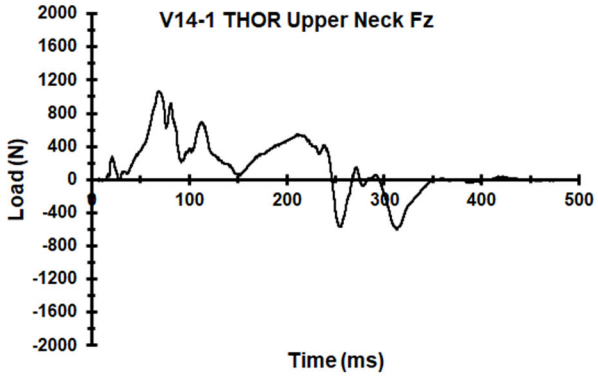
V14-1 THOR Upper Neck Fz
Load (N)
Time (ms)

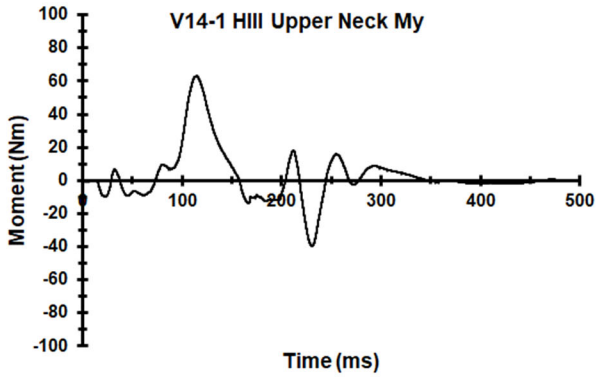
V14-1 HIII Upper Neck My
Moment (Nm)
Time (ms)

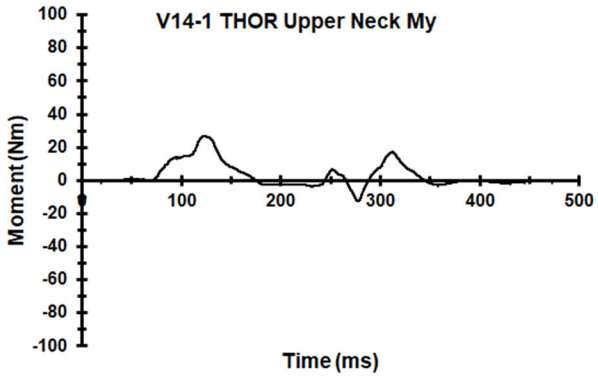
V14-1 THOR Upper Neck My
Moment (Nm)
Time (ms)

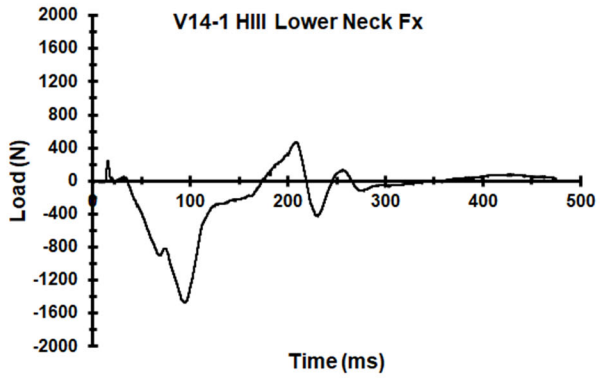
V14-1 HIII Lower Neck Fx
Load (N)
Time (ms)

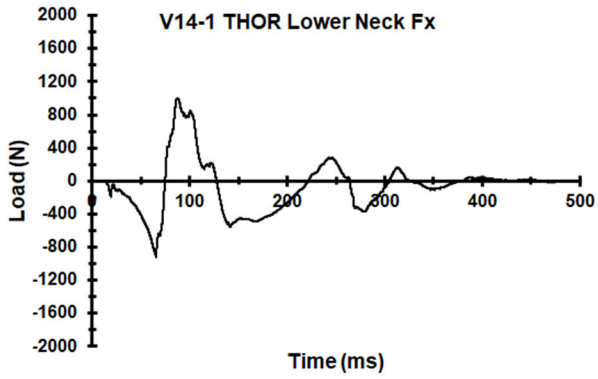
V14-1 THOR Lower Neck Fx
Load (N)
Time (ms)

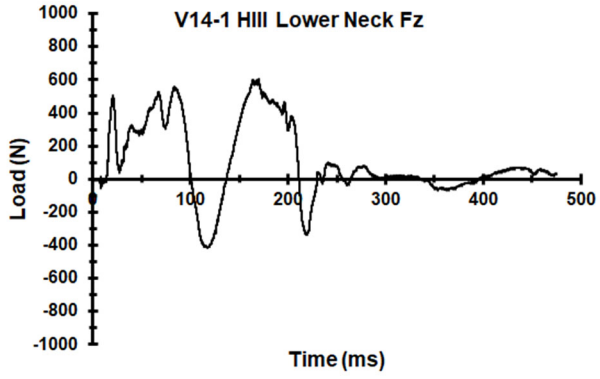
V14-1 HIII Lower Neck Fz
Load (N)
Time (ms)

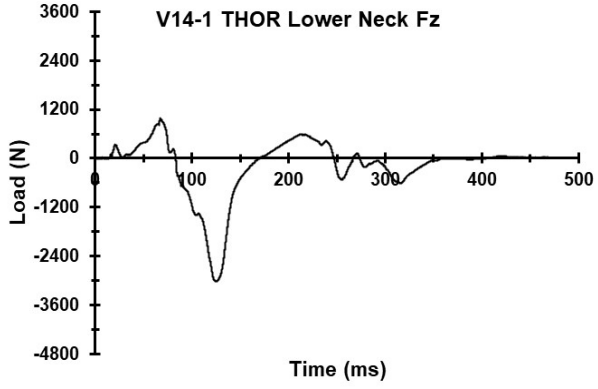
V14-1 THOR Lower Neck Fz
Load (N)
Time (ms)

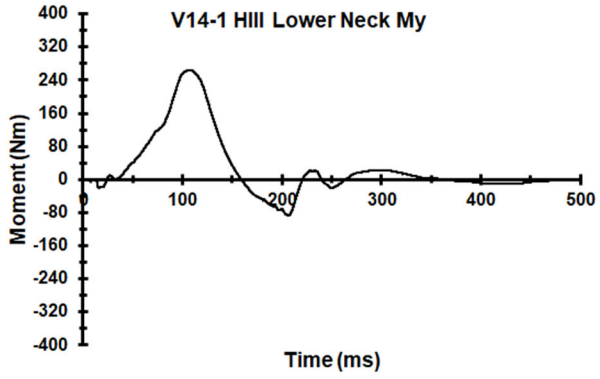
V14-1 HIII Lower Neck My
Moment (Nm)
Time (ms)

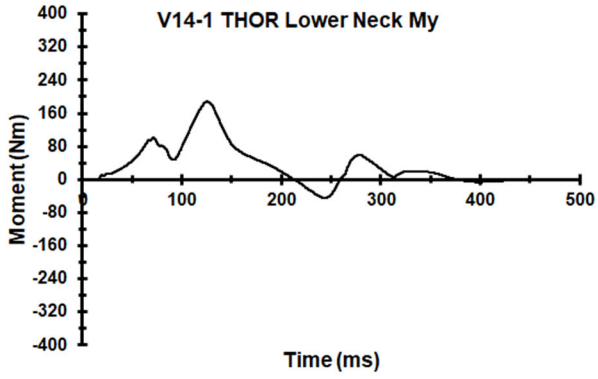
V14-1 THOR Lower Neck My
Moment (Nm)
Time (ms)

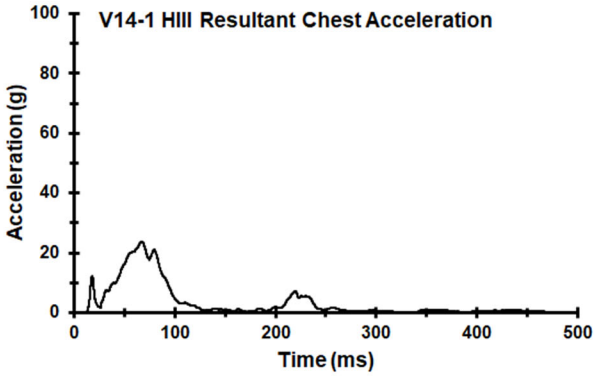
V14-1 HIII Resultant Chest Acceleration
Acceleration (g)
Time (ms)

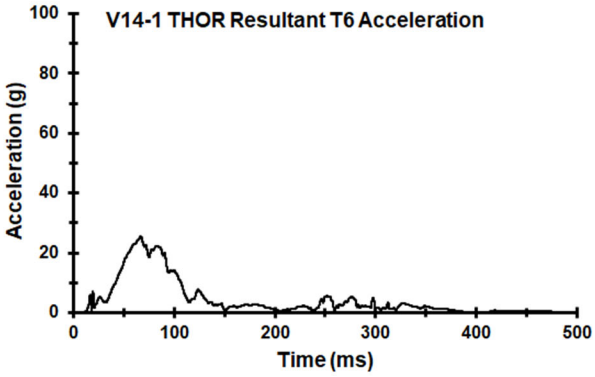
V14-1 THOR Resultant T6 Acceleration
Acceleration (g)
Time (ms)

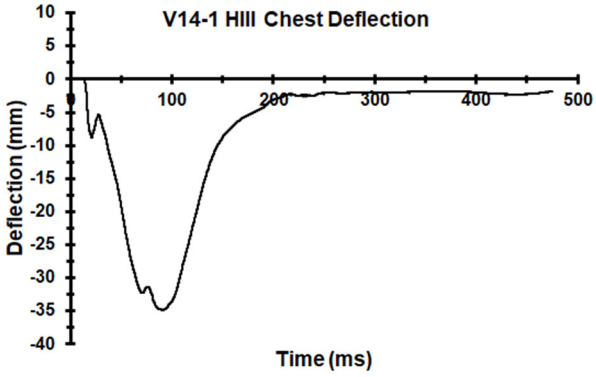
V14-1 HIII Chest Deflection
Deflection (mm)
Time (ms)

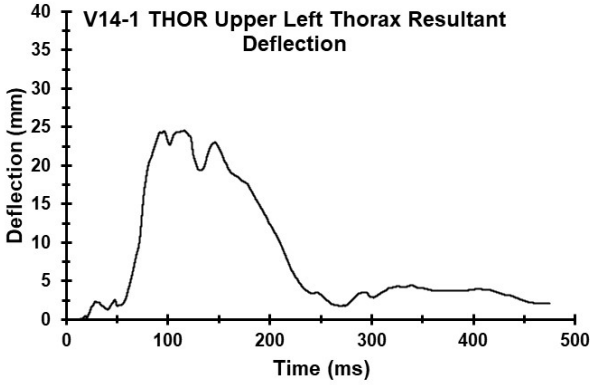
V14-1 THOR Upper Left Thorax Resultant Deflection
Deflection (mm)
Time (ms)

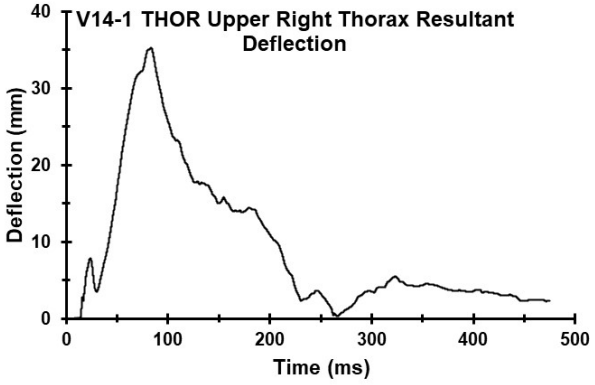
V14-1 THOR Upper Right Thorax Resultant Deflection
Deflection (mm)
Time (ms)

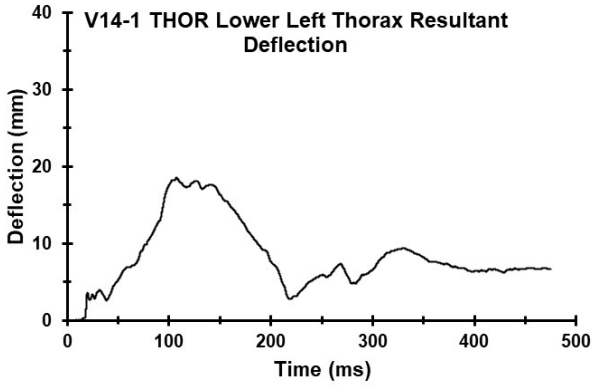
V14-1 THOR Lower Left Thorax Resultant Deflection
Deflection (mm)
Time (ms)

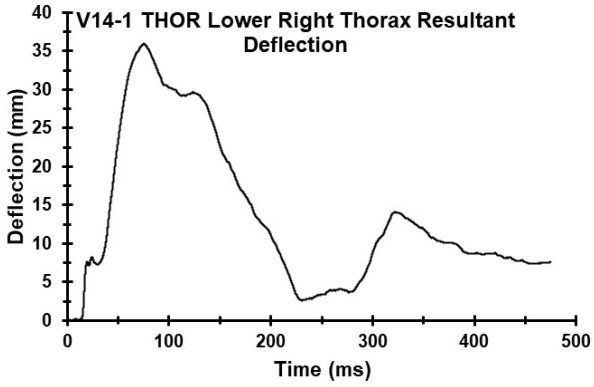
V14-1 THOR Lower Right Thorax Resultant Deflection
Deflection (mm)
Time (ms)

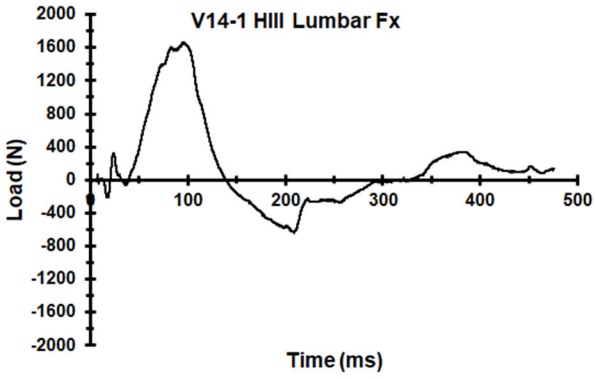
V14-1 HIII Lumbar Fx
Load (N)
Time (ms)

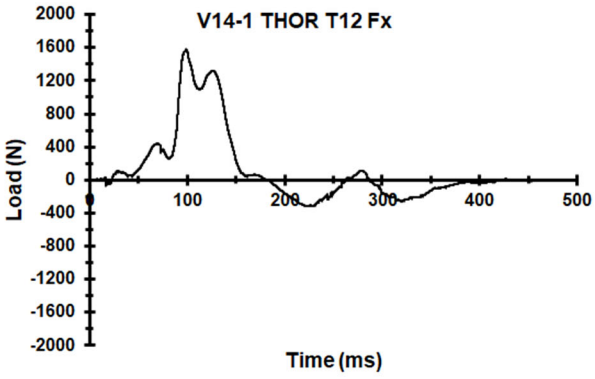
V14-1 THOR T12 Fx
Load (N)
Time (ms)

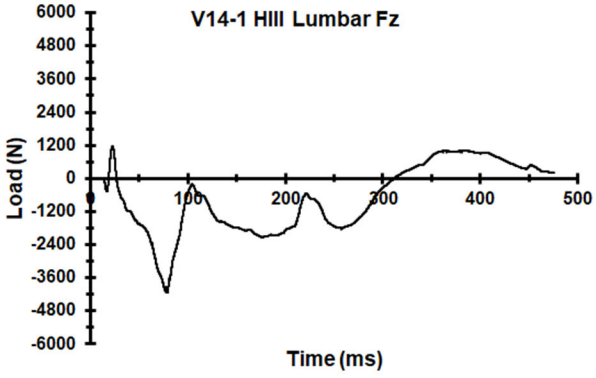
V14-1 HIII Lumbar Fz
Load (N)
Time (ms)

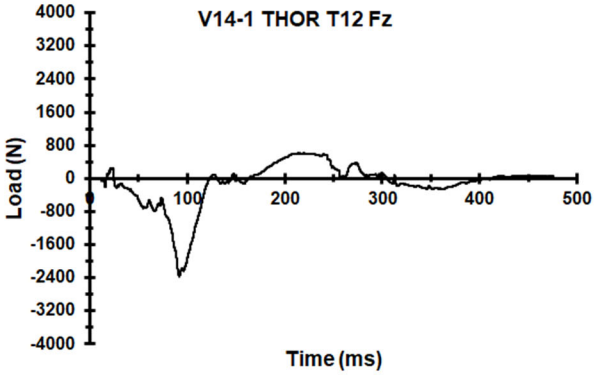
V14-1 THOR T12 Fz
Load (N)
Time (ms)

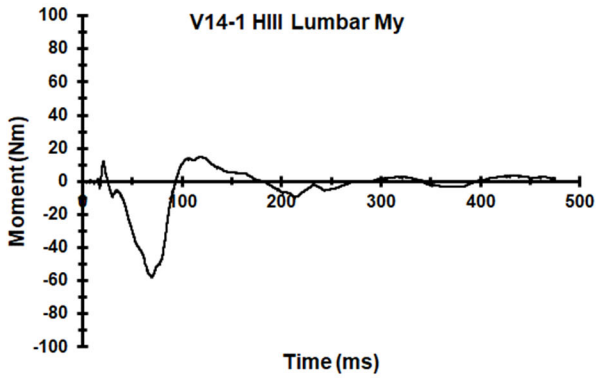
V14-1 HIII Lumbar My
Moment (Nm)
100
80
60
40
20
0
-20
-40
-60
-80
-100
100
200
300
400
500
Time (ms)

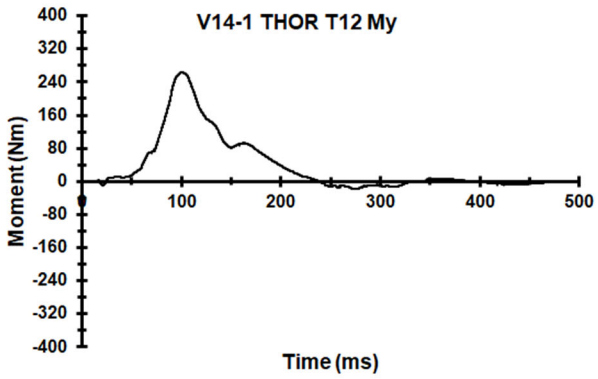
V14-1 THOR T12 My
Moment (Nm)
400
320
240
160
80
0
-80
-160
-240
-320
-400
100
200
300
400
500
Time (ms)

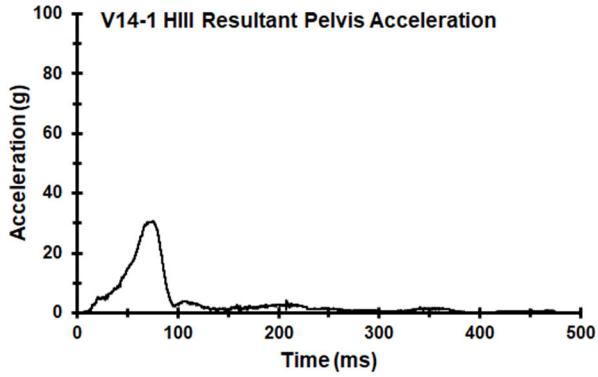
V14-1 HIII Resultant Pelvis Acceleration
Acceleration (g)
100
80
60
40
20
0
0
100
200
300
400
500
Time (ms)

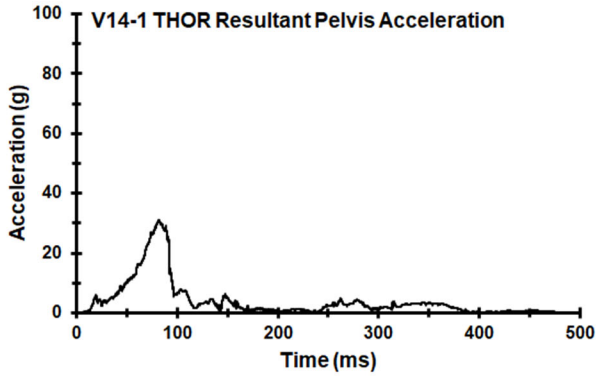
V14-1 THOR Resultant Pelvis Acceleration
Acceleration (g)
100
80
60
40
20
0
0
100
200
300
400
500
Time (ms)

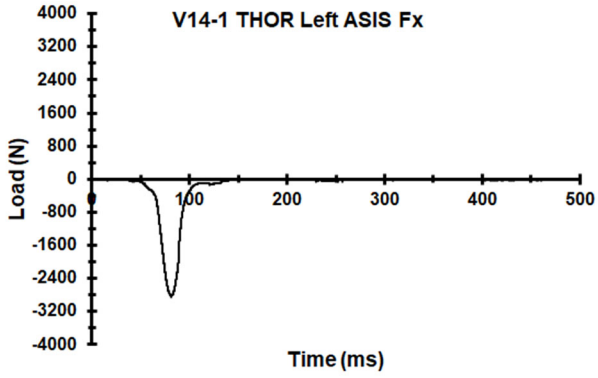
V14-1 THOR Left ASIS Fx
Load (N)
4000
3200
2400
1600
800
0
-800
-1600
-2400
-3200
-4000
100
200
300
400
500
Time (ms)

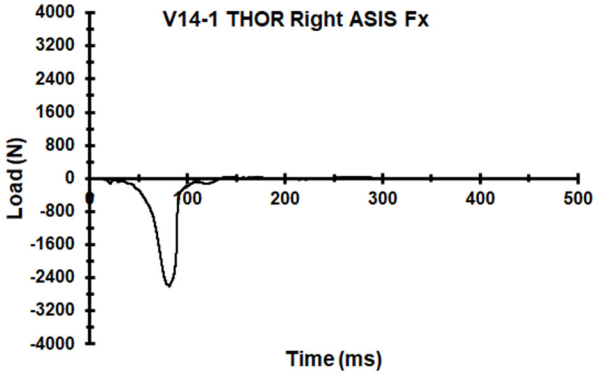
V14-1 THOR Right ASIS Fx
Load (N)
4000
3200
2400
1600
800
0
-800
-1600
-2400
-3200
-4000
100
200
300
400
500
Time (ms)

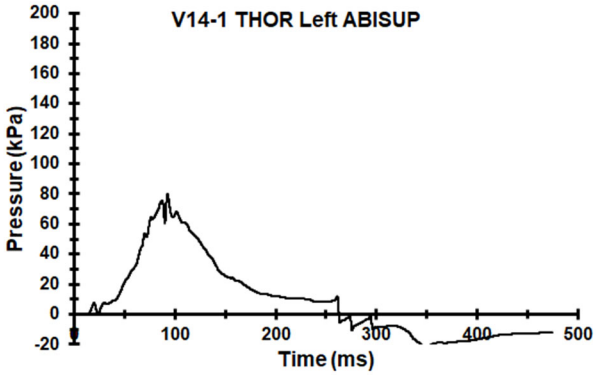
V14-1 THOR Left ABISUP
Pressure (kPa)
200
180
160
140
120
100
80
60
40
20
0
-20
100
200
300
400
500
Time (ms)

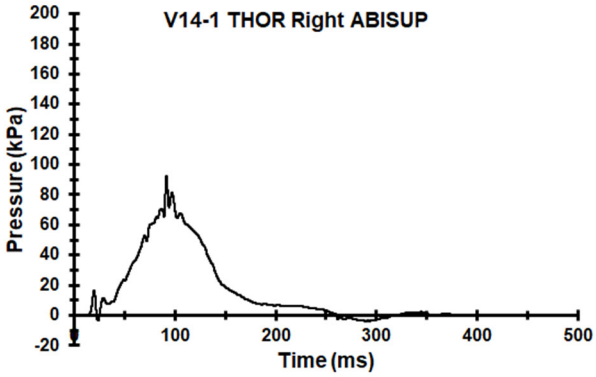
V14-1 THOR Right ABISUP
Pressure (kPa)
200
180
160
140
120
100
80
60
40
20
0
-20
100
200
300
400
500
Time (ms)

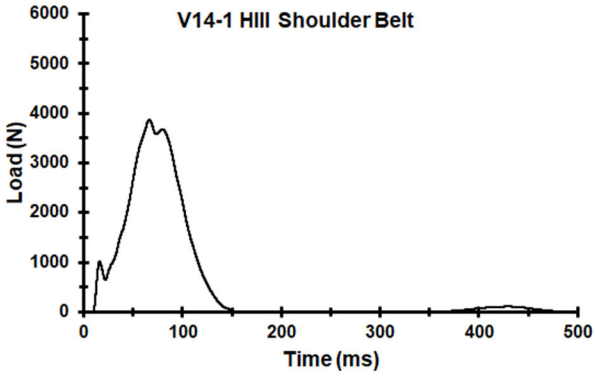
V14-1 HIII Shoulder Belt
Load (N)
6000
5000
4000
3000
2000
1000
0
0
100
200
300
400
500
Time (ms)

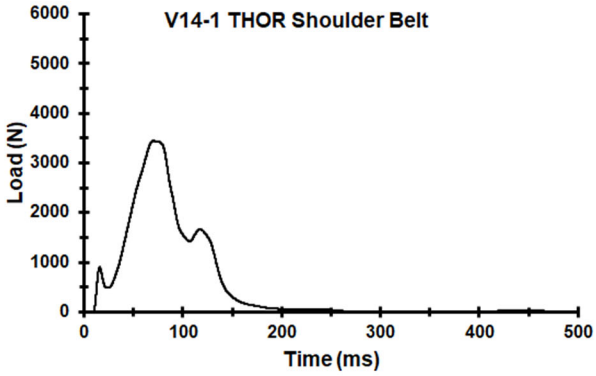
V14-1 THOR Shoulder Belt
Load (N)
6000
5000
4000
3000
2000
1000
0
0
100
200
300
400
500
Time (ms)

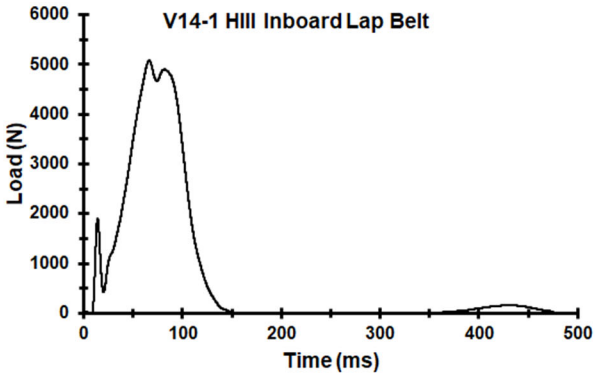
V14-1 HIII Inboard Lap Belt
Load (N)
Time (ms)
0
1000
2000
3000
4000
5000
6000
0
100
200
300
400
500

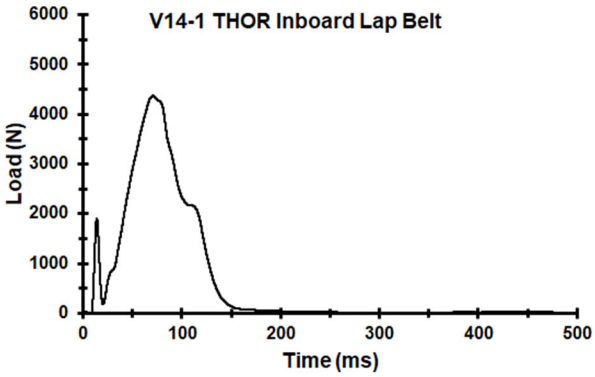
V14-1 THOR Inboard Lap Belt
Load (N)
Time (ms)
0
1000
2000
3000
4000
5000
6000
0
100
200
300
400
500

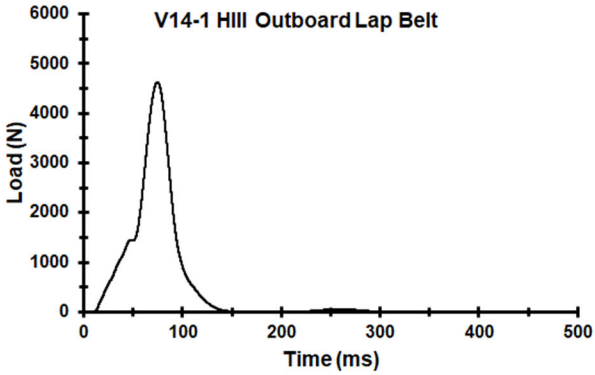
V14-1 HIII Outboard Lap Belt
Load (N)
Time (ms)
0
1000
2000
3000
4000
5000
6000
0
100
200
300
400
500

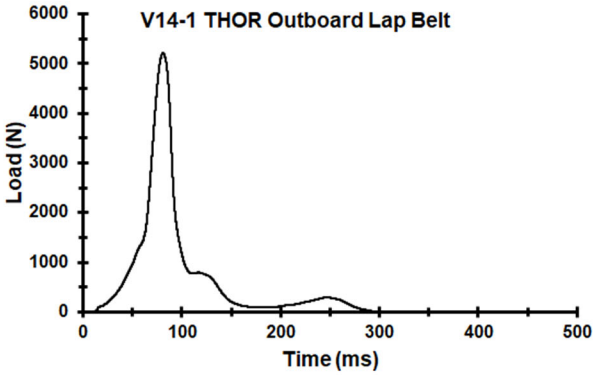
V14-1 THOR Outboard Lap Belt
Load (N)
Time (ms)
0
1000
2000
3000
4000
5000
6000
0
100
200
300
400
500

Appendix X. Select Data Traces From Test FRS-V14-2

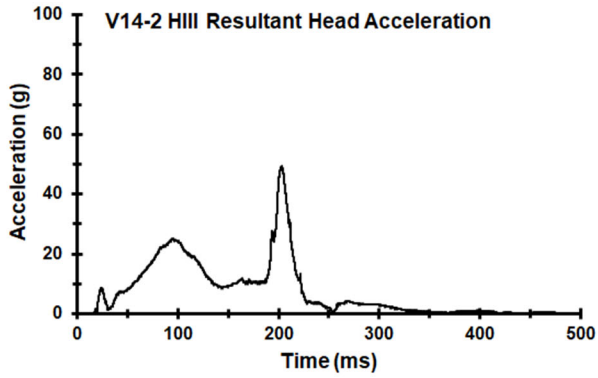
V14-2 HIII Resultant Head Acceleration
Acceleration (g)
Time (ms)

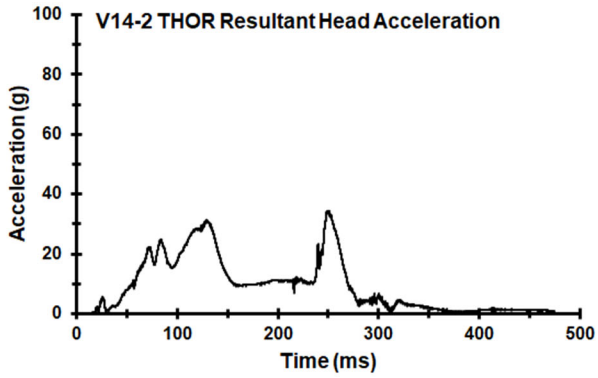
V14-2 THOR Resultant Head Acceleration
Acceleration (g)
Time (ms)

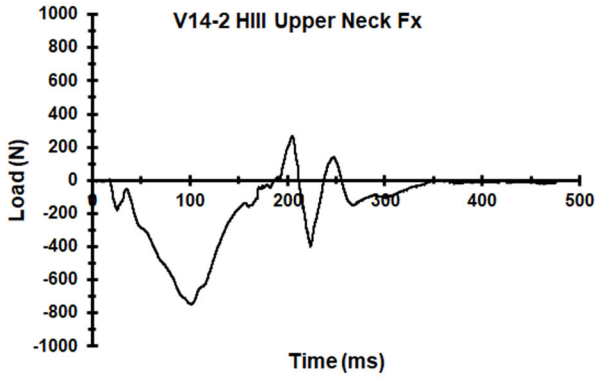
V14-2 HIII Upper Neck Fx
Load (N)
Time (ms)

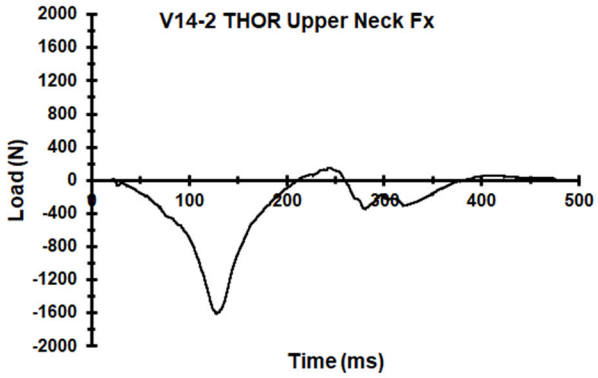
V14-2 THOR Upper Neck Fx
Load (N)
Time (ms)

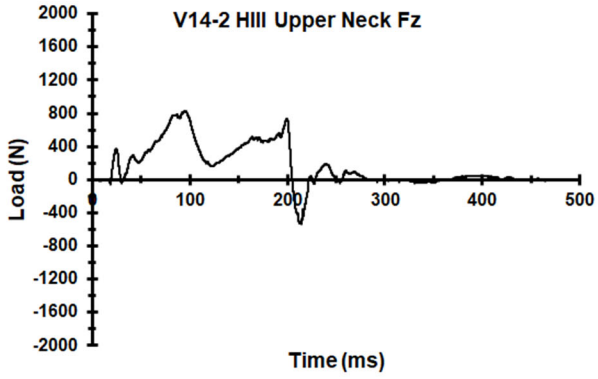
V14-2 HIII Upper Neck Fz
Load (N)
Time (ms)

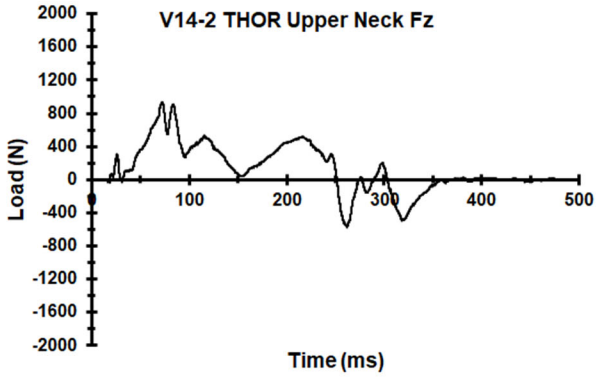
V14-2 THOR Upper Neck Fz
Load (N)
Time (ms)

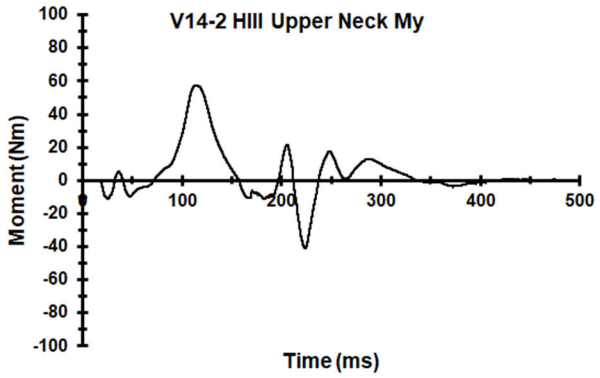
V14-2 HIII Upper Neck My
Moment (Nm)
Time (ms)

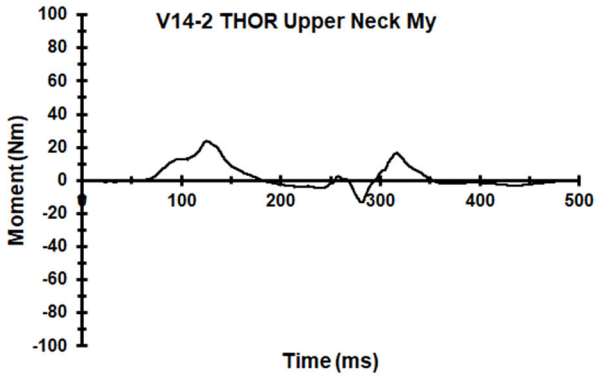
V14-2 THOR Upper Neck My
Moment (Nm)
Time (ms)

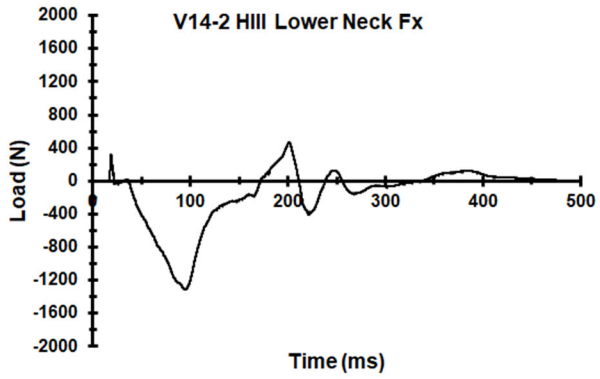
V14-2 HIII Lower Neck Fx
Load (N)
Time (ms)

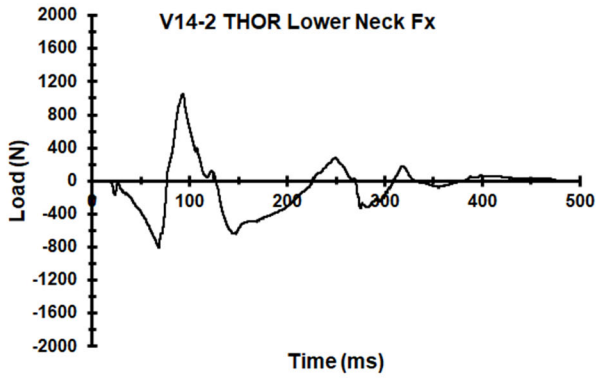
V14-2 THOR Lower Neck Fx
Load (N)
Time (ms)

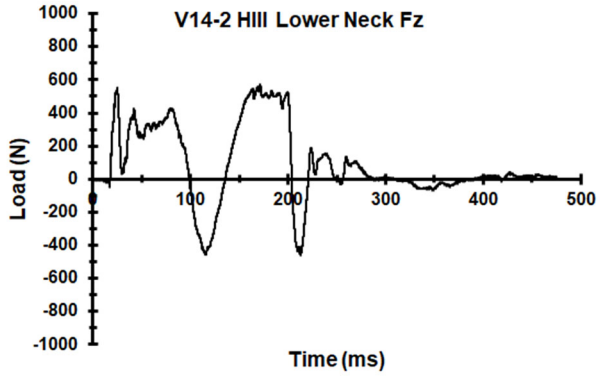
V14-2 HIII Lower Neck Fz
Load (N)
Time (ms)

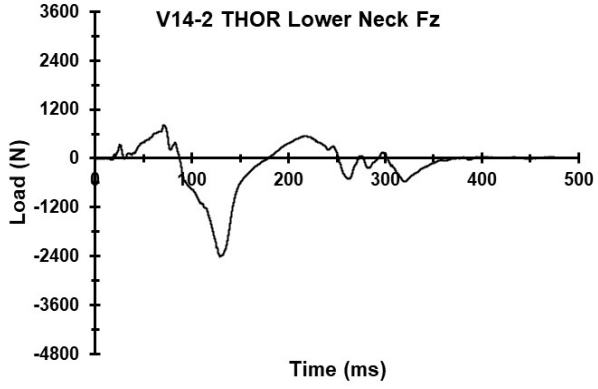
V14-2 THOR Lower Neck Fz
Load (N)
Time (ms)

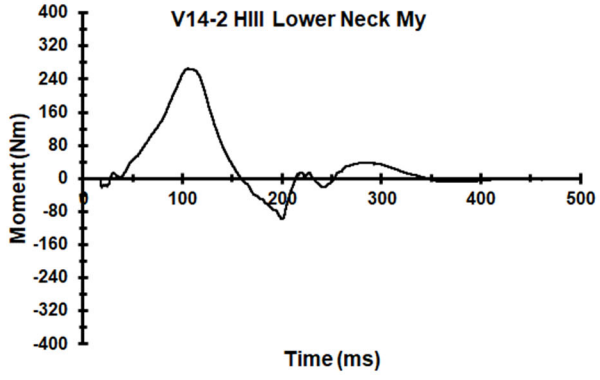
V14-2 HIII Lower Neck My
Moment (Nm)
Time (ms)

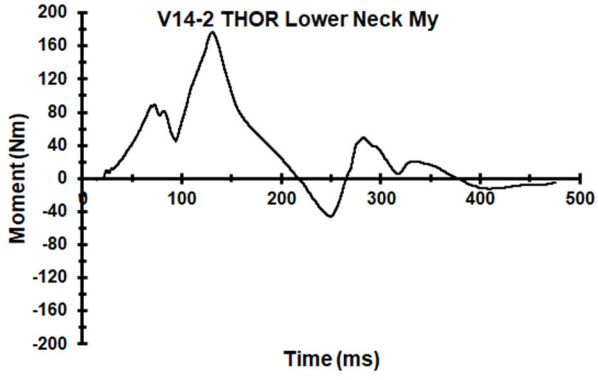
V14-2 THOR Lower Neck My
Moment (Nm)
Time (ms)

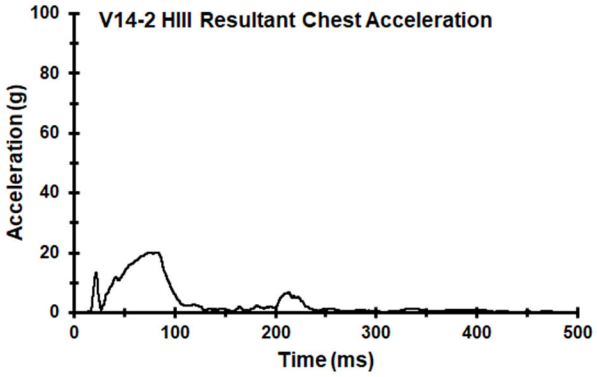
V14-2 HIII Resultant Chest Acceleration
Acceleration (g)
Time (ms)

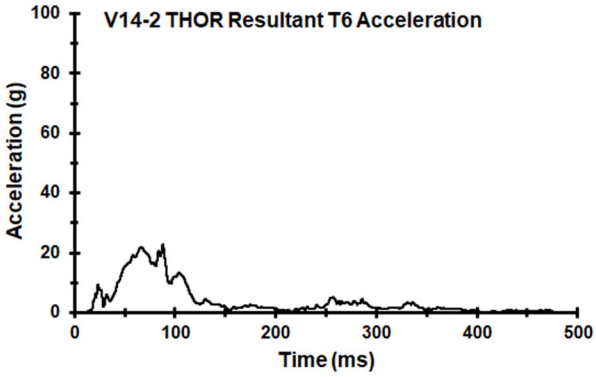
V14-2 THOR Resultant T6 Acceleration
Acceleration (g)
Time (ms)

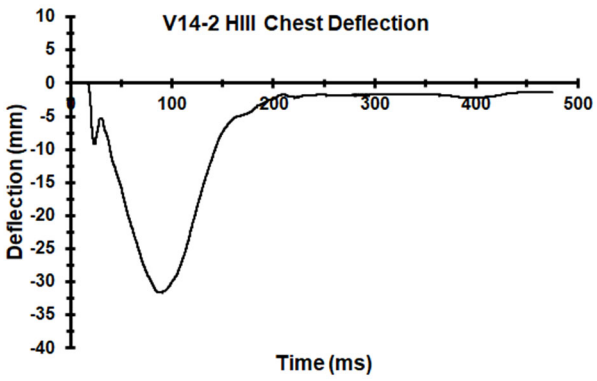
V14-2 HIII Chest Deflection
Deflection (mm)
Time (ms)

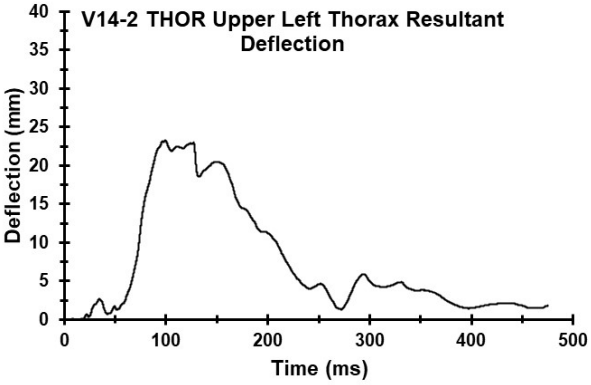
V14-2 THOR Upper Left Thorax Resultant Deflection
Deflection (mm)
Time (ms)

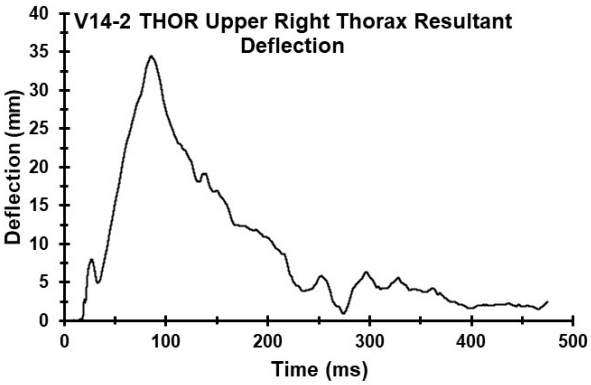
V14-2 THOR Upper Right Thorax Resultant Deflection
Deflection (mm)
Time (ms)

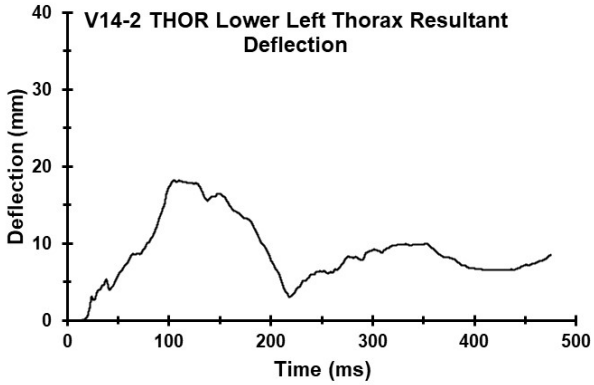
V14-2 THOR Lower Left Thorax Resultant Deflection
Deflection (mm)
0
10
20
30
40
0
100
200
300
400
500
Time (ms)

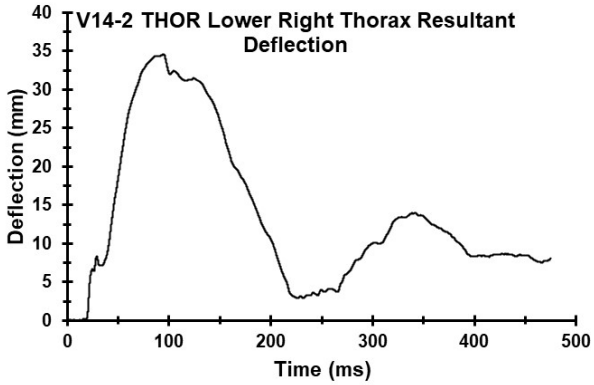
V14-2 THOR Lower Right Thorax Resultant Deflection
Deflection (mm)
0
5
10
15
20
25
30
35
40
0
100
200
300
400
500
Time (ms)

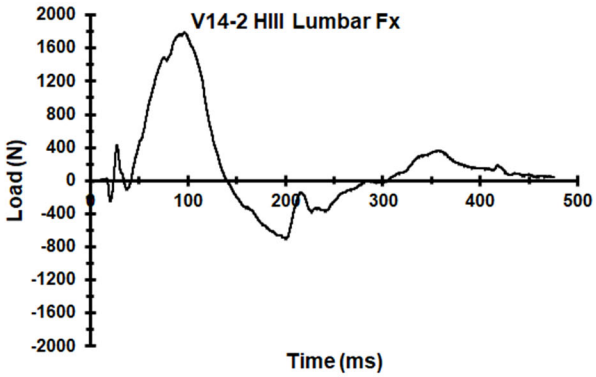
V14-2 HIII Lumbar Fx
Load (N)
2000
1600
1200
800
400
0
-400
-800
-1200
-1600
-2000
0
100
200
300
400
500
Time (ms)

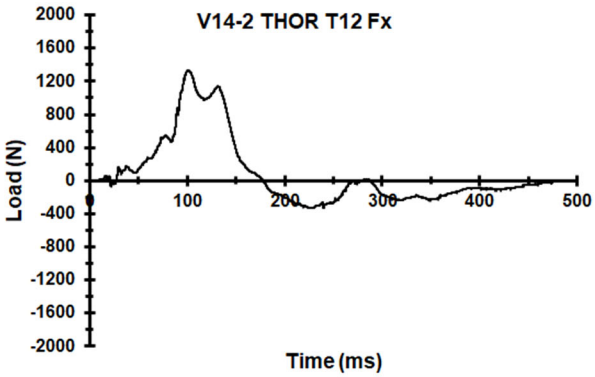
V14-2 THOR T12 Fx
Load (N)
2000
1600
1200
800
400
0
-400
-800
-1200
-1600
-2000
0
100
200
300
400
500
Time (ms)

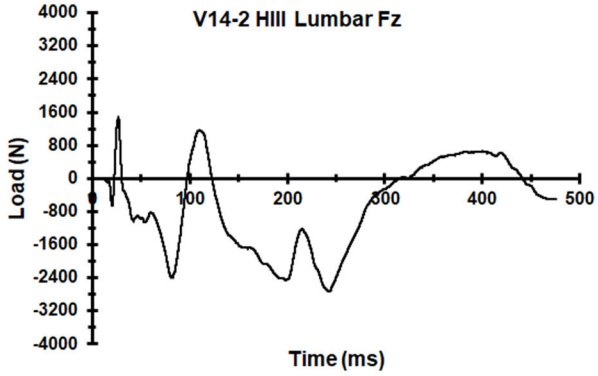
V14-2 HIII Lumbar Fz
Load (N)
Time (ms)

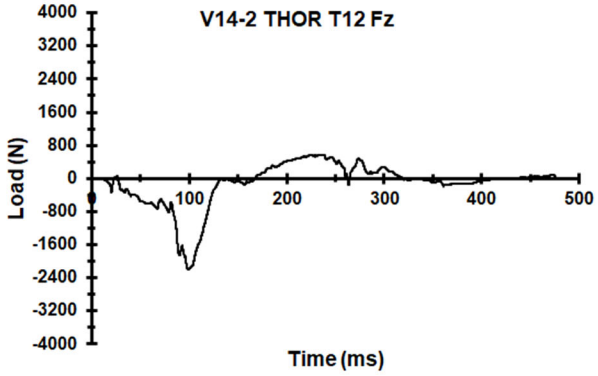
V14-2 THOR T12 Fz
Load (N)
Time (ms)

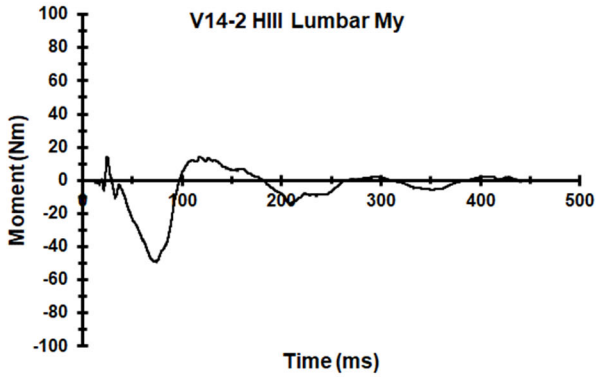
V14-2 HIII Lumbar My
Moment (Nm)
Time (ms)

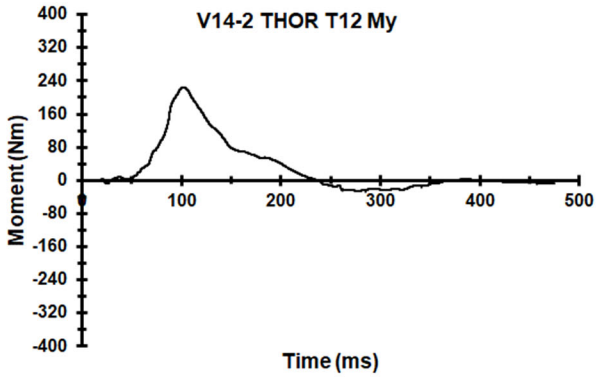
V14-2 THOR T12 My
Moment (Nm)
Time (ms)

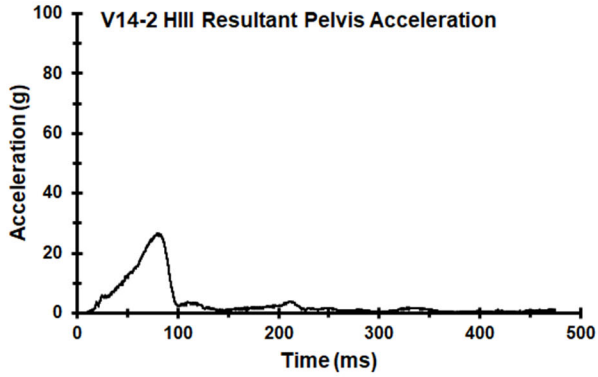
V14-2 HIII Resultant Pelvis Acceleration
Acceleration (g)
Time (ms)

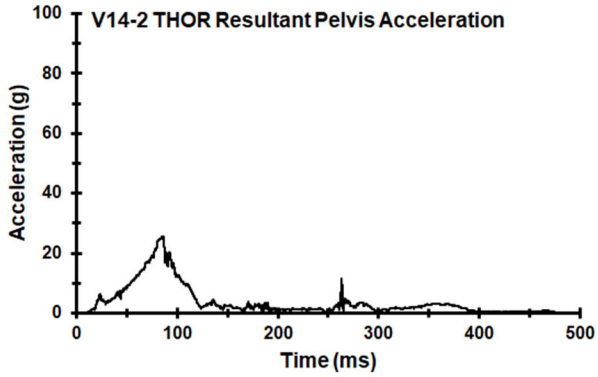
V14-2 THOR Resultant Pelvis Acceleration
Acceleration (g)
Time (ms)

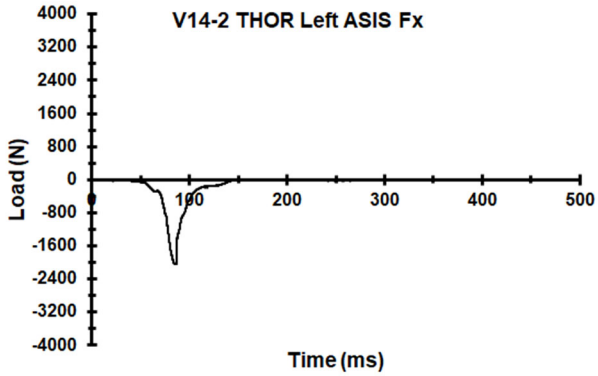
V14-2 THOR Left ASIS Fx
Load (N)
Time (ms)

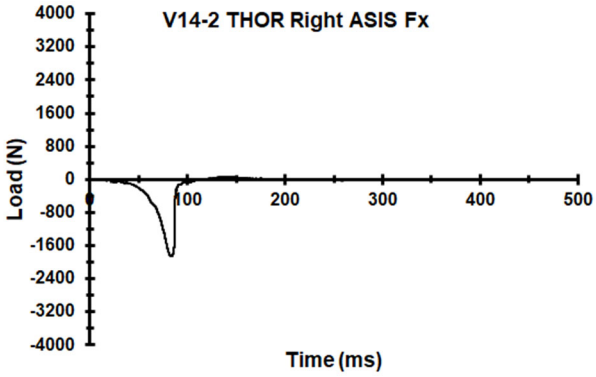
V14-2 THOR Right ASIS Fx
Load (N)
4000
3200
2400
1600
800
0
-800
-1600
-2400
-3200
-4000
100
200
300
400
500
Time (ms)

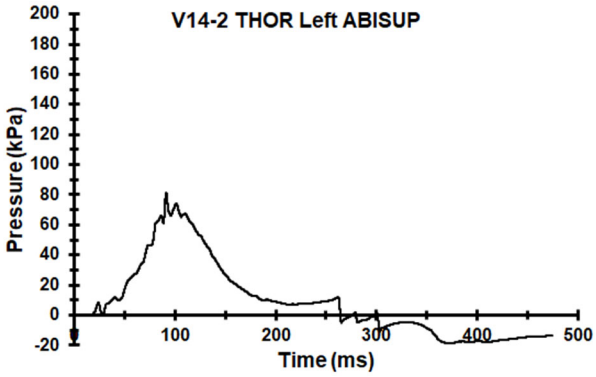
V14-2 THOR Left ABISUP
Pressure (kPa)
200
180
160
140
120
100
80
60
40
20
0
-20
100
200
300
400
500
Time (ms)

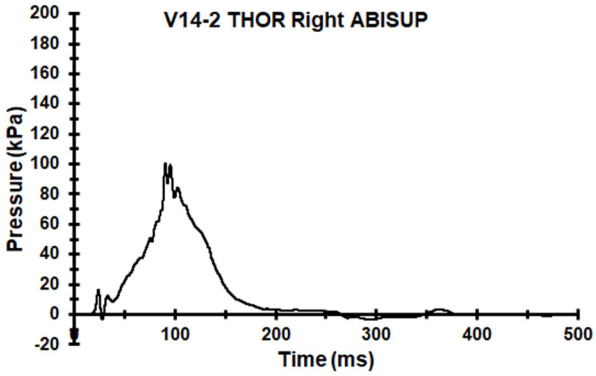
V14-2 THOR Right ABISUP
Pressure (kPa)
200
180
160
140
120
100
80
60
40
20
0
-20
100
200
300
400
500
Time (ms)

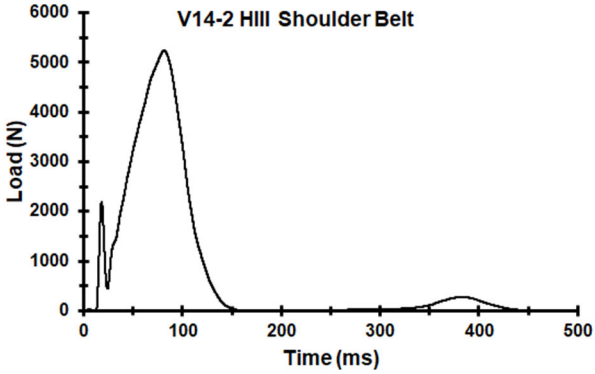
V14-2 HIII Shoulder Belt
Load (N)
Time (ms)

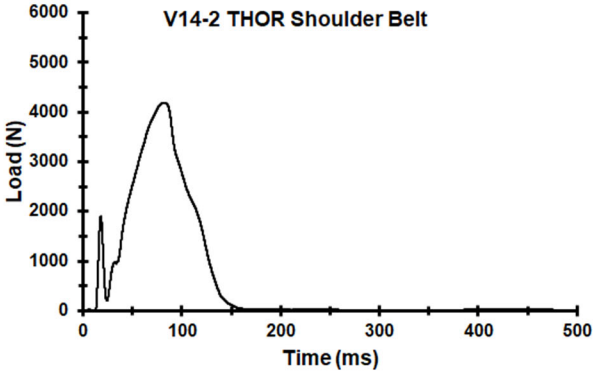
V14-2 THOR Shoulder Belt
Load (N)
Time (ms)

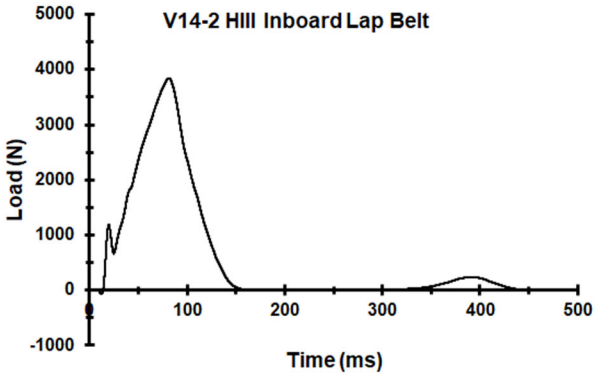
V14-2 HIII Inboard Lap Belt
Load (N)
Time (ms)

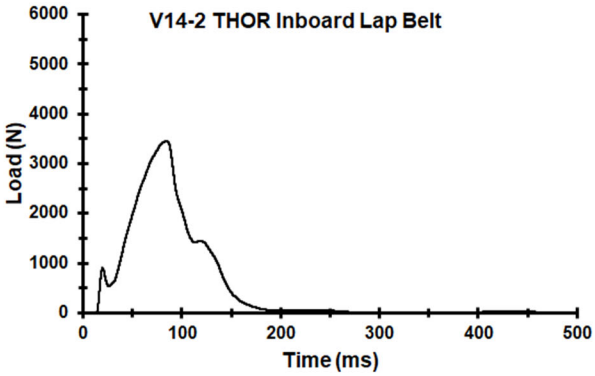
V14-2 THOR Inboard Lap Belt
Load (N)
Time (ms)

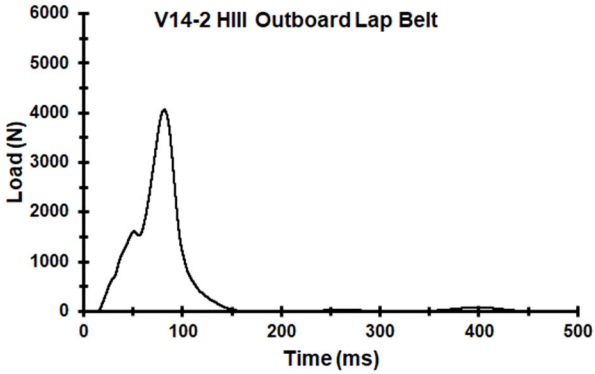
V14-2 HIII Outboard Lap Belt
Load (N)
Time (ms)

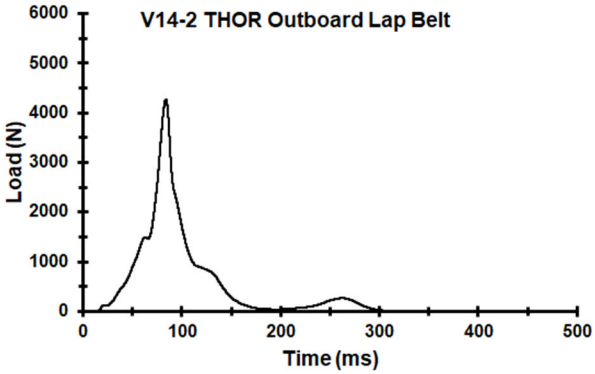
V14-2 THOR Outboard Lap Belt
Load (N)
Time (ms)

Appendix Y. Select Data Traces From Test FRS-V14-3

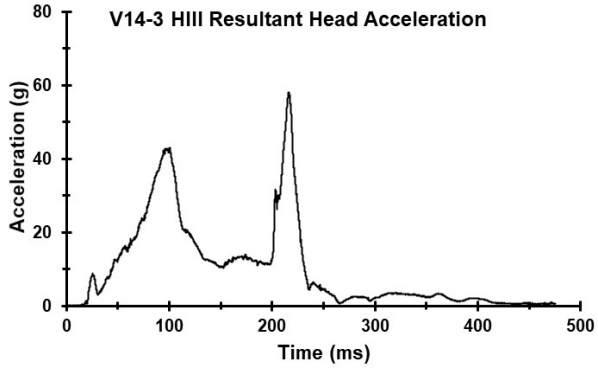
V14-3 HIII Resultant Head Acceleration
Acceleration (g)
Time (ms)

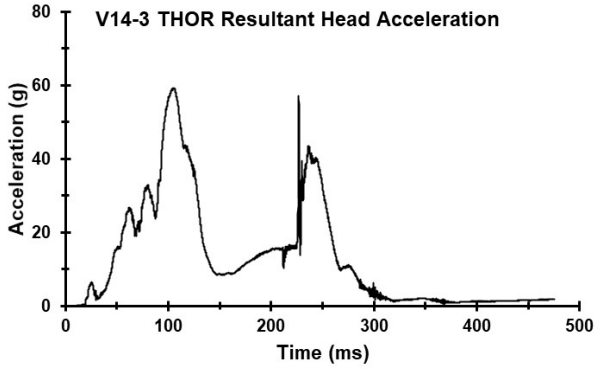
V14-3 THOR Resultant Head Acceleration
Acceleration (g)
Time (ms)

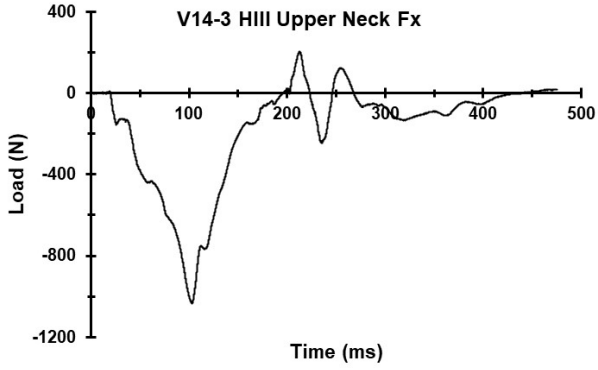
V14-3 HIII Upper Neck Fx
Load (N)
Time (ms)

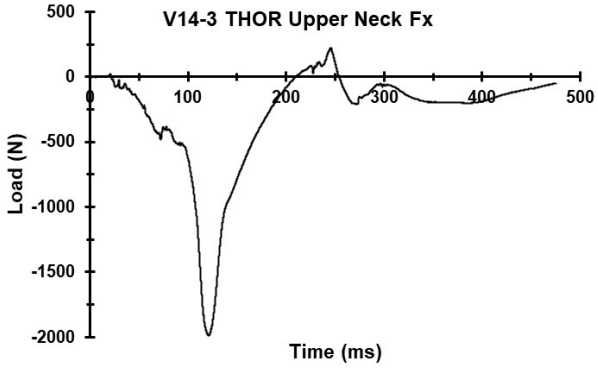
V14-3 THOR Upper Neck Fx
Load (N)
Time (ms)

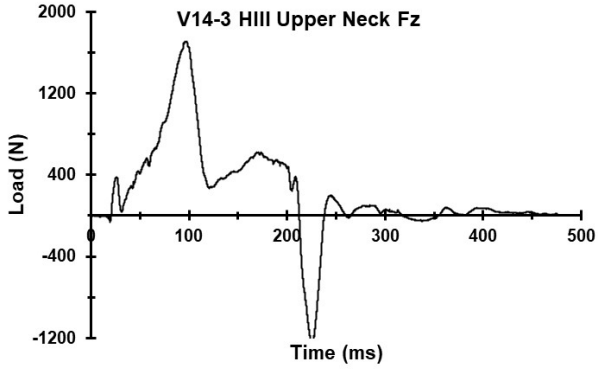
V14-3 HIII Upper Neck Fz
Load (N)
Time (ms)

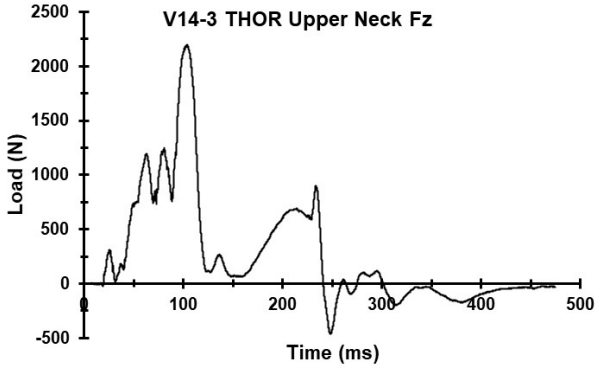
V14-3 THOR Upper Neck Fz
Load (N)
Time (ms)

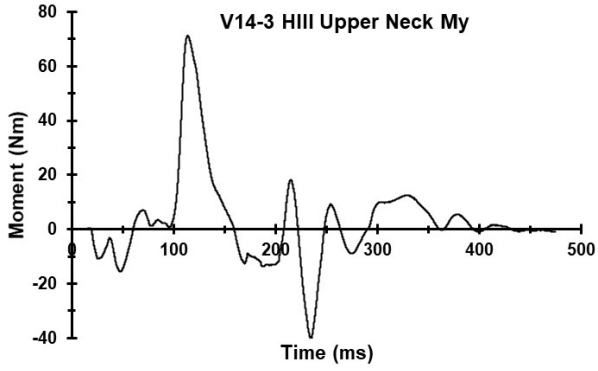
V14-3 HIII Upper Neck My
Moment (Nm)
Time (ms)

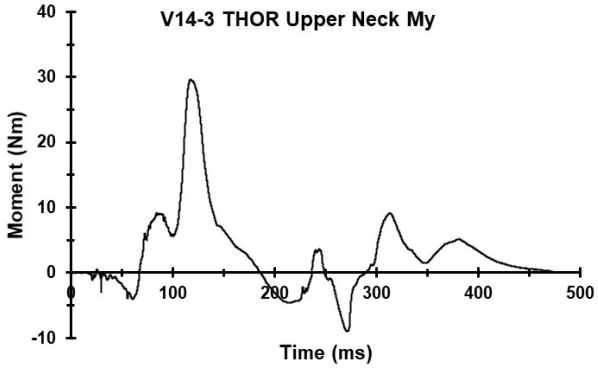
V14-3 THOR Upper Neck My
Moment (Nm)
Time (ms)

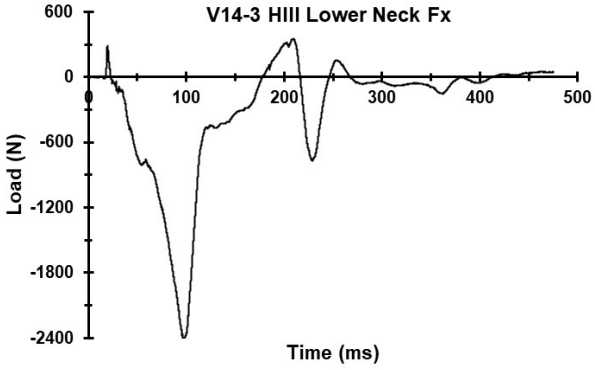
V14-3 HIII Lower Neck Fx
Load (N)
Time (ms)

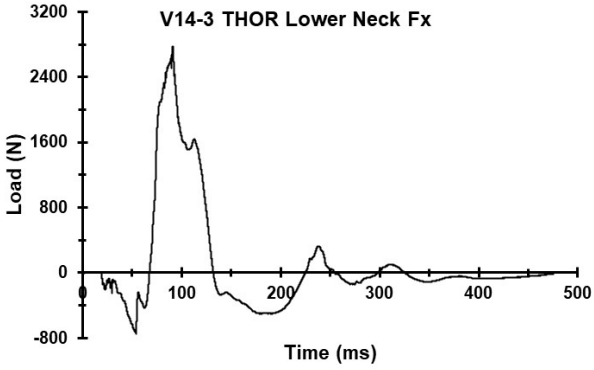
V14-3 THOR Lower Neck Fx
Load (N)
Time (ms)

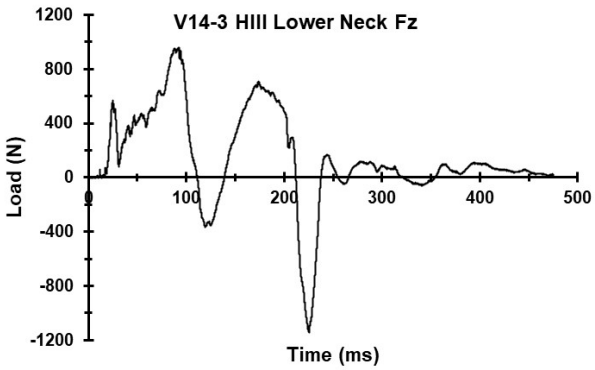
V14-3 HIII Lower Neck Fz
Load (N)
Time (ms)

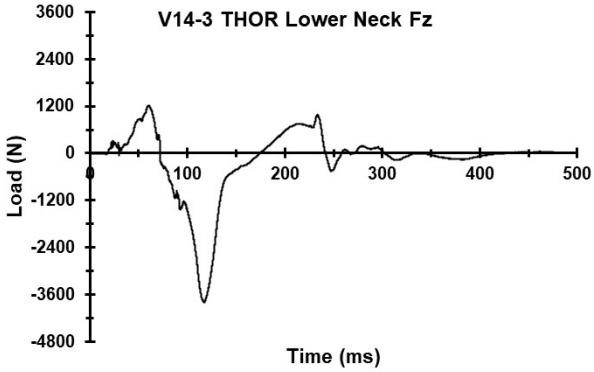
V14-3 THOR Lower Neck Fz
Load (N)
Time (ms)

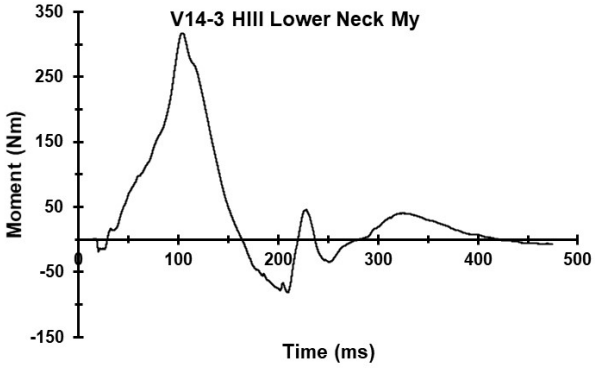
V14-3 HIII Lower Neck My
Moment (Nm)
Time (ms)

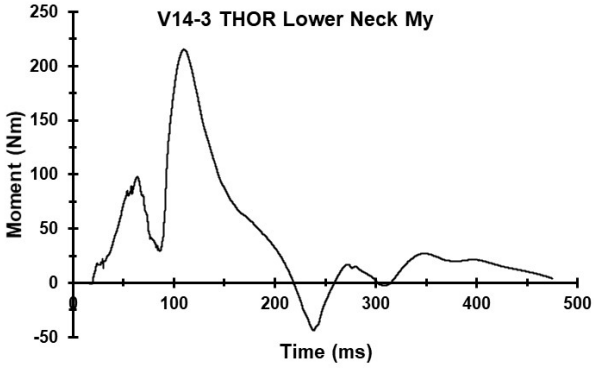
V14-3 THOR Lower Neck My
Moment (Nm)
Time (ms)

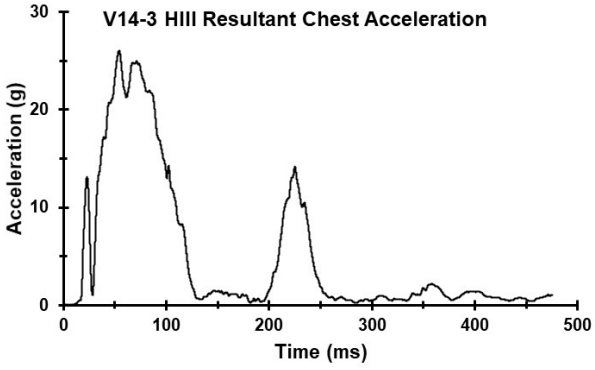
V14-3 HIII Resultant Chest Acceleration
Acceleration (g)
Time (ms)

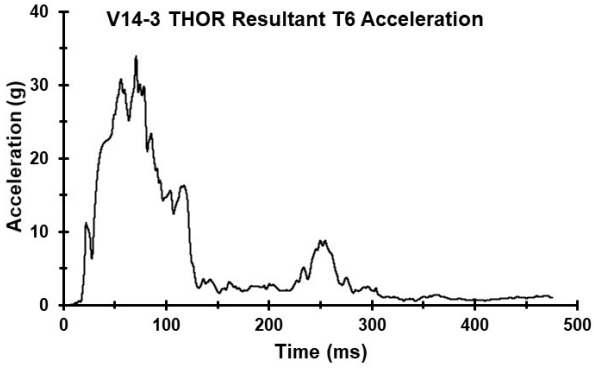
V14-3 THOR Resultant T6 Acceleration
Acceleration (g)
Time (ms)

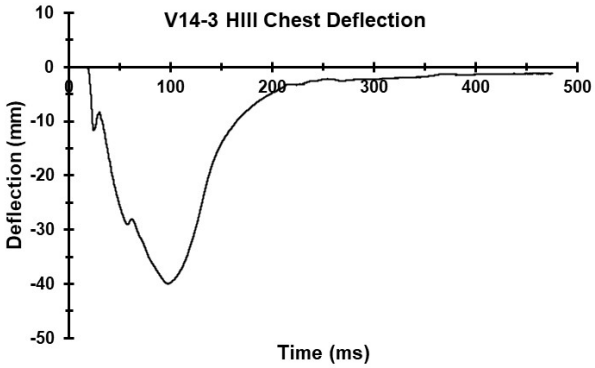
V14-3 HIII Chest Deflection
Deflection (mm)
Time (ms)
10
0
-10
-20
-30
-40
-50
0
100
200
300
400
500

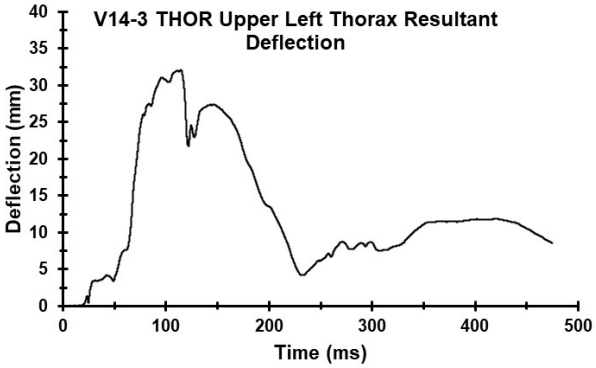
V14-3 THOR Upper Left Thorax Resultant Deflection
Deflection (mm)
Time (ms)
40
35
30
25
20
15
10
5
0
0
100
200
300
400
500

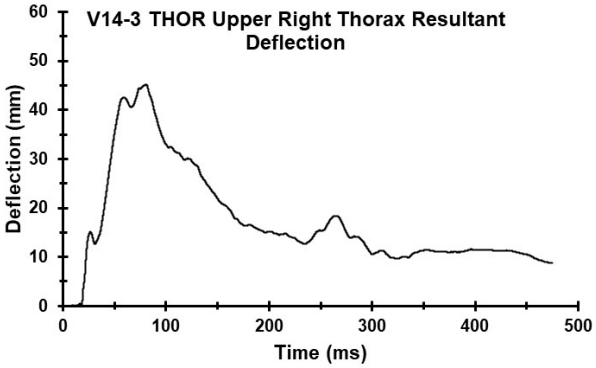
V14-3 THOR Upper Right Thorax Resultant Deflection
Deflection (mm)
Time (ms)
60
50
40
30
20
10
0
0
100
200
300
400
500

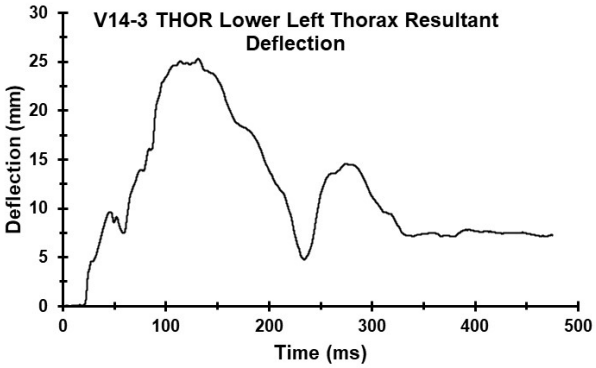
V14-3 THOR Lower Left Thorax Resultant Deflection
Deflection (mm)
Time (ms)
30
25
20
15
10
5
0
0
100
200
300
400
500

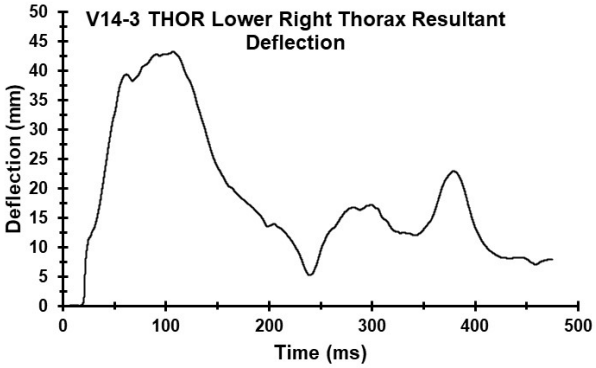
V14-3 THOR Lower Right Thorax Resultant Deflection
Deflection (mm)
Time (ms)
50
45
40
35
30
25
20
15
10
5
0
0
100
200
300
400
500

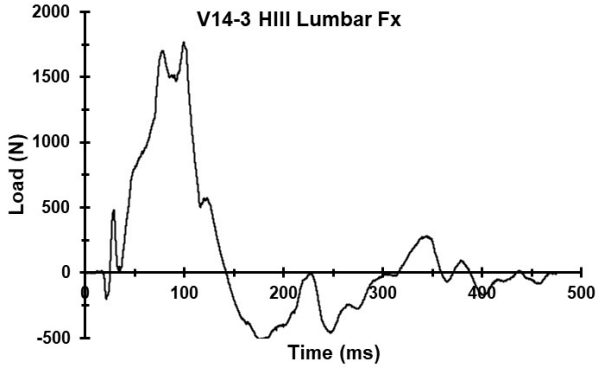
V14-3 HIII Lumbar Fx
Load (N)
2000
1500
1000
500
0
-500
0
100
200
300
400
500
Time (ms)

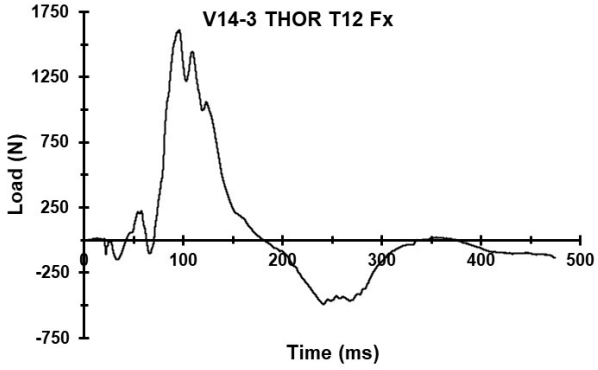
V14-3 THOR T12 Fx
Load (N)
1750
1250
750
250
-250
-750
0
100
200
300
400
500
Time (ms)

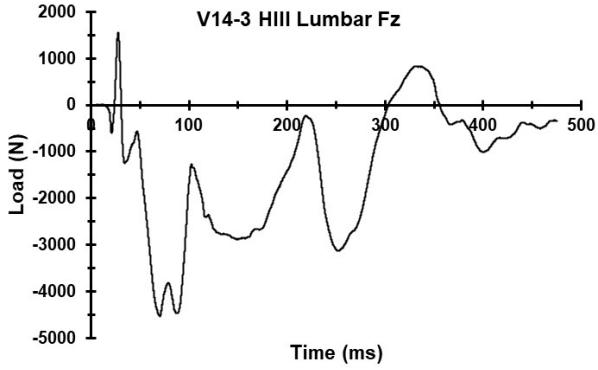
V14-3 HIII Lumbar Fz
Load (N)
2000
1000
0
-1000
-2000
-3000
-4000
-5000
0
100
200
300
400
500
Time (ms)

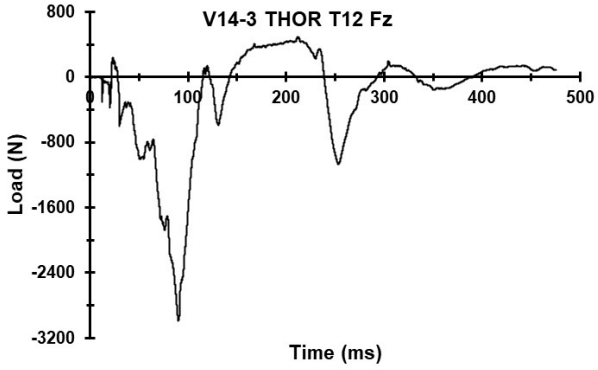
V14-3 THOR T12 Fz
Load (N)
800
0
-800
-1600
-2400
-3200
0
100
200
300
400
500
Time (ms)

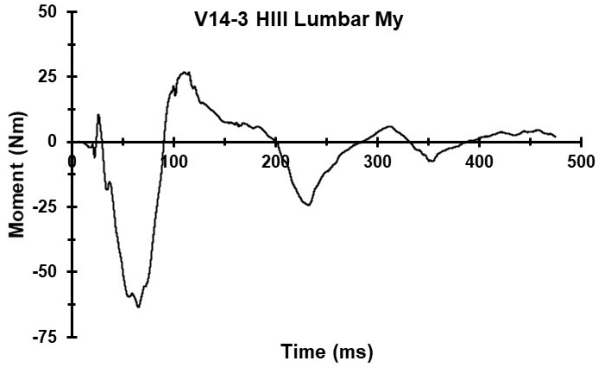
V14-3 HIII Lumbar My
Moment (Nm)
50
25
0
-25
-50
-75
0
100
200
300
400
500
Time (ms)

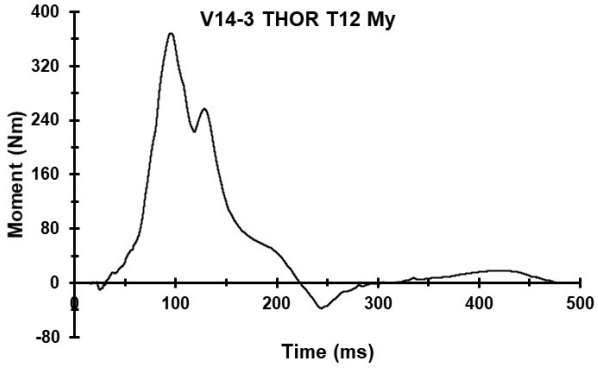
V14-3 THOR T12 My
Moment (Nm)
400
320
240
160
80
0
-80
0
100
200
300
400
500
Time (ms)

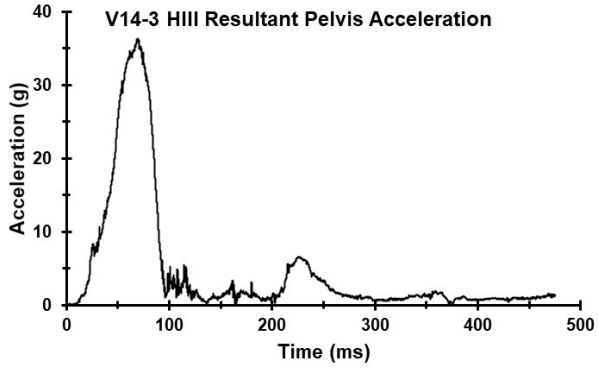
V14-3 HIII Resultant Pelvis Acceleration
Acceleration (g)
40
30
20
10
0
0
100
200
300
400
500
Time (ms)

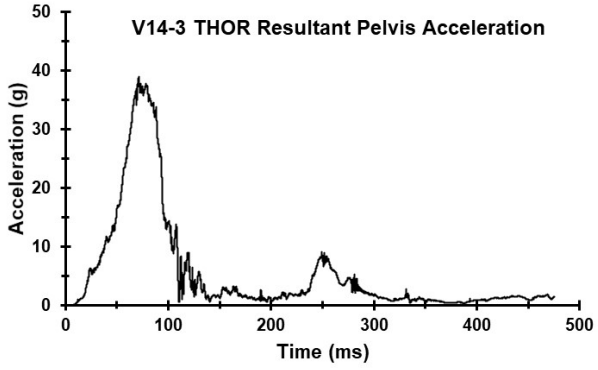
V14-3 THOR Resultant Pelvis Acceleration
Acceleration (g)
50
40
30
20
10
0
0
100
200
300
400
500
Time (ms)

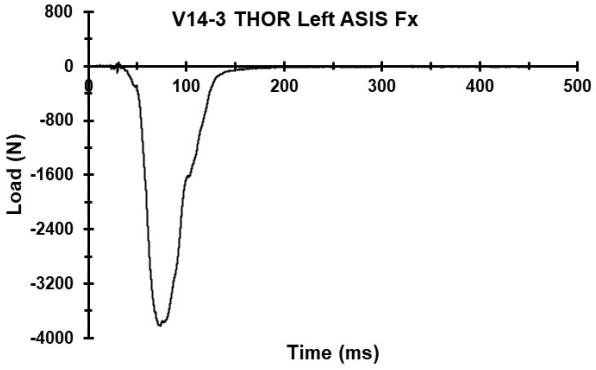
V14-3 THOR Left ASIS Fx
800
0
-800
-1600
-2400
-3200
-4000
Load (N)
100
200
300
400
500
Time (ms)

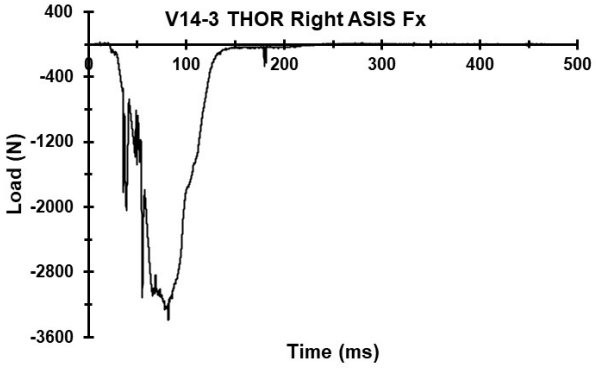
V14-3 THOR Right ASIS Fx
400
-400
-1200
-2000
-2800
-3600
Load (N)
100
200
300
400
500
Time (ms)

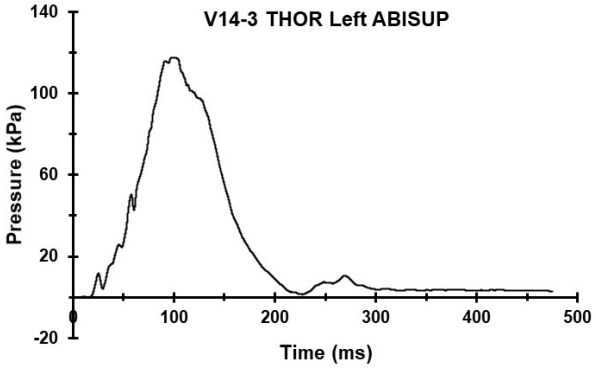
V14-3 THOR Left ABISUP
140
100
60
20
-20
Pressure (kPa)
100
200
300
400
500
Time (ms)

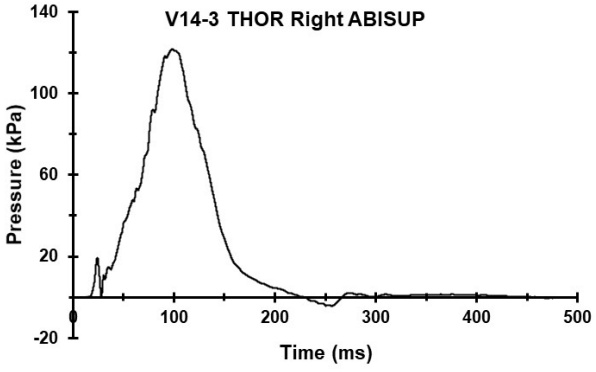
V14-3 THOR Right ABISUP
140
100
60
20
-20
Pressure (kPa)
100
200
300
400
500
Time (ms)

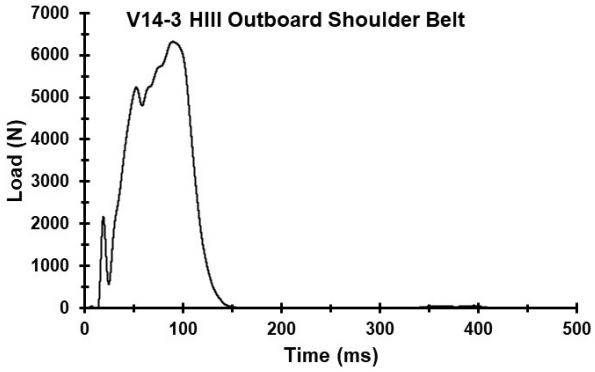
V14-3 HIII Outboard Shoulder Belt
Load (N)
7000
6000
5000
4000
3000
2000
1000
0
0
100
200
300
400
500
Time (ms)

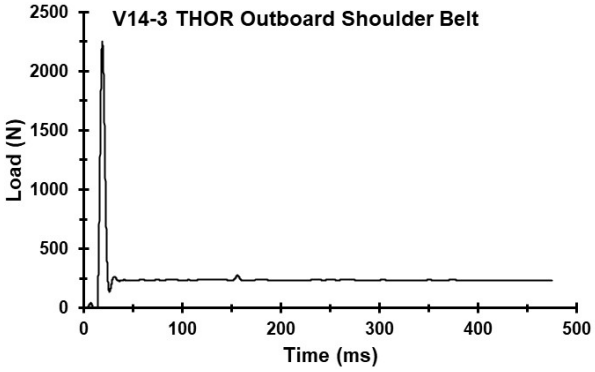
V14-3 THOR Outboard Shoulder Belt
Load (N)
2500
2000
1500
1000
500
0
0
100
200
300
400
500
Time (ms)

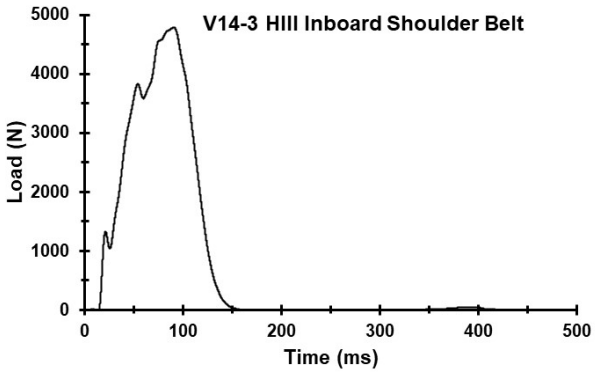
V14-3 HIII Inboard Shoulder Belt
Load (N)
5000
4000
3000
2000
1000
0
0
100
200
300
400
500
Time (ms)

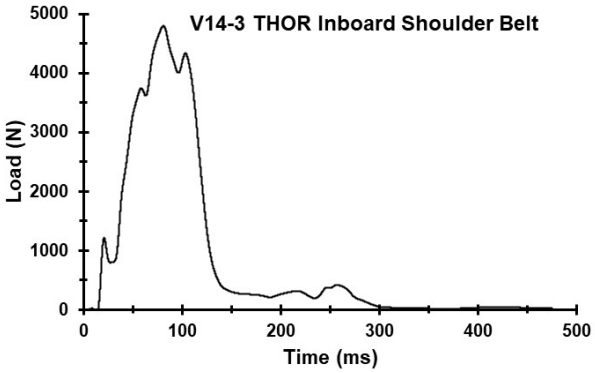
V14-3 THOR Inboard Shoulder Belt
Load (N)
5000
4000
3000
2000
1000
0
0
100
200
300
400
500
Time (ms)

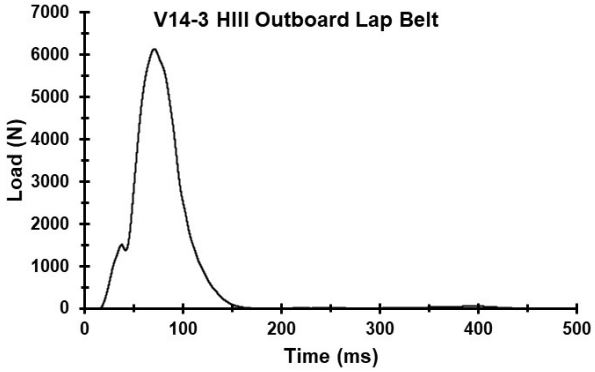
V14-3 HIII Outboard Lap Belt
Load (N)
7000
6000
5000
4000
3000
2000
1000
0
0
100
200
300
400
500
Time (ms)

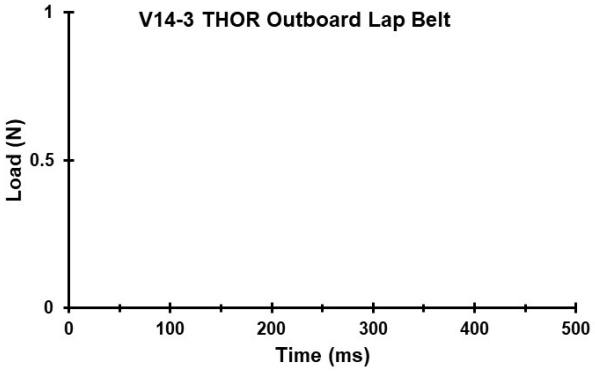
V14-3 THOR Outboard Lap Belt
Load (N)
1
0.5
0
0
100
200
300
400
500
Time (ms)

Appendix Z. Select Data Traces From Test FRS-V14-4

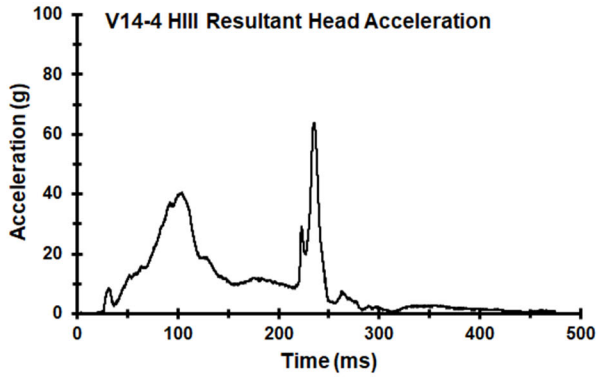
V14-4 HIII Resultant Head Acceleration
Acceleration (g)
Time (ms)

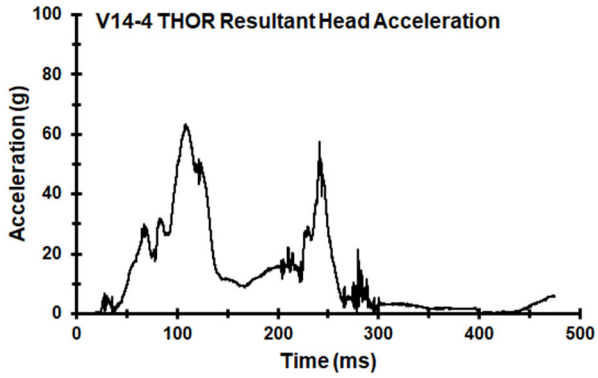
V14-4 THOR Resultant Head Acceleration
Acceleration (g)
Time (ms)

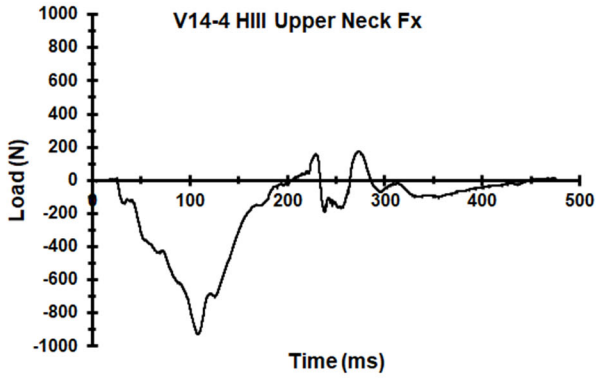
V14-4 HIII Upper Neck Fx
Load (N)
Time (ms)

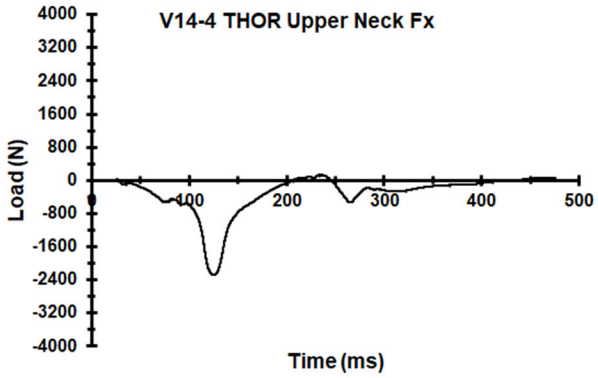
V14-4 THOR Upper Neck Fx
Load (N)
Time (ms)

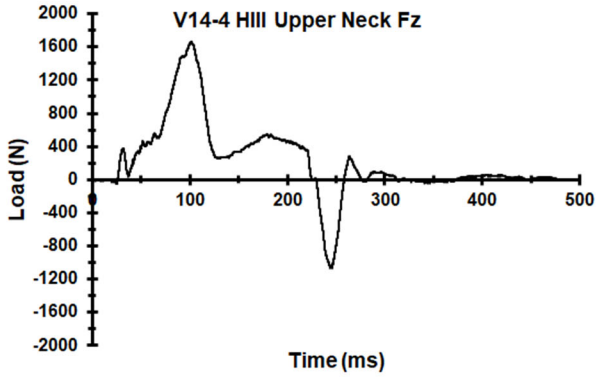
V14-4 HIII Upper Neck Fz
Load (N)
Time (ms)

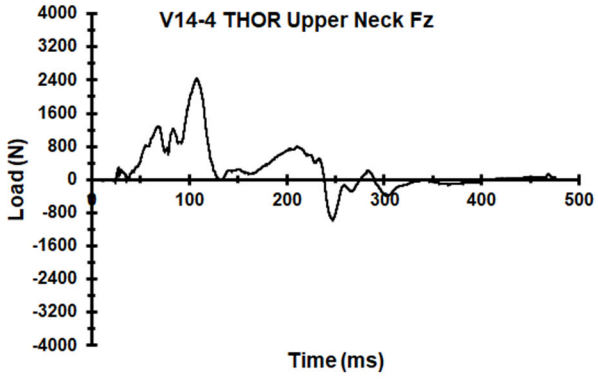
V14-4 THOR Upper Neck Fz
Load (N)
Time (ms)

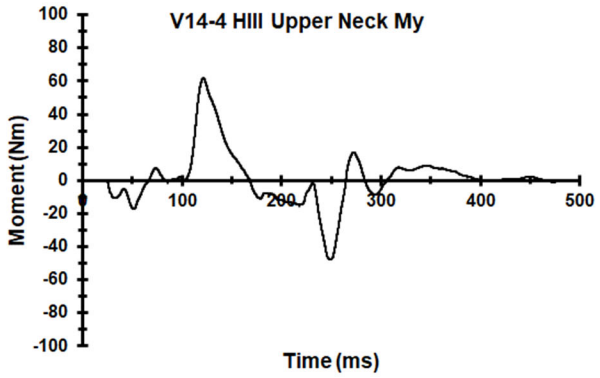
V14-4 HIII Upper Neck My
Moment (Nm)
Time (ms)

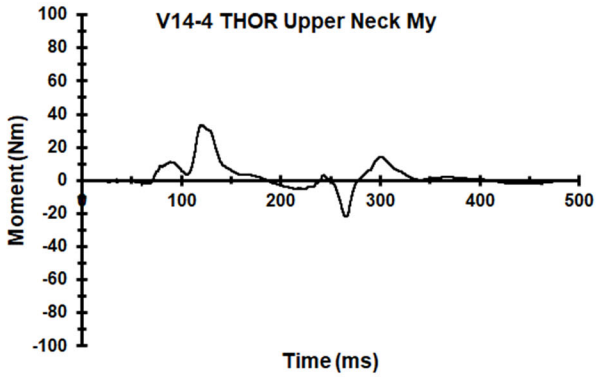
V14-4 THOR Upper Neck My
Moment (Nm)
Time (ms)

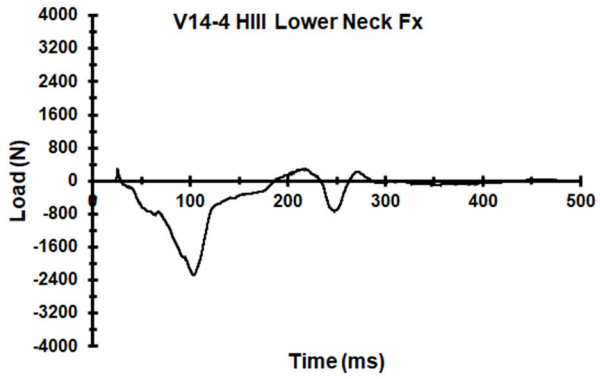
V14-4 HIII Lower Neck Fx
Load (N)
Time (ms)

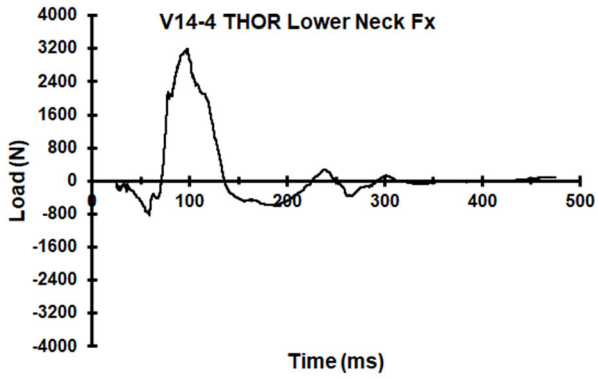
V14-4 THOR Lower Neck Fx
Load (N)
Time (ms)

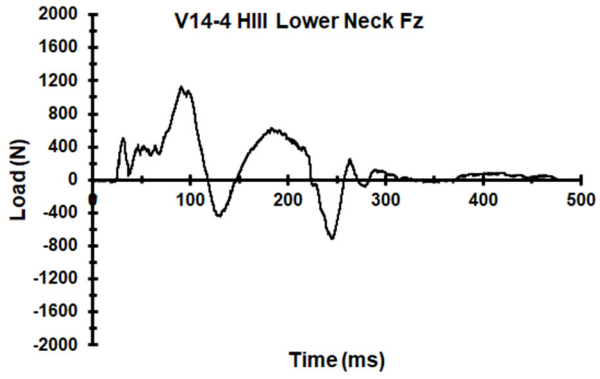
V14-4 HIII Lower Neck Fz
Load (N)
Time (ms)

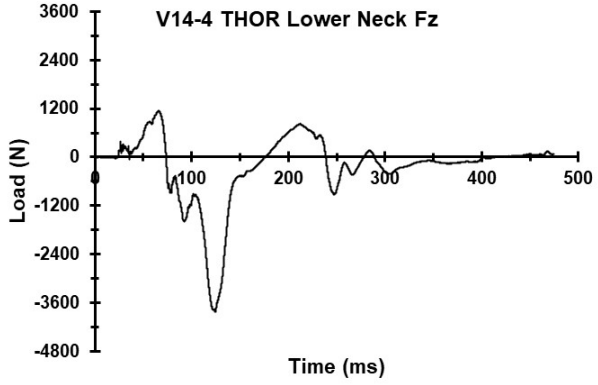
V14-4 THOR Lower Neck Fz
Load (N)
Time (ms)

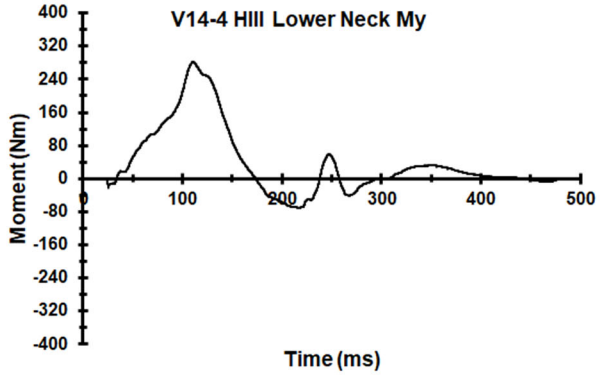
V14-4 HIII Lower Neck My
Moment (Nm)
Time (ms)

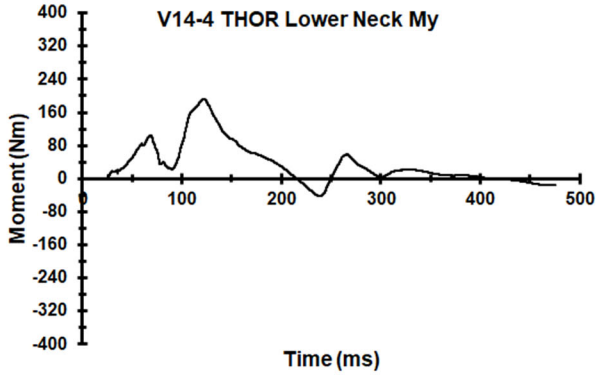
V14-4 THOR Lower Neck My
Moment (Nm)
Time (ms)

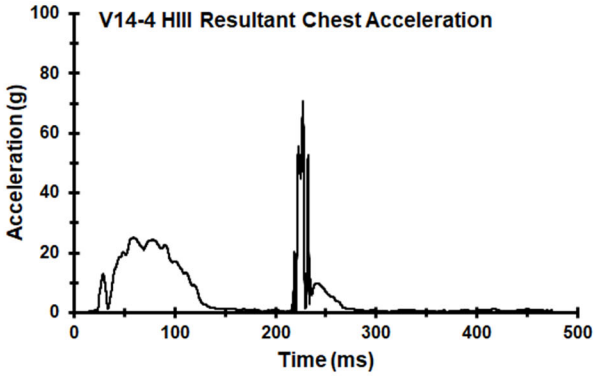
V14-4 HIII Resultant Chest Acceleration
Acceleration (g)
Time (ms)

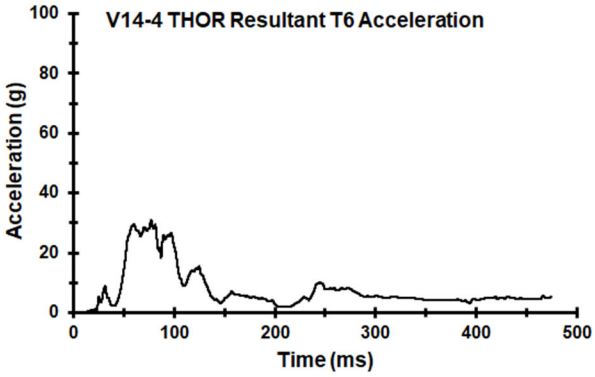
V14-4 THOR Resultant T6 Acceleration
Acceleration (g)
Time (ms)

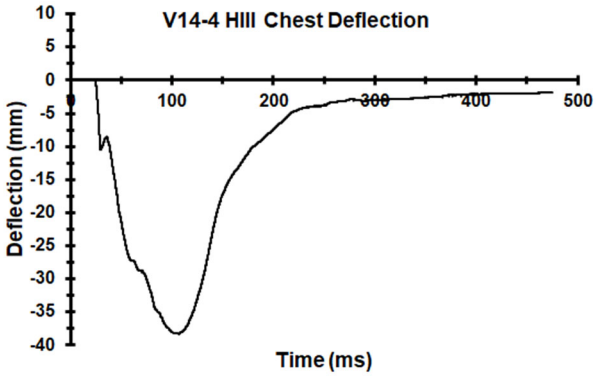
V14-4 HIII Chest Deflection
Deflection (mm)
Time (ms)

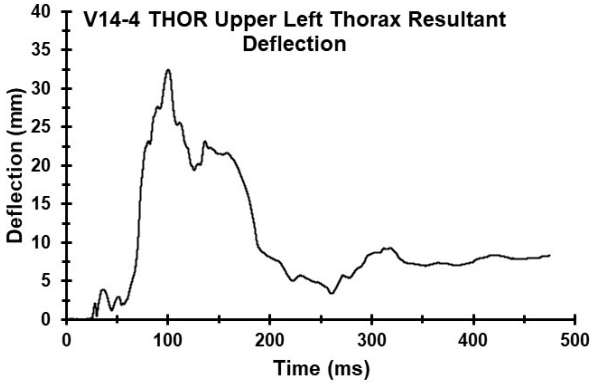
V14-4 THOR Upper Left Thorax Resultant Deflection
Deflection (mm)
Time (ms)

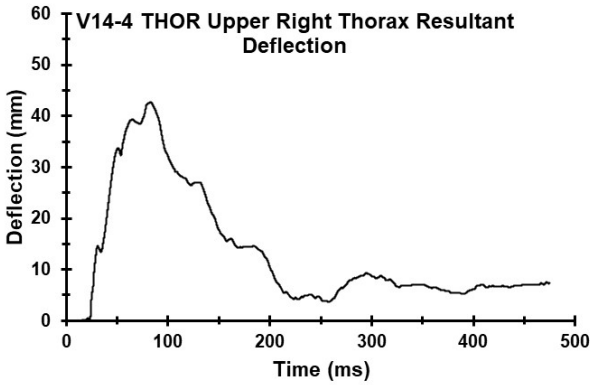
V14-4 THOR Upper Right Thorax Resultant Deflection
Deflection (mm)
Time (ms)

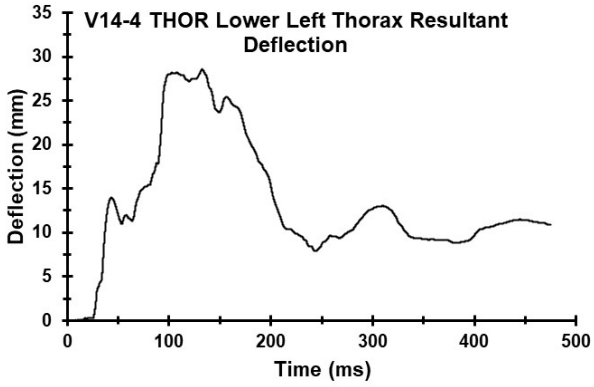
V14-4 THOR Lower Left Thorax Resultant Deflection
Deflection (mm)
Time (ms)

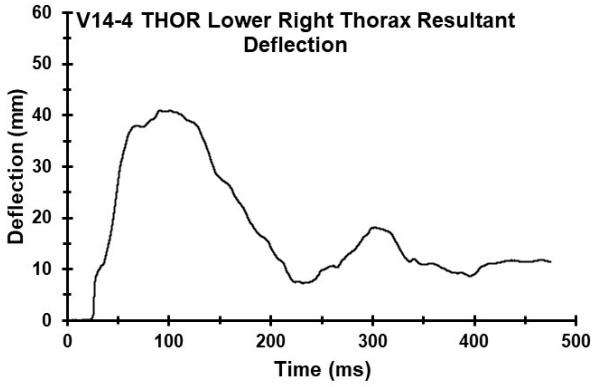
V14-4 THOR Lower Right Thorax Resultant Deflection
Deflection (mm)
Time (ms)

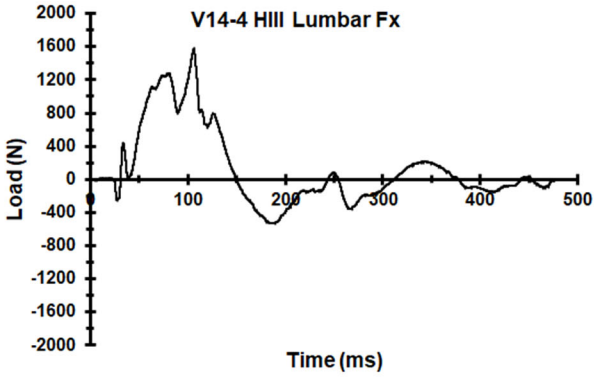
V14-4 HIII Lumbar Fx
Load (N)
Time (ms)

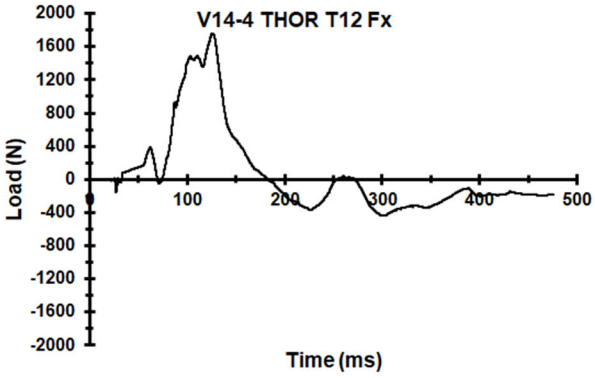
V14-4 THOR T12 Fx
Load (N)
Time (ms)

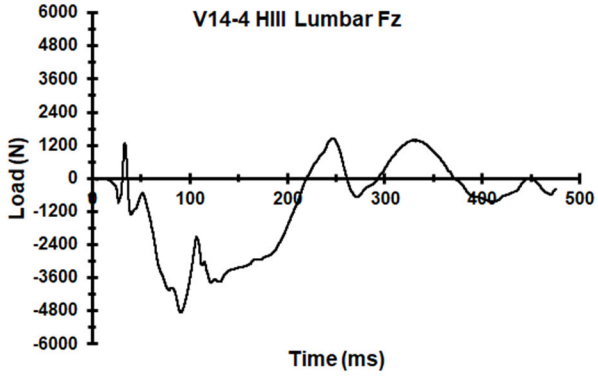
V14-4 HIII Lumbar Fz
Load (N)
6000
4800
3600
2400
1200
0
-1200
-2400
-3600
-4800
-6000
0
100
200
300
400
500
Time (ms)

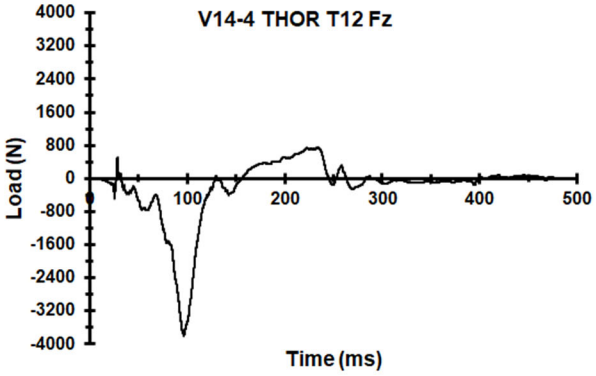
V14-4 THOR T12 Fz
Load (N)
4000
3200
2400
1600
800
0
-800
-1600
-2400
-3200
-4000
0
100
200
300
400
500
Time (ms)

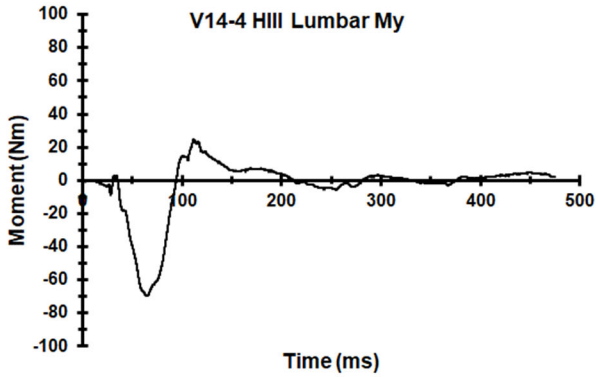
V14-4 HIII Lumbar My
Moment (Nm)
100
80
60
40
20
0
-20
-40
-60
-80
-100
0
100
200
300
400
500
Time (ms)

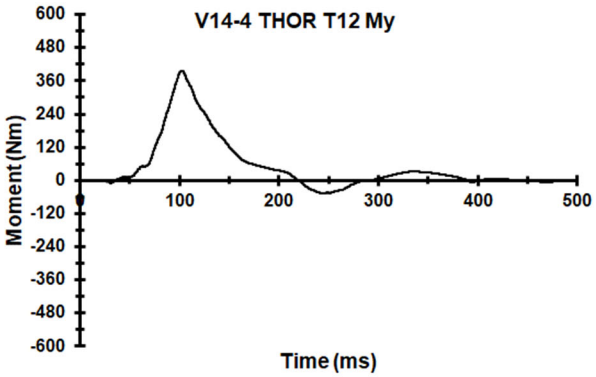
V14-4 THOR T12 My
Moment (Nm)
600
480
360
240
120
0
-120
-240
-360
-480
-600
0
100
200
300
400
500
Time (ms)

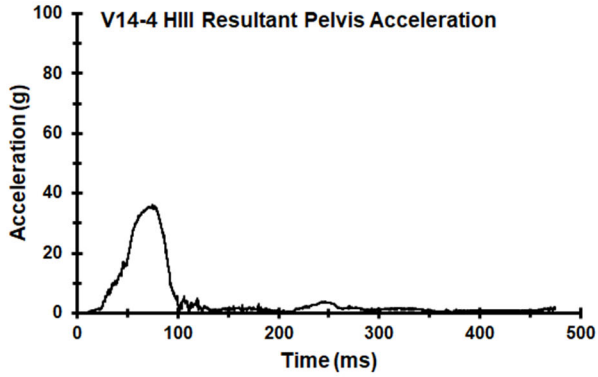
V14-4 HIII Resultant Pelvis Acceleration
Acceleration (g)
100
80
60
40
20
0
0
100
200
300
400
500
Time (ms)

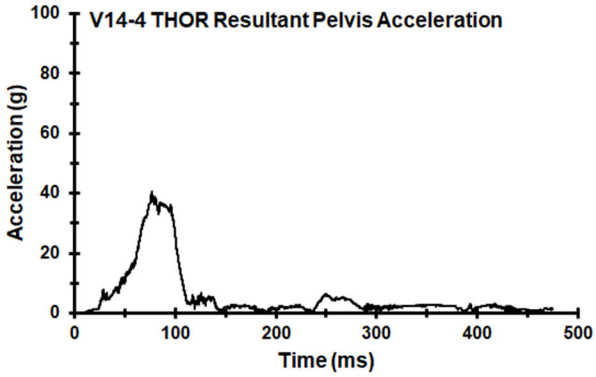
V14-4 THOR Resultant Pelvis Acceleration
Acceleration (g)
100
80
60
40
20
0
0
100
200
300
400
500
Time (ms)

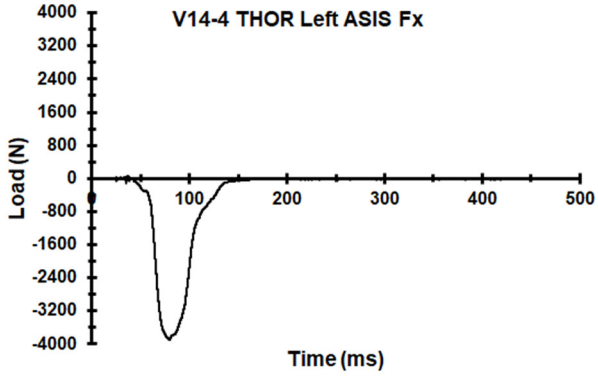
V14-4 THOR Left ASIS Fx
Load (N)
4000
3200
2400
1600
800
0
-800
-1600
-2400
-3200
-4000
100
200
300
400
500
Time (ms)

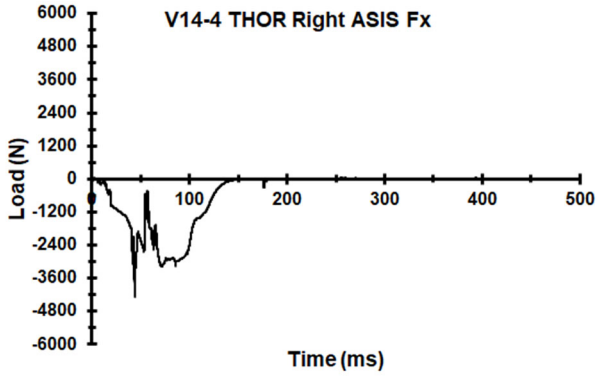
V14-4 THOR Right ASIS Fx
Load (N)
6000
4800
3600
2400
1200
0
-1200
-2400
-3600
-4800
-6000
100
200
300
400
500
Time (ms)

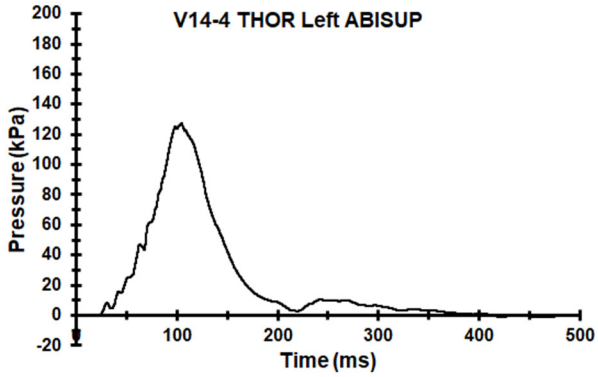
V14-4 THOR Left ABISUP
Pressure (kPa)
200
180
160
140
120
100
80
60
40
20
0
-20
100
200
300
400
500
Time (ms)

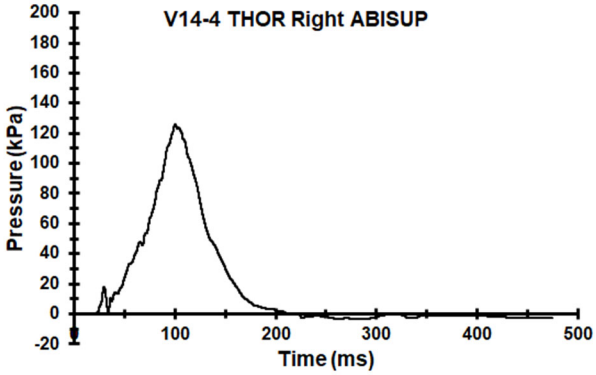
V14-4 THOR Right ABISUP
Pressure (kPa)
200
180
160
140
120
100
80
60
40
20
0
-20
100
200
300
400
500
Time (ms)

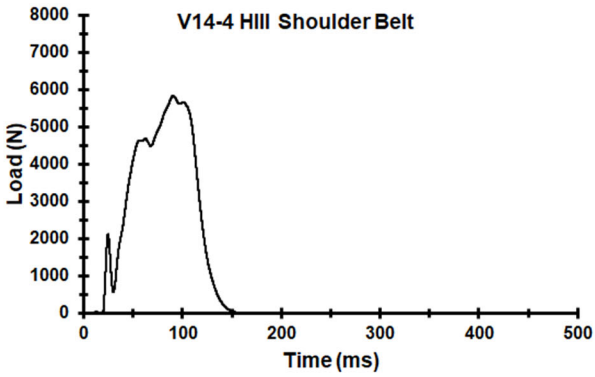
V14-4 HIII Shoulder Belt
Load (N)
8000
7000
6000
5000
4000
3000
2000
1000
0
0
100
200
300
400
500
Time (ms)

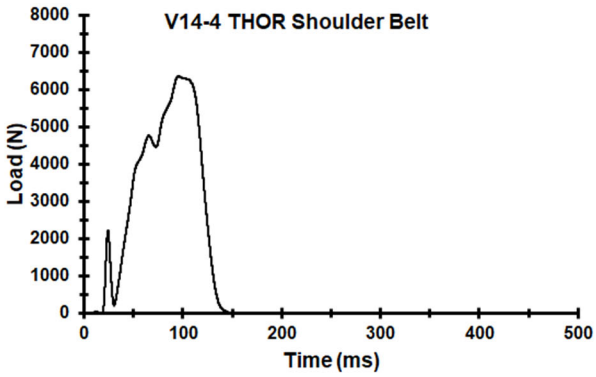
V14-4 THOR Shoulder Belt
Load (N)
8000
7000
6000
5000
4000
3000
2000
1000
0
0
100
200
300
400
500
Time (ms)

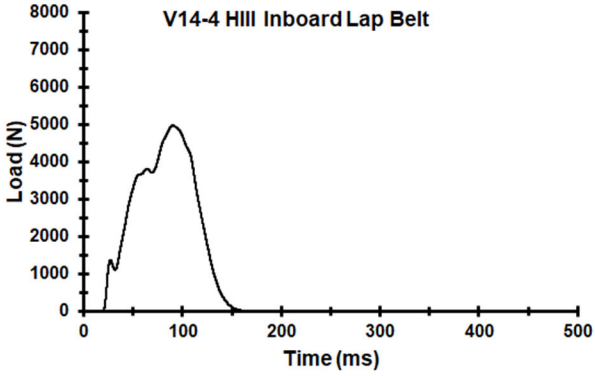
V14-4 HIII Inboard Lap Belt
Load (N)
8000
7000
6000
5000
4000
3000
2000
1000
0
0
100
200
300
400
500
Time (ms)

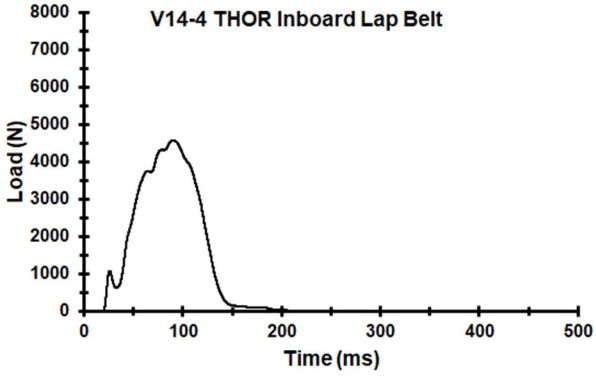
V14-4 THOR Inboard Lap Belt
Load (N)
8000
7000
6000
5000
4000
3000
2000
1000
0
0
100
200
300
400
500
Time (ms)

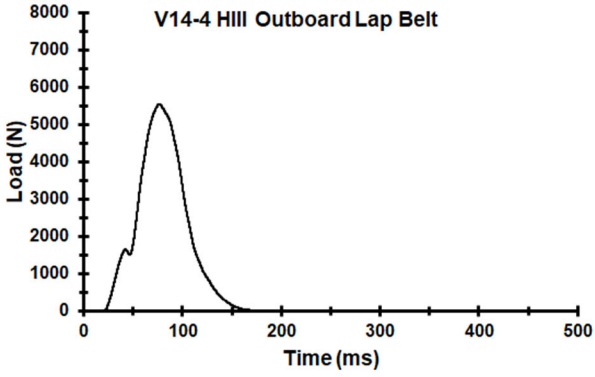
V14-4 HIII Outboard Lap Belt
Load (N)
8000
7000
6000
5000
4000
3000
2000
1000
0
0
100
200
300
400
500
Time (ms)

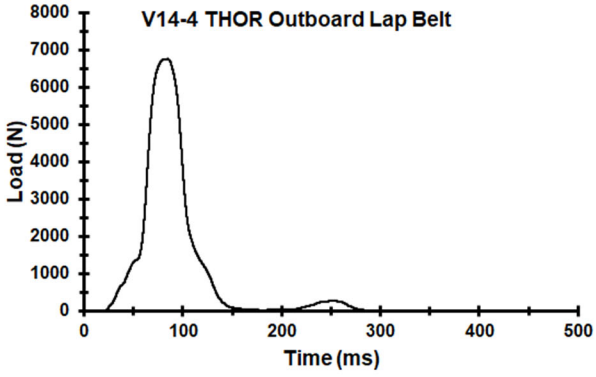
V14-4 THOR Outboard Lap Belt
Load (N)
8000
7000
6000
5000
4000
3000
2000
1000
0
0
100
200
300
400
500
Time (ms)

Appendix AA. Select Data Traces From Test FRS-V15-1

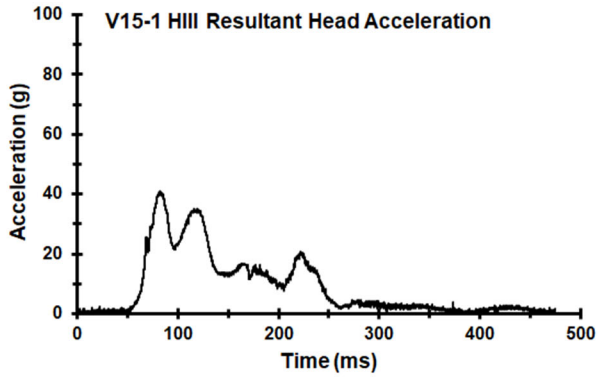
V15-1 HIII Resultant Head Acceleration
Acceleration (g)
Time (ms)

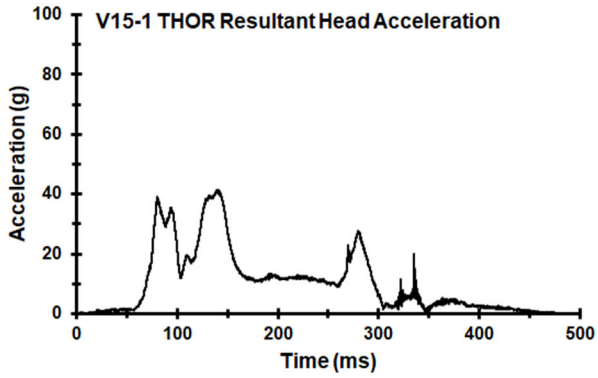
V15-1 THOR Resultant Head Acceleration
Acceleration (g)
Time (ms)

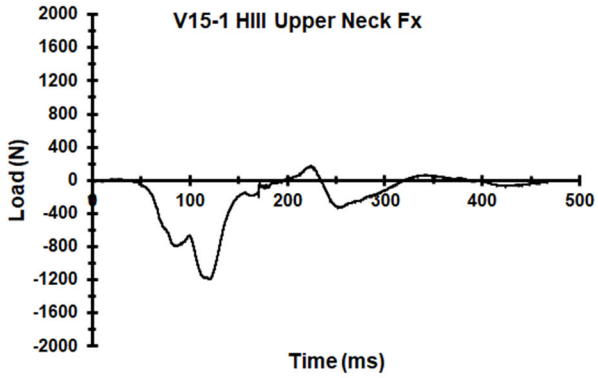
V15-1 HIII Upper Neck Fx
Load (N)
Time (ms)

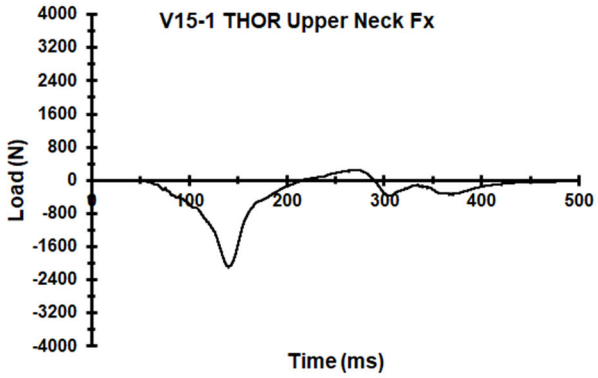
V15-1 THOR Upper Neck Fx
Load (N)
Time (ms)

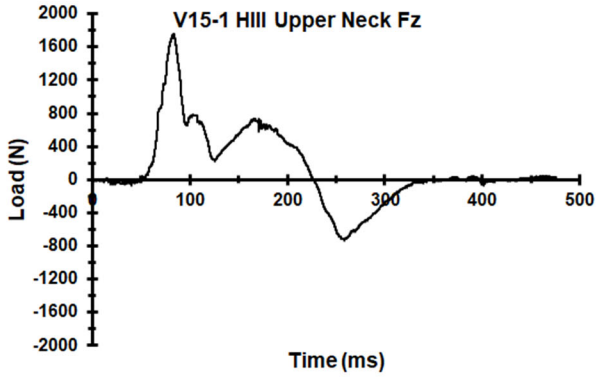
V15-1 HIII Upper Neck Fz
Load (N)
Time (ms)

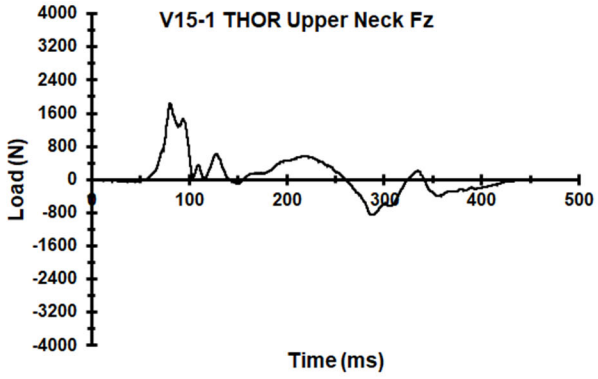
V15-1 THOR Upper Neck Fz
Load (N)
Time (ms)

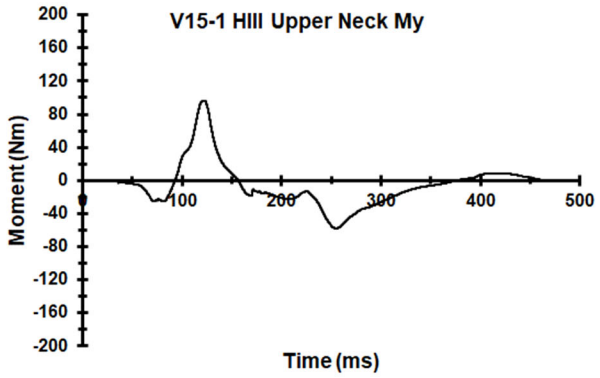
V15-1 HIII Upper Neck My
Moment (Nm)
Time (ms)

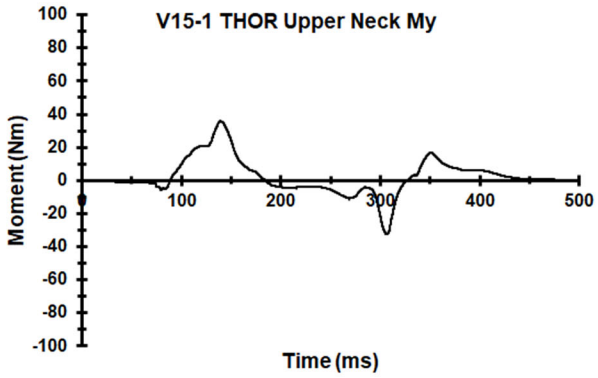
V15-1 THOR Upper Neck My
Moment (Nm)
Time (ms)

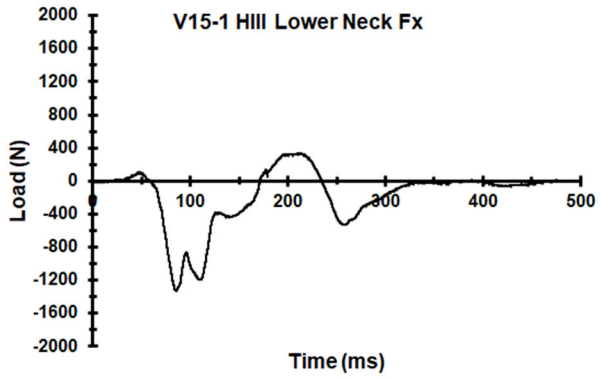
V15-1 HIII Lower Neck Fx
Load (N)
Time (ms)

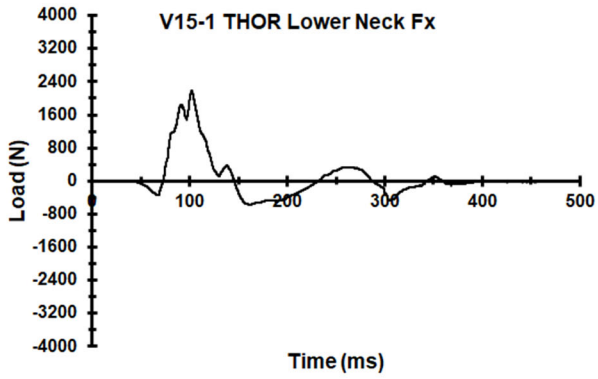
V15-1 THOR Lower Neck Fx
Load (N)
Time (ms)

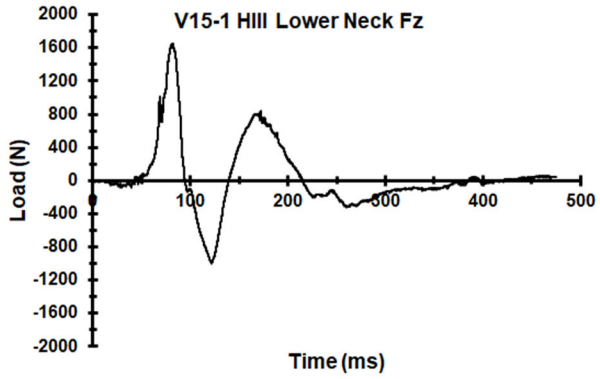
V15-1 HIII Lower Neck Fz
Load (N)
Time (ms)

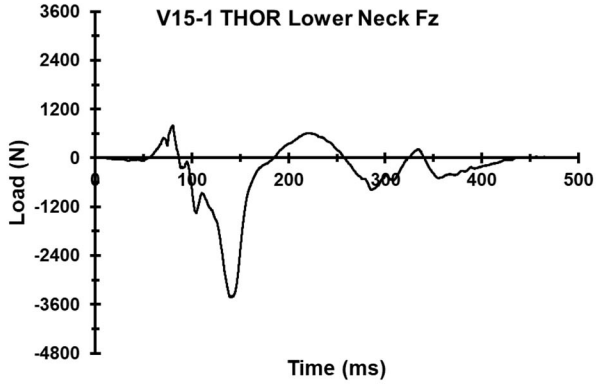
V15-1 THOR Lower Neck Fz
Load (N)
Time (ms)

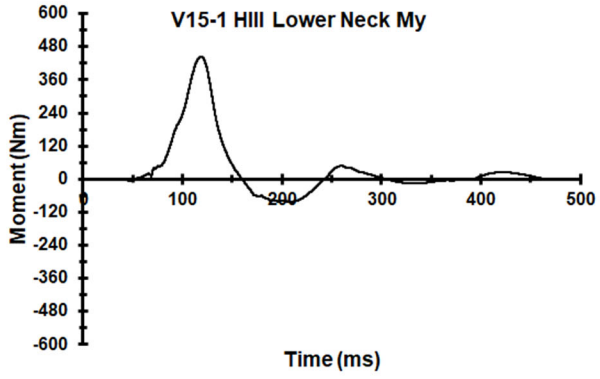
V15-1 HIII Lower Neck My
Moment (Nm)
Time (ms)

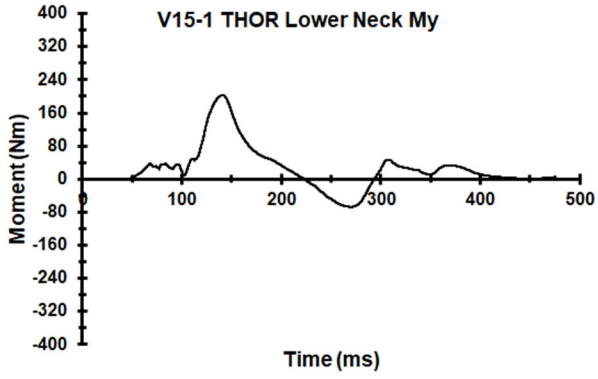
V15-1 THOR Lower Neck My
Moment (Nm)
Time (ms)

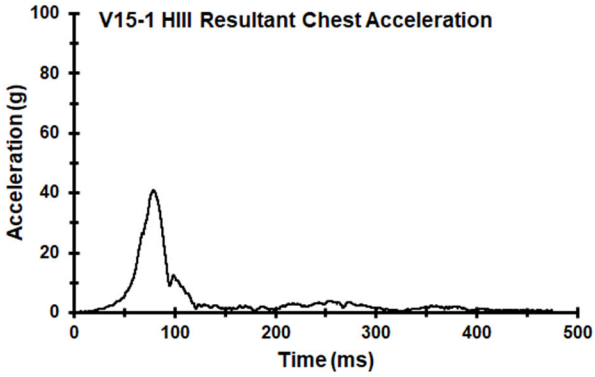
V15-1 HIII Resultant Chest Acceleration
Acceleration (g)
Time (ms)

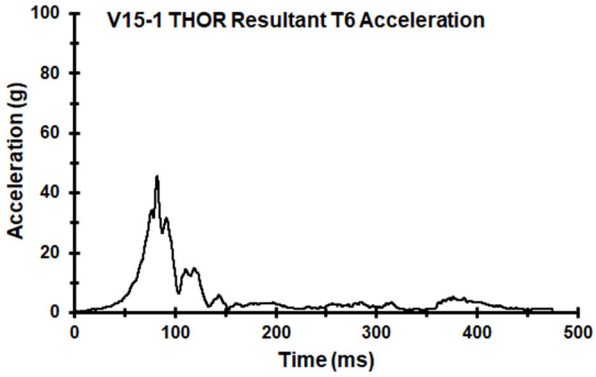
V15-1 THOR Resultant T6 Acceleration
Acceleration (g)
Time (ms)

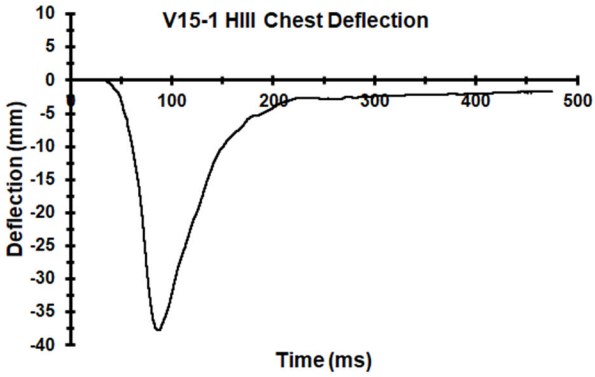
V15-1 HIII Chest Deflection
Deflection (mm)
Time (ms)

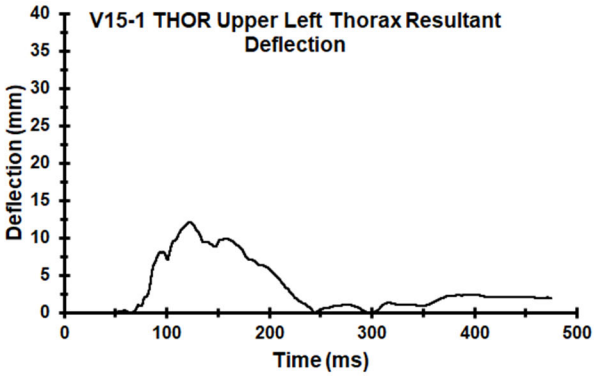
V15-1 THOR Upper Left Thorax Resultant Deflection
Deflection (mm)
Time (ms)

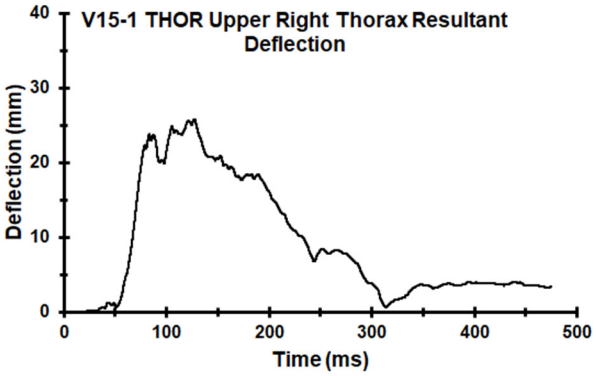
V15-1 THOR Upper Right Thorax Resultant Deflection
Deflection (mm)
Time (ms)

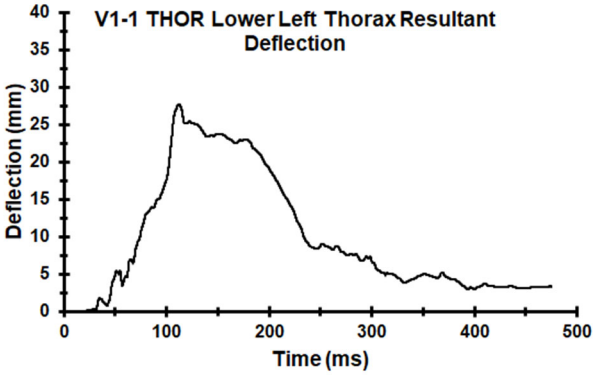
V1-1 THOR Lower Left Thorax Resultant Deflection
Deflection (mm)
Time (ms)

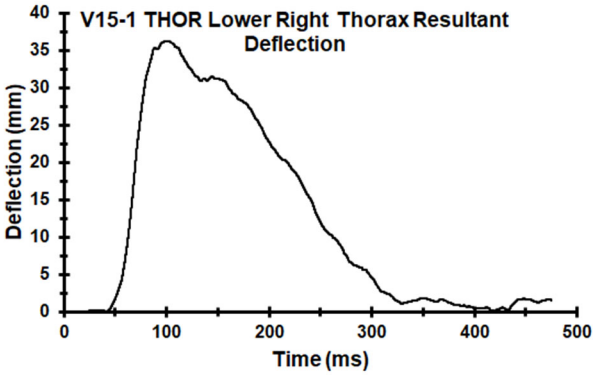
V15-1 THOR Lower Right Thorax Resultant Deflection
Deflection (mm)
Time (ms)

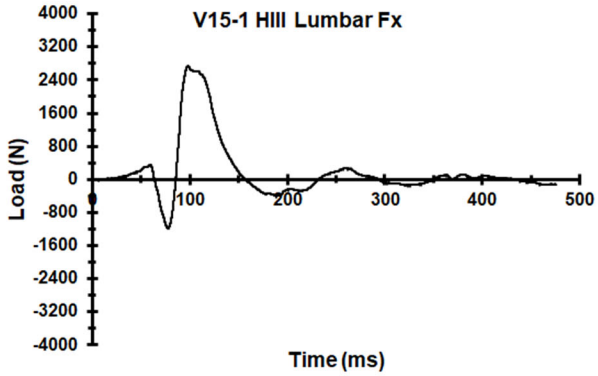
V15-1 HIII Lumbar Fx
Load (N)
Time (ms)

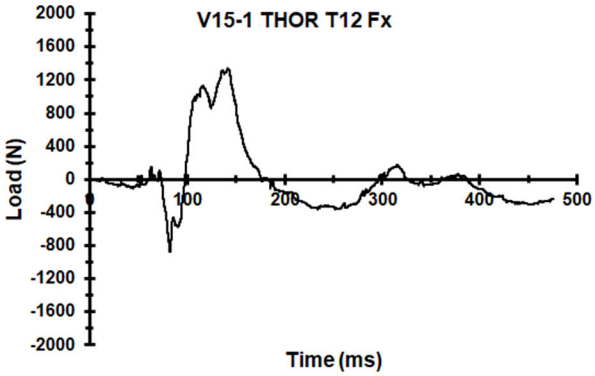
V15-1 THOR T12 Fx
Load (N)
Time (ms)

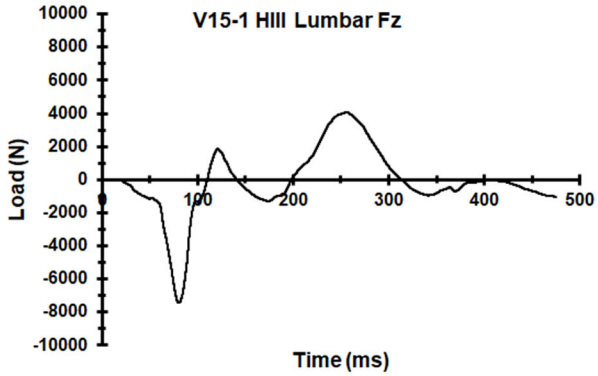
V15-1 HIII Lumbar Fz
Load (N)
Time (ms)

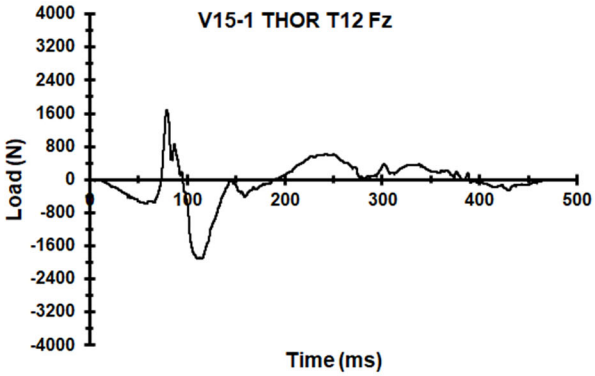
V15-1 THOR T12 Fz
Load (N)
Time (ms)

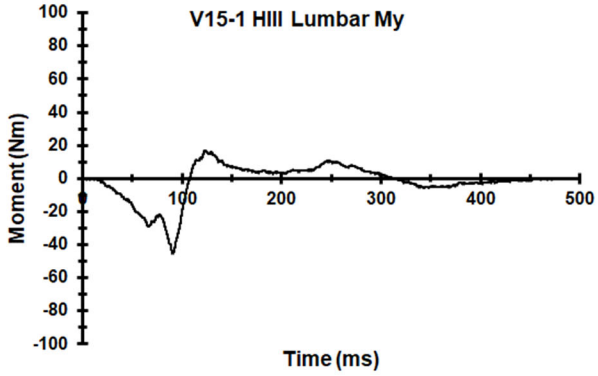
V15-1 HIII Lumbar My
Moment (Nm)
Time (ms)

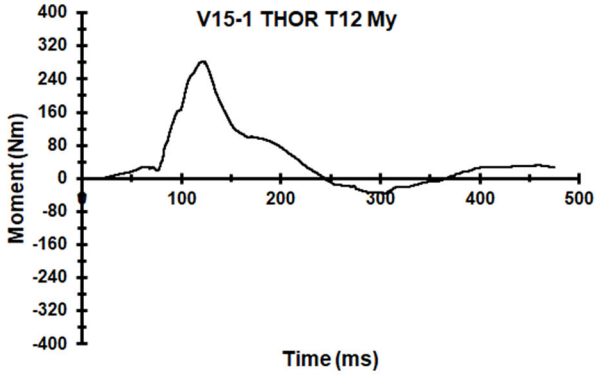
V15-1 THOR T12 My
Moment (Nm)
Time (ms)

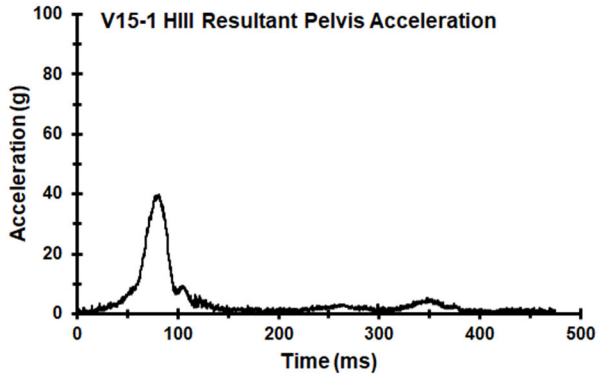
V15-1 HIII Resultant Pelvis Acceleration
Acceleration (g)
Time (ms)

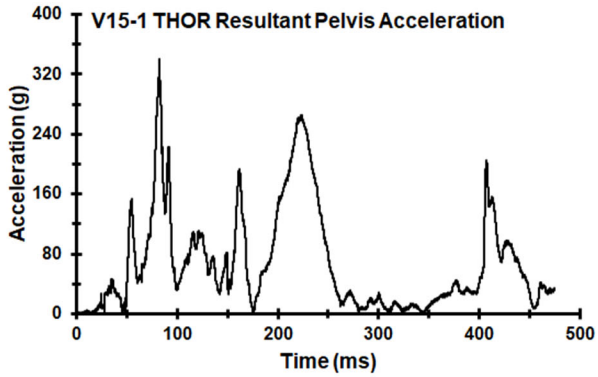
V15-1 THOR Resultant Pelvis Acceleration
Acceleration (g)
Time (ms)

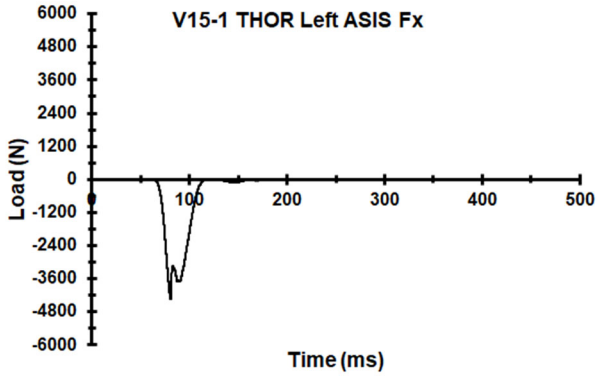
V15-1 THOR Left ASIS Fx
Load (N)
Time (ms)

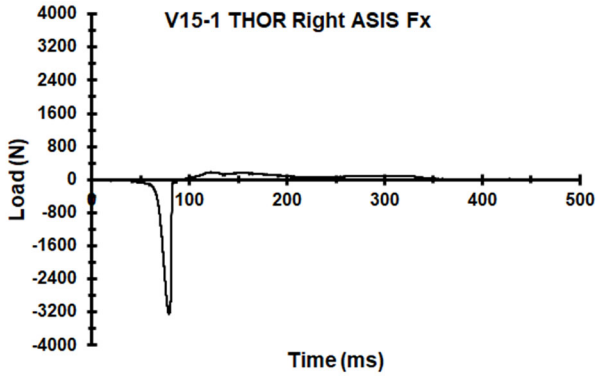
V15-1 THOR Right ASIS Fx
Load (N)
Time (ms)

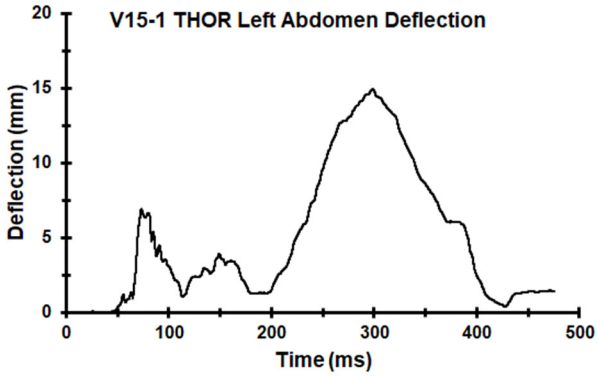
V15-1 THOR Left Abdomen Deflection
Deflection (mm)
0
5
10
15
20
0
100
200
300
400
500
Time (ms)

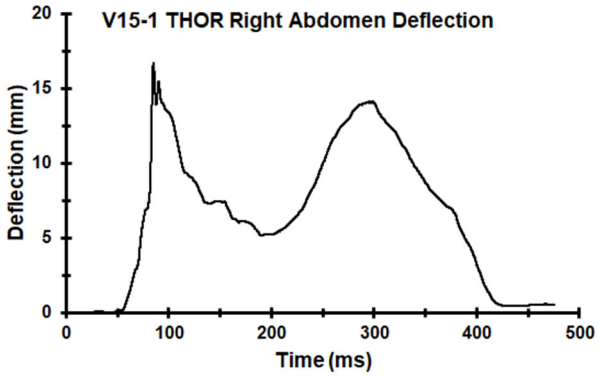
V15-1 THOR Right Abdomen Deflection
Deflection (mm)
0
5
10
15
20
0
100
200
300
400
500
Time (ms)

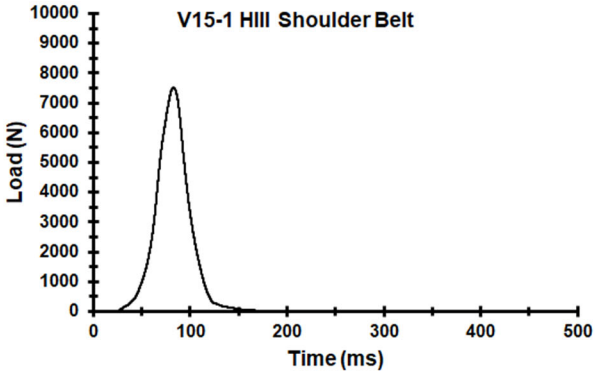
V15-1 HIII Shoulder Belt
Load (N)
0
1000
2000
3000
4000
5000
6000
7000
8000
9000
10000
0
100
200
300
400
500
Time (ms)

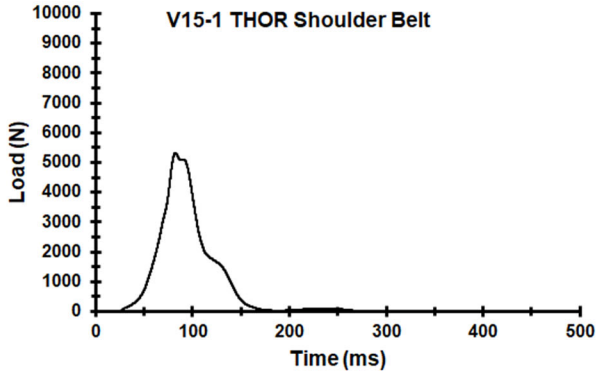
V15-1 THOR Shoulder Belt
Load (N)
0
1000
2000
3000
4000
5000
6000
7000
8000
9000
10000
0
100
200
300
400
500
Time (ms)

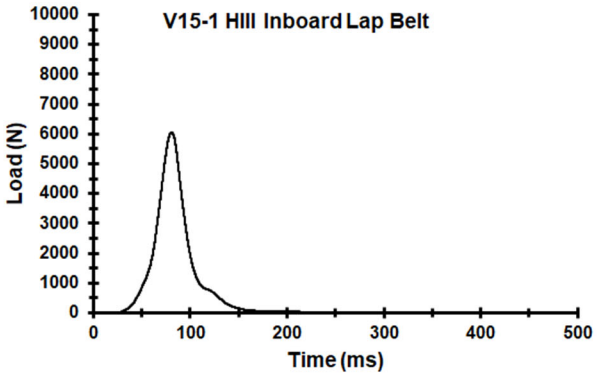
V15-1 HIII Inboard Lap Belt
Load (N)
Time (ms)
10000
9000
8000
7000
6000
5000
4000
3000
2000
1000
0
0
100
200
300
400
500

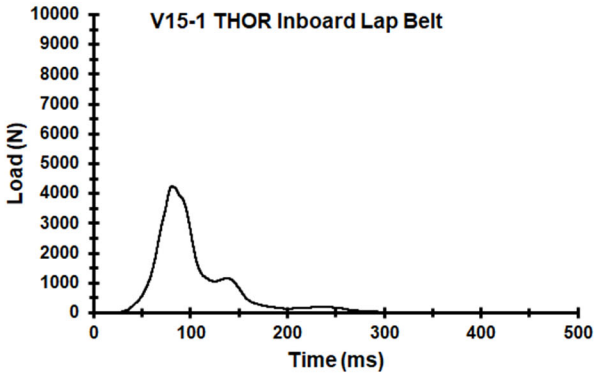
V15-1 THOR Inboard Lap Belt
Load (N)
Time (ms)
10000
9000
8000
7000
6000
5000
4000
3000
2000
1000
0
0
100
200
300
400
500

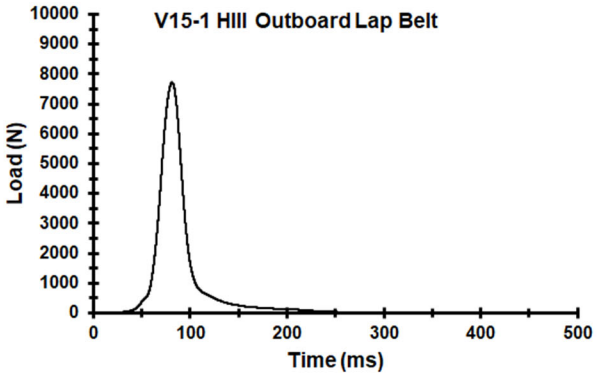
V15-1 HIII Outboard Lap Belt
Load (N)
Time (ms)
10000
9000
8000
7000
6000
5000
4000
3000
2000
1000
0
0
100
200
300
400
500

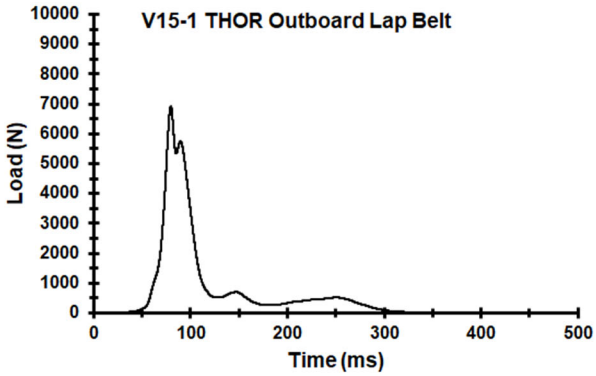
V15-1 THOR Outboard Lap Belt
Load (N)
Time (ms)
10000
9000
8000
7000
6000
5000
4000
3000
2000
1000
0
0
100
200
300
400
500

Appendix BB. Select Data Traces From Test FRS-V15-2

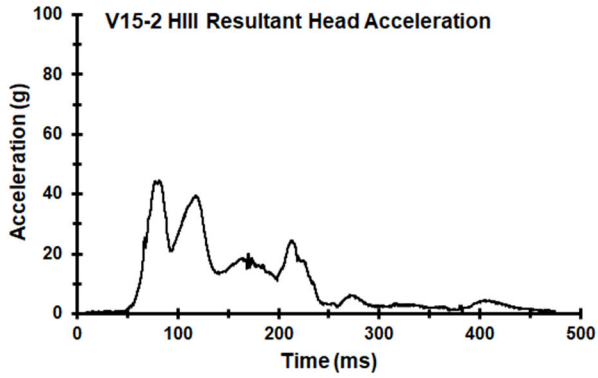
V15-2 HIII Resultant Head Acceleration
Acceleration (g)
Time (ms)

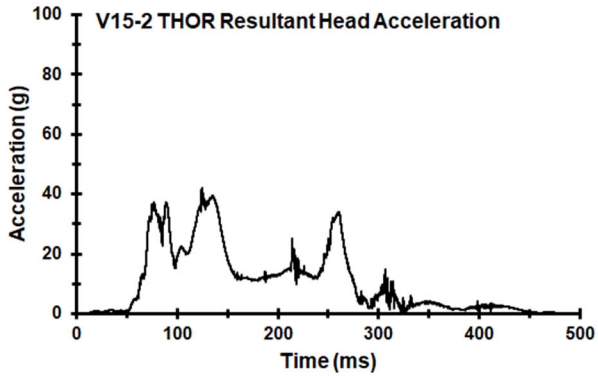
V15-2 THOR Resultant Head Acceleration
Acceleration (g)
Time (ms)

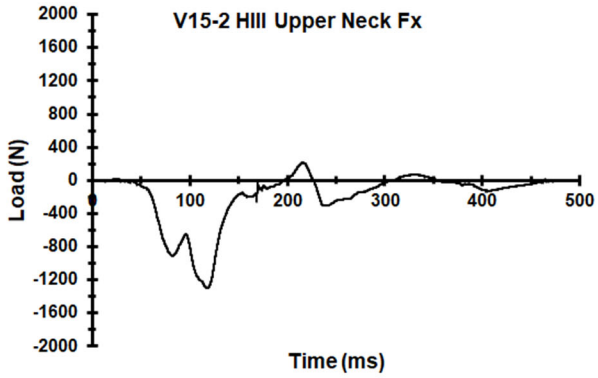
V15-2 HIII Upper Neck Fx
Load (N)
Time (ms)

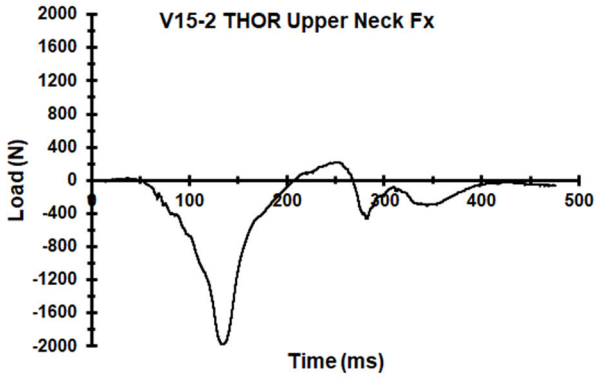
V15-2 THOR Upper Neck Fx
Load (N)
Time (ms)

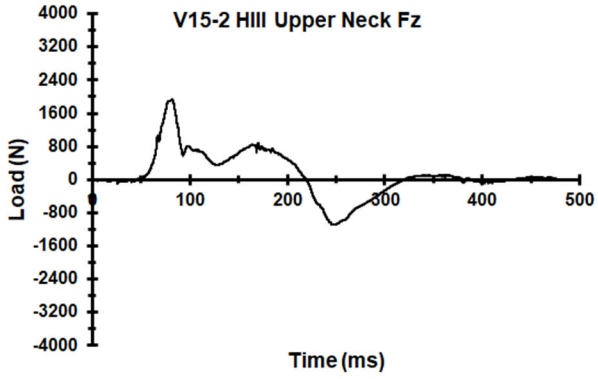
V15-2 HIII Upper Neck Fz
Load (N)
Time (ms)

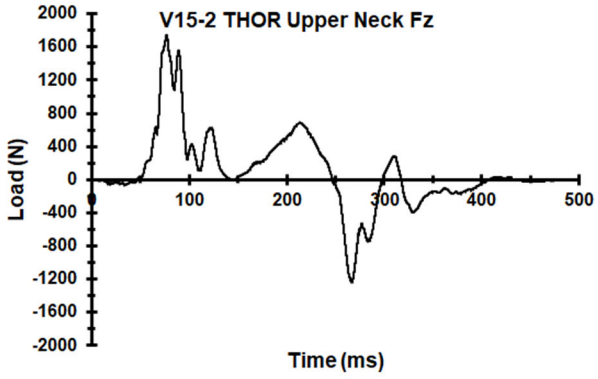
V15-2 THOR Upper Neck Fz
Load (N)
Time (ms)

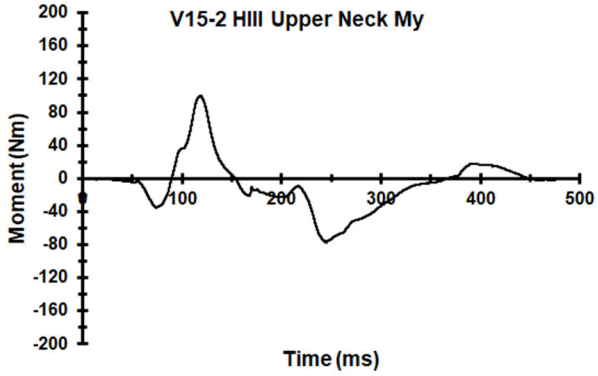
V15-2 HIII Upper Neck My
Moment (Nm)
200
160
120
80
40
0
-40
-80
-120
-160
-200
100
200
300
400
500
Time (ms)

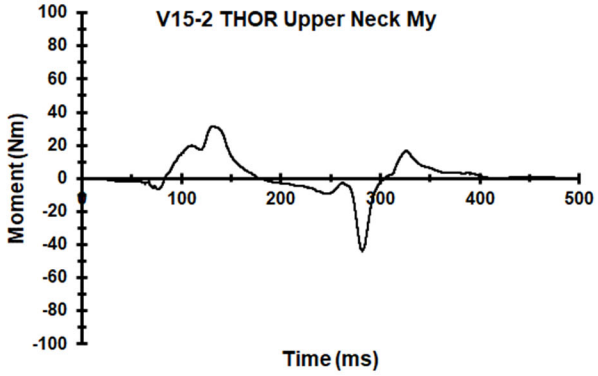
V15-2 THOR Upper Neck My
Moment (Nm)
100
80
60
40
20
0
-20
-40
-60
-80
-100
100
200
300
400
500
Time (ms)

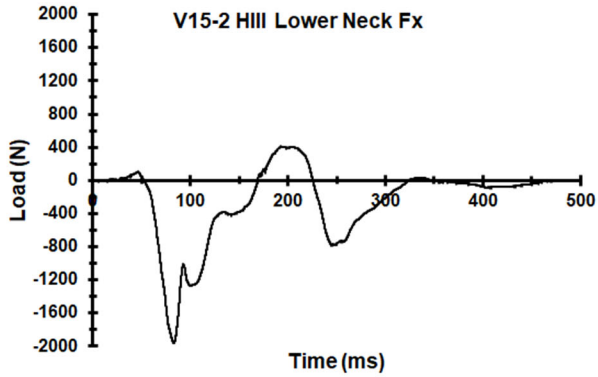
V15-2 HIII Lower Neck Fx
Load (N)
2000
1600
1200
800
400
0
-400
-800
-1200
-1600
-2000
100
200
300
400
500
Time (ms)

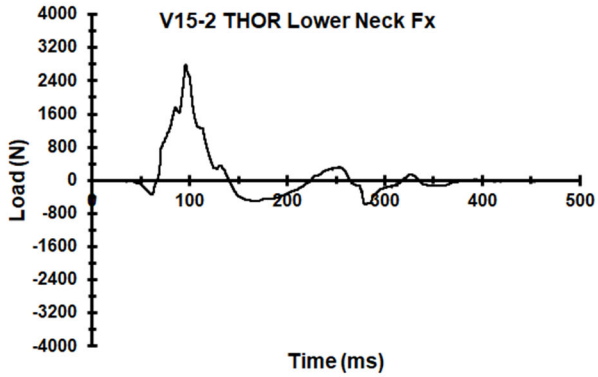
V15-2 THOR Lower Neck Fx
Load (N)
4000
3200
2400
1600
800
0
-800
-1600
-2400
-3200
-4000
100
200
300
400
500
Time (ms)

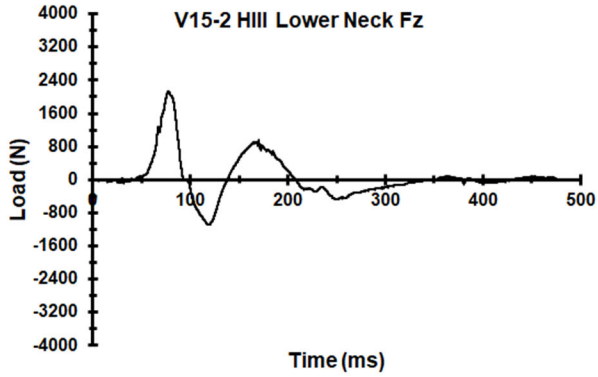
V15-2 HIII Lower Neck Fz
Load (N)
4000
3200
2400
1600
800
0
-800
-1600
-2400
-3200
-4000
100
200
300
400
500
Time (ms)

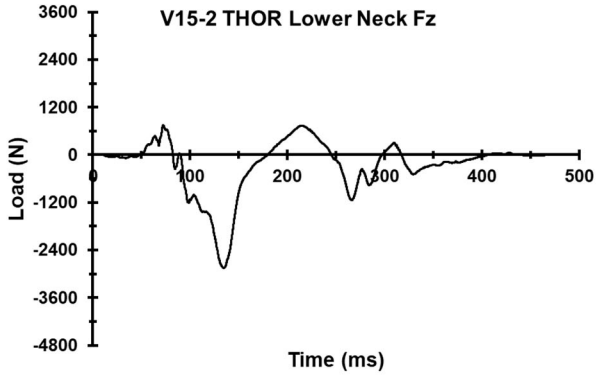
V15-2 THOR Lower Neck Fz
Load (N)
3600
2400
1200
0
-1200
-2400
-3600
-4800
100
200
300
400
500
Time (ms)

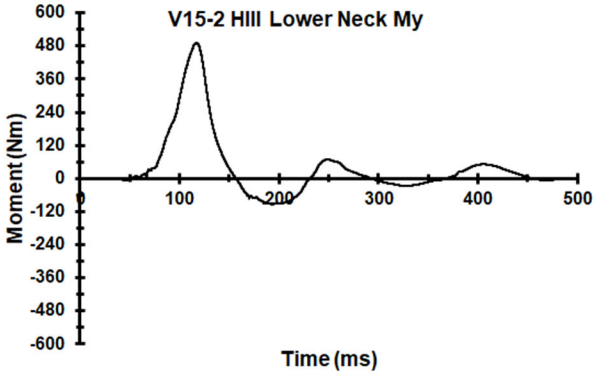
V15-2 HIII Lower Neck My
Moment (Nm)
600
480
360
240
120
0
-120
-240
-360
-480
-600
0
100
200
300
400
500
Time (ms)

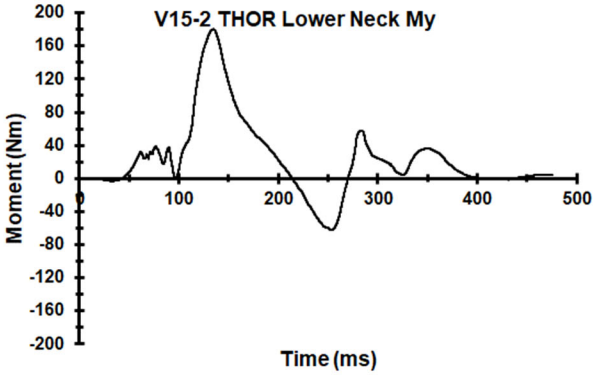
V15-2 THOR Lower Neck My
Moment (Nm)
200
160
120
80
40
0
-40
-80
-120
-160
-200
0
100
200
300
400
500
Time (ms)

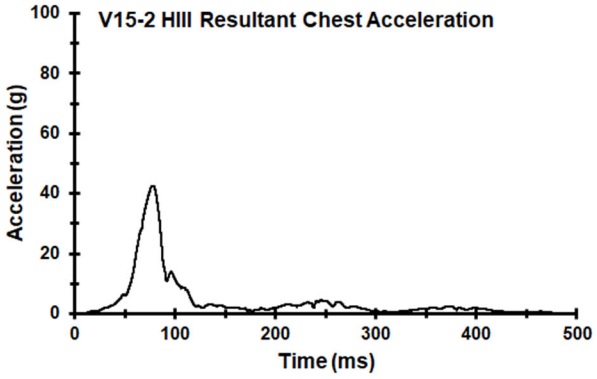
V15-2 HIII Resultant Chest Acceleration
Acceleration (g)
100
80
60
40
20
0
0
100
200
300
400
500
Time (ms)

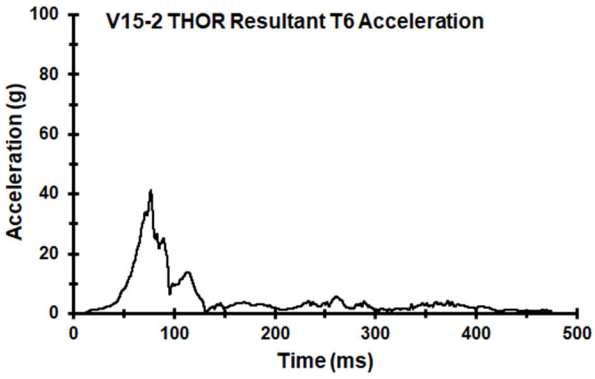
V15-2 THOR Resultant T6 Acceleration
Acceleration (g)
100
80
60
40
20
0
0
100
200
300
400
500
Time (ms)

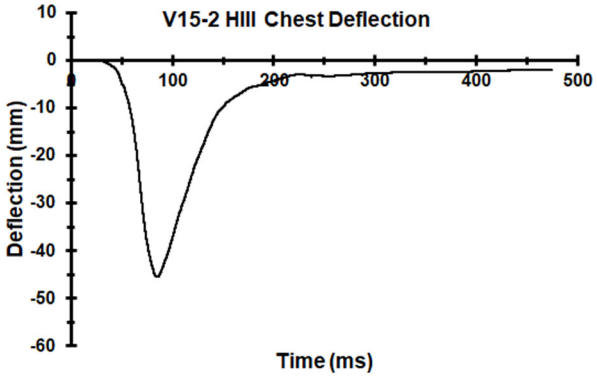
V15-2 HIII Chest Deflection
Deflection (mm)
10
0
-10
-20
-30
-40
-50
-60
0
100
200
300
400
500
Time (ms)

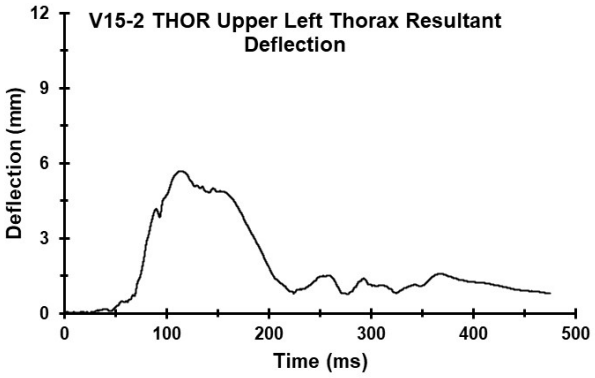
V15-2 THOR Upper Left Thorax Resultant Deflection
Deflection (mm)
12
9
6
3
0
0
100
200
300
400
500
Time (ms)

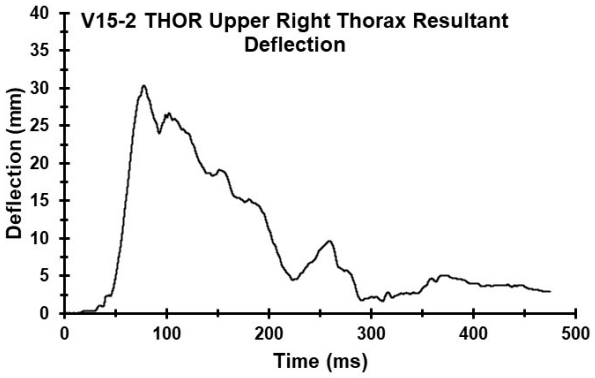
V15-2 THOR Upper Right Thorax Resultant Deflection
Deflection (mm)
40
35
30
25
20
15
10
5
0
0
100
200
300
400
500
Time (ms)

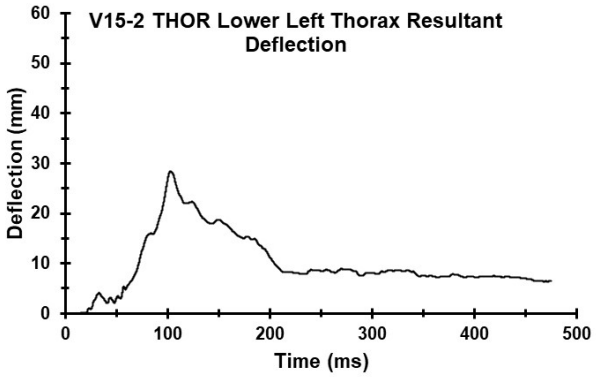
V15-2 THOR Lower Left Thorax Resultant Deflection
Deflection (mm)
60
50
40
30
20
10
0
0
100
200
300
400
500
Time (ms)

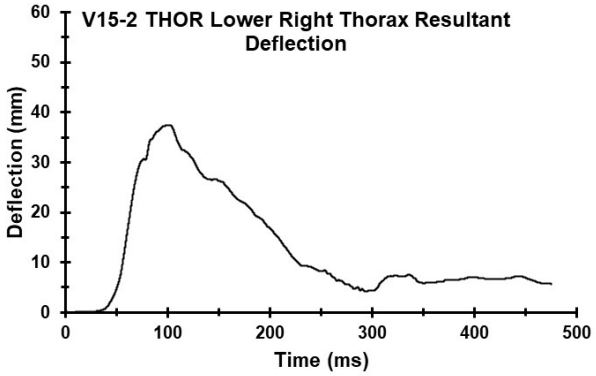
V15-2 THOR Lower Right Thorax Resultant Deflection
Deflection (mm)
60
50
40
30
20
10
0
0
100
200
300
400
500
Time (ms)

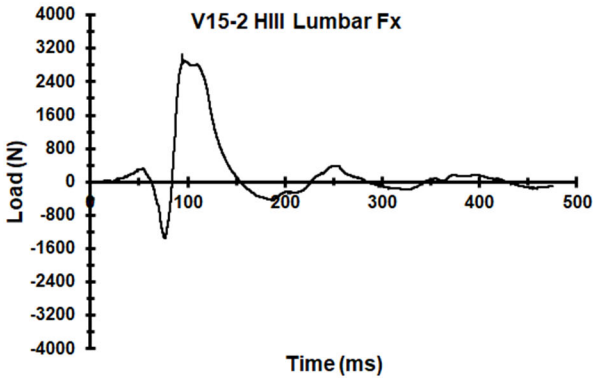
V15-2 HIII Lumbar Fx
Load (N)
4000
3200
2400
1600
800
0
-800
-1600
-2400
-3200
-4000
0
100
200
300
400
500
Time (ms)

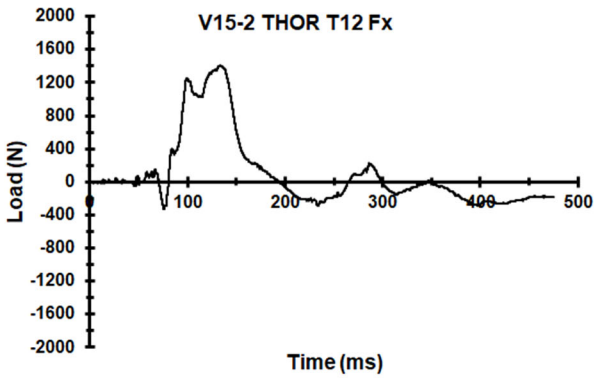
V15-2 THOR T12 Fx
Load (N)
2000
1600
1200
800
400
0
-400
-800
-1200
-1600
-2000
0
100
200
300
400
500
Time (ms)

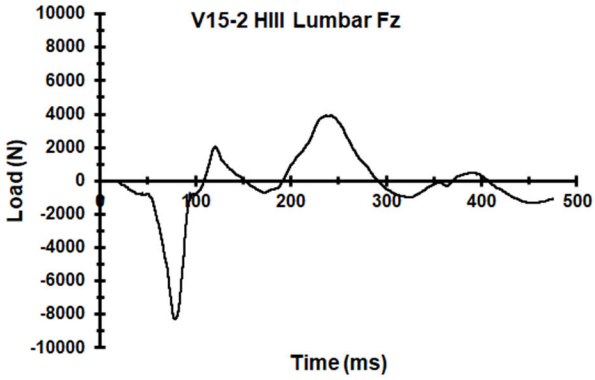
V15-2 HIII Lumbar Fz
Load (N)
Time (ms)

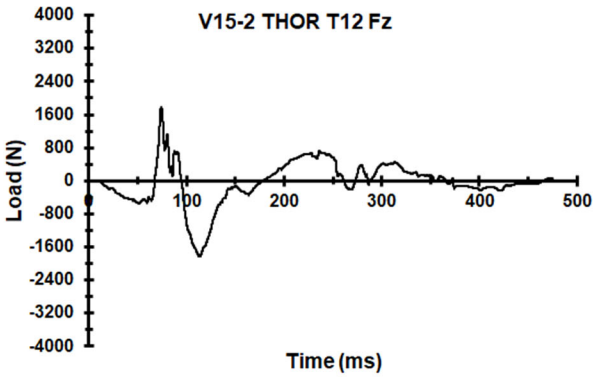
V15-2 THOR T12 Fz
Load (N)
Time (ms)

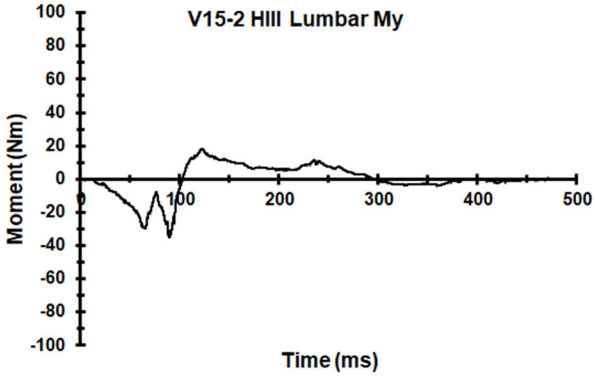
V15-2 HIII Lumbar My
Moment (Nm)
Time (ms)

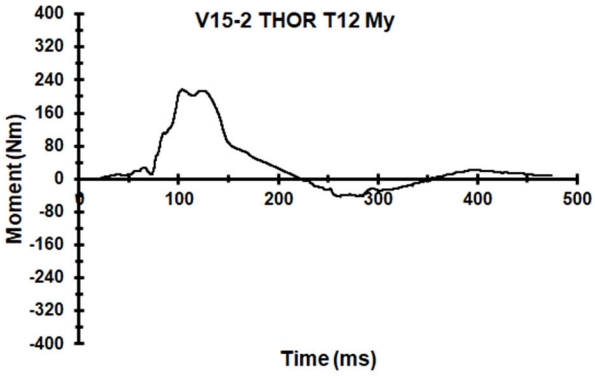
V15-2 THOR T12 My
Moment (Nm)
Time (ms)

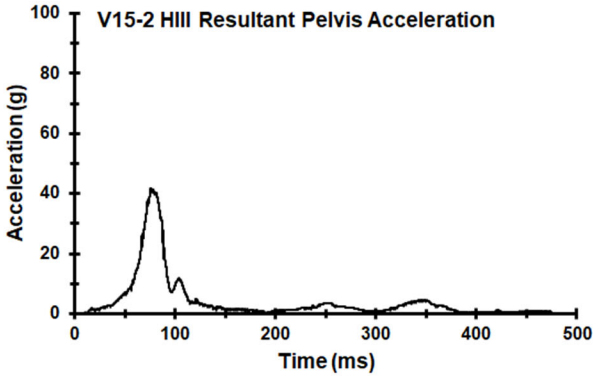
V15-2 HIII Resultant Pelvis Acceleration
Acceleration (g)
Time (ms)

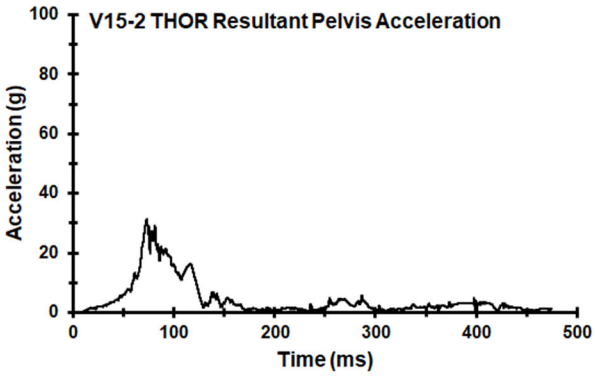
V15-2 THOR Resultant Pelvis Acceleration
Acceleration (g)
Time (ms)

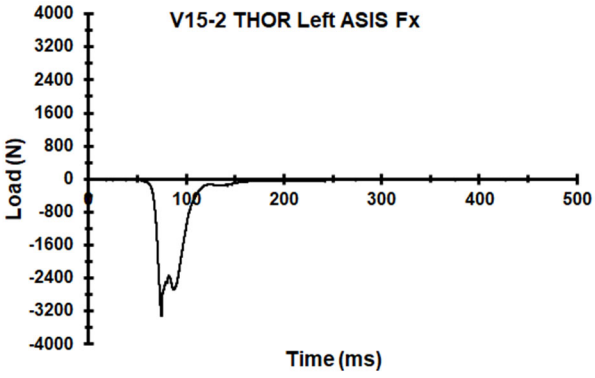
V15-2 THOR Left ASIS Fx
Load (N)
Time (ms)

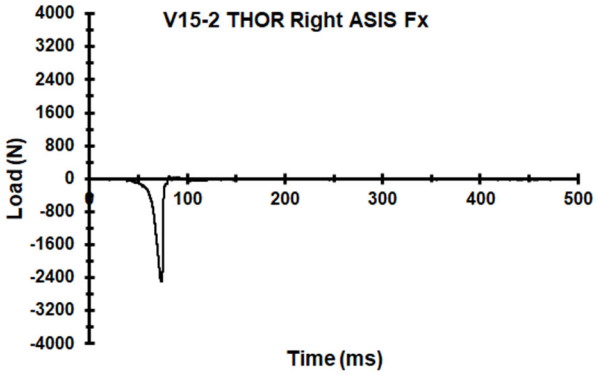
V15-2 THOR Right ASIS Fx
Load (N)
4000
3200
2400
1600
800
0
-800
-1600
-2400
-3200
-4000
100
200
300
400
500
Time (ms)

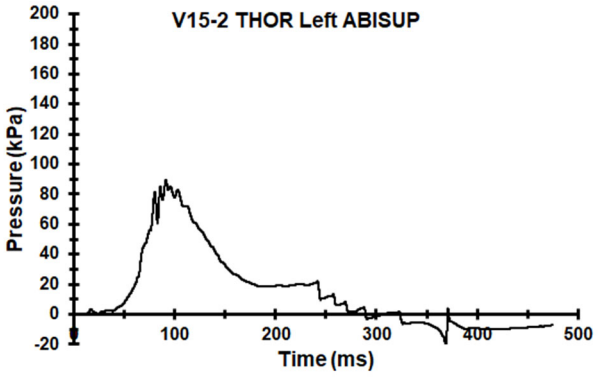
V15-2 THOR Left ABISUP
Pressure (kPa)
200
180
160
140
120
100
80
60
40
20
0
-20
100
200
300
400
500
Time (ms)

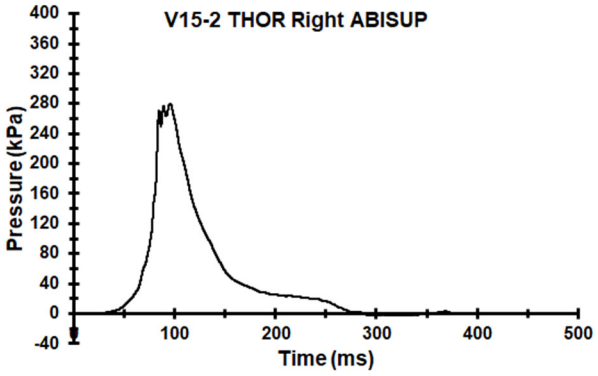
V15-2 THOR Right ABISUP
Pressure (kPa)
400
360
320
280
240
200
160
120
80
40
0
-40
100
200
300
400
500
Time (ms)

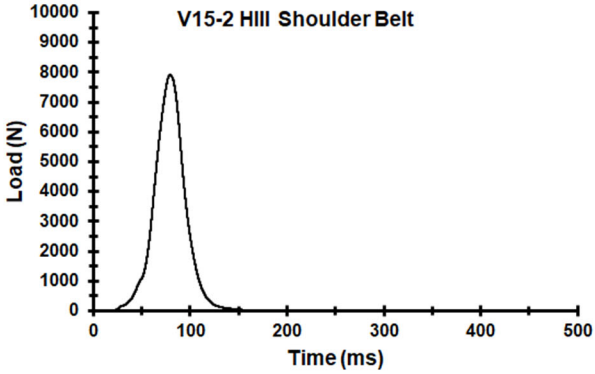
V15-2 HIII Shoulder Belt
Load (N)
Time (ms)

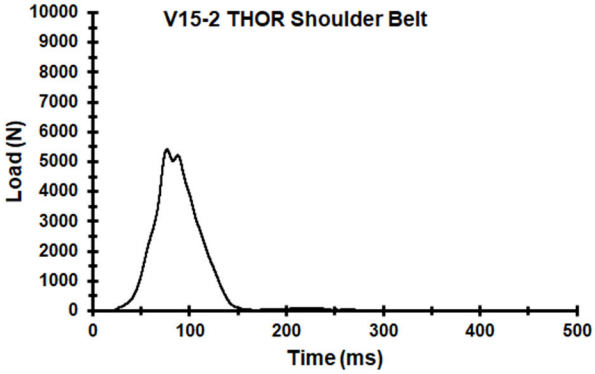
V15-2 THOR Shoulder Belt
Load (N)
Time (ms)

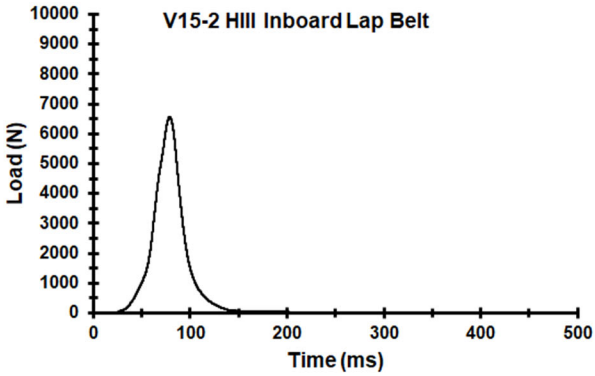
V15-2 HIII Inboard Lap Belt
Load (N)
Time (ms)

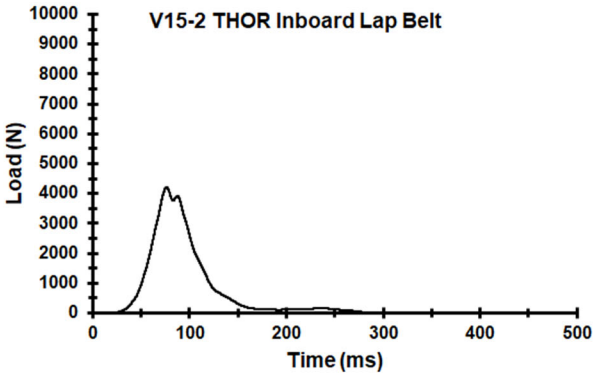
V15-2 THOR Inboard Lap Belt
Load (N)
Time (ms)

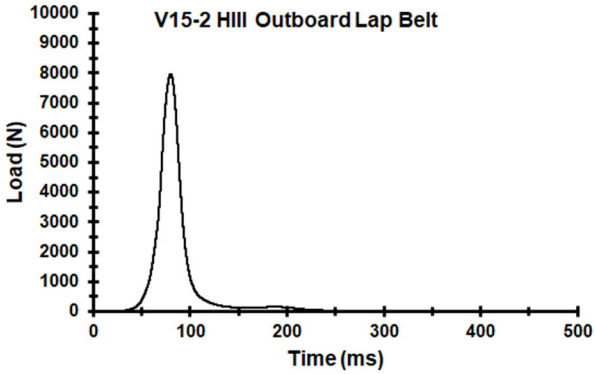
V15-2 HIII Outboard Lap Belt
Load (N)
Time (ms)

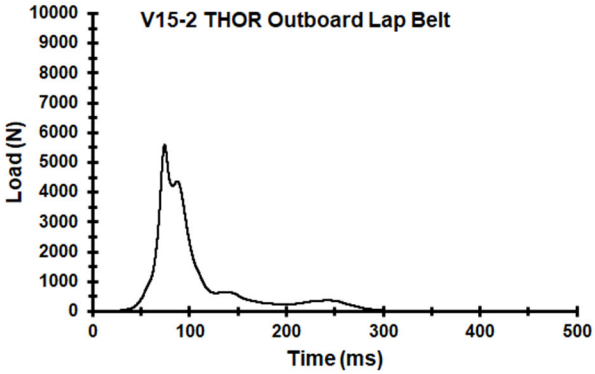
V15-2 THOR Outboard Lap Belt
Load (N)
Time (ms)

Appendix CC. Select Data Traces From Test FRS-V15-3

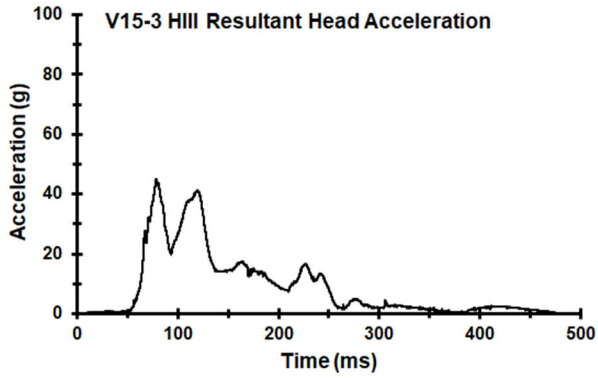
V15-3 HIII Resultant Head Acceleration
Acceleration (g)
Time (ms)

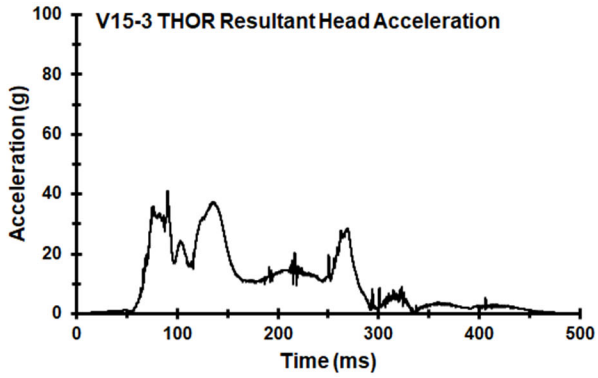
V15-3 THOR Resultant Head Acceleration
Acceleration (g)
Time (ms)

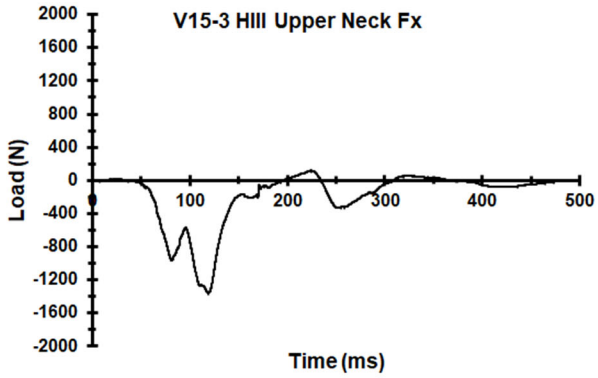
V15-3 HIII Upper Neck Fx
Load (N)
Time (ms)

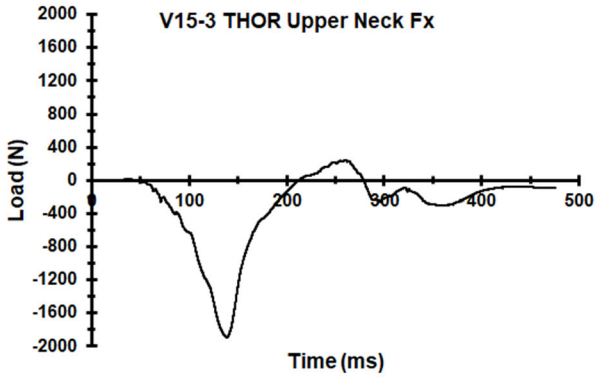
V15-3 THOR Upper Neck Fx
Load (N)
Time (ms)

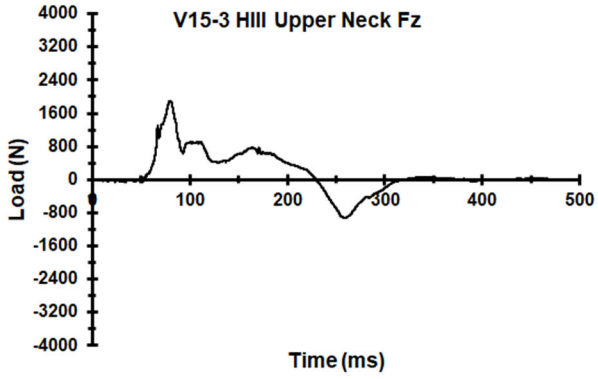
V15-3 HIII Upper Neck Fz
Load (N)
Time (ms)

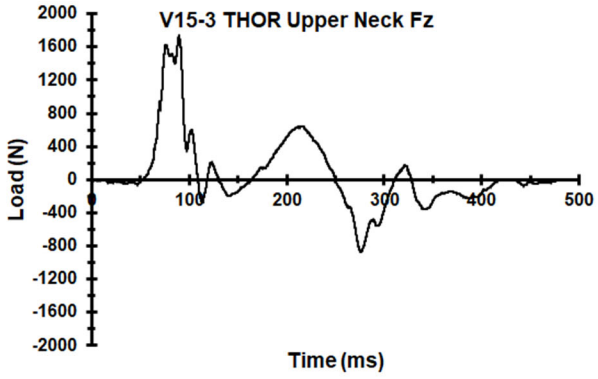
V15-3 THOR Upper Neck Fz
Load (N)
Time (ms)

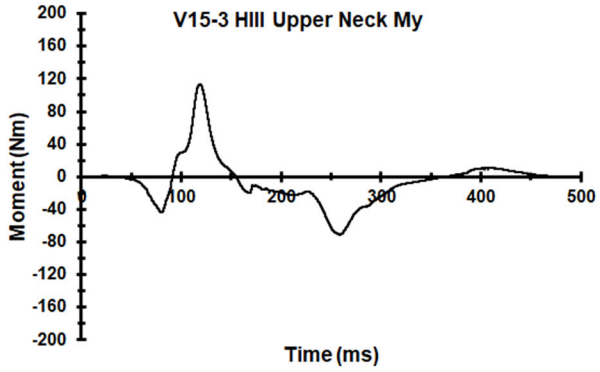
V15-3 HIII Upper Neck My
Moment (Nm)
200
160
120
80
40
0
-40
-80
-120
-160
-200
0
100
200
300
400
500
Time (ms)

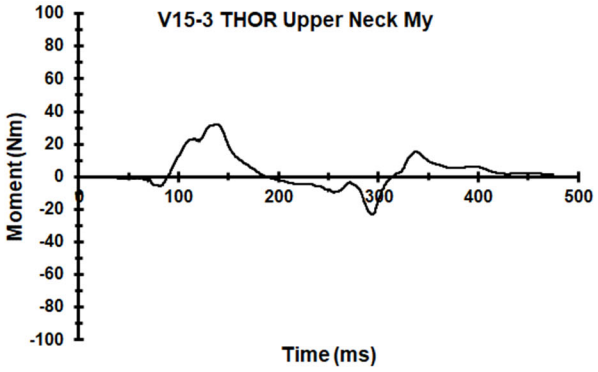
V15-3 THOR Upper Neck My
Moment (Nm)
100
80
60
40
20
0
-20
-40
-60
-80
-100
0
100
200
300
400
500
Time (ms)

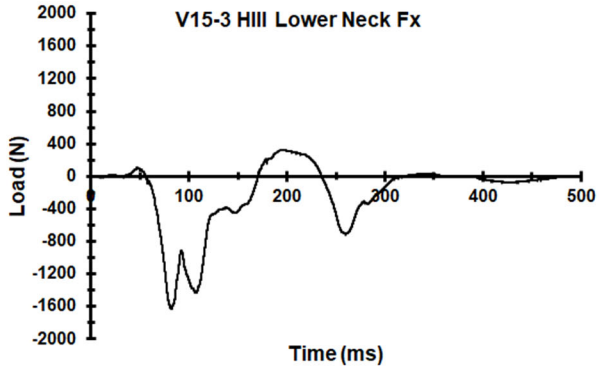
V15-3 HIII Lower Neck Fx
Load (N)
2000
1600
1200
800
400
0
-400
-800
-1200
-1600
-2000
0
100
200
300
400
500
Time (ms)

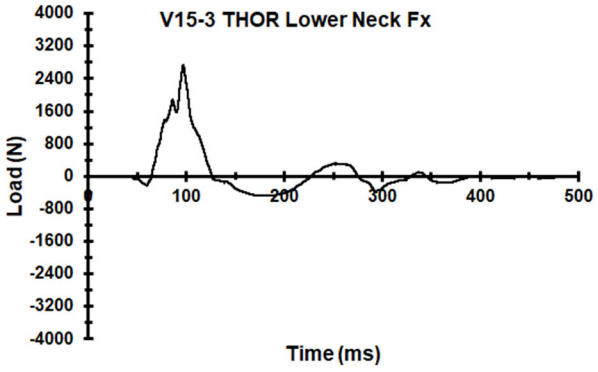
V15-3 THOR Lower Neck Fx
Load (N)
4000
3200
2400
1600
800
0
-800
-1600
-2400
-3200
-4000
0
100
200
300
400
500
Time (ms)

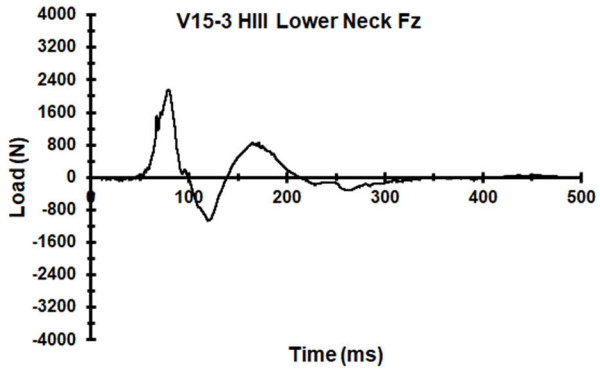
V15-3 HIII Lower Neck Fz
Load (N)
4000
3200
2400
1600
800
0
-800
-1600
-2400
-3200
-4000
0
100
200
300
400
500
Time (ms)

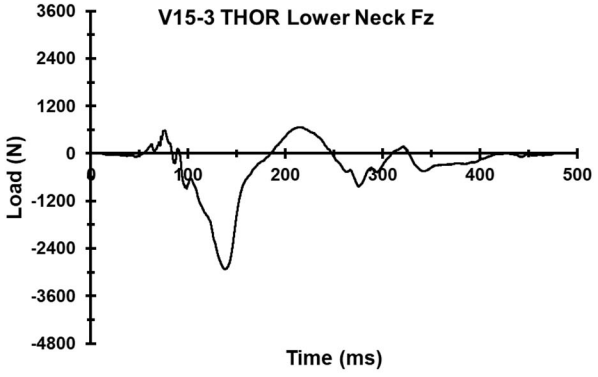
V15-3 THOR Lower Neck Fz
Load (N)
3600
2400
1200
0
-1200
-2400
-3600
-4800
0
100
200
300
400
500
Time (ms)

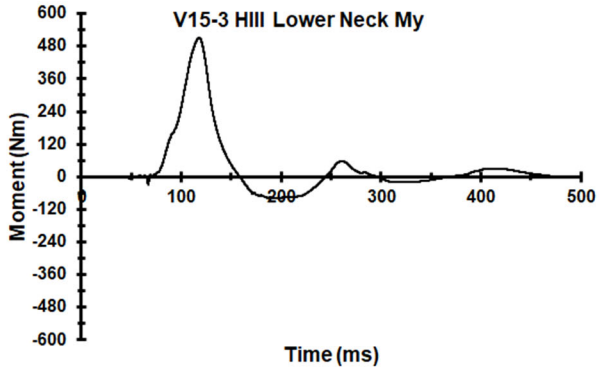
V15-3 HIII Lower Neck My
Moment (Nm)
600
480
360
240
120
0
-120
-240
-360
-480
-600
0
100
200
300
400
500
Time (ms)

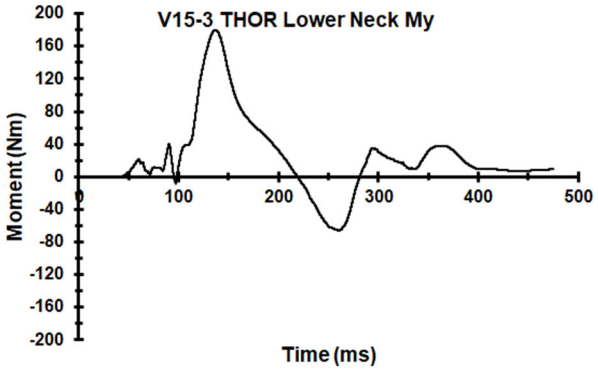
V15-3 THOR Lower Neck My
Moment (Nm)
200
160
120
80
40
0
-40
-80
-120
-160
-200
0
100
200
300
400
500
Time (ms)

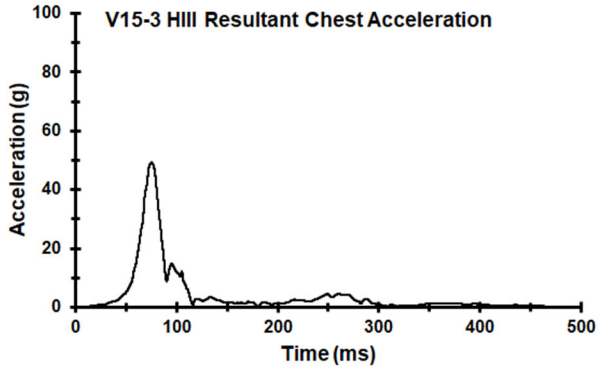
V15-3 HIII Resultant Chest Acceleration
Acceleration (g)
100
80
60
40
20
0
0
100
200
300
400
500
Time (ms)

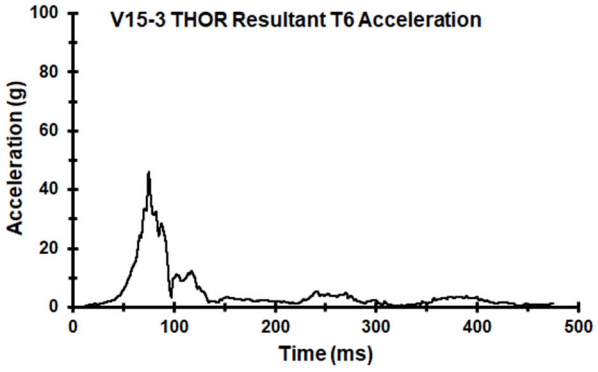
V15-3 THOR Resultant T6 Acceleration
Acceleration (g)
100
80
60
40
20
0
0
100
200
300
400
500
Time (ms)

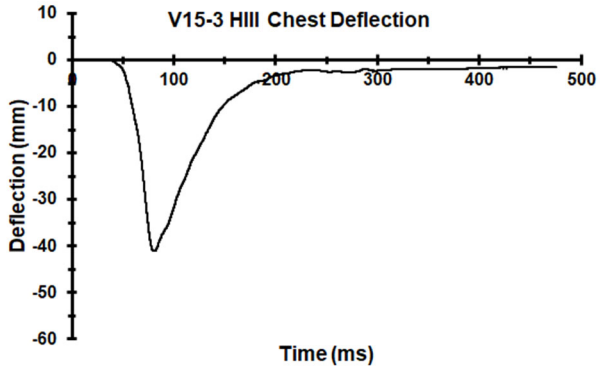
V15-3 HIII Chest Deflection
Deflection (mm)
10
0
-10
-20
-30
-40
-50
-60
0
100
200
300
400
500
Time (ms)

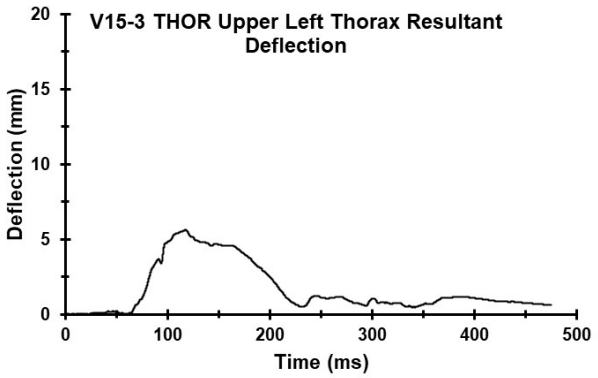
V15-3 THOR Upper Left Thorax Resultant Deflection
Deflection (mm)
20
15
10
5
0
0
100
200
300
400
500
Time (ms)

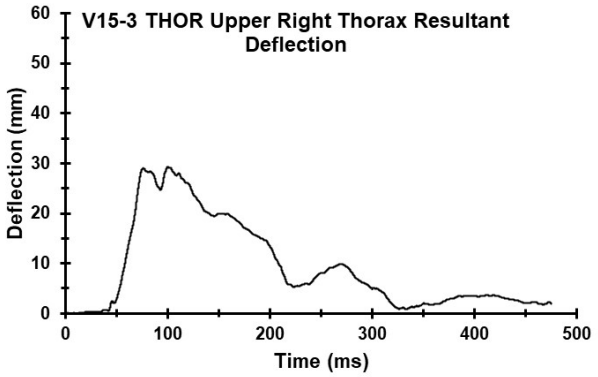
V15-3 THOR Upper Right Thorax Resultant Deflection
Deflection (mm)
60
50
40
30
20
10
0
0
100
200
300
400
500
Time (ms)

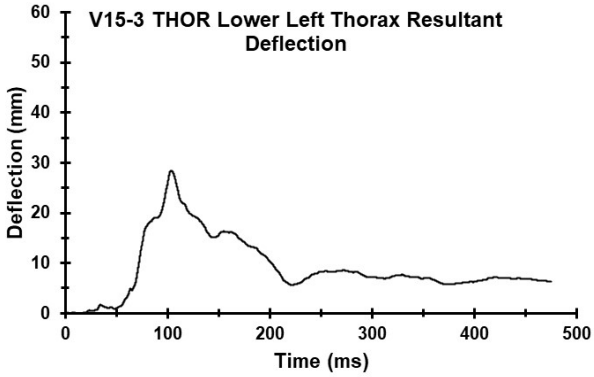
V15-3 THOR Lower Left Thorax Resultant Deflection
Deflection (mm)
60
50
40
30
20
10
0
0
100
200
300
400
500
Time (ms)

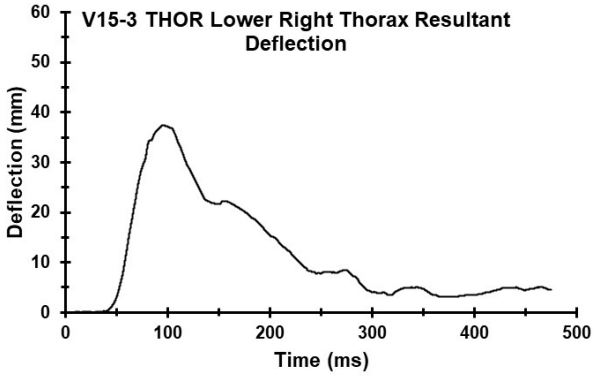
V15-3 THOR Lower Right Thorax Resultant Deflection
Deflection (mm)
60
50
40
30
20
10
0
0
100
200
300
400
500
Time (ms)

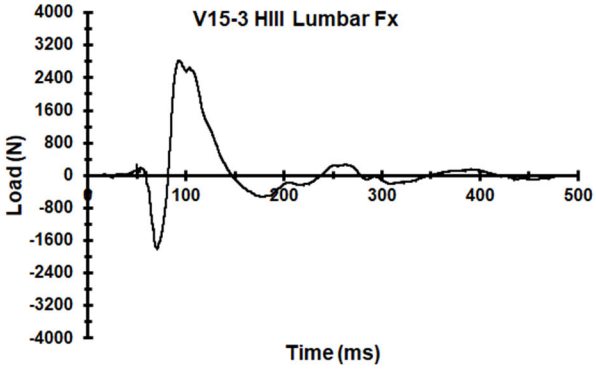
V15-3 HIII Lumbar Fx
Load (N)
4000
3200
2400
1600
800
0
-800
-1600
-2400
-3200
-4000
0
100
200
300
400
500
Time (ms)

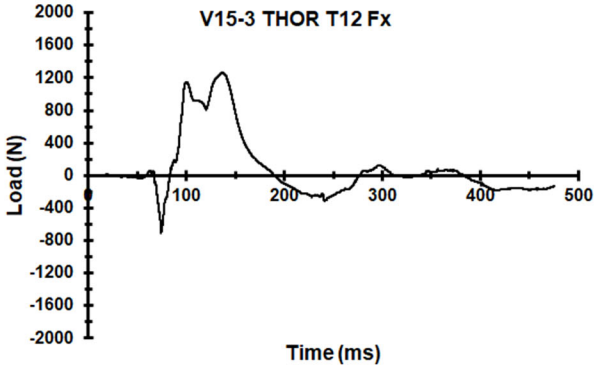
V15-3 THOR T12 Fx
Load (N)
2000
1600
1200
800
400
0
-400
-800
-1200
-1600
-2000
0
100
200
300
400
500
Time (ms)

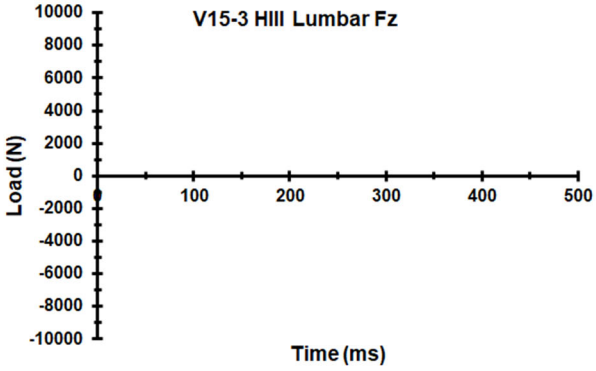
V15-3 HIII Lumbar Fz
Load (N)
10000
8000
6000
4000
2000
0
-2000
-4000
-6000
-8000
-10000
0
100
200
300
400
500
Time (ms)

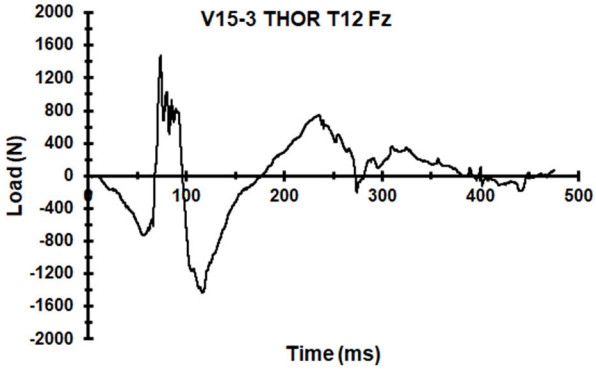
V15-3 THOR T12 Fz
Load (N)
2000
1600
1200
800
400
0
-400
-800
-1200
-1600
-2000
0
100
200
300
400
500
Time (ms)

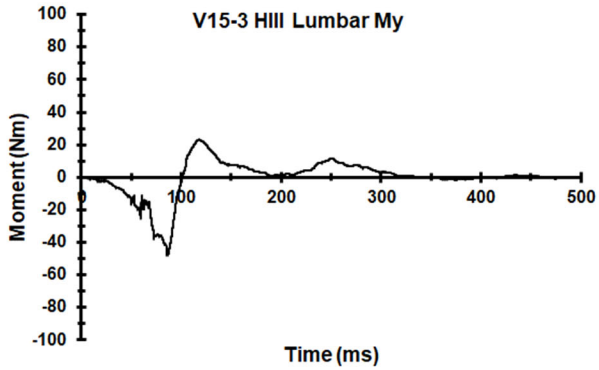
V15-3 HIII Lumbar My
Moment (Nm)
100
80
60
40
20
0
-20
-40
-60
-80
-100
0
100
200
300
400
500
Time (ms)

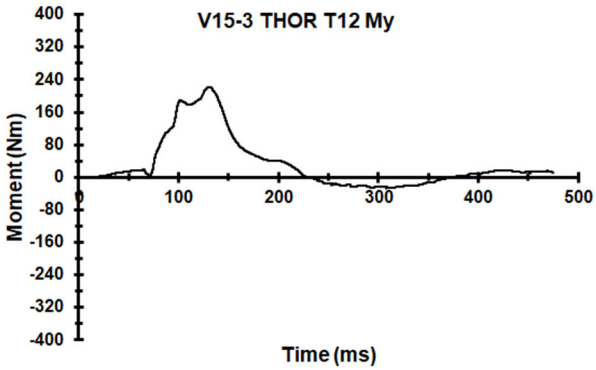
V15-3 THOR T12 My
Moment (Nm)
400
320
240
160
80
0
-80
-160
-240
-320
-400
0
100
200
300
400
500
Time (ms)

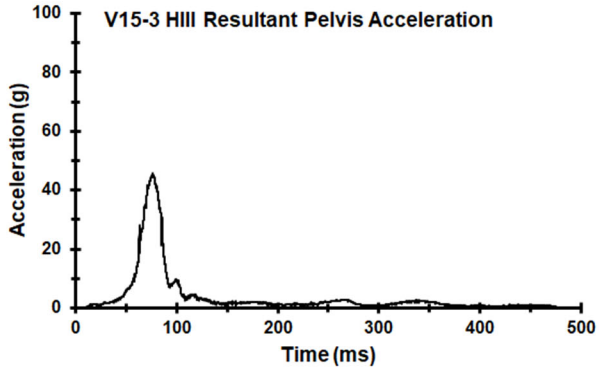
V15-3 HIII Resultant Pelvis Acceleration
Acceleration (g)
100
80
60
40
20
0
0
100
200
300
400
500
Time (ms)

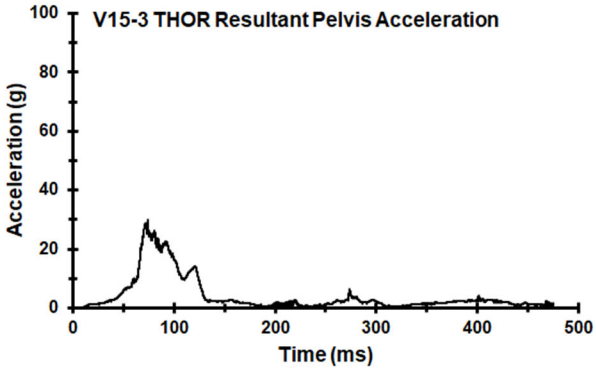
V15-3 THOR Resultant Pelvis Acceleration
Acceleration (g)
100
80
60
40
20
0
0
100
200
300
400
500
Time (ms)

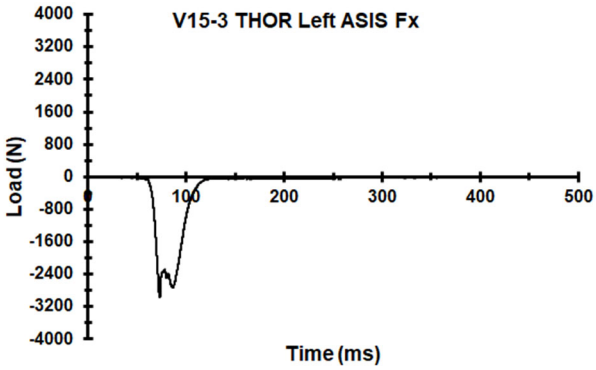
V15-3 THOR Left ASIS Fx
Load (N)
4000
3200
2400
1600
800
0
-800
-1600
-2400
-3200
-4000
0
100
200
300
400
500
Time (ms)

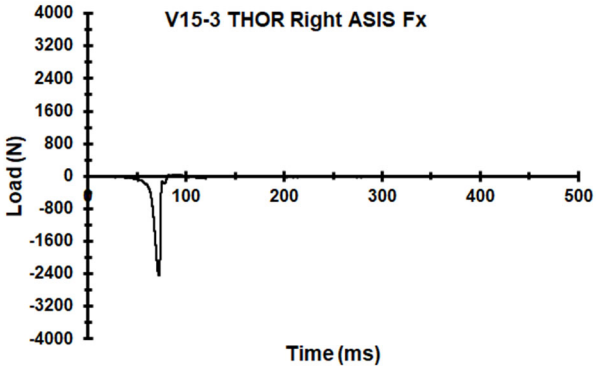
V15-3 THOR Right ASIS Fx
Load (N)
4000
3200
2400
1600
800
0
-800
-1600
-2400
-3200
-4000
0
100
200
300
400
500
Time (ms)

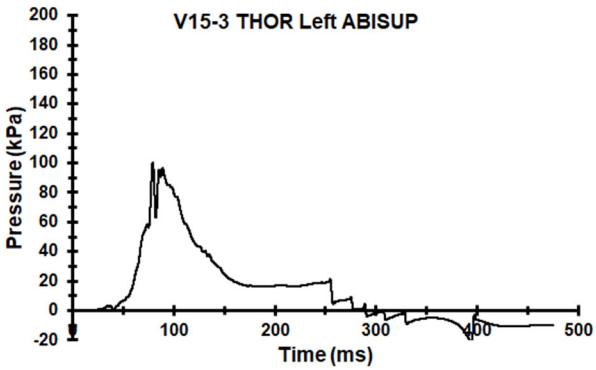
V15-3 THOR Left ABISUP
Pressure (kPa)
200
180
160
140
120
100
80
60
40
20
0
-20
100
200
300
400
500
Time (ms)

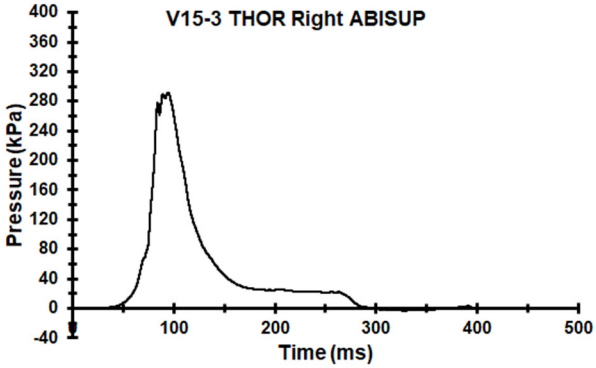
V15-3 THOR Right ABISUP
Pressure (kPa)
400
360
320
280
240
200
160
120
80
40
0
-40
100
200
300
400
500
Time (ms)

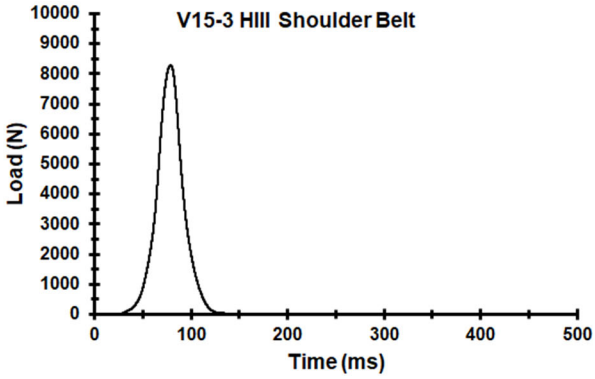
V15-3 HIII Shoulder Belt
Load (N)
10000
9000
8000
7000
6000
5000
4000
3000
2000
1000
0
0
100
200
300
400
500
Time (ms)

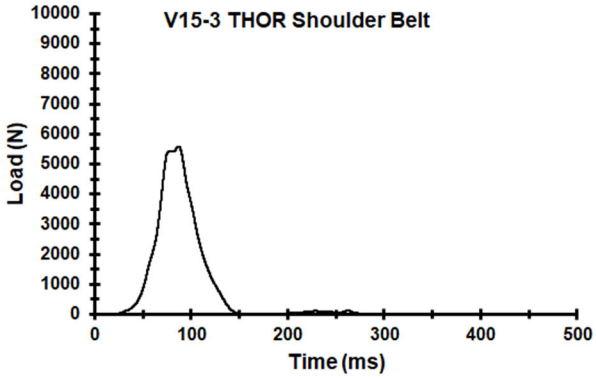
V15-3 THOR Shoulder Belt
Load (N)
10000
9000
8000
7000
6000
5000
4000
3000
2000
1000
0
0
100
200
300
400
500
Time (ms)

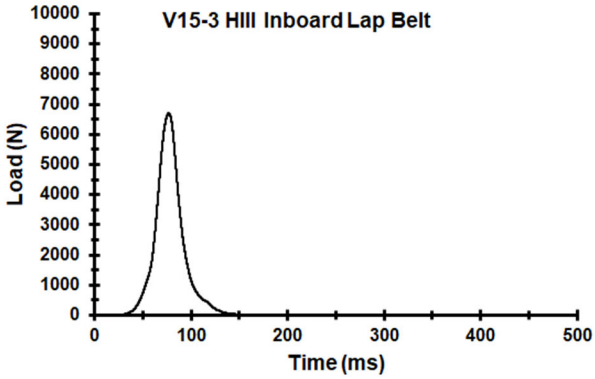
V15-3 HIII Inboard Lap Belt
Load (N)
Time (ms)
0
1000
2000
3000
4000
5000
6000
7000
8000
9000
10000
0
100
200
300
400
500

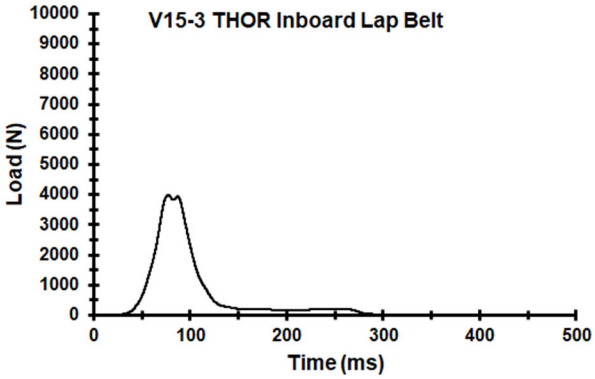
V15-3 THOR Inboard Lap Belt
Load (N)
Time (ms)
0
1000
2000
3000
4000
5000
6000
7000
8000
9000
10000
0
100
200
300
400
500

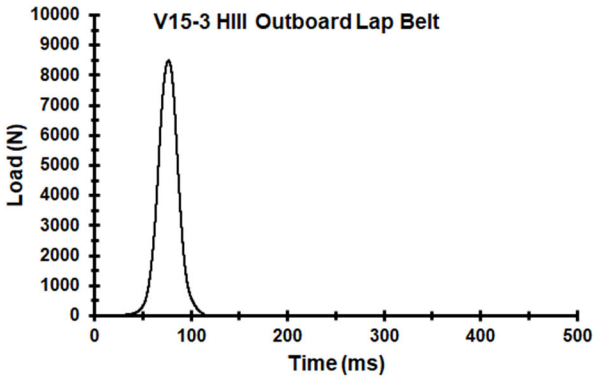
V15-3 HIII Outboard Lap Belt
Load (N)
Time (ms)
0
1000
2000
3000
4000
5000
6000
7000
8000
9000
10000
0
100
200
300
400
500

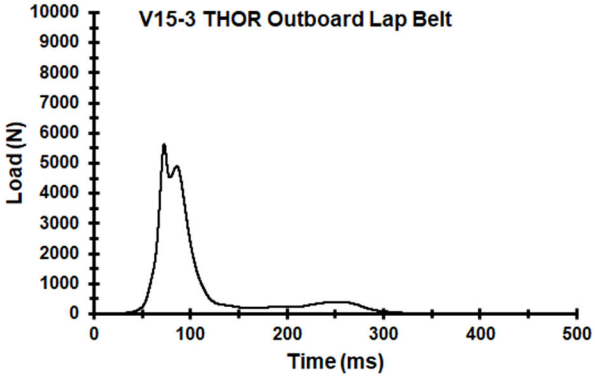
V15-3 THOR Outboard Lap Belt
Load (N)
Time (ms)
0
1000
2000
3000
4000
5000
6000
7000
8000
9000
10000
0
100
200
300
400
500

Appendix DD. Select Data Traces From Test FRS-V15-4

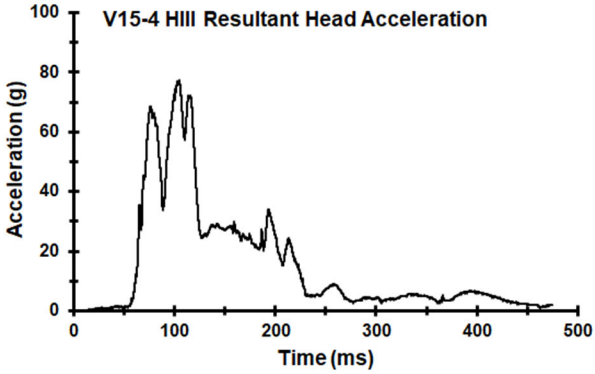
V15-4 HIII Resultant Head Acceleration
Acceleration (g)
Time (ms)

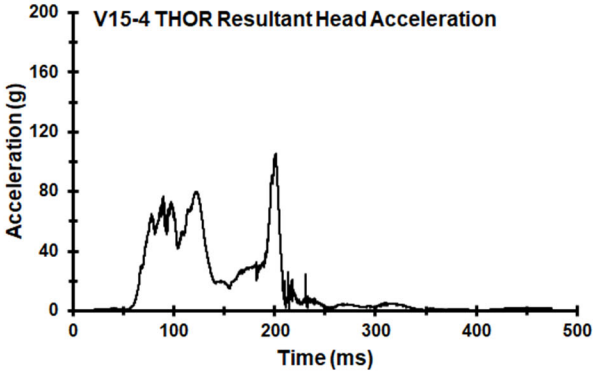
V15-4 THOR Resultant Head Acceleration
Acceleration (g)
Time (ms)

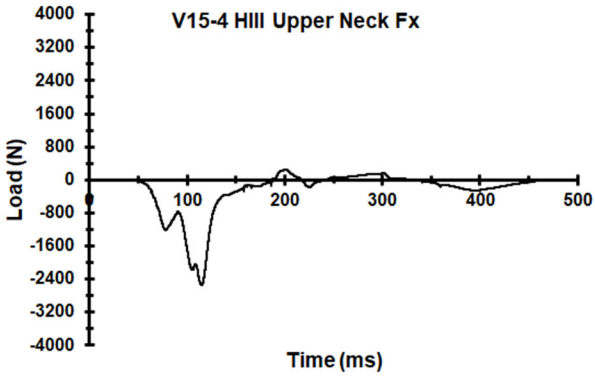
V15-4 HIII Upper Neck Fx
Load (N)
Time (ms)

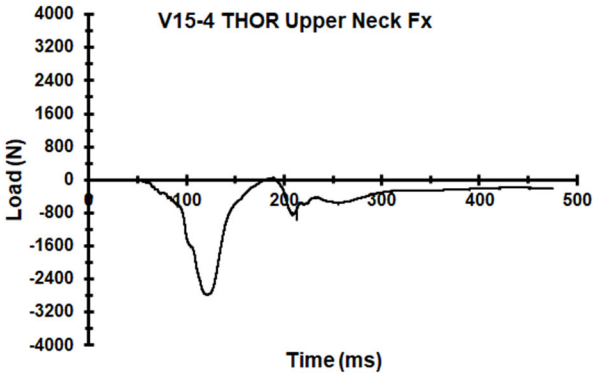
V15-4 THOR Upper Neck Fx
Load (N)
Time (ms)

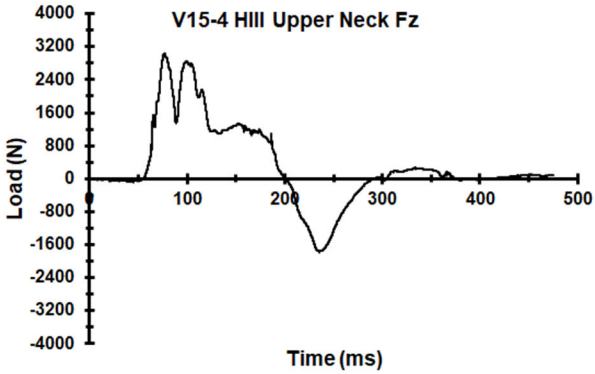
V15-4 HIII Upper Neck Fz
Load (N)
Time (ms)

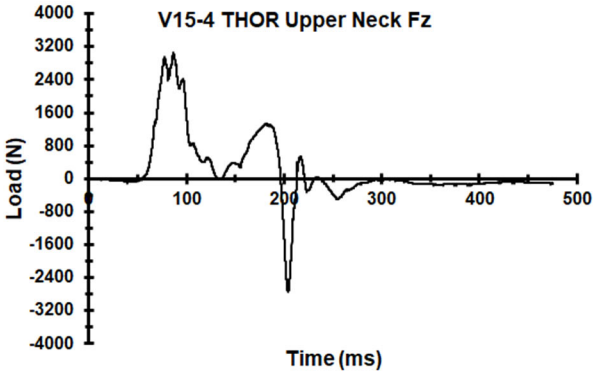
V15-4 THOR Upper Neck Fz
Load (N)
Time (ms)

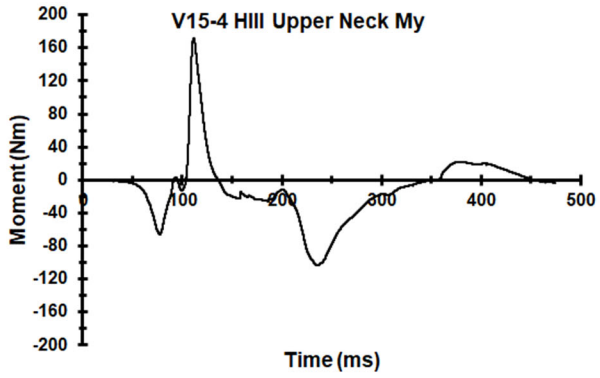
V15-4 HIII Upper Neck My
Moment (Nm)
200
160
120
80
40
0
-40
-80
-120
-160
-200
0
100
200
300
400
500
Time (ms)

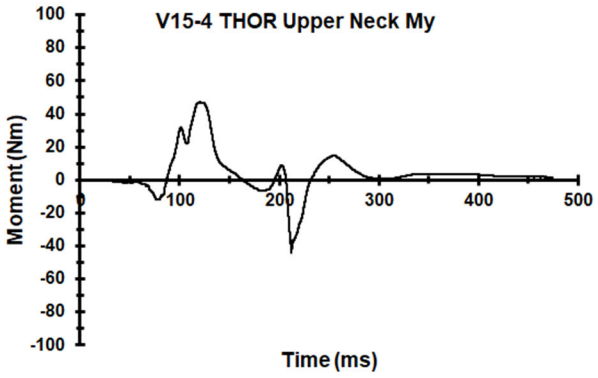
V15-4 THOR Upper Neck My
Moment (Nm)
100
80
60
40
20
0
-20
-40
-60
-80
-100
0
100
200
300
400
500
Time (ms)

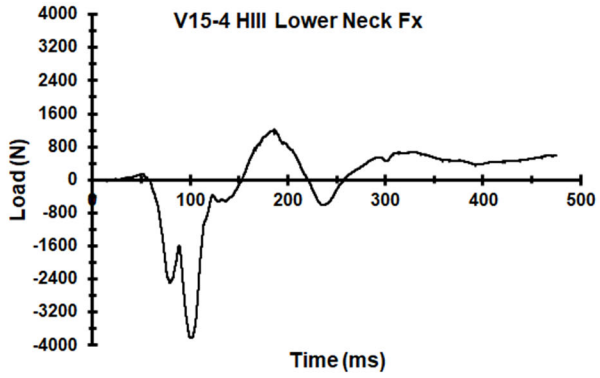
V15-4 HIII Lower Neck Fx
Load (N)
4000
3200
2400
1600
800
0
-800
-1600
-2400
-3200
-4000
0
100
200
300
400
500
Time (ms)

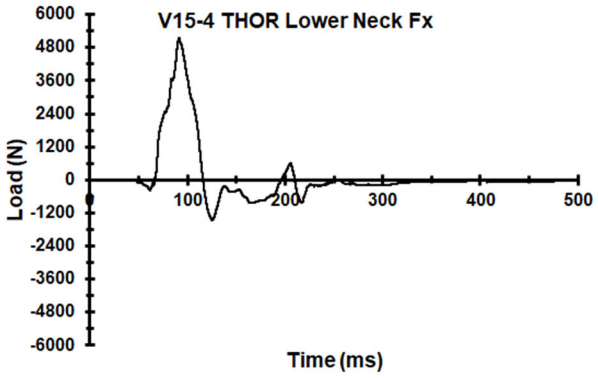
V15-4 THOR Lower Neck Fx
Load (N)
6000
4800
3600
2400
1200
0
-1200
-2400
-3600
-4800
-6000
0
100
200
300
400
500
Time (ms)

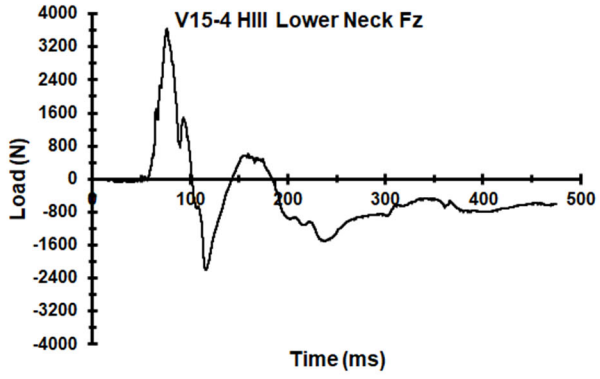
V15-4 HIII Lower Neck Fz
Load (N)
4000
3200
2400
1600
800
0
-800
-1600
-2400
-3200
-4000
0
100
200
300
400
500
Time (ms)

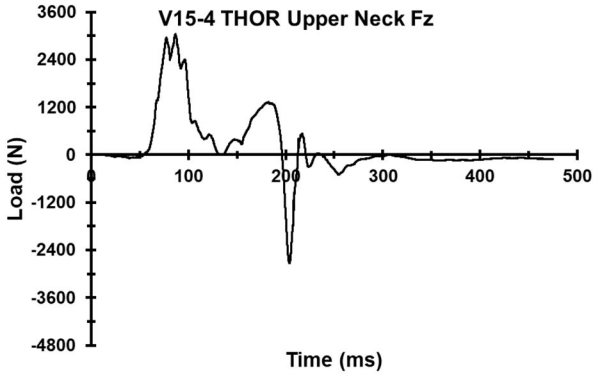
V15-4 THOR Upper Neck Fz
Load (N)
3600
2400
1200
0
-1200
-2400
-3600
-4800
0
100
200
300
400
500
Time (ms)

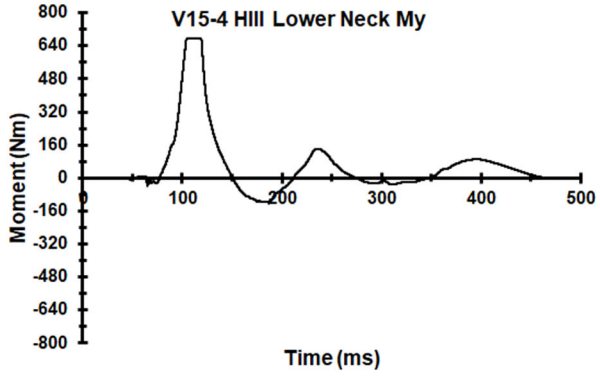
V15-4 HIII Lower Neck My
Moment (Nm)
800
640
480
320
160
0
-160
-320
-480
-640
-800
0
100
200
300
400
500
Time (ms)

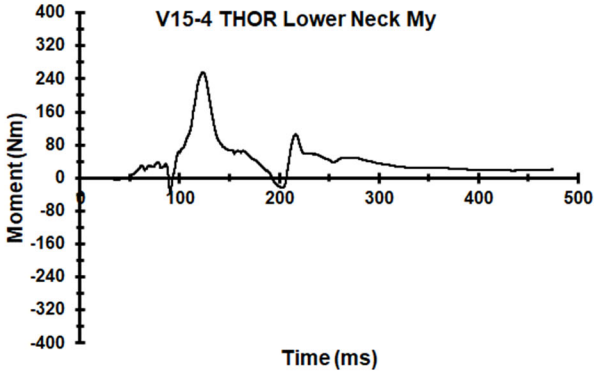
V15-4 THOR Lower Neck My
Moment (Nm)
400
320
240
160
80
0
-80
-160
-240
-320
-400
0
100
200
300
400
500
Time (ms)

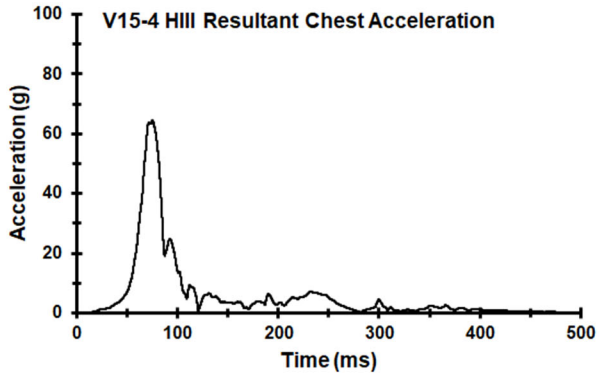
V15-4 HIII Resultant Chest Acceleration
Acceleration (g)
100
80
60
40
20
0
0
100
200
300
400
500
Time (ms)

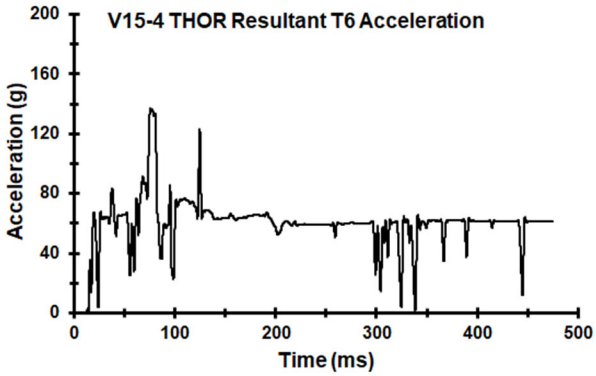
V15-4 THOR Resultant T6 Acceleration
Acceleration (g)
200
160
120
80
40
0
0
100
200
300
400
500
Time (ms)

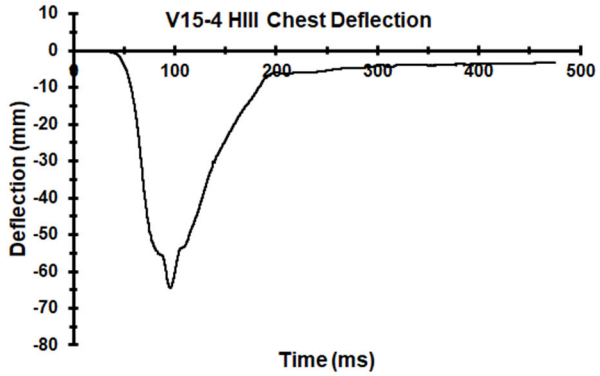
V15-4 HIII Chest Deflection
Deflection (mm)
10
0
-10
-20
-30
-40
-50
-60
-70
-80
0
100
200
300
400
500
Time (ms)

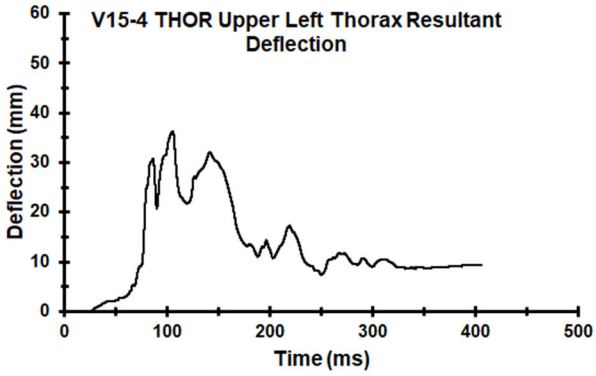
V15-4 THOR Upper Left Thorax Resultant Deflection
Deflection (mm)
60
50
40
30
20
10
0
0
100
200
300
400
500
Time (ms)

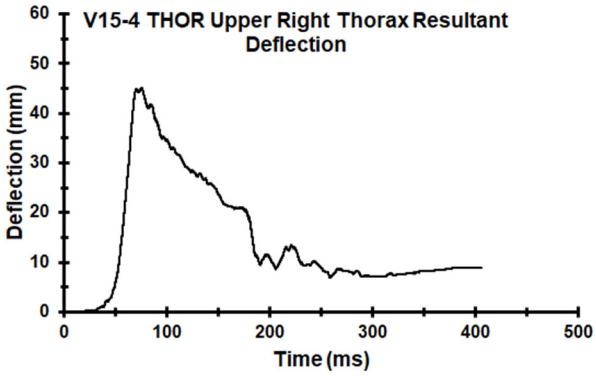
V15-4 THOR Upper Right Thorax Resultant Deflection
Deflection (mm)
60
50
40
30
20
10
0
0
100
200
300
400
500
Time (ms)

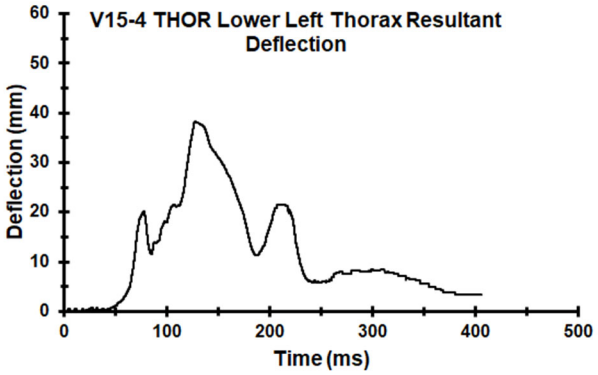
V15-4 THOR Lower Left Thorax Resultant Deflection
Deflection (mm)
60
50
40
30
20
10
0
0
100
200
300
400
500
Time (ms)

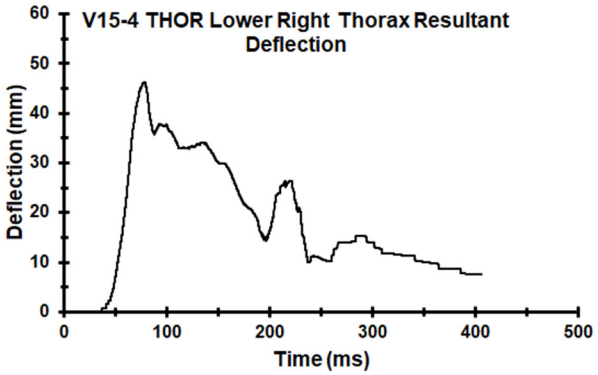
V15-4 THOR Lower Right Thorax Resultant Deflection
Deflection (mm)
60
50
40
30
20
10
0
0
100
200
300
400
500
Time (ms)

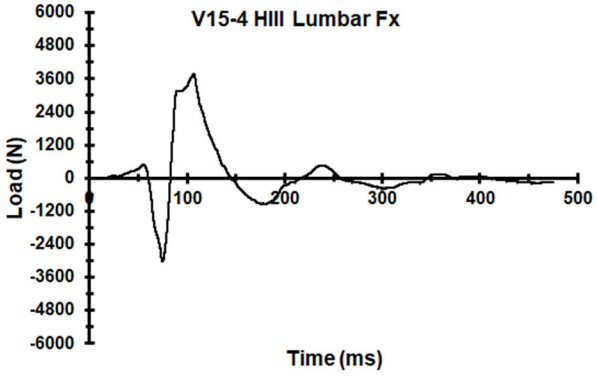
V15-4 HIII Lumbar Fx
Load (N)
6000
4800
3600
2400
1200
0
-1200
-2400
-3600
-4800
-6000
0
100
200
300
400
500
Time (ms)

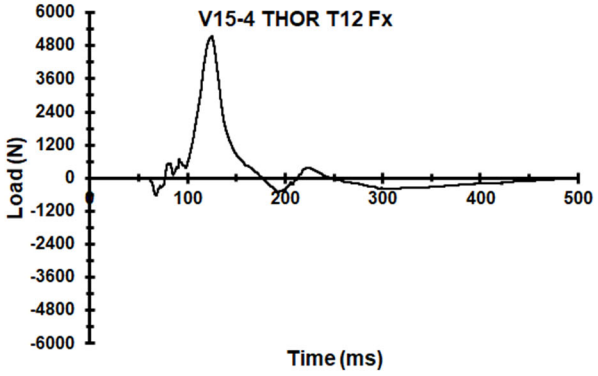
V15-4 THOR T12 Fx
Load (N)
6000
4800
3600
2400
1200
0
-1200
-2400
-3600
-4800
-6000
0
100
200
300
400
500
Time (ms)

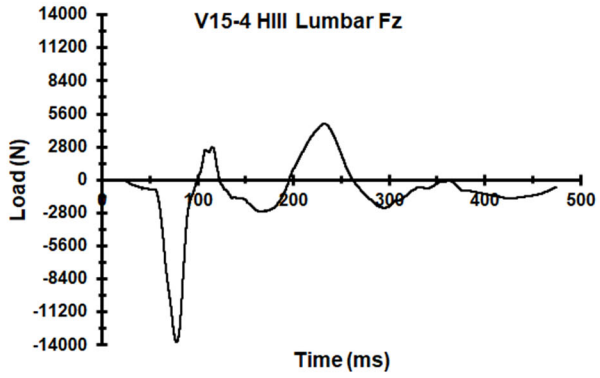
V15-4 HIII Lumbar Fz
Load (N)
14000
11200
8400
5600
2800
0
-2800
-5600
-8400
-11200
-14000
0
100
200
300
400
500
Time (ms)

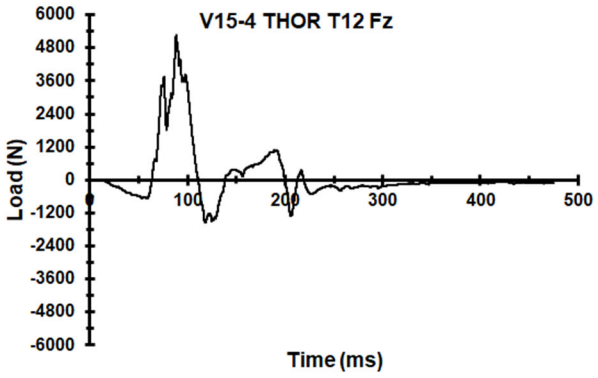
V15-4 THOR T12 Fz
Load (N)
6000
4800
3600
2400
1200
0
-1200
-2400
-3600
-4800
-6000
0
100
200
300
400
500
Time (ms)

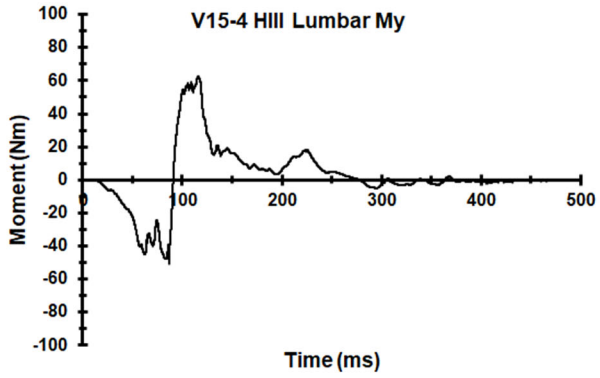
V15-4 HIII Lumbar My
Moment (Nm)
100
80
60
40
20
0
-20
-40
-60
-80
-100
0
100
200
300
400
500
Time (ms)

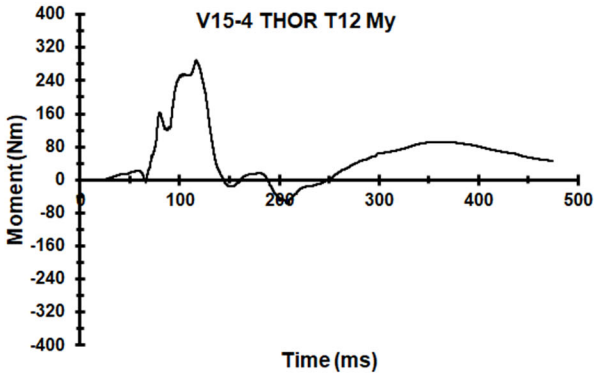
V15-4 THOR T12 My
Moment (Nm)
400
320
240
160
80
0
-80
-160
-240
-320
-400
0
100
200
300
400
500
Time (ms)

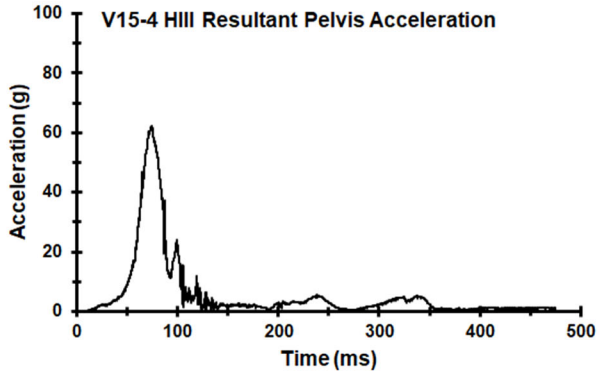
V15-4 HIII Resultant Pelvis Acceleration
Acceleration (g)
100
80
60
40
20
0
0
100
200
300
400
500
Time (ms)

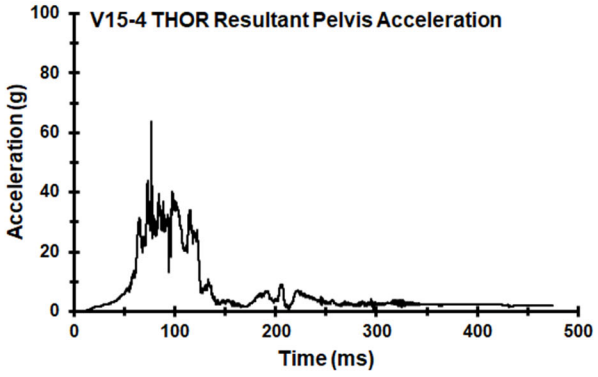
V15-4 THOR Resultant Pelvis Acceleration
Acceleration (g)
100
80
60
40
20
0
0
100
200
300
400
500
Time (ms)

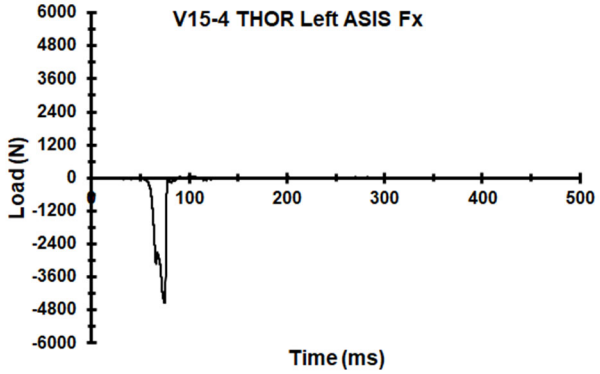
V15-4 THOR Left ASIS Fx
Load (N)
6000
4800
3600
2400
1200
0
-1200
-2400
-3600
-4800
-6000
100
200
300
400
500
Time (ms)

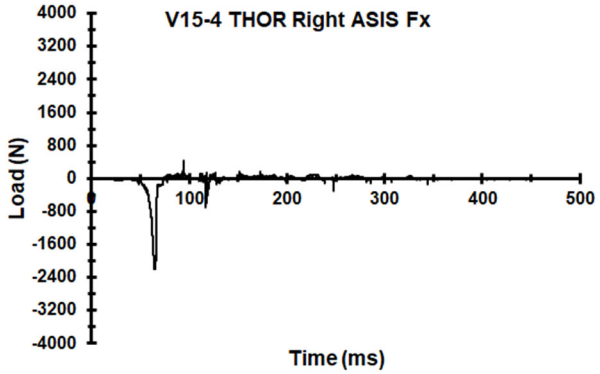
V15-4 THOR Right ASIS Fx
Load (N)
4000
3200
2400
1600
800
0
-800
-1600
-2400
-3200
-4000
100
200
300
400
500
Time (ms)

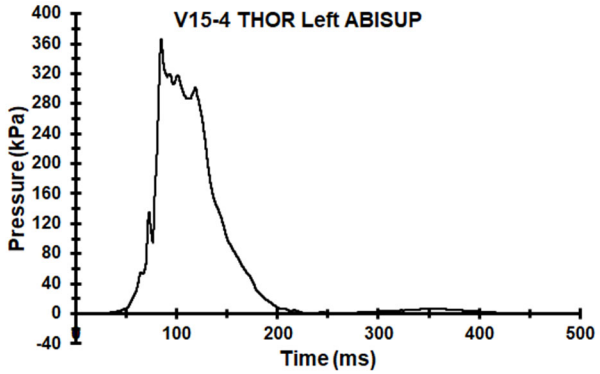
V15-4 THOR Left ABISUP
Pressure (kPa)
400
360
320
280
240
200
160
120
80
40
0
-40
100
200
300
400
500
Time (ms)

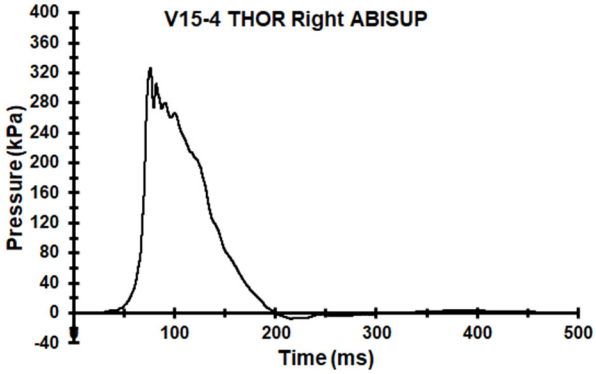
V15-4 THOR Right ABISUP
Pressure (kPa)
400
360
320
280
240
200
160
120
80
40
0
-40
100
200
300
400
500
Time (ms)

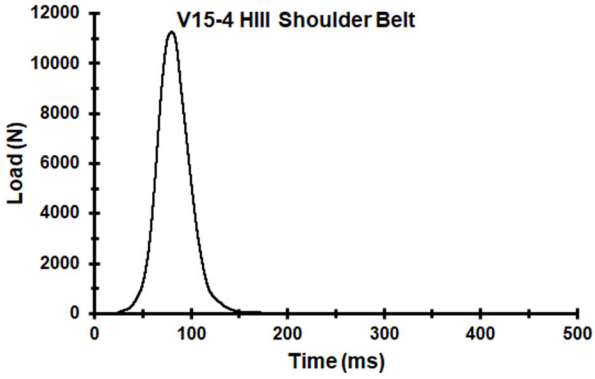
V15-4 HIII Shoulder Belt
Load (N)
12000
10000
8000
6000
4000
2000
0
0
100
200
300
400
500
Time (ms)

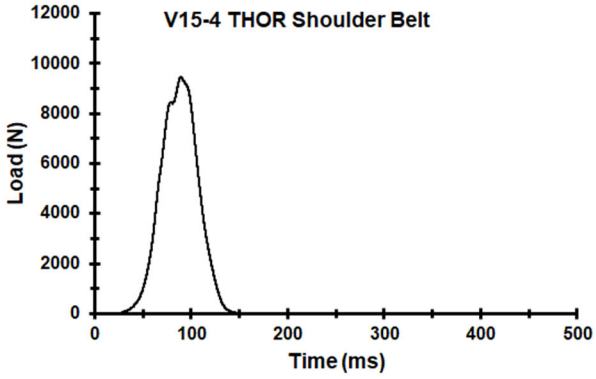
V15-4 THOR Shoulder Belt
Load (N)
12000
10000
8000
6000
4000
2000
0
0
100
200
300
400
500
Time (ms)

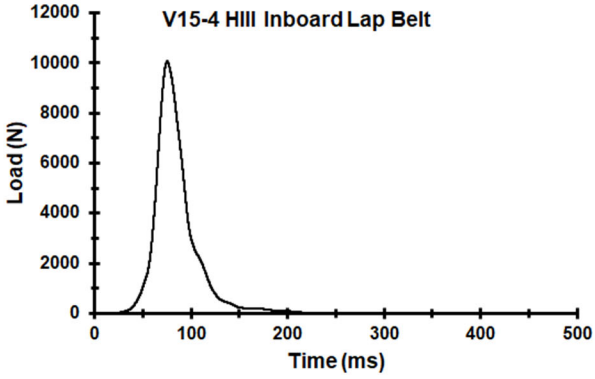
V15-4 HIII Inboard Lap Belt
Load (N)
12000
10000
8000
6000
4000
2000
0
0
100
200
300
400
500
Time (ms)

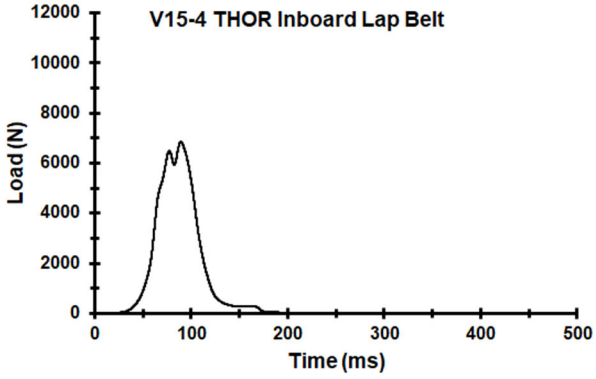
V15-4 THOR Inboard Lap Belt
Load (N)
12000
10000
8000
6000
4000
2000
0
0
100
200
300
400
500
Time (ms)

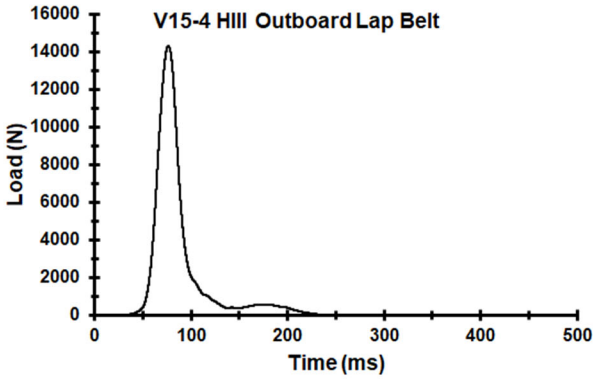
V15-4 HIII Outboard Lap Belt
Load (N)
16000
14000
12000
10000
8000
6000
4000
2000
0
0
100
200
300
400
500
Time (ms)

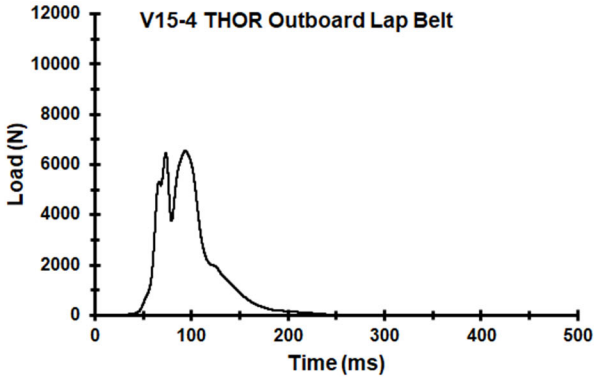
V15-4 THOR Outboard Lap Belt
Load (N)
12000
10000
8000
6000
4000
2000
0
0
100
200
300
400
500
Time (ms)

Appendix EE. Select Data Traces From Test FRS-V19-1

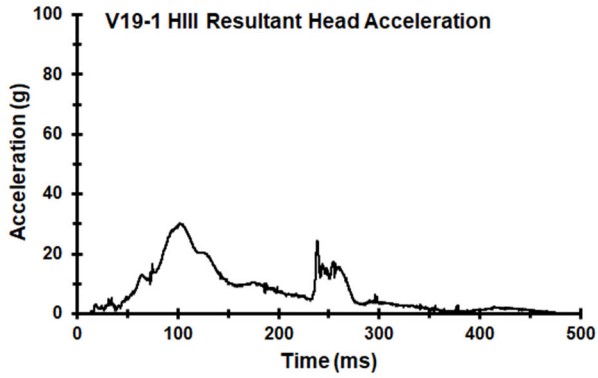
V19-1 HIII Resultant Head Acceleration
Acceleration (g)
Time (ms)

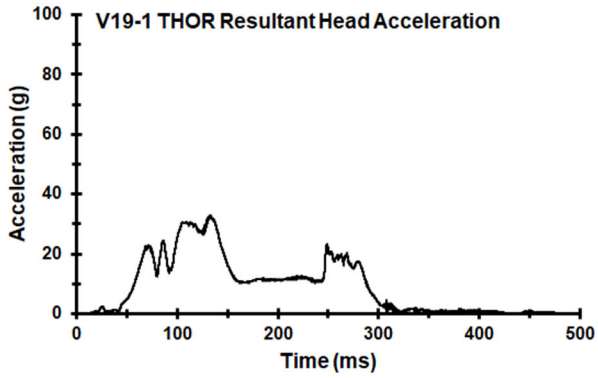
V19-1 THOR Resultant Head Acceleration
Acceleration (g)
Time (ms)

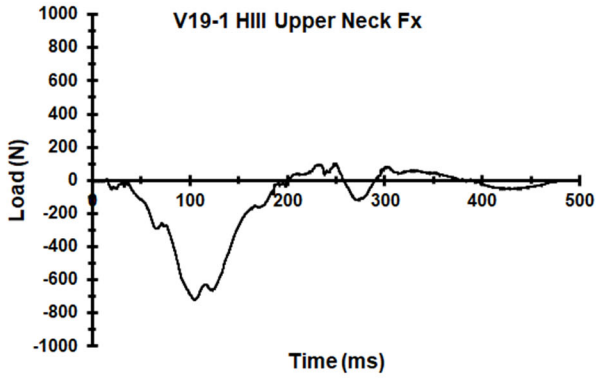
V19-1 HIII Upper Neck Fx
Load (N)
Time (ms)

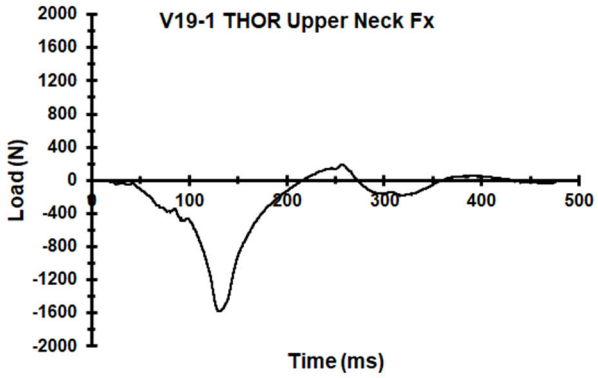
V19-1 THOR Upper Neck Fx
Load (N)
Time (ms)

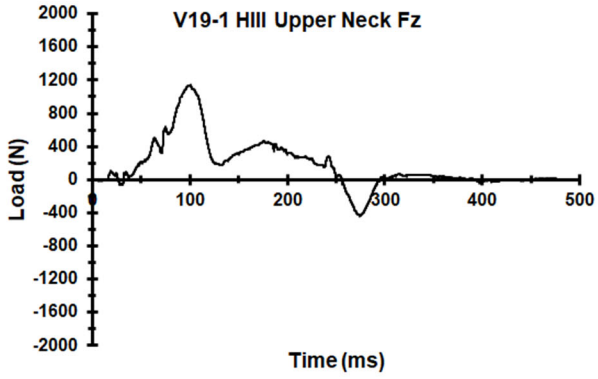
V19-1 HIII Upper Neck Fz
Load (N)
Time (ms)

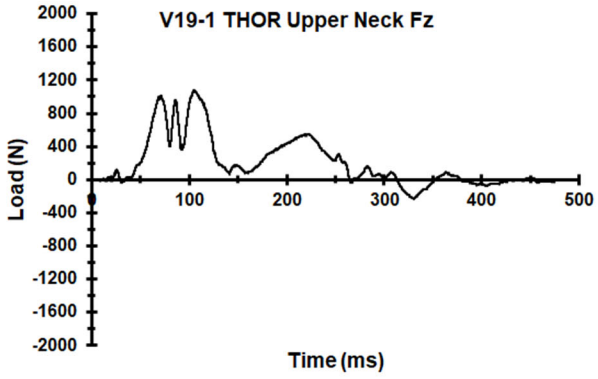
V19-1 THOR Upper Neck Fz
Load (N)
Time (ms)

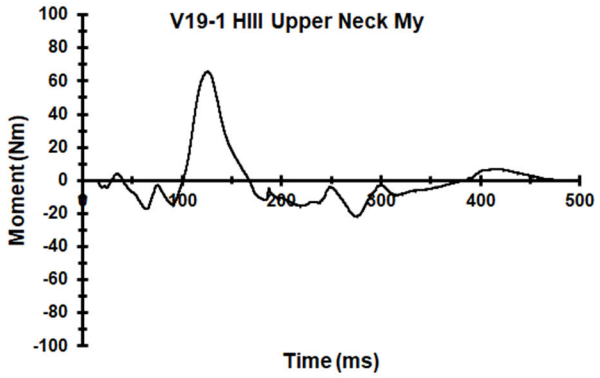
V19-1 HIII Upper Neck My
Moment (Nm)
Time (ms)

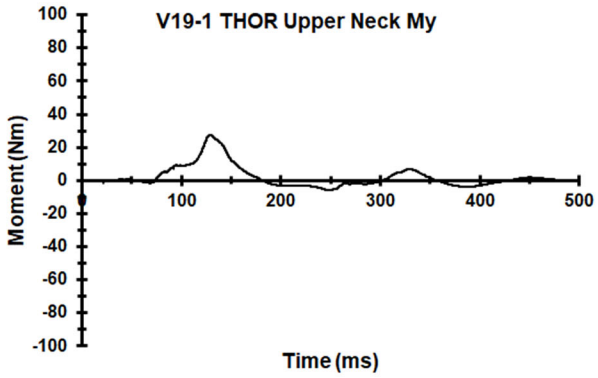
V19-1 THOR Upper Neck My
Moment (Nm)
Time (ms)

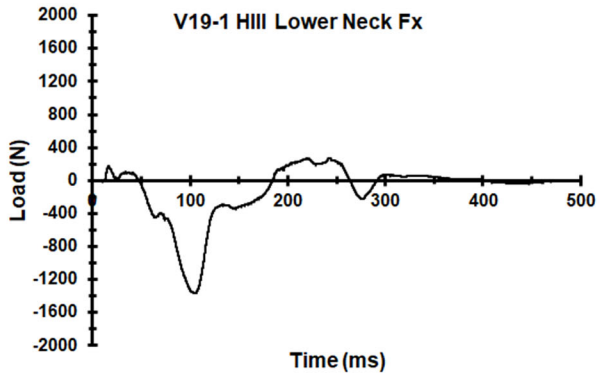
V19-1 HIII Lower Neck Fx
Load (N)
Time (ms)

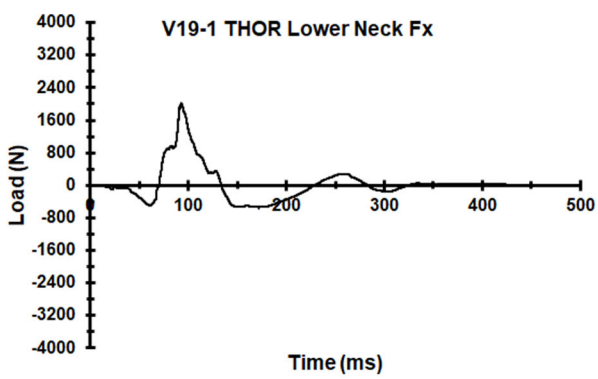
V19-1 THOR Lower Neck Fx
Load (N)
Time (ms)

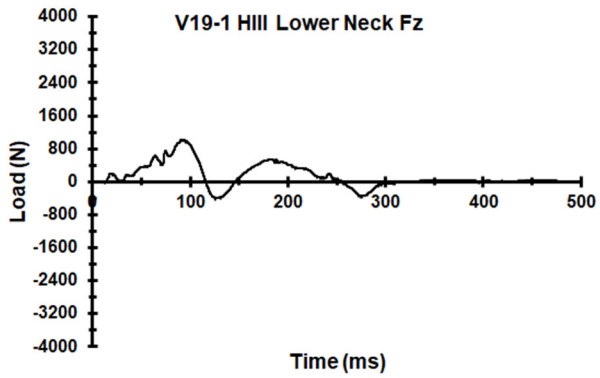
V19-1 HIII Lower Neck Fz
Load (N)
Time (ms)

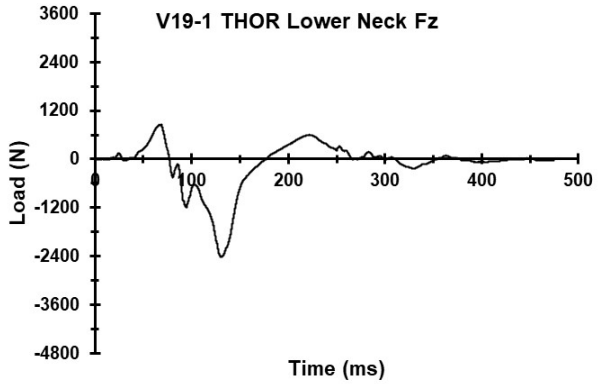
V19-1 THOR Lower Neck Fz
Load (N)
Time (ms)

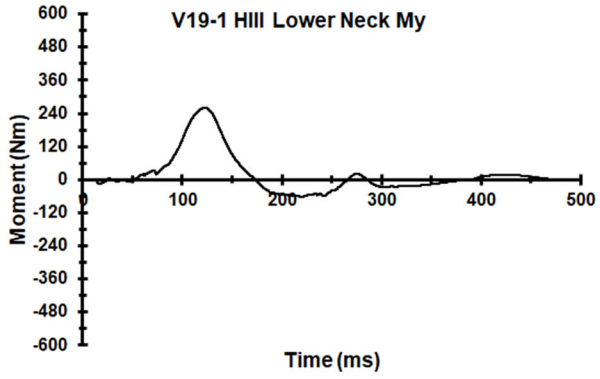
V19-1 HIII Lower Neck My
Moment (Nm)
Time (ms)

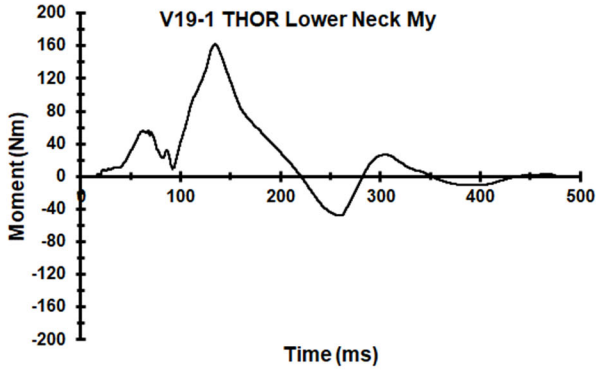
V19-1 THOR Lower Neck My
Moment (Nm)
Time (ms)

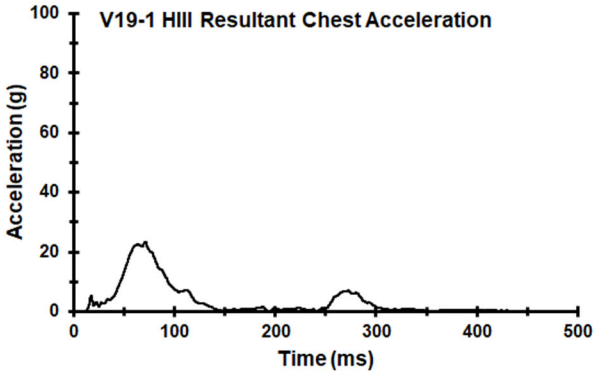
V19-1 HIII Resultant Chest Acceleration
Acceleration (g)
100
80
60
40
20
0
0
100
200
300
400
500
Time (ms)

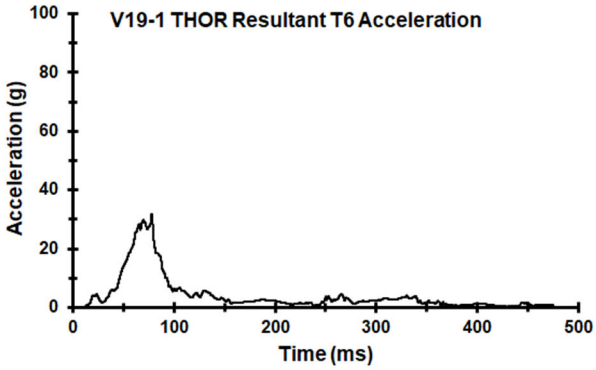
V19-1 THOR Resultant T6 Acceleration
Acceleration (g)
100
80
60
40
20
0
0
100
200
300
400
500
Time (ms)

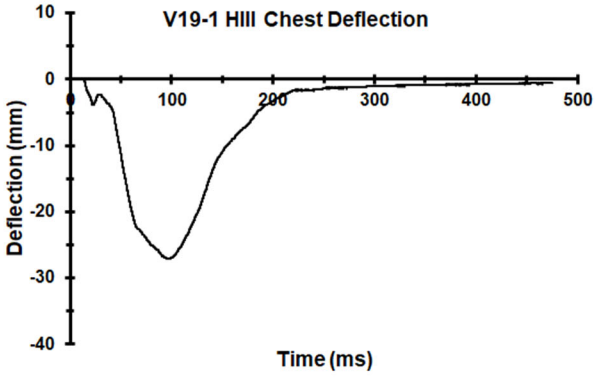
V19-1 HIII Chest Deflection
Deflection (mm)
10
0
-10
-20
-30
-40
0
100
200
300
400
500
Time (ms)

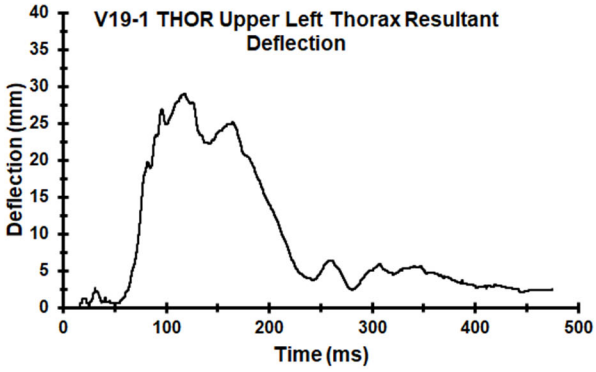
V19-1 THOR Upper Left Thorax Resultant Deflection
Deflection (mm)
40
35
30
25
20
15
10
5
0
0
100
200
300
400
500
Time (ms)

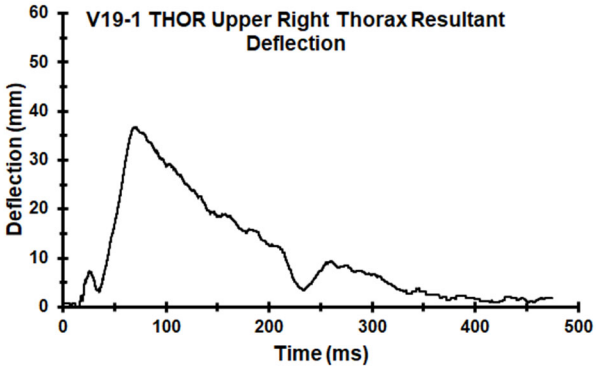
V19-1 THOR Upper Right Thorax Resultant Deflection
Deflection (mm)
60
50
40
30
20
10
0
0
100
200
300
400
500
Time (ms)

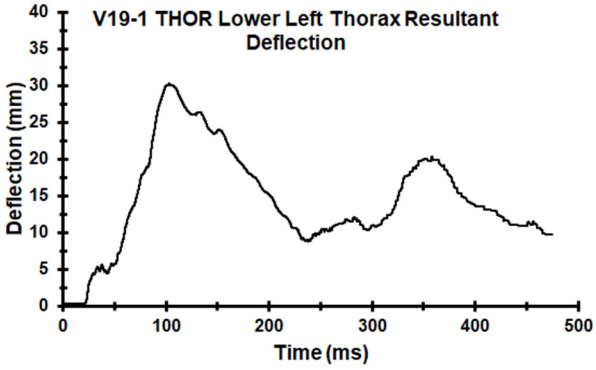
V19-1 THOR Lower Left Thorax Resultant Deflection
Deflection (mm)
Time (ms)

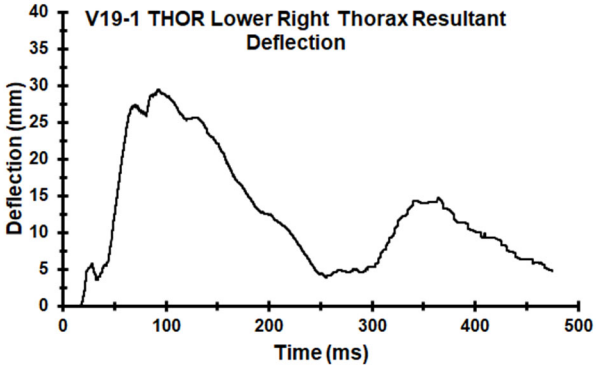
V19-1 THOR Lower Right Thorax Resultant Deflection
Deflection (mm)
Time (ms)

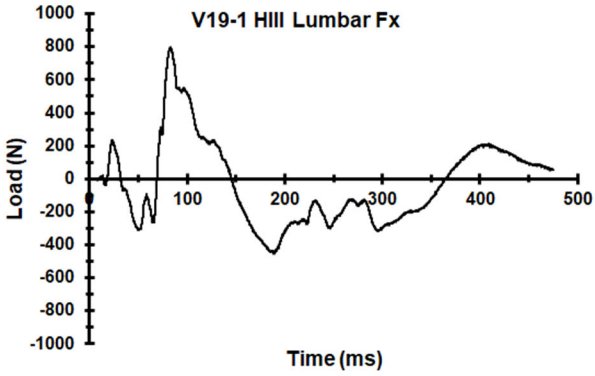
V19-1 HIII Lumbar Fx
Load (N)
Time (ms)

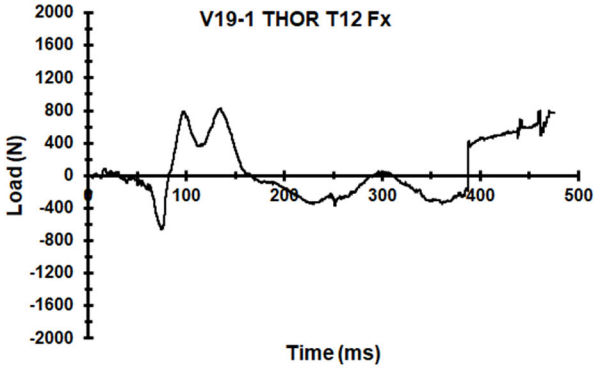
V19-1 THOR T12 Fx
Load (N)
Time (ms)

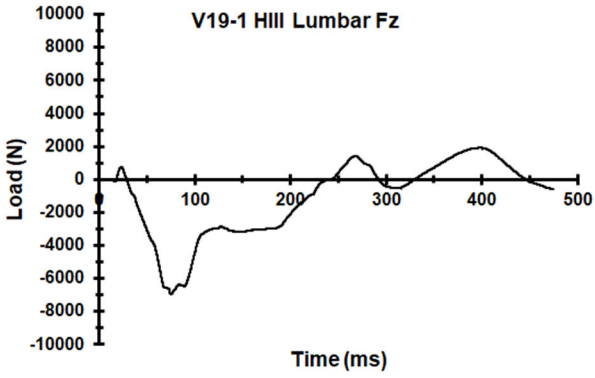
V19-1 HIII Lumbar Fz
Load (N)
Time (ms)

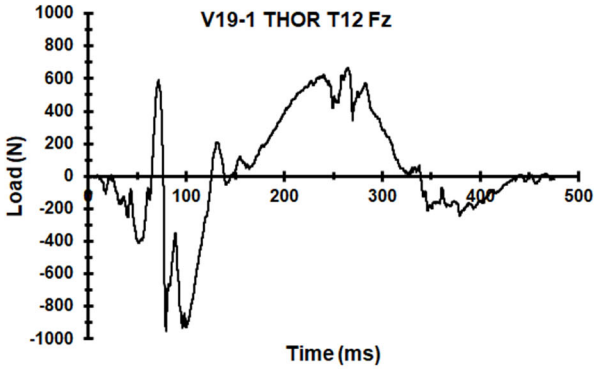
V19-1 THOR T12 Fz
Load (N)
Time (ms)

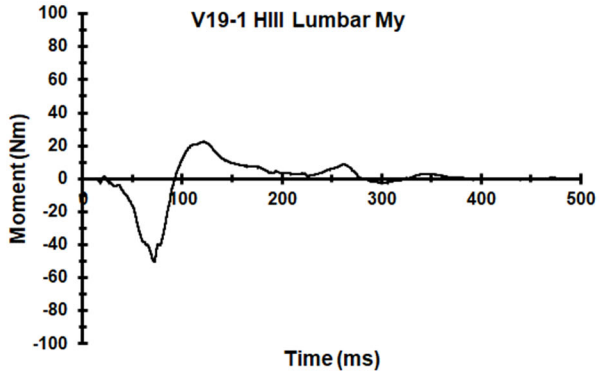
V19-1 HIII Lumbar My
Moment (Nm)
100
80
60
40
20
0
-20
-40
-60
-80
-100
0
100
200
300
400
500
Time (ms)

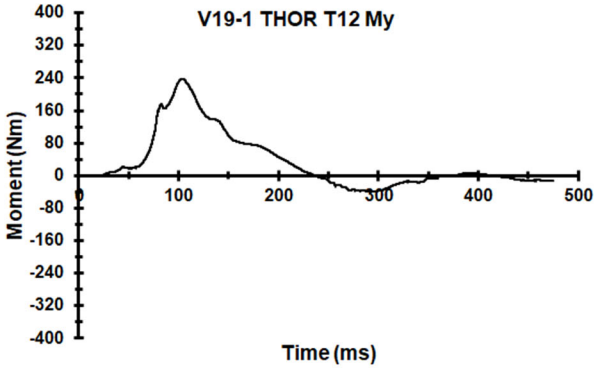
V19-1 THOR T12 My
Moment (Nm)
400
320
240
160
80
0
-80
-160
-240
-320
-400
0
100
200
300
400
500
Time (ms)

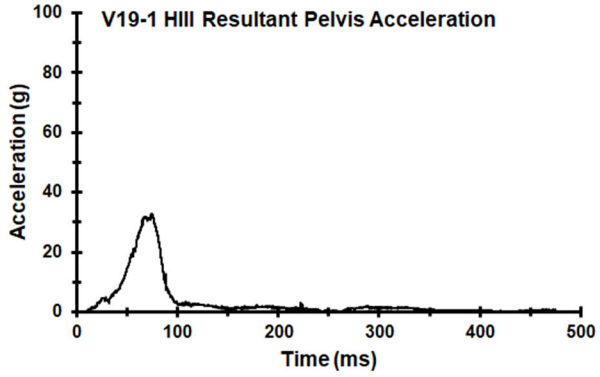
V19-1 HIII Resultant Pelvis Acceleration
Acceleration (g)
100
80
60
40
20
0
0
100
200
300
400
500
Time (ms)

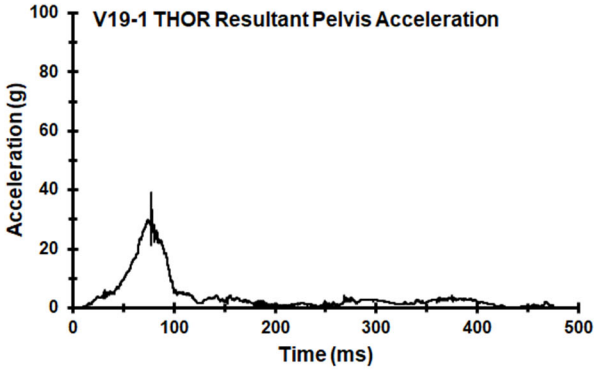
V19-1 THOR Resultant Pelvis Acceleration
Acceleration (g)
100
80
60
40
20
0
0
100
200
300
400
500
Time (ms)

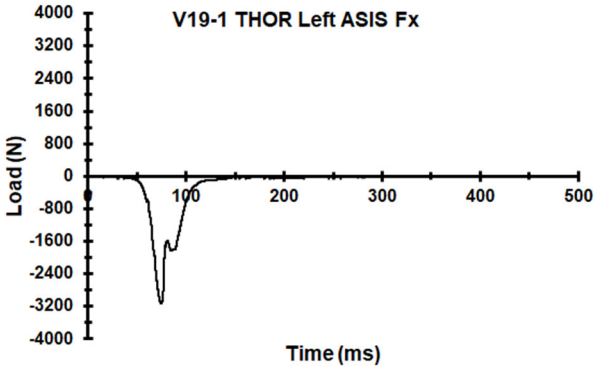
V19-1 THOR Left ASIS Fx
Load (N)
4000
3200
2400
1600
800
0
-800
-1600
-2400
-3200
-4000
0
100
200
300
400
500
Time (ms)

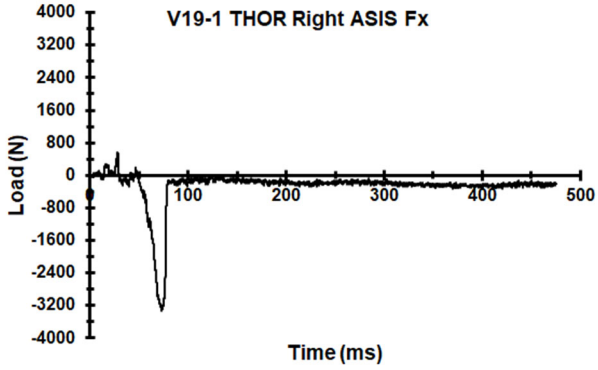
V19-1 THOR Right ASIS Fx
Load (N)
4000
3200
2400
1600
800
0
-800
-1600
-2400
-3200
-4000
100
200
300
400
500
Time (ms)

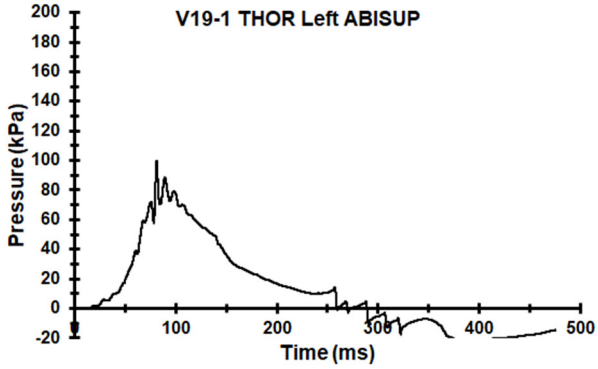
V19-1 THOR Left ABISUP
Pressure (kPa)
200
180
160
140
120
100
80
60
40
20
0
-20
100
200
300
400
500
Time (ms)

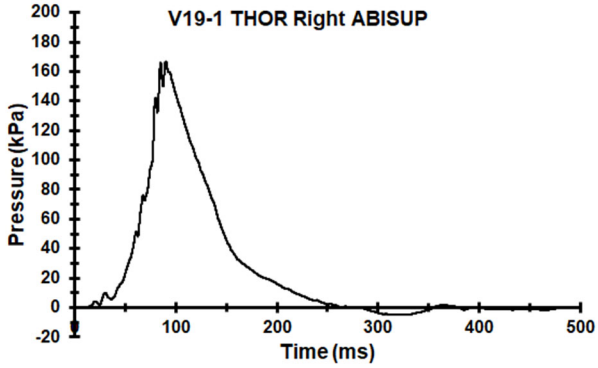
V19-1 THOR Right ABISUP
Pressure (kPa)
200
180
160
140
120
100
80
60
40
20
0
-20
100
200
300
400
500
Time (ms)

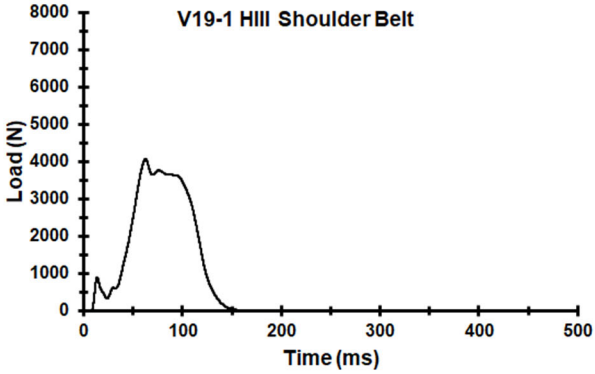
V19-1 HIII Shoulder Belt
Load (N)
Time (ms)

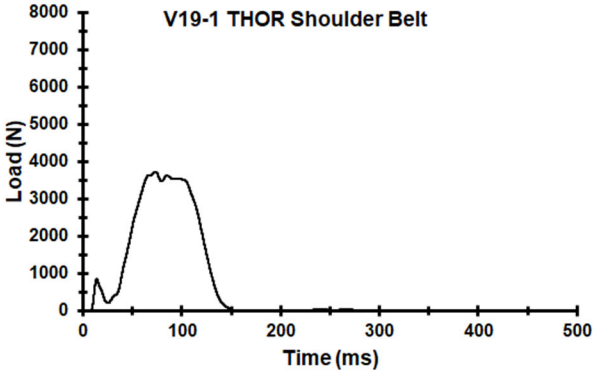
V19-1 THOR Shoulder Belt
Load (N)
Time (ms)

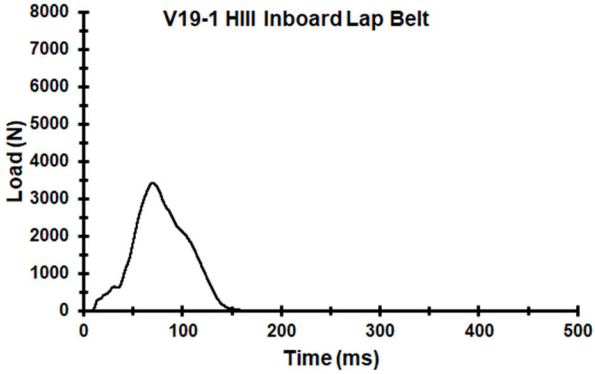
V19-1 HIII Inboard Lap Belt
Load (N)
Time (ms)

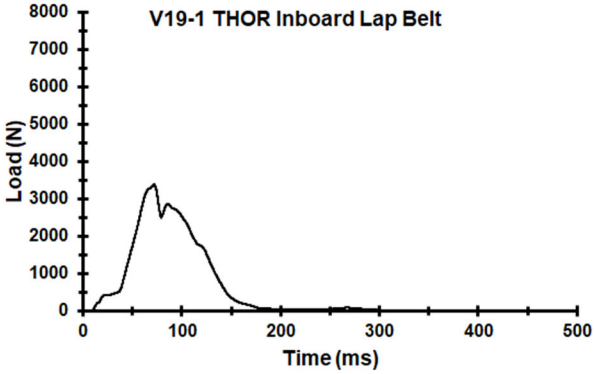
V19-1 THOR Inboard Lap Belt
Load (N)
Time (ms)

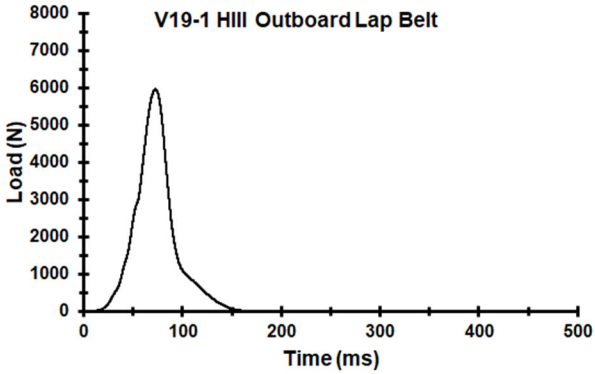
V19-1 HIII Outboard Lap Belt
Load (N)
Time (ms)

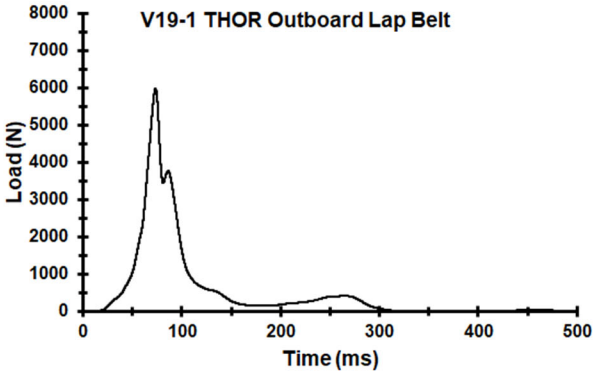
V19-1 THOR Outboard Lap Belt
Load (N)
Time (ms)

Appendix FF. Select Data Traces From Test FRS-V19-2

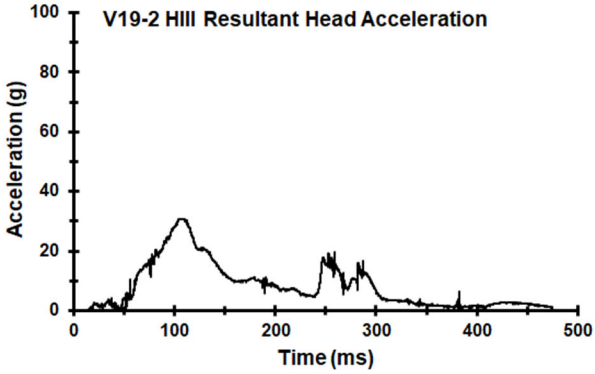
V19-2 HIII Resultant Head Acceleration
Acceleration (g)
Time (ms)

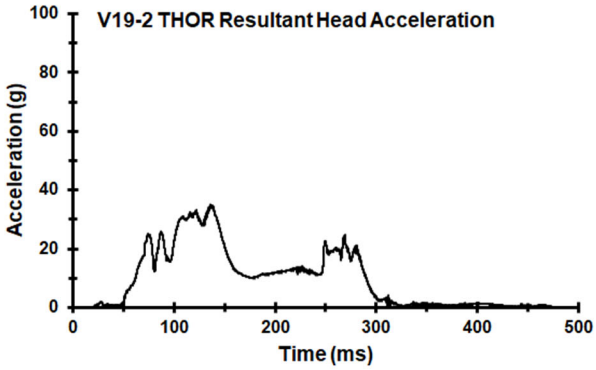
V19-2 THOR Resultant Head Acceleration
Acceleration (g)
Time (ms)

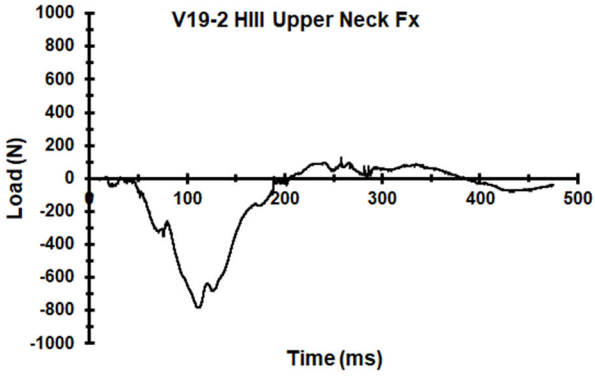
V19-2 HIII Upper Neck Fx
Load (N)
Time (ms)

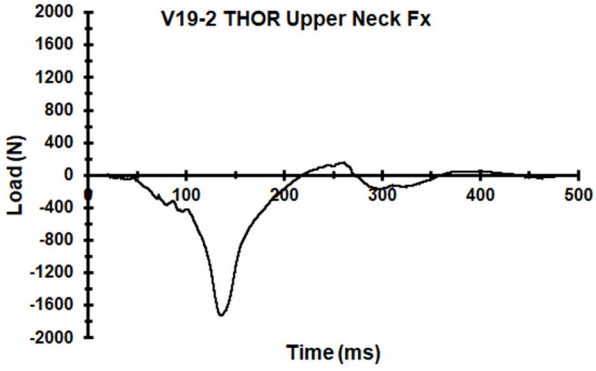
V19-2 THOR Upper Neck Fx
Load (N)
Time (ms)

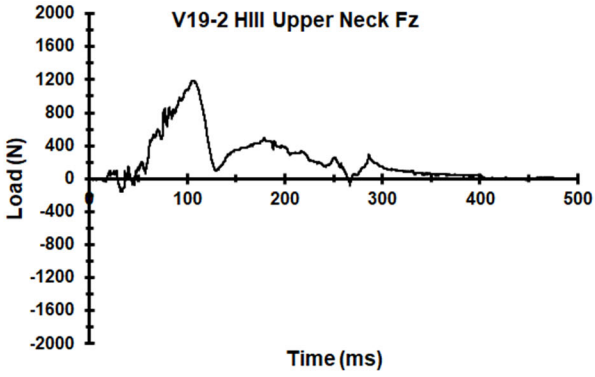
V19-2 HIII Upper Neck Fz
Load (N)
Time (ms)

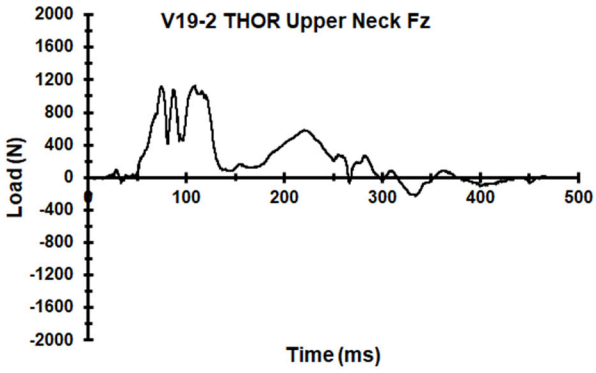
V19-2 THOR Upper Neck Fz
Load (N)
Time (ms)

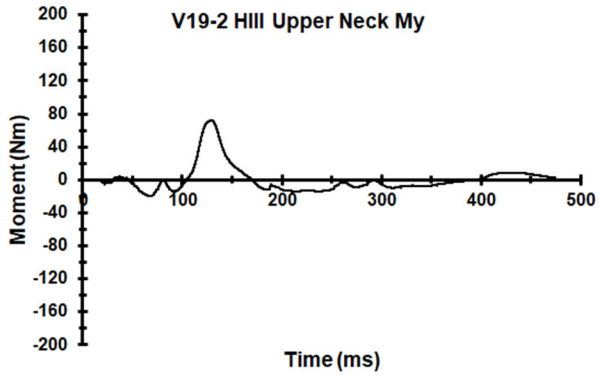
V19-2 HIII Upper Neck My
Moment (Nm)
200
160
120
80
40
0
-40
-80
-120
-160
-200
0
100
200
300
400
500
Time (ms)

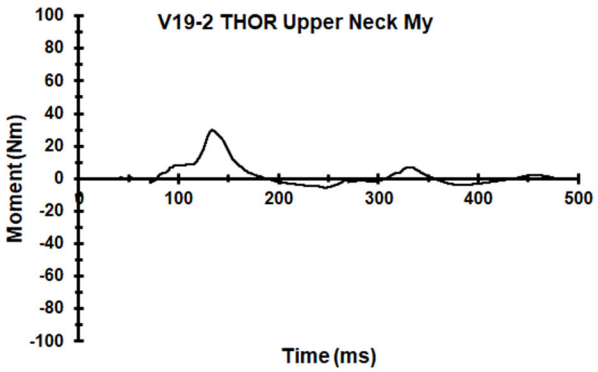
V19-2 THOR Upper Neck My
Moment (Nm)
100
80
60
40
20
0
-20
-40
-60
-80
-100
0
100
200
300
400
500
Time (ms)

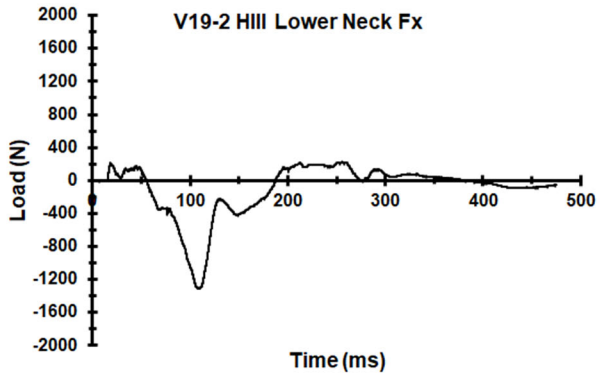
V19-2 HIII Lower Neck Fx
Load (N)
2000
1600
1200
800
400
0
-400
-800
-1200
-1600
-2000
0
100
200
300
400
500
Time (ms)

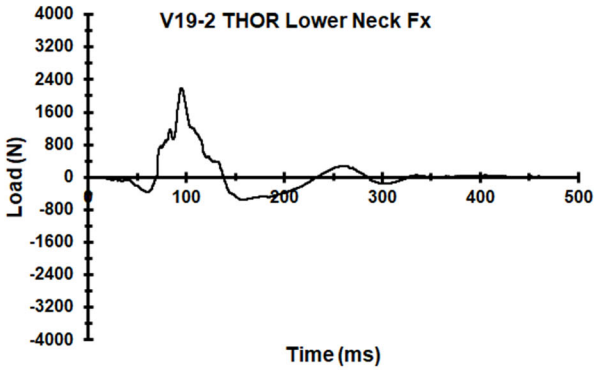
V19-2 THOR Lower Neck Fx
Load (N)
4000
3200
2400
1600
800
0
-800
-1600
-2400
-3200
-4000
0
100
200
300
400
500
Time (ms)

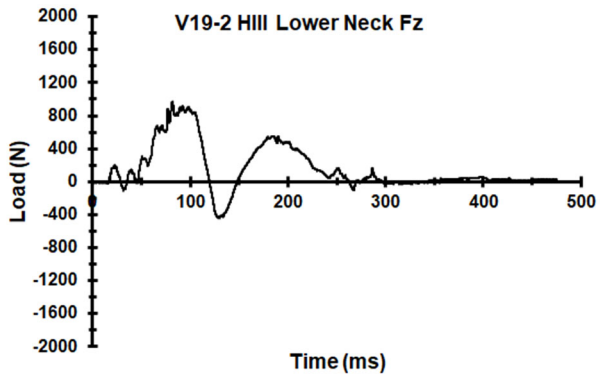
V19-2 HIII Lower Neck Fz
Load (N)
2000
1600
1200
800
400
0
-400
-800
-1200
-1600
-2000
0
100
200
300
400
500
Time (ms)

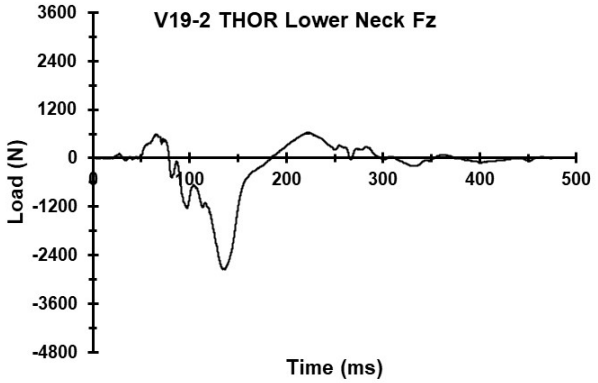
V19-2 THOR Lower Neck Fz
Load (N)
3600
2400
1200
0
-1200
-2400
-3600
-4800
0
100
200
300
400
500
Time (ms)

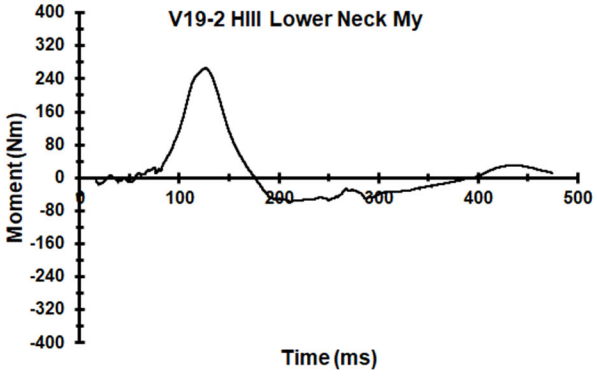
V19-2 HIII Lower Neck My
Moment (Nm)
400
320
240
160
80
0
-80
-160
-240
-320
-400
0
100
200
300
400
500
Time (ms)

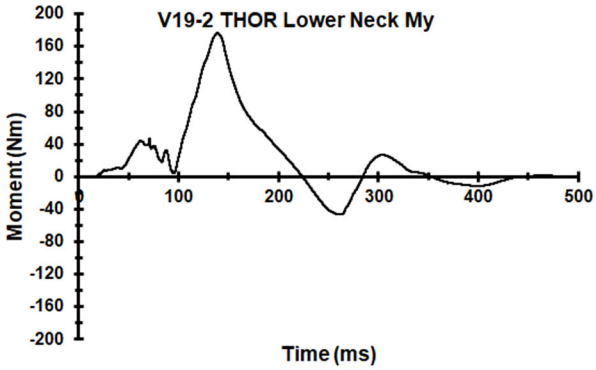
V19-2 THOR Lower Neck My
Moment (Nm)
200
160
120
80
40
0
-40
-80
-120
-160
-200
0
100
200
300
400
500
Time (ms)

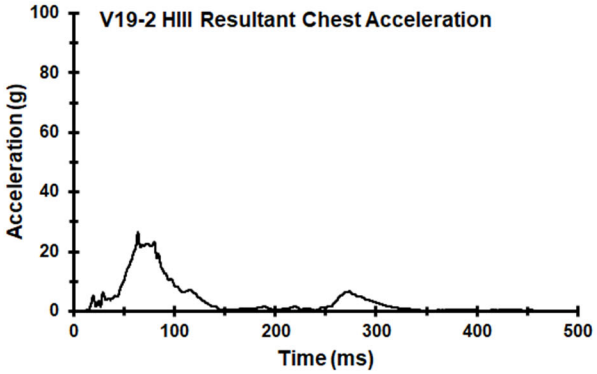
V19-2 HIII Resultant Chest Acceleration
Acceleration (g)
100
80
60
40
20
0
0
100
200
300
400
500
Time (ms)

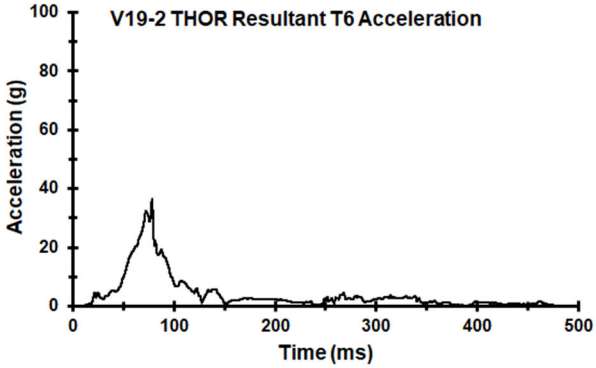
V19-2 THOR Resultant T6 Acceleration
Acceleration (g)
100
80
60
40
20
0
0
100
200
300
400
500
Time (ms)

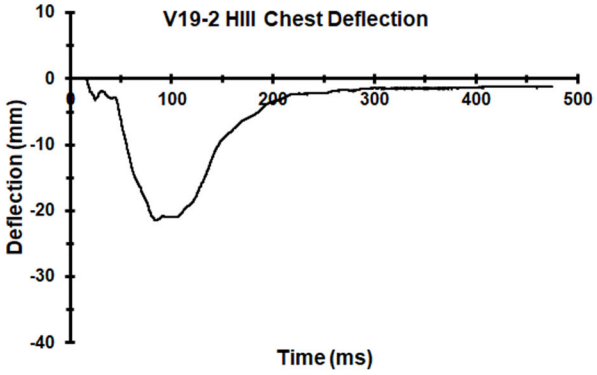
V19-2 HIII Chest Deflection
Deflection (mm)
10
0
-10
-20
-30
-40
0
100
200
300
400
500
Time (ms)

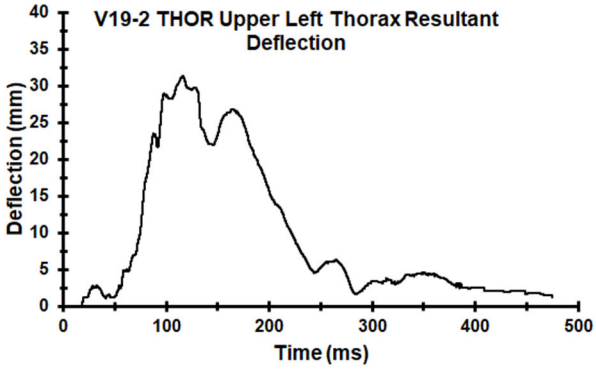
V19-2 THOR Upper Left Thorax Resultant Deflection
Deflection (mm)
40
35
30
25
20
15
10
5
0
0
100
200
300
400
500
Time (ms)

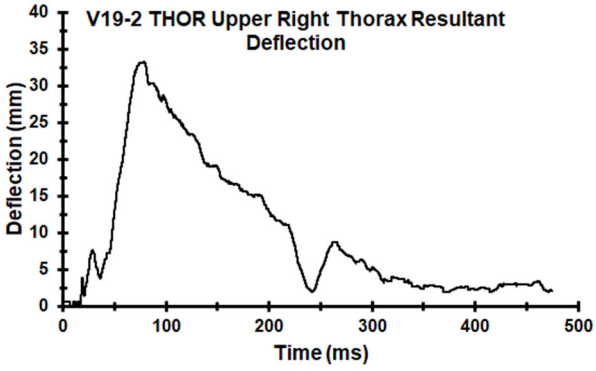
V19-2 THOR Upper Right Thorax Resultant Deflection
Deflection (mm)
40
35
30
25
20
15
10
5
0
0
100
200
300
400
500
Time (ms)

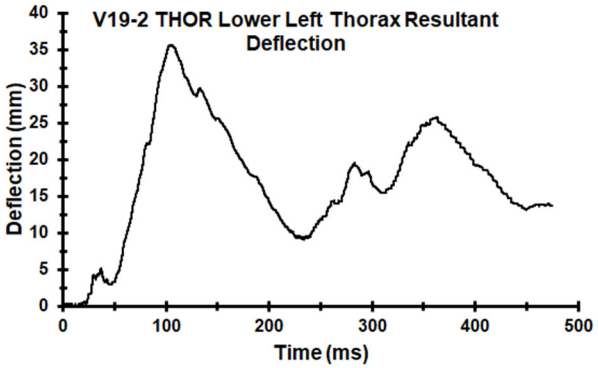
V19-2 THOR Lower Left Thorax Resultant Deflection
Deflection (mm)
Time (ms)

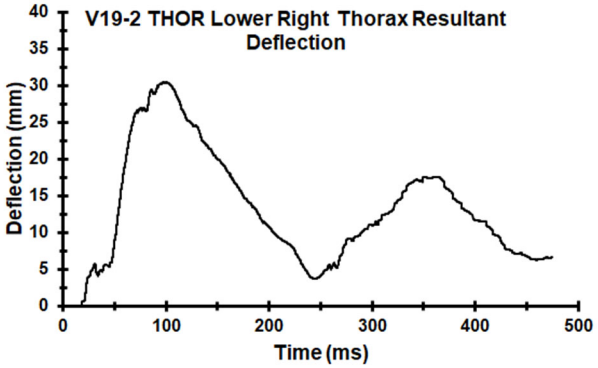
V19-2 THOR Lower Right Thorax Resultant Deflection
Deflection (mm)
Time (ms)

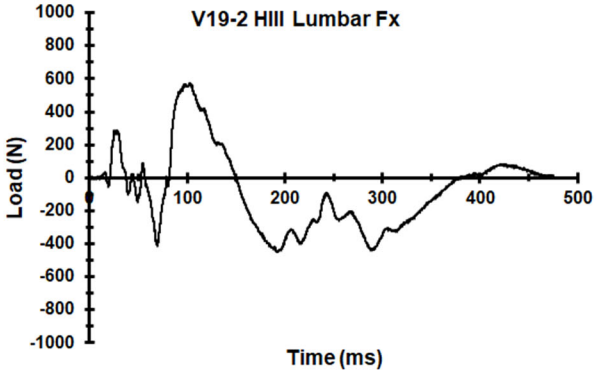
V19-2 HIII Lumbar Fx
Load (N)
Time (ms)

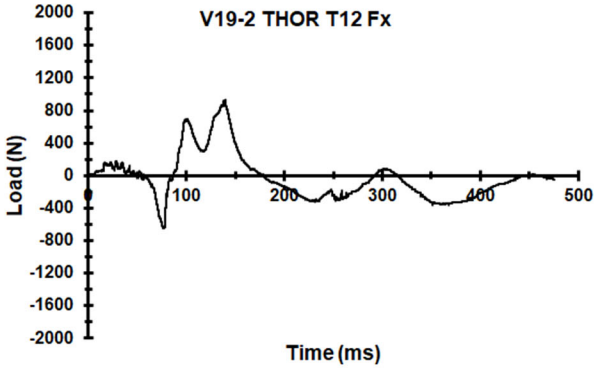
V19-2 THOR T12 Fx
Load (N)
Time (ms)

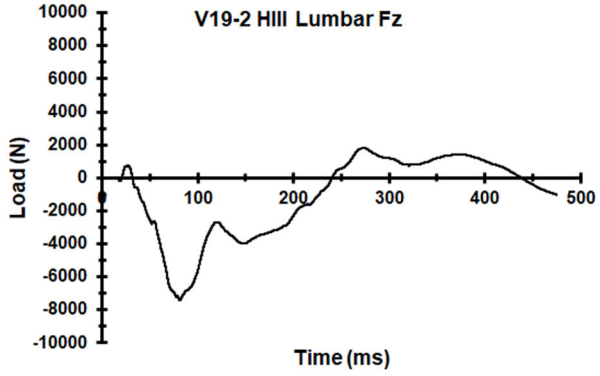
V19-2 HIII Lumbar Fz
Load (N)
Time (ms)

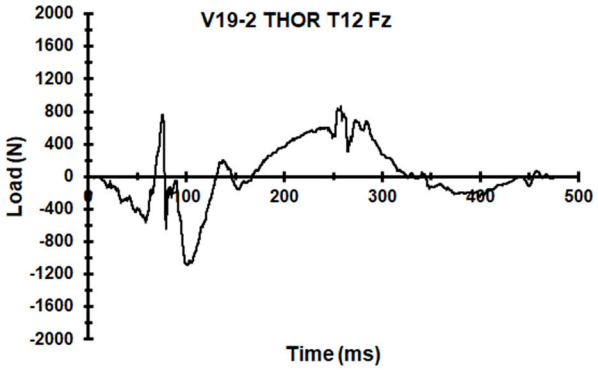
V19-2 THOR T12 Fz
Load (N)
Time (ms)

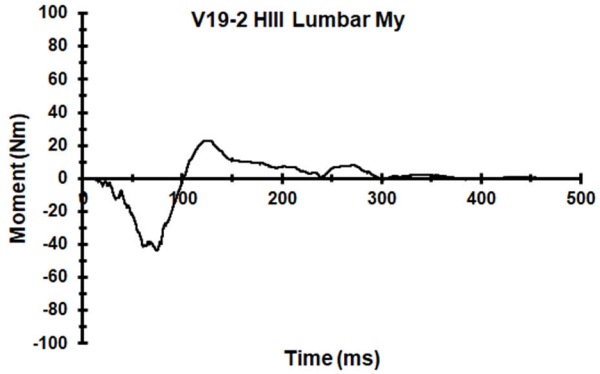
V19-2 HIII Lumbar My
Moment (Nm)
Time (ms)

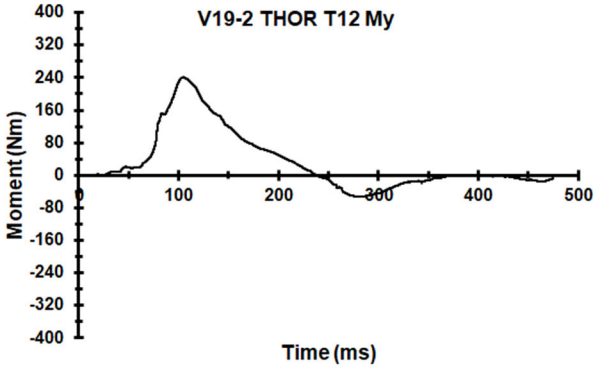
V19-2 THOR T12 My
Moment (Nm)
Time (ms)

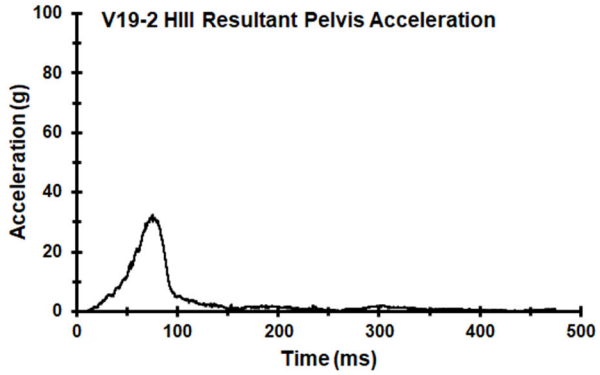
V19-2 HIII Resultant Pelvis Acceleration
Acceleration (g)
Time (ms)

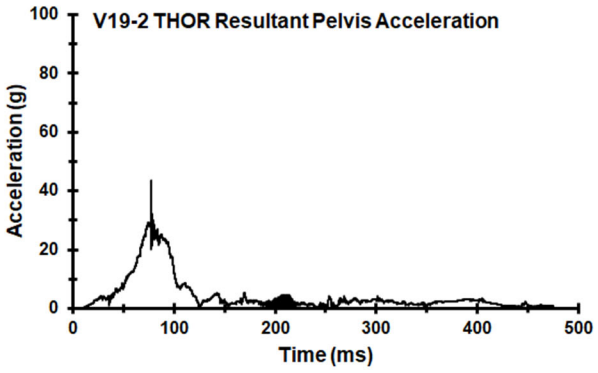
V19-2 THOR Resultant Pelvis Acceleration
Acceleration (g)
Time (ms)

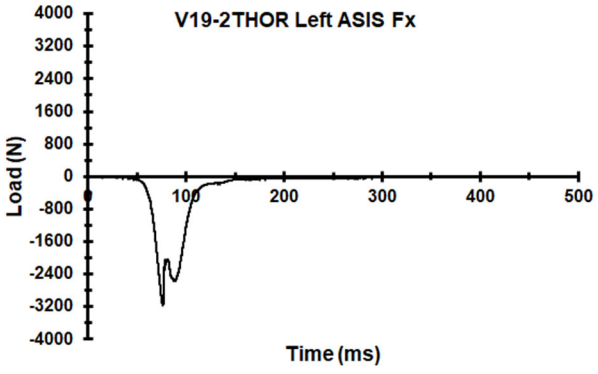
V19-2THOR Left ASIS Fx
Load (N)
Time (ms)

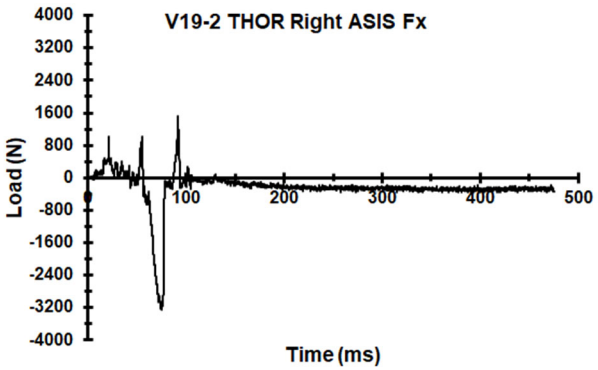
V19-2 THOR Right ASIS Fx
Load (N)
4000
3200
2400
1600
800
0
-800
-1600
-2400
-3200
-4000
100
200
300
400
500
Time (ms)

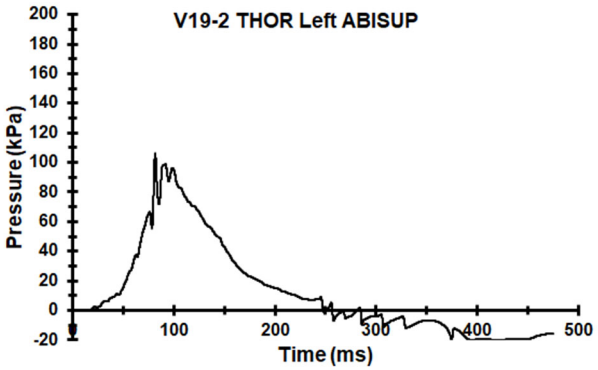
V19-2 THOR Left ABISUP
Pressure (kPa)
200
180
160
140
120
100
80
60
40
20
0
-20
100
200
300
400
500
Time (ms)

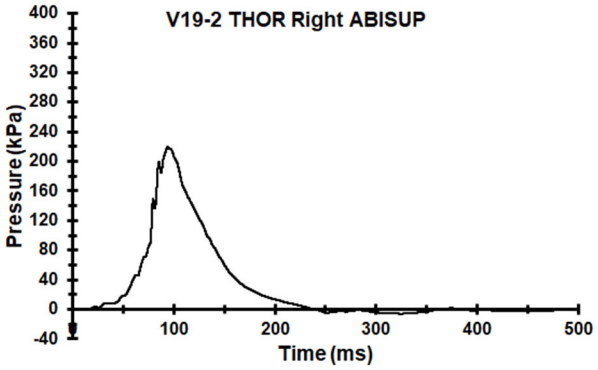
V19-2 THOR Right ABISUP
Pressure (kPa)
400
360
320
280
240
200
160
120
80
40
0
-40
100
200
300
400
500
Time (ms)

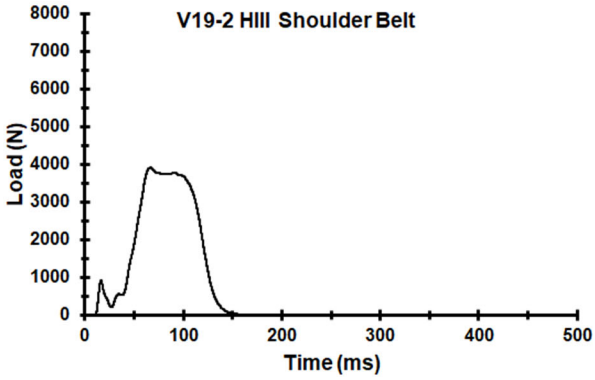
V19-2 HIII Shoulder Belt
Load (N)
8000
7000
6000
5000
4000
3000
2000
1000
0
0
100
200
300
400
500
Time (ms)

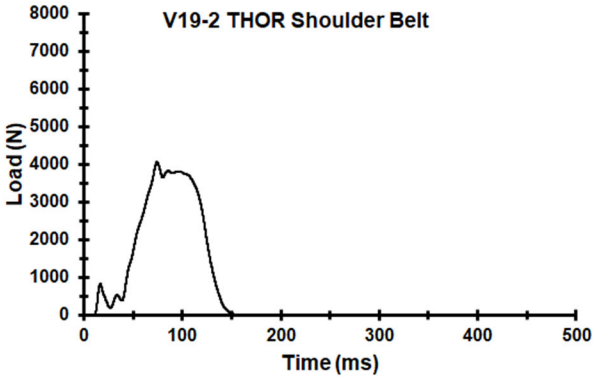
V19-2 THOR Shoulder Belt
Load (N)
8000
7000
6000
5000
4000
3000
2000
1000
0
0
100
200
300
400
500
Time (ms)

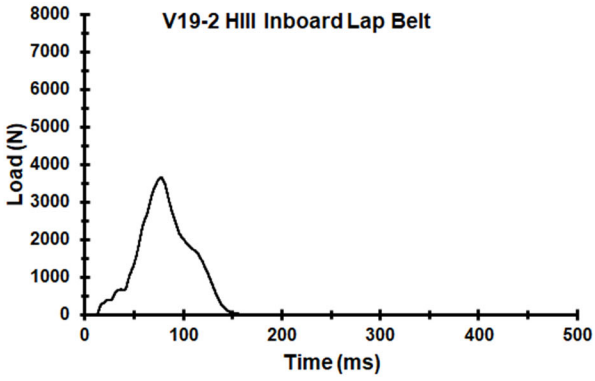
V19-2 HIII Inboard Lap Belt
Load (N)
8000
7000
6000
5000
4000
3000
2000
1000
0
0
100
200
300
400
500
Time (ms)

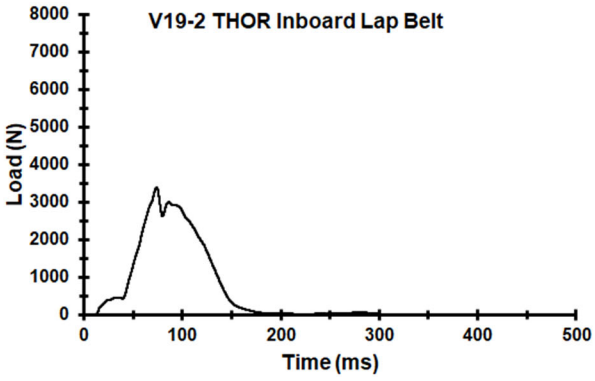
V19-2 THOR Inboard Lap Belt
Load (N)
8000
7000
6000
5000
4000
3000
2000
1000
0
0
100
200
300
400
500
Time (ms)

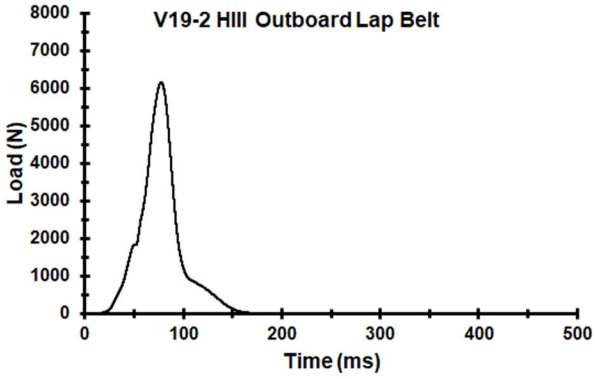
V19-2 HIII Outboard Lap Belt
Load (N)
8000
7000
6000
5000
4000
3000
2000
1000
0
0
100
200
300
400
500
Time (ms)

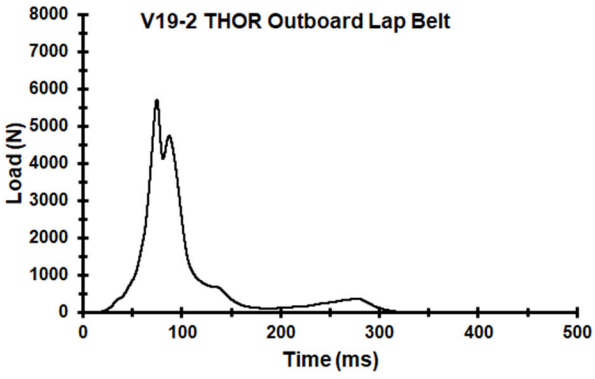
V19-2 THOR Outboard Lap Belt
Load (N)
8000
7000
6000
5000
4000
3000
2000
1000
0
0
100
200
300
400
500
Time (ms)

Appendix GG. Select Data Traces From Test FRS-V19-3

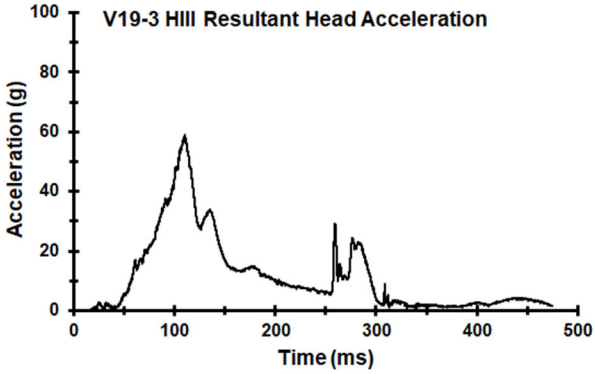
V19-3 HIII Resultant Head Acceleration
Acceleration (g)
Time (ms)

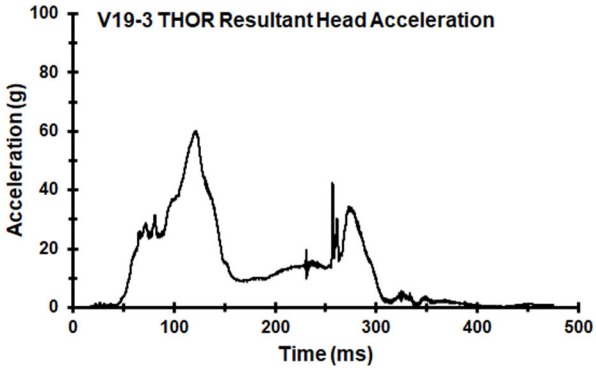
V19-3 THOR Resultant Head Acceleration
Acceleration (g)
Time (ms)

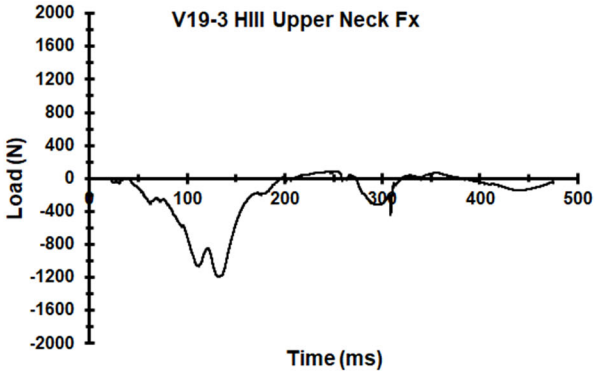
V19-3 HIII Upper Neck Fx
Load (N)
Time (ms)

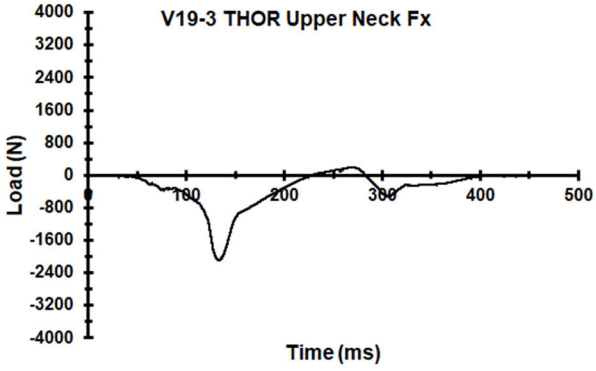
V19-3 THOR Upper Neck Fx
Load (N)
Time (ms)

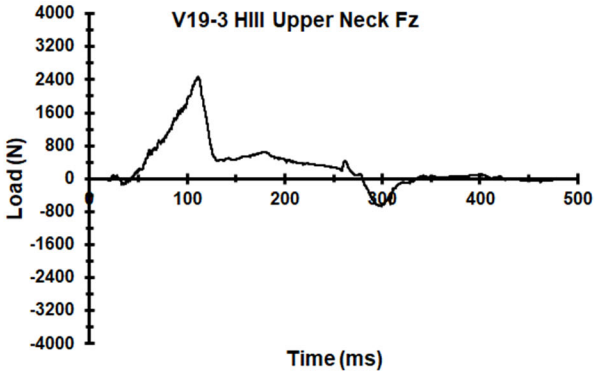
V19-3 HIII Upper Neck Fz
Load (N)
Time (ms)

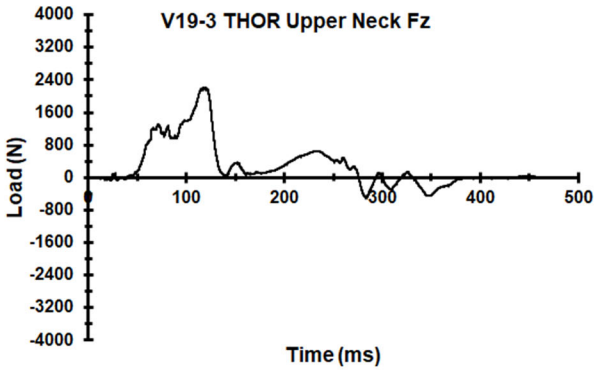
V19-3 THOR Upper Neck Fz
Load (N)
Time (ms)

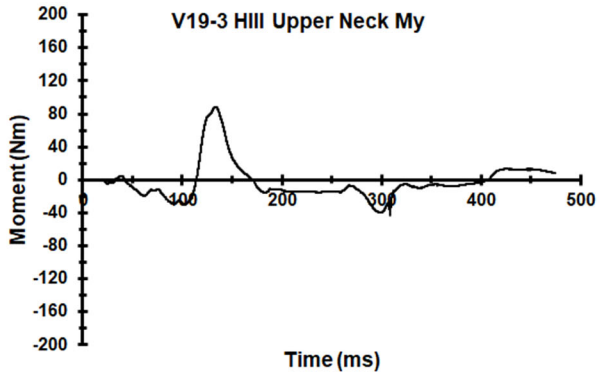
V19-3 HIII Upper Neck My
Moment (Nm)
200
160
120
80
40
0
-40
-80
-120
-160
-200
0
100
200
300
400
500
Time (ms)

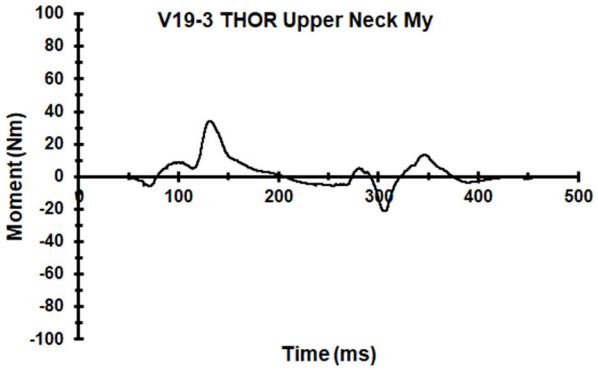
V19-3 THOR Upper Neck My
Moment (Nm)
100
80
60
40
20
0
-20
-40
-60
-80
-100
0
100
200
300
400
500
Time (ms)

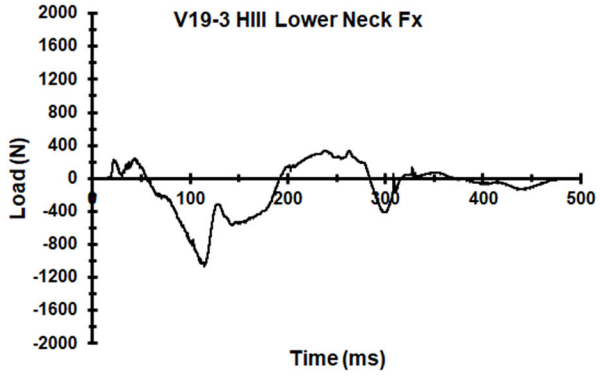
V19-3 HIII Lower Neck Fx
Load (N)
2000
1600
1200
800
400
0
-400
-800
-1200
-1600
-2000
0
100
200
300
400
500
Time (ms)

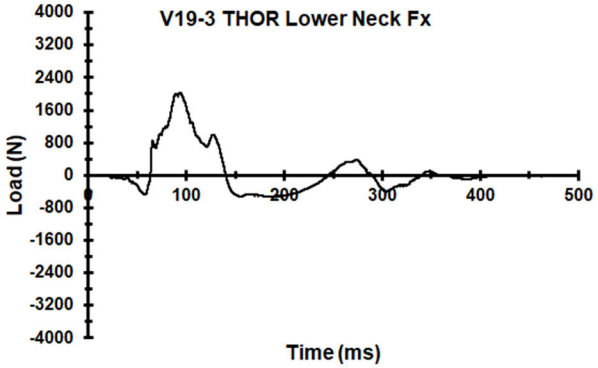
V19-3 THOR Lower Neck Fx
Load (N)
4000
3200
2400
1600
800
0
-800
-1600
-2400
-3200
-4000
0
100
200
300
400
500
Time (ms)

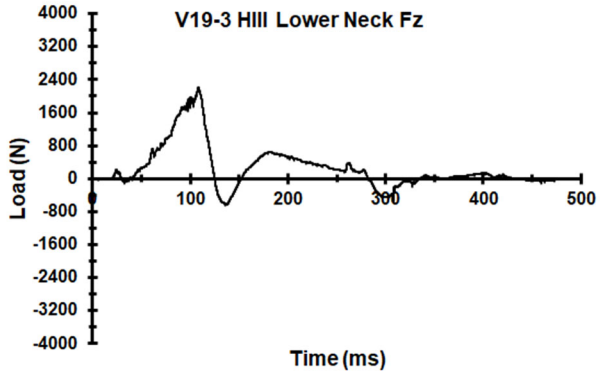
V19-3 HIII Lower Neck Fz
Load (N)
4000
3200
2400
1600
800
0
-800
-1600
-2400
-3200
-4000
0
100
200
300
400
500
Time (ms)

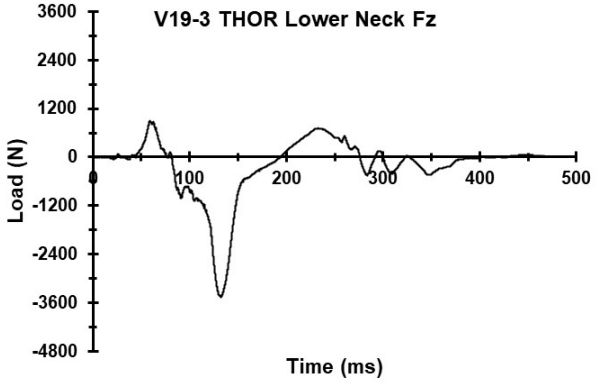
V19-3 THOR Lower Neck Fz
Load (N)
3600
2400
1200
0
-1200
-2400
-3600
-4800
0
100
200
300
400
500
Time (ms)

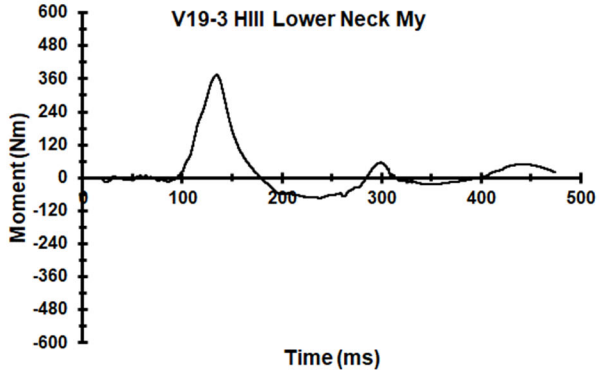
V19-3 HIII Lower Neck My
Moment (Nm)
600
480
360
240
120
0
-120
-240
-360
-480
-600
0
100
200
300
400
500
Time (ms)

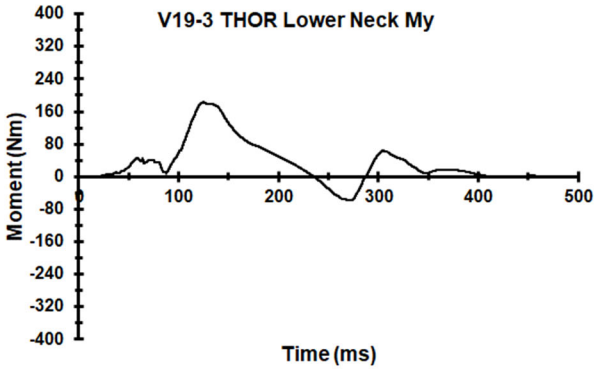
V19-3 THOR Lower Neck My
Moment (Nm)
400
320
240
160
80
0
-80
-160
-240
-320
-400
0
100
200
300
400
500
Time (ms)

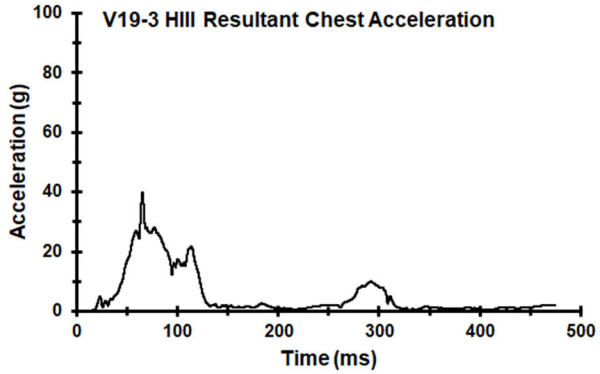
V19-3 HIII Resultant Chest Acceleration
Acceleration (g)
100
80
60
40
20
0
0
100
200
300
400
500
Time (ms)

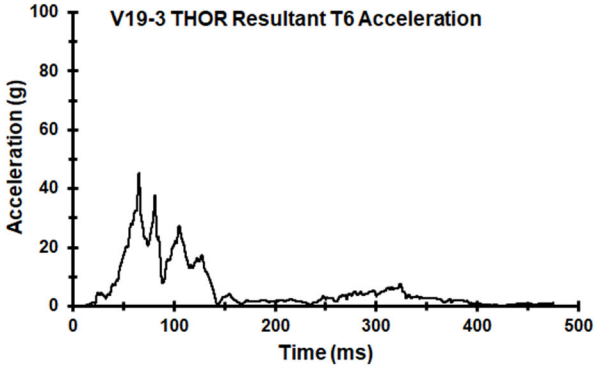
V19-3 THOR Resultant T6 Acceleration
Acceleration (g)
100
80
60
40
20
0
0
100
200
300
400
500
Time (ms)

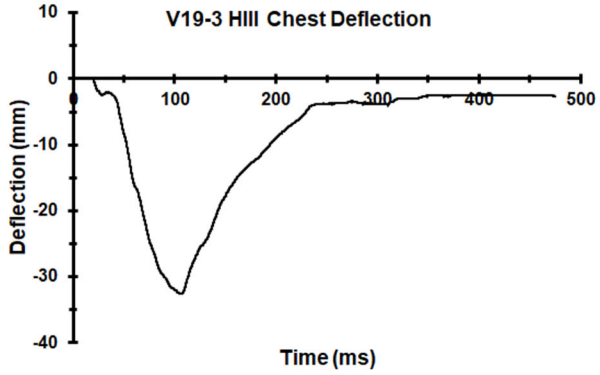
V19-3 HIII Chest Deflection
Deflection (mm)
10
0
-10
-20
-30
-40
0
100
200
300
400
500
Time (ms)

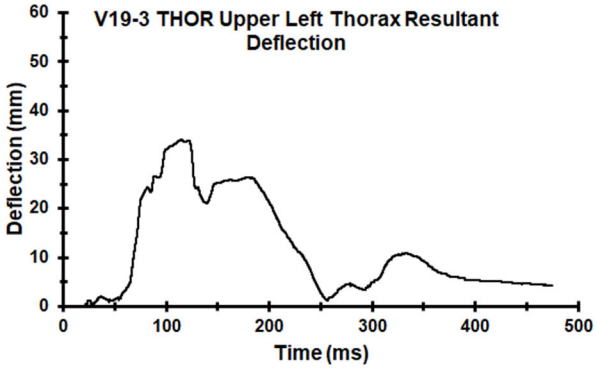
V19-3 THOR Upper Left Thorax Resultant Deflection
Deflection (mm)
60
50
40
30
20
10
0
0
100
200
300
400
500
Time (ms)

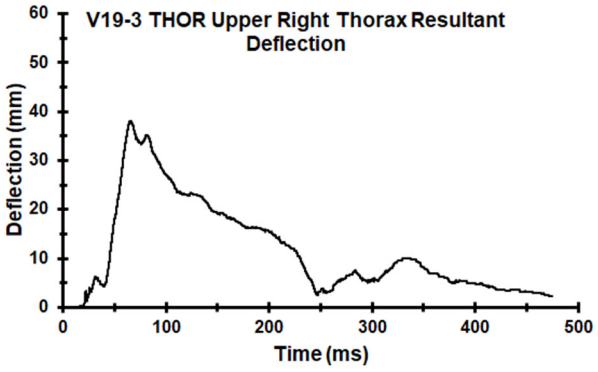
V19-3 THOR Upper Right Thorax Resultant Deflection
Deflection (mm)
60
50
40
30
20
10
0
0
100
200
300
400
500
Time (ms)

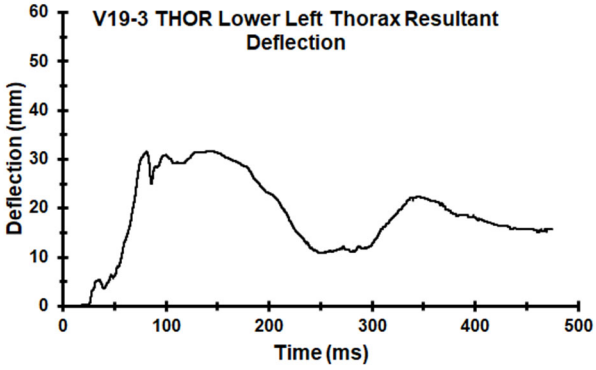
V19-3 THOR Lower Left Thorax Resultant Deflection
Deflection (mm)
60
50
40
30
20
10
0
0
100
200
300
400
500
Time (ms)

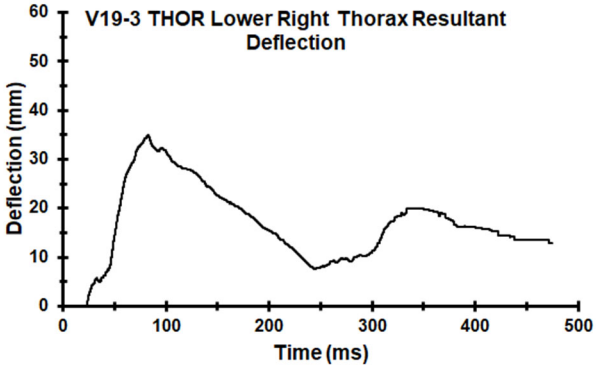
V19-3 THOR Lower Right Thorax Resultant Deflection
Deflection (mm)
60
50
40
30
20
10
0
0
100
200
300
400
500
Time (ms)

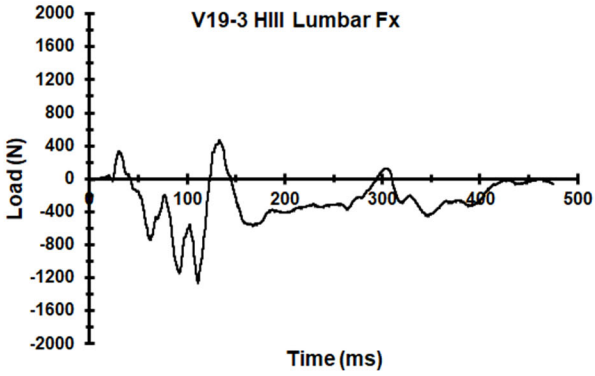
V19-3 HIII Lumbar Fx
Load (N)
2000
1600
1200
800
400
0
-400
-800
-1200
-1600
-2000
0
100
200
300
400
500
Time (ms)

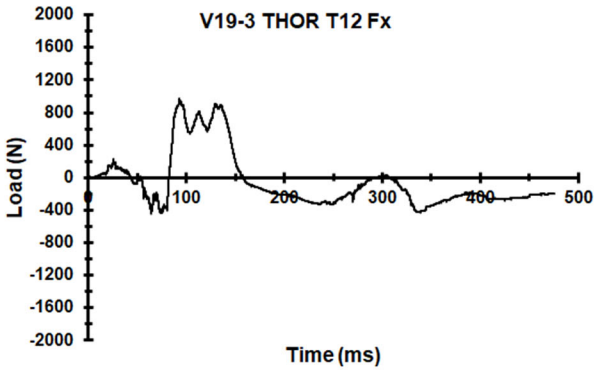
V19-3 THOR T12 Fx
Load (N)
2000
1600
1200
800
400
0
-400
-800
-1200
-1600
-2000
0
100
200
300
400
500
Time (ms)

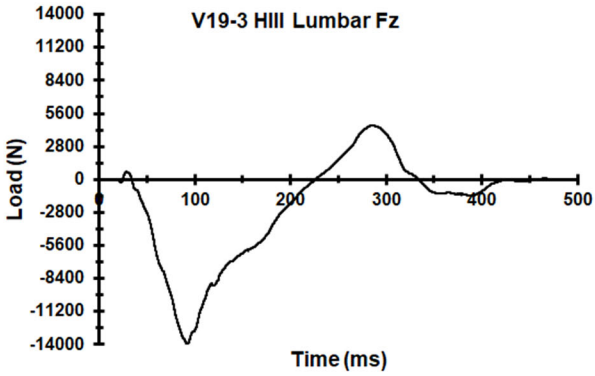
V19-3 HIII Lumbar Fz
Load (N)
14000
11200
8400
5600
2800
0
-2800
-5600
-8400
-11200
-14000
0
100
200
300
400
500
Time (ms)

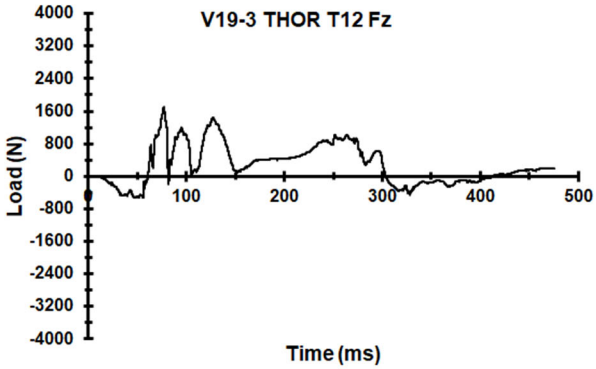
V19-3 THOR T12 Fz
Load (N)
4000
3200
2400
1600
800
0
-800
-1600
-2400
-3200
-4000
0
100
200
300
400
500
Time (ms)

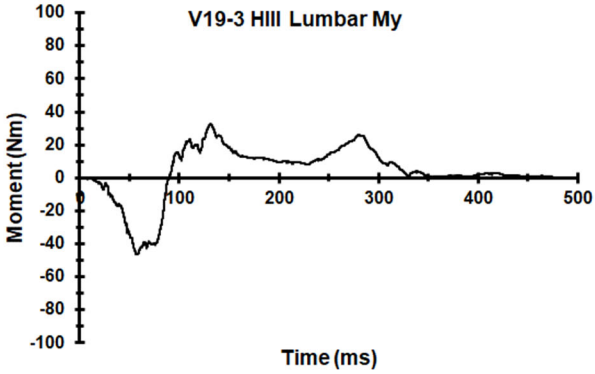
V19-3 HIII Lumbar My
Moment (Nm)
Time (ms)

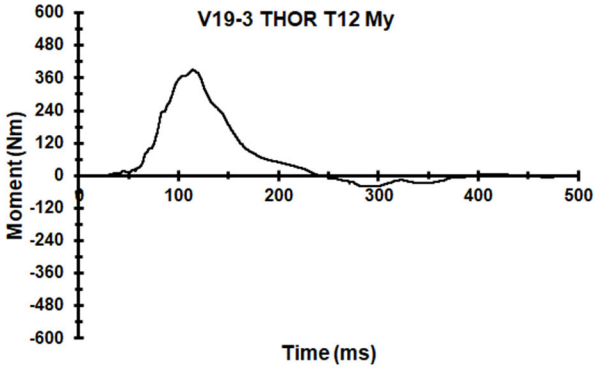
V19-3 THOR T12 My
Moment (Nm)
Time (ms)

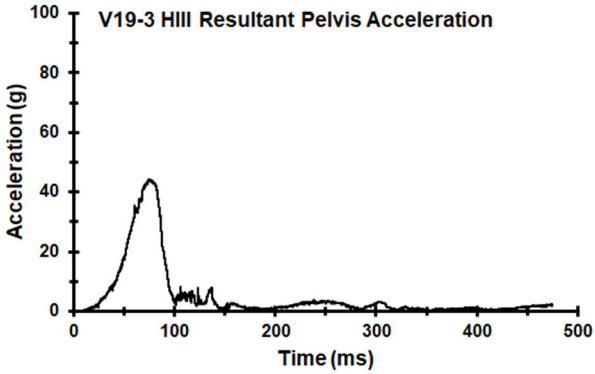
V19-3 HIII Resultant Pelvis Acceleration
Acceleration (g)
Time (ms)

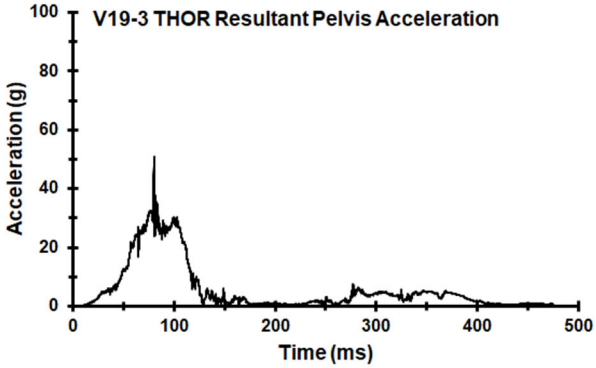
V19-3 THOR Resultant Pelvis Acceleration
Acceleration (g)
Time (ms)

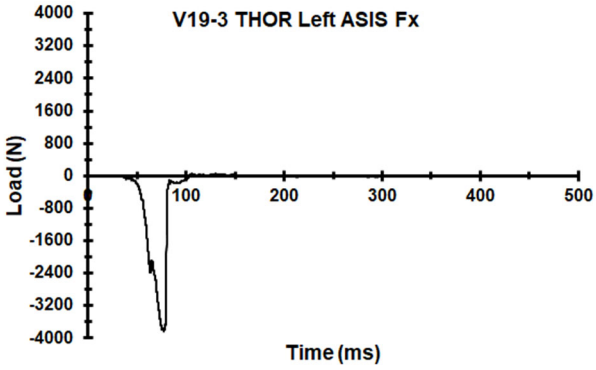
V19-3 THOR Left ASIS Fx
Load (N)
Time (ms)

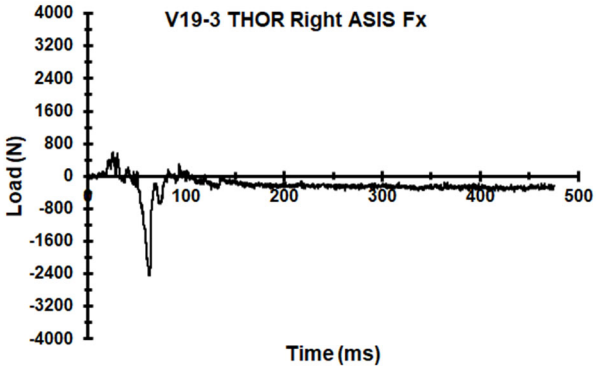
V19-3 THOR Right ASIS Fx
Load (N)
Time (ms)

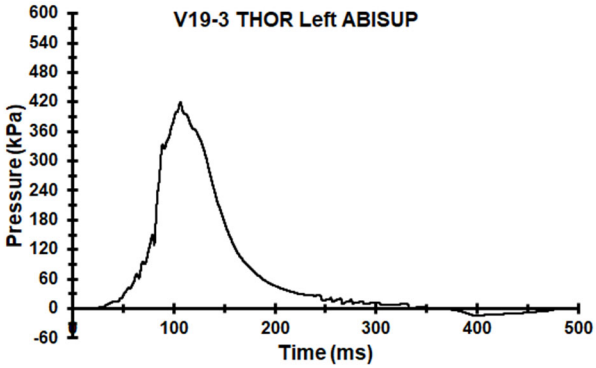
V19-3 THOR Left ABISUP
Pressure (kPa)
600
540
480
420
360
300
240
180
120
60
0
-60
100
200
300
400
500
Time (ms)

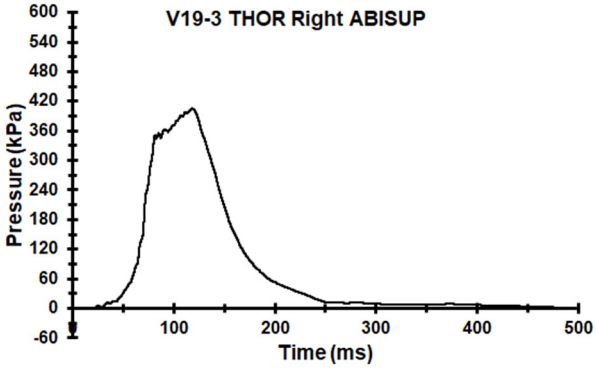
V19-3 THOR Right ABISUP
Pressure (kPa)
600
540
480
420
360
300
240
180
120
60
0
-60
100
200
300
400
500
Time (ms)

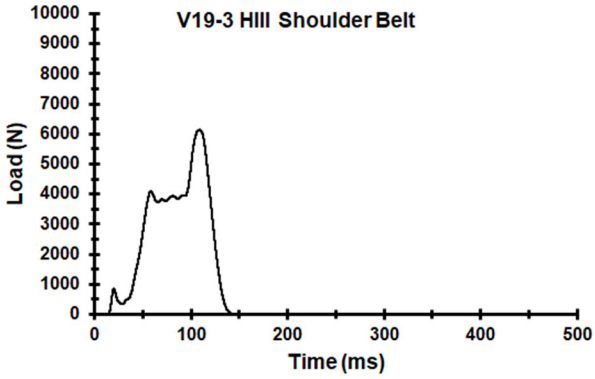
V19-3 HIII Shoulder Belt
Load (N)
10000
9000
8000
7000
6000
5000
4000
3000
2000
1000
0
0
100
200
300
400
500
Time (ms)

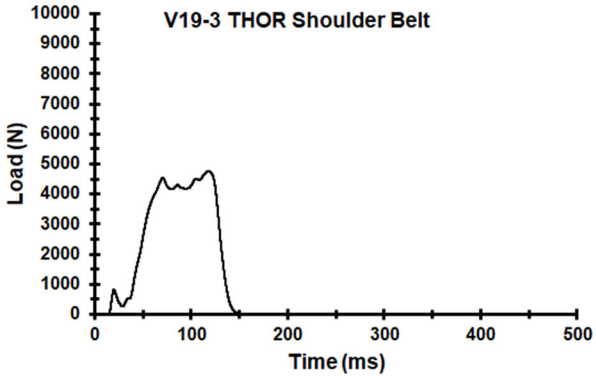
V19-3 THOR Shoulder Belt
Load (N)
10000
9000
8000
7000
6000
5000
4000
3000
2000
1000
0
0
100
200
300
400
500
Time (ms)

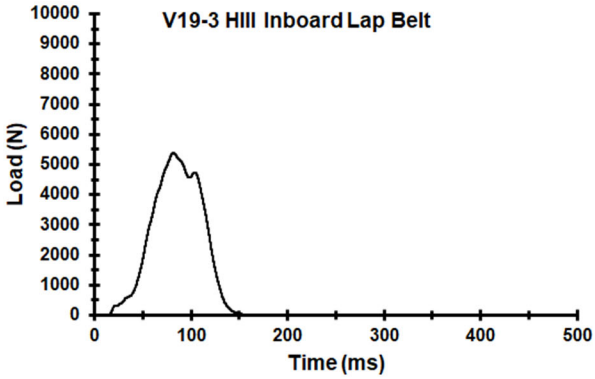
V19-3 HIII Inboard Lap Belt
Load (N)
Time (ms)
0
1000
2000
3000
4000
5000
6000
7000
8000
9000
10000
0
100
200
300
400
500

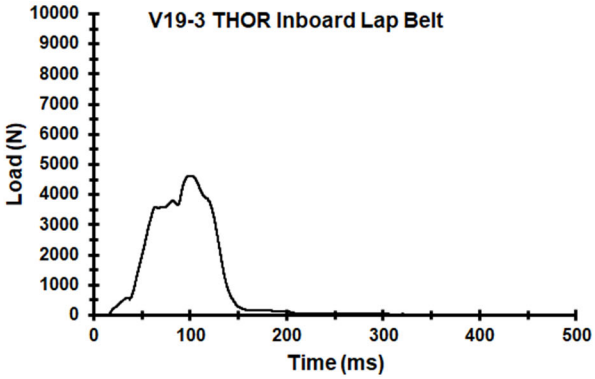
V19-3 THOR Inboard Lap Belt
Load (N)
Time (ms)
0
1000
2000
3000
4000
5000
6000
7000
8000
9000
10000
0
100
200
300
400
500

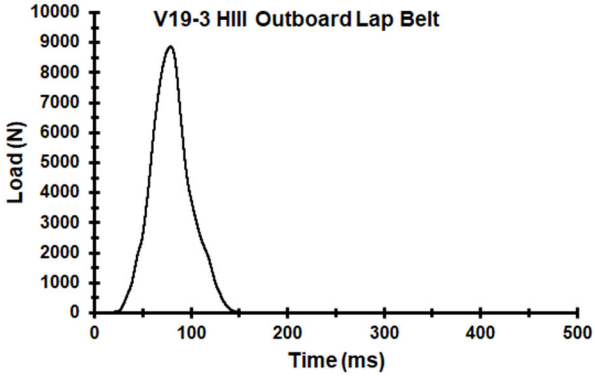
V19-3 HIII Outboard Lap Belt
Load (N)
Time (ms)
0
1000
2000
3000
4000
5000
6000
7000
8000
9000
10000
0
100
200
300
400
500

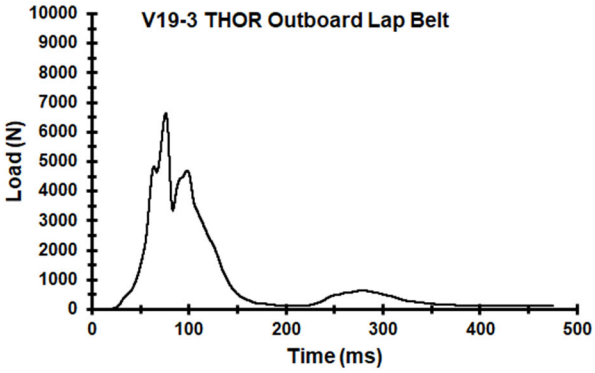
V19-3 THOR Outboard Lap Belt
Load (N)
Time (ms)
0
1000
2000
3000
4000
5000
6000
7000
8000
9000
10000
0
100
200
300
400
500

Appendix HH. Select Data Traces From Test FRS-V19-4

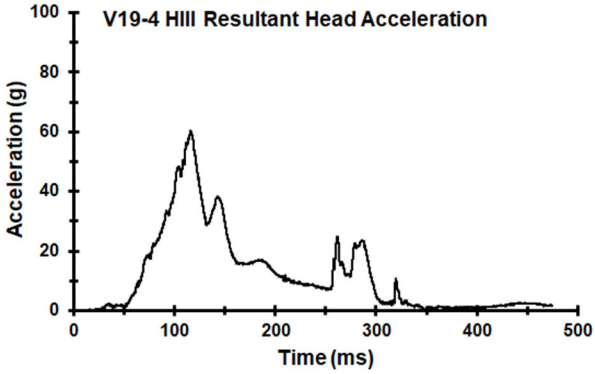
V19-4 HIII Resultant Head Acceleration
Acceleration (g)
Time (ms)

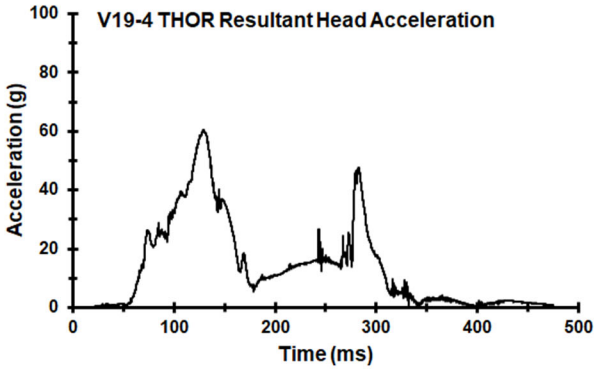
V19-4 THOR Resultant Head Acceleration
Acceleration (g)
Time (ms)

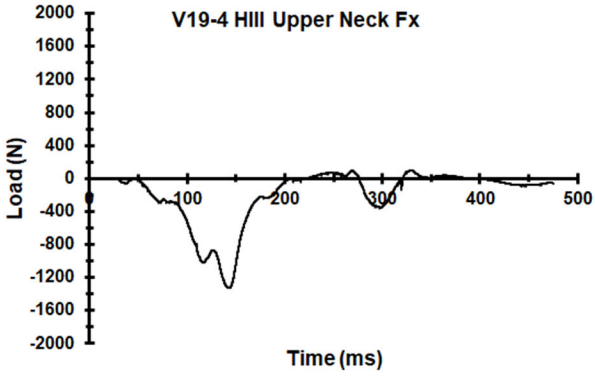
V19-4 HIII Upper Neck Fx
Load (N)
Time (ms)

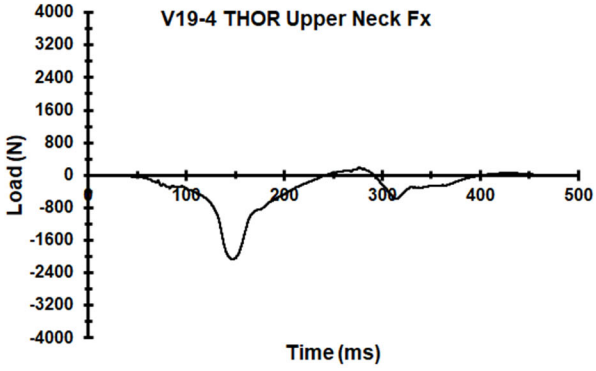
V19-4 THOR Upper Neck Fx
Load (N)
Time (ms)

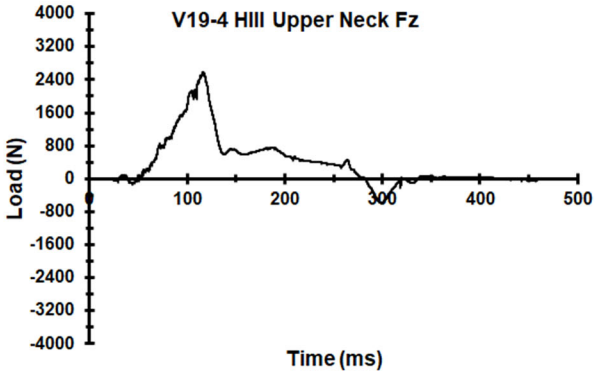
V19-4 HIII Upper Neck Fz
Load (N)
Time (ms)

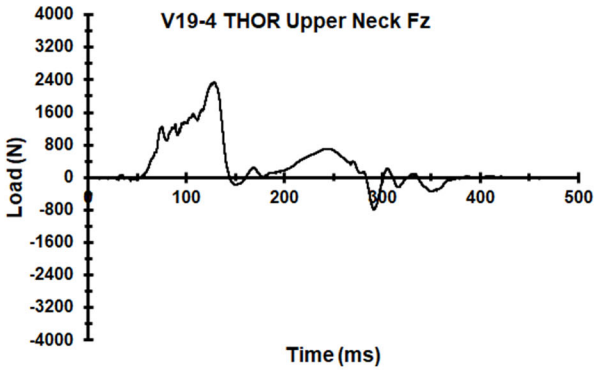
V19-4 THOR Upper Neck Fz
Load (N)
Time (ms)

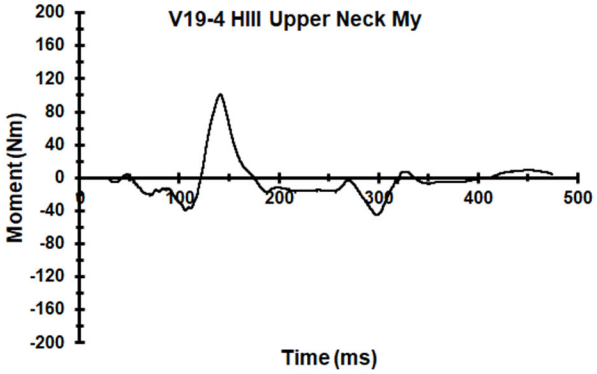
V19-4 HIII Upper Neck My
Moment (Nm)
Time (ms)

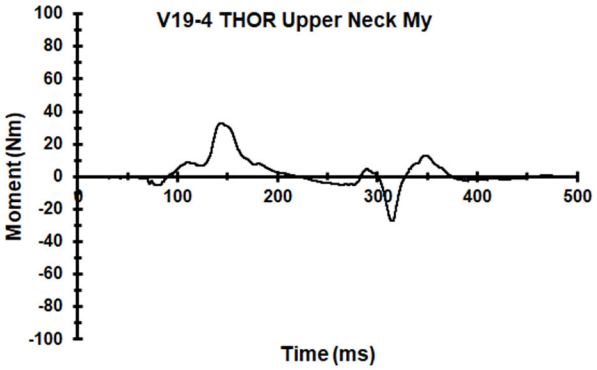
V19-4 THOR Upper Neck My
Moment (Nm)
Time (ms)

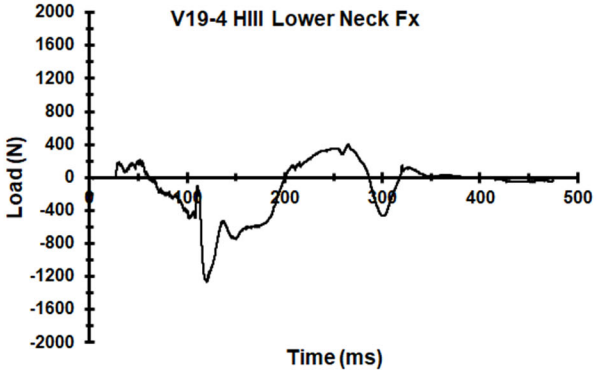
V19-4 HIII Lower Neck Fx
Load (N)
Time (ms)

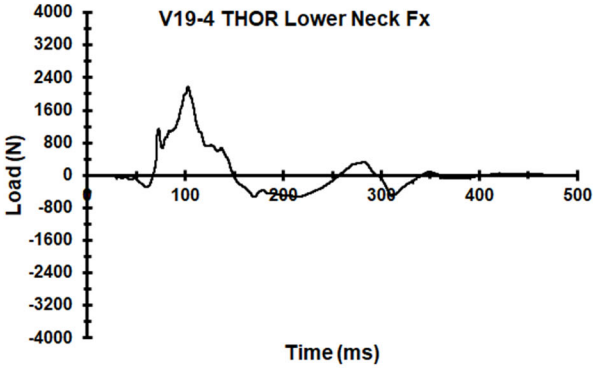
V19-4 THOR Lower Neck Fx
Load (N)
Time (ms)

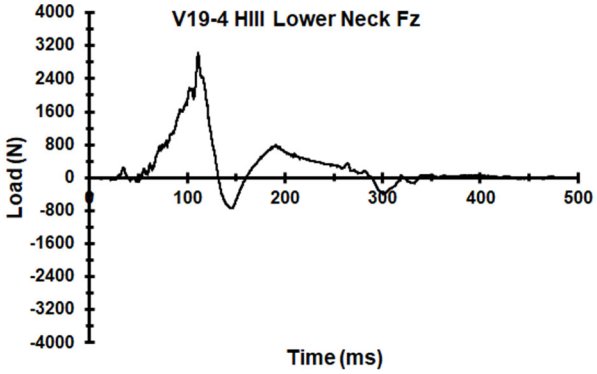
V19-4 HIII Lower Neck Fz
Load (N)
Time (ms)

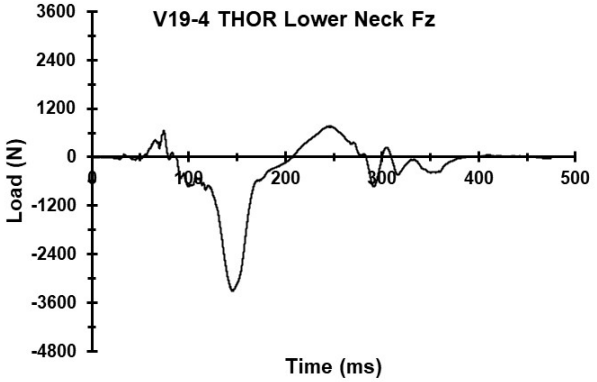
V19-4 THOR Lower Neck Fz
Load (N)
Time (ms)

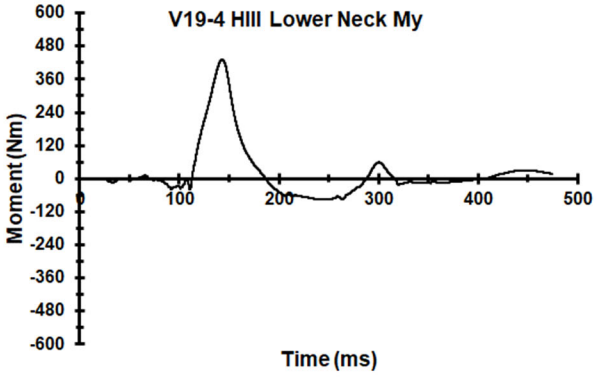
V19-4 HIII Lower Neck My
Moment (Nm)
Time (ms)

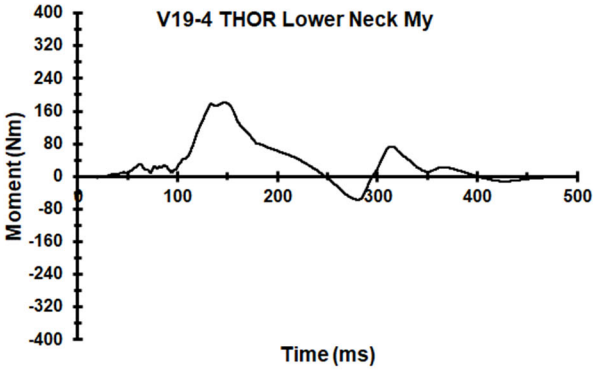
V19-4 THOR Lower Neck My
Moment (Nm)
Time (ms)

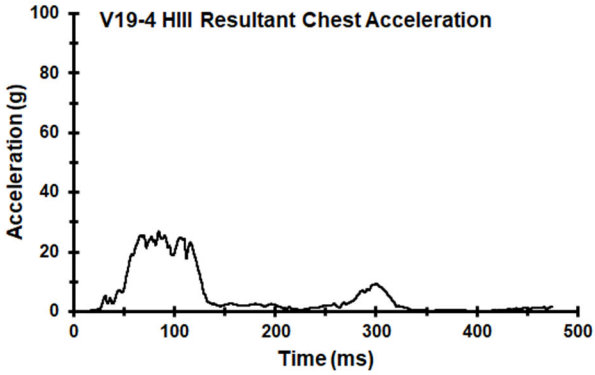
V19-4 HIII Resultant Chest Acceleration
Acceleration (g)
Time (ms)

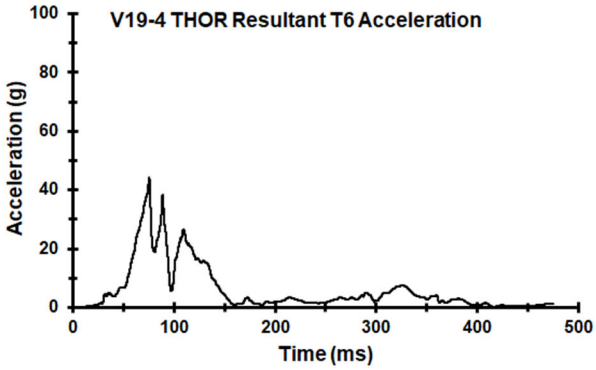
V19-4 THOR Resultant T6 Acceleration
Acceleration (g)
Time (ms)

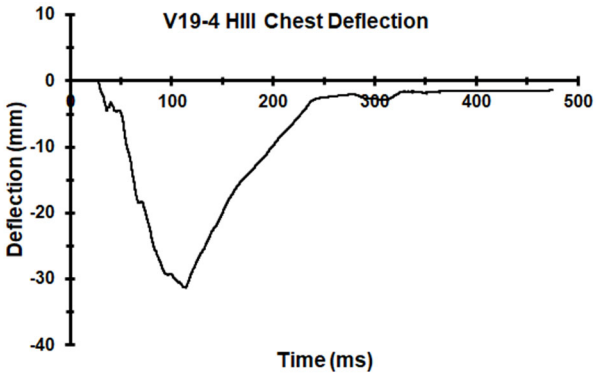
V19-4 HIII Chest Deflection
Deflection (mm)
Time (ms)

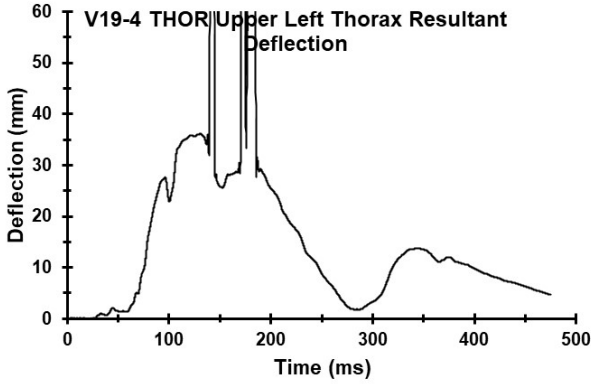
V19-4 THOR Upper Left Thorax Resultant Deflection
Deflection (mm)
Time (ms)

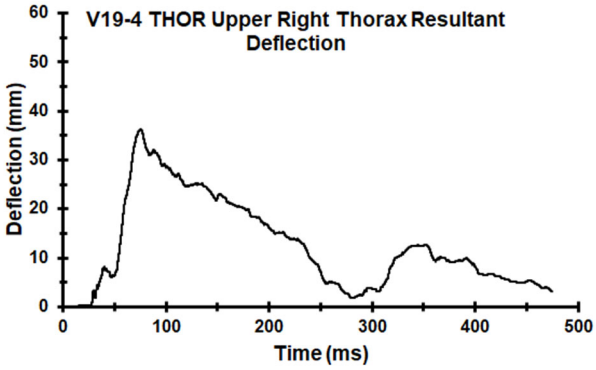
V19-4 THOR Upper Right Thorax Resultant Deflection
Deflection (mm)
Time (ms)

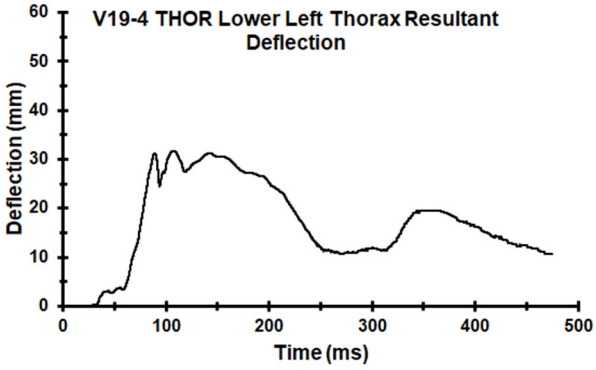
V19-4 THOR Lower Left Thorax Resultant Deflection
Deflection (mm)
60
50
40
30
20
10
0
0
100
200
300
400
500
Time (ms)

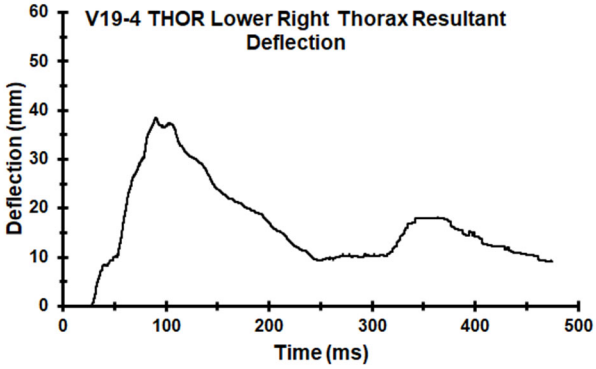
V19-4 THOR Lower Right Thorax Resultant Deflection
Deflection (mm)
60
50
40
30
20
10
0
0
100
200
300
400
500
Time (ms)

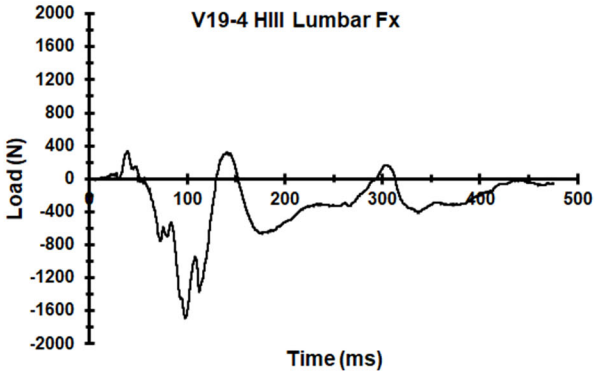
V19-4 HIII Lumbar Fx
Load (N)
2000
1600
1200
800
400
0
-400
-800
-1200
-1600
-2000
0
100
200
300
400
500
Time (ms)

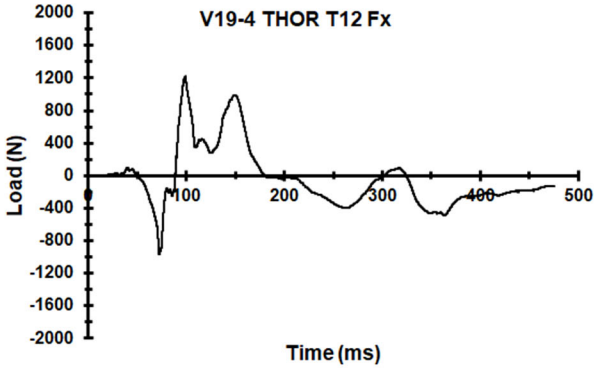
V19-4 THOR T12 Fx
Load (N)
2000
1600
1200
800
400
0
-400
-800
-1200
-1600
-2000
0
100
200
300
400
500
Time (ms)

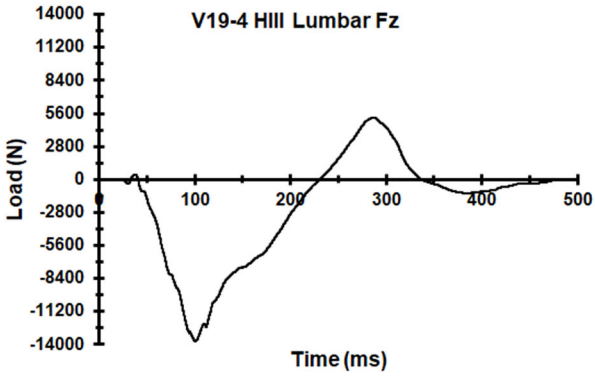
V19-4 HIII Lumbar Fz
Load (N)
14000
11200
8400
5600
2800
0
-2800
-5600
-8400
-11200
-14000
0
100
200
300
400
500
Time (ms)

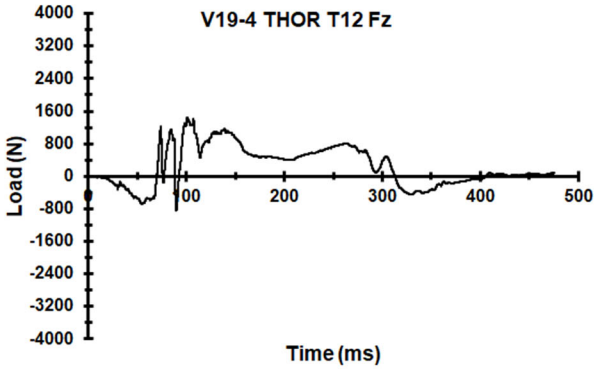
V19-4 THOR T12 Fz
Load (N)
4000
3200
2400
1600
800
0
-800
-1600
-2400
-3200
-4000
0
100
200
300
400
500
Time (ms)

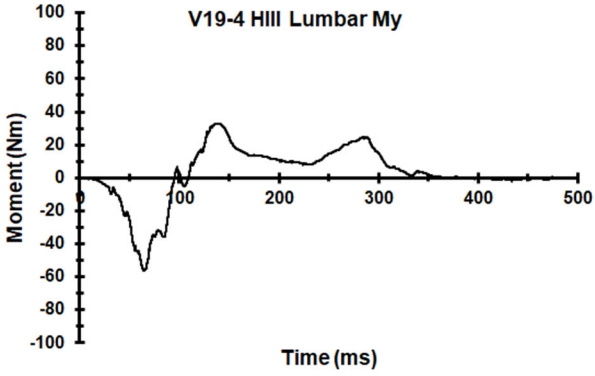
V19-4 HIII Lumbar My
Moment (Nm)
100
80
60
40
20
0
-20
-40
-60
-80
-100
0
100
200
300
400
500
Time (ms)

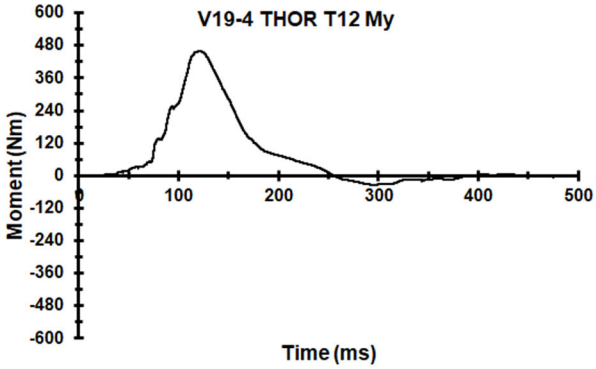
V19-4 THOR T12 My
Moment (Nm)
600
480
360
240
120
0
-120
-240
-360
-480
-600
0
100
200
300
400
500
Time (ms)

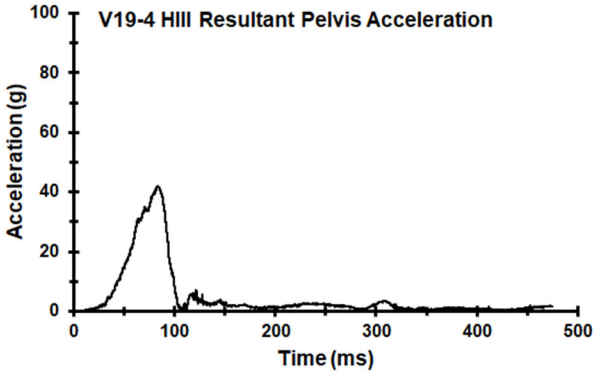
V19-4 HIII Resultant Pelvis Acceleration
Acceleration (g)
100
80
60
40
20
0
0
100
200
300
400
500
Time (ms)

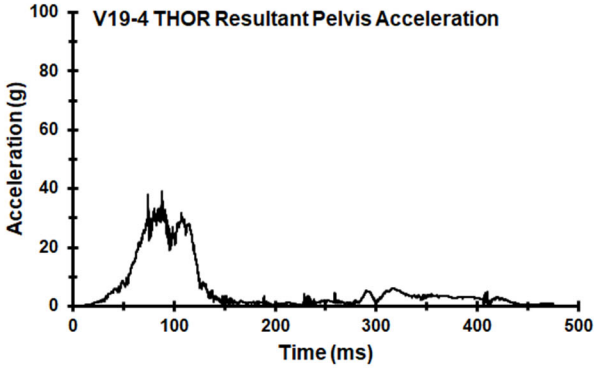
V19-4 THOR Resultant Pelvis Acceleration
Acceleration (g)
100
80
60
40
20
0
0
100
200
300
400
500
Time (ms)

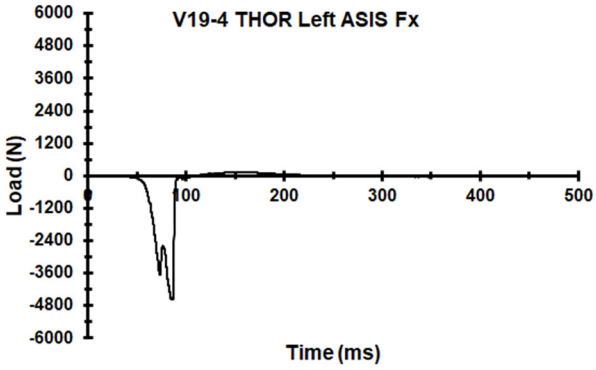
V19-4 THOR Left ASIS Fx
Load (N)
6000
4800
3600
2400
1200
0
-1200
-2400
-3600
-4800
-6000
0
100
200
300
400
500
Time (ms)

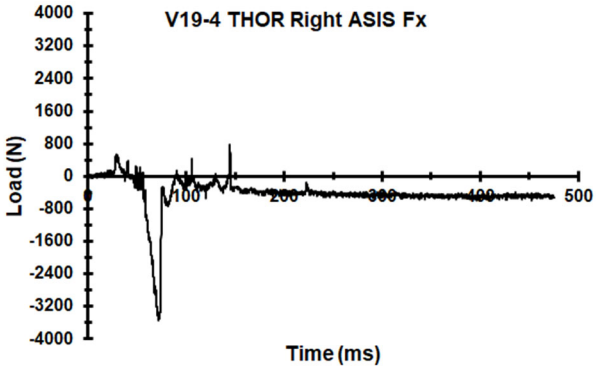
V19-4 THOR Right ASIS Fx
Load (N)
4000
3200
2400
1600
800
0
-800
-1600
-2400
-3200
-4000
0
100
200
300
400
500
Time (ms)

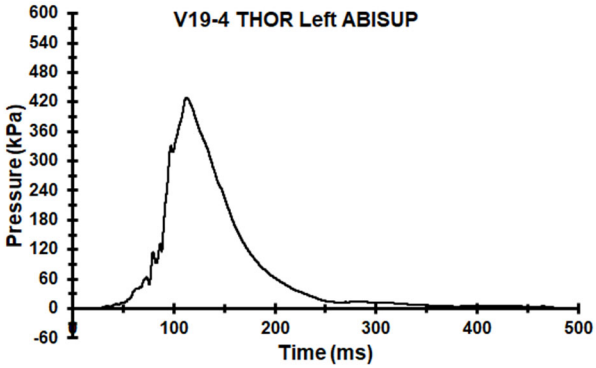
V19-4 THOR Left ABISUP
Pressure (kPa)
600
540
480
420
360
300
240
180
120
60
0
-60
100
200
300
400
500
Time (ms)

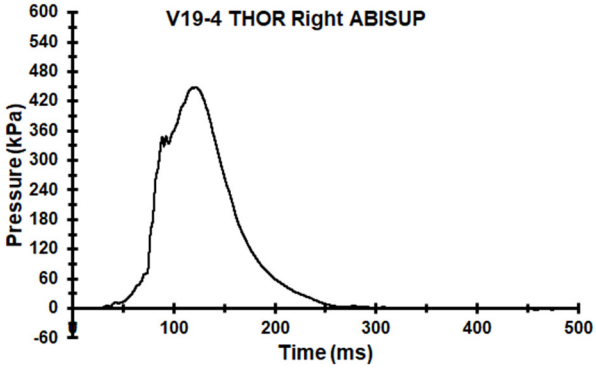
V19-4 THOR Right ABISUP
Pressure (kPa)
600
540
480
420
360
300
240
180
120
60
0
-60
100
200
300
400
500
Time (ms)

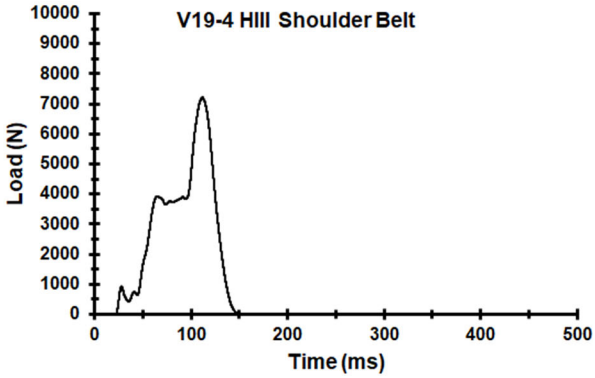
V19-4 HIII Shoulder Belt
Load (N)
10000
9000
8000
7000
6000
5000
4000
3000
2000
1000
0
0
100
200
300
400
500
Time (ms)

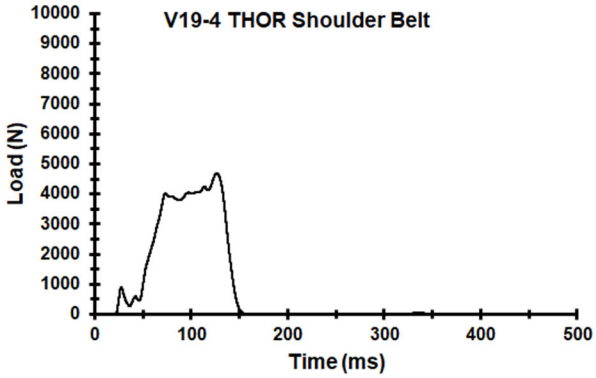
V19-4 THOR Shoulder Belt
Load (N)
10000
9000
8000
7000
6000
5000
4000
3000
2000
1000
0
0
100
200
300
400
500
Time (ms)

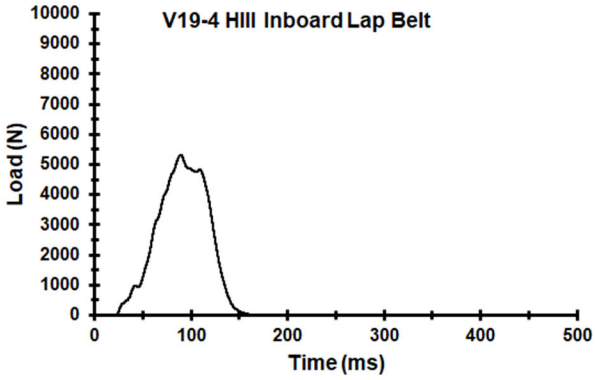
V19-4 HIII Inboard Lap Belt
Load (N)
Time (ms)
0
1000
2000
3000
4000
5000
6000
7000
8000
9000
10000
0
100
200
300
400
500

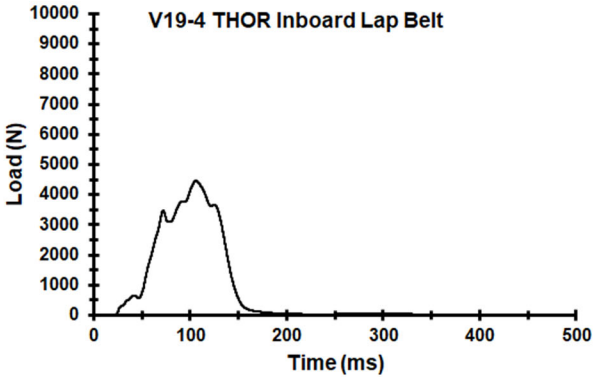
V19-4 THOR Inboard Lap Belt
Load (N)
Time (ms)
0
1000
2000
3000
4000
5000
6000
7000
8000
9000
10000
0
100
200
300
400
500

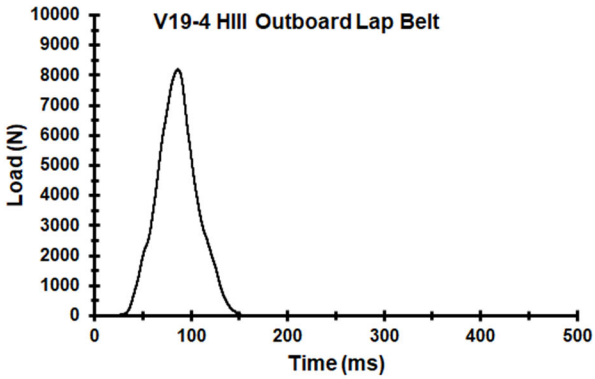
V19-4 HIII Outboard Lap Belt
Load (N)
Time (ms)
0
1000
2000
3000
4000
5000
6000
7000
8000
9000
10000
0
100
200
300
400
500

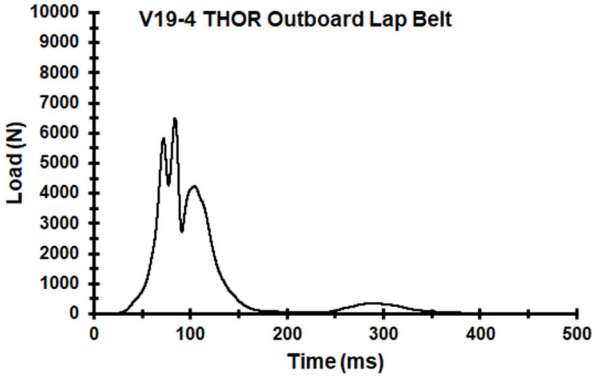
V19-4 THOR Outboard Lap Belt
Load (N)
Time (ms)
0
1000
2000
3000
4000
5000
6000
7000
8000
9000
10000
0
100
200
300
400
500

Appendix II. PeakTables of Data Peaks Organized by Vehicle Series

Table II-1. Data Peaks for Test Series FRS-V1

Parameters	Units	V1-1		V1-2		V1-3	
		HIII	THOR	HIII	THOR	HIII	THOR
Head A_R	g	28*	35	30*	37	55	64
Upper Neck Fx	N	224*	155*	233*	153*	161*	107*
	N	-610	-1454	-637	-1298	-1086	-1335
Upper Neck Fz	N	978	1287	1064	1467	2303	2877
	N	-314*	-577*	-278*	-639*	-716*	-584*
Upper Neck My	Nm	52	26	55	23	80	23
	Nm	-21*	-8*	-22*	-8*	-60*	-21*
Lower Neck Fx	N	289*	955	278*	1499	333	801
	N	-1198	-670	-1302	-656	-2155	-630
Lower Neck Fz	N	919	758	1043	715	2542	2567
	N	-257	-1848	-335	-1714	-509	-1593
Lower Neck My	Nm	199	132	216	142	335	160
	Nm	-63*	-44*	-64*	-46*	-73	-37*
Chest A_R	g	21	28	24	34	29	43
Chest Deflection	mm	27		26		43	
ULT R_{max}	mm		27		25		22
URT R_{max}	mm		40		36		55
LLT R_{max}	mm		17*		17*		13*
LRT R_{max}	mm		34		33		41
Lumbar Fx	N	1096	804	1319	888	2202	1326
	N	-537*	-285	-537	-325*	-1280	-301
Lumbar Fz	N		566		582*	1545	1027
	N		-2027		-2643	-3820	-3679
Lumbar My	Nm	28	256	27	263	261	301
	Nm	-65	-17*	-76	-16*	-86*	-34*
Left ABISUP	kPa		118		114		127
Right ABISUP	kPa		191		161		158
Left ASIS Fx	N		-2261		-2477		-3916
Right ASIS Fx	N		-2164		-2705		-3301
Pelvis A_R	g	29	33	32	22	48	55
Shoulder Belt	N	3796	3295	3808	3446		6897
Inboard Lap Belt	N	3061	2906	2895	3070	5346	5432
Outboard Lap Belt	N	4148	3927	4418	3928	5783	6466

*Peak value when the ATD head made contact with the seat or returned to the seat.

Table II-2. Data Peaks for Test Series FRS-V6

Parameters	Units	V6-1		V6-2		V6-4	
		HIII	THOR	HIII	THOR	HIII	THOR
Head A_R	g	46	38	46	33	78	66
Upper Neck Fx	N	147*	146*	166*	163*	130*	202*
	N	-1298	-1179	-1343	-1460	-1538	-2114
Upper Neck Fz	N	1652	1424	1613	1191	3230	2683
	N	-82*	-163*	-90*	-242*	-239*	-451*
Upper Neck My	Nm	105	24	108	29	113	39
	Nm	-35*	-10	-34*	-10*	-38*	-16*
Lower Neck Fx	N	655*	1899	680*	2330	587*	3067
	N	-2073	-634	-2106	-459	-3542	-687
Lower Neck Fz	N	1678	1151	1473	639	2808	1818
	N	-601	-1866	-595	-1984	-660	-3711
Lower Neck My	Nm	405	147	412	167	520	185
	Nm	-107*	-35*	-138*	-48*	-161*	-45*
Chest A_R	g	33	39	31	30	39	47
Chest Deflection	mm	39		37		55	
ULT R_{max}	mm		20		24		27
URT R_{max}	mm		42		32		46
LLT R_{max}	mm		18*		16*		13
LRT R_{max}	mm		32		29		37
Lumbar Fx	N	1318	756	1508	706	1483	1549
	N	-970	-310*	-1072	-358	-1143	-636
Lumbar Fz	N	1615	708*	1466	687*	1830	686*
	N	-1769	-873	-1775	-620	-2337	-1343
Lumbar My	Nm	200	157	186	199	198	253
	Nm	-52*	-37*	-45*	-58*	-2	-7*
Left ABISUP	kPa		68		76		132
Right ABISUP	kPa		70		77		116
Left ASIS Fx	N		-2853		-2883		-4792
Right ASIS Fx	N		-2216		-2145		-3860
Pelvis A_R	g	34	36	34	29	44	49
Shoulder Belt	N	6497	5170	6416	5010	9477	8880
Inboard Lap Belt	N	5006	3917	5098	3610	7109	6129
Outboard Lap Belt	N	5839	5280	5584	5371	7226	7446

*Peak value when the ATD head made contact with the seat or returned to the seat.

Table II-3. Data Peaks for Test Series FRS-V10

Parameters	Units	V10-1		V10-2		V10-3	
		HIII	THOR	HIII	THOR	HIII	THOR
Head A_R	g	46	51*	42	72*	74*	73*
Upper Neck Fx	N	205*	259	166*	166*	364	77*
	N	-1660	-1729	-1478	-1498	-2322	-2675
Upper Neck Fz	N	1473	1804	1294	1333	2731	2510
	N	-1107*	-1642*	-782*	-3262*	-2076*	-803*
Upper Neck My	Nm	115	32	111	29	153	48
	Nm	-86*	-14*	-78*	-12*	-103*	-27*
Lower Neck Fx	N	344	1513	284	1689	1257	2163
	N	-1784	-795	-1509	-589	-3151	-1019*
Lower Neck Fz	N	1471	1735	1650	1531	2671	1679*
	N	-742	-2937	-761	-3061*	-2012*	-4801
Lower Neck My	Nm	514	172	478	145	828	217
	Nm	-85	-46*	-77	-38*	-93	-9*
Chest A_R	g	36	49	41	49	51	57
Chest Deflection	mm	41		35		63	
ULT R_{max}	mm		19		23		26
URT R_{max}	mm		48		42		44
LLT R_{max}	mm		11		15		24
LRT R_{max}	mm		40		32		41
Lumbar Fx	N	1940	1259	1593	1337	3101	2890
	N	-2476	-689	-2407	-715	-3081	-738
Lumbar Fz	N	1189	2391	1057	2156	1999	5190
	N	-767	-823	-1132	-1057*	-705	-1155
Lumbar My	Nm	273	222	263	187	370	312
	Nm	-80*	-40*	-61*	-29*	-78*	-79*
Left ABISUP	kPa		224		254		383
Right ABISUP	kPa		221		187		375
Left ASIS Fx	N		-3110		-2579		-2700
Right ASIS Fx	N		-3127		-3289		-3022
Pelvis A_R	g	33	32	37	29	43	41
Shoulder Belt	N	7431	5956	7631	5996	10329	8934
Inboard Lap Belt	N	5266	4865	5922	5025	7746	6454
Outboard Lap Belt	N	6885	5375	8047	5054	10415	7770

*Peak value when the ATD head made contact with the seat or returned to the seat.

Table II-4. Data Peaks for Test Series FRS-V13

Parameters	Units	V13-1		V13-2		V13-3	
		HIII	THOR	HIII	THOR	HIII	THOR
Head A_R	g	38	95*	74	119*	43*	62*
Upper Neck Fx	N	308*	46	119*	84*	244*	69*
	N	-1405	-2034	-2346	-2625	-1485	-1430
Upper Neck Fz	N	1201	1463	2783	2287	1290	1446
	N	-758*	-1219*	-720*	-2525*	-671*	-1258*
Upper Neck My	Nm	99	35	142	40	101	30
	Nm	-78*	-27*	-86*	-46*	-87*	-27*
Lower Neck Fx	N	354	2761	1128*	5644	501	2148
	N	-1866	-700	-3991	-1492*	-1614	-763
Lower Neck Fz	N	1297	1420	2028	1779	1490	1575
	N	-1258*	-3123	-1973	-3388	-1422*	-2154
Lower Neck My	Nm	465	169	677	168	492	151
	Nm	-81*	-24*	-127	-36*	-99	-32*
Chest A_R	g	34	35	47	54	35	35
Chest Deflection	mm	35		79		39	
ULT R_{max}	mm				32		22
URT R_{max}	mm		41		43		45
LLT R_{max}	mm		19		26		19
LRT R_{max}	mm		34		37		36
Lumbar Fx	N	3094	2313	2524	6297	3714	2977
	N	-1040	-786	-1306	-1022	-1610	-150*
Lumbar Fz	N	1461*	2000	2444*	5520	1034	1836
	N	-8198	-941	-10424	-1501	-1771	-1849
Lumbar My	Nm	29	207	68	230	234	143
	Nm	-45	-58*	-49	-135	-51*	-65*
Left ABISUP	kPa		239		352		250
Right ABISUP	kPa		189		294		248
Left ASIS Fx	N		-2807		-4328		-2439
Right ASIS Fx	N		-3490		-3955		-1843
Pelvis A_R	g	37	32	48	47	34	26
Shoulder Belt	N	6613	5192	9509	8908	6710	4987
Inboard Lap Belt	N	4705	3959	6900	5975	4857	4208
Outboard Lap Belt	N	6827	5523	9715		6980	4213

*Peak value when the ATD head made contact with the seat or returned to the seat.

Table II-5. Data Peaks for Test Series FRS-V14

Parameters	Units	V14-1		V14-2		V14-3		V14-4	
		HIII	THOR	HIII	THOR	HIII	THOR	HIII	THOR
Head A_R	g	41*	35	49*	34*	58*	59	64*	63
Upper Neck Fx	N	231*	158*	267*	151*	205*	223*	178*	135*
	N	-806	-1815	-747	-1599	-1035	-1988	-930	-2275
Upper Neck Fz	N	1003	1066	829	934	1712	2197	1667	2453
	N	-472*	-588*	-524*	-564*	-1276*	-460*	-1061*	-964*
Upper Neck My	Nm	63	27	58	24	71	30	62	33
	Nm	-40*	-13*	-41*	-13*	-40*	-9*	-48*	-22*
Lower Neck Fx	N	468*	1005	470*	1058	355*	2780	289	3198
	N	-1469	-910	-1314	-804	-2410	-750	-2273	-802
Lower Neck Fz	N	606	981	571	815	956	1223	1126	1149
	N	-415	-3026	-456*	-2415	-1143*	-3807	-707*	-3835
Lower Neck My	Nm	264	188	265	176	317	215	282	192
	Nm	-86*	-44*	-99*	-46*	-81*	-44*	-71	-43*
Chest A_R	g	24	26	20	23	26	34	25	31
Chest Deflection	mm	35		32		40		38	
ULT R_{max}	mm		25		23		32		32
URT R_{max}	mm		35		34		45		43
LLT R_{max}	mm		19		18		25		29
LRT R_{max}	mm		36		35		43		41
Lumbar Fx	N	1661	1578	1793	1335	1768	1612	1579	1762
	N	-634*	-317	-700*	-332	-513	-490*	-533	-438*
Lumbar Fz	N	1149	611	1506	569	1552	491	1444*	744*
	N	-4139	-2350	-2738*	-2203	-4540	-2986	-4851	-3778
Lumbar My	Nm	15	263	14	225	27	368	25	397
	Nm	-57	-19*	-49	-26*	-64	-38*	-70	-47*
Left ABISUP	kPa		80		82		118		127
Right ABISUP	kPa		93		100		122		126
Left ASIS Fx	N		-2825		-2041		-3821		-3893
Right ASIS Fx	N		-2581		-1854		-3390		-3176
Pelvis A_R	g	31	31	27	26	36	39	36	41
Shoulder Belt	N	5080	4371	5242	4192	6318		5845	6368
Inboard Lap Belt	N	3874	3446	3840	3458	4787	4793	4986	4571
Outboard Lap Belt	N	4632	5213	4065	4277	6139		5551	6767

*Peak value when the ATD head made contact with the seat or returned to the seat.

Table II-6. Data Peaks for Test Series FRS-V15

Parameters	Units	V15-1		V15-2		V15-3		V15-4	
		HIII	THOR	HIII	THOR	HIII	THOR	HIII	THOR
Head A_R	g	41	41	45	42	45	41	77	105*
Upper Neck Fx	N	173*	253*	218*	221*	118*	242*	253*	53
	N	-1193	-2078	-1298	-1976	-1359	-1889	-2542	-2777
Upper Neck Fz	N	1750	1852	1933	1739	1900	1740	3043	3048
	N	-720*	-844*	-1086*	-1231*	-918*	-875*	-1759*	-2730*
Upper Neck My	Nm	97	36	100	31	114	32	172	47
	Nm	-58*	-33	-76*	-43*	-71*	-23*	-104*	-43*
Lower Neck Fx	N	334*	2196	410	2798	324	2753	1220	5155
	N	-1328	-569	-1964	-570*	-1633	-475	-3826	-1445
Lower Neck Fz	N	1654	804	2135	742	2161	665	3640	1347
	N	-987	-3429	-1085	-2864	-1058	-2928	-2193	-4712
Lower Neck My	Nm	444	203	492	180	512	180	677	255
	Nm	-81*	-67*	-93	-62*	-78	-65*	-120	-35
Chest A_R	g	41	46	43	41	49	46	65	
Chest Deflection	mm	38		45		41		64	
ULT R_{max}	mm								36
URT R_{max}	mm		33		30		29		43
LLT R_{max}	mm		27		28		28		35
LRT R_{max}	mm		37		37		37		46
Lumbar Fx	N	2736	1349	3052	1407	2834	1263	3799	5155
	N	-1190	-873	-1357	-330	-1792	-695	-3015	-639
Lumbar Fz	N	4065*	1673	3928*	1788		1478	4773*	5287
	N	-7434	-1908	-8271	-1823		-1432	-13718	-1540
Lumbar My	Nm	17	283	18	217	23	222	62	290
	Nm	-45	-36*	-35	-42*	-48	-26*	-51	-57*
Left ABISUP	kPa				90		100		366
Right ABISUP	kPa				280		292		326
Left ASIS Fx	N		-4348		-3322		-2969		-4517
Right ASIS Fx	N		-3230		-2496		-2437		-2201
Pelvis A_R	g	40	33	42	31	46	30	62	41
Shoulder Belt	N	7524	5325	7923	5423	8302	5587	11254	9454
Inboard Lap Belt	N	6057	4253	6559	4209	6713	3994	10068	6853
Outboard Lap Belt	N	7723	6921	7970	5598	8496	5631	14338	6559

*Peak value when the ATD head made contact with the seat or returned to the seat.

Table II-7. Data Peaks for Test Series FRS-V19

Parameters	Units	V19-1		V19-2		V19-3		V19-4	
		HIII	THOR	HIII	THOR	HIII	THOR	HIII	THOR
Head A_R	g	30	33	31	35	59	60	60	61
Upper Neck Fx	N	103*	191*	129*	157*	84*	204*	100*	189*
	N	-720	-1578	-783	-1718	-1190	-2094	-1326	-2057
Upper Neck Fz	N	1139	1084	1188	1132	2471	2216	2594	2338
	N	-428*	-228*	-156	-216*	-650*	-495*	-581*	-782*
Upper Neck My	Nm	66	28	72	30	89	34	101	33
	Nm	-22*	-6*	-20	-6*	-41*	-21*	-45*	-27*
Lower Neck Fx	N	271*	2023	225	2196	335	2034	400*	2181
	N	-1368	-539	-1310	-553	-1062	-529	-1255	-526
Lower Neck Fz	N	1015	854	973	629	2220	896	3028	763
	N	-404	-2423	-430	-2754	-632	-3472	-740	-3312
Lower Neck My	Nm	260	162	266	177	374	183	433	182
	Nm	-62	-48*	-57*	-46*	-73	-58*	-74*	-57*
Chest A_R	g	23	32	27	37	40	45	27	44
Chest Deflection	mm	27		21		33		31	
ULT R_{max}	mm		29		31		33		36
URT R_{max}	mm		36		33		36		35
LLT R_{max}	mm		33		39		34		34
LRT R_{max}	mm		30		30		35		39
Lumbar Fx	N	799	830	574	929	464	974	339	1219
	N	-447	-658	-451	-652	-1255	-434	-1681	-970
Lumbar Fz	N	1923*	666*	1795*	861*	4593*	1700	5273*	1433
	N	-6967	-946	-7403	-1082	-13954	-532	-13684	-848
Lumbar My	Nm	23	238	23	241	33	390	33	460
	Nm	-50	-39*	-44	-52*	-46	-39*	-56	-34*
Left ABISUP	kPa		100		106		420		428
Right ABISUP	kPa		167		220		405		449
Left ASIS Fx	N		-3120		-3141		-3822		-4587
Right ASIS Fx	N		-3323		-3226		-2438		-3509
Pelvis A_R	g	33	30	32	44	44	51	42	39
Shoulder Belt	N	4072	3735	3915	4068	6143	4749	7213	4689
Inboard Lap Belt	N	3424	3388	3658	3411	5395	4629	5328	4455
Outboard Lap Belt	N	5973	5982	6173	5723	8880	6639	8202	6505

*Peak value when the ATD head made contact with the seat or returned to the seat.

Appendix JJ. Tables of IARVs and Injury Risk Organized by Vehicle Test Series

Table JJ-1. IARVs and Injury Risk for Test Series FRS-V1

Parameters	Units	1		2		3	
		HIII	THOR	HIII	THOR	HIII	THOR
HIC15	-	48.53	90.26	58.04	89.63	309.08	367.56
BrIC	-	0.5	0.6	0.5	0.6	0.7	0.7
PBrIC	%	11.4	1.7	15.1	2.2	35.4	18.9
Max Nij	-	0.2	0.5	0.2	0.5	0.5	0.7
Nij Risk	%	5.9	3.2	6.1	3.6	9.5	11.4
Neck Tension Risk	%	0.0	-	0.0	-	0.4	-
Neck Comp Risk	%	0.0	-	0.0	-	0.0	-
Max Chest Dx	mm	27	-	26	-	43	-
Chest 3ms Clip	g	20.8	27.6	22.8	31.6	27.8	42.3
Chest Risk	%	3.2	-	2.9	-	16.3	-
Chest Max Rmax	Mm	-	39.6	-	36.2	-	55.0
Chest Rmax Risk	%	-	27.3	-	21.6	-	57.0
PC Score	-	-	6.0	-	5.9	-	7.1
PC Score Risk	%	-	23.9	-	22.5	-	45.1

Table JJ-2. IARVs and Injury Risk for Test Series FRS-V6

Parameter	Units	1		2		4	
		HIII	THOR	HIII	THOR	HIII	THOR
HIC15	-	190.0	89.0	189.5	87.2	607.3	416.4
BrIC	-	0.8	0.8	0.8	0.7	0.9	1.0
PBrIC	%	42.6	27.5	41.0	11.4	59.1	57.2
Max Nij	-	0.5	0.5	0.5	0.5	0.6	0.8
Nij Risk	%	8.9	3.8	9.2	3.9	10.9	15.4
Max cNij	-	-	0.6	-	0.5	-	1.0
cNij Risk	%	-	32.1	-	27.6	-	78.2
Neck Tension Risk	%	0.0	-	0.0	-	0.0	-
Neck Comp Risk	%	0.1	-	0.1	-	3.5	-
Max Chest Dx	mm	39.2	-	36.6	-	55.0	-
Chest 3ms Clip	g	32.2	37.7	30.4	28.6	38.2	45.2
Chest Risk	%	11.6	-	9.2	-	35.7	-
Chest Max Rmax	mm	-	41.7	-	32.1	-	46.4
Chest Rmax Risk	%	-	30.9	-	15.7	-	40.0
PC Score	-	-	6.1	-	5.1	-	6.5
PC Score Risk	%	-	25.6	-	13.0	-	33.9

Table JJ-3. IARVs and Injury Risk for Test Series FRS-V10

Parameter	Units	1		2		3	
		HIII	THOR	HIII	THOR	HIII	THOR
HIC15	-	184.4	98.2	152.0	231.5	604.8	426.0
BrIC	-	0.9	0.9	0.8	0.9	1.1	1.1
PBrIC	%	51.9	38.4	44.9	37.5	76.8	66.9
Max Nij	-	0.7	0.6	0.6	0.8	1.1	0.9
Nij Risk	%	14.7	6.1	12.4	16.5	24.6	25.3
Max cNij	-	-	0.7	-	0.8	-	0.9
cNij Risk	%	-	43.6	-	65.5	-	76.1
Neck Tension Risk	%	0.0	-	0.0	-	0.0	-
Neck Comp Risk	%	0.1	-	0.0	-	1.1	-
Max Chest Dx	mm	41	-	35	-	63	-
Chest 3ms Clip	g	35.0	43.8	38.8	46.6	48.2	53.1
Chest Risk	%	13.6	-	7.9	-	50.4	-
Chest Max Rmax	mm	-	47.7	-	42.3	-	44.0
Chest Rmax Risk	%	-	42.5	-	32.1	-	35.3
PC Score	-	-	6.6	-	6.1	-	7.1
PC Score Risk	%	-	34.8	-	26.6	-	45.5

Table JJ-4. IARVs and Injury Risk for Test Series FRS-V13

Parameter	Units	1		2		3	
		HIII	THOR	HIII	THOR	HIII	THOR
HIC15	-	114.9	381.0	583.2	807.7	161.5	197.4
BrIC	-	0.7	0.7	0.9	0.8	0.8	0.7
PBrIC	%	29.4	17.9	57.6	31.3	37.0	9.0
Max Nij	-	0.5	0.6	0.9	0.8	0.6	0.6
Nij Risk	%	10.1	7.3	18.0	15.6	11.6	6.4
Max cNij	-	-	0.6	-	0.8	-	0.6
cNij Risk	%	-	34.3	-	62.5	-	36.2
Neck Tension Risk	%	0.0	-	0.0	-	0.0	-
Neck Comp Risk	%	0.0	-	1.3	-	0.0	-
Max Chest Dx	mm	35.4	-	79.0	-	38.7	-
Chest 3ms Clip	g	33.4	32.2	45.7	49.2	34.5	34.4
Chest Risk	%	8.2	-	77.2	-	11.1	-
Chest Max Rmax	mm	-	40.7	-	43.2	-	45.0
Chest Rmax Risk	%	-	29.2	-	33.8	-	37.2
PC Score	-	-	6.6	-	6.9	-	6.8
PC Score Risk	%	-	35.5	-	41.1	-	38.9

Table JJ-5. IARVs and Injury Risk for Test Series FRS-V14

Parameter	Units	1		2		3		4	
		HIII	THOR	HIII	THOR	HIII	THOR	HIII	THOR
HIC15	-	102.3	96.0	150.5	73.1	210.0	353.9	179.2	387.4
BrIC	-	0.6	0.6	0.6	0.6	0.6	0.8	0.6	0.8
PBrIC	%	19.3	1.9	19.5	0.6	23.1	21.1	17.7	33.0
Max Nij	-	0.3	0.5	0.3	0.5	0.4	0.7	0.5	0.8
Nij Risk	%	6.4	4.1	6.3	3.4	7.6	10.2	9.5	15.9
Max cNij	-	-	0.5	-	0.5	-	0.8	-	0.9
cNij Risk	%	-	25.8	-	21.0	-	60.2	-	69.4
Neck Tension Risk	%	0.0	-	0.0	-	0.0	-	0.0	-
Neck Comp Risk	%	0.0	-	0.0	-	0.1	-	0.1	-
Max Chest Dx	mm	35	-	32	-	40	-	38.3	-
Chest 3ms Clip	g	23.4	24.8	20.0	21.6	25.4	30.3	25.0	28.9
Chest Risk	%	7.7	-	5.5	-	12.4	-	10.7	-
Chest Max Rmax	mm	-	35.9	-	34.6	-	42.5	-	42.8
Chest Rmax Risk	%	-	21.2	-	19.2	-	37.6	-	33.0
PC Score	-	-	5.7	-	5.3	-	7.4	-	7.1
PC Score Risk	%	-	20.1	-	14.8	-	50.5	-	45.3

Table JJ-6. IARVs and Injury Risk for Test Series FRS-V15

Parameter	Units	1		2		3		4	
		HIII	THOR	HIII	THOR	HIII	THOR	HIII	THOR
HIC15	-	126.8	149.1	163.9	129.9	143.2	112.4	609.2	707.3
BrIC	-	0.7	0.7	0.7	0.7	0.8	0.7	1.0	1.0
PBrIC	%	31.0	10.3	33.8	8.7	42.1	14.6	69.5	52.8
Max Nij	-	0.5	0.6	0.7	0.7	0.6	0.6	1.0	0.9
Nij Risk	%	9.6	6.2	13.6	10.1	12.1	5.2	23.8	27.0
Max cNij	-	-	0.6	-	0.6	-	0.6	-	1.1
cNij Risk	%	-	38.5	-	38.3	-	28.9	-	85.5
Neck Tension Risk	%	0.0	-	0.0	-	0.0	-	0.0	-
Neck Comp Risk	%	0.1	-	0.2	-	0.2	-	2.3	-
Max Chest Dx	mm	37.7	-	45.4	-	41.0	-	64.4	-
Chest 3ms Clip	g	40.3	40.0	42.2	37.0	48.7	38.5	63.3	134.6
Chest Risk	%	10.1	-	19.3	-	13.6	-	54.0	-
Chest Max Rmax	mm	-	37.3	-	37.5	-	37.4	-	46.4
Chest Rmax Risk	%	-	23.3	-	23.7	-	23.6	-	39.9
PC Score	-	-	5.7	-	5.3	-	5.2	-	7.8
PC Score Risk	%	-	19.6	-	14.9	-	13.3	-	58.9

Table JJ-7. IARVs and Injury Risk for Test Series FRS-V19

Parameter	Units	1		2		3		4	
		HIII	THOR	HIII	THOR	HIII	THOR	HIII	THOR
HIC15	-	67.9	76.1	73.1	87.0	308.3	346.9	328.5	357.7
BrIC	-	0.7	0.6	0.6	0.6	0.9	0.7	0.9	0.7
PBrIC	%	26.5	2.7	22.9	3.6	48.5	13.5	51.9	12.6
Max Nij	-	0.3	0.5	0.3	0.5	0.4	0.8	0.5	0.7
Nij Risk	%	6.5	3.8	6.8	4.2	8.3	16.9	9.7	11.1
Max cNij	-	-	0.5	-	0.5	-	0.9	-	0.9
cNij Risk	%	-	21.7	-	24.3	-	73.8	-	67.0
Neck Tension Risk	%	0.0	-	0.0	-	0.0	-	0.0	-
Neck Comp Risk	%	0.0	-	0.0	-	0.6	-	0.8	-
Max Chest Dx	mm	27.0	-	21.4	-	32.6	-	31.3	-
Chest 3ms Clip	g	22.6	28.9	22.6	31.0	33.4	35.0	25.3	38.6
Chest Risk	%	3.3	-	1.6	-	6.1	-	5.3	-
Chest Max Rmax	mm	-	35.9	-	38.9	-	36.3	-	38.5
Chest Rmax Risk	%	-	21.1	-	26.0	-	21.7	-	25.4
PC Score	-	-	5.8	-	5.6	-	6.2	-	6.7
PC Score Risk	%	-	20.9	-	18.7	-	27.3	-	37.1

Appendix KK. PeakTables of Differences Between Data Peaks and IARVs of Repeat Tests

Table KK-1. Comparison of Data Peaks Between Tests V14-3 & V14-4

Parameters	Units	V14-3		V14-4		% Difference	
		HIII	THOR	HIII	THOR	HIII	THOR
Head A_R	g	58	59	64	63	9.4	6.6
Upper Neck Fx	N	205	223	178	135	14.5	49.3
	N	-1035	-1988	-930	-2275	10.7	13.5
Upper Neck Fz	N	1712	2197	1667	2453	2.7	11.0
	N	-1276	-460	-1061	-964	18.4	70.8
Upper Neck My	Nm	71	30	62	33	14.6	11.5
	Nm	-40	-9	-48	-22	16.9	83.4
Lower Neck Fx	N	355	2780	289	3198	20.7	14.0
	N	-2410	-750	-2273	-802	5.9	6.7
Lower Neck Fz	N	956	1223	1126	1149	16.3	6.2
	N	-1143	-3807	-707	-3835	47.1	0.7
Lower Neck My	Nm	317	215	282	192	11.9	11.7
	Nm	-81	-44	-71	-43	13.5	1.6
Chest A_R	g	26	34	25	31	3.7	8.6
Chest Deflection	mm	40		38		4.3	
ULT R_{max}	mm		32		32		
URT R_{max}	mm		45		43		5.5
LLT R_{max}	mm		25		29		12.1
LRT R_{max}	mm		43		41		5.4
Lumbar/T12 Fx	N	1768	1612	1579	1762	11.3	8.9
	N	-513	-490	-533	-438	3.7	11.2
Lumbar/T12 Fz	N	1552	491	1444	744	7.3	41.0
	N	-4540	-2986	-4851	-3778	6.6	23.4
Lumbar/T12 My	Nm	27	368	25	397	7.3	7.6
	Nm	-64	-38	-70	-47	9.2	22.3
Left ABISUP	kPa		118		127		7.8
Right ABISUP	kPa		122		126		3.4
Left ASIS Fx	N		-3821		-3893		1.9
Right ASIS Fx	N		-3390		-3176		6.5
Pelvis A_R	g	36	39	36	41	0.7	4.0
Shoulder Belt	N	6318		5845	6368	7.8	
Inboard Lap Belt	N	4787	4793	4986	4571	4.1	4.7
Outboard Lap Belt	N	6139		5551	6767	10.1	

Table KK-2. Comparison of IARVs and Injury Risks Between Tests V14-3 & V14-4

Parameters	Units	V14-3		V14-4		% Difference	
		HIII	THOR	HIII	THOR	HIII	THOR
HIC15	-	210.0	353.9	179.2	387.4	15.8	9.0
BrIC	-	0.6	0.8	0.6	0.8	10.4	10.1
PBrIC	%	23.1	21.1	17.7	33.0	26.1	43.9
Max Nij	-	0.4	0.7	0.5	0.8	29.1	12.5
Nij Risk	%	7.6	10.2	9.5	15.9	22.5	44.0
Neck Tension Risk	%	0.1		0.1		0.0	
Neck Comp Risk	%	0.0		0.0			
Max Chest Dx	mm	40.0		38.3		4.3	
Chest 3ms Clip	g	25.4	30.3	25.0	28.9	1.5	4.8
Chest Risk	%	12.4		10.7		15.0	
Chest Max Rmax	mm		45.2		42.8		5.5
Chest Rmax Risk	%		37.6		33.0		13.0
PC Score	-		7.4		7.1		3.5
PC Score Risk	%		50.5		45.3		10.9

Table KK-3. Comparison of Peak Excursions Between Tests V14-3 & V14-4

Parameter	Units	V14-3		V14-4		% Difference	
		HIII	THOR	HIII	THOR	HIII	THOR
Head X	cm	42.5	54.2	43.3	51.3	1.9	5.6
Head Z	cm	19.9	41.0	20.2	42.1	1.6	2.8
Shoulder X	cm	22.4	43.7	22.7	42.6	1.2	2.5
Shoulder Z	cm	1.2	2.2	1.4	2.9	13.3	29.1
Hip X	cm	15.5	23.0	16.8	25.2	7.8	8.9
Hip Z	cm	-1.2	1.8	-1.9	2.0	46.1	10.1
Knee X	cm	19.3	28.2	18.2	28.4	5.9	0.6
Knee Z	cm	12.4	19.0	14.6	1.6	16.1	169.2

Table KK-4. Comparison of Data Peaks Between Tests V15-1 & V15-2

Parameters	Units	V15-1		V15-2		% Difference	
		HIII	THOR	HIII	THOR	HIII	THOR
Head A_R	g	41	41	45	42	8.7	1.3
Upper Neck Fx	N	173	253	218	221	22.8	13.7
	N	-1193	-2078	-1298	-1976	8.4	5.0
Upper Neck Fz	N	1750	1852	1933	1739	9.9	6.3
	N	-720	-844	-1086	-1231	40.5	37.3
Upper Neck My	Nm	97	36	100	31	3.1	13.0
	Nm	-58	-33	-76	-43	26.7	28.7
Lower Neck Fx	N	334	2196	410	2798	20.5	24.1
	N	-1328	-569	-1964	-570	38.6	0.0
Lower Neck Fz	N	1654	804	2135	742	25.4	8.0
	N	-987	-3429	-1085	-2864	9.5	18.0
Lower Neck My	Nm	444	203	492	180	10.2	11.7
	Nm	-81	-67	-93	-62	13.3	8.4
Chest A_R	g	41	46	43	41	4.0	10.9
Chest Deflection	mm	38		45		18.7	
ULT R_{max}	mm						
URT R_{max}	mm		33		30		7.6
LLT R_{max}	mm		27		28		4.9
LRT R_{max}	mm		37		37		0.6
Lumbar/T12 Fx	N	2736	1349	3052	1407	10.9	4.3
	N	-1190	-873	-1357	-330	13.1	90.4
Lumbar/T12 Fz	N	4065	1673	3928	1788	3.4	6.6
	N	-7434	-1908	-8271	-1823	10.7	4.5
Lumbar/T12 My	Nm	17	283	18	217	8.0	26.4
	Nm	-45	-36	-35	-42	25.2	17.3
Left ABISUP	kPa				90		
Right ABISUP	kPa				280		
Left ASIS Fx	N		-4348		-3322		26.8
Right ASIS Fx	N		-3230		-2496		25.6
Pelvis A_R	g	40	33	42	31	4.9	4.3
Shoulder Belt	N	7524	5325	7923	5423	5.2	1.8
Inboard Lap Belt	N	6057	4253	6559	4209	7.9	1.0
Outboard Lap Belt	N	7723	6921	7970	5598	3.1	21.1

Table KK-5. Comparison of IARVs and Injury Risks Between Tests V15-1 & V15-2

Parameters	Units	V15-1		V15-2		% Difference	
		HIII	THOR	HIII	THOR	HIII	THOR
HIC15	-	126.8	149.1	163.9	129.9	25.5	13.8
BrIC	-	0.7	0.7	0.7	0.7	3.8	2.2
PBrIC	%	31.0	10.3	33.8	8.7	8.8	16.8
Max Nij	-	0.5	0.6	0.7	0.7	32.7	14.5
Nij Risk	%	9.6	6.2	13.6	10.1	34.0	47.2
Neck Tension Risk	%	0.1		0.2		66.7	
Neck Comp Risk	%	0.0		0.0			
Max Chest Dx	mm	37.7		45.4		18.7	
Chest 3ms Clip	g	40.3	40.0	42.2	37.0	4.7	7.9
Chest Risk	%	10.1		19.3		62.5	
Chest Max Rmax	mm		37.3		37.5		0.6
Chest Rmax Risk	%		23.3		23.7		1.5
PC Score	-		5.7		5.3		6.8
PC Score Risk	%		19.6		14.9		27.2

Table KK-6. Comparison of Peak Excursions Between Tests V15-1 & V15-2

Parameter	Units	V15-1		V15-2		% Difference	
		HIII	THOR	HIII	THOR	HIII	THOR
Head X	cm	36.7	51.0	38.1	48.5	3.9	5.0
Head Z	cm	18.4	32.5	20.6	31.0	10.9	4.7
Shoulder X	cm	25.0	42.3	25.2	41.1	1.1	2.9
Shoulder Z	cm	1.0	4.7	1.8	3.3	50.2	36.2
Hip X	cm	22.7	23.9	25.2	26.3	10.1	9.7
Hip Z	cm	-2.2	3.4	-2.7	2.5	20.0	31.3
Knee X	cm	23.6	28.6	26.1	29.1	10.3	2.0
Knee Z	cm	12.6	13.2	8.8	7.3	35.3	58.0

Table KK-7. Comparison of Data Peaks Between Tests V19-3 & V19-4

Parameter	Units	V19-3		V19-4		% Difference	
		HIII	THOR	HIII	THOR	HIII	THOR
Head A_R	g	59	60	60	61	2.5	0.7
Upper Neck Fx	N	84	204	100	189	16.7	7.2
	N	-1190	-2094	-1326	-2057	10.7	1.8
Upper Neck Fz	N	2471	2216	2594	2338	4.9	5.4
	N	-650	-495	-581	-782	11.3	45.0
Upper Neck My	Nm	89	34	101	33	13.4	3.6
	Nm	-41	-21	-45	-27	8.5	24.4
Lower Neck Fx	N	335	2034	400	2181	17.7	7.0
	N	-1062	-529	-1255	-526	16.6	0.5
Lower Neck Fz	N	2220	896	3028	763	30.8	16.1
	N	-632	-3472	-740	-3312	15.8	4.7
Lower Neck My	Nm	374	183	433	182	14.6	0.6
	Nm	-73	-58	-74	-57	1.5	1.1
Chest A_R	g	40	45	27	44	38.4	2.1
Chest Deflection	mm	33		31		4.1	
ULT R_{max}	mm		33		36		7.7
URT R_{max}	mm		36		35		3.6
LLT R_{max}	mm		34		34		0.7
LRT R_{max}	mm		35		39		9.5
Lumbar/T12 Fx	N	464	974	339	1219	31.2	22.4
	N	-1255	-434	-1681	-970	29.0	76.3
Lumbar/T12 Fz	N	4593	1700	5273	1433	13.8	17.0
	N	-13954	-532	-13684	-848	2.0	45.8
Lumbar/T12 My	Nm	33	390	33	460	0.0	16.4
	Nm	-46	-39	-56	-34	19.3	13.0
Left ABISUP	kPa		420		428		1.8
Right ABISUP	kPa		405		449		10.1
Left ASIS Fx	N		-3822		-4587		18.2
Right ASIS Fx	N		-2438		-3509		36.0
Pelvis A_R	g	44	51	42	39	5.2	25.8
Shoulder Belt	N	6143	4749	7213	4689	16.0	1.3
Inboard Lap Belt	N	5395	4629	5328	4455	1.2	3.8
Outboard Lap Belt	N	8880	6639	8202	6505	7.9	2.0

Table KK-8. Comparison of IARVs and Injury Risks Between Tests V19-3 & V19-4

Parameters	Units	V19-3		V19-4		% Difference	
		HIII	THOR	HIII	THOR	HIII	THOR
HIC15	-	308.3	346.8	328.5	357.7	6.3	3.1
BrIC	-	0.9	0.7	0.9	0.7	3.4	1.1
PBrIC	%	48.5	13.5	51.9	12.6	6.7	7.0
Max Nij	-	0.4	0.8	0.5	0.7	17.7	11.5
Nij Risk	%	8.3	16.9	9.7	11.1	14.6	41.3
Neck Tension Risk	%	0.6		0.8		28.6	
Neck Comp Risk	%	0.0		0.0		0.0	
Max Chest Dx	mm	32.6		31.3		4.1	
Chest 3ms Clip	g	33.4	35.0	25.3	38.6	27.5	9.8
Chest Risk	%	6.1		5.3		13.9	
Chest Max Rmax	mm		36.3		38.5		6.0
Chest Rmax Risk	%		21.7		25.4		15.5
PC Score	-		6.2		6.7		8.5
PC Score Risk	%		27.3		37.1		30.6

Table KK-9. Comparison of Peak Excursions Between Tests V19-3 & V19-4

Parameters	Units	V19-3		V19-4		% Difference	
		HIII	THOR	HIII	THOR	HIII	THOR
Head X	cm	60.9	65.5	60.4	68.9	0.9	5.1
Head Z	cm	29.1	28.7	41.3	28.2	34.6	1.6
Shoulder X	cm	41.3	58.4	40.7	60.9	1.4	4.1
Shoulder Z	cm	3.0	4.4	3.5	4.2	15.5	3.5
Hip X	cm	21.2	29.8	17.3	30.4	20.4	2.0
Hip Z	cm	-1.4	0.9	0.9	0.9	944.0	4.3
Knee X	cm	22.9	36.4	18.8	34.8	19.9	4.5
Knee Z	cm	16.5	8.4	16.9	3.3	2.0	86.6

Appendix LL. ATD X-Z VICON Excursion Plots for Generic Tests

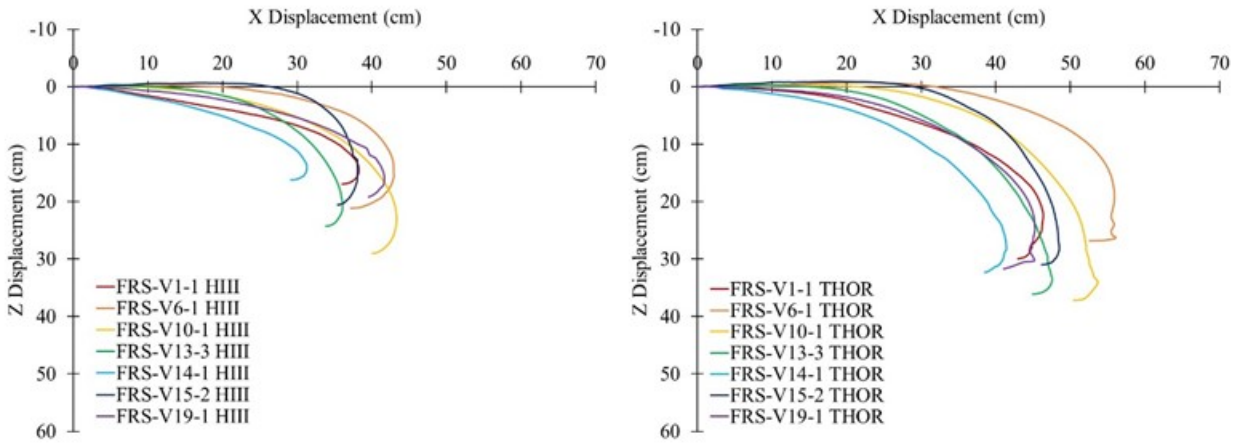

Figure LL-1. HIII (Left) and THOR (Right) Head Excursions (Generic Tests)

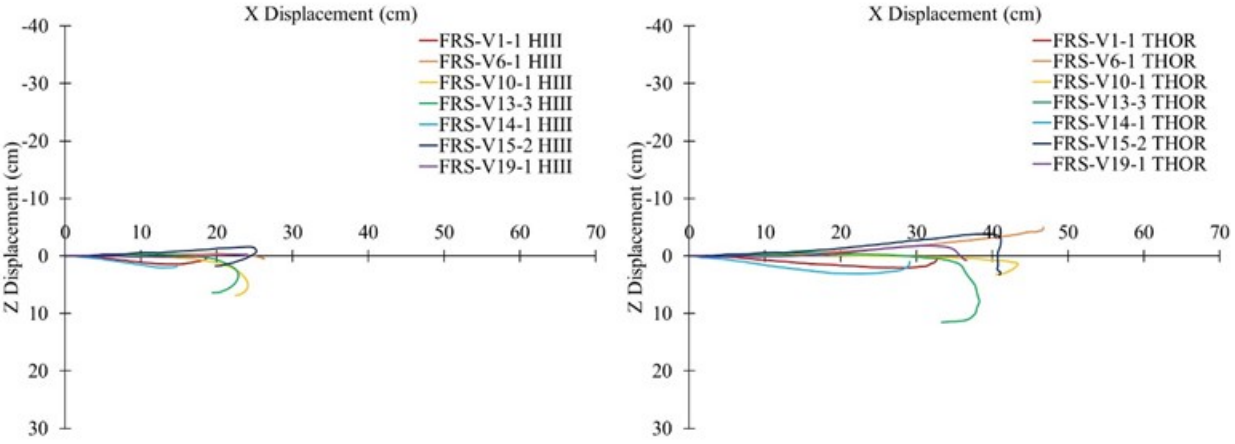

Figure LL-2. HIII (Left) and THOR (Right) Shoulder Excursions (Generic Tests)

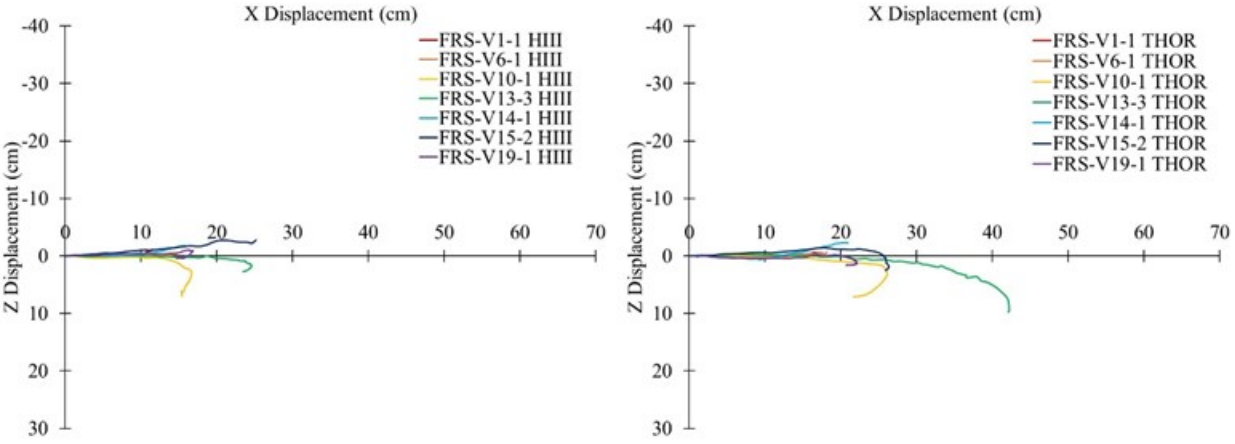

Figure LL-3. HIII (Left) and THOR (Right) Hip Excursions (Generic Tests)

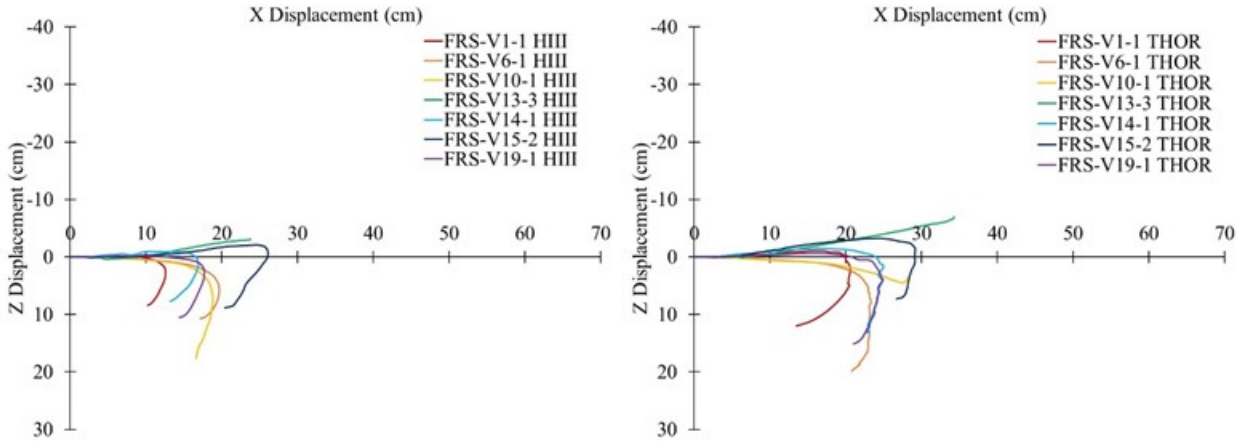

Figure LL-4 HIII (Left) and THOR (Right) Knee Excursions (Generic Tests)

Appendix MM. ATD X-Z VICON Excursion Plots for Scaled Tests

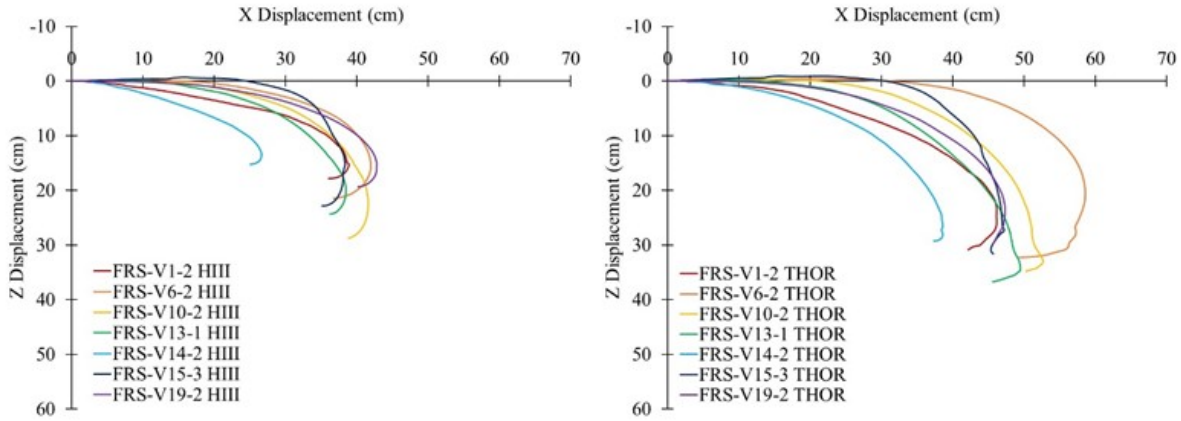

Figure MM-1. HIII (Left) and THOR (Right) Head Excursions (Scaled/Specific Tests)

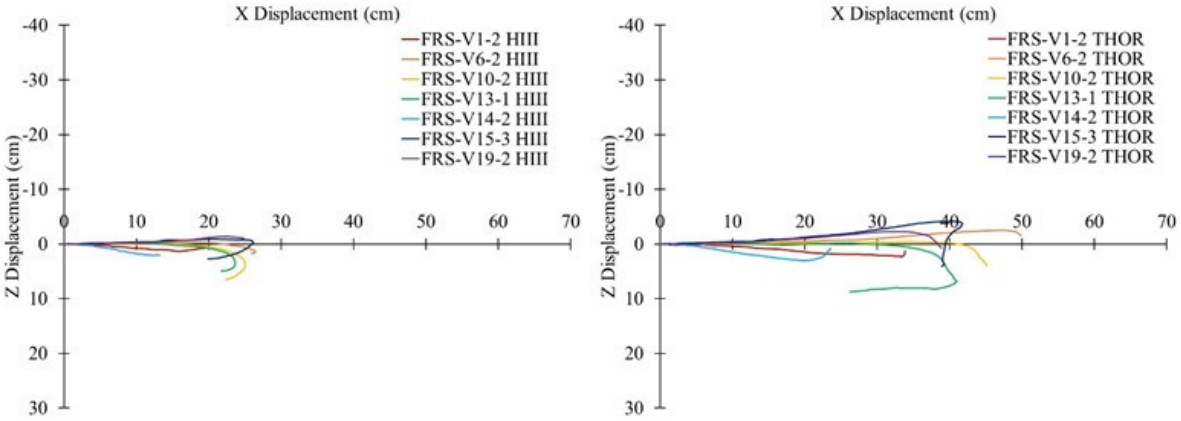

Figure MM-2. HIII (Left) and THOR (Right) Shoulder Excursions (Scaled/Specific Tests)

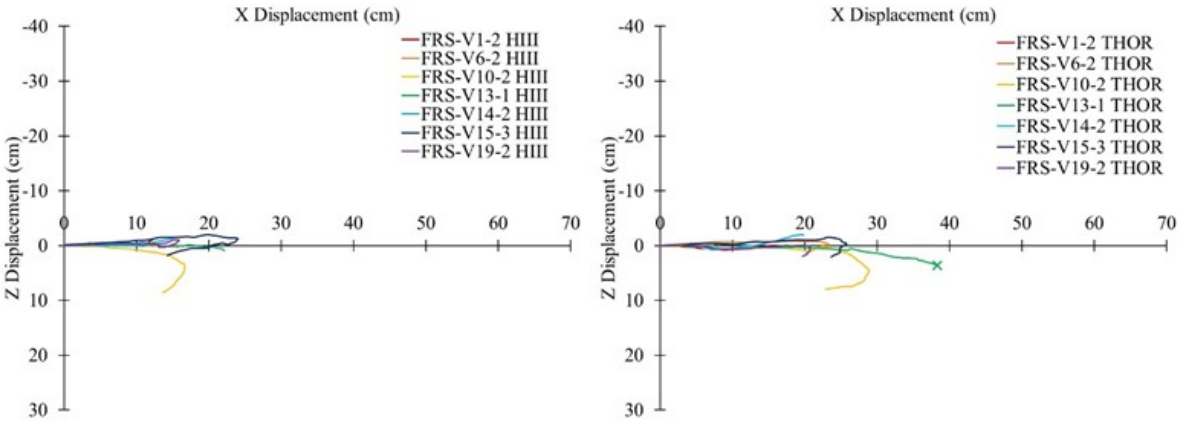

Figure MM-3. HIII (Left) and THOR (Right) Hip Excursions (Scaled/Specific Tests)

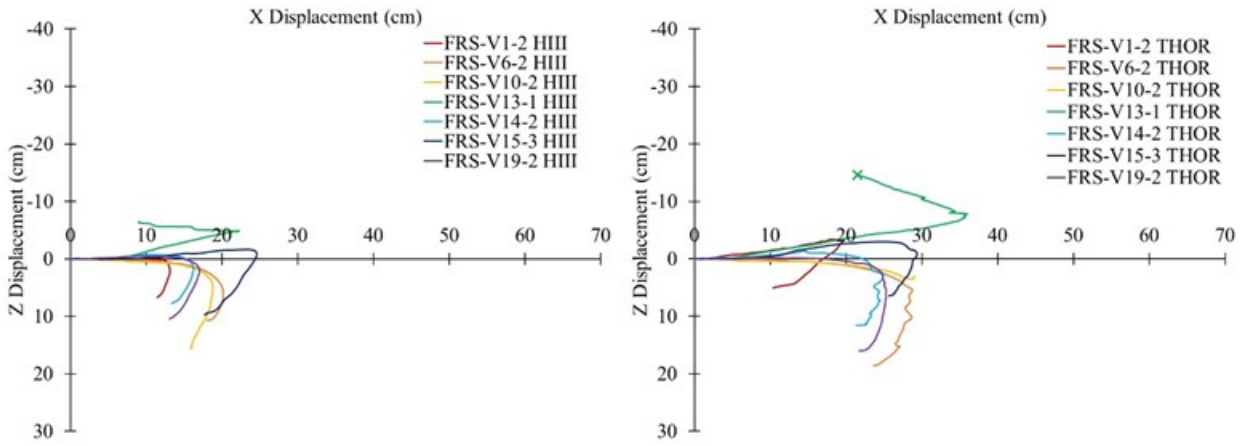

Figure MM-4. HIII (Left) and THOR (Right) Knee Excursions (Scaled/Specific Tests)

Appendix NN. ATD X-Z VICON Excursion Plots for NCAP85 TESTS

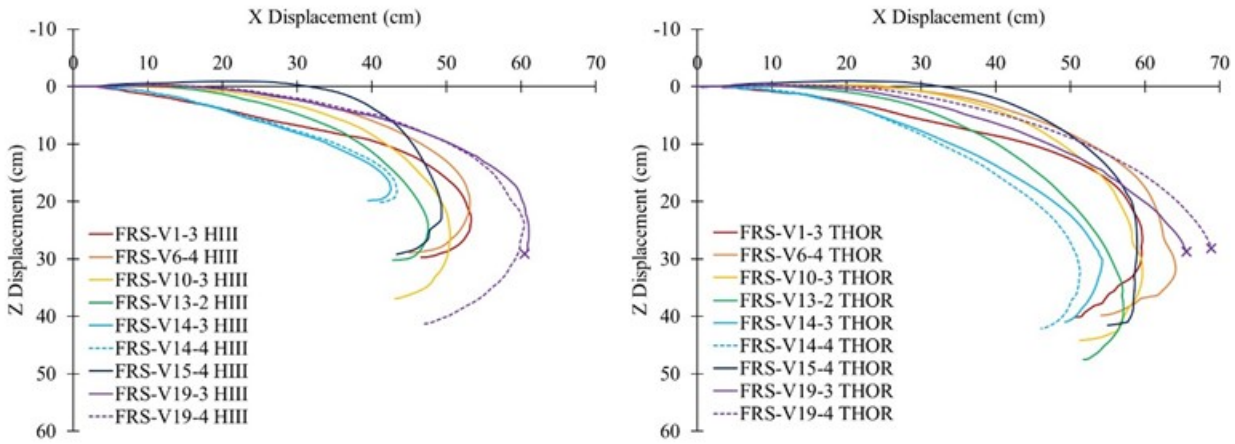

Figure NN-1. HIII (Left) and THOR (Right) Head Excursions (NCAP85 Tests)

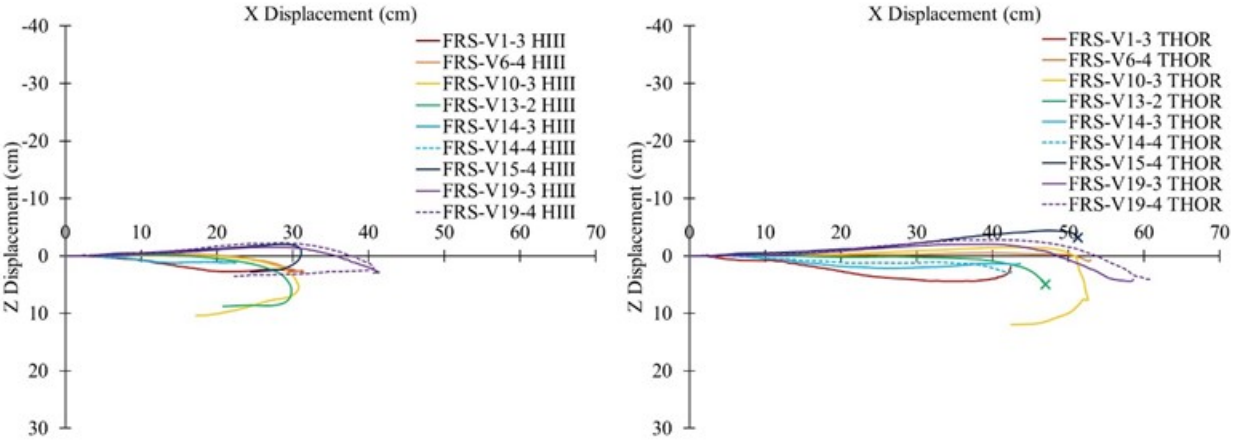

Figure NN-2. HIII (Left) and THOR (Right) Shoulder Excursions (NCAP85 Tests)

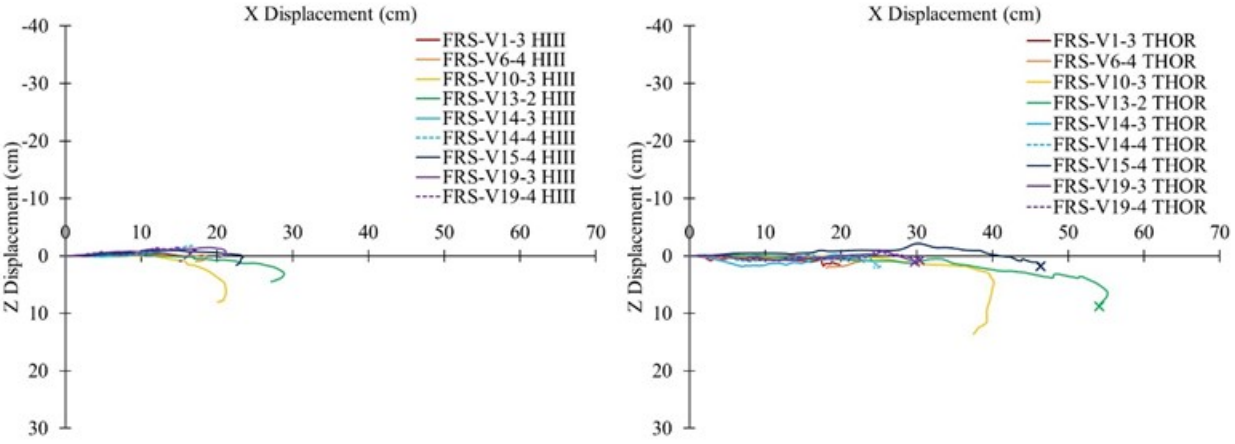

Figure NN-3. HIII (Left) and THOR (Right) Hip Excursions (NCAP85 Tests)

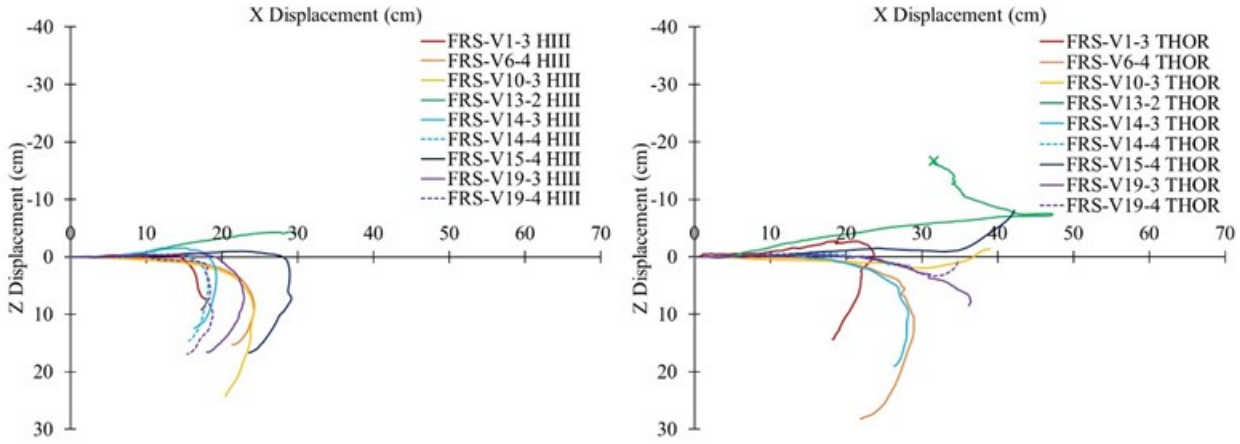

Figure NN-4. HIII (Left) and THOR (Right) Knee Excursions (NCAP85 Tests)

Appendix OO. TABLES OF ATD Peak X AND Z VICON Excursions Organized by Vehicle

Table OO-1. FRS-V1 Test Series Peak X and Z Direction Excursions in CM

	1		2		3	
	HIII	THOR	HIII	THOR	HIII	THOR
Head X	38.26	46.34	38.88	46.16	53.30	59.64
Head Z	16.94	29.97	17.85	30.87	29.71	40.14
Shoulder X	18.64	32.75	19.66	33.83	31.27	42.39
Shoulder Z	1.44	2.07	1.32	2.28	2.74	4.41
Hip X	11.49	17.90	12.26	17.97	16.44	19.86
Hip Z	-1.15	-0.64	-1.07	0.80	0.19	1.72
Knee X	12.56	20.58	13.14	19.57	17.99	23.68
Knee Z	8.39	11.97	6.70	5.06	9.21	14.36

Table OO-2. FRS-V6 Test Series Peak X and Z Direction Excursions in CM

	1		2		4	
	HIII	THOR	HIII	THOR	HIII	THOR
Head X	42.94	56.06	41.96	58.57	53.15	64.10
Head Z	21.20	26.82	21.47	32.26	28.89	39.82
Shoulder X	26.23	46.73	26.43	49.91	31.58	52.94
Shoulder Z	0.52	-5.01	1.72	-2.51	2.94	0.96
Hip X	14.76	18.13	15.82	23.39	18.67	22.90
Hip Z	-0.23	-0.73	0.31	-0.82	0.96	2.04
Knee X	19.66	23.30	20.18	28.78	24.29	28.98
Knee Z	10.69	19.83	10.72	18.60	15.28	28.20

Table OO-3. FRS-V10 Test Series Peak X and Z Direction Excursions in CM

	1		2		3	
	HIII	THOR	HIII	THOR	HIII	THOR
Head X	43.31	53.66	41.60	52.67	50.47	59.63
Head Z	29.02	37.20	28.73	34.92	36.92	44.14
Shoulder X	24.09	43.35	25.01	45.15	30.81	52.60
Shoulder Z	6.83	3.18	6.50	4.00	10.39	11.96
Hip X	16.65	26.13	16.66	28.90	21.21	40.18
Hip Z	7.00	7.11	8.59	7.90	8.02	13.61
Knee X	18.80	28.09	18.79	29.05	24.24	39.01
Knee Z	17.62	4.51	15.58	3.51	24.25	1.94

Table OO-4. FRS-V13 Test Series Peak X and Z Direction Excursions in CM

	1		2		3	
	HIII	THOR	HIII	THOR	HIII	THOR
Head X	38.48	49.46	47.53	57.11	36.09	47.55
Head Z	24.30	36.74	30.20	47.51	24.29	36.09
Shoulder X	23.64	41.00	29.84	46.97*	22.83	38.26
Shoulder Z	4.95	8.74	8.78	4.99*	6.38	11.55
Hip X	22.15	38.32*	28.88	55.20*	24.56	42.20
Hip Z	0.93	3.62*	4.51	8.79*	2.70	9.74
Knee X	22.28	36.02*	29.81	47.27*	23.80	34.28
Knee Z	-6.44	-14.64*	-4.36	-16.70*	-3.06	-6.97

*Sightlines lost before peak excursions

Table OO-5. FRS-V14 Test Series Peak X and Z Direction Excursions in CM

	1		2		3		4	
	HIII	THOR	HIII	THOR	HIII	THOR	HIII	THOR
Head X	31.29	41.42	26.64	38.58	42.53	54.25	43.35	51.28
Head Z	16.24	32.33	15.26	29.25	19.88	40.97	20.19	42.11
Shoulder X	14.76	29.09	13.20	23.56	22.44	43.67	22.72	42.58
Shoulder Z	2.04	3.10	2.10	3.04	1.22	2.19	1.40	2.93
Hip X	15.90	20.89	15.22	19.81	15.52	23.03	16.78	25.18
Hip Z	-1.80	-2.33	-1.50	-2.04	-1.16	1.83	-1.86	2.03
Knee X	16.88	24.95	16.23	24.92	19.28	28.23	18.18	28.40
Knee Z	7.63	13.17	7.68	11.57	12.42	18.97	14.59	1.58

Table OO-6. FRS-V15 Test Series Peak X and Z Direction Excursions in CM

	1		2		3		4	
	HIII	THOR	HIII	THOR	HIII	THOR	HIII	THOR
Head X	36.66	50.98	38.10	48.51	38.36	47.18	49.35	58.93
Head Z	18.43	32.50	20.56	31.00	22.83	31.63	29.18	41.55
Shoulder X	24.96	42.34	25.23	41.13	26.13	41.76	31.14	51.27*
Shoulder Z	1.05	4.69	1.75	3.25	2.73	4.06	2.81	-4.42*
Hip X	22.73	23.90	25.15	26.35	24.06	25.76	23.47	46.33*
Hip Z	-2.25	3.44	-2.75	2.51	1.77	2.04	1.58	1.77*
Knee X	23.56	28.57	26.11	29.15	24.60	29.37	29.13	42.19
Knee Z	12.61	13.25	8.83	7.29	9.70	6.44	16.69	-8.14

*Sightlines lost before peak excursions

Table OO-7. FRS-V19 Test Series Peak X and Z Direction Excursions in CM

	1		2		3		4	
	HIII	THOR	HIII	THOR	HIII	THOR	HIII	THOR
Head X	41.68	45.25	42.82	47.32	60.94*	65.45*	60.41	68.86*
Head Z	19.20	31.70	19.36	33.00	29.09*	28.65*	41.28	28.19*
Shoulder X	24.04	36.58	24.85	38.91	41.29	58.43	40.71	60.89
Shoulder Z	-0.26	0.75	-1.37	-2.24	3.03	4.35	3.54	4.20
Hip X	16.88	22.19	15.89	20.76	21.16	29.79*	17.25	30.38*
Hip Z	0.43	1.66	-1.09	1.94	-1.43	0.94*	0.93	0.90*
Knee X	17.70	24.91	17.03	25.30	22.93	36.36	18.78	34.76
Knee Z	10.49	15.08	10.43	16.02	16.54	8.42	16.88	3.33

*Sightlines lost before peak excursions

Appendix PP. ATD X-Z Peak HIP Excursion Frames for Generic Tests

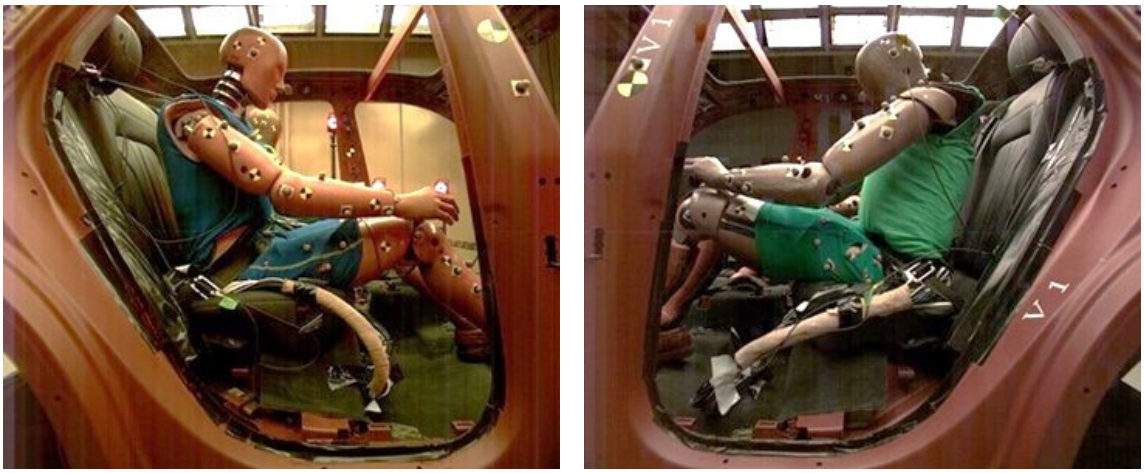

Figure PP-1. Test FRS-V1-1 HIII (Left) and THOR (Right) at Peak Hip Excursion

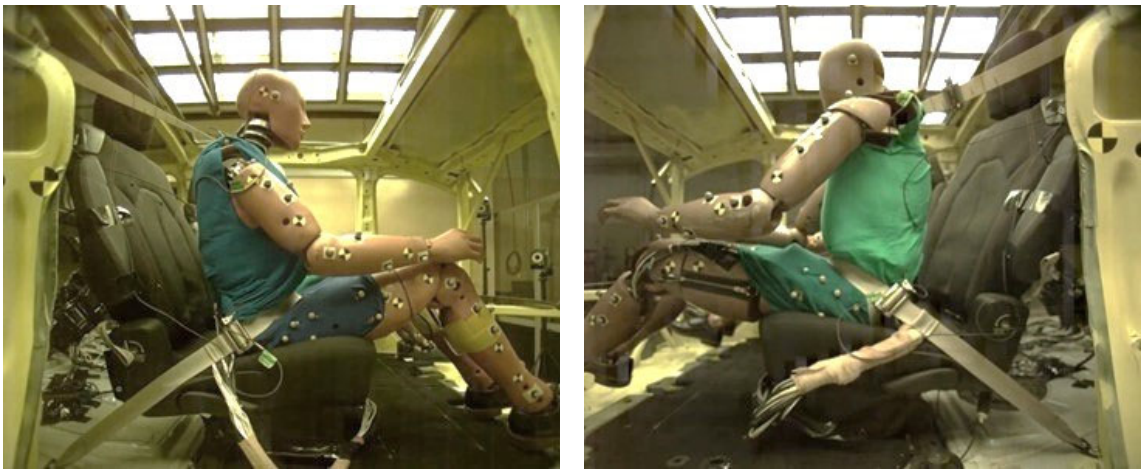

Figure PP-2. Test FRS-V6-1 HIII (Left) and THOR (Right) at Peak Hip Excursion

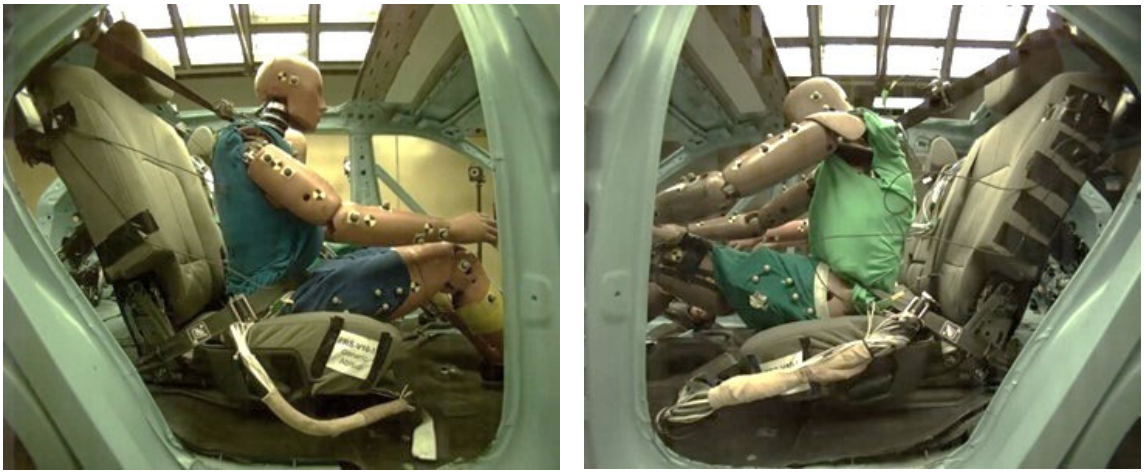

Figure PP-3. Test FRS-V10-1 HIII (Left) and THOR (Right) at Peak Hip Excursion

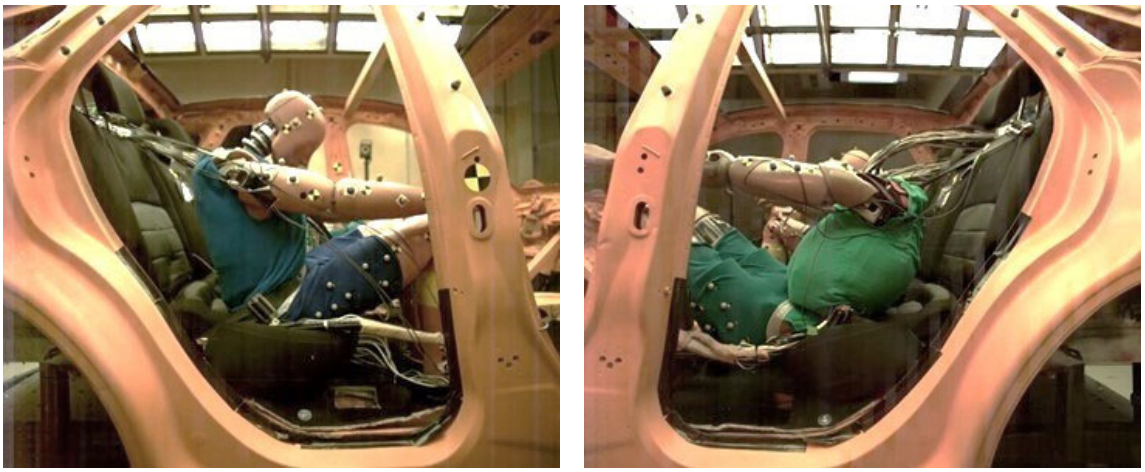

Figure PP-4. Test FRS-V13-3 HIII (Left) and THOR (Right) at Peak Hip Excursion

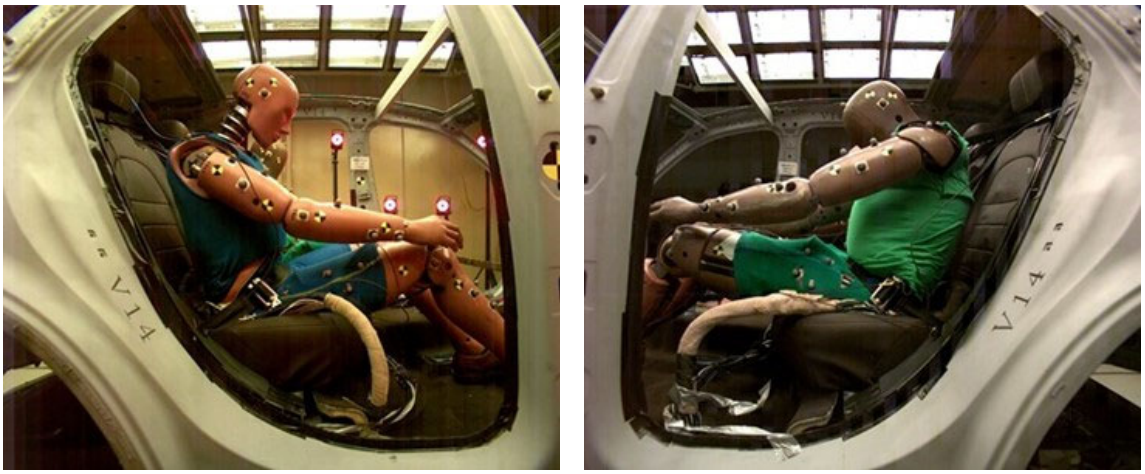

Figure PP-5. Test FRS-V14-1 HIII (Left) and THOR (Right) at Peak Hip Excursion

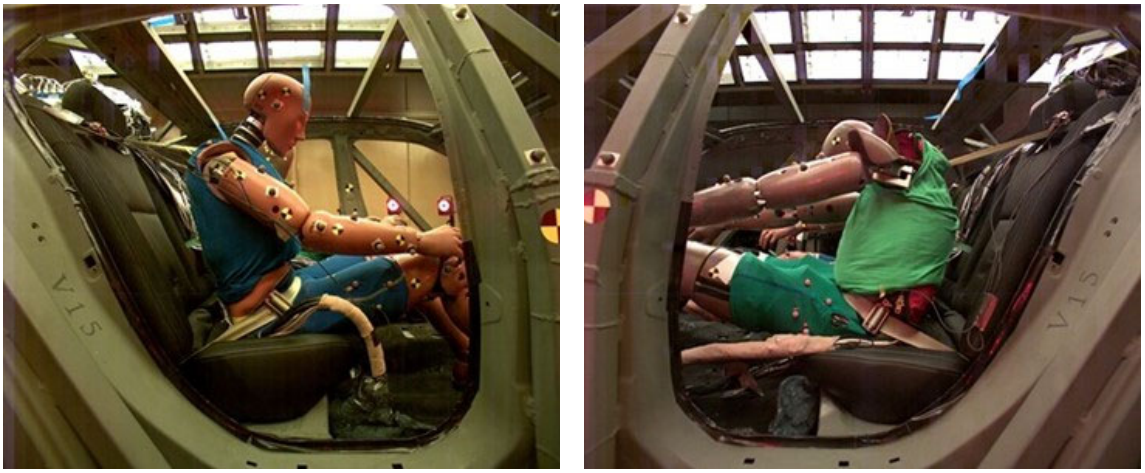

Figure PP-6. Test FRS-V15-2 HIII (Left) and THOR (Right) at Peak Hip Excursion

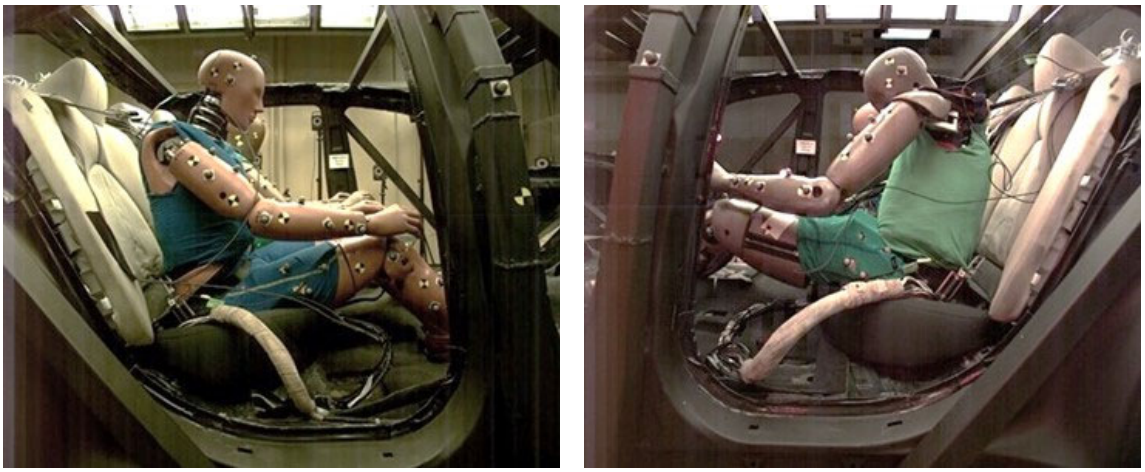

Figure PP-7. Test FRS-V19-1 HIII (Left) and THOR (Right) at Peak Hip Excursion

Appendix QQ. ATD X-Z Peak HIP X Excursion Frames for Scaled Tests

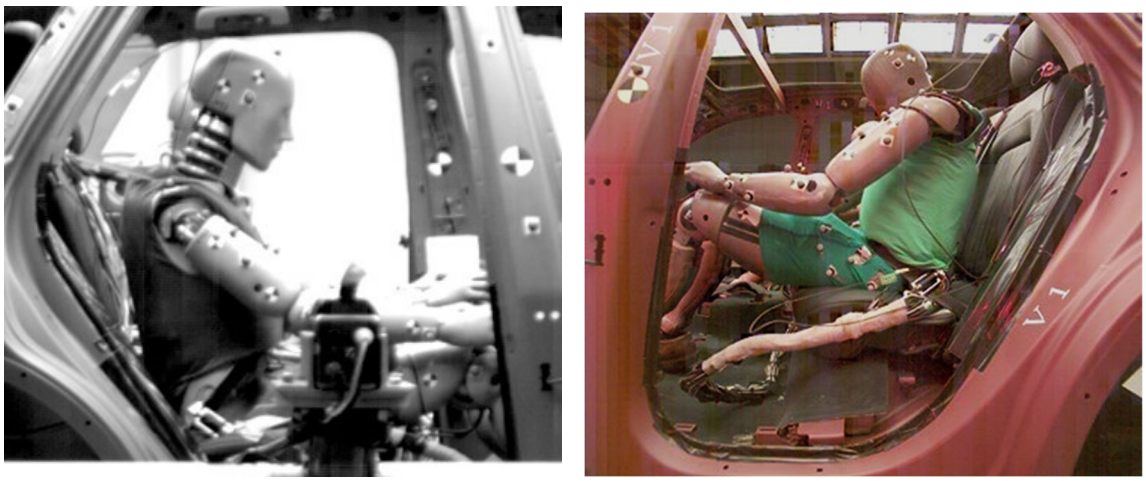

Figure QQ-1. Test FRS-V1-2 HIII (Left) and THOR (Right) at Peak Hip Excursion

Figure QQ-2. Test FRS-V6-2 HIII (Left) and THOR (Right) at Peak Hip Excursion

Figure QQ-3. Test FRS-V10-2 HIII (Left) and THOR (Right) at Peak Hip Excursion

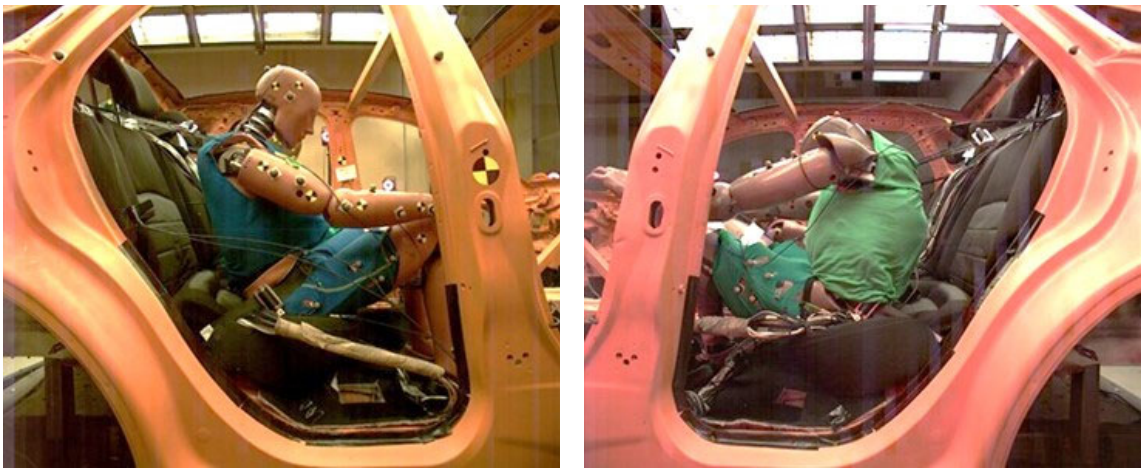

Figure QQ-4. Test FRS-V13-1 HIII (Left) and THOR (Right) at Peak Hip Excursion

Figure QQ-5. Test FRS-V14-2 HIII (Left) and THOR (Right) at Peak Hip Excursion

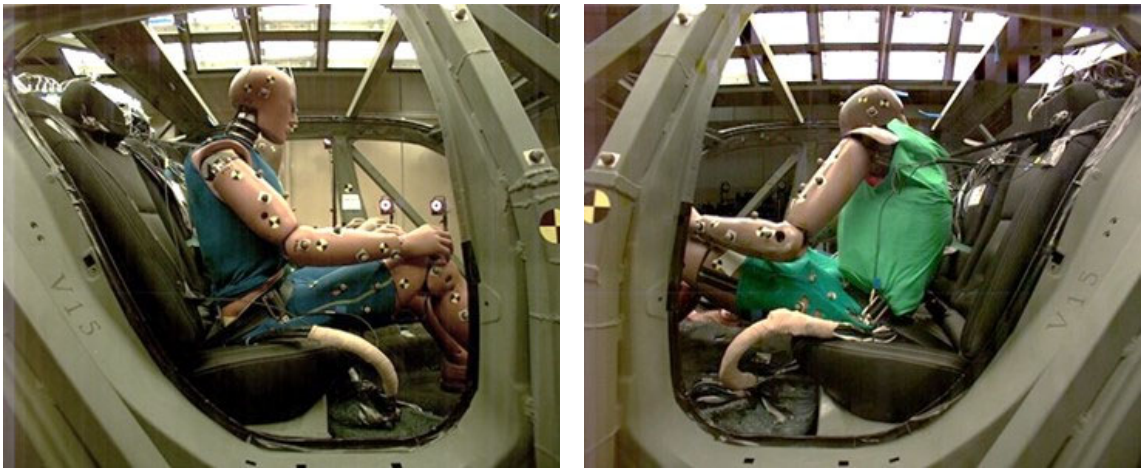

Figure QQ-6. Test FRS-V15-3 HIII (Left) and THOR (Right) at Peak Hip Excursion

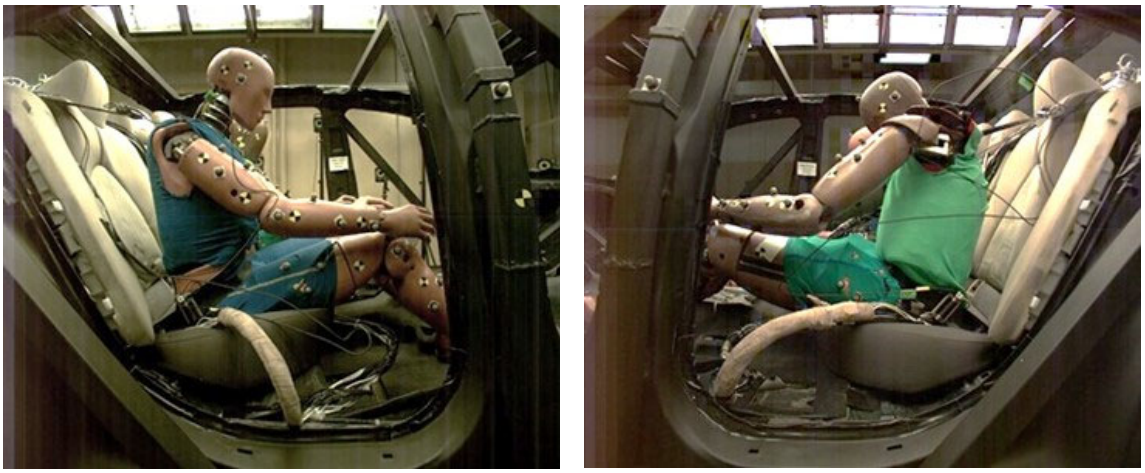

Figure QQ-7. Test FRS-V19-2 HIII (Left) and THOR (Right) at Peak Hip Excursion

Appendix RR. ATD X-Z Peak HIP X Excursion Frames for NCAP85 TESTS

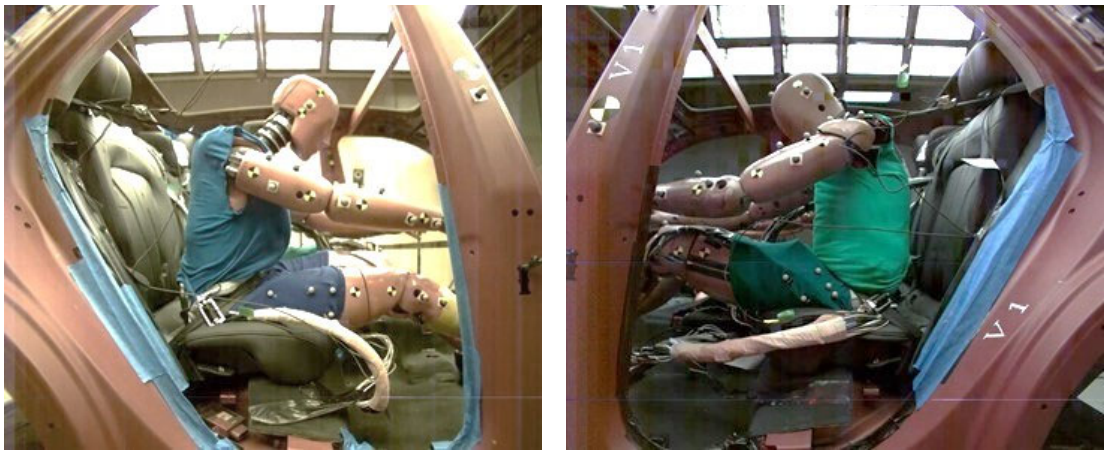

Figure RR-1. Test FRS-V1-3 HIII (Left) and THOR (Right) at Peak Hip Excursion

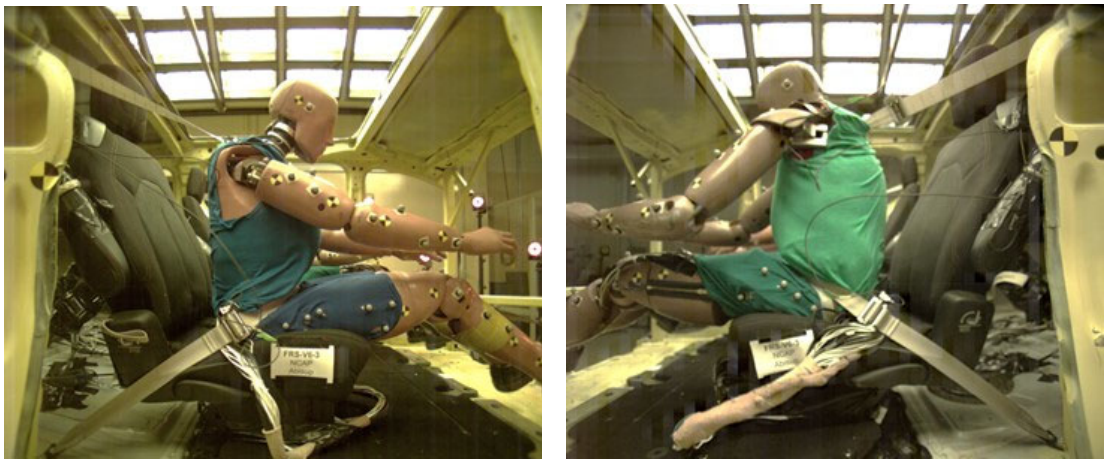

Figure RR-2. Test FRS-V6-3 HIII (Left) and THOR (Right) at Peak Hip Excursion

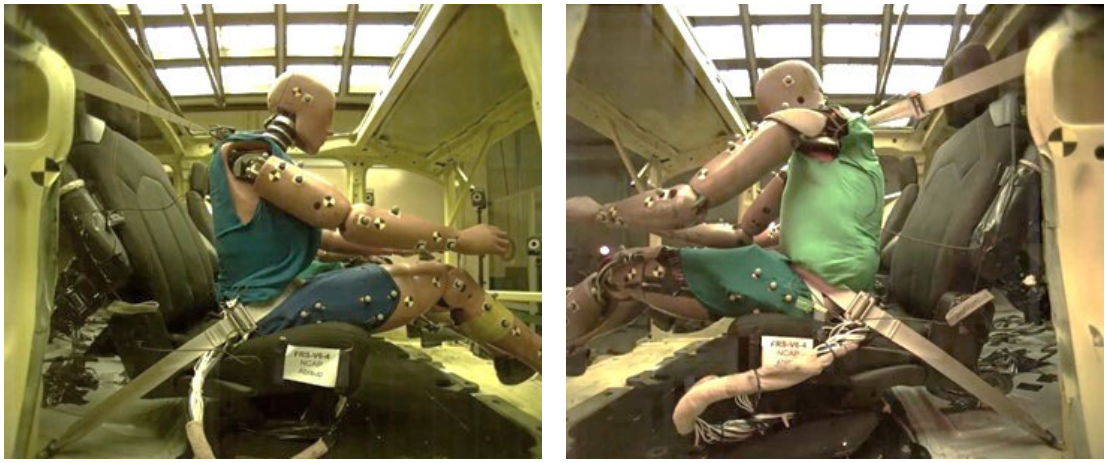

Figure RR-3. Test FRS-V6-4 HIII (Left) and THOR (Right) at Peak Hip Excursion

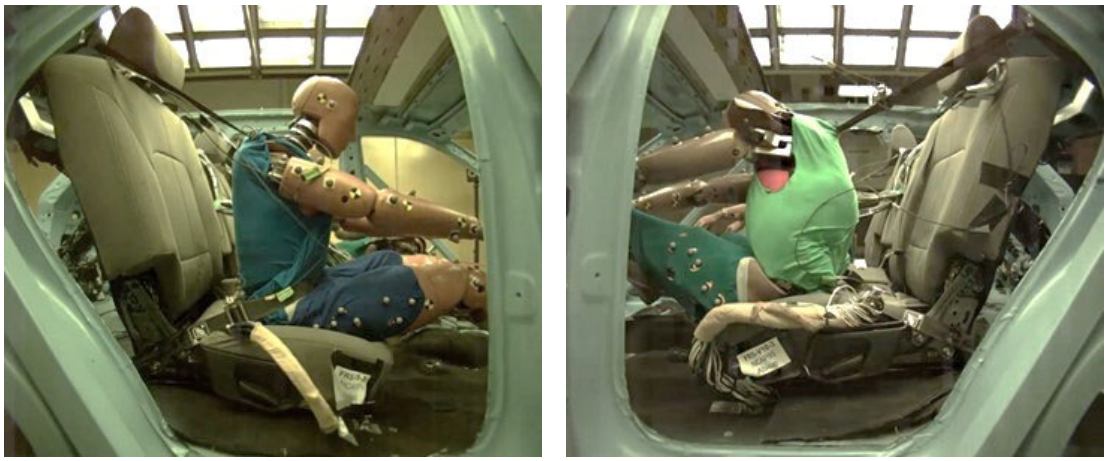

Figure RR-4. Test FRS-V10-3 HIII (Left) and THOR (Right) at Peak Hip Excursion

Figure RR-5. Test FRS-V13-2 HIII (Left) and THOR (Right) at Peak Hip Excursion

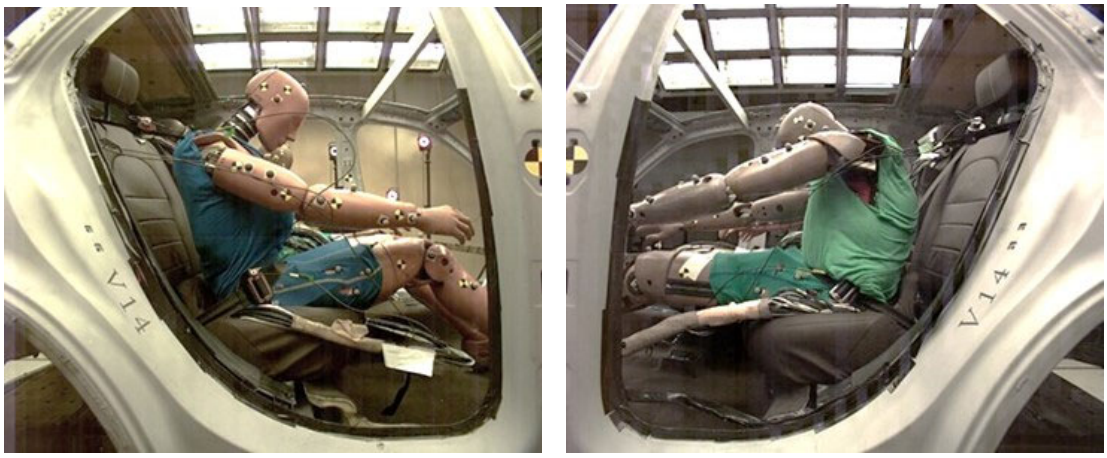

Figure RR-6. Test FRS-V14-3 HIII (Left) and THOR (Right) at Peak Hip Excursion

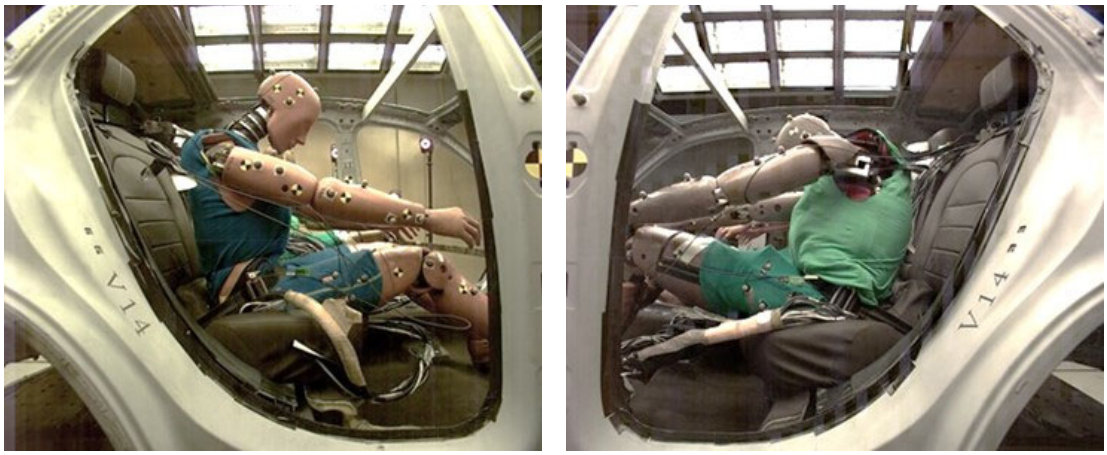

Figure RR-7. Test FRS-V14-4 HIII (Left) and THOR (Right) at Peak Hip Excursion

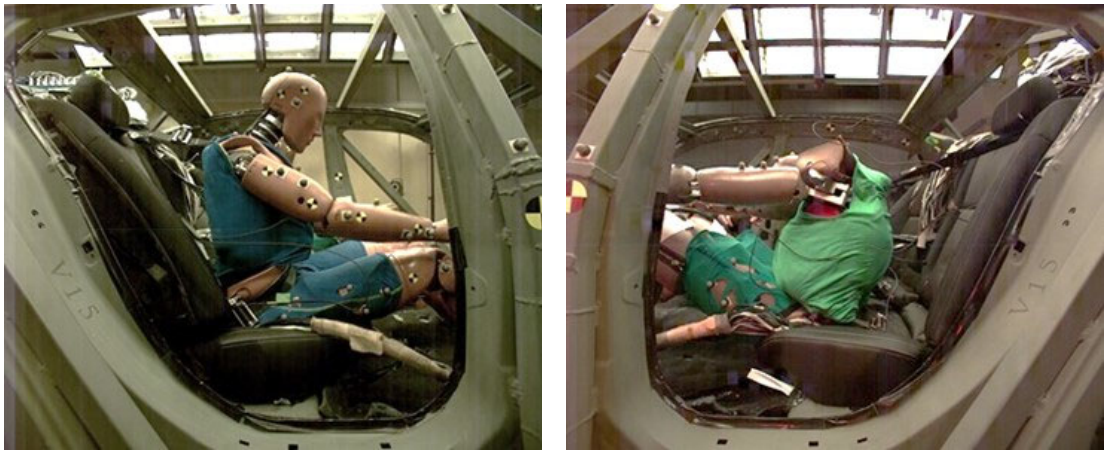

Figure RR-8. Test FRS-V15-4 HIII (Left) and THOR (Right) at Peak Hip Excursion

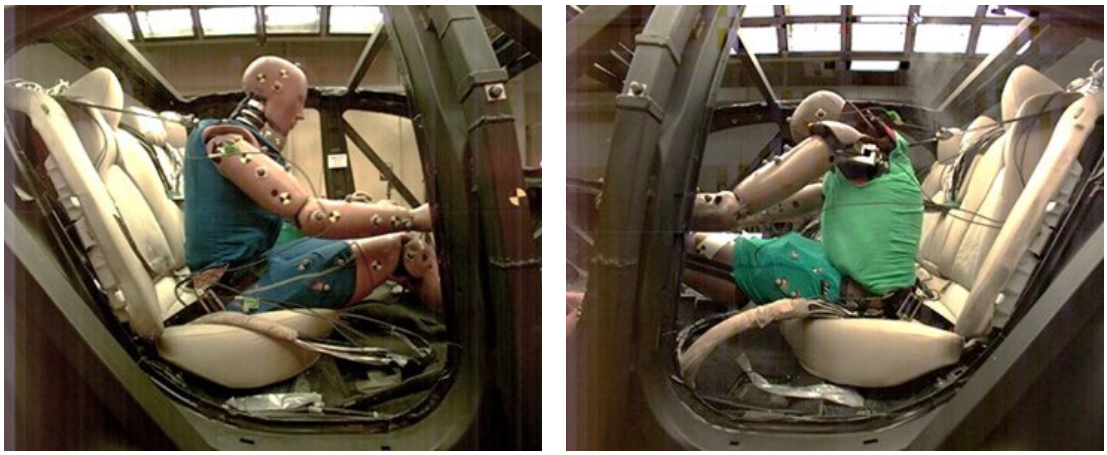

Figure RR-9. Test FRS-V19-3 HIII (Left) and THOR (Right) at Peak Hip Excursion

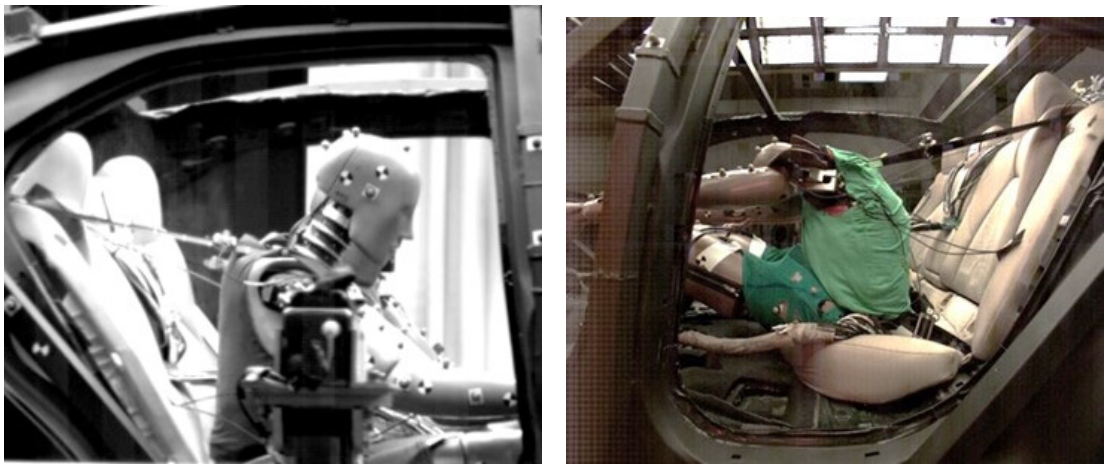

Figure RR-10. Test FRS-V19-4 HIII (Left) and THOR (Right) at Peak Hip Excursion

DOT HS 813 269
September 2022

U.S. Department
of Transportation

**National Highway
Traffic Safety
Administration**

15472-071422-v3